Contract No:

This document was prepared in conjunction with work accomplished under Contract No. DE-AC09-08SR22470 with the U.S. Department of Energy.

Disclaimer:

This work was prepared under an agreement with and funded by the U.S. Government. Neither the U. S. Government or its employees, nor any of its contractors, subcontractors or their employees, makes any express or implied: 1. warranty or assumes any legal liability for the accuracy, completeness, or for the use or results of such use of any information, product, or process disclosed; or 2. representation that such use or results of such use would not infringe privately owned rights; or 3. endorsement or recommendation of any specifically identified commercial product, process, or service. Any views and opinions of authors expressed in this work do not necessarily state or reflect those of the United States Government, or its contractors, or subcontractors.

We put science to work.™

Savannah River National Laboratory™

OPERATED BY SAVANNAH RIVER NUCLEAR SOLUTIONS

A U.S. DEPARTMENT OF ENERGY NATIONAL LABORATORY • SAVANNAH RIVER SITE • AIKEN, SC

PDRD (SR13046) Tritium Production Final Report

Authors: Steve Sheetz
Mark Jones
Jason Wilson

End-user: Bob Snyder

SRNL-STI-2013-00547, Revision 0
September 2013

Prepared for the U.S. Department of Energy
under contract number DE-AC09-08SR22470.

SRNL.DOE.GOV

This page intentionally left blank.

EXECUTIVE SUMMARY

Utilizing the results of Texas A&M University (TAMU) senior design projects on tritium production in four different small modular reactors (SMR), the Savannah River National Laboratory's (SRNL) developed an optimization model evaluating tritium production versus uranium utilization under a FY2013 plant directed research development (PDRD) project. The model is a tool that can evaluate varying scenarios and various reactor designs to maximize the production of tritium per unit of unobligated United States (US) origin uranium that is in limited supply.

The primary module in the model compares the consumption of uranium for various production reactors against the base case of Watts Bar I running a nominal load of 1,696 tritium producing burnable absorber rods (TPBARs) with an average refueling of 41,000 kg low enriched uranium (LEU) on an 18 month cycle. After inputting an initial year, starting inventory of unobligated uranium and tritium production forecast, the model will compare and contrast the depletion rate of the LEU between the entered alternatives. This is an annual tritium production rate of approximately 0.059 grams of tritium per kilogram of LEU (g-T/kg-LEU). To date, the Nuclear Regulatory Commission (NRC) license has not been amended to accept a full load of TPBARs so the nominal tritium production has not yet been achieved.

The alternatives currently loaded into the model include the three light water SMRs evaluated in TAMU senior projects including, mPower, Holtec and NuScale designs. Initial evaluations of tritium production in light water reactor (LWR) based SMRs using optimized loads TPBARs is on the order 0.02-0.06 grams of tritium per kilogram of LEU used.

The TAMU students also chose to model tritium production in the GE-Hitachi SPRISM, a pool-type sodium fast reactor (SFR) utilizing a modified TPBAR type target. The team was unable to complete their project so no data is available. In order to include results from a fast reactor, the SRNL Technical Advisory Committee (TAC) ran a Monte Carlo N-Particle (MCNP) model of a basic SFR for comparison. A 600MWth core surrounded by a lithium blanket produced approximately 1,000 grams of tritium annually with a 13% enriched, 6 year core. This is similar results to a mid-1990's study where the Fast Flux Test Facility (FFTF), a 400 MWth reactor at the Idaho National Laboratory (INL), could produce about 1,000 grams with an external lithium target. Normalized to the LWRs values, comparative tritium production for an SFR could be approximately 0.31 g-T/kg LEU.

A summary of the key values is shown in the table below.

Table ES-1: Estimated Tritium Production by Reactor Design

Reactor	Watts Bar 1 Base Case	Watts Bar 1 NRC Approved	NuScale	Holtec	mPower	Sodium Fast Reactor
Power (MWth)	**3,459**	**3,459**	**160**	**446**	**530**	**600**
Annual Tritium (g-T)	**1,696**	**704**	**105**	**297**	**559**	**1,001**
Annual LEU Use – Normalized (kg)	**28,533**	**27,000**	**5,797**	**5,481**	**8,896**	**3241**
Tritium/LEU (g-T/kg-LEU)	**0.059**	**0.026**	**0.018**	**0.054**	**0.063**	**0.31**

Initial Observations

Figure ES-1 is an example of output from Tritium Enterprise model comparing uranium consumption for various production reactor types for a steady annual tritium requirement of 1.0 kilogram. Note that tritium production scenarios used in this report do not reflect actual tritium requirements. The production scenarios were defined at 0.5 kg increments and utilized to test the model and to demonstrate the effects of various reactor designs on uranium usage.

From the evaluation of the reactor designs, and output from the model, some initial observations include:

- When loaded with an optimal complement of TPBARs LWRs small and large produce roughly the same quantity of tritium per kilogram of uranium basis.
- If the long-term requirement for tritium approximates the optimized annual production from Watts Bar 1 and is relatively constant over time, an equivalent fleet of light water SMRs offers little benefit on the impact of the unobligated reserves.
- Small LWRs can optimize uranium utilization in two primary cases. If stockpile requirements trend lower, a fleet of SMRs could “follow” the decreasing requirements by utilizing just the number of cores required, instead of running a full core of US uranium in Watts Bar with just a fraction of the TPBARs in pile. Should the tritium requirements increase incrementally above what Watts Bar can produce, one or more SMRs could be loaded to produce the delta without having to start a second full sized Tennessee Valley Authority (TVA) reactor.
- Fast spectrum reactors, such as an SFR, demonstrate the potential to increase uranium utilization by 5-fold or greater. SFRs may be able to de-power the reactor by adjusting the reflectors, so that tritium production can be reduced to follow a lower demand, while extending the core life; thereby further conserving the uranium.

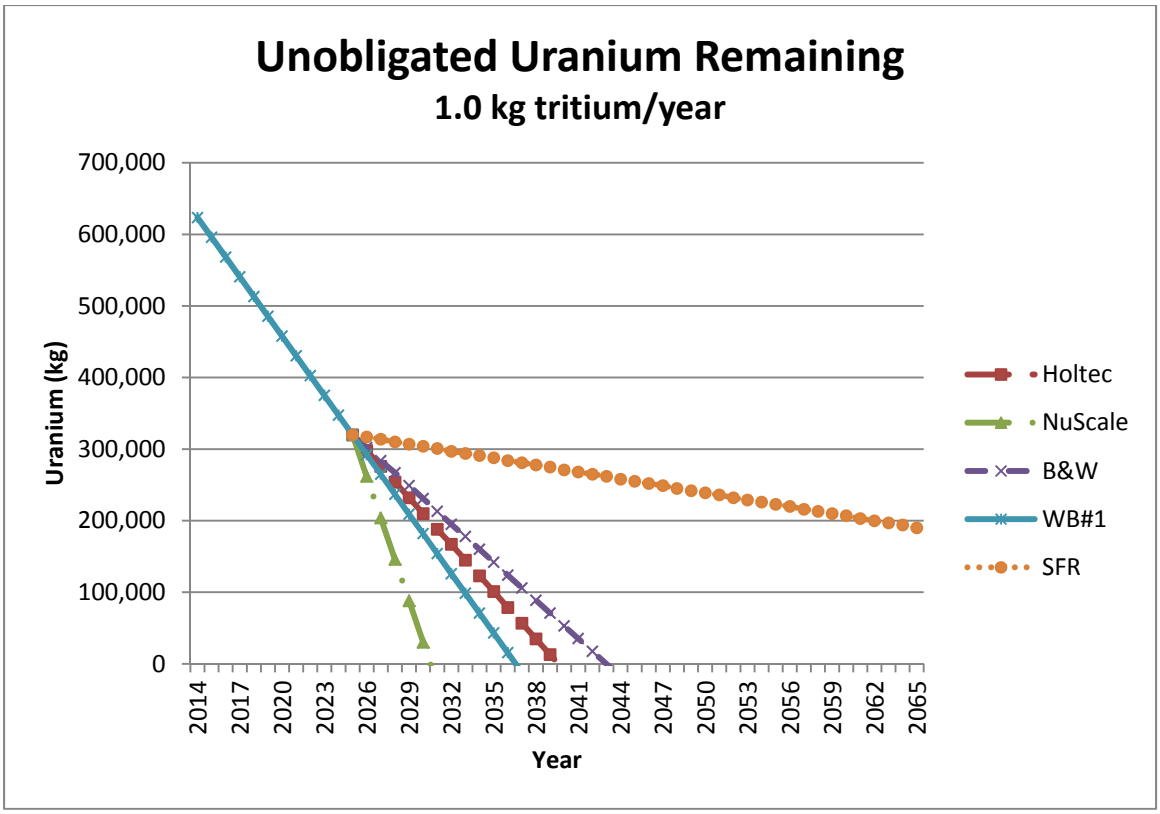

Figure ES-1 Tritium Enterprise Model Comparing Uranium Consumption for Various Production Reactor Types

Summary of future needs

- Approve and load the model on a classified system so actual tritium production values and forecast needs can be entered to more accurately reflect different options on the consumption of US origin, unobligated uranium.
- Work with interested SMR vendors to more accurately model their cores, their fuel management schemes, and reactor design to develop more accurate estimates of their tritium producing capacity.
- Pursue SFR options with advanced lithium target design.
- Leverage an approved Lab Directed R&D (LDRD) program at SRNL for extraction of tritium from a liquid lithium target.
- Develop business cases for cost-effective tritium production for the next 50 years.

Table of Contents

EXECUTIVE SUMMARY iii
ACRONYMS x
1.0 INTRODUCTION – PDRD TASK AND SCOPE 1
2.0 REVIEW OF THE TEXAS A&M STUDENT REPORT ON TRITIUM PRODUCTION IN SMRs 1
2.1 B&W mPower 2
2.1.1 Overview 2
2.1.2 Process 2
2.1.3 Conclusions and Path Forward 3
2.2 Holtec HI-SMUR™ 4
2.2.1 Overview 4
2.2.2 Process 4
2.2.3 Conclusions and Path Forward 5
2.3 NuScale 6
2.3.1 Overview 6
2.3.2 Process 6
2.3.3 Conclusions and Path Forward 7
2.4 GE-SPRISM 8
2.4.1 Overview 8
2.4.2 Process 8
2.4.3 Conclusions and Path Forward 8
3.0 INDEPENT ANALYSIS OF SODIUM FAST REACTORS 9
4.0 TRITIUM ENTERPRISE MODEL DEVELOPMENT 15
4.1 Tritium Production Model 15
4.2 Simulation and Modeling 15
4.3 Base Model 16
4.4 Venapps 20
5.0 DISCUSSION OF RESULTS 26
5.1 Model comparison with Watts Bar 1 27
5.2 Model results for SMR Scenarios 28
6.0 Conclusions 31
6.1 Observations 31
6.2 Summary of Future Needs 32

7.0 REFERENCES 32

8.0 APPENDIX 32

8.1 Appendix A - Tritium Production Model 32

8.2 Appendix B - Texas A&M Studies 57

List of Figures

Figure ES-1 Tritium Enterprise Model Comparing Uranium Consumption for Various Production Reactor Types v

Figure 3-1: MCNP layout configuration for simple lithium blanket 10

Figure 3-2: Tritium production rate in units of Tritium per Fission in an external blanket as a function of lithium blanket thickness 11

Figure 3-3: MCNP layout configuration for "sandwich" lithium/moderator blanket with the lithium volume surrounding the moderator greatly exaggerated in this drawing 12

Figure 3-4: Tritium production rate in units of Tritium per Fission in a "sandwich" configured external blanket as a function of Be moderator thickness 13

Figure 3-5: Tritium production rate in units of Tritium per Fission in a "sandwich" configured external blanket as a function of NaOH moderator thickness 13

Figure 4-1 Base Structure 16

Figure 4-2 Base Input/Output Structure 17

Figure 4-3 Comparison Structure 17

Figure 4-4 Excel Input Sheet 18

Figure 4-5 Comparison Output Charts 19

Figure 4-6 Example of Post Processed Excel Chart 19

Figure 4-7 Title Screen 21

Figure 4-8 Main Menu 22

Figure 4-9 Scenario Setup 23

Figure 4-10 Setup Screen 24

Figure 4-11Unobligated Uranium Remaining 25

Figure 4-12 Additional Charts 26

Figure 5-1 Unobligated Uranium Remaining – 1.0 kg tritium/year 29

Figure 5-2 Unobligated Uranium Remaining – 1.5 kg tritium/year 29

Figure 5-3 Unobligated Uranium Remaining – 2.0 kg tritium/year 30

Figure 5-4 Unobligated Uranium Remaining – 0.5 kg tritium/year 31

List of Tables

Table ES-1: Estimated Tritium Production by Reactor Design..... iv

Table 3-1 Summary of Potential Tritium Production..... 14

Table 5-1 Watts Bar 1 Tritium Production Summary 27

Table 5-2 Summary of the Key Values of Reactor Types..... 28

ACRONYMS

DOE	Department of Energy
FTTF	Fast Flux Test Facility
LDRD	Laboratory Directed Research and Development
LEU	Low Enriched Uranium
LWR	Light Water Reactor
MNCP	Monte Carlo N-Particle
NRC	Nuclear Regulatory Commission
PDRD	Plant Directed Research and Development
PNNL	Pacific Northwest National Laboratory
PWR	Pressurized Water Reactor
SFR	Sodium Fast Reactor
SMR	Small Modular Reactor
SRNL	Savannah River National Laboratory
TAC	Technical Advisory Committee
TAMU	Texas A&M University
TPBAR	Tritium Producing Burnable Absorber Rods
TVA	Tennessee Valley Authority
US	United States
WABAs	Wet Annular Burnable Absorbers
WB1	Watts Bar 1(Tennessee Valley Authority nuclear reactor)

1.0 INTRODUCTION – PDRD TASK AND SCOPE

New nuclear reactor technology is emerging in the United States (US). This new technology has potential to have a positive effect on the long-term supply of US origin uranium needed to produce the tritium for the US nuclear stockpile. Senior level projects at TAMU, sponsored by adjunct professor, Dr. David Senor of Pacific Northwest National Laboratory (PNNL), evaluated four different reactor designs on their capacity to produce tritium. The output of these senior projects will define the potential tritium production in these units but they are not expected to develop strategies that optimize tritium production and maximize the utilization of US origin uranium in the out years.

SRNL originally proposed to collaborate with PNNL and TAMU on their senior projects, utilizing SRNL's tritium experience, SMR design knowledge, and existing agreements with each of selected designs (NuScale Power, Generation mPower, Holtec, GE-Hitachi) to support them. Due to delays in funding until February 15, 2013, it was deemed too late in the school year for SRNL's involvement with the students to add value to their project so the PDRD budget was reduced to $190k. So SRNL utilized the results from the Texas A&M senior design projects that are evaluating potential tritium production in four different SMR designs, and developed an optimization model that evaluates tritium production versus uranium utilization. The goal is to maximize the production of tritium per unit of US origin uranium that is in limited supply.

2.0 REVIEW OF THE TEXAS A&M STUDENT REPORT ON TRITIUM PRODUCTION IN SMRs

The TAMU study involved four student teams who analyzed four different proposed SMR concepts for tritium production. The four teams conducted studies on core neutronics, thermal hydraulics, safety and economics. The SMRs analyzed included the Babcock and Wilcox mPower, Oregon State's NuScale, Holtec's HI-SMUR^{TM}, and the GE SPRISM reactor. The first three reactor types are light water SMRs while SPRISM is a fast spectrum system.

For each concept evaluated in the A&M study, the students:

- Developed a baseline design representing the proposed reactor,
- Evaluated the tritium production potential of the reactor using TPBARs,
- Conducted reactor physics analyses (either CASMO4, MCNP, Simulate3), thermal hydraulic, and safety evaluations (RELAP in most cases or GOTHIC for NuScale),
- Evaluated the safety of the modified SMR by estimating the reactor feedback changes and by performing thermal hydraulic safety analysis for a design basis loss of flow accident or loss of off-site power, plus other events, and
- Performed a preliminary economic analysis of the tritium production by taking into account the fuel enrichment cost, the effective value of tritium, reactor capital cost for some of the cases, and revenue from the sale of electricity in most cases.

The first three reactors in the list (mPower, NuScale, and Holtec) are all light water SMR's that all employ currently operational 17x17 fuel assemblies of varying lengths in their design. The

last reactor in the list, the GE-Hitachi SPRISM is a liquid metal fast neutron reactor. For each of the reactors evaluated in these studies, the students evaluated tritium production capabilities of the reactors using TPBARs.

A brief review of the student results follows and includes an overview of each study, how each defined the process, and a critique of the results with a path forward to improve the data. Results from the three LWR teams are close to expectations for production. The GE-Hitachi SPRISM team results are incomplete and therefore the results are not included in the enterprise model for further evaluation. The complete results of the TAMU studies are included for reference in Appendix B.

There was limited time available for the student study, and in order to confirm some estimates on fast spectrum systems, the TAC subgroup reviewed other relevant studies. Tritium production was proposed in the FFTF in the mid-nineties, and the results were published in several reports. FFTF is a 400 MWth sodium cooled fast reactor developed by the US Department of Energy (DOE) to test advanced fast reactor fuels and was considered generally representative of a fast spectrum SMR. Independent neutronic analyses were also conducted to verify the production capabilities of a representative advanced SFR SMRs.

2.1 B&W mPower

2.1.1 *Overview*

For the analysis of the B&W mPower reactor, the group of students set out with the objectives of using the mPower SMR to produce tritium through the use of TPBARs, with a design goal of producing 1150 grams of tritium per year. The goal of the group was to design the mPower reactor to produce maximum amount of tritium while still being able to operate over a desired cycle length. This design attempted to fulfill the objective for tritium production before examining electricity production, cost effectiveness, and research and development benefits

B&W mPower

2.1.2 *Process*

To reach the goal for tritium production with the TPBARs in the mPower SMR, the group accomplished these tasks by using CASMO4 and a Team 9 Nuclide Program (T9NP). The T9NP was a FORTRAN program that was developed by the group to solve for the amount of tritium that would be produced based on the neutron scalar flux within the reactor. The fuel assemblies that were used for the mPower design are shortened 17X17 fuel assemblies; the group used an example from a B&W presentation to model the fuel assemblies within the reactor. These assemblies have 16 burnable absorber rods each as well as

24 guide tubes. In order to produce tritium in the mPower SMR, the burnable absorber rods were replaced with TPBARs that were shortened to fit in an mPower assembly. This is different than what is currently done at Watts Barr. Currently the TPBARs are placed in guide tubes in fuel assemblies that do not have control or shutdown rods to be inserted into these guide tubes. Using the negative reactivity from the TPBARs in place of the burnable absorbers could lead to using lower enriched fuel than currently utilized for WB1, but since the TPBAR's neutron absorption properties do not drop off at the same rate as boron poison rods, this could lead to requiring a higher enriched fuel than planned for the mPower design.

CASMO4 was chosen by this group also because of its simplicity and students' previous knowledge and experience with the program. However, the version that was available for their use was only the student version, which did not have access to the full isotope data library. This limitation did not allow access to lithium-6 and lithium-7, which were needed to model the TPBAR. The only available lithium for them to use in their models was natural lithium, which had a fixed weight percentage of lithium-6 and lithium-7 (7.5% and 92.5%, respectively); where the lithium aluminate in the TPBAR is enriched with lithium-6. To account for this boron-10 was used as a surrogate material to make up the balance of lithium-6 deficiency due to the limitations in the code. The team determined by the neutron absorption cross sections of boron-10 and lithium-6 that boron-10 could be used to mimic lithium-6 in the reactor by adjusting the boron-10 density. The method used to validate this was the case they ran different enrichments of boron-10 in the TPBARs and compared it to natural lithium in the TPBAR. This method showed that there was a difference between the natural lithium and boron-10 equivalent. However, the difference is under 8%, and increases as the burn-up increases. This is expected since the boron-10 does not build up any poisons when it is depleted and the TPBARs will produce helium-3. The next thing that was completed was to optimize the cycle length and lithium-6 enrichment and fuel enrichment levels. They ran simulations in CASMO4 for varying fuel and lithium-6 enrichments. The group used fuel enrichments varying from 3% to 5% and lithium-6 enrichments from 8% to 34%. In order to examine the effect of helium-3 buildup in the TPBARs throughout the cycle of the reactor, the group modeled the TPBARs that contained 12% helium-3. To evaluate the effect of the helium-3 concentrations the group ran the same simulations as above with the varying fuel and lithium-6 enrichments to determine fuel and lithium-6 enrichments to be used. With this amount of lithium-6 it was determined that the reactor was still viable but the effect was fairly significant.

2.1.3 *Conclusions and Path Forward*

After this analysis was completed the team concluded that a single mPower reactor with all 69 assemblies containing 16 TPBARs, the core would produce 1116.9 grams of tritium per two year cycle and 559 grams of tritium per year. This level of tritium production was achieved by using 4% enriched fuel and a lithium-6 enrichment in the TPBARs of 22% and a cycle length of two years. The design goal of 1150 grams of tritium per year was not met with a single core. If a "twin pack" design is considered the production doubles to 1116.9 grams of tritium per year but still falls short of the 1150 grams of tritium per year.

The amount of tritium that the group concluded could be produced in a single mPower reactor deviates from the actual production since they were not able to use enriched lithium in their modified TPBARs. Even though they used boron-10 with a correction factor to get the same cross section and density as lithium-6 and implemented helium-3 into the rods, the buildup of helium-3 from zero to a steady state value that will be reached between the production of helium-3 through decay of tritium and helium-3 absorption of a neutron and being converted back to tritium.

A further analysis would need to be done on the shorter TPBARs since the pressure limit currently imposed on TPBARs is 1.2 grams per bar, and in the case of the TPBARs used in this analysis it would be 0.86 grams per shortened TPBAR for the mPower reactor. With this consideration the production of tritium from a single mPower reactor would be limited to 949.4 grams of tritium per two year cycle. A further examination would need to be done with replacing the wet annular burnable absorbers (WABAs) with TPBARs and still maintaining safety and shutdown margins.

2.2 Holtec HI-SMUR™

2.2.1 *Overview*

For the analysis of the Holtec Inherently-Safe Modular Underground Reactor (HI-SMUR™), this group of students set out with the objective of modifying the HI-SMUR™ design for production of tritium through the use of TPBARs. The project was to modify the design to see what increase in cost from an unmodified reactor would be necessary to produce tritium in one or multiple HI-SMUR™at a rate of 1150 and to evaluate how much of the cost can be offset by electricity production.

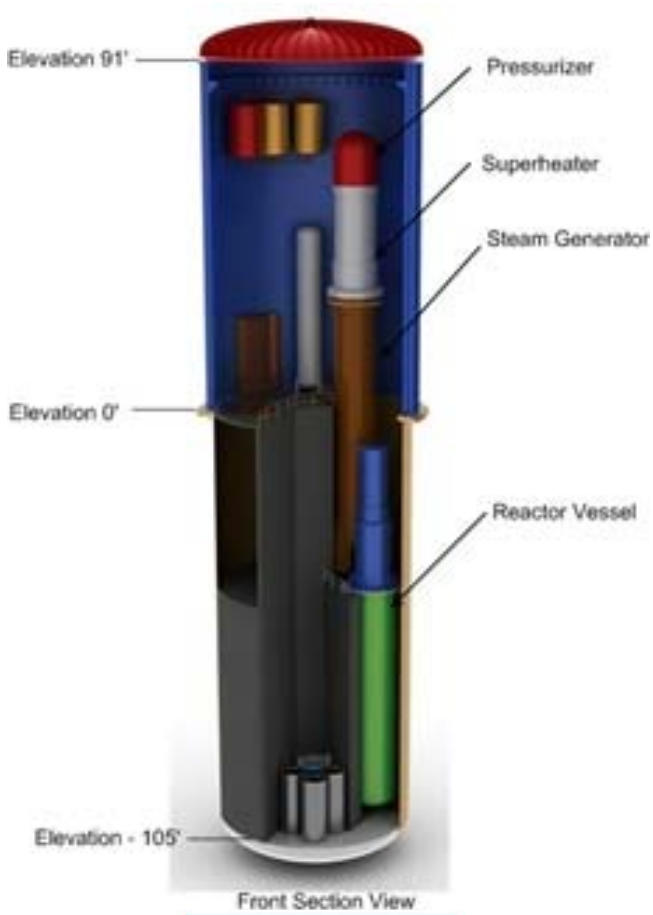

Holtec – HI-SMUR

2.2.2 *Process*

In order to reach to production goal set forth with TPBARs in the HI-SMUR™, the group approached the task by looking at a loss of coolant accident safety analysis to impose a maximum limit on the number of TPBARs in the core. Then they used neutronic analysis by using MCNP to design the optimal core arrangement for tritium production and cost effectiveness. The group of students was unable to acquire a core design for the HI-SMUR™ because it was considered proprietary information. So they modeled the core configuration after the NuScale SMR. To calculate tritium production rate and was compared using two methods.

- The first method used MCNP to calculate the thermal neutron flux radial variations in the lithium pellet and iterate with the Tritium Production Model. This was used to determine the number of TPBARs required in each assembly to meet the goal because it accounted for the depletion of the lithium.
- The second method utilizes a cell averaged flux tally in MCNP coupled with a neutron reaction multiplier, not accounting for depletion, to compare with result from the Tritium Production Model.

The Tritium Production Model was an Excel program that used simple production and loss equations along with inputs of lithium-6 absorption cross section, half-life of tritium, and decay constant, as well as the initial enrichment of lithium-6 and the thermal flux, and gave values for the amount of lithium-6 and tritium produced for time steps throughout the cycle. Even though Monte Carlo N-Particle (MCNP) is capable of keeping decay product inventories during calculations, the group decided to use the Tritium Production Model because of the long computing time needed for MCNP. An increase in the neutron flux was seen at the inner surface of the TPBAR and helium gas annulus because of the scattering of fast neutrons. The group did not use the fast neutron flux in either of the two methods, only the thermal neutron flux.

Due to time constraints the group was unable to do this full iterative process to determine the number of TPBARs per assembly and the lithium-6 enrichment levels. They chose to estimate these values to keep tritium production under 1.2 grams per TPBAR. This led to them choosing 24 TPBARs per assembly and a lithium-6 enrichment level of 12.2%.

2.2.3 *Conclusions and Path Forward*

After all the analysis was completed the group concluded that a single HI-SMUR™ with all 32 assemblies holding 24 TPBARs, the single unit would produce 296.67 grams per year with the first method, and 694.48 grams per year with the second method. The group expected the second method results to be higher than the results from the first method, since the second method did not take into account for the depletion of lithium-6. If you look at their assumption of a max tritium production per TPBAR of 1.2 grams per TPBAR and apply it to the number of TPBARS in the core, you would obtain a maximum production of 921.6 grams of tritium per reactor core for any given cycle or 307.2 grams of tritium per year with the three year cycle used by this group. If you compare this maximum to the two results that were obtained by the group it is clearly shows that the first method is close to the maximum production per TPBAR and that the second method is over twice the limit for tritium production per TPBAR. At the first method's rate of production it would take four HI-SMUR™s to reach the production goal of 1150 grams of tritium per year.

Although this group was able to use lithium-6 over a surrogate material, they failed to account for the production of helium-3 by the decay of tritium. With helium-3 having such a large neutron cross section, ignoring the buildup of helium-3 in the TPBARs will greatly increase the neutron flux that was seen inside of the bars. Also since they took into account the loss of tritium through decay and did not account for the production of tritium from helium-3 the loss term was greater than was actually needed.

Since the HI-SMUR™ uses standard length 17x17 fuel assemblies, there will not need to be any shortening of the TPBARs for use within this reactor. The only modification that might have to be investigated for the TPBARs is that the group had them inserted in fuel rod positions instead of guide tube positions, which is what is currently done at Watts Barr. The guide tubes are used for control rod insertion therefore, this can only be done if the fuel assembly does not have a control rod assembly above it and it appears from the report that all 32 fuel assemblies have control rods.

2.3 NuScale

2.3.1 *Overview*

For the analysis of the NuScale reactor, the group of students set out with the objectives of using the NuScale SMR to produce tritium through the use of TPBARs, without exceeding the tritium production limits in a single TPBAR. The limit of tritium per TPBAR that was used by the group was 1.2 grams per TPBAR, for a full pressurized water reactor (PWR) assembly, and subsequently 0.65 grams for a shortened TPBAR to fit in the NuScale design. The 1.2 grams per TPBAR was used, in order to meet design limitations on internal pressure of the TPBAR and meet the burn-up of the lithium pellets. The lower number for the NuScale sized TPBAR was arrived at by looking at the decrease in active absorber region available in the NuScale SMR leading to the maximum amount of tritium being produced to 0.65 grams per TPBAR.

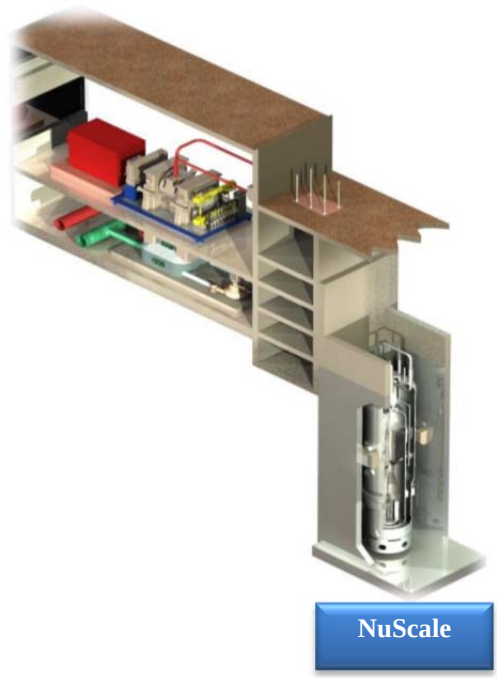

2.3.2 *Process*

Their goal in this was to design a reactor that ran at a constant power level while keeping the enrichment below 4.95%, and to keep the tritium produced as close as possible to the limit of 0.65 grams per TPBAR. To accomplish these tasks the group used DRAGON and CASMO4 to do the neutronic analysis. CASMO4 was chosen by the students because of its simplicity and students' previous knowledge and experience with the program. However, the version that was available for their use was only the student version, which did not have access to the full isotope data library. This limitation did not allow access to lithium-6 and lithium-7, which were needed to model the TPBAR. The only available lithium for them to use in their models was natural lithium, which had a fixed weight percentage of lithium-6 and lithium-7 (7.5% and 92.5%, respectively); where the lithium aluminate in the TPBAR is enriched with lithium-6. From this they developed two alternative methods to simulate the TPBARs in CASMO4. The two methods are as follows:

- The first method used natural lithium to account for the correct amount of lithium-7, which led to a deficit of the amount of lithium-6. To account for this deficit the group used boron-10 to account for the remainder of the lithium-6. Boron-10 was used because it was available in their version of CASMO4 and also because boron-10 and lithium-6 have similar microscopic absorption cross sections. They then calculated a correction factor from the microscopic absorption cross sections and applied it to the total macroscopic cross sections, which led to having a total neutron cross section that was approximately a third of what was expected. Another problem that arose from this method was that boron-10 has a different decay chain than lithium-6, which does not take into account the buildup of helium-3, a neutron poison prevalent in lithium-6 decay chain.
- The second method developed used natural lithium to account for the correct amount of lithium-6 mass per TPBAR, while ignoring the lithium-7 mass. Since natural lithium's enrichment of lithium-6 is so low, an abundant amount was needed to meet the lithium-6 mass requirements. This led to a vast excess of lithium-7, nearly three times the amount in a normal TPBAR. This was deemed feasible since the absorption cross section of lithium-7 was so low, and lithium-6 was more importantly neutronically.

These two methods were run in CASMO4 and compared to a run in DRAGON to compare the k-infinite of an assembly over a burn-up of 60 GWD/MTU. The DRAGON run consisted of a 17x17 fuel assembly with 3.8% fuel enrichment and 24, 18.7% enriched TPBARs. The CASMO4 runs comparing the other methods were done with the same fuel enrichment and the same number of TPBARs in the assembly. From this comparison the method that compared the best with the DRAGON run was method two.

2.3.3 *Conclusions and Path Forward*

After all of the analysis was completed by the group they concluded that a single NuScale reactor with 12 of the 37 assemblies holding 24 TPBARs each would produce 161.27 grams of tritium per 18 month cycle, or 109.22 grams per year. In order to reach the goal that was set forth to the group of producing 1150 grams of tritium per year, eleven tritium producing NuScale reactors would be needed to reach this goal.

The amount of tritium that the group calculated to be produced in these reactors deviates from the actual production since they were not able to use the correct lithium-6 to lithium-7 ratio. Even though lithium-7 has very little impact on the neutronics, having three times the amount of lithium-7 in the TPBAR will have some effect just by tripling the amount that will be seen by the neutrons. Another factor that would lead to the production numbers being different is the group assumed all lithium-6 neutron absorption resulted in obtainable tritium. Where there would be some of the produced tritium would leak into the core to the coolant/moderator and with the relatively short half-life of tritium (12.3 years), there would be some decay of the tritium that was produced. Another term that could induce a change in the tritium produced was the assumption that a half-length TPBAR would produce greater than half of what they used for a full TPBAR.

A further analysis of a half-length TPBAR is needed, along with optimizing the production over the planned reactor cycle of 24 months instead of the 18 month cycle length that was used. This model also did not take into account burnable absorbers that are used in the core to flatten the neutron flux for a more even burn-up of the fuel, and consequently the TPBARs. This biggest improvement that is needed is a more accurate portrayal of the TPBARs lithium-6 to lithium-7 ratio to make better estimates to what could be produced within a NuScale SMR.

2.4 GE-SPRISM

2.4.1 *Overview*

For the analysis of the GE-SPRISM the students investigated the feasibility of using the SPRISM for tritium production. They began with the intention of choosing a fuel type, fuel composition, and a TPBAR position distribution such that tritium production was maximized. Also, two methods of tritium production inside the reactor were to be investigated: a breeder blanket application and a homogenous coolant mixture application. The investigation into the homogenous coolant mixture was halted, since its application was outside the scope of this project. Also, exploring all three fuel types for the SPRISM, different fuel compositions, and various TPBAR position distributions proved to be ambitious for accomplishment within the allotted time for the project.

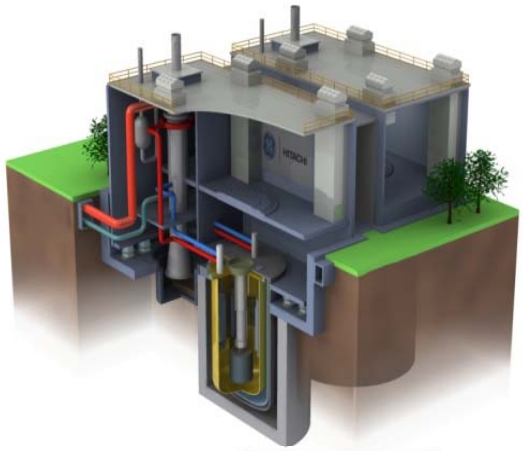

GE-SPRISM

2.4.2 *Process*

In order to reach the production levels of 1150 grams of tritium per year, the group set out with two main goals. The first goal was to modify the loading of the SPRISM to enable the production of tritium in the outermost breeder blanket. The second goal was to optimize the power production of the reactor with its tritium production. To accomplish these goals the group used MCNP for the neutronics. The group used an MCNP model of 1/6th core that they obtained from a thesis. The TPBARs were then modified to for height and dimensions to fit in a breeder fuel assembly, as well as a driver fuel assembly. This came out to 6096 TPBARs in the core in breeder fuel assemblies and 13056 TPBARs in the driver fuel assemblies, for a total of 19152 TPBARs in the core. With these TPBARs in the core they obtained neutron flux at the TPBAR locations and took an average of this flux to calculate the tritium production. This assumption was used instead of determining the efficiency of each assembly type because of the lack of results available due to time constraints and the large time required to run the code.

2.4.3 *Conclusions and Path Forward*

With these assumptions the total tritium production rate in the core was found to be negligible. Using both driver and breeder assemblies the production rate was less than one gram every 18 months. With this amount of TPBARs in the core, if viable neutronically and within safety

margins, if you could reach a production of a 0.25 grams per TPBAR in 18 month cycles, the reactor would be producing 4788 grams of tritium in a cycle, which is equivalent to 3192 grams of tritium per year. This design was not optimized for tritium production; the code was ran once and those numbers were used to draw their conclusions on the tritium production. This was an inadequate evaluation of the tritium production capabilities of this reactor and further analysis would need to be done to get an accurate portrayal of what this reactor is capable of.

3.0 INDEPENT ANALYSIS OF SODIUM FAST REACTORS

With the incomplete evaluation of tritium in the GE-Hitachi (GE-H) PRISM SFR by the TAMU team, the SRNL TAC was asked to conduct a high-level scoping analysis of what a small SFR could produce. Their evaluation was based on a pool-type sodium cooled reactor based off the Experimental Breeder Reactor II (EBR-II) which ran for 30 years at the Idaho National Laboratory. This pool design is the basis for many emerging SFR designs including the GE-Hitachi PRISM, Toshiba 4S, Terrapower and others.

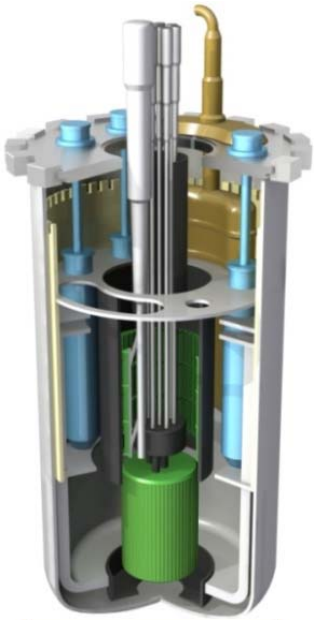

GE-H PRISM

In order to confirm the estimates of fast spectrum tritium production potential, a series of scoping level calculations with MCNP was carried out using a representative, but simplified fast reactor configuration. Fast spectrum systems generally have lower parasitic absorption, more neutrons produced per fission, and a larger fission to absorption cross section ratio in the fuel. Neutron leakage from a fast reactor is also greater than water cooled thermal reactors, due to the smaller scattering cross section for fast neutrons. These factors indicate that fast spectrum systems will potentially have greater tritium production capacity than thermal systems.

EBR-II
INL

Production of tritium in a fast reactor will require moderation of the neutrons that are going to be absorbed in the lithium targets, as is done for poison control rod of the GE-H PRISM reactor. If that is done in the core, it could significantly increase the power density of fuel near the region where the neutrons are slowed down, and a significant redesign may be required.

Production of tritium in a fast reactor will require moderation of the leakage neutrons that are going to be absorbed in the lithium targets, as is done for poison control rod of the GE SPRISM reactor. If that is done in the core, it could significantly increase the

power density of fuel near the region where the neutrons are slowed down, and a significant redesign may be required.

An alternative approach was examined to see if significant tritium production could be obtained with little or no change to the basic fast reactor core design. That approach is to utilize only a lithium blanket region for tritium production as is proposed for fusion reactors. This approach is plausible due to the large neutron leakage component of fast reactors. An MCNP model was constructed with a fast core 1.2 meters in diameter and 1.2 meters in height, see Figure 3-1. The core was modeled as a homogenized volume consisting of 50% U10Zr (13% enriched uranium) with an average density of 10.3 gm/cc, 25% stainless steel with an average density of 7.86 gm/cc and 25% sodium with an average density of 0.92 gm/cc. Surrounding the core were various stainless steel volumes as well as a 30 cm thick sodium down-coming flow (an RSR like system). Both natural lithium (7.59% Li-6) and depleted lithium (2% Li-6) were examined for tritium production rate per fission in the fast core as a function of the lithium blanket thickness. Figure 3-2 shows the results of those calculations. Calculated production rates are significant, with ½ atom of tritium per fission for a 40 cm naturally enriched lithium blanket and similar rates for an 80 cm depleted lithium blanket. Since the thermal neutron absorption mean free path for natural lithium is only 3 mm, it appears that the large lithium blanket thickness is driven by the moderating ability of lithium.

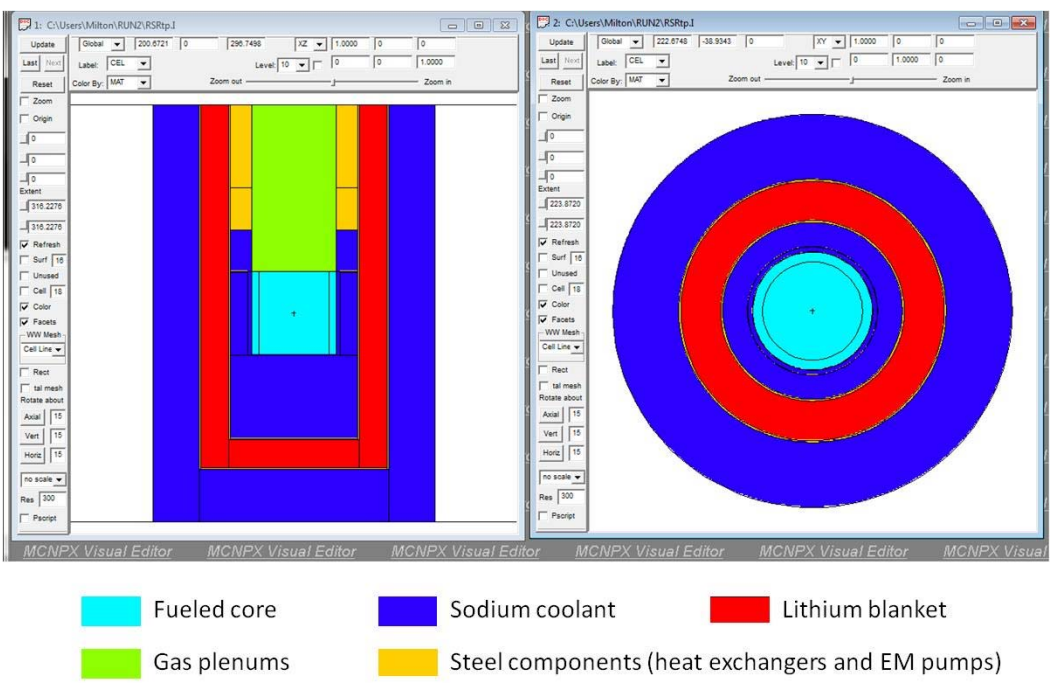

Figure 3-1: MCNP layout configuration for simple lithium blanket

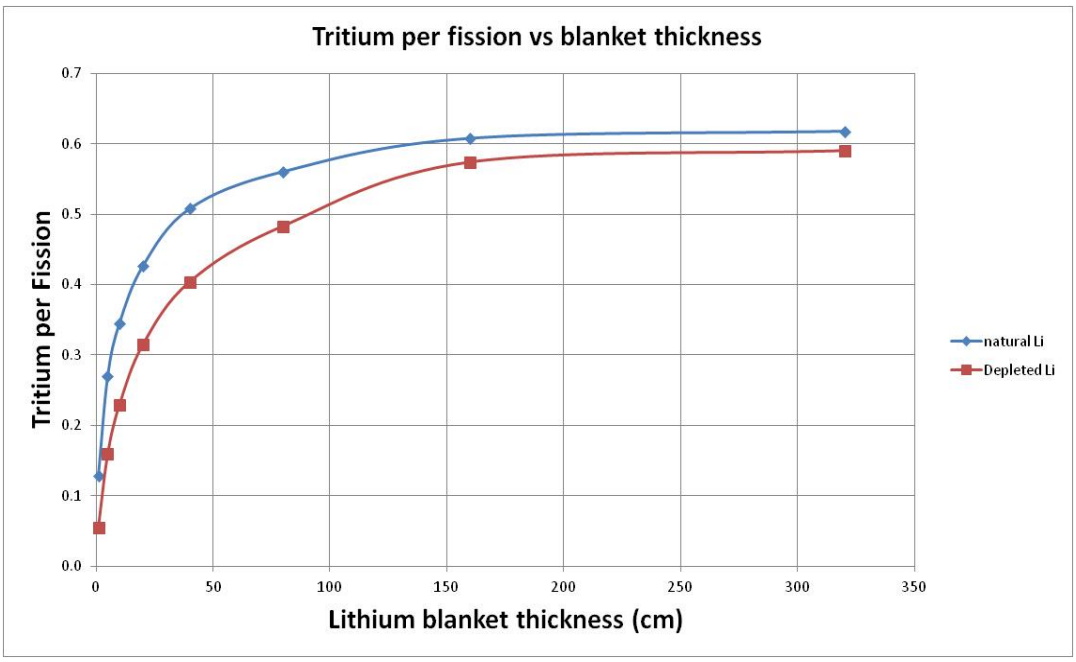

Figure 3-2: Tritium production rate in units of Tritium per Fission in an external blanket as a function of lithium blanket thickness

Two alternative blanket designs were examined; one was a "sandwich" blanket configuration with 2.5 cm of lithium on both sides of an improved moderator, see Figure 3-3. This sandwich configuration was then examined to find the tritium production per fission as a function of the moderator thickness. The first moderator examined was beryllium. Figure 3-4 show the results of those calculations. In this configuration, a production maximum is observed. That rollover occurs at about 18 cm beryllium thickness with a peak production rate for natural lithium of 0.52 tritium per fission and 0.43 tritium per fission for depleted lithium. The second moderator was NaOH, since sodium hydroxide does not chemically react with either the lithium or the sodium in the system. Figure 3-5 show the results of those calculations. Like the beryllium sandwich, a production rollover was observed at 5 cm NaOH thickness, but even there the production rates for tritium were approximately 0.5 tritium atoms per fission.

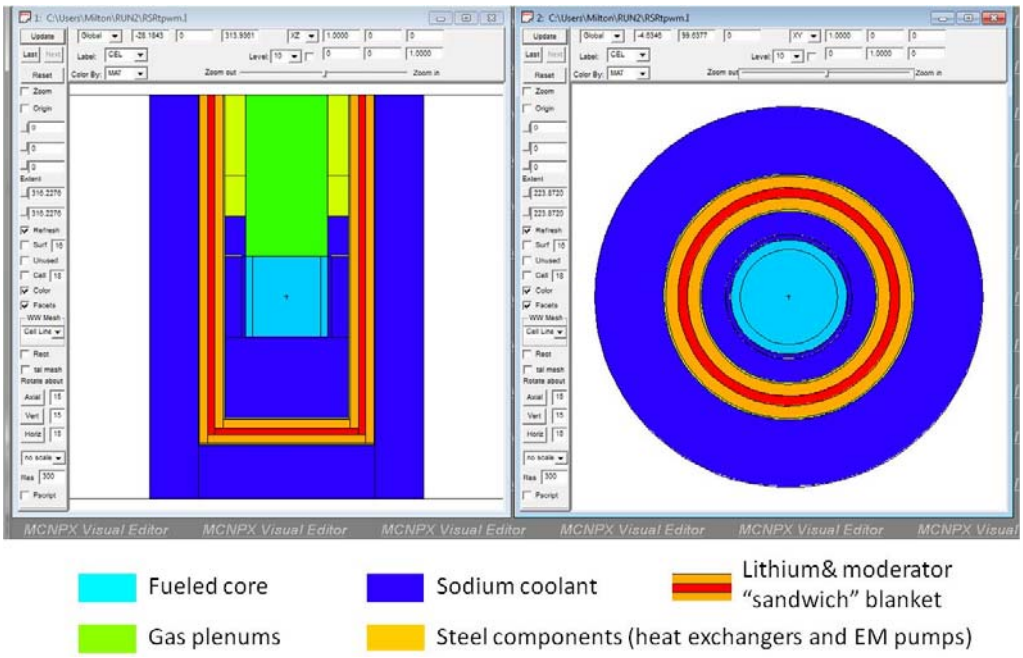

Figure 3-3: MCNP layout configuration for "sandwich" lithium/moderator blanket with the lithium volume surrounding the moderator greatly exaggerated in this drawing

Two additional calculations were undertaken; the first was to see what production rate we would expect midway through the reactor core's lifetime. It is anticipated that the core could achieve 20% heavy metal burnup, and the core size and enrichment is adjusted to achieve this burnup with only a modest shift in reactivity over the lifetime. The anticipated production rate at 10% burnup is calculated to improve by 5% (0.523 vs 0.499) at midway through the reactor's lifetime. The second calculation was to examine the production rate if the core was fueled with DU and Pu-239. Calculations for that core showed a 20% improvement in the production rate (0.602 vs. 0.499).

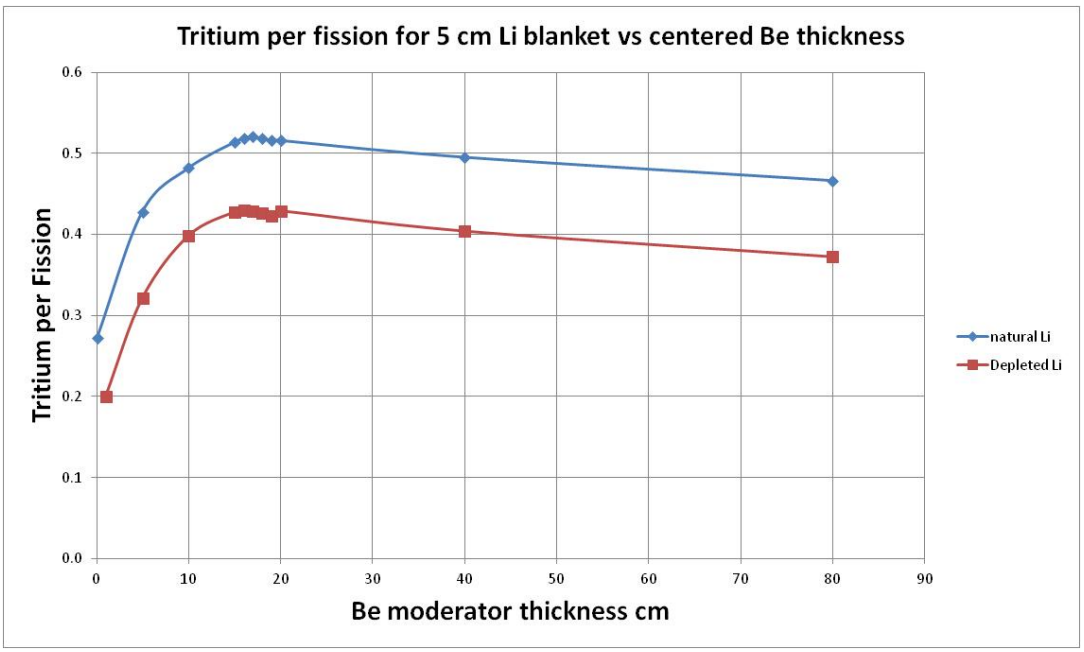

Figure 3-4: Tritium production rate in units of Tritium per Fission in a "sandwich" configured external blanket as a function of Be moderator thickness

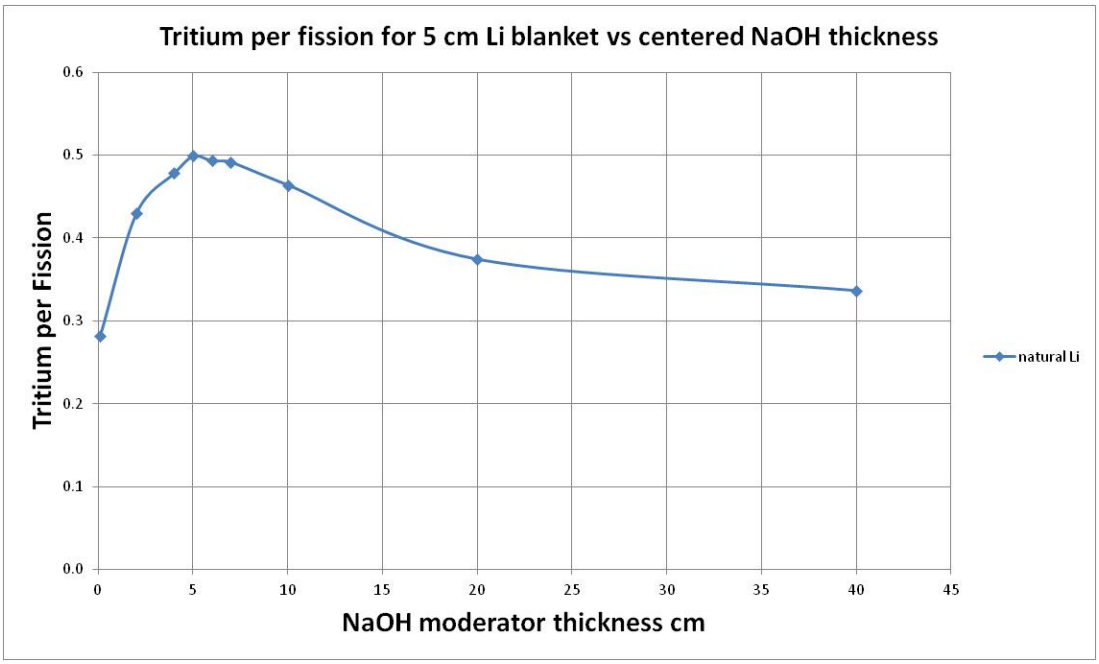

Figure 3-5: Tritium production rate in units of Tritium per Fission in a "sandwich" configured external blanket as a function of NaOH moderator thickness

The Tritium production rate per unit power can be derived from tritium production per fission with the simple equation:

$$\text{Tritium_production_rate} := \frac{\text{TpF} \cdot 3 \frac{\text{gm}}{\text{mole}}}{200\,\text{MeV} \cdot N_a}$$

Where TpF is the tritium production per fission, 3 gm/mole is the mass per mole of tritium, 200 MeV is the recoverable energy per fission and N_a is Avogadro's number ($0.6022*10^{24}$/mole). Inserting a TpF value of 0.5, one obtains a tritium production rate of 2.453 gm/MW_{th}*year or 1 kg/year for 407 MW_{th}. These values assume a 100% duty cycle. The production rate scales with the TpF yield and with reactor power. These values differ from those in Table 3-1 only by the duty cycle used in that table – 0.85.

The production of tritium through the use of an external lithium blanket appears to be a viable option for the fast reactor design. The production rate estimates from this analysis indicate that the blanket approach could provide at least a factor of three higher production rates than light water reactors, although both systems can probably be improved. The use of an external blanket permits the recovery of tritium on a frequency independent of the reactor refueling cycle. The use of hydrogenous moderator significantly reduces the blanket thickness; however hydrogenous moderators generally have more parasitic absorption and introduce other materials compatibility issues.

Table 3-1 Summary of Potential Tritium Production

Reactor Type	**B&W M-Power**	**Holtec**	**Nu-Scale**	**SPRISM**	**FFTF**	**RSR-Li-Blanket**
Study Team	TAMU	TAMU	TAMU	TAMU	PNNL	M Vernon
kg-Trit/yr	1.1	1.2	1.2	1.00E-04	1.5	1.00
MW.th	530	446	160	1000	400	600
No. Cores	1	4	11	1	1	1
plant capacity factor	1	1	1	1	0.75	0.85
days/yr	730	365	365	365	365	365
MW-days	386900	651160	642400	365000	109500	186150
kg-HM	386.9	651.16	642.4	365	109.5	186.15
kg-Trit/kg-HM	0.0028	0.0018	0.0019	0.0000	0.01	0.0054
gm-Trit/kg-HM	2.84	1.84	1.87	2.74E-04	13.70	5.38
gm-Trit/MWd	**0.0028**	**0.0018**	**0.0019**	**0.0000**	**0.0137**	**0.0054**
NOTES						
Trit-Estimate	B-10 Not Li-6	Li-6 w MCNP	B-10 Not Li-6	Li-6 w MCNP	Unknown	Li-6 w MCNP
Li-Enrich	Li-6 22% Enr	Li-6 12% Enr	Li-6 18% enr	-		Natural
Target	T-bars	T-bars	T-bars	T-bars	T-bars Mod	Li Blnkt Cool
Fuel Enrich	4-5%	4-5%	4-5%	Nat U+Pu+Nitride	42% Pu Enr	13% fissile

4.0 TRITIUM ENTERPRISE MODEL DEVELOPMENT

4.1 Tritium Production Model

A model of US tritium production alternatives was built for the purpose of demonstrating the impact of different production methods on production capabilities. In particular, the focus of this model was on the ability of emerging SMR technology to maximize the utilization of US origin uranium for tritium production in the out years. The specific production alternatives considered included:

- Watts Bar 1 unit running a nominal load of 1,696 tritium producing burnable absorber rods (TPBARs) with an average refueling of 41,000 LEU on an 18-month cycle (base case), as well as reduced production rate cases
- Babcock & Wilcox (B&W) Company's mPower™ light water reactor (LWR) SMR with an optimized load of TPBARs
- Holtec International's Inherently Safe Modular Underground Reactor (HI-SMUR™) LWR SMR with an optimized load of TPBARs
- NuScale Power's LWR SMR with an optimized load of TPBARs
- GE-Hitachi's SPRISM pool-type SFR utilizing a modified TPBAR type target

Watts Bar I unit tritium production data was estimated based on information available in the public domain. Details were deliberately kept at a minimum to avoid crossing into the classified realm. SMR tritium production data was based on the results of senior design projects conducted at TAMU that were sponsored by PNNL and coordinated with SRNL.

The model is not intended to provide accurate projections at its current state of development, but rather to demonstrate the usefulness of such a tool for helping formulate US tritium production strategy. It will need to be further enhanced to incorporate the necessary level of detail, which will likely ultimately require classification.

4.2 Simulation and Modeling

The Tritium Production Model was developed using Vensim® from Ventana Systems, Inc. Vensim® is a visual modeling tool that allows you to conceptualize, document, simulate, analyze, and optimize models of dynamic systems. Vensim® provides a simple and flexible way of building simulation models from causal loop or stock and flow diagrams.

Ventana Systems provides a free Vensim® Model Reader available on their website. The model can publish such that it can be used by individuals without a copy of the Vensim® software.

System dynamics models contain a number of stocks, shown in diagrams as rectangles, and flows, displayed as double-lined arrows. Any flow directed to the stock increases its level, and the flow going out of the stock decreases its level. The amount of flow in and out is regulated by rates, visualized as "valves". So-called connectors, visualized as circles, are used as helper elements to specify user-defined functions and parameters. They are linked to other nodes in the diagram and serve as "information flows". The information flows control the water valves, and often the stocks in the model are the original values.

The challenge in developing simulation software is to end up with something that can easily, reliably, and intuitively model a wide range of systems. Simulation models are typically built both to obtain an understanding of the system dynamics and compare alternatives. The model is developed for the purpose understanding of the behavior of the system, or to evaluate various strategies (within the limits imposed by a criterion or set of criteria) for operating the system. A general rule of thumb is to build the simplest model that solves the problem.

Model development is typically an iterative process, as was the case with the Tritium Production Model. A prototype was developed in the early phase of the project to answer the question, "Is this what you want?" Review of the prototype suggested additional options and complexities to be added to the model. A second prototype followed the same process. These iterations are the foundation for the Base Model described below.

4.3 Base Model

Three different structures were developed to characterize the relationships between the various elements from which tritium production is comprised and to display the model results. The structures are used to answer two different questions. The Base structure (**Error! Reference source not found.**) evaluates the interdependencies between tritium production, electric power generation, and the amount of unobligated uranium consumed.

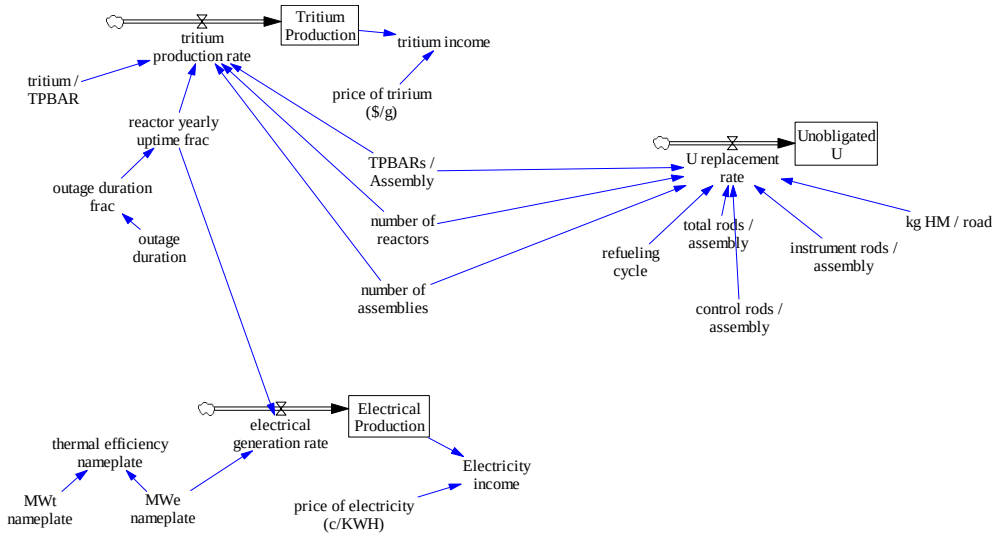

Figure 4-1 Base Structure

Input variables or constants can modified from within the equations coded into this structure. The results of a simulation can be viewed using the standard Vensim output tools or the created Base Input/Output structure (Figure 4-2) along with being to modify certain input variables.

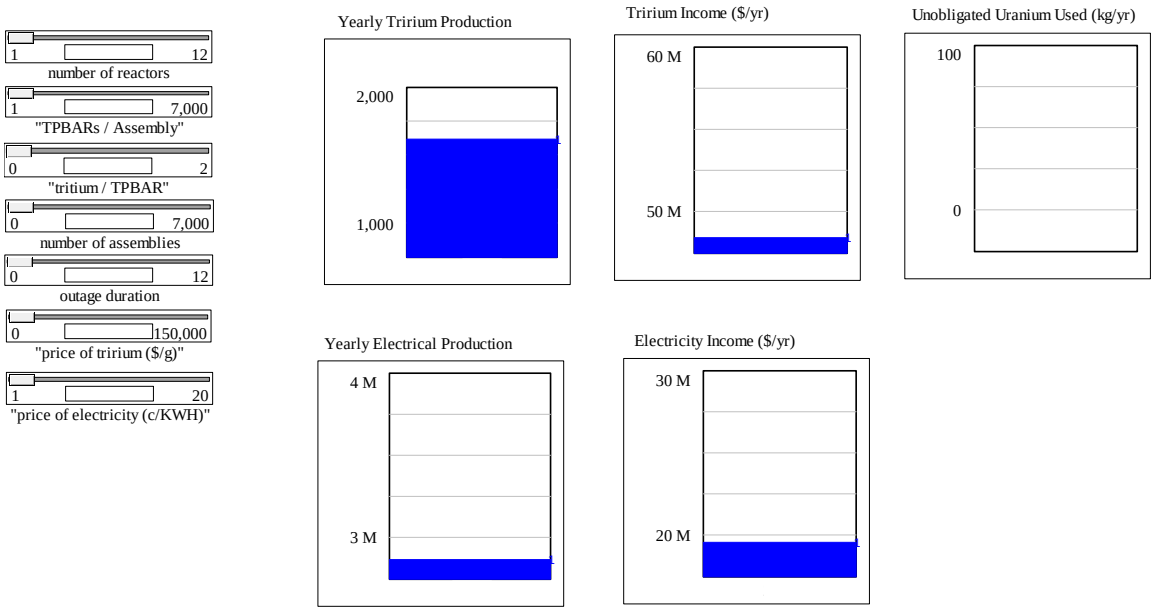

Figure 4-2 Base Input/Output Structure

The Comparison structure (Figure 4-3) compares the results of the four (4) TAMU evaluated SMRs and the Watts Bar #1 reactor.

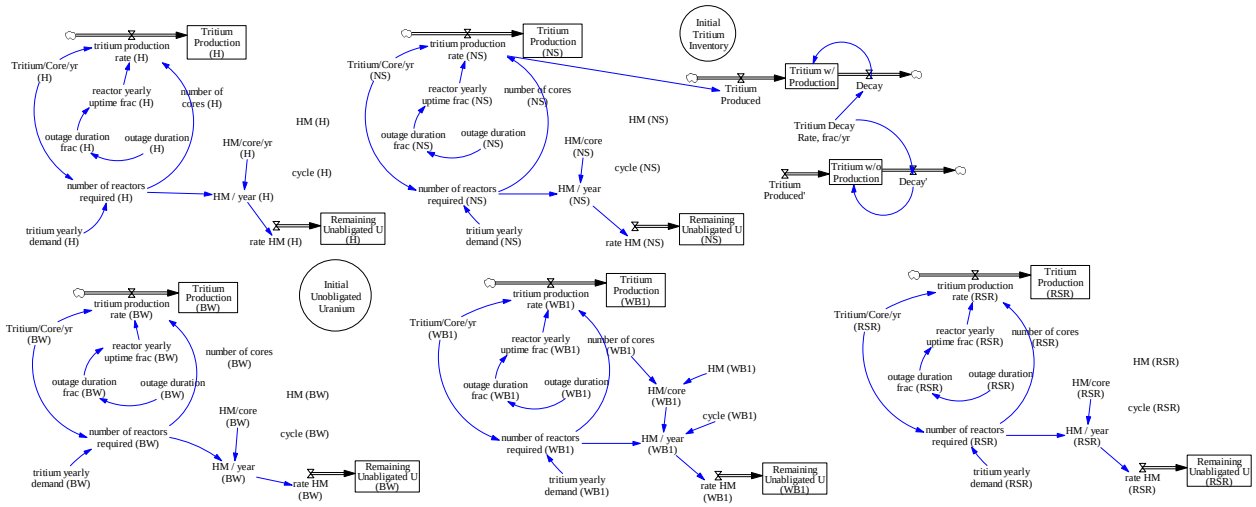

Figure 4-3 Comparison Structure

Input for this structure uses a Microsoft Excel worksheet. Vensim reads values from Excel using row and column designations. This gives non-Vensim users easier access to the model. Figure 4-4 below is a copy of the Excel worksheet.

	A	B	C	D	E	F	G	H
1	**Reactor Type**	**B&W m-Power**	**Holtec HI_SMUR**	**Nu_Scale**	**SPRISM**	**FFTF**	**Sodium Fast Reacto**	**Watts Bar #1**
2	kg-Trit/yr	1.117	1.187	1.15	1.00E-04	1.5	1.001	1.696
3	MWt	530	446	160	1,000	400	600	
4	No. Cores	2	4	11	1	1	1	1
5	Capacity Factor	1	1	1	1	0.75	0.85	
6	days/yr	365	365	365	365	365	365	
7	MW-days	386,900	651,160	642,400	365,000	109,500	186,150	
8	kg-HM	386.9	651.16	642.4	365	109.5	186.15	1022
9	kg-Trit/kg_HM	0.0029	0.0018	0.0018	0	0.01	0.0054	
10	gm-Trit/kg-HM	2.89	1.82	1.79	2.74E-04	13.7	5.38	
11	gm-Trit/Myd	0.0029	0.0018	0.0018	0	0.0137	0.0054	
12	gm-Trit/core/yr	559	296.75	105	0.1	1,500	1,001	1,696
13	MWe	180	160	45				1,000
14	Assemblies	69	32	37				193
15	TPBARs/Core							1,696
16	Cycle (mon)	24	36	18			72	18
17	kg-HM/core	193.45	162.8	58.4	365	109.5	186.2	
18	Array size	17x17	17x17	17x17	17x17			
19		289	289	289	289			
20	g Trit/TPBAR/yr							1
21	kg LEU	17,791.46	21,924.98	63,763.33			19,446	41,500
22	kg LEU/core/yr	8896	5481	5797			3241	
23								
24								
25		**BW**	**H**	**NS**	**S**		**SFR**	**WB1**
26								
27		Table 2, Interim Report: Evaluation of Tritium Production with Small Modular Reactors						
28		other sources						

Figure 4-4 Excel Input Sheet

The output can be model generated charts (Figure) or the data saved to a tab delimited file that can be post processed in Excel.

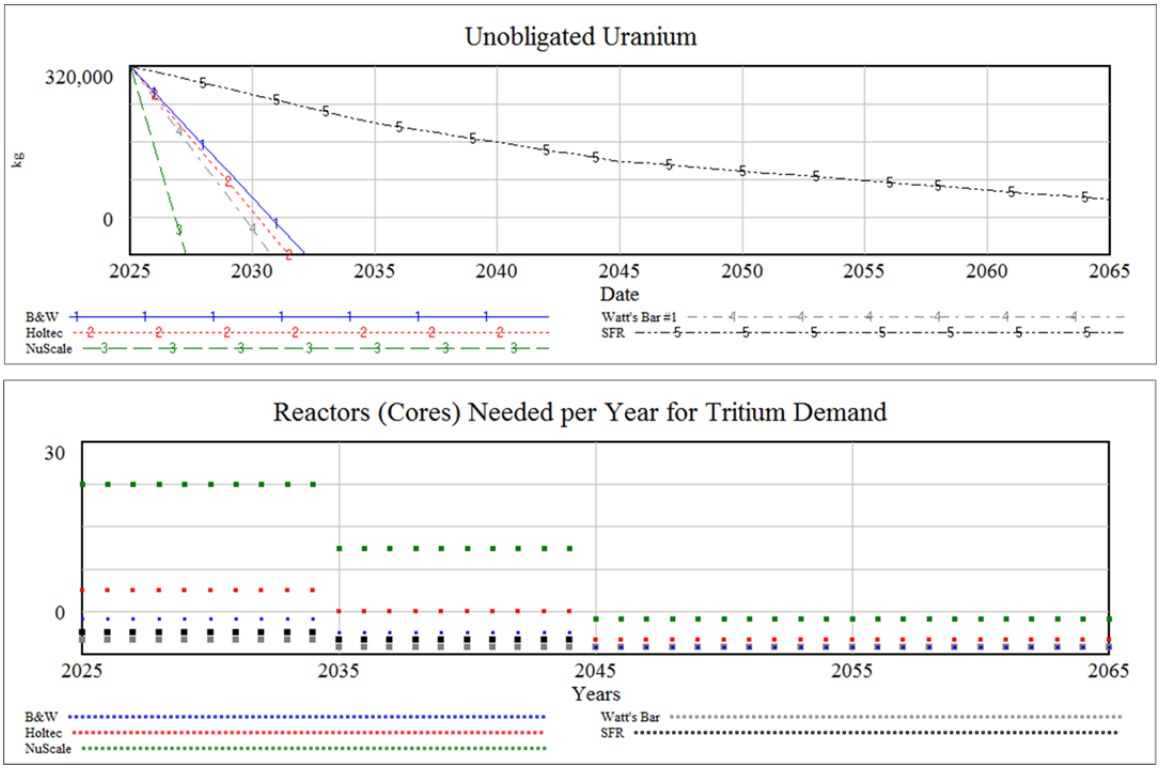

Figure 4-5 Comparison Output Charts

Post processed Excel charts can be of any design. An example (Figure 4-6) is shown below.

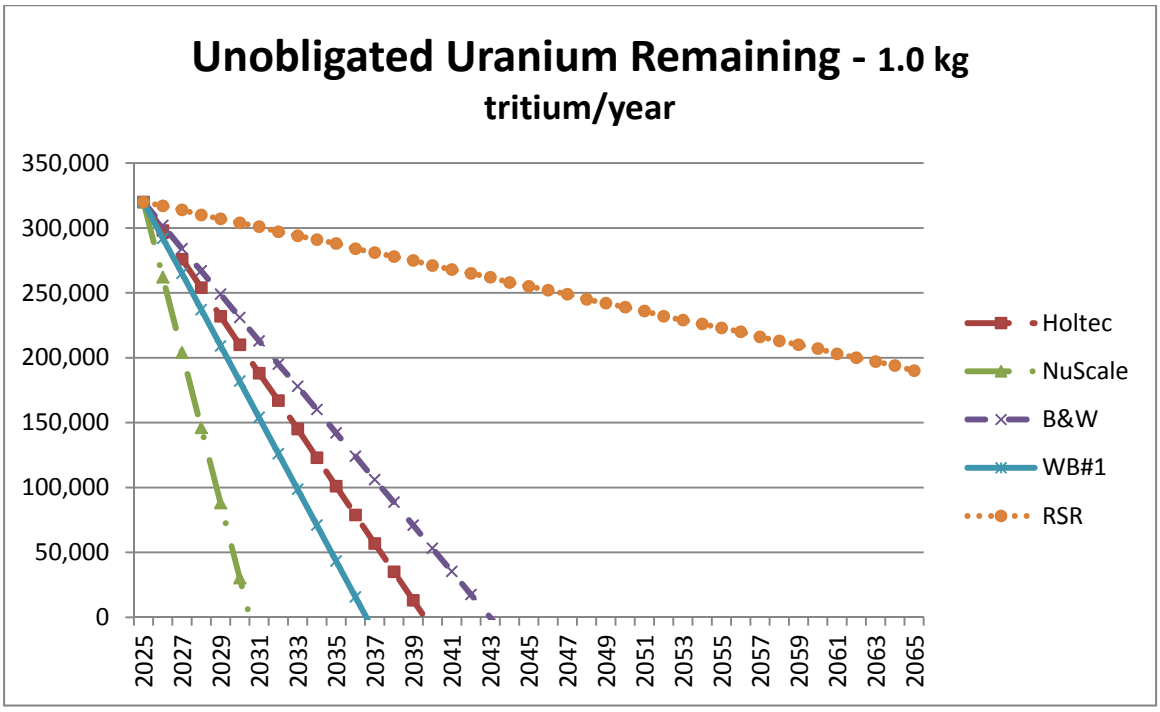

Figure 4-6 Example of Post Processed Excel Chart

Input for assorted 40-year tritium production curves uses an Excel worksheet. Vensim reads values from Excel using row and column designations. The model is set up to simulate years 2025 through 2065 for the 40-year curves. The data could have been added directly into the model using internal databases if so desired.

Different methods for data input and output were incorporated into the model to demonstrate some of the many capabilities of the software.

4.4 Venapps

Vensim Applications (Venapps) are simplified, push button interfaces that allow users access to a Vensim model without going through the Vensim modeling environment (i.e. Base Model). Other generic names for a Venapp are "Management Flight Simulators," "Scenario Generators.", "Decision Support Systems," "Executive Support Systems," "Learning Environments," "Games," "Menu Driven Interfaces," and "Packaged Applications,".

A Venapp uses a model and a set of rules for interacting with the model to give users simplified access to that model. To the user, the Venapp appears as a series of buttons, menus, or a sequence of screens allowing him or her to use and analyze the model in straightforward and meaningful way.

A Venapp is developed to:

- Give non-Vensim users easy access to models.
- Simplify scenario generation.
- Support interactive gaming.
- Provide on-line commentary on a model.
- Focus attention on specific aspects of a model.
- Provide control over what can be changed in making simulations of a model.

The Tritium Production Venapp could be considered a prototype due to fact that the iteration process of model develop has not been completed. The Venapp has been demonstrated but no feedback has been incorporated in this design. Figure through Figure show screen shots of the Venapp.

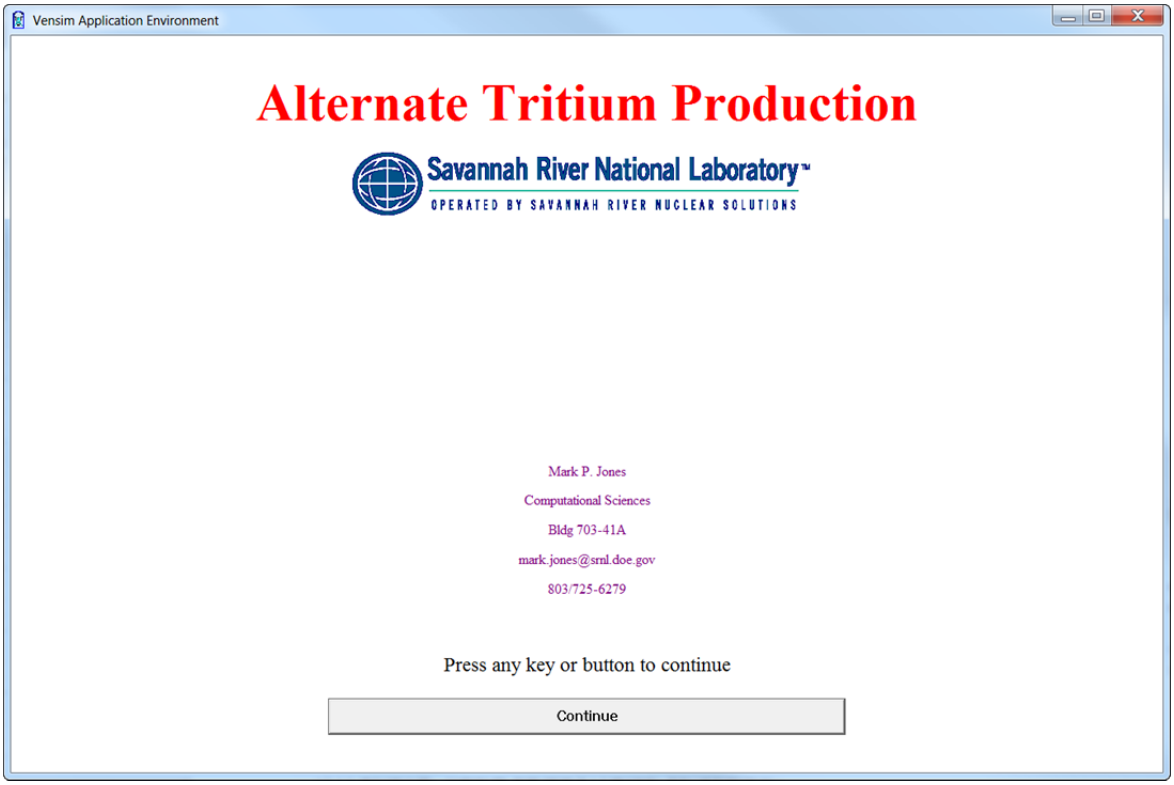

Figure 4-7 Title Screen

Figure 4-8 Main Menu

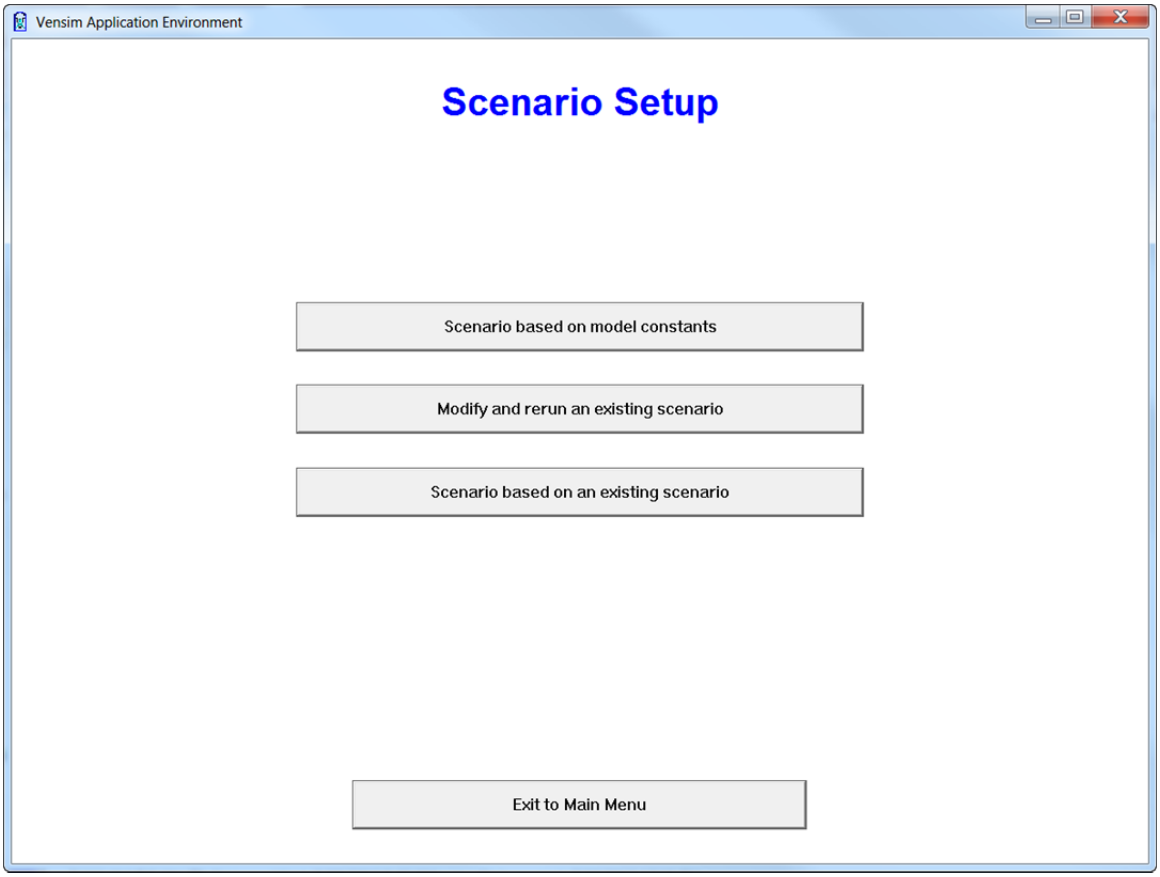

Figure 4-9 Scenario Setup

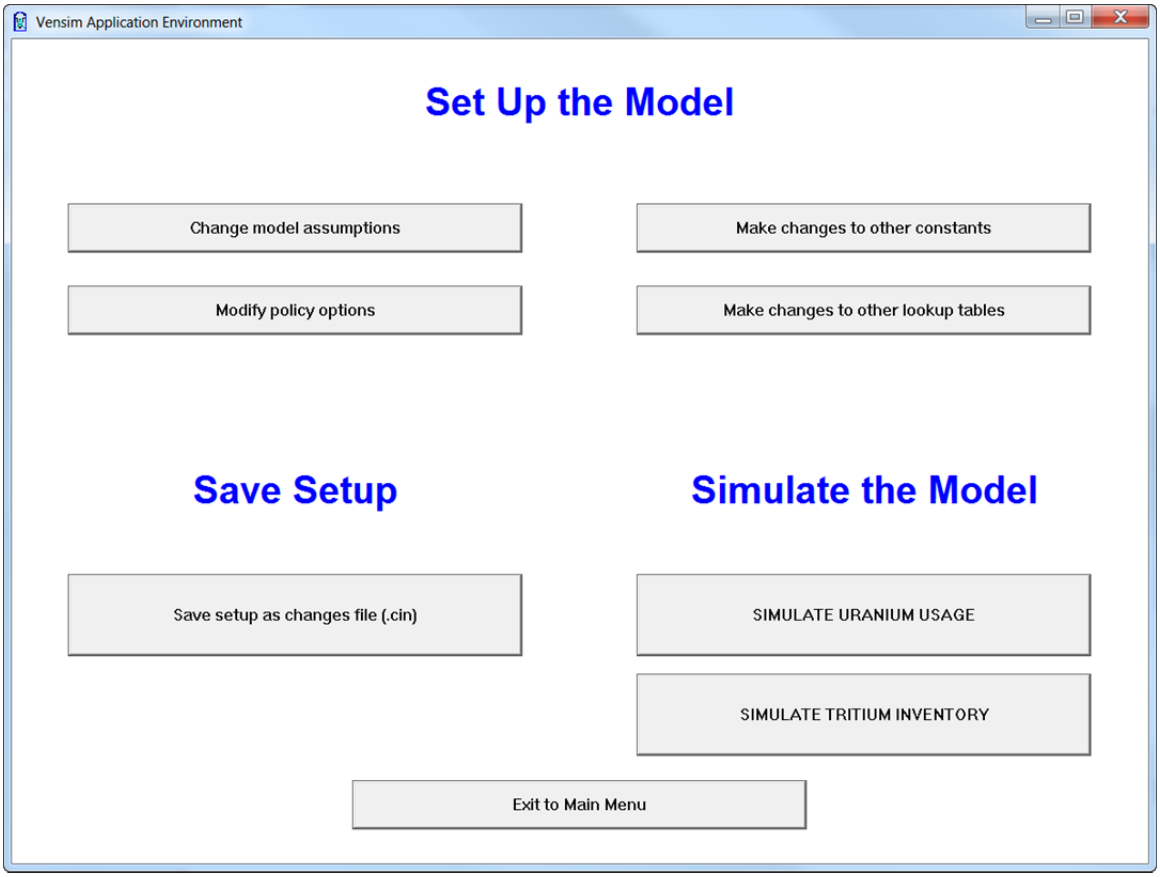

Figure 4-10 Setup Screen

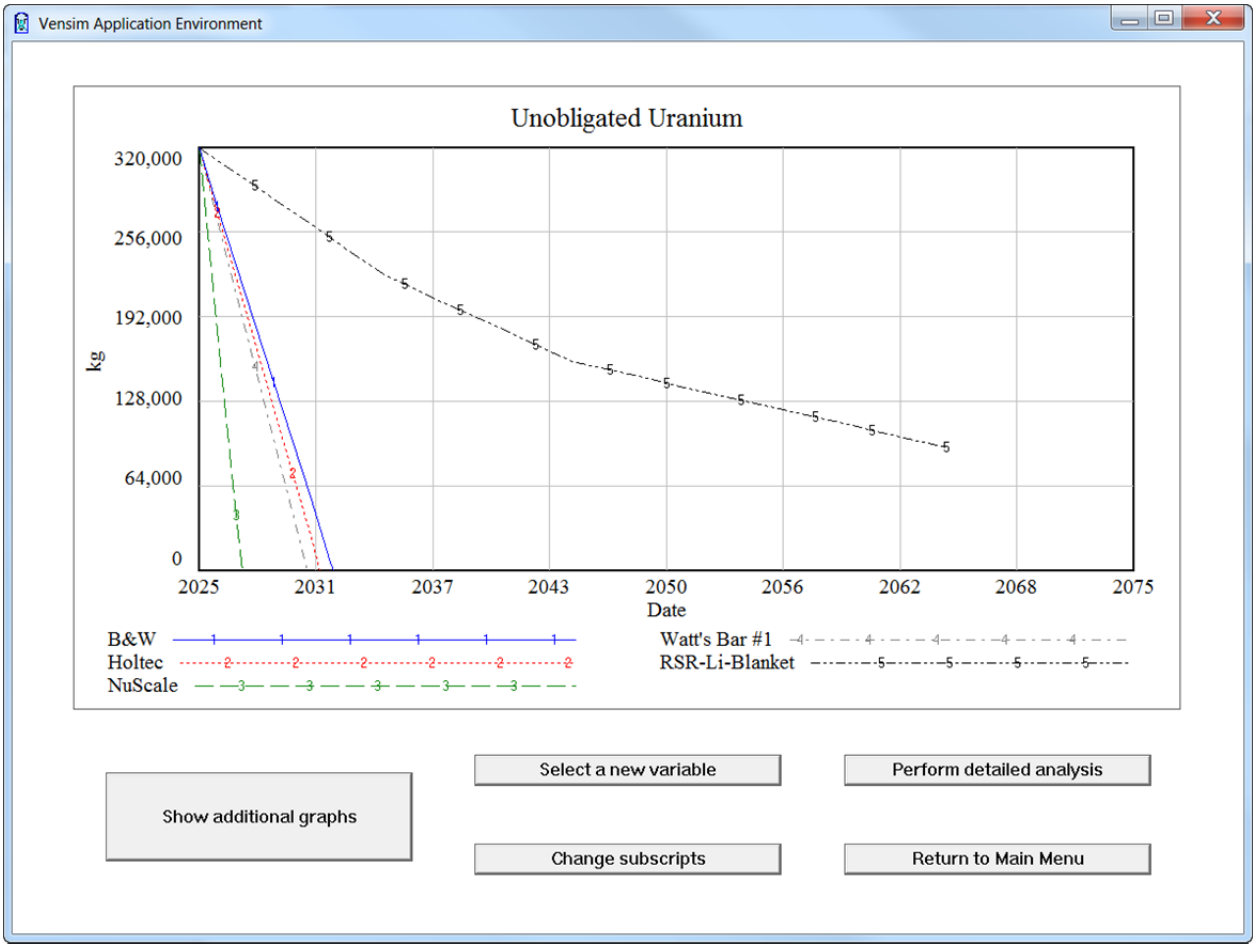

Figure 4-11Unobligated Uranium Remaining

Figure 4-12 Additional Charts

5.0 DISCUSSION OF RESULTS

The model is a tool that can evaluate varying scenarios and various reactor designs to maximize the production of tritium per unit of unobligated US origin uranium that is in limited supply. In order to demonstrate the enterprise model and make an initial evaluation of uranium consumption, a variety of production scenarios in half kilogram increments have be selected that bracket possible "break points" in production that contrast the potential benefits of various reactor types.

Note that if the model were loaded on a classified computer system, more accurate requirements for future uranium supply could be evaluated since more exacting tritium production values per TPBAR could be entered and actual tritium forecasts needed to maintain the stockpile could be used. The four scenarios chosen are:

- Low – 1 kg: Contrasts U consumption in a large reactor at a reduced production rate versus "tailored" production with smaller reactors.
- Medium – 1.5 kg: Contrast production at close to optimized production in a large reactor versus using multiple smaller reactors.

- High – 2 kg: Contrasts impact of needing a second larger reactor to meet production requirements versus bringing on incremental production with small reactors.
- Very low – 0.5 kg: Should stock pile requirements diminish over time and tritium requirements trend lower, this scenario highlights benefits of closely matching the optimized production of a fleet of small reactors with actual tritium needs.

The primary module in the model compares the consumption of uranium for various production reactors against the base case of Watts Bar 1 running a nominal load of 1,696 TPBARs with an average refueling of 41,000 kg LEU on an 18 month cycle. After inputting an initial year, starting inventory of unobligated uranium and tritium production forecast, the model will compare and contrast the depletion rate of the LEU between the entered alternatives. This is an annual tritium production rate of approximately 0.059 grams of tritium per kilogram of LEU (g-T/kg-LEU).

5.1 Model comparison with Watts Bar 1

This evaluation will use the forecast nominal production of tritium for Watts Bar 1 as the base case. With an expected full load of TPBARs of approximately 1,696, WB1 will nominally produce 0.059 gram of tritium per kilogram of LEU used in the core.

The initial assumptions for WB1 production that will be used in the model include:

- Starting US origin uranium available is 600,000 kg in 2014.
- Average consumption in Watts Bar 1 is 41,500 kg per 18 month cycle or 27,667 on an annualized basis.
- Average of 1 gram of tritium per TPBAR
- Alternate reactors begin production in 2025
- Remaining LEU in 2025 is approximately 320,000 kg

Table 5-1 compares estimated tritium production for the 544 TPBARs currently in pile. At a little more than one half of a kilogram per year, production will be about 0.02 grams of tritium per kilogram of LEU utilized. Other intermediate loadings values are included for comparison, as WB1 ramps up to its targeted full production rate.

Table 5-1 Watts Bar 1 Tritium Production Summary

Watts Bar 1 Tritium Production Summary		
TPBARs Loaded	**Grams of Tritium per kilogram of LEU**	**Grams of Tritium per year**
1696	0.059	1,696
880	0.033	880
704	0.026	704
544	0.020	544

The alternatives currently loaded into the model include the three light water SMRs evaluated in TAMU senior projects including, mPower, Holtec and NuScale designs. Initial evaluations of tritium production in light water reactor (LWR) based SMRs using optimized loads of TPBARs are on the order 0.02-0.06 grams of tritium per kilogram of LEU used. In place of the GE-Hitachi

PRISM, the data from the MCNP model of an intermediate size SFR prepared by the SRNL TAC has been utilized. It is a 600MWth core surrounded by a lithium blanket produced approximately 1,000 grams of tritium annually with a 13% enriched, 6 year core. This is similar results to a mid-1990's study where the Fast Flux Test Facility, a 400 MWth reactor at INL, could produce about 1,000 grams with an external lithium target. Normalized to the LWRs values, comparative tritium production for an SFR could be approximately 0.31 g-T/kg LEU.

A summary of the key values is shown in Table 5-2 below.

Table 5-2 Summary of the Key Values of Reactor Types

Reactor	**WB1 Base Case**	**WB1 NRC approved**	**NuScale**	**Holtec**	**mPower**	**Sodium Fast Reactor**
Power (MWth)	**3,459**	**3,459**	**160**	**446**	**530**	**600**
Annual Tritium (g-T)	**1,696**	**704**	**105**	**297**	**559**	**1,001**
Annual LEU Use – Normalized (kg)	**28,533**	**27,000**	**5,797**	**5,481**	**8,896**	**3241**
Tritium/LEU (g-T/kg-LEU)	**0.059**	**0.026**	**0.018**	**0.054**	**0.063**	**0.31**

5.2 Model results for SMR Scenarios

Assuming an average production of 1 g per year of tritium per TPBAR, the maximum amount of tritium the Watts Bar 1 reactor can produce is approximately 1.7 kg with up to 1,696 TPBARs in pile. One must recall that no matter how many TPBARs are loaded into WB1; a full core of US origin uranium must be used.

The low annual production scenario of 1 kilogram in Figure 5-1 shows the impact of having to load a large reactor with a full core of US origin uranium whether one TPBAR is loaded or a full complement. Although the light water SMRs are similar to, or even less efficient than, Watts Bar 1 in tritium production on a g-T/kg-LEU basis, they may be better able to conserve the US origin uranium by only loading the number of cores necessary to meet production needs. By following closely the tritium demand curve, they can fully utilize all of the uranium in their cores. Whereas at 1 kg Watts Bar is making less than 60% of its potential production while still loaded with a full core of uranium.

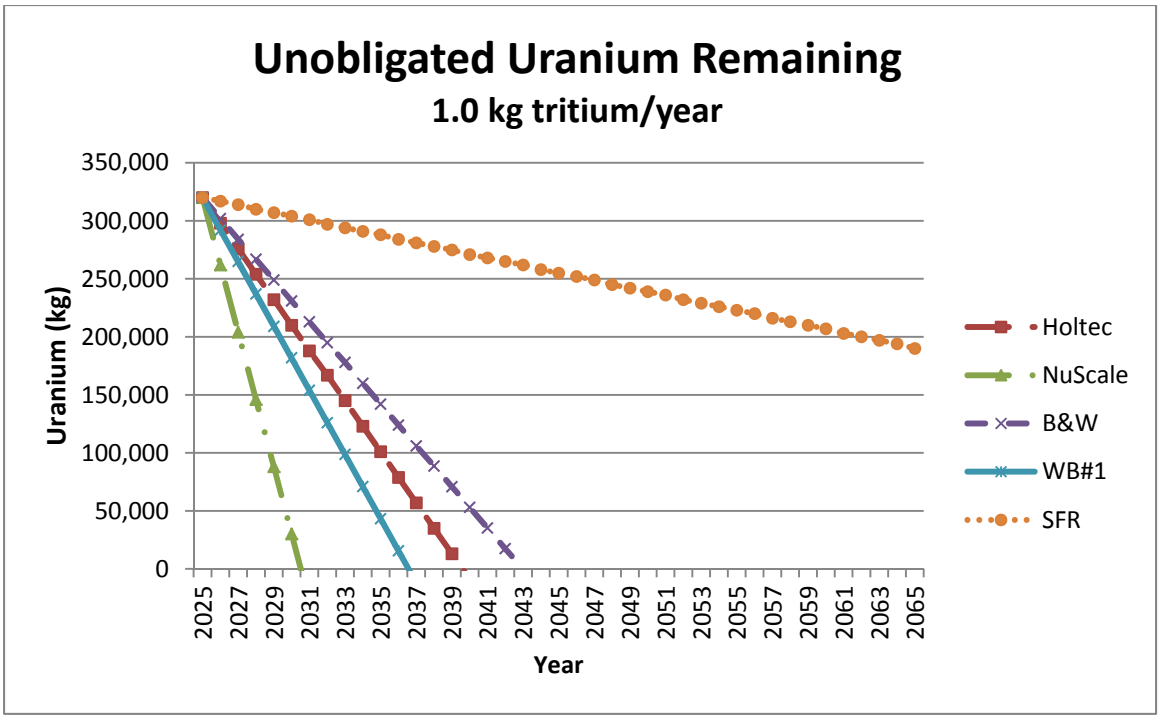

Figure 5-1 Unobligated Uranium Remaining – 1.0 kg tritium/year

With estimated production of 1 kg per year, this is a very efficient range for the SFR that was modeled. If brought into production in 2025, this design could very well provide tritium at this production rate for another 100 years using the current inventory of uranium.

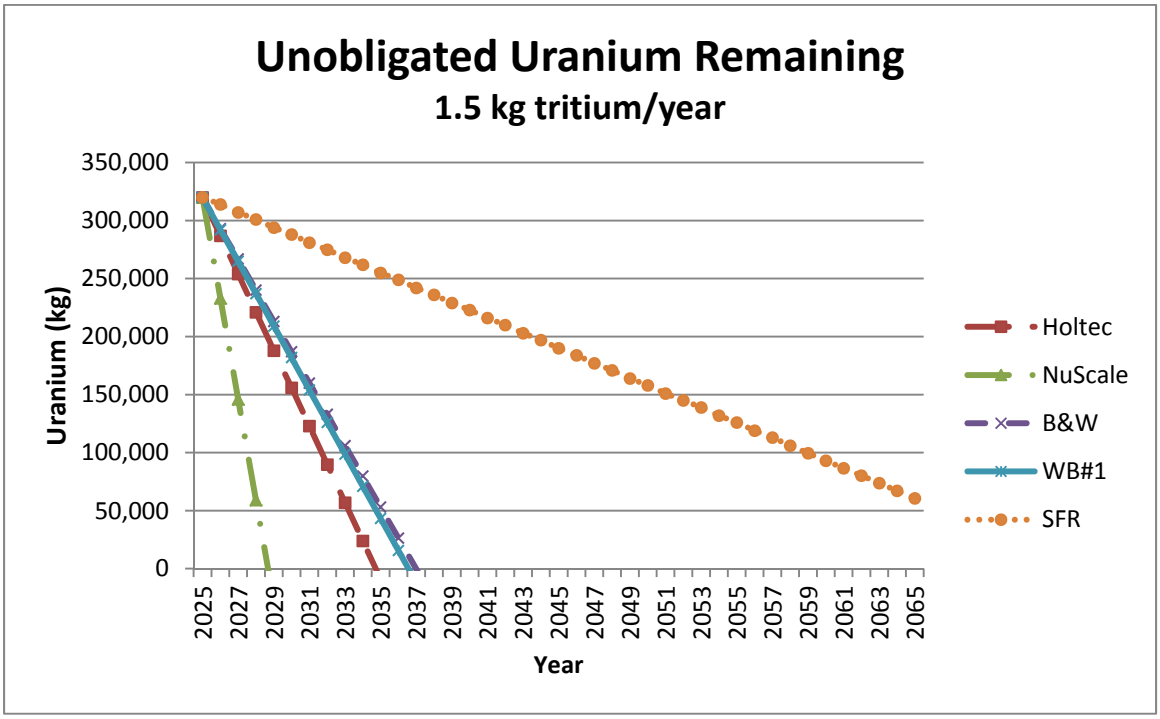

Figure 5-2 Unobligated Uranium Remaining – 1.5 kg tritium/year

The 1.5 kg scenario in Figure 5-2 shows WB1 production being more consistent with the light water SMRs since it is closer to its estimated maximum production rate of 0.059 g-T/kg-LEU. If the long term forecast for tritium were in this range, a fleet of small LWRs would offer little or no advantage in optimizing uranium utilization. With an estimated production of approximately 1 kg per year for a 600 MWth SFR, this scenario would require that a second reactor be brought on-line. Although this doubles its uranium consumption, it still far less than the amount required in WB1 and demonstrates the potential for much more efficient utilization of US uranium with an advanced reactor producing tritium.

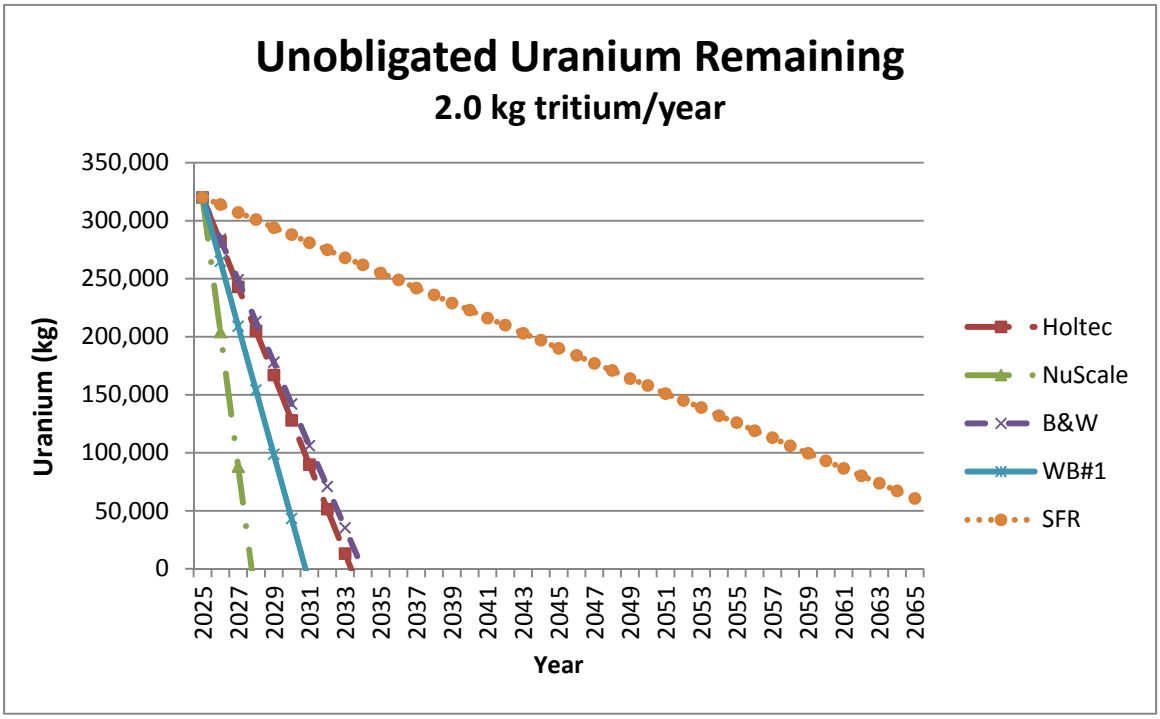

Figure 5-3 Unobligated Uranium Remaining – 2.0 kg tritium/year

At 2 kg production, the negative impact of using large reactors is once again evident in Figure 5-3 due to the large increase in uranium consumption for a modest increase in tritium production. Once the production capacity of the first unit is exceeded, a second reactor must be brought on line – essentially doubling the consumption rate of the US uranium. A fleet of SMR's could be used to provide a tailored production rate closely matching the needs by bringing only the requisite number of units on-line with US uranium. Alternatively, a few SMR's could be paired with WB1 to provide any incremental production increases that may be needed without doubling LEU usage.

Alternatively, should stock pile requirements diminish over time and tritium requirements trend to a much lower level, the consumption rate of uranium in small reactors is very favorable as shown in the 0.5 kg scenarios show in Figure 5-4. An advanced fast reactor continues to show great promise, but in this case light water SMRs also show the potential to more than double the life expectancy of the useable uranium supply.

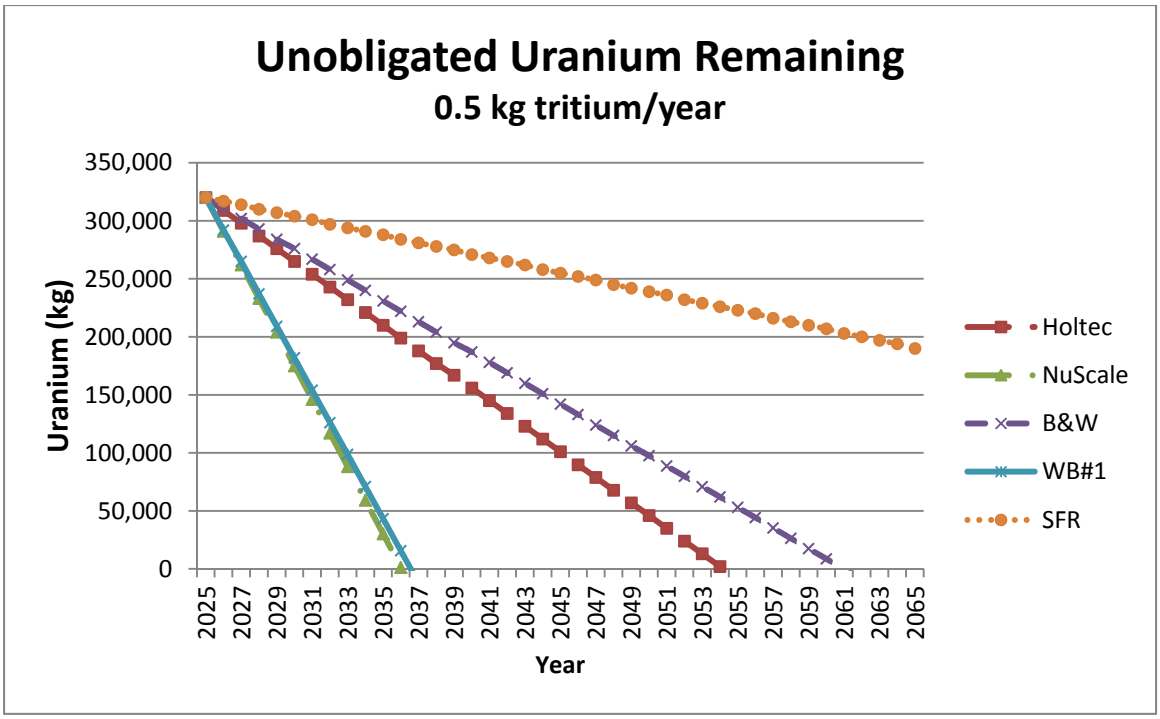

Figure 5-4 Unobligated Uranium Remaining – 0.5 kg tritium/year

6.0 Conclusions

6.1 Observations

From the evaluation of the reactor designs, and reviewing the output from the enterprise model on the various tritium production scenarios, some initial observations include:

- When loaded with an optimal complement of TPBARs, LWRs small and large produce roughly the same quantity of tritium per kilogram of uranium basis. Reactors with small cores will typically be somewhat less efficient because higher surface area equates to higher neutron leakage. Likely one contributing factor of the lower unit production rate of the NuScale SMR.
- If the long-term requirement for tritium approximates the optimized annual production from Watts Bar 1 – 1.7 kg-T/year and is relatively constant over time, an equivalent fleet of light water SMRs offers little or no benefit on the consumption of the unobligated uranium reserves.
- Small light water reactors can optimize uranium utilization in two primary cases – that is to follow the stockpile needs as requirements trend higher or lower. First, if stockpile requirements trend lower, a fleet of SMRs could "follow" the decreasing requirements by utilizing just the number of cores required, instead of running a full core of US uranium in WB1 with a reduced fraction of the TPBARs in pile. The unused SMRs could put their partially used US fuel aside and reload with open market uranium to produce power. Second, should the tritium requirements increase incrementally above what Watts Bar can produce, one or more SMRs could be loaded to produce the delta without having to start a second full sized TVA reactor.

- Fast spectrum reactors, such as a sodium fast reactor, demonstrate the potential to increase uranium utilization by 5-fold or greater. This is based on the SFR scoping model done for this report as well as the FFTF study done in the mid-1990 at Hanford. SFRs may be able to de-power the reactor by adjusting the reflectors, so that tritium production can be reduced to follow a lower demand, while extending the core life; thereby further conserving the uranium.

6.2 Summary of Future Needs

The model of the tritium production enterprise is a useful tool to compare various production requirements and their impact on US origin uranium. Further action is required to fully utilize the capabilities of this tool, as well as more fully vet the input data for the various reactor types.

Additional recommended activities include:

- Approve and load the model on a classified system so actual tritium production values and forecast needs can be entered to more accurately reflect different options on the consumption of US origin, unobligated uranium.
- Work with interested SMR vendors to more accurately model their cores, their fuel management schemes, and reactor design to develop more accurate estimates of their tritium producing capacity.
- Pursue SFR options with advance lithium target design.
- Leverage an approved LDRD program at SRNL for extraction of tritium from a liquid lithium target.
- Develop business cases for cost-effective tritium production for the next 50 years.
- Investigate using benefits of using “fissile” requirements, i.e. kg U235, versus more generic average LEU.
- Integrate this model into the Tritium Readiness Enterprise Model.

7.0 REFERENCES

Tritium and Enriched Uranium Management Plan through 2060: Report to Congress, Department of Energy.

Technical and Economic Viability of Future FFTF Operation; http://www5.hanford.gov/pdw/fsd/AR/FSD0001/FSD0027/D197320116/D197320116_17142_30.pdf

8.0 APPENDIX

8.1 Appendix A - Tritium Production Model

Vensim Analysis Tools

Structural Analysis Tools

- **Causes Tree —** creates a tree-type graphical representation showing the causes of the Workbench Variable.
- **Uses Tree —** create a tree-type graphical representation showing the uses of the Workbench Variable.

- **Loops —** displays a list of all feedback loops passing through the Workbench Variable.
- **Document —** reviews equations, definitions, units of measure, and selected values for the Workbench Variable.

Dataset Analysis Tools

- **Causes Strip Graph —** displays simple graphs in a strip, allowing you to trace causality by showing the direct causes (as shown) of the Workbench Variable.
- **Graph —** displays behavior in a larger graph than the **Strip Graph**, and contains different options for output than the **Strip Graph**.
- **Sensitivity Graph —** creates a sensitivity graph of one variable and its range of uncertainty generated from sensitivity testing.
- **Bar Graph —** creates a bar graph of a variable at a specific time, or displays a histogram of variables over all times or across sensitivity simulations at a time.
- **Table —** generates a table of values for the Workbench Variable.
- **Table Running Down —** table with time running down.
- **Runs Compare —** compares all Lookups and Constants in the first loaded dataset to those in the second loaded dataset.
- **Statistics —** provides summary statistics on the Workbench Variable and its causes or uses.

Other Tools

- **Units Check** — provides an alternative way to access the units checking feature.
- **Equation Editor —** provides an alternative way to access the equation for the Workbench Variable.
- **Venapp Editor‡ —** supports the visual editing of Venapps.
- **Text Editor —** a general purpose text editor. As shown, it is configured to edit *.vgd* files).

The **Tree Diagram**, the **Strip Graph**, the **Sensitivity Graph**, the **Table** and the **Statistics** tools can all be configured to show either causes or uses of the Workbench Variable.

Base Model

```
"outage duration frac (RSR)"=
        "outage duration (RSR)"/52
        ~       Dmnl
        ~               |

"HM (RSR)"=
        GET XLS CONSTANTS('Table_2_TAC.xlsx', 'Sheet1', 'G21')
        ~
        ~               |

"number of reactors required (RSR)"=
        INTEGER( "tritium yearly demand (RSR)"/"Tritium/Core/yr (RSR)" )+1
        ~
        ~               |

"number of cores (RSR)"=
        GET XLS CONSTANTS('Table_2_TAC.xlsx','Sheet1','G4')
        ~       core
        ~               |

"cycle (RSR)"=
        GET XLS CONSTANTS('Table_2_TAC.xlsx', 'Sheet1', 'G16')
        ~
        ~               |

"HM/core (RSR)"=
        GET XLS CONSTANTS('Table_2_TAC.xlsx', 'Sheet1', 'G22')
        ~
        ~               |

"Tritium Production (RSR)"= INTEG (
        "tritium production rate (RSR)",
                0)
        ~       g
        ~               |

"rate HM (RSR)"=
        "HM / year (RSR)"
        ~
        ~               |

"outage duration (RSR)"=
        1
        ~       week
        ~               |

"Remaining Unabligated U (RSR)"= INTEG (
        -"rate HM (RSR)",
                Initial Unobligated Uranium)
```

```
        ~
        ~               |

"reactor yearly uptime frac (RSR)"=
        1-"outage duration frac (RSR)"
        ~       Dmnl
        ~               |

"tritium yearly demand (RSR)":INTERPOLATE::=
        GET XLS DATA('Table_2_TAC.xlsx' , 'Sheet5', '1' , 'a2' )
        ~
        ~               |

"tritium production rate (RSR)"=
        "number of reactors required (RSR)"*"reactor yearly uptime frac
(RSR)"*"Tritium/Core/yr (RSR)"
        ~       g/yr
        ~               |

"HM / year (RSR)"=
        "HM/core (RSR)"*"number of reactors required (RSR)"
        ~
        ~               |

"Tritium/Core/yr (RSR)"=
        GET XLS CONSTANTS('Table_2_TAC.xlsx', 'Sheet1', 'G12')
        ~       g/core/yr
        ~               |

"tritium production rate (WB1)"=
        "number of reactors required (WB1)"*"reactor yearly uptime frac
(WB1)"*"Tritium/Core/yr (WB1)"
        ~       g/yr
        ~               |

"cycle (BW)"=
        GET XLS CONSTANTS('Table_2_TAC.xlsx', 'Sheet1', 'B16')
        ~
        ~               |

"cycle (H)"=
        GET XLS CONSTANTS('Table_2_TAC.xlsx', 'Sheet1', 'C16')
        ~
        ~               |

"cycle (NS)"=
        GET XLS CONSTANTS('Table_2_TAC.xlsx', 'Sheet1', 'D16')
        ~
        ~               |

"cycle (WB1)"=
```

```
        GET XLS CONSTANTS('Table_2_TAC.xlsx', 'Sheet1', 'H16')
        ~
        ~                   |

"HM / year (NS)"=
        "HM/core (NS)"*"number of reactors required (NS)"
        ~
        ~                   |

"HM / year (WB1)"=
        "HM/core (WB1)"*"number of reactors required (WB1)"*12/"cycle (WB1)"
        ~
        ~                   |

"HM / year (BW)"=
        "HM/core (BW)"*"number of reactors required (BW)"
        ~
        ~                   |

"HM / year (H)"=
        "HM/core/yr (H)"*"number of reactors required (H)"
        ~
        ~                   |

"Tritium w/o Production"= INTEG (
        Tritium Produced'-Decay'*"Tritium w/o Production",
                Initial Tritium Inventory)
        ~
        ~                   |

Decay=
        "Tritium Decay Rate, frac/yr"
        ~
        ~                   |

Decay'=
        "Tritium Decay Rate, frac/yr"
        ~
        ~                   |

"HM/core (BW)"=
        GET XLS CONSTANTS('Table_2_TAC.xlsx', 'Sheet1', 'B22')
        ~
        ~                   |

"HM/core/yr (H)"=
        GET XLS CONSTANTS('Table_2_TAC.xlsx', 'Sheet1', 'C22')
        ~
        ~                   |

"HM/core (NS)"=
```

```
        GET XLS CONSTANTS('Table_2_TAC.xlsx', 'Sheet1', 'D22')
        ~
        ~               |

"tritium production rate (BW)"=
        "number of reactors required (BW)"*"reactor yearly uptime frac (BW)"*"Tritium/Core/yr
(BW)"
        ~
        ~               |

"tritium production rate (H)"=
        "number of reactors required (H)"*"reactor yearly uptime frac (H)"*"Tritium/Core/yr
(H)"
        ~       g/yr
        ~               |

"tritium production rate (NS)"=
        "number of reactors required (NS)"*"reactor yearly uptime frac (NS)"*"Tritium/Core/yr
(NS)"
        ~       g/yr
        ~               |

"Tritium w/ Production"= INTEG (
        Tritium Produced-Decay*"Tritium w/ Production",
                Initial Tritium Inventory)
        ~
        ~               |

Tritium Produced'=
        0
        ~
        ~               |

"HM/core (WB1)"=
        "HM (WB1)"/"number of cores (WB1)"
        ~
        ~               |

Initial Tritium Inventory=
        50000
        ~       g
        ~               |

"Tritium Decay Rate, frac/yr"=
        0.055
        ~
        ~               |

Tritium Produced=
        "tritium production rate (NS)"
        ~
```

```
	~	|

"HM (WB1)"=
	GET XLS CONSTANTS('Table_2_TAC.xlsx', 'Sheet1', 'H21')
	~
	~	|

"tritium yearly demand (WB1)":INTERPOLATE::=
	GET XLS DATA('Table_2_TAC.xlsx' , 'Sheet5', '1' , 'a2' )
	~
	~	|

"Tritium Production (WB1)"= INTEG (
	"tritium production rate (WB1)",
		0)
	~	g
	~	|

"rate HM (WB1)"=
	"HM / year (WB1)"
	~
	~	|

"number of cores (WB1)"=
	GET XLS CONSTANTS('Table_2_TAC.xlsx','Sheet1','H4')
	~	core
	~	|

"Remaining Unabligated U (WB1)"= INTEG (
	-"rate HM (WB1)",
		Initial Unobligated Uranium)
	~
	~	|

"Tritium/Core/yr (WB1)"=
	GET XLS CONSTANTS('Table_2_TAC.xlsx', 'Sheet1', 'H12')
	~	g/core/yr
	~	|

"reactor yearly uptime frac (WB1)"=
	1-"outage duration frac (WB1)"
	~	Dmnl
	~	|

"number of reactors required (WB1)"=
	INTEGER( "tritium yearly demand (WB1)"/"Tritium/Core/yr (WB1)" )+1
	~
	~	|

"outage duration (WB1)"=
	1
```

```
	~	week
	~		|

"outage duration frac (WB1)"=
	"outage duration (WB1)"/52
	~	Dmnl
	~		|

"control rods / assembly"=
	25
	~
	~		|

electrical generation rate=
	MWe nameplate*reactor yearly uptime frac*8760
	~
	~		|

Electrical Production= INTEG (
	electrical generation rate,
		electrical generation rate)
	~
	~		|

Electricity income=
	Electrical Production*"price of electricity (c/KWH)"
	~
	~		|

"HM (BW)"=
	GET XLS CONSTANTS('Table_2_TAC.xlsx', 'Sheet1', 'B21')
	~
	~		|

"instrument rods / assembly"=
	1
	~
	~		|

"kg HM / road"=
	1.6
	~	kg
	~		|

MWe nameplate=
	180
	~
	~		|

refueling cycle=
	18
```

```
	~
	~		|

number of assemblies=
	69
	~
	~		|

"price of tririum ($/g)"=
	30000
	~	$/g
	~		|

Tritium Production= INTEG (
	tritium production rate,
		0)
	~
	~		|

thermal efficiency nameplate=
	MWe nameplate/MWt nameplate
	~
	~		|

number of reactors=
	1
	~
	~		|

"total rods / assembly"=
	13000
	~
	~		|

U replacement rate=
	("total rods / assembly"-"TPBARs / Assembly"-"control rods / assembly"-"instrument rods / assembly"\
		)*"kg HM / road"*number of assemblies*number of reactors*12/refueling cycle
	~	kg/yr
	~		|

MWt nameplate=
	450
	~
	~		|

outage duration=
	1
	~	week
	~		|
```

```
tritium income=
	"price of tririum ($/g)"*Tritium Production
	~
	~	|

tritium production rate=
	number of assemblies*"TPBARs / Assembly"*"tritium / TPBAR"*reactor yearly uptime
frac\
		*number of reactors
	~
	~	|

Unobligated U= INTEG (
	U replacement rate,
		0)
	~	kg/yr
	~	|

outage duration frac=
	outage duration/52
	~	Dmnl
	~	|

reactor yearly uptime frac=
	1-outage duration frac
	~	Dmnl
	~	|

"price of electricity (c/KWH)"=
	7
	~
	~	|

"TPBARs / Assembly"=
	25
	~
	~	|

"tritium / TPBAR"=
	1
	~	g
	~	|

"rate HM (H)"=
	"HM / year (H)"
	~
	~	|

"rate HM (NS)"=
	"HM / year (NS)"
	~
```

```
	~		|

"reactor yearly uptime frac (BW)"=
	1-"outage duration frac (BW)"
	~
	~		|

"number of reactors required (NS)"=
	INTEGER( "tritium yearly demand (NS)"/"Tritium/Core/yr (NS)" )+1
	~
	~		|

"outage duration (BW)"=
	1
	~
	~		|

"Remaining Unabligated U (BW)"= INTEG (
	-"rate HM (BW)",
		Initial Unobligated Uranium)
	~
	~		|

"Remaining Unabligated U (H)"= INTEG (
	-"rate HM (H)",
		Initial Unobligated Uranium)
	~
	~		|

"Remaining Unabligated U (NS)"= INTEG (
	-"rate HM (NS)",
		Initial Unobligated Uranium)
	~
	~		|

"number of cores (BW)"=
	GET XLS CONSTANTS('Table_2_TAC.xlsx','Sheet1','B4')
	~
	~		|

"Tritium Production (BW)"= INTEG (
	"tritium production rate (BW)",
		0)
	~
	~		|

"rate HM (BW)"=
	"HM / year (BW)"
	~
	~		|
```

```
"number of reactors required (BW)"=
        INTEGER( "tritium yearly demand (BW)"/"Tritium/Core/yr (BW)" )+1
        ~
        ~               |

"number of reactors required (H)"=
        INTEGER( "tritium yearly demand (H)"/"Tritium/Core/yr (H)" )+1
        ~
        ~               |

"Tritium/Core/yr (BW)"=
        GET XLS CONSTANTS('Table_2_TAC.xlsx', 'Sheet1', 'B12')
        ~
        ~               |

Initial Unobligated Uranium=
        320000
        ~       kg
        ~               |

"outage duration frac (BW)"=
        "outage duration (BW)"/52
        ~
        ~               |

"HM (H)"=
        GET XLS CONSTANTS('Table_2_TAC.xlsx', 'Sheet1', 'C21')
        ~
        ~               |

"HM (NS)"=
        GET XLS CONSTANTS('Table_2_TAC.xlsx', 'Sheet1', 'D21')
        ~
        ~               |

"number of cores (NS)"=
        GET XLS CONSTANTS('Table_2_TAC.xlsx','Sheet1','D4')
        ~       core
        ~               |

"outage duration frac (NS)"=
        "outage duration (NS)"/52
        ~       Dmnl
        ~               |

"outage duration (NS)"=
        1
        ~       week
        ~               |

"tritium yearly demand (H)":INTERPOLATE::=
```

```
        GET XLS DATA('Table_2_TAC.xlsx' , 'Sheet5', '1' , 'a2' )
        ~
        ~               |

"reactor yearly uptime frac (NS)"=
        1-"outage duration frac (NS)"
        ~       Dmnl
        ~               |

"Tritium Production (NS)"= INTEG (
        "tritium production rate (NS)",
                0)
        ~       g
        ~               |

"tritium yearly demand (NS)":INTERPOLATE::=
        GET XLS DATA('Table_2_TAC.xlsx' , 'Sheet5', '1' , 'a2' )
        ~
        ~               |

"tritium yearly demand (BW)":INTERPOLATE::=
        GET XLS DATA('Table_2_TAC.xlsx' , 'Sheet5', '1' , 'a2' )
        ~
        ~               |

"Tritium/Core/yr (NS)"=
        GET XLS CONSTANTS('Table_2_TAC.xlsx', 'Sheet1', 'D12')
        ~       g/core/yr
        ~               |

"number of cores (H)"=
        GET XLS CONSTANTS('Table_2_TAC.xlsx','Sheet1','C4')
        ~       core
        ~               |

"outage duration (H)"=
        1
        ~       week
        ~               |

"outage duration frac (H)"=
        "outage duration (H)"/52
        ~       Dmnl
        ~               |

"reactor yearly uptime frac (H)"=
        1-"outage duration frac (H)"
        ~       Dmnl
        ~               |

"Tritium Production (H)"= INTEG (
```

```
        "tritium production rate (H)",
                0)
        ~       g
        ~               |

"Tritium/Core/yr (H)"=
        GET XLS CONSTANTS('Table_2_TAC.xlsx', 'Sheet1', 'C12')
        ~       g/core/yr
        ~               |

*********************************************************
        .Control
*********************************************************~
                Simulation Control Parameters
        |

FINAL TIME  = 40
        ~       Year
        ~       The final time for the simulation.
        |

INITIAL TIME  = 0
        ~       Year
        ~       The initial time for the simulation.
        |

SAVEPER  =
      TIME STEP
        ~       Year [0,?]
        ~       The frequency with which output is stored.
        |

TIME STEP  = 1
        ~       Year [0,?]
        ~       The time step for the simulation.
        |

\\\---/// Sketch information - do not modify anything except names
V300  Do not put anything below this section - it will be ignored
*Comparison
$192-192-192,0,Times New Roman|12||0-0-0|0-0-0|0-0-255|-1--1--1|-1--1--1|120,120,100,0
10,1,"Tritium/Core/yr (H)",-711,-86,67,22,8,3,0,0,0,0,0,0
10,2,"reactor yearly uptime frac (H)",-566,-39,65,22,8,3,0,0,0,0,0,0
10,3,"outage duration frac (H)",-649,47,64,22,8,3,0,0,0,0,0,0
10,4,"outage duration (H)",-499,49,64,22,8,3,0,0,0,0,0,0
10,5,"number of cores (H)",-414,-37,42,22,8,3,0,0,0,0,0,0
10,6,"Tritium Production (H)",-386,-140,56,32,3,131,0,0,0,0,0,0
12,7,48,-662,-154,10,8,0,3,0,0,-1,0,0,0
1,8,10,6,4,0,0,22,0,0,0,-1--1--1,,1|(-491,-154)|
1,9,10,7,100,0,0,22,0,0,0,-1--1--1,,1|(-602,-154)|
11,10,48,-547,-154,6,8,34,3,0,0,1,0,0,0
```

10,11,"tritium production rate (H)",-547,-124,75,22,40,3,0,0,-1,0,0,0
1,12,1,11,1,0,0,0,0,64,0,-1--1--1,,1|(-654,-122)|
1,13,2,11,0,0,0,0,0,64,0,-1--1--1,,1|(-558,-74)|
1,14,3,2,1,0,0,0,0,64,0,-1--1--1,,1|(-633,-11)|
1,15,4,3,1,0,0,0,0,64,0,-1--1--1,,1|(-552,82)|
10,16,"tritium yearly demand (H)",-693,225,56,22,8,3,0,0,0,0,0,0
10,17,"number of reactors required (H)",-595,141,78,22,8,3,0,0,0,0,0,0
1,18,16,17,1,0,0,0,0,64,0,-1--1--1,,1|(-611,201)|
1,19,1,17,1,0,0,0,0,64,0,-1--1--1,,1|(-679,104)|
10,20,"HM (H)",-205,8,34,12,8,3,0,0,0,0,0,0
10,21,"HM/core/yr (H)",-328,59,50,22,8,3,0,0,0,0,0,0
10,22,"HM / year (H)",-336,150,59,12,8,3,0,0,0,0,0,0
1,23,21,22,0,0,0,0,0,64,0,-1--1--1,,1|(-330,102)|
1,24,17,22,0,0,0,0,0,64,0,-1--1--1,,1|(-462,144)|
10,25,"Tritium/Core/yr (BW)",-721,410,67,22,8,3,0,0,0,0,0,0
10,26,"reactor yearly uptime frac (BW)",-528,443,73,22,8,3,0,0,0,0,0,0
10,27,"outage duration frac (BW)",-636,510,64,22,8,3,0,0,0,0,0,0
10,28,"outage duration (BW)",-469,513,64,22,8,3,0,0,0,0,0,0
10,29,"number of cores (BW)",-343,454,67,22,8,3,0,0,0,0,0,0
10,30,"Tritium Production (BW)",-402,342,56,29,3,131,0,0,0,0,0,0
12,31,48,-646,333,10,8,0,3,0,0,-1,0,0,0
1,32,34,30,4,0,0,22,0,0,0,-1--1--1,,1|(-499,333)|
1,33,34,31,100,0,0,22,0,0,0,-1--1--1,,1|(-594,333)|
11,34,48,-547,333,6,8,34,3,0,0,1,0,0,0
10,35,"tritium production rate (BW)",-547,363,75,22,40,3,0,0,-1,0,0,0
1,36,25,35,1,0,0,0,0,64,0,-1--1--1,,1|(-655,374)|
1,37,27,26,1,0,0,0,0,64,0,-1--1--1,,1|(-619,451)|
1,38,28,27,1,0,0,0,0,64,0,-1--1--1,,1|(-534,546)|
10,39,"Tritium/Core/yr (NS)",-77,-89,67,22,8,3,0,0,0,0,0,0
10,40,"reactor yearly uptime frac (NS)",68,-42,70,22,8,3,0,0,0,0,0,0
10,41,"outage duration frac (NS)",-15,44,64,22,8,3,0,0,0,0,0,0
10,42,"outage duration (NS)",136,40,64,22,8,3,0,0,0,0,0,0
10,43,"number of cores (NS)",220,-40,67,22,8,3,0,0,0,0,0,0
10,44,"Tritium Production (NS)",248,-143,56,32,3,131,0,0,0,0,0,0
12,45,48,-28,-157,10,8,0,3,0,0,-1,0,0,0
1,46,48,44,4,0,0,22,0,0,0,-1--1--1,,1|(142,-157)|
1,47,48,45,100,0,0,22,0,0,0,-1--1--1,,1|(31,-157)|
11,48,48,87,-157,6,8,34,3,0,0,1,0,0,0
10,49,"tritium production rate (NS)",87,-127,75,22,40,3,0,0,-1,0,0,0
1,50,39,49,1,0,0,0,0,64,0,-1--1--1,,1|(-20,-125)|
1,51,40,49,0,0,0,0,0,64,0,-1--1--1,,1|(75,-77)|
1,52,41,40,1,0,0,0,0,64,0,-1--1--1,,1|(1,-14)|
1,53,42,41,1,0,0,0,0,64,0,-1--1--1,,1|(75,78)|
10,54,"tritium yearly demand (NS)",137,225,56,22,8,3,0,0,0,0,0,0
10,55,"number of reactors required (NS)",68,146,78,22,8,3,0,0,0,0,0,0
1,56,54,55,1,0,0,0,0,64,0,-1--1--1,,1|(103,198)|
1,57,39,55,1,0,0,0,0,64,0,-1--1--1,,1|(-80,84)|
10,58,"HM (NS)",429,5,40,12,8,3,0,0,0,0,0,0
10,59,"HM/core (NS)",306,56,39,22,8,3,0,0,0,0,0,0
10,60,"HM / year (NS)",299,147,43,22,8,3,0,0,0,0,0,0
1,61,59,60,0,0,0,0,0,64,0,-1--1--1,,1|(303,94)|

1,62,55,60,0,0,0,0,0,64,0,-1--1--1,,1|(194,146)|
10,63,"HM (BW)",-214,524,43,12,8,3,0,0,0,0,0,0
10,64,"HM/core (BW)",-346,566,39,22,8,3,0,0,0,0,0,0
10,65,"HM / year (BW)",-354,672,43,22,8,3,0,0,0,0,0,0
1,66,64,65,0,0,0,0,0,64,0,-1--1--1,,1|(-348,612)|
10,67,"tritium yearly demand (BW)",-680,682,59,22,8,3,0,0,0,0,0,0
10,68,"number of reactors required (BW)",-553,606,78,22,8,3,0,0,0,0,0,0
1,69,67,68,1,0,0,0,0,64,0,-1--1--1,,1|(-637,637)|
1,70,25,68,1,0,0,0,0,64,0,-1--1--1,,1|(-712,544)|
1,71,68,65,1,0,0,0,0,64,0,-1--1--1,,1|(-443,615)|
1,72,26,35,0,0,0,0,0,64,0,-1--1--1,,1|(-535,409)|
10,73,Initial Unobligated Uranium,-162,338,68,68,2,131,0,0,0,0,0,0
10,74,"Remaining Unabligated U (BW)",-64,680,61,30,3,131,0,0,0,0,0,0
1,75,76,74,4,0,0,22,0,0,0,-1--1--1,,1|(-164,674)|
11,76,1756,-209,674,6,8,34,3,0,0,1,0,0,0
10,77,"rate HM (BW)",-209,704,35,22,40,3,0,0,-1,0,0,0
1,78,73,74,0,0,0,0,0,64,1,-1--1--1,,1|(-109,519)|
1,79,65,77,0,0,0,0,0,64,0,-1--1--1,,1|(-284,686)|
10,80,"Remaining Unabligated U (H)",-129,212,61,30,3,131,0,0,0,0,0,0
1,81,82,80,4,0,0,22,0,0,0,-1--1--1,,1|(-229,206)|
11,82,1788,-274,206,6,8,34,3,0,0,1,0,0,0
10,83,"rate HM (H)",-274,236,52,12,40,3,0,0,-1,0,0,0
10,84,"Remaining Unabligated U (NS)",548,213,61,30,3,131,0,0,0,0,0,0
1,85,86,84,4,0,0,22,0,0,0,-1--1--1,,1|(448,207)|
11,86,1804,403,207,6,8,34,3,0,0,1,0,0,0
10,87,"rate HM (NS)",403,237,57,12,40,3,0,0,-1,0,0,0
1,88,22,83,0,0,0,0,0,64,0,-1--1--1,,1|(-309,187)|
1,89,60,87,0,0,0,0,0,64,0,-1--1--1,,1|(351,192)|
1,90,73,80,0,0,0,0,0,64,1,-1--1--1,,1|(-142,264)|
1,91,73,84,0,0,0,0,0,64,1,-1--1--1,,1|(188,276)|
10,92,"reactor yearly uptime frac (WB1)",225,429,79,22,8,3,0,0,0,0,0,0
10,93,"outage duration frac (WB1)",140,516,64,22,8,3,0,0,0,0,0,0
10,94,"outage duration (WB1)",293,511,64,22,8,3,0,0,0,0,0,0
10,95,"number of cores (WB1)",377,431,67,22,8,3,0,0,0,0,0,0
10,96,"Tritium Production (WB1)",405,328,56,32,3,131,0,0,0,0,0,0
12,97,48,129,314,10,8,0,3,0,0,-1,0,0,0
1,98,100,96,4,0,0,22,0,0,0,-1--1--1,,1|(299,314)|
1,99,100,97,100,0,0,22,0,0,0,-1--1--1,,1|(188,314)|
11,100,48,244,314,6,8,34,3,0,0,1,0,0,0
10,101,"tritium production rate (WB1)",244,344,75,22,40,3,0,0,-1,0,0,0
1,102,92,101,0,0,0,0,0,64,0,-1--1--1,,1|(232,393)|
1,103,93,92,1,0,0,0,0,64,0,-1--1--1,,1|(156,456)|
1,104,94,93,1,0,0,0,0,64,0,-1--1--1,,1|(231,551)|
10,105,"tritium yearly demand (WB1)",294,696,64,22,8,3,0,0,0,0,0,0
10,106,"number of reactors required (WB1)",225,617,78,22,8,3,0,0,0,0,0,0
1,107,105,106,1,0,0,0,0,64,0,-1--1--1,,1|(260,669)|
10,108,"HM (WB1)",586,476,48,12,8,3,0,0,0,0,0,0
10,109,"HM/core (WB1)",463,527,39,22,8,3,0,0,0,0,0,0
1,110,108,109,1,0,0,0,0,64,0,-1--1--1,,1|(526,489)|
10,111,"HM / year (WB1)",456,618,43,22,8,3,0,0,0,0,0,0
1,112,109,111,0,0,0,0,0,64,0,-1--1--1,,1|(460,565)|

1,113,106,111,0,0,0,0,0,64,0,-1--1--1,,1|(351,617)|
10,114,"Remaining Unabligated U (WB1)",705,684,61,30,3,131,0,0,0,0,0,0
1,115,116,114,4,0,0,22,0,0,0,-1--1--1,,1|(605,678)|
11,116,1180,560,678,6,8,34,3,0,0,1,0,0,0
10,117,"rate HM (WB1)",560,708,35,22,40,3,0,0,-1,0,0,0
1,118,111,117,0,0,0,0,0,64,0,-1--1--1,,1|(502,658)|
10,119,"Tritium/Core/yr (WB1)",41,400,67,22,8,3,0,0,0,0,0,0
1,120,119,106,1,0,0,0,0,64,0,-1--1--1,,1|(57,542)|
1,121,73,114,0,0,0,0,0,64,1,-1--1--1,,1|(265,508)|
10,122,Initial Tritium Inventory,541,-157,53,53,2,131,0,0,0,0,0,0
10,123,"Tritium w/ Production",737,-76,50,24,3,131,0,0,0,0,0,0
12,124,48,510,-73,10,8,0,3,0,0,-1,0,0,0
1,125,127,123,4,0,0,22,0,0,0,-1--1--1,,1|(648,-73)|
1,126,127,124,100,0,0,22,0,0,0,-1--1--1,,1|(558,-73)|
11,127,48,603,-73,6,8,34,3,0,0,1,0,0,0
10,128,Tritium Produced,603,-43,40,22,40,3,0,0,-1,0,0,0
12,129,48,934,-80,10,8,0,3,0,0,-1,0,0,0
1,130,132,129,4,0,0,22,0,0,0,-1--1--1,,1|(887,-80)|
1,131,132,123,100,0,0,22,0,0,0,-1--1--1,,1|(813,-80)|
11,132,48,845,-80,6,8,34,3,0,0,1,0,0,0
10,133,Decay,845,-60,27,12,40,3,0,0,-1,0,0,0
10,134,"Tritium Decay Rate, frac/yr",760,28,60,22,8,3,0,0,0,0,0,0
1,135,134,133,0,0,0,0,0,64,0,-1--1--1,,1|(802,-15)|
1,136,133,123,1,0,0,0,0,64,0,-1--1--1,,1|(810,-138)|
1,137,122,123,0,0,0,0,0,64,1,-1--1--1,,1|(631,-119)|
1,138,55,49,1,0,0,0,0,64,0,-1--1--1,,1|(240,13)|
1,139,17,11,1,0,0,0,0,64,0,-1--1--1,,1|(-432,33)|
1,140,68,35,1,0,0,0,0,64,0,-1--1--1,,1|(-425,505)|
1,141,106,101,1,0,0,0,0,64,0,-1--1--1,,1|(356,488)|
1,142,49,128,0,0,0,0,0,64,0,-1--1--1,,1|(355,-83)|
10,143,"Tritium w/o Production",820,105,50,24,3,131,0,0,0,0,0,0
1,144,145,143,4,0,0,22,0,0,0,-1--1--1,,1|(731,108)|
11,145,828,686,108,6,8,34,3,0,0,1,0,0,0
10,146,Tritium Produced',686,138,42,22,40,3,0,0,-1,0,0,0
12,147,48,1017,101,10,8,0,3,0,0,-1,0,0,0
1,148,150,147,4,0,0,22,0,0,0,-1--1--1,,1|(970,101)|
1,149,150,143,100,0,0,22,0,0,0,-1--1--1,,1|(896,101)|
11,150,48,928,101,6,8,34,3,0,0,1,0,0,0
10,151,Decay',928,121,29,12,40,3,0,0,-1,0,0,0
1,152,151,143,1,0,0,0,0,64,0,-1--1--1,,1|(865,186)|
1,153,134,151,1,0,0,0,0,64,0,-1--1--1,,1|(908,48)|
1,154,122,143,0,0,0,0,0,64,1,-1--1--1,,1|(681,-24)|
1,155,95,109,0,0,0,0,0,64,0,-1--1--1,,1|(414,473)|
10,156,"cycle (H)",-206,105,40,12,8,3,0,0,0,0,0,0
10,157,"cycle (BW)",-220,598,48,12,8,3,0,0,0,0,0,0
10,158,"cycle (NS)",408,95,45,12,8,3,0,0,0,0,0,0
10,159,"cycle (WB1)",582,564,53,12,8,3,0,0,0,0,0,0
1,160,159,111,0,0,0,0,0,64,0,-1--1--1,,1|(532,584)|
1,161,119,101,1,0,0,0,0,64,0,-1--1--1,,1|(122,358)|
10,162,"reactor yearly uptime frac (RSR)",1026,414,77,22,8,3,0,0,0,0,0,0
10,163,"outage duration frac (RSR)",941,501,64,22,8,3,0,0,0,0,0,0

10,164,"outage duration (RSR)",1094,496,64,22,8,3,0,0,0,0,0,0
10,165,"number of cores (RSR)",1178,416,67,22,8,3,0,0,0,0,0,0
10,166,"Tritium Production (RSR)",1206,313,56,32,3,131,0,0,0,0,0,0
12,167,48,930,299,10,8,0,3,0,0,-1,0,0,0
1,168,170,166,4,0,0,22,0,0,0,-1--1--1,,1|(1100,299)|
1,169,170,167,100,0,0,22,0,0,0,-1--1--1,,1|(989,299)|
11,170,48,1045,299,6,8,34,3,0,0,1,0,0,0
10,171,"tritium production rate (RSR)",1045,329,75,22,40,3,0,0,-1,0,0,0
1,172,162,171,0,0,0,0,0,64,0,-1--1--1,,1|(1033,378)|
1,173,163,162,1,0,0,0,0,64,0,-1--1--1,,1|(957,441)|
1,174,164,163,1,0,0,0,0,64,0,-1--1--1,,1|(1032,536)|
10,175,"tritium yearly demand (RSR)",1095,681,62,22,8,3,0,0,0,0,0,0
10,176,"number of reactors required (RSR)",1026,602,78,22,8,3,0,0,0,0,0,0
1,177,175,176,1,0,0,0,0,64,0,-1--1--1,,1|(1061,654)|
10,178,"HM (RSR)",1387,461,46,12,8,3,0,0,0,0,0,0
10,179,"HM/core (RSR)",1264,512,39,22,8,3,0,0,0,0,0,0
10,180,"HM / year (RSR)",1257,603,43,22,8,3,0,0,0,0,0,0
1,181,179,180,0,0,0,0,0,64,0,-1--1--1,,1|(1261,550)|
1,182,176,180,0,0,0,0,0,64,0,-1--1--1,,1|(1152,602)|
10,183,"Remaining Unabligated U (RSR)",1506,669,61,30,3,131,0,0,0,0,0,0
1,184,185,183,4,0,0,22,0,0,0,-1--1--1,,1|(1406,663)|
11,185,444,1361,663,6,8,34,3,0,0,1,0,0,0
10,186,"rate HM (RSR)",1361,693,35,22,40,3,0,0,-1,0,0,0
1,187,180,186,0,0,0,0,0,64,0,-1--1--1,,1|(1303,643)|
10,188,"Tritium/Core/yr (RSR)",842,385,67,22,8,3,0,0,0,0,0,0
1,189,188,176,1,0,0,0,0,64,0,-1--1--1,,1|(858,527)|
1,190,176,171,1,0,0,0,0,64,0,-1--1--1,,1|(1157,473)|
10,191,"cycle (RSR)",1383,549,51,12,8,3,0,0,0,0,0,0
1,192,188,171,1,0,0,0,0,64,0,-1--1--1,,1|(923,343)|
1,193,73,183,0,0,0,0,0,64,1,-1--1--1,,1|(667,502)|
\\\---/// Sketch information - do not modify anything except names
V300 Do not put anything below this section - it will be ignored
*Base
$192-192-192,0,Times New Roman|12||0-0-0|0-0-0|0-0-255|-1--1--1|-1--1--1|120,120,100,0
10,1,"TPBARs / Assembly",569,252,44,22,8,3,0,0,0,0,0,0
10,2,"tritium / TPBAR",142,151,34,22,8,3,0,0,0,0,0,0
10,3,reactor yearly uptime frac,289,202,58,22,8,3,0,0,0,0,0,0
10,4,"price of tririum ($/g)",545,167,64,22,8,3,0,0,0,0,0,0
10,5,tritium income,621,92,59,12,8,3,0,0,0,0,0,0
10,6,number of reactors,571,324,42,22,8,3,0,0,0,0,0,0
10,7,number of assemblies,559,409,46,22,8,3,0,0,0,0,0,0
10,8,outage duration frac,202,283,64,22,8,3,0,0,0,0,0,0
10,9,outage duration,272,346,35,22,8,3,0,0,0,0,0,0
10,10,thermal efficiency nameplate,211,599,75,22,8,3,0,0,0,0,0,0
10,11,MWt nameplate,125,669,43,22,8,3,0,0,0,0,0,0
10,12,MWe nameplate,276,668,43,22,8,3,0,0,0,0,0,0
10,13,"price of electricity (c/KWH)",511,675,78,22,8,3,0,0,0,0,0,0
10,14,Electricity income,686,626,44,22,8,3,0,0,0,0,0,0
10,15,refueling cycle,850,364,37,22,8,3,0,0,0,0,0,0
10,16,"total rods / assembly",958,329,46,22,8,3,0,0,0,0,0,0
10,17,"control rods / assembly",984,432,57,22,8,3,0,0,0,0,0,0

10,18,"instrument rods / assembly",1112,357,70,22,8,3,0,0,0,0,0,0
10,19,"kg HM / road",1241,314,55,12,8,3,0,0,0,0,0,0
10,20,Tritium Production,469,73,48,25,3,131,0,0,0,0,0,0
10,21,Unobligated U,1103,219,51,27,3,131,0,0,0,0,0,0
10,22,Electrical Production,554,555,50,26,3,131,0,0,0,0,0,0
12,23,48,217,68,10,8,0,3,0,0,-1,0,0,0
1,24,26,20,4,0,0,22,0,0,0,-1--1--1,,1|(375,68)|
1,25,26,23,100,0,0,22,0,0,0,-1--1--1,,1|(272,68)|
11,26,48,324,68,6,8,34,3,0,0,1,0,0,0
10,27,tritium production rate,324,98,64,22,40,3,0,0,-1,0,0,0
12,28,48,329,545,10,8,0,3,0,0,-1,0,0,0
1,29,31,22,4,0,0,22,0,0,0,-1--1--1,,1|(465,545)|
1,30,31,28,100,0,0,22,0,0,0,-1--1--1,,1|(377,545)|
11,31,48,421,545,6,8,34,3,0,0,1,0,0,0
10,32,electrical generation rate,421,575,62,22,40,3,0,0,-1,0,0,0
12,33,48,888,218,10,8,0,3,0,0,-1,0,0,0
1,34,36,21,4,0,0,22,0,0,0,-1--1--1,,1|(1016,218)|
1,35,36,33,100,0,0,22,0,0,0,-1--1--1,,1|(933,218)|
11,36,48,975,218,6,8,34,3,0,0,1,0,0,0
10,37,U replacement rate,975,248,60,22,40,3,0,0,-1,0,0,0
1,38,1,27,0,0,0,0,0,64,0,-1--1--1,,1|(452,178)|
1,39,2,27,0,0,0,0,0,64,0,-1--1--1,,1|(211,131)|
1,40,3,27,0,0,0,0,0,64,0,-1--1--1,,1|(303,156)|
1,41,8,3,0,0,0,0,0,64,0,-1--1--1,,1|(239,247)|
1,42,9,8,0,0,0,0,0,64,0,-1--1--1,,1|(242,319)|
1,43,4,5,0,0,0,0,0,64,0,-1--1--1,,1|(582,129)|
1,44,20,5,0,0,0,0,0,64,0,-1--1--1,,1|(532,80)|
1,45,6,27,0,0,0,0,0,64,0,-1--1--1,,1|(452,215)|
1,46,6,37,0,0,0,0,0,64,0,-1--1--1,,1|(757,289)|
1,47,1,37,0,0,0,0,0,64,0,-1--1--1,,1|(757,250)|
1,48,7,27,0,0,0,0,0,64,0,-1--1--1,,1|(445,259)|
1,49,7,37,0,0,0,0,0,64,0,-1--1--1,,1|(754,333)|
1,50,15,37,0,0,0,0,0,64,0,-1--1--1,,1|(906,310)|
1,51,16,37,0,0,0,0,0,64,0,-1--1--1,,1|(964,295)|
1,52,17,37,0,0,0,0,0,64,0,-1--1--1,,1|(979,346)|
1,53,18,37,0,0,0,0,0,64,0,-1--1--1,,1|(1049,306)|
1,54,19,37,0,0,0,0,0,64,0,-1--1--1,,1|(1120,283)|
1,55,3,32,0,0,0,0,0,64,0,-1--1--1,,1|(352,381)|
1,56,11,10,0,0,0,0,0,64,0,-1--1--1,,1|(162,638)|
1,57,12,10,0,0,0,0,0,64,0,-1--1--1,,1|(248,639)|
1,58,12,32,0,0,0,0,0,64,0,-1--1--1,,1|(342,625)|
1,59,22,14,0,0,0,0,0,64,0,-1--1--1,,1|(617,589)|
1,60,13,14,0,0,0,0,0,64,0,-1--1--1,,1|(608,648)|
\\\---/// Sketch information - do not modify anything except names
V300 Do not put anything below this section - it will be ignored
*Comparison Output
$192-192-192,0,Times New Roman|12||0-0-0|0-0-0|0-0-255|-1--1--1|-1--1--1|120,120,100,0
12,1,4527720,691,-206,548,183,3,188,0,0,1,0,0,0
Reactors
12,2,2691896,692,154,549,171,3,188,0,0,1,0,0,0
HM

12,3,3934352,692,510,549,172,3,188,0,0,1,0,0,0
U-U
\\\---/// Sketch information - do not modify anything except names
V300 Do not put anything below this section - it will be ignored
*Decay Curve
$192-192-192,0,Times New Roman|12||0-0-0|0-0-0|0-0-255|-1--1--1|-1--1--1|120,120,100,0
12,1,3999888,832,381,599,364,3,188,0,0,1,0,0,0
Trit-Inv
\\\---/// Sketch information - do not modify anything except names
V300 Do not put anything below this section - it will be ignored
*Base Input/Output
$192-192-192,0,Times New Roman|12||0-0-0|0-0-0|0-0-255|-1--1--1|-1--1--1|120,120,100,0
12,1,15272760,185,92,126,20,3,252,0,0,0,0,0,0
number of reactors,1,12,1
12,2,1383744,185,159,126,19,3,252,0,0,0,0,0,0
"TPBARs / Assembly",1,7000,5
12,3,1580350,184,230,127,21,3,252,0,0,0,0,0,0
"tritium / TPBAR",0,2,0.1
12,4,1776904,186,298,127,20,3,252,0,0,0,0,0,0
number of assemblies,0,7000,10
12,5,1580274,185,364,127,19,3,252,0,0,0,0,0,0
outage duration,0,12,0.06
12,6,269708,185,432,125,20,3,252,0,0,0,0,0,0
"price of tririum ($/g)",0,150000,500
12,7,269700,186,508,126,20,3,252,0,0,0,0,0,0
"price of electricity (c/KWH)",1,20,1
12,8,0,569,61,116,16,8,135,0,0,-1,0,0,0
Yearly Tririum Production
12,9,0,901,50,94,16,8,135,0,0,-1,0,0,0
Tririum Income ($/yr)
12,10,0,1298,52,144,20,8,135,0,0,-1,0,0,0
Unobligated Uranium Used (kg/yr)
12,11,0,561,452,122,21,8,135,0,0,-1,0,0,0
Yearly Electrical Production
12,12,0,922,449,105,15,8,135,0,0,-1,0,0,0
Electricity Income ($/yr)
12,13,204180,597,232,150,150,3,44,0,0,1,0,0,0
YTProd
12,14,204182,950,227,150,150,3,44,0,0,1,0,0,0
tritium$
12,15,204184,1303,225,150,150,3,44,0,0,1,0,0,0
UU/yr
12,16,204186,589,624,150,150,3,44,0,0,1,0,0,0
ElecProd
12,17,204188,961,621,150,150,3,44,0,0,1,0,0,0
Elec$
12,18,0,350,347,38,322,3,135,0,0,-1,0,0,0
1

Venapp

```
! Venapp Tritium Production Model
! the exclamation mark marks something as a comment (the item is not functional in the venapp)
! remove the exclamation marks (below) to restore functionality
!
:SCREEN WELCOME
SCREENFONT,Times New Roman|12|B|0-0-0|-1--1--1
PIXELPOS,0
!*|COMMAND,"",0,0,0,0,,,"SPECIAL>SETTITLE|Venapp Template Example"
COMMAND,"",0,0,0,0,,,SPECIAL>LOADMODEL|base model rev 4b.mdl
COMMAND,"",0,0,0,0,,,SPECIAL>READCUSTOM|T3a.vgd
COMMAND,"",0,0,0,0,,,SPECIAL>LOADTOOLSET|default.vts
COMMAND,"",0,0,0,0,,,SPECIAL>CLEARRUNS
COMMAND,"",0,0,0,0,,,SPECIAL>LOADRUN|Current1.vdf
COMMAND,"",0,0,0,0,,,SETTING>SHOWWARNING|0
TEXTONLY,"Alternate Tritium Production",50,5,0,0,C||36|B|255-0-0,
!*|TEXTONLY,"Vensim Application Template",0,20,100,0,C|Arial|22|B|0-0-255,
TEXTONLY,"Mark P. Jones",0,58,100,0,C||10||128-0-128|,
TEXTONLY,"Computational Sciences",0,62,100,0,C||10||128-0-128|,
TEXTONLY,"Bldg 703-41A",0,66,100,0,C||10||128-0-128|,
TEXTONLY,"mark.jones@srnl.doe.gov",0,70,100,0,C||10||128-0-128|,
TEXTONLY,"803/725-6279",0,74,100,0,C||10||128-0-128|,
TEXTONLY,"Press any key or button to continue",0,84,100,0,C||14|||,
BUTTON,"Continue",50,90,45,5,C,,,MAIN
ANYKEY,"",0,0,0,0,0,,,MAIN
BITMAP,"base model rev 40000.bmp",29,15,41,10,C,,,
!
:SCREEN MAIN
SCREENFONT,Times New Roman|12|B|0-0-0|-1--1--1
PIXELPOS,0
TEXTONLY,"Alternate Tritium Production",50,5,0,0,C|Times New Roman|30|B|200-55-0,
TEXTONLY,"Main Menu",50,18,0,0,C|Arial|24|B|0-0-255,
RECTANGLE,"",20,30,60,46,C||||0-0-255
BUTTON,"Review Model Structure",50,35,50,6,C,,,STRUCTURE
BUTTON,"Review Process Flow",50,44,50,6,C,,,PROCESS
BUTTON,"Simulate the Model",50,55,50,6,C,,,SETUPSCENARIO
Results",50,65,50,6,C,,SPECIAL>ALIASSCREEN|ARETURN|MAIN,ANALYSIS
BUTTON,"Exit",50,90,40,6,C,Qq,SPECIAL>ASKYESNO|Do you really want to exit?&MENU>EXIT,
!
:SCREEN STRUCTURE
SCREENFONT,Times New Roman|12|B|0-0-0|-1--1--1
PIXELPOS,0
SKETCH,"SK1",0,0,93,88,,5,1,
COMMAND,"",18,77,20,6,L,,SPECIAL>SETTITLE|*MV|%s - View:%s
BUTTON,"Previous",7,92,10,6,L,,SKETCH>PREVVIEW|SK1&SPECIAL>SETTITLE|*MV|%s - View:%s,
BUTTON,"Next",19,92,10,6,L,,SKETCH>NEXTVIEW|SK1&SPECIAL>SETTITLE|*MV|%s - View:%s,
BUTTON,"Exit to Main Menu",71,92,22,6,L,,,MAIN
```

```
!
:SCREEN PROCESS
SCREENFONT,Times New Roman|10||0-0-0|-1--1--1
PIXELPOS,0
BITMAP,"material flow.bmp",43,4,40,50,,,,
BITMAP,"fuel cycle.bmp",7,18,30,24,,,,
BUTTON,"Exit to Main Menu",7,49,22,6,L,,,MAIN
!
:SCREEN INPUT/OUTPUT1
SCREENFONT,Times New Roman|10||0-0-0|-1--1--1
PIXELPOS,0
TEXTONLY,"Scenario Options",49,3,0,0,C|Arial|24|B|0-0-255,,,
TEXTONLY,"Number of Reactors (Cores)",2,4,0,0,L,,,
TEXTONLY,"TPBARs / Assembly",2,19,0,0,L,,,
TEXTONLY,"grams Trtium / TPBAR / Year",2,34,0,0,L,,,
SLIDEVAR,"number of reactors",2,7,15,10,H,[1|15|1],,
SLIDEVAR,"TPBARs / Assembly",2,22,15,10,H,[0|50|1],,
SLIDEVAR,"trtium / TPBAR",2,37,15,10,H,[0|1.6|.1],,
TEXTONLY,"Number of Assemblies",2,49,0,0,L,,,
TEXTONLY,"Price for Tritium ($/g)",2,64,0,0,L,,,
TEXTONLY,"Price of Electricity (cents / KWH)",2,79,0,0,L,,,
SLIDEVAR,"number of assemblies",2,52,15,10,H,[0|200|1],,
SLIDEVAR,"price of tritium ($/g)",2,67,15,10,H,[10000|250000|10000],,
SLIDEVAR,"price of electricity (¢/KWH)",2,82,15,10,H,[3|20|1],,
TEXTONLY,"Yearly Tritium Production (g)",27,19,0,0,L|Times New Roman|12|B|0-0-255,,,
TEXTONLY,"Tritium Income ($/yr)",47,19,12,3,L|Times New Roman|12|B|0-0-255,,,
TEXTONLY,"Unobligated Uranium Used (kg/yr)",67,19,0,0,|Times New Roman|12|B|0-0-255,,,
TEXTONLY,"Yearly Electrical Production (MW)",27,57,0,0,|Times New Roman|12|B|0-0-255,,,
TEXTONLY,"Electricity Income ($/yr)",47,57,0,0,|Times New Roman|12|B|0-0-255,,,
TEXTONLY,"Summary of Input Variables",67,57,0,0,|Times New Roman|12|B|0-0-255,,,
BUTTON,"Exit to Main Menu",87,17,9,5,L,,,MAIN
TOOL,"GR1",27,23,18,30,,,CUSTOM>YTProd,
TOOL,"GR1",67,23,18,30,,,CUSTOM>UU/yr,
TOOL,"GR1",47,23,18,30,,,CUSTOM>tritium$,
TOOL,"GR1",27,62,18,30,,,CUSTOM>ElecProd,
TOOL,"GR1",47,62,18,30,,,CUSTOM>Elec$,
BUTTON,"SIMULATE",92,11,9,5,C,,,RUNNING1
!
:SCREEN RUNNING1
SCREENFONT,Times New Roman|10||0-0-0|-1--1--1
PIXELPOS,0
TEXTONLY,"Yearly Tritium Production (g)",27,19,0,0,L|Times New Roman|12|B|0-0-255,,,
TEXTONLY,"Tritium Income ($/yr)",47,19,12,3,L|Times New Roman|12|B|0-0-255,,,
TEXTONLY,"Unobligated Uranium Used (kg/yr)",67,19,0,0,|Times New Roman|12|B|0-0-255,,,
TEXTONLY,"Yearly Electrical Production (MW)",27,57,0,0,|Times New Roman|12|B|0-0-255,,,
TEXTONLY,"Electricity Income ($/yr)",47,57,0,0,|Times New Roman|12|B|0-0-255,,,
TEXTONLY,"Summary of Input Variables",67,57,0,0,|Times New Roman|12|B|0-0-255,,,
BUTTON,"Exit to Main Menu",87,17,9,5,L,,,MAIN
TOOL,"GR1",27,23,18,30,,,CUSTOM>YTProd,
TOOL,"GR1",67,23,18,30,,,CUSTOM>UU/yr,
TOOL,"GR1",47,23,18,30,,,CUSTOM>tritium$,
```

```
TOOL,"GR1",27,62,18,30,,,CUSTOM>ElecProd,
TOOL,"GR1",47,62,18,30,,,CUSTOM>Elec$,
TEXTONLY,"Scenario Options",49,3,0,0,C|Arial|24|B|0-0-255,,,
WIPTOOL,"",4,24,15,29,,,SIMULATE>RUNNAME|Tritium Production,
!
:SCREEN INPUT/OUTPUT2
SCREENFONT,Times New Roman|10||0-0-0|-1--1--1
PIXELPOS,0
TEXTONLY,"Scenario Options",49,1,0,0,C|Arial|24|B|0-0-255,,,
RADIOVAR,"Watt's Bar",12,22,0,0,,,,
TEXTONLY,"Watt's Bar",4,22,,,,,"",
TEXTONLY,"NuScale",4,31,0,0,,,,
TEXTONLY,"B & W",4,41,0,0,,,,
TEXTONLY,"Holtec",4,48,0,0,,,,
TEXTONLY,"Advanced Reactor",4,56,0,0,,,,
RADIOVAR,"NuScale",12,31,0,0,,,,
RADIOVAR,"B&W",12,40,0,0,,,,
RADIOVAR,"Holtec",12,48,0,0,,,,
RADIOVAR,"Advanced",12,55,0,0,,,,
TEXTONLY,"Number of Reactors (Cores)",3,72,0,0,L,,,
SLIDEVAR,"number of reactors",3,75,15,10,H,[1|15|1],,
BUTTON,"Exit to Main Menu",5,89,10,5,L,,,MAIN
TEXTONLY,"Yearly Tritium Production (g)",27,10,,,L|Times New Roman|12|B|0-0-255,,"",
TEXTONLY,"Tritium Income ($/yr)",47,10,12,3,L|Times New Roman|12|B|0-0-255,,,
TEXTONLY,"Unobligated Uranium Used (kg/yr)",64,10,0,0,|Times New Roman|12|B|0-0-255,,,
TEXTONLY,"Yearly Electrical Production (MW)",25,58,,,|Times New Roman|12|B|0-0-255,,"",
TEXTONLY,"Electricity Income ($/yr)",47,58,0,0,|Times New Roman|12|B|0-0-255,,,
TEXTONLY,"Summary of Input Variables",66,58,0,0,|Times New Roman|12|B|0-0-255,,,
!
:SCREEN INPUT/OUTPUT3
SCREENFONT,Times New Roman|10||0-0-0|-1--1--1
PIXELPOS,0
TOOL,"GR1",7,4,53,31,,,CUSTOM>Reactors,
TOOL,"GR1",6,68,53,30,,,CUSTOM>HM,
TOOL,"GR1",7,36,52,30,,,CUSTOM>U-U,
!
:SCREEN SETUPSCENARIO
SCREENFONT,Times New Roman|12|B|0-0-0|-1--1--1
PIXELPOS,0
TEXTONLY,"Scenario Setup",50,5,0,0,C|Arial|24|B|0-0-255,
BUTTON,"Scenario based on model constants",50,32,50,6,C,Ss,SIMULATE>READRUNCHG&SIMULATE>RUNNAME|?Name the n\
ew scenario,SETUPSIM
BUTTON,"Modify and rerun an existing scenario",50,42,50,6,C,Mm,SIMULATE>RUNNAME|?Select the scenario to mod\
ify|E&SIMULATE>READRUNCHG|!,SETUPSIM
BUTTON,"Scenario based on an existing scenario",50,52,50,6,C,Ss,SIMULATE>READRUNCHG|?Select scenario for ba\
sis&SIMULATE>RUNNAME|?Name the new scenario,SETUPSIM
```

```
!BUTTON,"Scenario based on changes (.cin) file",50,62,50,6,C,Ss,SIMULATE>READCIN|?Choose a changes fi\
le&SIMULATE>RUNNAME|?Name the new scenario,SETUPSIM
BUTTON,"Exit to Main Menu",50,90,40,6,C,EeXx,,MAIN
!
:SCREEN SETUPSIM
SCREENFONT,Times New Roman|12|B|0-0-0|-1--1--1
PIXELPOS,0
TEXTONLY,"Set Up the Model",50,5,0,0,C|Arial|24|B|0-0-255,
TEXTONLY,"Simulate the Model",75,52,0,0,C|Arial|24|B|0-0-255,
TEXTONLY,"Save Setup",25,52,0,0,C|Arial|24|B|0-0-255,
BUTTON,"Change model assumptions",25,20,40,6,C,,,INPUT1
BUTTON,"Modify policy options",25,30,40,6,C,,,INPUT2
BUTTON,"Make changes to other constants",75,20,40,6,C,,SIMULATE>GETCNSTCHG
BUTTON,"Make changes to other lookup tables",75,30,40,6,C,,SIMULATE>GETTABCHG
BUTTON,"Save setup as changes file (.cin)",25,65,40,10,C,,SIMULATE>WRITECIN|?Name the changes file,
BUTTON,"SIMULATE URANIUM USAGE",75,65,40,10,C,,,RUNNING
BUTTON,"Exit to Main Menu",50,90,40,6,C,,,MAIN
BUTTON,"SIMULATE TRITIUM INVENTORY",75,77,40,10,C,,,RUNNING2
!
:SCREEN RUNNING
SCREENFONT,Times New Roman|12|B|0-0-0|-1--1--1
PIXELPOS,0
TOOL,"GR1",3,4,53,31,,,CUSTOM>Reactors,
TOOL,"GR1",2,68,53,30,,,CUSTOM>HM,
TOOL,"GR1",3,36,52,30,,,CUSTOM>U-U,
!WIPTOOL,"GR1",5,5,90,80,,,CUSTOM>U-U
COMMAND,"",0,0,0,0,,,MENU>RUN1|O
COMMAND,"",0,0,0,0,,,SPECIAL>SETWBITEM|U-U
CLOSESCREEN,"",0,0,0,0,,,,OUTPUT1
TOOL,"GR1",57,4,53,30,,,"CUSTOM>Trit-Inv",
!
:SCREEN OUTPUT1
SCREENFONT,Times New Roman|12|B|0-0-0|-1--1--1
PIXELPOS,0
TOOL,"GR1",5,5,90,70,,,CUSTOM>U-U
!TOOL,"GR1",5,5,90,70,,,WORKBENCH>Graph
BUTTON,"Show additional graphs",20,82,25,10,C,,,OUTPUT3
BUTTON,"Select a new variable",50,80,25,0,C,,SPECIAL>VARSELECT|New variable to use,OUTPUT1
BUTTON,"Change subscripts",50,90,25,0,C,8,SPECIAL>SUBSCRIPT|?Choose a subscript to control selection on,OUT\
PUT1
BUTTON,"Perform detailed analysis",80,80,25,0,C,,SPECIAL>ALIASSCREEN|ARETURN|OUTPUT1,ANALYSIS
BUTTON,"Return to Main Menu",80,90,25,0,C,,,MAIN
!
:SCREEN OUTPUT2
SCREENFONT,Times New Roman|12|B|0-0-0|-1--1--1
PIXELPOS,0
```

```
TOOL,"GR1",5,5,90,70,,,WORKBENCH>Table
BUTTON,"Show graph",20,82,25,10,C,,,OUTPUT1
BUTTON,"Select a new variable",50,80,25,0,C,,SPECIAL>VARSELECT|New variable to use,OUTPUT2
BUTTON,"Change subscripts",50,90,25,0,C,8,SPECIAL>SUBSCRIPT|?Choose a subscript to control selection on,OUT\
PUT2
BUTTON,"Perform detailed analysis",80,80,25,0,C,,SPECIAL>ALIASSCREEN|ARETURN|OUTPUT2,ANALYSIS
BUTTON,"Return to Main Menu",80,90,25,0,C,,,MAIN
!
:SCREEN OUTPUT3
SCREENFONT,Times New Roman|12|B|0-0-0|-1--1--1
PIXELPOS,0
TOOL,"GR1",5,5,88,42,,,CUSTOM>HM,
!TOOL,"GR1",5,5,90,70,,,WORKBENCH>Graph
!BUTTON,"Show additional graphs",20,82,25,10,C,,,OUTPUT3
BUTTON,"Return to Main Menu",80,90,25,0,C,,,MAIN
TOOL,"GR1",5,48,88,40,,,CUSTOM>Reactors,
!
:SCREEN RUNNING2
SCREENFONT,Times New Roman|12|B|0-0-0|-1--1--1
PIXELPOS,0
TOOL,"GR1",3,4,53,31,,,"CUSTOM>Trit-Inv",
!WIPTOOL,"GR1",5,5,90,80,,,CUSTOM>U-U
COMMAND,"",0,0,0,0,,,MENU>RUN1|O
COMMAND,"",0,0,0,0,,,SPECIAL>SETWBITEM|Trit-Inv
CLOSESCREEN,"",0,0,0,0,,,,OUTPUT4
!
:SCREEN OUTPUT4
SCREENFONT,Times New Roman|12|B|0-0-0|-1--1--1
PIXELPOS,0
TOOL,"GR1",5,5,88,82,,,CUSTOM>Trit-Inv,
!TOOL,"GR1",5,5,90,70,,,WORKBENCH>Graph
BUTTON,"Return to Main Menu",80,90,25,0,C,,,MAIN
!
```

8.2 Appendix B - Texas A&M Studies

1. Modification of NuScale Design for Tritium Production
2. A Feasibility Study of Tritium Production in the GE SPRISM Reactor
3. Design and Analysis of the Application of the B&W mPower SMR of Tritium Production
4. Modified Holtec Inherently-Safe Modular Underground Reactor (HI-SMUR) for Tritium Production

Modification of NuScale Design for Tritium Production

Modification of NuScale SMR Design for Tritium Production

NUEN 410 Senior Final Report

Thomas Moore, Daniel Clark, Ali Alnuaimi

4/22/2013

Texas A&M University

Department of Nuclear Engineering

ADVISOR APPROVAL

X

Karen Vierow Ph.D- Technical Advisor
Texas A&M University

X

David Senor Ph.D- Technical Advisor
Pacific Northwest National Laboratories

X

Jean Ragusa Ph. D- Technical Advisor
Texas A&M University

TEAM MEMBERS

X

Thomas Moore

X

Daniel Clark

X

Ali Alnuaimi

TABLE OF CONTENT

1. EXECUTIVE SUMMARY - ALL 1

2. INTRODUCTION - ALL 3

3. OBJECTIVES 5

4. APPROACH AND ANALYSIS - ALL 6

4.1 NEUTRONIC ANALYSIS - Daniel Clark 6

4.1.1 NuScale Core Overview 6

4.1.2 Tritium-Producing Burnable Absorber Rods Overview 8

4.1.3 Design Overview 11

4.1.4 CASMO4 and DRAGON 12

4.1.5 TPBAR Modeling 13

4.1.6 DRAGON Comparison 16

4.1.7 Core Map Design 17

4.1.8 TPBAR Placement and Tritium Production 18

4.2 Thermal Hydraulic Analysis - Thomas Moore 20

4.2.1 Overview 20

4.2.2 GOTHIC 21

4.2.3 Model 1 22

4.2.4 Model 2 23

4.2.5 Model 3 28

4.3 Core Integration - Daniel Clark & Thomas Moore 31

4.3.1 Overview 31

4.3.2 Iteration 31

4.3.3 Iteration Results 32

4.4 Safety Analysis - Ali Alnuaimi 36

4.4.1 Introduction 36

4.4.2 Probabilistic Risk Assessment (PRA) 36

4.4.3 Loss of Offsite AC Power 39

4.4.4 Total Loss of AC Power 41

4.4.5 DNBR Analysis 43

4.4.6 TPBARS Safety Analysis 45

4.4.7 Safety Analysis Results 46

4.4.8 Scenario A Results 49

4.4.9 Scenario B Results 49

4.4.10 DNBR Results 52

4.5 Economic Analysis - Ali Alnuaimi 53

4.5.1 Introduction 53

4.5.2 Methodology 53

4.5.3 Detailed Design and Engineering Costs (DD&E) 54

4.5.4 Direct Costs 54

4.5.5 Additional Costs 55

5. CONCLUSIONS AND RECOMMENDATIONS - ALL 57

5.1 Summary 57

5.2 Improvements 58

5.3 Future Works 59

6. REFERENCES 61

7. APPENDIX 62

1. EXECUTIVE SUMMARY - ALL

The need for a cost effective way of producing tritium is the driving force for this project. The purpose of this project is to design a small modular reactor (SMR) dedicated to the production of tritium. This reactor will be designed to replace the production of tritium in commercial reactors. In this project, the NuScale SMR design will be modified to produce tritium through the use of Tritium-Producing Burnable Absorber Rod (TPBAR). The core will be optimized to producing tritium, minimizing the number of SMR's required to meet the United States tritium needs.

The project team used advanced computer programs such as CASMO4, DRAGON and GOTHIC to analyze the different aspects of the reactor. CASMO4 was used, in conjunction with DRAGON, to neutronically adapt and optimize a NuScale SMR to producing tritium. GOTHIC was then used to complete a thermal hydraulic analysis of the final core design ensure the safety of the core with respect to the coolant and cladding temperatures. Through the integration of these two analyses, a stable coolant mass flow rate determined for the core. After a final core design was established, an Excel program was used to perform a probabilistic risk assessment in order to determine the safety margin.

The final number of nuclear reactors required to produce the necessary tritium was deemed to be 11. The maximum number of reactors available in a NuScale facility is 12. The neutronics and thermal hydraulics portions of the project calculated a final mass flow rate through the core to be 185.67 (kg/cm2 hour). This was done through a process of iteration. An Event Tree Analysis (ETA) was performed to analyze two different scenarios and the NuScale reactor was found to perform better than traditional reactors in these scenarios. DNBR was calculated by using W-3 correlation and the NuScale reactor was able to achieve DNBR values above 1.3 for a wide range

of flow qualities. Safety analysis found that the number of TPBARs used is limited due to leakage issues of tritium into the coolant that are being experienced in other similar reactors. The economic analysis found that the estimation of the NuScale cost is about $4 billion for the whole site, which is pretty competitive compared to other reactors. The cost of NuScale was approximated to be 7.5% lower than the NOAK costs.

2. INTRODUCTION - ALL

The United States standing as a dominant world power requires that it maintain a large stockpile of thermo-nuclear weapons. The signature component of these weapons is its tritium core. Tritium's relatively low half-life of 12.3 years leads to a quick core deterioration. To stay functional, the weapon cores must be constantly re-fabricated using fresh tritium. Prior to 1988, tritium was produced exclusively at the Savannah River Site located in South Carolina. Following the shutdown of this tritium production facility, the United States searched for a new approach to satisfy its tritium needs. The government first looked to dedicated tritium producing reactors and accelerators; however, both were determined to be too costly. In 1995, the Department of Energy turned to commercial light water reactors in order to meet tritium demands. Pacific Northwest National Laboratory (PNNL) was chosen to be the design authority in this regard. PNNL's solution was the Tritium-Producing Burnable Absorber Rod (TPBAR). These TPBAR's are designed to be placed in commercial light water reactors and burned for 18 months. When the reactor is shut down for refueling, the irradiated TPBAR's are removed and replaced with fresh ones. The irradiated TPBAR's are then sent away for post irradiation examination and tritium removal.

Currently, the reactor being used to produce tritium is the Tennessee Valley Authority's Watts Bar Nuclear Unit 1. There is a constant conflict between need for tritium production and the want for maximum electrical power output. To remove this strain, PNNL is searching for the possibility of a Small Modular Reactor (SMR) dedicated to producing tritium. The purpose of this project was to design a tritium producing SMR using the NuScale Modular Reactor Design. If proven viable, NuScale and PNNL could collaborate on creating a dedicated SMR facility to produce the tritium necessary for the nuclear weapons stockpile. This would provide PNNL with

a viable option for producing tritium toward the end of the Watts Bar Facilities lifetime or in the event of an incident that precludes the production of tritium.[1]

3. OBJECTIVES - ALL

The purpose of this project was to modify the NuScale SMR design to produce tritium through the use of TPBAR's. The final model of the reactor core was designed to accurately produce the as much tritium as possible without exceeding tritium production limits in a single TPBAR. The final reactor design was analyzed using both neutronic and thermal hydraulic methods. The final design was also verified to satisfy safety and environmental requirements designated by the Nuclear Regulatory Commission (NRC).

4. APPROACH AND ANALYSIS - ALL

4.1 NEUTRONIC ANALYSIS - Daniel Clark

4.1.1 NuScale Core Overview

The core configuration of the NuScale SMR consists of 37 assemblies surrounded with reflectors on all sides. Sixteen of the 37 assemblies contain a control rod cluster. These 16 control rod assemblies are divided into two groups; a regulating group and a shutdown group. The regulating group consists of four assemblies, all of which are symmetrically located in the center of the core. The control rod clusters in this regulating group are used during normal plant operation to flatten the overall neutron flux pattern and control power. The remaining 12 assemblies comprise the shutdown group. The group is used during core shutdown and scram events. Each control rod cluster is comprised of 24 standard boron carbide control rods. A visual representation of the core assembly map can be seen in Figure 1.

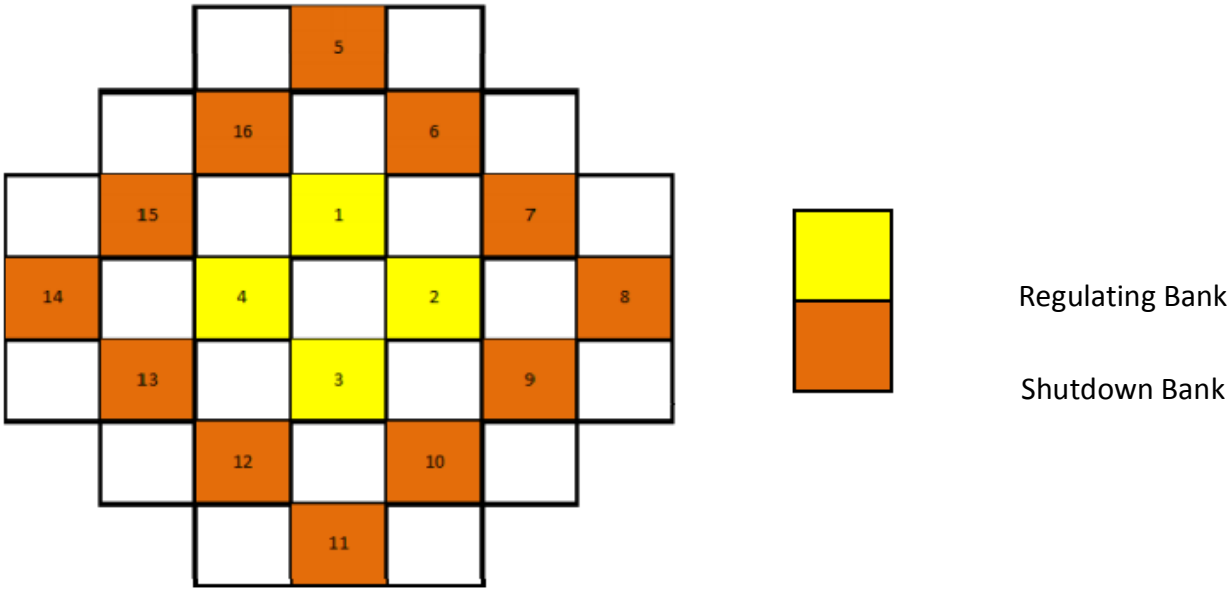

FIGURE 1. Core assembly map showing position of control rod clusters.[2]

Each fuel assembly is a standard 17x17 PWR fuel assembly with 24 guide tube locations, used for control rods and burnable absorber rods, and a central instrument tube. The assemblies are nominally half the height of standard PWR fuel assemblies (approximately 72 inches) and each contains five spacer grids. The fuel is standard uranium oxide fuel with zirconium alloy cladding. The U-235 enrichment is limited to the U.S. manufacturer limit of 4.95 percent. A list of baseline fuel design parameters is presented in Table I.

TABLE I. Reactor core and fuel parameters.[2]

Core Parameters	Dimensions
Fuel Pins (Standard 17 x 17 PWR Enriched UO_2 Fuel with Zircaloy Cladding)	
Rod outside diameter	0.374 inches
Pellet outside diameter	0.322 inches
Clad thickness	0.0224 inches
Active height	1/2 standard height
Fuel Assembly (17x 17 Square Array)	
Assembly pitch	8.466 inches
Pin pitch	0.496 inches
Control Rods (B_4C Absorber)	
Absorber material diameter	0.339 inches
Control rod outside diameter	0.378 inches
Control rod length	1/2 standard height

The NuScale SMR operates at 160 MWth, or equivalently to 51.13 kW/liter. From the NuScale information provided, the primary coolant loop was found to operate at a pressure of 1850 psig. From this information, it was also estimated that the average coolant temperature and average fuel temperatures were approximately 580 K and 890 K respectively. The mass fluent rate was determined to be approximately 106.9 kg/cm^2 hour. These values were used for the initial neutronics analysis, but more exact values were obtained during the core integration process.

4.1.2 Tritium-Producing Burnable Absorber Rods Overview

Tritium-producing burnable absorber rods, or TPBARs, are designed to produce tritium when irradiated in a pressurized water reactor. TPBARs are similar in size and nuclear characteristics to standard, commercial PWR burnable absorber rods. The exterior of the TPBAR is a standard stainless-steel tube while the internal components have been designed and selected to produce and retain tritium during irradiation. A standard TPBAR is approximately 152 inches from tip to tip, and the nominal outer diameter is 0.381 inches. Figure 2 illustrates the concentric, cylindrical, internal components of a TPBAR.

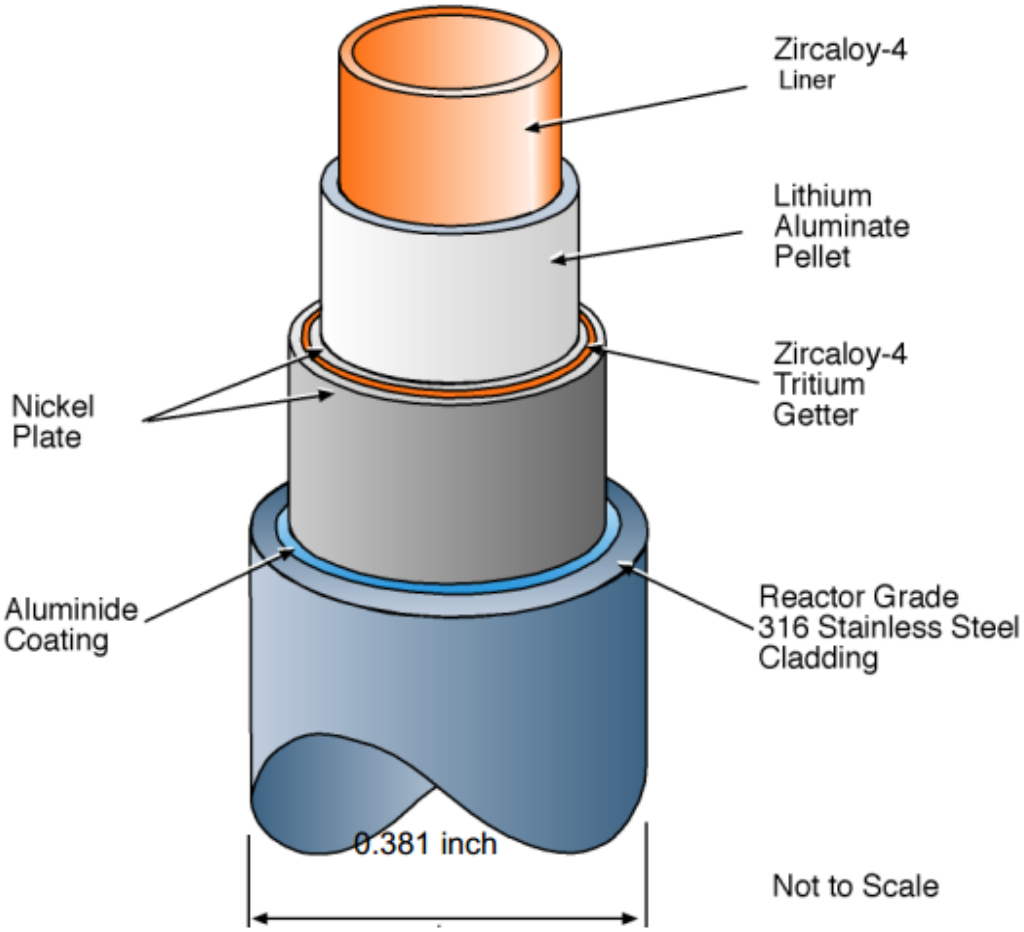

FIGURE 2. Cylindrical cross-section of a TPBAR.[4]

The metal getter tube within the stainless-steel cladding encircles a stack of ceramic lithium aluminate pellets that are enriched with the lithium-6 isotope. This lithium isotope, when irradiated in a PWR, absorbs neutrons, simulating a burnable absorber, and produces the hydrogen isotope tritium. The tritium produced in the lithium aluminate pellets then chemically reacts with the metal getter, capturing the tritium as a metal hydride. For neutronic accuracy, the lithium absorber pellet in the TPBARs is modeled explicitly while all other internal structures have been homogenized into the "cladding" region. Table II provides dimensions of the pellet and homogenized cladding as well as the material number densities of the "cladding" region. The amount of lithium-6 in the TPBARs ranges from 0.04125 to 0.02675 grams per inch.

TABLE II. TPBAR dimensions and homogenized cladding materials.[5]

Homogenized Cladding Material Dimensions	
	Mark 9.2 and Mark 10 Design
Homogenized Cladding OD (in)	0.381
Homogenized Cladding Inner Diameter (ID) (in)	0.302
Pellet OD (in)	0.302
Pellet ID (in)	0.223
Homogenized Cladding Material Number Densities	
	Mark 9.2 and Mark 10 Design
Cr (Atoms/b-cm)	8.2004E-03
Fe (Atoms/b-cm)	2.8330E-02
Ni (Atoms/b-cm)	2.7095E-02
Mo (Atoms/b-cm)	6.3490E-04
Mn (Atoms/b-cm)	6.6525E-04
Zr (Atoms/b-cm)	9.7431E-03

The active absorber region for a traditional TPBAR is 132 inches. However, the NuScale SMR is half height when compared to the standard PWRs for which the TPBARs were originally designed. For use in this project, the active absorber height of the TPBARs is the same as that of the fuel elements, namely 72 inches. When loaded into an assembly, the TPBARs are inserted in

guide-tube positions, and cannot be used in control rod banks. Between four and 24 TPBARs are permitted per assembly. For this project, all TPBAR assemblies contain 24 TPBARs and have the loading scheme shown in Figure 3.

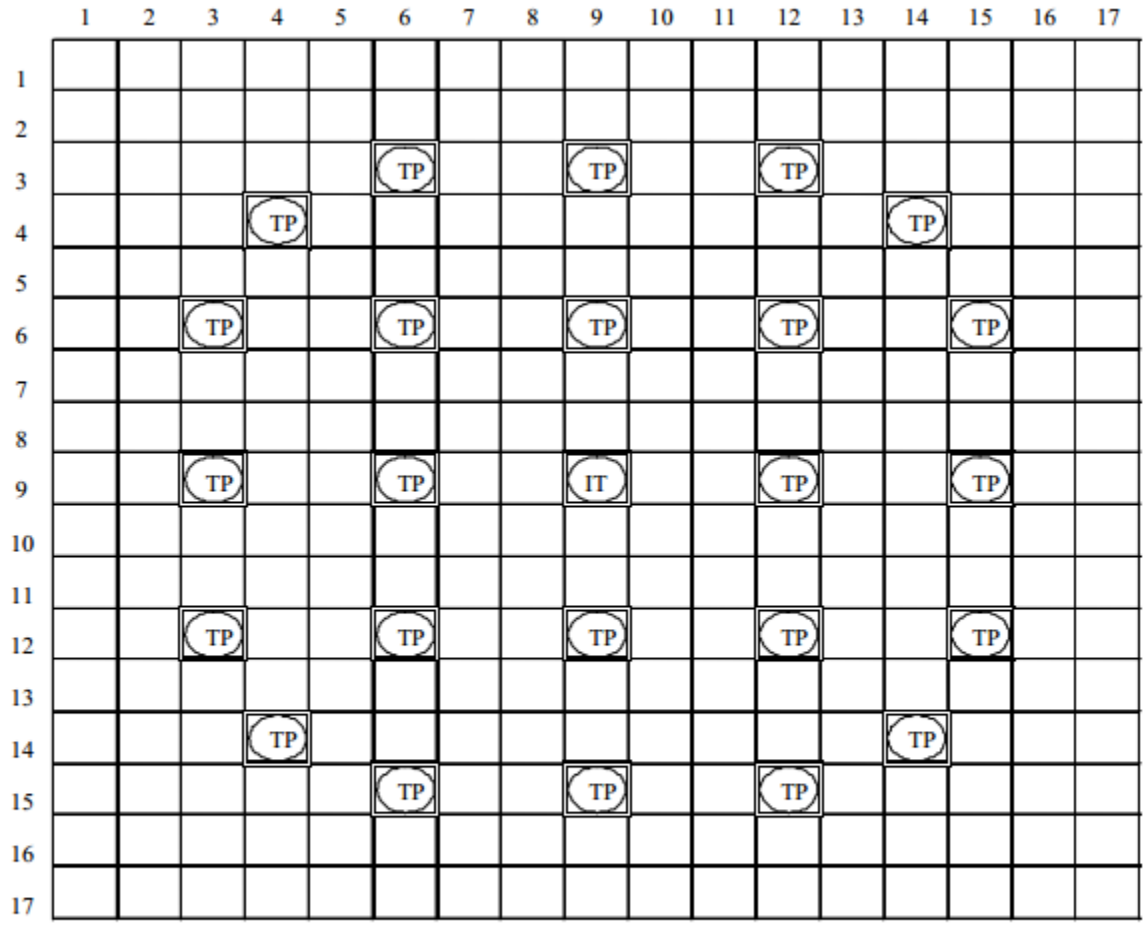

#	Naming convention
IT	Instrument Tube (Assembly center)
TP	TPBARs

FIGURE 3. 24 TPBAR loading pattern.[4]

In order to meet design limitations on rod internal pressure and burn-up of the lithium pellets, the maximum amount of tritium that can be produced in a TPBAR in a typical PWR is limited to 1.2 grams over the full design life of the rod (approximately 600 equivalent full-power days). However, due to the decrease in active absorber region in the NuScale SMR, the maximum

amount of tritium that can be produced was estimated to be approximately 0.65 grams. This being said, it is a long and complex process to determine the actual maximum amount of tritium that can be produced in a single TPBAR, and is beyond the scope of this project. A full analysis by Pacific Northwest National Laboratories is required to determine the actual maximum amount of tritium that could be produced in a single, half-height TPBAR.

4.1.3 Design Overview

As previously stated, the purpose of this design project was to adapt the NuScale Small Modular Reactor (SMR) to producing tritium. In terms of neutronics, the goal was to design a reactor core that ran at a constant power level for an appropriate amount of time in order to provide a certain neutron exposure to the TPBARs. In designing the core, there were three major objectives: achieve an acceptable cycle length, keep fuel enrichment below 4.95 percent, and keep the amount of tritium produced per TPBAR below the upper limit. In order to keep true to the NuScale design, as well as for simplicities sake, most parameters and core features were left unaltered. This encompasses the reactor core and fuel parameters as well as the thermal output and primary coolant parameter. The core features that were incorporated into the design process are the core map and the placement of TPBARs. The programs used to complete the neutronic analysis were DRAGON and CASMO4 (along with cms.link and Simulate3). The code functions and uses, as well as the design features, are discussed in detail in the following sections.

4.1.4 CASMO4 and DRAGON

CASMO4 is a multi-group, two-dimensional transport theory code that incorporates burn-up, and is commonly used for neutronics analysis in the nuclear field. In combination with cms.link and Simulate3, CASMO4 can be used to perform an accurate three-dimensional analysis of the nuclear core region. CASMO4 was chosen as the program to analyze the core because of its simplicity and the students' previous knowledge and experience with the program. However, due to strict licensing, the only version of CASMO4 available for use was the student version, which does not have access to the full isotope data library. Because of this limited access, two isotopes needed to model the TPBARs, lithium-6 and lithium-7, were not available for use. Only natural lithium was available, which has a fixed weight percentage of lithium-6 and lithium-7 (07.5% and 92.5% respectively); whereas the lithium aluminate in absorber is enriched in lithium-6. Two alternative methods were devised to accurately simulate the TPBARs in CASMO4, and will be discussed in the following section. In order to determine accuracy of these methods, DRAGON was used. Dragon is a neutronic analysis code similar to CASMO4, but with a few key differences. DRAGON is an open source code, so using it allows access to the full isotope data libraries; however, this freedom comes at a price. Because it is open source, it is less streamlined and has a more complicated input, thus it has a much higher learning curve. And while it is possible to model entire cores through the use of DRAGON, it was beyond the students' breadth of knowledge and expertise. For this reason, DRAGON was only used to analyze a TPBAR assembly and determine the best method for which to proceed in CASMO4.

4.1.5 TPBAR Modeling

Knowing there was an upper limit to the amount of tritium that could be produced in each TPBAR, the lowest linear density for the amount of lithium-6 per bar was chosen (0.02675 grams/inch) when first modeling the TPBARs. Using the known bar dimensions, lithium aluminate density, and molar masses, the lithium-6 enrichment for this linear density was found to correspond to approximately 18.7 percent. However, only natural lithium was available for use in CASMO4, which as previously stated corresponds to approximately 7.5 percent lithium-6. Therefore, in order to correctly model the TPBARs, a method for simulating enriched lithium was needed. Two such methods were developed. The first method involved using natural lithium to account for the correct amount of the lithium-7 isotope, which lead to an inadequate amount of lithium-6. Boron-10 was then used to account for the remainder of lithium-6. Boron-10 was chosen because it is one of the most common burnable poisons and thus was available in CASMO4. Not only that, but boron-10 and lithium-6 have similar microscopic absorption cross sections. By plotting these absorption cross sections and matching the area under the curve, a correction factor of 0.07695 was found and then used to match the macroscopic cross sections. A plot of the microscopic cross sections can be seen in Figure 4.

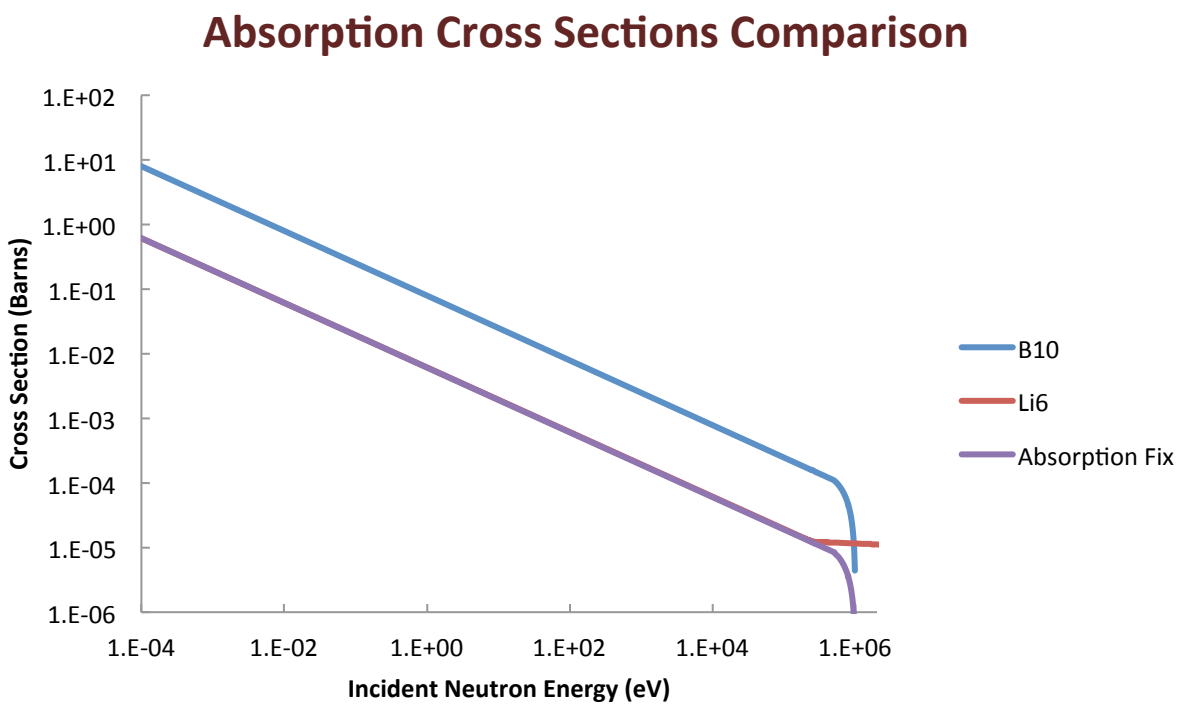

FIGURE 4. Comparison of lithium-6 and boron-10 neutron absorption cross sections.

By equating the macroscopic absorption cross sections, a TPBAR was created using natural lithium and boron-10 so that it correctly simulated the neutron absorption of an actual TPBAR. However, because the fix was determined for the absorption cross sections, the total cross sections did not match. Figure 5 depicts the total cross section comparison.

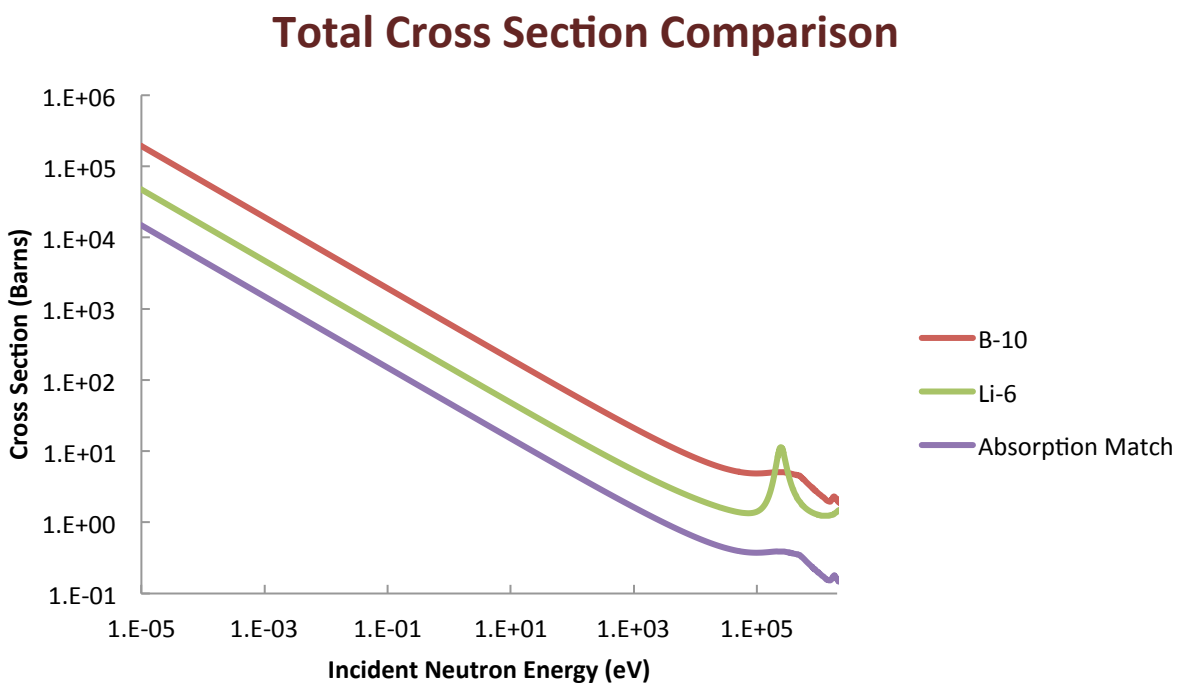

FIGURE 5. Comparison of lithium-6 and boron-10 total neutron cross sections.

This lead to a total neutron cross section that was approximately a third of what it should be. Another problem associated with this method is the fact that boron-10 has a different decay chain than lithium-6, and thus does not take into account the buildup of helium-3, a poison prevalent in the lithium-6 neutron absorption decay chain. For these reasons, this method was considered a plausible solution, but needed further examining. The second method developed to simulate an actual TPBAR uses natural lithium to meet the needed mass of lithium-6 per bar, while ignoring the lithium-7 mass. However, because natural lithium's enrichment is so low, an abundant amount was needed to meet the lithium-6 mass requirements. This lead to a vast excess of lithium-7, nearly three times the amount that would be in an actual TPBAR. This was seen as a possible problem, but because of lithium-7's low absorption cross section, and because lithium-6 is more important neutronically, it was deemed a feasible model. Both of these alternative ways of simulating TPBARs were then modeled in CASMO4 in a 17x17 assembly with 3.8 percent

fuel enrichment, containing 24 TPBARs. Tables of all TPBAR compositions can be seen in the appendix.

4.1.6 DRAGON Comparison

Using DRAGON, an actual 17x17 TPBAR assembly with 3.8 percent fuel enrichment and 24, 18.7 percent lithium-6 enriched TPBARs was modeled. The k-infinite of this assembly was then compared to the k-infinite of two CASMO4 assemblies over a burn-up of 60 MWd/t. The results can be seen in Figure 6.

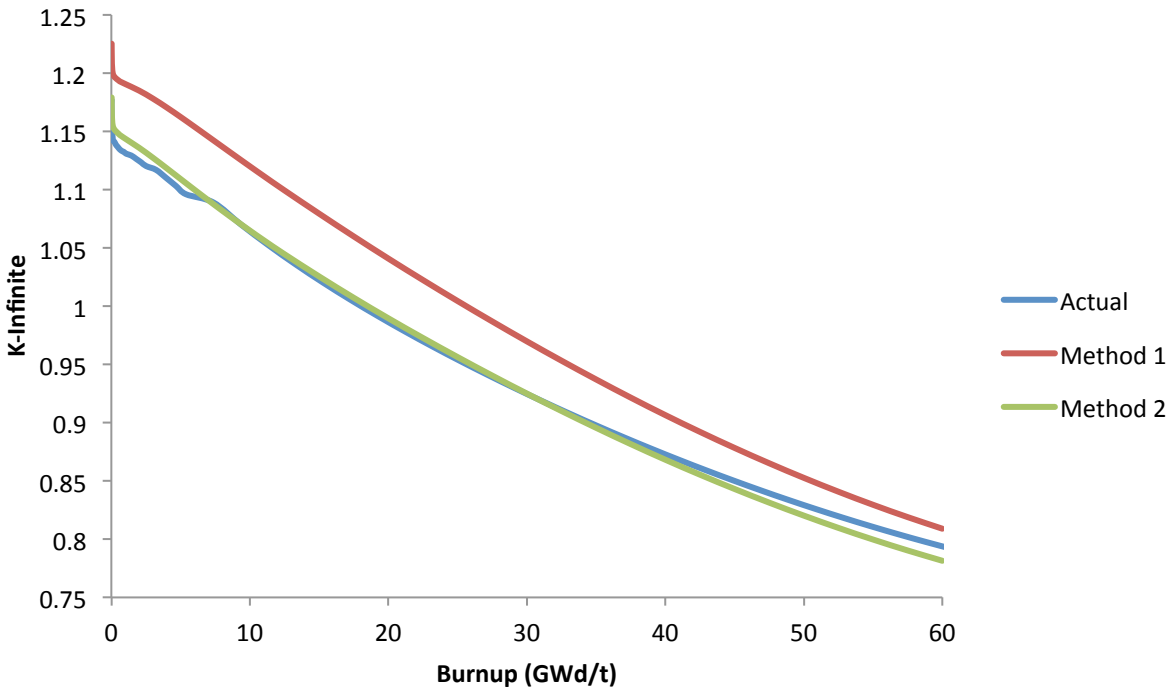

FIGURE 6. Comparison of k-infinites for TPBAR simulation methods and actual assembly.

From Figure 6, it can be seen that the second simulation method very closely mimics an actual TPBAR assembly. For this reason, method two was chosen when modeling the TPBAR assemblies is CASM04. A comparison of depletion rates for important isotopes for all three methods can be seen in Figure 26 in the appendix.

4.1.7 Core Map Design

Because no core map was provided by NuScale Power, LLC, a large portion of the neutronics design section revolved around generating a functioning core map. Based off Dr. Ragusa's notes, a generalized core map was developed and analyzed using different fuel enrichments. This core map can be seen in Figure 7.

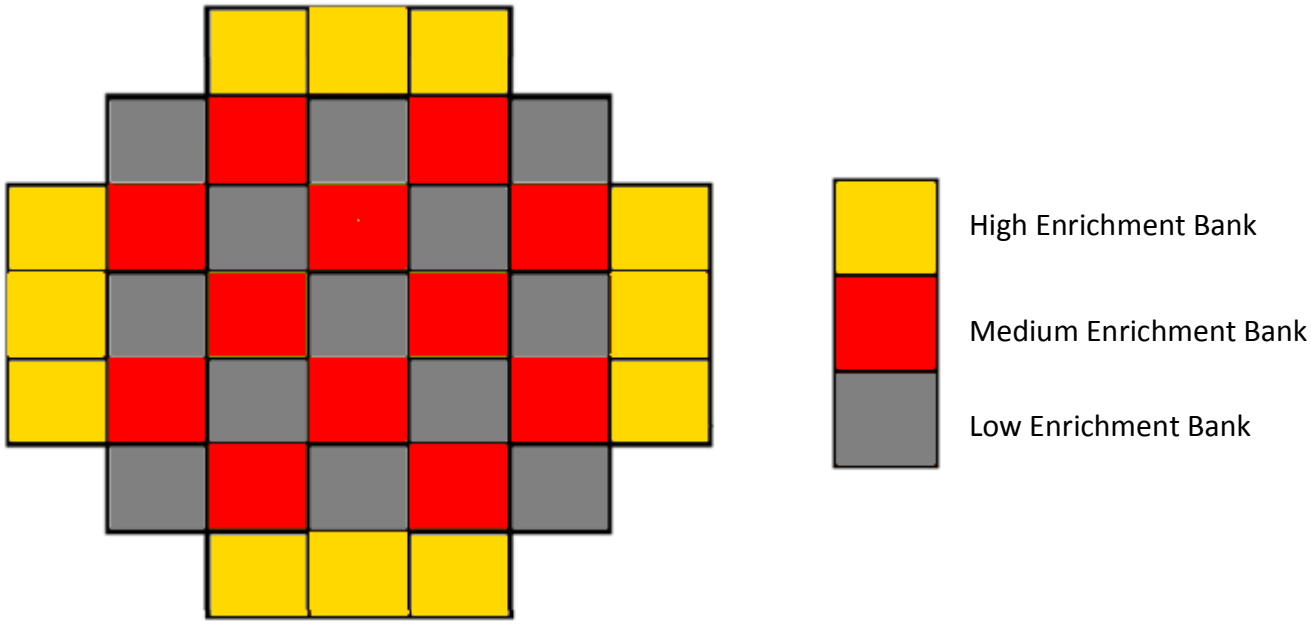

FIGURE 7. General NuScale core map.

When choosing fuel enrichments, two parameters had to be met; the core must be able to operate at 160 MWth for between 18 and 24 months and the maximum relative power fraction of a single assembly must remain below 2.0. Using the thermal power output and mass of heavy metal in the core, it was possible to convert months into burn-up (GWd/t). The results of this calculation showed that the average burn-up required to meet this cycle length was between approximately 10 and 14 GWd/t. In order to account for the addition of neutron poison that would be added with the addition of TPBARs, the target burn-up for this TPBAR free core model was set at 18 GWd/t. Using Simulate3, the three enrichments that were found to meet the these criteria were

3.3 percent, 3.8 percent, and 4.5 percent. Analyzing the output yielded the maximum burn-up for this core mapping scheme to be 18.371 GWd/t, and the maximum relative power fraction of a single assembly to be 1.622. Although a somewhat simplified one, this core map met both of the parameters above, and was used for the remainder of the analysis.

4.1.8 TPBAR Placement and Tritium Production

Using the second method mentioned for simulating TPBARs in CASMO4, Simulate3 was then used to test different TPBAR assembly placements in the core. Due to control rods, a number of the assemblies were unable to have TPBARs. A map of all possible placement slots can be seen in Figure 8.

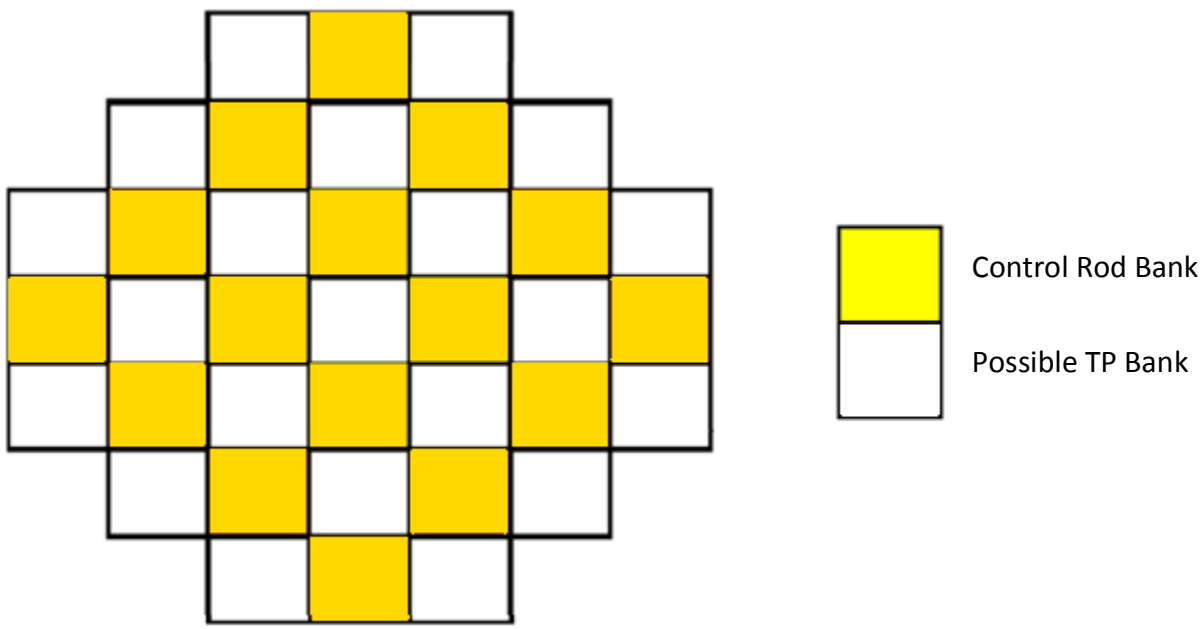

FIGURE 8. Position of empty banks applicable for TPBAR placement.

When analyzing the possible TPBAR assembly positions, the most important constraint was to ensure that the average amount of tritium produced per bar in an assembly does not exceed the maximum allowable amount of tritium production. As previously stated, the maximum amount

of tritium that can be produced per TPBAR in the NuScale reactor is approximately 0.65 grams over the full design life of the rods (approximately 600 equivalent full-power days). When calculating the amount of tritium produced in each assembly with TPBARs, it was assumed that all lithium-6 neutron absorption produced a tritium atom. In order to calculate this, the average two-group neutron flux of each assembly at each burn-up step was output by the Simulate3 model. Equation 1 shows the relation between thermal neutron flux and lithium-6 burn-up for each time step.

$$A_{n+1} = A_n \emptyset_{th} \sigma_A \Delta t \qquad (1)$$

Where $A_{n+1}$is the number of lithium-6 atoms at the beginning of the next time step, A_n is the number of lithium-6 atoms at the current, $\emptyset_{th}$ is the thermal neutron flux, σ_A is the neutron absorption cross section of lithium-6, and Δt is the change in time. Using Equation 1 and the thermal neutron flux, the amount of lithium-6 atoms used for each burn-up step was calculated. By summing the lithium used over the previous steps, it was possible to determine the remaining amount of lithium-6 atoms after each step, and thus relate the total core burn-up to the amount of lithium-6 atom burn-up in the TPBARs. Using Equation 2, the number of lithium-6 atoms burned was then related to the mass of tritium produced.

$$m_{H3} = M_{H3} \frac{A_{Li6}}{N_A} \qquad (2)$$

Where m_{H3} is the mass of tritium produced, M_{H3} is the molar mass of tritium, A_{Li6} is the number of lithium-6 atoms burned, and N_A is Avogadro's Number. Using these relations and the neutron fluxes provided by Simulate3, it was possible to determine how much tritium was being produced per TPBAR in each assembly. In order to determine which assemblies were viable TPBAR positions, a Simulate3 model was run with the lowest lithium-6 concentration TPBARs placed in all available assemblies. From this model, it was determined that all possible interior

assemblies exceeded the maximum amount of tritium production for all acceptable cycle lengths. For this reason, they were disqualified as possible TPBAR placement slots. This left only the exterior assemblies as possible TPBAR placement slots. Using the above relations and a Simulate3 model with the lowest lithium-6 concentration TPBARs placed only in the external assemblies, the maximum amount of tritium production in an assembly was determined to be 0.43 grams per bar. This maximum, which does not exceed the upper limit, validated the external assemblies as acceptable TPBAR placements slots. In order to optimize the core and produce as much tritium as possible without exceeding the limit, the amount of lithium-6 in each TPBAR was incrementally increased until the maximum amount of tritium produced was just below the limit. This point was reached at the maximum allowable amount of lithium-6 per TPBAR, 0.04125 grams per inch. With this loading, the maximum amount of tritium produced per bar in an assembly was 0.64 grams over an 18 month cycle, just below the design maximum of 0.65 grams. This configuration had a maximum achievable burn-up of 15.205 GWd/t and a maximum relative power fraction of 1.840, both of which satisfy the criteria previously stated and validated this as the optimal TPBAR loading scheme.

4.2 Thermal Hydraulic Analysis - Thomas Moore

4.2.1 Overview

The goal of the thermal hydraulics portion of this project was to design a NuScale style SMR for the production of tritium through the use of tritium producing burnable absorber rods. As was stated in the neutronics portion of this project, the aim to resemble the NuScale reactor was desired for several reasons. By keeping the reactor similar to the NuScale reactor, less work would be required when licensing these tritium producing designated reactors. In addition, the

closer the designed model is to the NuScale reactor, the more efficiently it could be built and maintained by NuScale Power. The design of this reactor aims to provide PNNL with a reactor design that will efficiently produce tritium at the cheapest possible price with the maximum amount of safety. In reference to safety, the NuScale reactor was chosen for its passive safety features. The NuScale reactor has no pumps pushing water through the primary system. The design is based on natural convection of the coolant through the core. A major portion of the thermal hydraulics portion of this project is to assure that the core will remain at a safe temperature throughout normal operating conditions. To ensure this, the neutronics portion and the thermal hydraulics portion of this project will be optimizing on a mass flow rate that is suitable to both parts of this project. To model the mass flow rate through the reactor a thermal hydraulics code was used.

4.2.2 GOTHIC

The thermal hydraulic program GOTHIC was chosen to perform the aforementioned tasks. This specific program was chosen for many reasons. First, GOTHIC is also being used by NuScale to design their reactor. For this reason, the design team thought that it would be best to use this program so that comparisons could be made if the models were compared. Also, the team member performing the thermal hydraulics portion of this project was familiar with the program. This helped cut down on the time that would have been required to learn a new program. GOTHIC solves all the necessary conservation equations and has the ability to design the geometries present in the primary side of a nuclear reactor. GOTHIC also has the capability to model natural convection which is necessary when modeling a NuScale style SMR.

4.2.3 Model 1

One of the most daunting tasks when building a computer model of something as complex as the primary system of a nuclear reactor is making a layout of that is organized and well thought through. Having the correct volumes and the correct geometries is only the beginning. Next the subdivisions of the volumes must be decided. How will each physical volume be modeled in the computer program? How much detail is required in each volume? How will each volume be connected to each other? These are only some of the questions that needed to be faced before modeling can actually begin. After many brainstorming sessions aiming to answer these questions and many more, an initial model was created. This model consisted of two volumes; one for the reactor pressure vessel, and another for the active core region and riser. This model is shown in Figure 1.

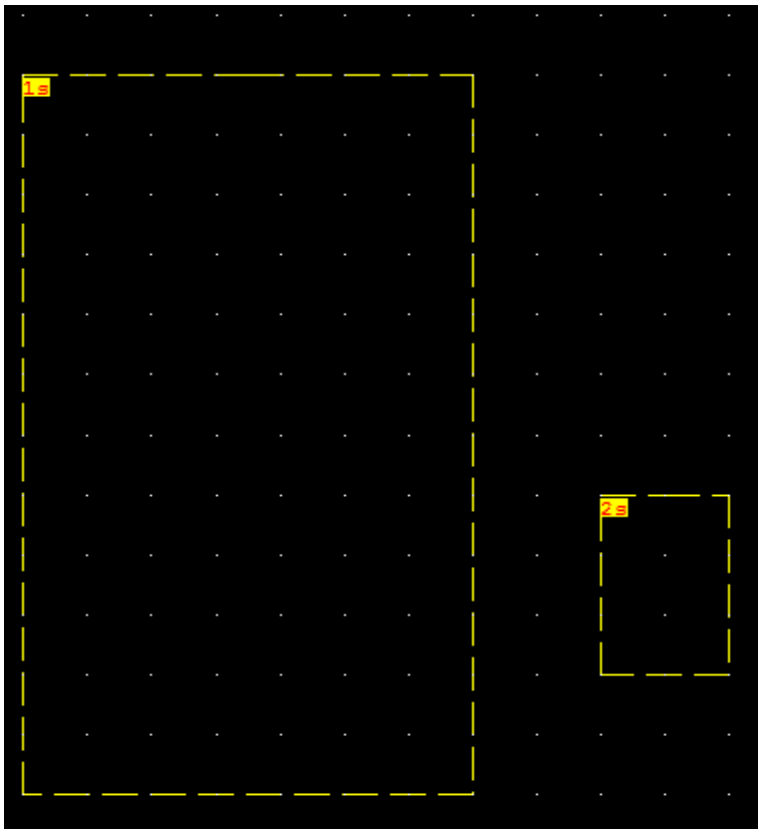

FIGURE 9. The first GOTHIC model created to perform the thermal hydraulic analysis.

This model has several issues that rendered it unused. First, modeling the reactor in this way does not allow for changes in subdivision. The upper and lower plenum would hold the same discretization of the riser and downcomer. Over discretization of the first volume (the volume that consists of the riser, upper plenum, lower plenum, and downcomer) would cause the model to run much slower than necessary. Another issue with this model is the possible transition of matter and energy through the baffle separating the downcomer and the riser. GOTHIC calculates blockages as a percentage porosity blockage. The only way to stop the transition of matter and energy is to fully block an entire group of cells in a vertical column. Since this was not possible geometrically, the model would not work.

4.2.4 Model 2

Once the first model was discarded, a new model was devised. A visual representation of this model is shown below in Figure 2.

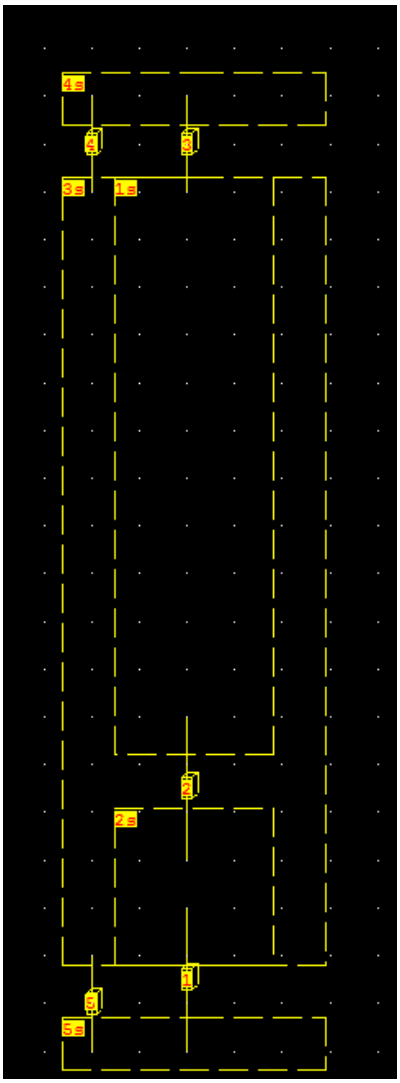

FIGURE 10. The second GOTHIC model created to perform the thermal hydraulic analysis.

The second GOTHIC model created to perform the thermal hydraulic analysis consists of many more volumes. This solved the problem of mass and energy being able to move from the riser to the downcomer in an unphysical way. Having more volumes also allowed the usage of different discretization in each volume. The active core region needed a specific discretization to match that of a fuel assembly while the riser needed only a very coarse mesh. One problem still remained however. When using three dimensional connectors in GOTHIC the grid lines in each

cell must match up. To better describe this issue reference Figure 3 taken from the GOTHIC user manual.

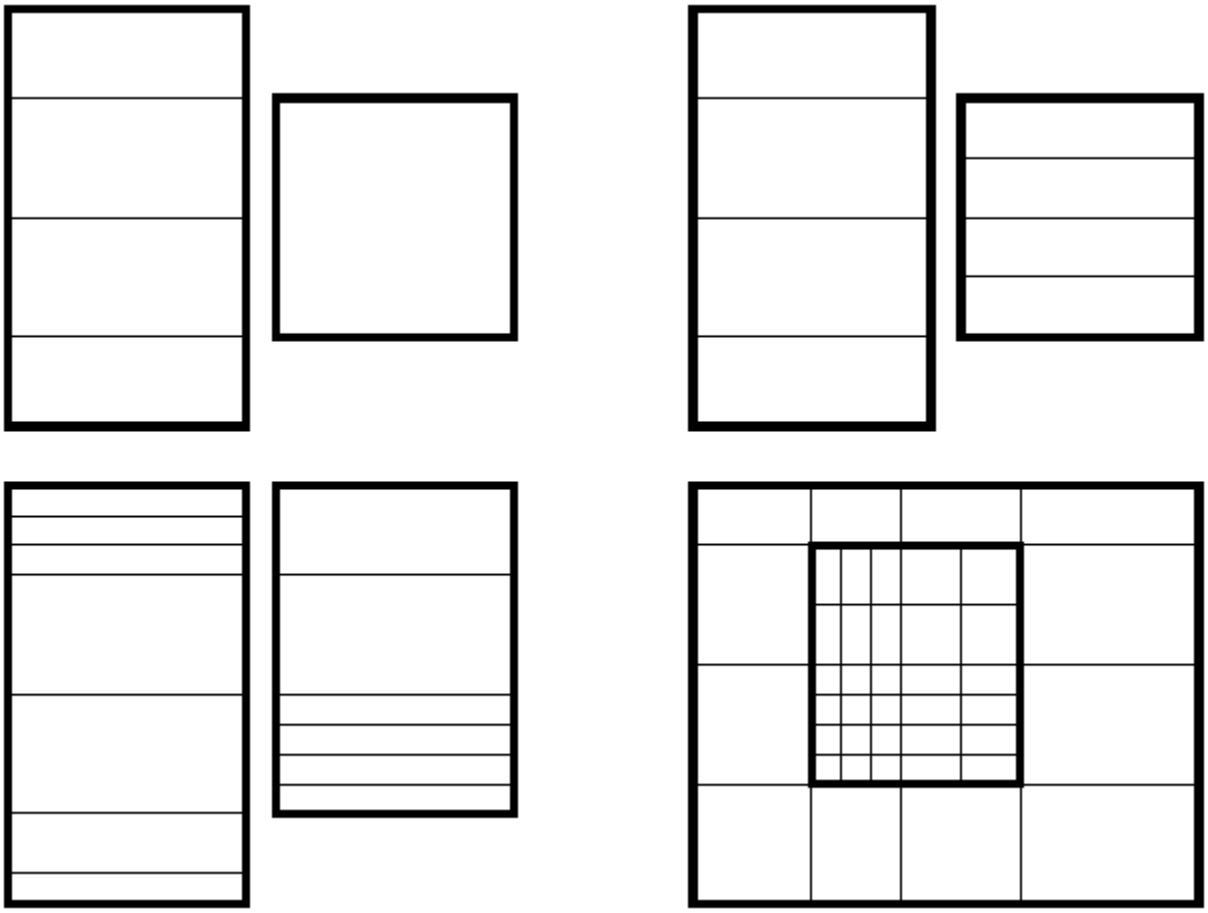

FIGURE 11. Examples of acceptable flow connecter grids.[6]

Notice that a model may have finer grid lines in between the corresponding grid lines, but the coarse grid lines must be scaled to the finer grid lines. The reference used to model this reactor was sent to the group from NuScale. Figure 4 shows the dimensions of the reactor pressure vessel as well as the baffle and barrel.

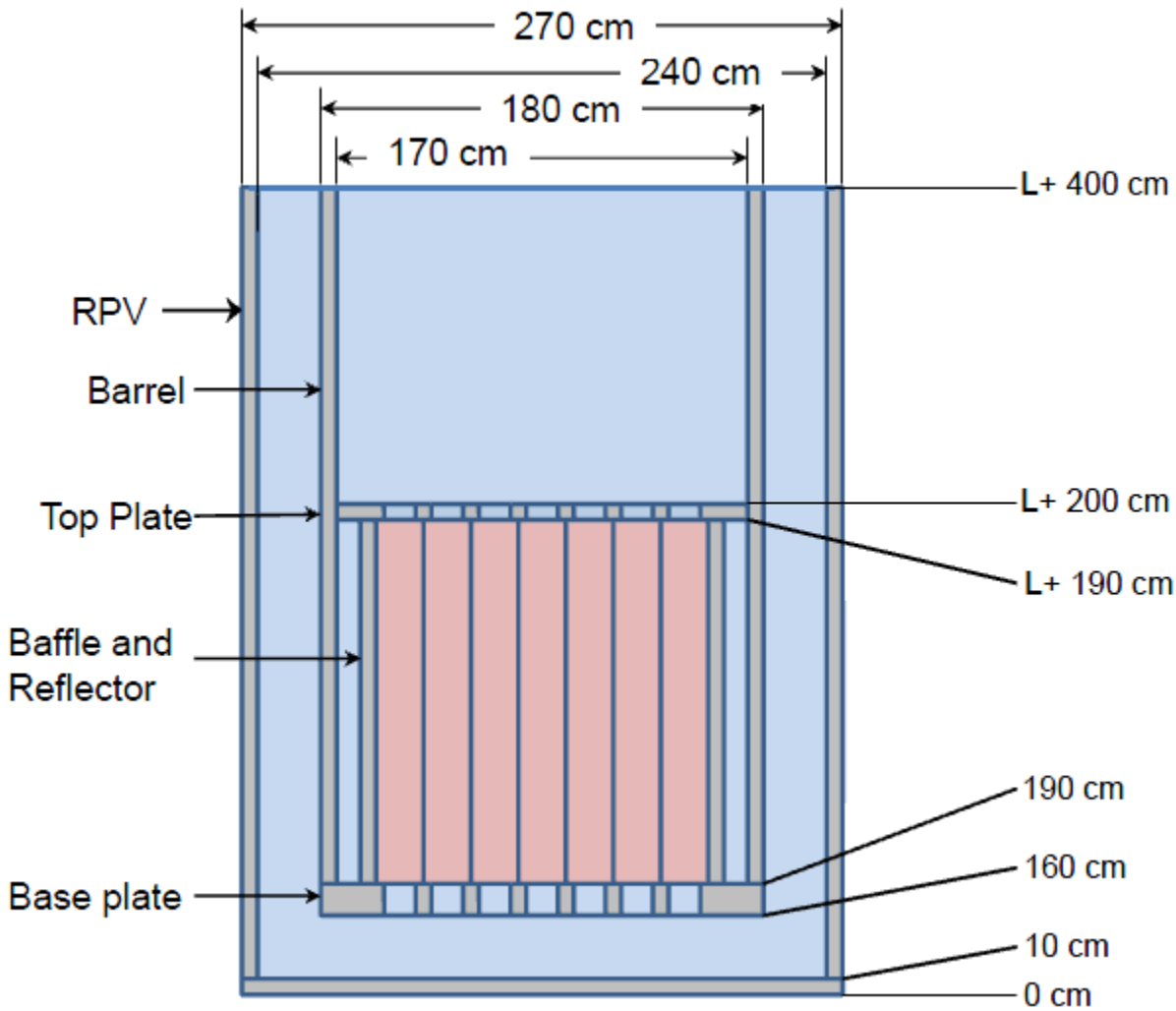

FIGURE 12. Reference model for the creation of GOTHIC model.[2]

The above dimensions were given to the group from NuScale. Due to the geometry, the downcomer volume had and outer radius of 240 cm but also had to have grid lines every 30 cm so that it would match up with active core region and riser. The active core region had grid lines every 20 cm so that it could match the assemblies. Due to this the lower plenum had to be discretized every 10 cm. This slowed down run time, but it did not reduce the quality of the model. With this said, the model was deemed physically sound. Once the volumes were created and subdivided, the next step was to input the blockages into the model. The first blockages made were to recreate the shape of the core to be cylindrical instead of rectangular. GOTHIC

inherently turns all three dimensional volumes into rectangles, so a simply cylindrical blockage was create for all the volumes. Next, the downcomer needed an interior cylindrical blockage where the riser and active core region would be. A top and front view of the downcomer is shown in Figure 5 as an example to what the blockages look like.

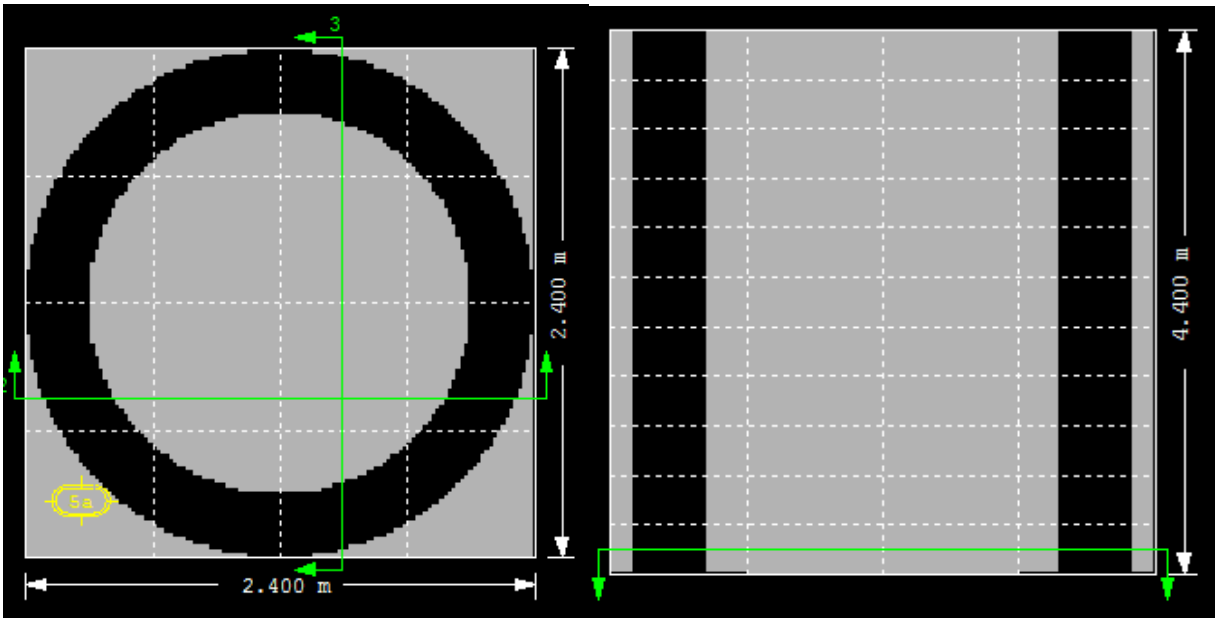

FIGURE 13. The downcomer top and front views, from left to right.

The next step in creating this model was to input the fuel assemblies through the use of thermal conductors. The data to input the thermal conductors was taken from the neutronics portion of the project. The thermal output of the core from neutronics is 160 MW, with an average water temperature of 310℃, a pressure of 12856.653 kPa, and a fuel temperature of 620 ℃. The data for the fuel pins and assemblies was taken from Table I. With this data the surface area per fuel assembly was calculated. To do this the rod outside diameter was used to calculate the surface area of a single fuel pin. This surface area was then multiplied by the number of fuel pins per assembly to calculate the correct amount of heat transfer to the coolant. The next step was to calculate the internal heat rate of the fuel rod. This was done by using the total thermal output of the core and dividing it by the volume of the fuel pins the fuel assembly. With the geometry,

initial conditions, and thermal components all set the model was ready to run. The first run yielded inconclusive results. Instead of creating natural convection, the flow of the coolant throughout the core was oscillating. From this problem a test model was created.

4.2.5 Model 3

This model simplified the model from a full reactor to a core region with boundary conditions representing the rest of the reactor. Not only does creating a simplified model yield quicker results, it also allows an easier path to pinpointing the problem at hand. An image of the test setup is shown below in Figure 7.

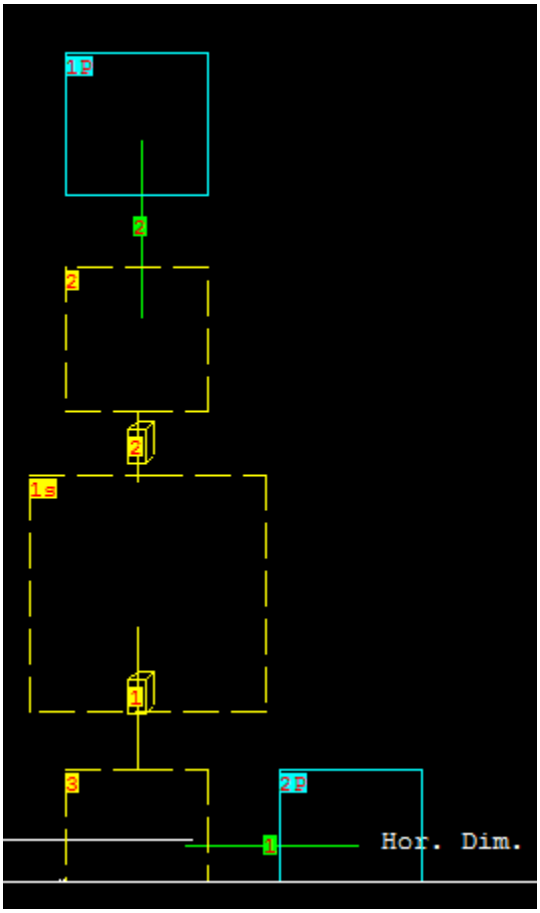

Figure 14. Test model used to determine issues with main GOTHIC model.

Volume 1S is the active core region where volume 2 and 3 are the riser and lower plenum respectively. Notice that boundary condition 2P is horizontal from volume 3. When using flow paths the user is required to input elevations of both ends of the flow path. Even though the model appears to be horizontal, the code describing the relationship between volume 3 and boundary condition 2P is that volume 3 is vertically above boundary condition 2P.

From this test analysis, it was determined that the thermal conductor input was incorrect. Instead of providing a constant heat flux throughout the run, it was only providing heat for a short period of time. Another issue was that the coolant was not interacting with the fuel rods. After much time and effort working on this test analysis the issue was found to be incorrect inputs for the thermal conductors. Instead of allowing for heat transfer to occur on the outside of the rods, the entire fuel rod was being viewed as a thermal boundary condition. After this fix, heat transfer between the fuel and the coolant began to occur in the core.

The next step was to have the fuel elements be properly modeled by the thermal conductors. To model this, the thermal conductors were split into two regions, one for the fuel and one for the cladding. The fuel had volumetric heat generation while the cladding only interacted with the fuel and the coolant. After the test model was run and natural convection was modeled, the thermal conductors were returned to the full model. Figure 8 shows the natural circulation occurring in the center of the core.

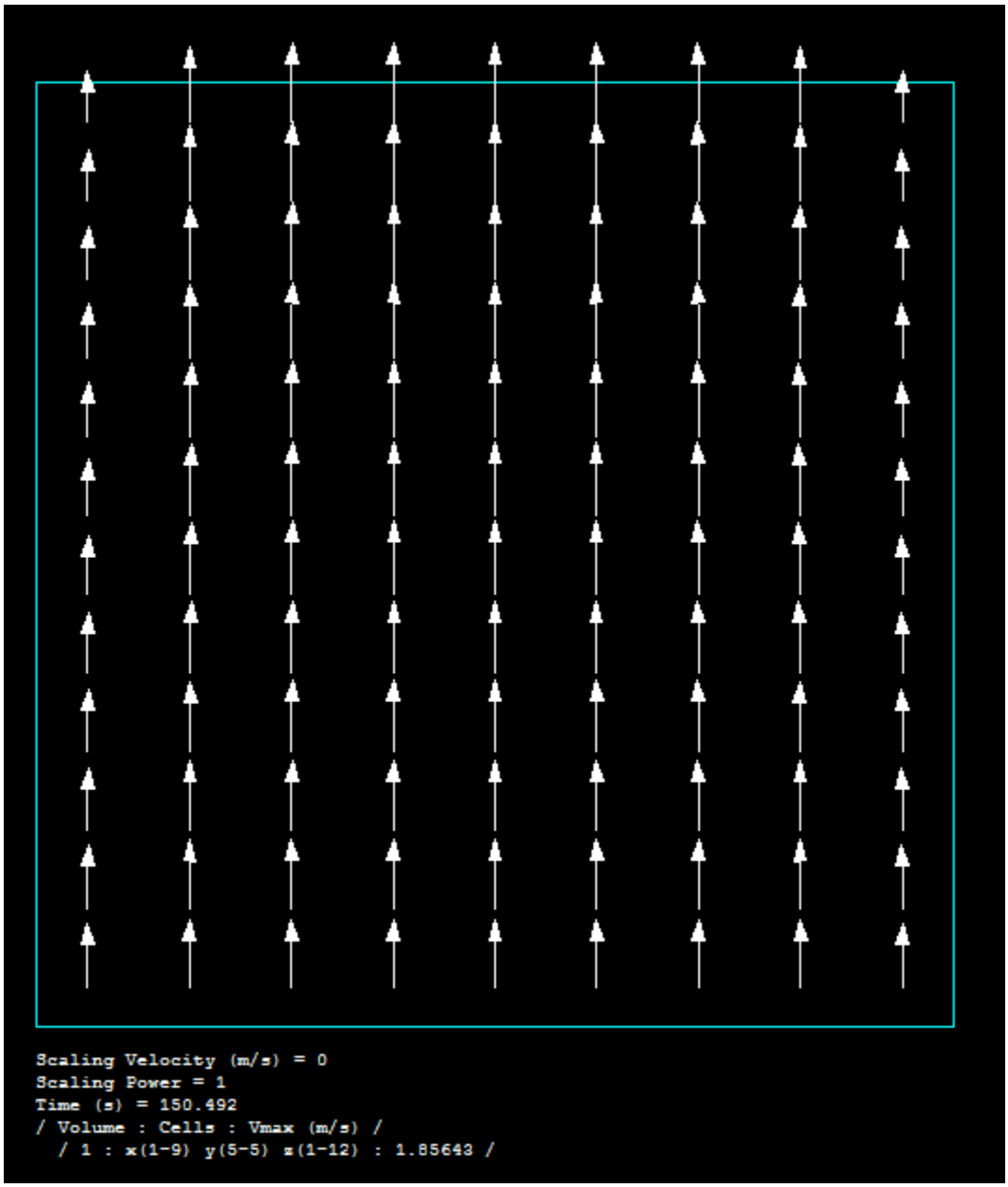

Figure 15. Natural convection is shown occurring in the center of the active core region.

The arrows in the figure are located at the center location of each cell. Notice that the flow is uniform throughout the core except for at the edges. The edges have less coolant traveling through the cells due to the cylindrical blockage of the volume. Once the thermal conductors were working as expected, the inputs were transferred to the full model. The full model was then

run. The simulation ended early before the natural convection could come to a steady state. The preliminary results were analyzed and it was noticed that the pressure in the system was increasing drastically causing the simulation to crash. To fix this problem, a boundary condition was added to act as the reactors pressurizers to ensure that pressures would remain in plausible values. The model was then run once more and no errors occurred. The simulation was then analyzed for the mass flux for the core to be given over to the neutronics portion for project integration. The final model was proven to accurately portray natural convection throughout the reactor model.

4.3 Core Integration - Daniel Clark & Thomas Moore

4.3.1 Overview

Upon completion of the individual neutronics and thermal hydraulic analyses, an integration process was begun to determine accurate average coolant temperatures, average fuel temperatures, and average coolant mass flux. This integration was a necessary step in determining the natural circulation of the coolant, something on which this system heavily relies. To correctly account for the interdependence of neutronics and thermal hydraulics, a step iteration process was used. This iteration process was needed to ensure that the neutronics and thermal hydraulic models did infact agreed with one another, and proved that the models were functioning properly. The outcome of this integration process led to a fully functioning reactor primary system model that encompasses both the neutronics and thermal hydraulics analyses.

4.3.2 Iteration

Through a collaboration of the Simulate3 and GOTHIC models, a step iteration process was created that accurately calculated the average coolant temperature, average fuel temperature, and

average coolant mass flux. In this process, the initial average coolant and fuel temperatures were taken from the Simulate3 model and given to the GOTHIC model, which would then return new a average coolant mass flux. By re-running the Simulate3 model with this new coolant mass flux, new average coolant and fuel temperatures were obtained. This iteration process was run until the difference in both the average coolant and fuel temperature converged to less than one degree between time steps. The step iteration process can be seen in Table III.

TABLE III. Iteration of Simulate3 and GOTHIC models.

Average Coolant Flux (kg/cm^2 hour)	Average Coolant Temperature (C)	Average Fuel Temperature (C)
106.9	306.04	613.99
183.6	297.08	606.52
185.76	296.92	606.36

4.3.3 Iteration Results

After the completion of the final simulation of the reactor running at steady state the results were collected. In Table III the three rows each represent an iteration performed. An iteration consisted of running Simulate3 and collecting the results (average coolant and fuel temperature). These results were then put into the GOTHIC model so that the average coolant flux could be calculated. The average coolant and fuel temperatures drove the natural convection throughout the reactor. Another value that was analyzed is the mass flow rate throughout the core. This is vital in removing heat from the fuel rods. The final value to be analyzed is the temperature of the fuel during steady state operation. This value will then be compared with the melting temperature to provide a level of safety for the core.

Figure 9 below shows the inlet and outlet temperatures of the core. During the first 100 seconds of the simulation the thermal conductors were turned off. Over the next 100 seconds the thermal

conductors slowly get ramped until they are running at full power. The final 800 seconds show the reactor running under steady state conditions.

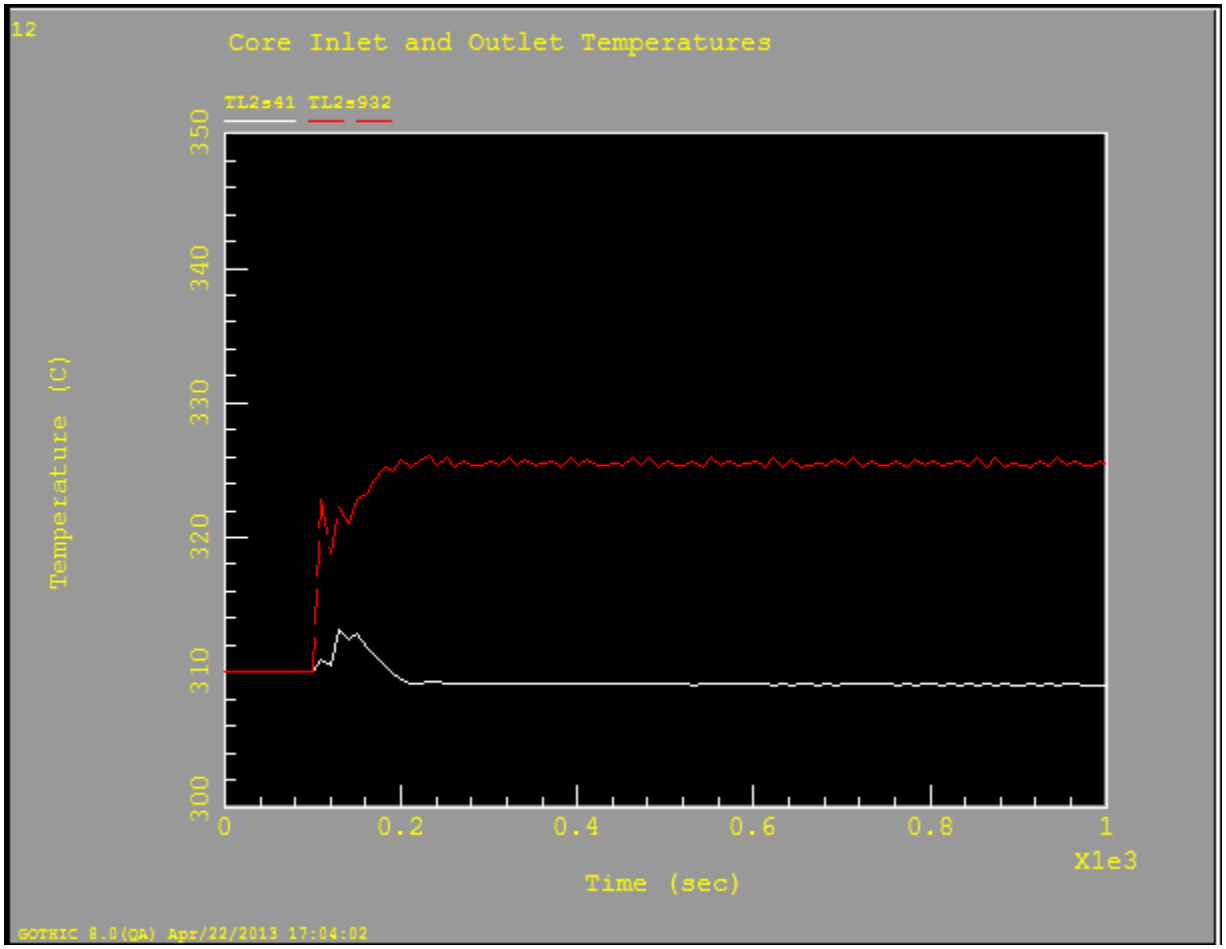

Figure 16. Inlet and outlet temperatures of the core are shown during steady state operation.

This temperature gradient is the cause of the natural convection in the core. Notice that once steady state is reached, the coolant temperatures very slightly throughout the entirety of the simulation. This analysis shows a level of uncertainty in this portion of the project to be on the order of 1 degree Celsius. This level uncertainty is carried over to the analysis of the mass flow rate shown in Figure 10.

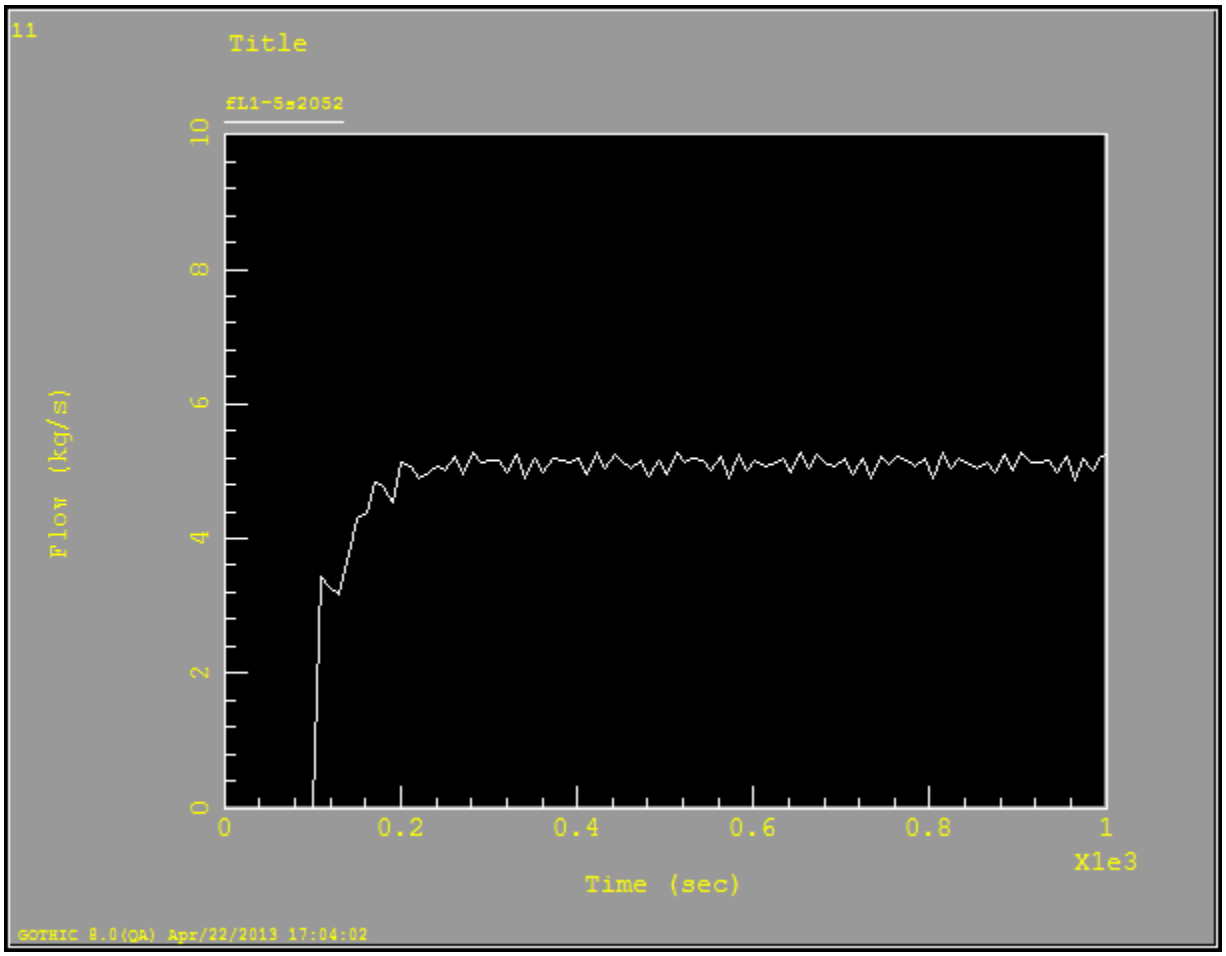

Figure 17. The mass flow through a single cell entering the core is shown.

The mass flow shown above is the mass flow rate through a single volume entering the core region. The units need only be changed for iteration with the neutronics portion of the project. The mass flow rate in this single volume corresponds to a mass flux through the entire core of 185.76 $\frac{kg}{cm^2 h}$. This mass flux is the final iterated mass flux between the thermal hydraulics portion of the project and neutronics portion.

The temperature of the fuel is one of the most important values to analyze when safety is concerned. The steady state fuel temperature on the outside of the core is shown in Figure 11.

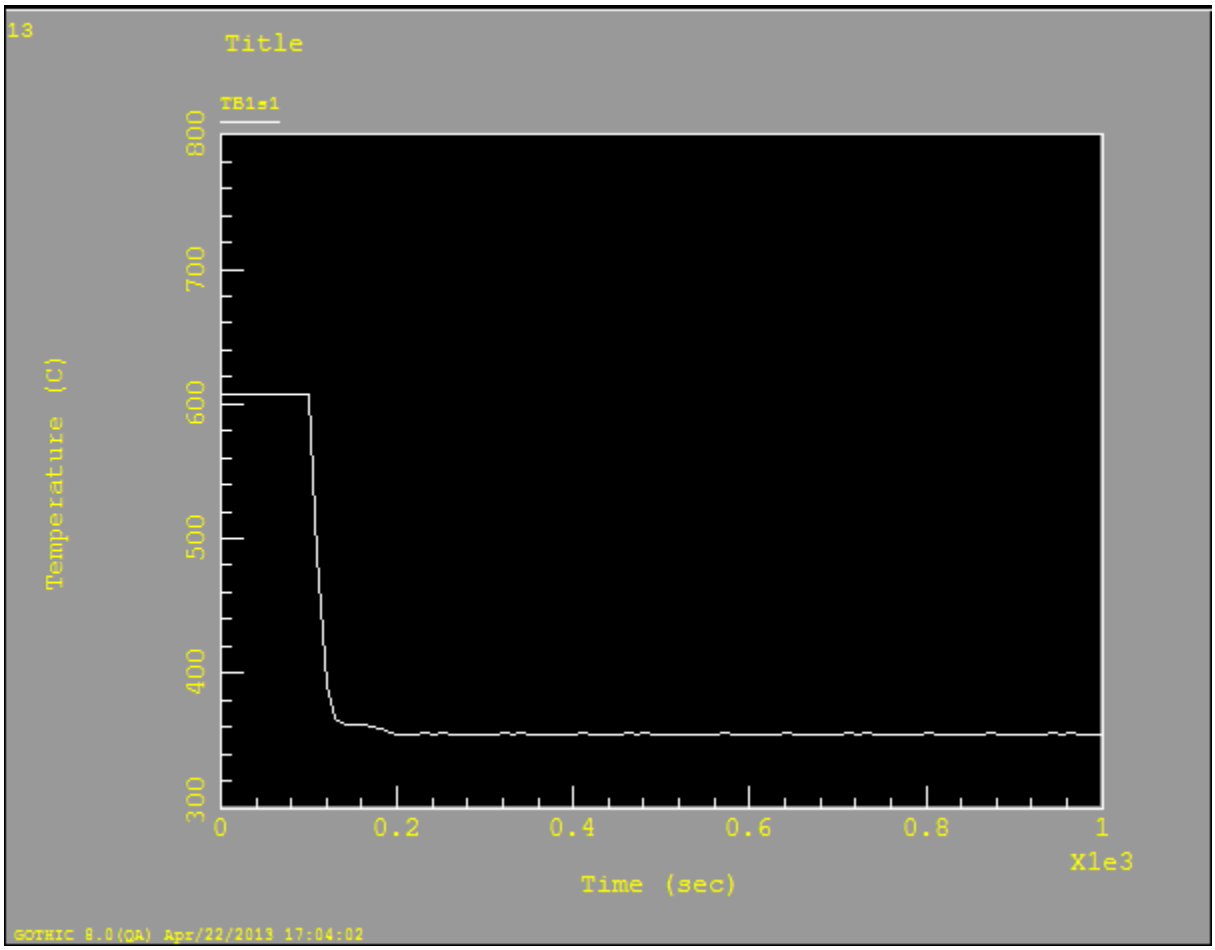

Figure 18. Outside temperature of the fuel is shown.

This fuel outer temperature is the same as the clad temperature. Notice that during steady state operation the clad temperature remains constant. Also note that the clad temperature drops to a very low temperature during operation. This clad temperature is close to the coolant maximum temperature which corresponds with common nuclear reactors. One important thing to note is that the average fuel temperature is quite low in this model in comparison to existing reactors. One reason for this is that there was no fuel-clad gap modeled in the fuel.

Using the average coolant temperatures, average fuel temperatures, and average coolant flux found in the last iteration step, it was determined that the maximum amount of tritium produced per bar in an assembly was 0.63 grams over an 18 month cycle. This value was less than a tenth

of a gram difference than the maximum amount of tritium produced using the initial mass flux and still conforms to the maximum limit of 0.65 grams. As such, this amount of tritium production is considered acceptable. Using the final coolant mass flux, the maximum achievable burn-up and maximum relative power fraction were determined to be 16.053 GWd/t and 1.846 respectively. Both of these values satisfy the criteria previously stated and validated this as the optimal, functioning core.

4.4 Safety Analysis - Ali Alnuaimi

4.4.1 Introduction

Safety analysis for any new reactor is required by the NRC to ensure that the reactor will not pose a threat to the public during its operation. The two types of safety analyses are deterministic risk assessment and probabilistic risk assessment (PRA). The safety analysis is also used to identify hazards and estimate the probabilities of failures and accidents. This analysis is used to prepare plan of actions in order to avoid future accidents or reduce the severity of the outcomes. This project focuses mainly on the PRA analysis because of the limited tools available to university students. The three sections of the safety analysis for this project are, Probabilistic Risk Assessment, Departure from Nucleate Boiling Ratio (DNBR) analysis, and TPBARs safety analysis.

4.4.2 Probabilistic Risk Assessment (PRA)

One important part of the probabilistic risk assessment is the Event Tree Analysis (ETA). An event tree simulates the series of events with respect to time and provides an inductive logic tool to identify the different possible outcomes of initiating events. They are similar to decision trees but the difference is that human intervention is not required to alter the outcome of the initiating

event. The initiating event can be defined as the failure of a system and the subsequent events are all determined by the overall performance of the individual system components.[7] Since the NuScale reactor has different components that may fail during an accident, we will focus mainly on the major important systems that may fail. For a nuclear reactor, we have different types of initiating events. As a result, different event trees should be constructed and evaluated in order to analyze the possible consequences. In order to be conservative with the safety analysis using ETA, each system has only one success rate where everything in that system is fine and a failure rate at which all the system components have failed. This approach allows us to calculate the probabilities of the worst possible scenarios. Figure 19 below shows a classical event tree with generic systems System 1 and System 2. The accident sequence for each tree branch is identified at the right end of each branch. For example the sequences I S1 S2 in the tree denote the accident sequence when initiating event I occur and System 1 succeeds to respond to the initiating event but System 2 fails when this initiating event occurs.

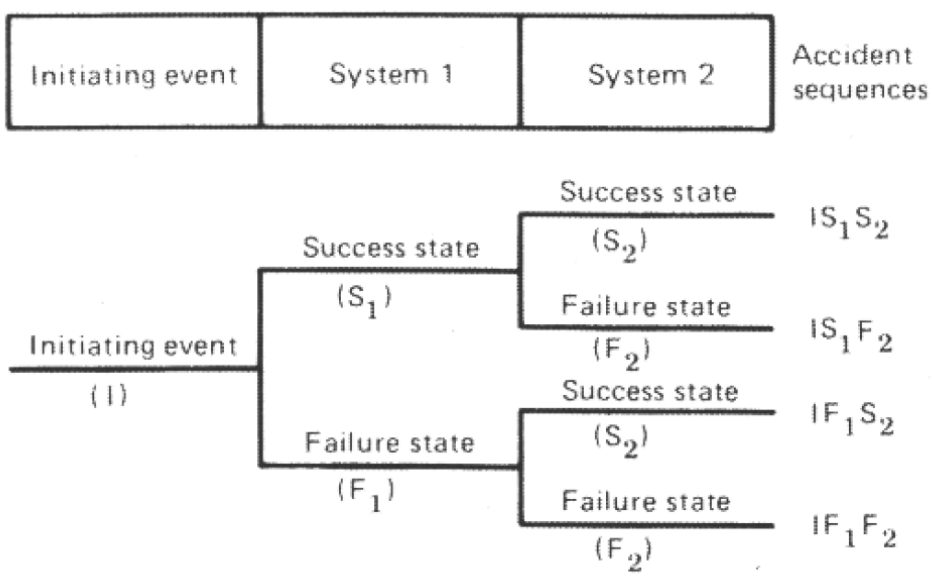

Figure 19. This plot illustrates the event tree branching of two systems.

It be should be emphasized that in reality the system states on any branch is dependent on the previous occurred events. For the simplicity of the analysis, an assumption that each event probability is independent of the path will be made since NRC data provide probabilities for individual events. This will not produce high variations in the results but this difference should be taken into account in real assessment of the NuScale Reactors. It should be noted that a major disadvantage of the above event tree is that it does not account for the timing of the events. The failure logic may change during an accident and is dependent on the time at which the accident takes place. This case for example occurs in the operation of the ECCS (emergency core cooling system) in nuclear reactors. As a result, a more complicated event tree is used to account for the timing of the event and it is called Dynamic Event Tree (DET). In the following section, the probability mathematical calculations will be discussed.

The probability of any event is usually a number between 0 and 1 as can be seen in the following equation:

$$0 \leq P(E) \leq 1. \tag{3}$$

Where P(E) is the probability of the generic outcome E. In Nuclear systems analysis, we are interested in the probabilities of different event occurring at the same period of time. The probability of two events occurring is given by the equation below:

$$P(E_1 E_2) = P(E_1|E_2)P(E_2) = P(E_2|E_1)P(E_1) \tag{4}$$

Where E_1 is the first outcome and E_2 is the second outcomes. $P(E_1 \text{ I } E_2)$ is the probability of event E_1 given event E_2 has occurred. This is very helpful for the event tree analysis (ETA) since we are interesting in the overall probability of different sequence of events. Based on the

simplifying assumption that the events analyzed in this report are assumed to be independent, the probability of both events E_1 and E_2 to occur together can be written as the following equation:

$$P(E_1 E_2) = P(E_1)P(E_2) \quad (5)$$

This equation is a much simpler form of the earlier equation and it simplifies the Event Tree Analysis calculations. Any failure of any system occurs during a specific period of time. If the time period of the event is very short compared to the time of interest of the whole event, then this event can be considered an instantaneous event and therefore time independent. As a result, the analysis of this project is based on the assumption that the events are time independent. Components that function in a dynamic state fail more frequently than static components. Once the event tree has been constructed, the next task is to compute the probabilities of the system failure. Because NuScale is a PWR type reactor, this report will focus on analyzing some PWR accidents and perform event tree analysis for each of these events. The probability data for this analysis was obtained from the Reactor Safety Study that was done by the NRC.[8] After each accident analysis, the report will include a section explaining why the NuScale reactor is expected to perform better compared to traditional nuclear reactors.

4.4.3 Loss of Offsite AC Power

This accident is very important to analyze because it has a sequence to core melt. This accident is defined by having a total loss of all feedwater (auxiliary and main) and therefore a loss of normal and alternate plant heat removal systems. If both of these systems fail to operate, the steam generators are expected to be emptied within 1 hour. The loss of the plant heat removal systems will cause the discharge of the RCS coolant through the pressurizer relief valves and safety valves. This will result in the eventual uncovering of the reactor core and then core melt will be occurring within 2 to 3 hours. The containment ESFs may be able to lessen or mitigate the

release of radioactivity in this accident sequence but their usefulness is conditional on the recovery of AC power during the time period before the core melt. It can be noticed from the previous sequence that there are many probabilities involved in this accident and the most important ones should be considered for the safety evaluation.[8] All of the probabilities data for each sequence are obtained from the NRC Reactor Safety Study. During the early progress of this project a RAM COMMANDER program was used to create event trees for the different events and accidents but it was fairly limited to two branches per accident. The RAM COMMANDER program was replaced by a program created by Excel spreadsheets and it proved to be more effective for long accident sequences. The equation to calculate the overall probability of this accident scenario is represented below:

$$P_A = P_1 \ x \ P_2 \ x \ P_3 \ x \ P_4 \ x \ P_5 \ x \ P_6$$

P_1: The probability of losing the offsite AC power.

P_2: The probability of the non-recovery of the offsite AC power in 30 min to 1 hour, which means a loss of feedwater delivery provided by the plant power conversion system.

P_3: The probability of the auxiliary feedwater system failure.

P_4: The probability that the off-site AC power will not be recovered for the containment ESFS within 1-3 hours after the transient event.

P_5: The probability that the on-site emergency AC power will not be recovered within 1-3 hours after the accident.

P_6: The probability that the containment ruptures after a melt-through of the base of the containment. All of the important probabilities of this event are represented in the table below.

TABLE IV: This table shows the probabilities values obtained from the NRC Reactor Safety Study document for the previous equation.[8]

	Probability Values
P_1	$\sim 2x10^{-1}$
P_2	$\sim 2x10^{-1}$
P_3	$\sim 1.5x10^{-4}$
P_4	$\sim 5x10^{-1}$
P_5	≤ 1
P_6	~0.2

It can be noticed that P_5 has a very large range (less than or equal to 1). In order to be conservative in the safety analysis, a value of 1 will be chosen to produce the highest probability. An event tree analysis of this event and a discussion why the NuScale is expected to perform better in this type of accident are presented in the results section.

4.4.4 Total Loss of AC Power

This is another accident to be analyzed and it is important for an effective safety evaluation of the reactor. This accident will result in the loss of all standby diesel generators and also the loss of off-site power. The only remaining systems that will be able to operate are High Pressure Coolant Injection system (HPCI) and Reactor Core Isolation Cooling system (RCIC) and they will provide make up water to the reactor vessel. According to the NRC safety report, there will be a time period of 27 hours before the core melt if make-up water is available. If make-up water is not available, this period will be one half hour before the core melt. To calculate the

probability of core-melt due to the loss of AC power and also loss of make-up water, the following equation will be used:

$$P_B = P_1 \; x \; P_2 \; x \; P_3 \; x \; P_4 \; x \; P_5$$

Also, it is interesting to calculate the probability of core-melt due to the loss of AC power but with make-up water available in this case. This can be done by using the following equation:

$$P_C = P_1 \; x \; P_2 \; x \; P_6 \; x \; P_7 \qquad (8)$$

P_1: The probability of the loss of off-site power.

P_2: The probability of the loss of standby diesel engines.

P_3: The probability of the loss of HPCI and RCIC systems.

P_4: The probability of the non-recovery of off-site power in ~ ½ hour.

P_5: The probability of the non-recovery of diesel engines in ~ ½ hour.

P_6: The probability of the non-recovery of off-site power in 27 hours.

P_7: The probability of the non-recovery of diesel engines in 27 hours.

TABLE V: This table shows the probabilities values obtained from the NRC Reactor Safety Study document for the previous two equations.[8]

	Probability Values
P_1	~ $2x10^{-1}$
P_2	10^{-3}
P_3	~ $2x10^{-3}$
P_4	~0.2
P_5	~1
P_6	~$2x10^{-2}$
P_7	~0.1

It should be noted that the value of P_2 ranges from 10^{-4} to 10^{-3} but the latter value was chosen to have a more conservative analysis. It is very beneficial to notice the importance of the make-up water being available on the overall probability of the core melt. As can be seen in the result section, the availability of the make-up water reduces the probability of the core melt by one order of magnitude approximately. A core melt may occur because all AC power is lost in this accident sequence and not recovered fast enough to avoid excessive coolant loss through the Reactor Coolant System relief and safety valves. Also, a steam explosion may occur because the molten core drops to the lower part of the reactor vessel and makes contact with the residual vessel coolant. A rupture of the reactor vessel may happen because of the steam explosion the air oxidation will increase the magnitude of the radioactivity release of the containment.[7] A discussion about the expected performance of the NuScale reactor in these types of accidents and how its new design helps to lower these consequences can be found in the results sections.

4.4.5 DNBR Analysis

Determining the departure from nucleate ratio (DNBR) for any reactor design is very important to ensure the maximum safety for the reactor. The DNBR value should be above 1.3 for a safe reactor operation. Normal convection can result in nuclear boiling if the difference of the temperature increases. This will result in the formation of bubbles and the occurrence of the film boiling. Film boiling reduces heat transfer and causes melting in source situations. The critical heat flux is the value that causes the film boiling to occur and DNBR shows how close the reactor flux is to the critical flux. DNBR was calculated by using W-3 correlation and the equation below was used to calculate the critical heat flux.[7]

Before using the W-3 correlation, it should be noted the ranges of parameters where this correlation is valid. This correlation is valid for reactor pressures between 5.5-16 MPa. The NuScale pressure is around 12.8 MPa so the NuScale reactor satisfies the first condition. This correlation is also valid for Dh values between 1.5 and 1.8 cm and the calculated Dh value for the NuScale was found to be 1.6 cm. This correlation is also valid for reactor lengths of between 0.254 to 3.7 meters and the NuScale length is around 2 meters. Based on the previous discussion, we can safely assume that the W-3 correlation is applicable to the NuScale reactor.

$$q''_{cr} = \{(2.022 - 0.06238p) + (0.1722 - 0.01427p)\big) \exp[(18.177 - 0.5987p)x_e]\,[(0.1484 - 1.596x_e + 0.1729x_e|x_e|)2.326G + 3271][1.157 - 0.869x_e][0.2664 + 0.8357\exp(-124.1D_h)]\big[0.8258 + 0.0003413\big(h_f - h_{in}\big)\big] \quad (9)$$

Where p is the pressure in Mpa, G is the mass flow per subchannel per the flow area, x_e is the flow quality. The area can then calculated by using the following equation:

$$A_z = P^2 - \frac{\pi}{4}D^2 \quad (10)$$

Where D is the diameter of the rods and P is the pitch length. The value of G and D_h be calculated from the following two equations:

$$G_m = \frac{m'}{A_z} \quad (11)$$

$$D_h = \frac{4A_z}{\pi D_{out}} \quad (12)$$

Where m' is the mass flow per subchannel in kg/s. The axial heat flux was approximated by using the next equation. This value is needed for the final calculation of DNBR.

$$q''(z) = q_o * \cos\left(\frac{\pi z}{L}\right) \qquad (13)$$

Where L is the length of reactor and q_o is the actual heat flux of the reactor. Then the DNBR can be calculated by using the next equation:

$$DNBR = \frac{q''_{cr,n}}{q''(z)} \qquad (14)$$

This analysis assumed the uniformity of the flux throughout the reactor in order to simplify the mathematical calculations. The NuScale reactor was able to achieve DNBR values above 1.3 as can be seen in the results section.

4.4.6 TPBARS Safety Analysis

The effect of introducing TPBARs to the reactor design should be considered. TPBARs insertion into the reactor core does not greatly affect the reactor thermal-hydraulics or neutronics analyses that were discussed earlier in this report. As a result, TPBARs does not increase dramatically the probability values of the reactor accidents. Any small effects caused by the TPBARs should be within the fuel design limits. According to the Department of Energy (DOE) tritium production report, TPBARs may fail during a large break LOCA accident.[10] From the earlier discussion, LBLOCA cannot happen to the NuScale reactor, which means it is one of the most suitable reactor designs to incorporate the TPBARs into the reactor.

There are some technical challenges with TPBARs that limits that total number of TPBARs used in the reactor. Despite the new designs of TPBARs, some reactors such as Watts Bar 1 reactor have some problems where tritium is still leaking from the TPBARs at higher than expected rates into the water that is used to cool the reactor.[10] This resulted in using much fewer TPBARs than

anticipated. As a result, this technical problem is another limiting factor that limits the total number of TPBARs used[10]. As a result, less tritium is produced and this will affect the economics analysis. A tritium production facility may take more time to recover its costs because of this additional limiting factor for the total number of TPBARs used.

4.4.7 Safety Analysis Results

Figure 20 below shows the event tree analysis that was done for loss of off-site AC power (scenario A). The picture was split into two parts because it is too big to fit one page.

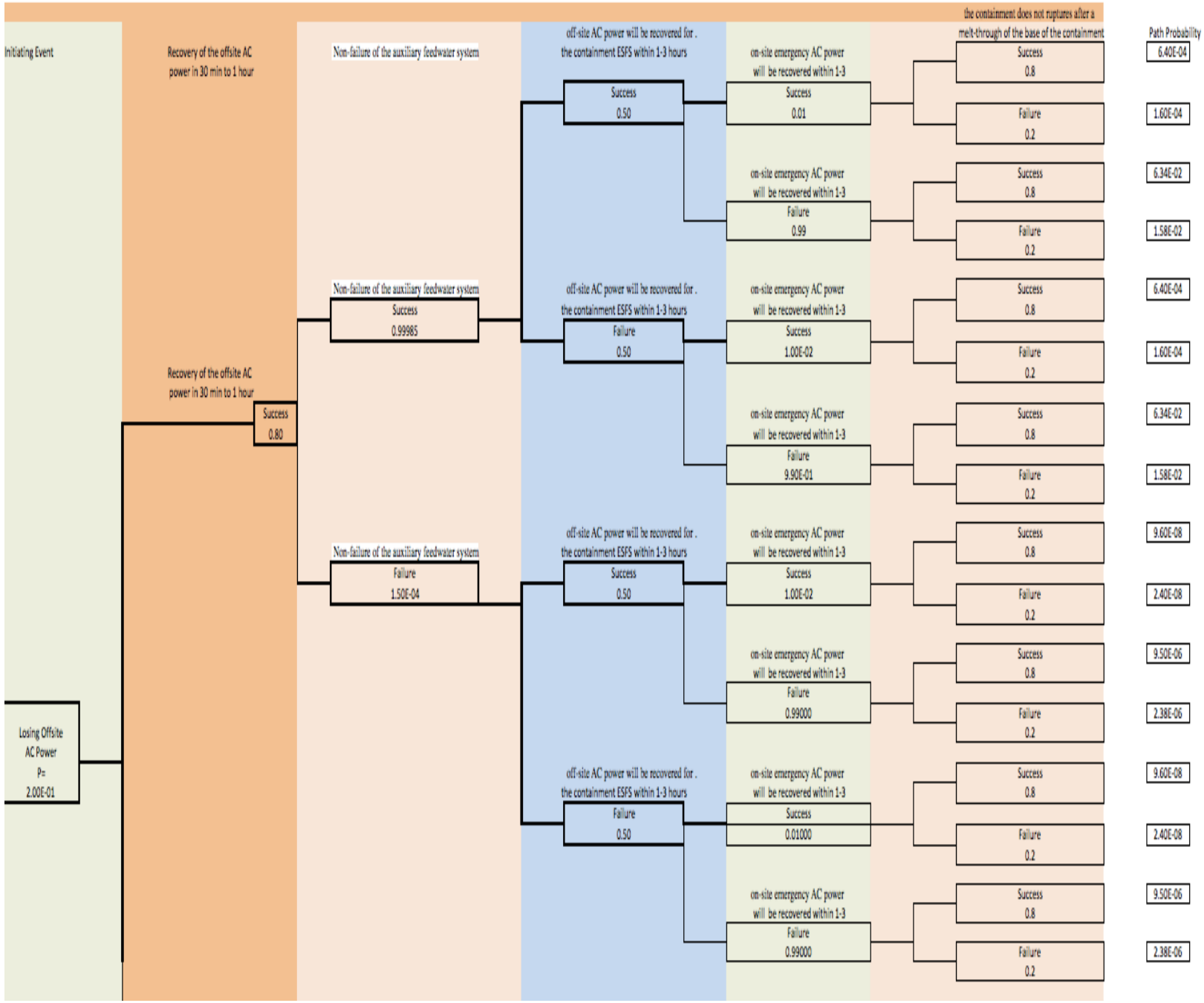

Figure 20. This figure shows the event tree analysis for a typical PWR when the off-site AC Power was lost.

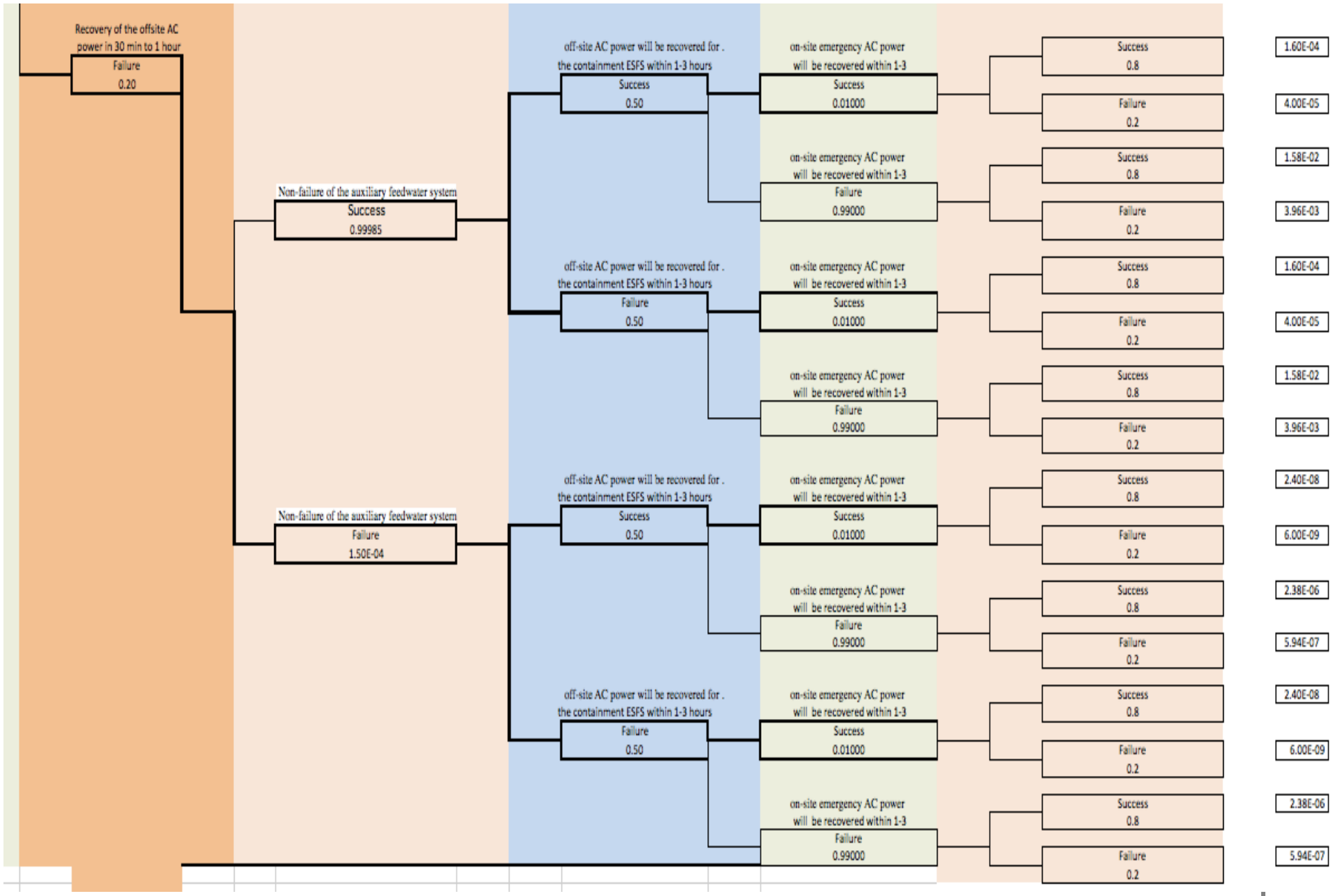

Figure 21. This figure shows the event tree analysis for a typical PWR when the off-site AC Power was lost.

As can be seen the figure above, the probability of the safety features to successfully operate during the accident is much higher than the worst-case scenario probability. This is true because these safety features are carefully designed to lower the risk and damage from such accidents.

4.4.8 Scenario A Results

NuScale reactor does not require off-site AC power to shutdown, which is one of the big advantages of the NuScale technology. NuScale reactor is designed such that the ECCS and supporting systems will be enough for a failsafe shutdown and operation. The safety valves in NuScale have been designed to align themselves to the safe condition without the use of batteries after a loss of all station power. This technology is also important for scenario such as Fukushima where many of the reactors had issues with failed diesel generators. Although no safety data for NuScale reactor is available at this time, its innovative design and technology will most probably lower the overall failure probabilities of the previous scenario.

4.4.9 Scenario B Results

This is a very interesting scenario since it involves calculating the probability of a core melt following a loss of AC power and also the loss of make-up water. The event tree analysis for this scenario can be seen in the following two pages.

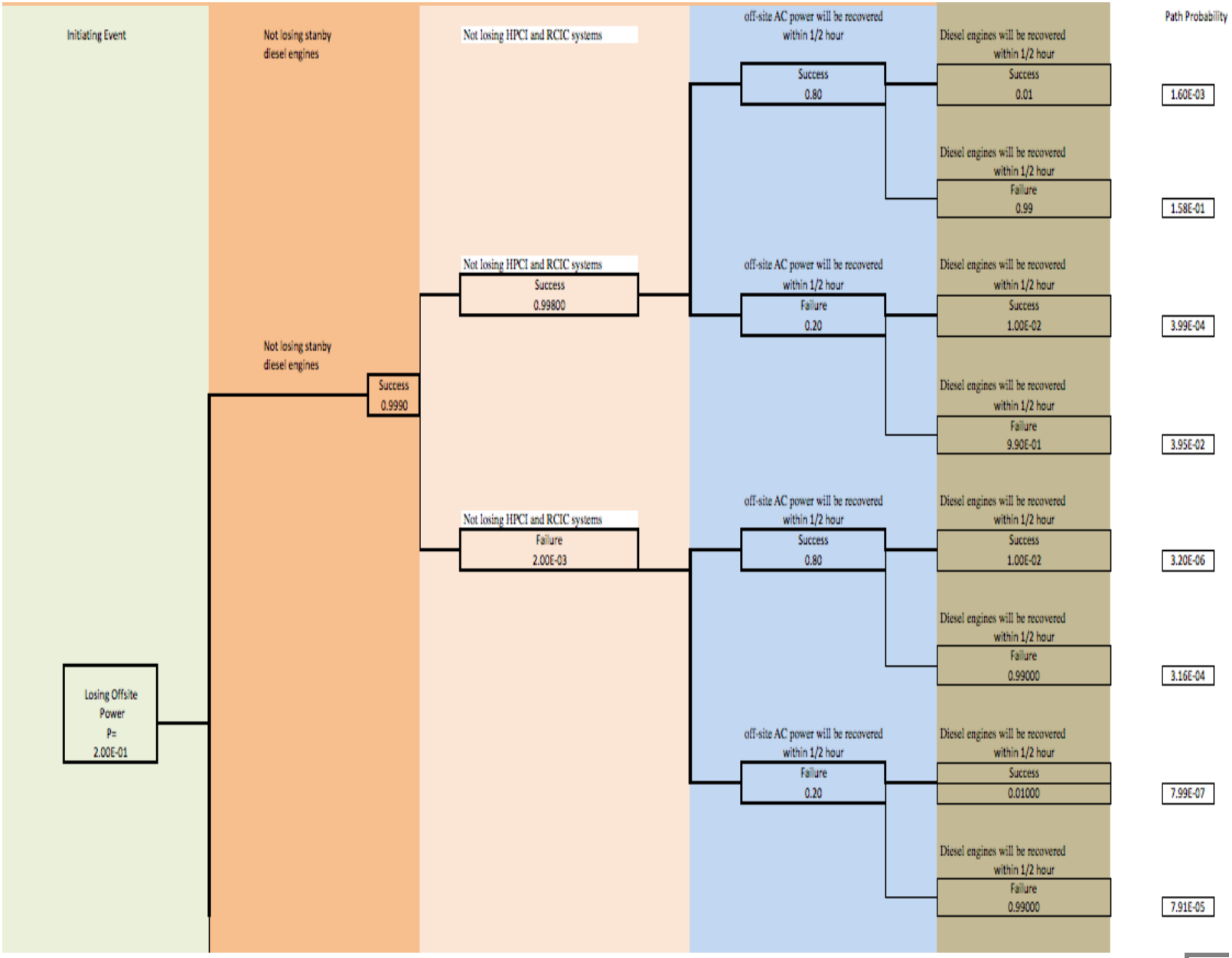

Figure 22. This figure shows the event tree analysis for a typical PWR when the off-site AC Power was lost and also the make-up water was lost.

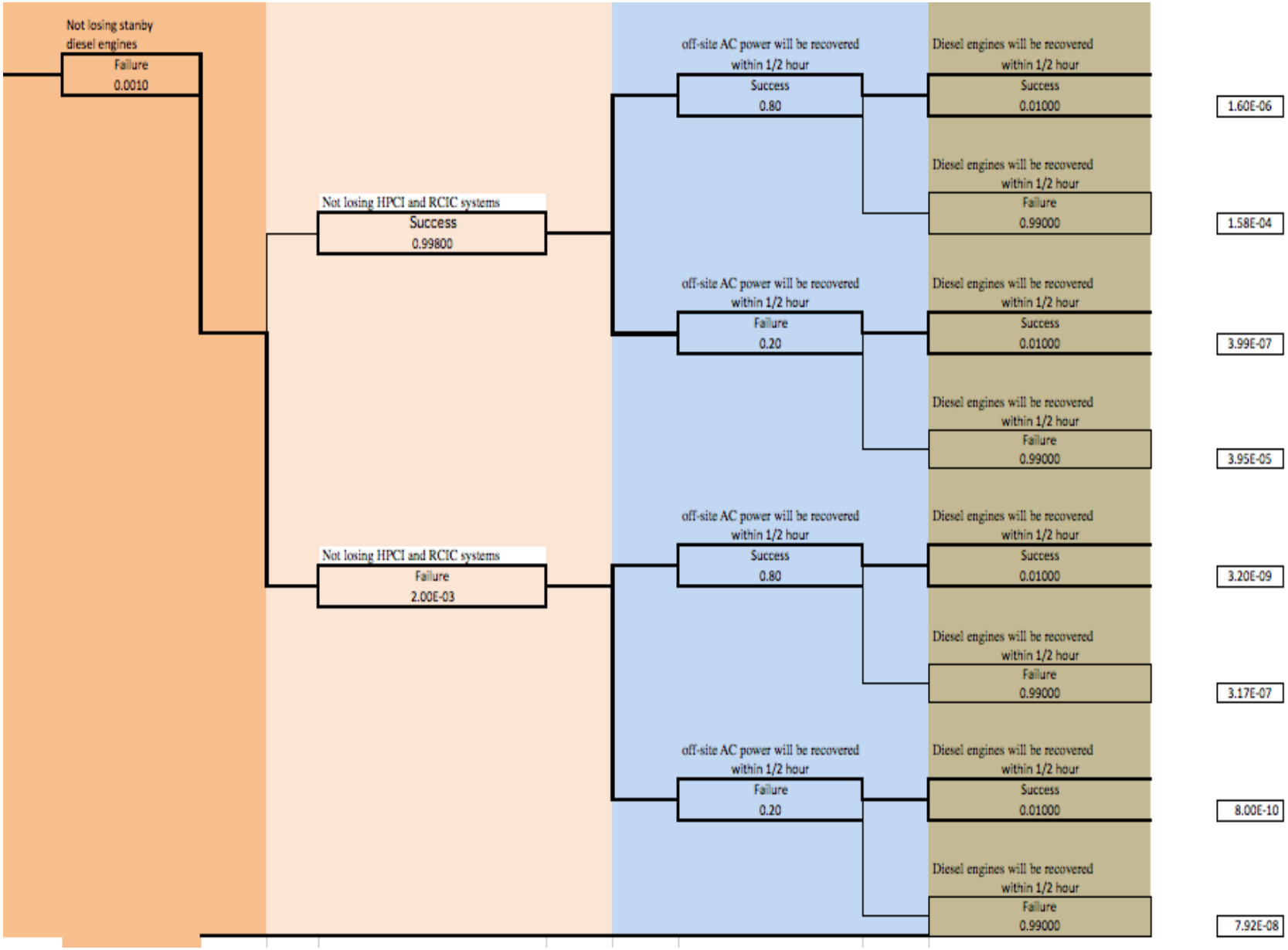

. **Figure 23**. This figure shows the event tree analysis for a typical PWR when the off-site AC Power was lost and also the make up water was lost.

The probability of the worst-case scenario is much lower than the previous scenario. We can also see that the probability of the systems successfully operating during this accident is much higher than the total failure probability. Because of the passive safety features of the NuScale technology, the probability of the core melt for NuScale is expected to be much lower than the traditional operating PWRs. This is due to the fact that losing the off-site AC power is expected to not have severe effects on the NuScale reactors due to the reasons mentioned earlier.

4.4.10 DNBR Results

The figure below shows the DNBR versus the flow quality for NuScale reactor.

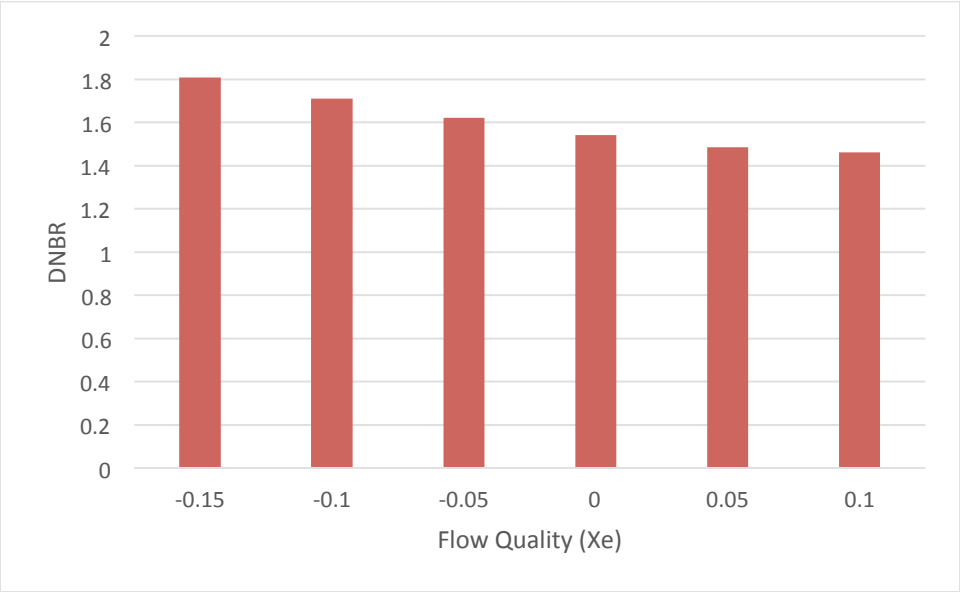

Figure 24. This figure shows the NuScale DNBR values versus the flow quality.

A negative flow quality means the coolant is in the subcooled state, which is the usual case for nuclear reactors. As can be seen from the figure above, the NuScale reactor was able to achieve DNBR values of above for vapor qualities below 0.15. As mentioned earlier, increasing vapor means a loss on the heat transfer amount and therefore approaching the critical heat flux. Typical nuclear reactors coolants do not usually reach higher qualities unless there is an accident.

4.5 Economic Analysis - Ali Alnuaimi

4.5.1 Introduction

One of the major objectives of the NuScale technology is to reduce the overall costs considerably. The next sections discuss the different costs of NuScale and their estimations. The goal of this analysis is to estimate the total cost of NuScale and show its competitiveness compared to other reactor types. The cost data for the NuScale reactor is not publicly available because it is a fairly new design.

4.5.2 Methodology

The economic analysis model in this project will be to use an available data for a similar SMR and adjust the costs slightly to represent the unique characteristics of the NuScale reactor. The chosen reactor is NOAK (Ninth of a Kind) with an electrical capacity of 600 MWe. Since the total electrical output of NuScale is 540 MWe and lower output means generally lower costs, the costs of NuScale will be approximated by 7.5% lower than the NOAK costs. NOAK reactor was chosen to be a reference during the cost calculation of the NuScale because both of these reactors are SMRs and produce roughly the same output. The NuScale reactor has a power output of 7.5% less than the NOAK so the individual costs were adjusted accordingly. This approach does not produce very accurate numbers but it can be used as a best-estimate approach. The NuScale reactor has a tritium production capability added to it by incorporating TPBARs in the reactor design and these costs were added to the NuScale calculations. NuScale will include an additional direct cost of TPBARS. The estimated cost for each TPBAR is $10000 and the reactor design has 3168 TPBARs. The different costs types are presented in the next sections.

4.5.3 Detailed Design and Engineering Costs (DD&E)

This cost includes the completion of the reactor detailed design, specification of system components and construction drawings. At study done by the energy policy institute at Chicago University estimates this cost to be $800 Million for new SMRs.[9]

4.5.4 Direct Costs

Direct costs include the costs of the containment and TPBARs and can be seen in the table below.

Table VI. This table compares the NOAK versus NuScale costs. It was projected that NuScale costs will be 7.5% less than NOAK costs.

Direct Costs	NOAK (in millions)	NuScale (in millions)
Balance of Plant Structures	$80	$74
Reactor Building	$200	$185
Non-reactor Structure	$120	$111
Reactor and Steam Generator	$1000	$925
Turbine Generator and Condenser	$300	$277.5
Electrical Equipment.	$200	$185
Cooling Systems	$100	$92.5
TPBARS Cost	$0	$31.68
Total	**$2000**	**$1881.68**

4.5.5 Additional Costs

The table below shows additional costs other than DD&E costs and Direct Costs.

Table VII. This table shows the other costs associated with building a new NuScale reactor.

Costs	NuScale (in millions)
Indirect Costs	$185
First Core Costs	$86.025
Owner's Costs	$185
Total	**$456.025**

The overnight cost can then be calculated using the following equation

$$OVC = C_{DD\&E} + C_{Direct} + C_{Indiect} + C_{O\&M} \quad (15)$$

Where OVC is the overnight cost, $C_{DD\&E}$ is the detailed design and engineering cost, C_{Direct} is the direct cost, $C_{Indirect}$ is the indirect cost, and $C_{O\&M}$ is the operation and management cost, which was obtained to be 1.37 Cents/kWh .[9] The overnight cost was calculated to be $3.137 billion. Assuming 8% interest during a two year construction period, the adjusted overnight cost can be calculated by the following equation

$$OVC_{Adjusted} = OVC_{Unadjusted}(1+i)^2 \quad (16)$$

where $OVC_{Adjusted}$ is the adjusted overnight cost and i is the interest rate. The adjusted overnight cost was calculated to be $3.7068 billion for the NuScale site. Since undergraduate students have little information on the reactor plant costs, this can be considered a rough estimate and additional hidden charges may raise the overnight cost to $4 billion.

5. CONCLUSIONS AND RECOMMENDATIONS – ALL

5.1 Summary

The final core configuration mentioned above met all core design goals, satisfied the heat transfer requirements, and was optimized for producing tritium. As such, this it is considered the final design. The final core configuration can be seen in Figure 9.

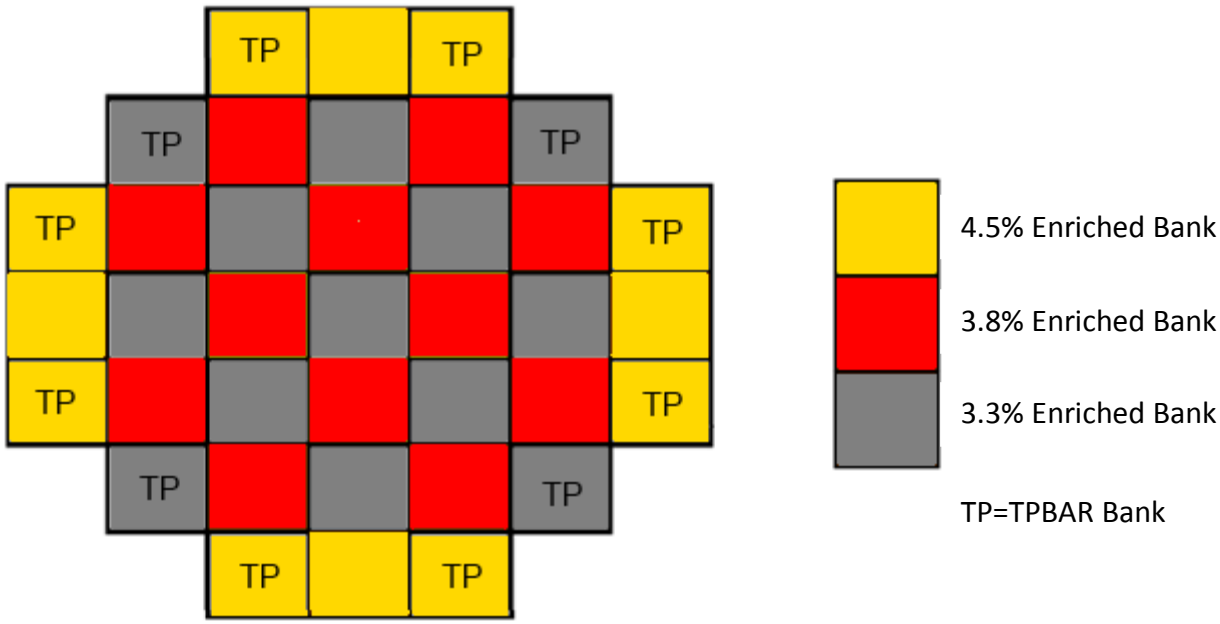

FIGURE 25. Final core mapping scheme including TPBAR placement.

The core cycle length for producing tritium is approximately 18 months at full power. With this loading scheme, each core produces approximately 161.27 grams of tritium per cycle, or equivalently 109.22 grams per year. In order to reach the designated goal of 1150 grams of tritium per year, eleven of these tritium producing SMRs are needed. When compared to the twelve SMRs in a traditional NuScale SMR power facility, this seems a reasonable conclusion.

Additionally, these cores produce the same amount of heat as the power producing versions of the NuScale SMRs. As such, using this thermal output to generate electricity could not only cut down on cost of operation for the tritium producing facility, but it would also put the heat generated to a beneficial use instead of merely using heat sink to remove the heat generated. The safety analysis results show that the NuScale response to accidents exceeds those of traditional reactors. An important advantage of the NuScale reactor is that LBLOCA accidents cannot happen to this type of reactors. Also, no external AC power is required for a safely shutdown of the reactor because of it's passive safety. The DNBR for the NuScale reactor was calculated to be above 1.3 for wide ranges of flow qualities. The safety analysis limits the number of TPBARs that can be used in the NuScale reactor because of the tritium leaking to the coolant that is experienced in some of the Tritium production reactors. The economic analysis shows that the total cost of the NuScale reactor is around $4 billion which makes this reactor very competitive compared with other reactors.

5.2 Improvements

Although this analysis is considered rigorous given the scope of the project, due to lack of resources and knowledge, there are a number of improvements that could be made. The first improvement that could be made is access to the full isotope libraries in CASMO4. Through this, the TPBARs could have been modeled more accurately, leading to a more accurate three-dimensional core model, and consequently, more accurate calculations of tritium production. The second improvement that could be made is a more accurate analysis of the half-height TPBARs. As stated previously, Pacific Northwest National Laboratories requires that they complete a full analysis of any TPBAR with an active absorber region other than that used for a

typical PWR, and is beyond the scope of this project. As such, the upper limit on tritium production in a single TPBAR used in this analysis is simply an estimation and could significantly vary from the actual limit, resulting in unaccounted error. The last improvement that could be made is in the calculation of tritium production. This analysis assumed that all lithium-6 neutron absorption resulted in obtainable tritium. In actuality, some of the tritium produced leaks into the core or experiences radioactive decay. Taking into account these factors was considered beyond the scope of this project, but would help more accurate depict the feasibility of using the NuScale SMR for tritium production.

5.3 Future Works

Although the current core design met all objectives, there are still a number of analyses that could be performed. These analyses were unable to be completed due to time constraints and lack of knowledge, but would be a good starting point for continuation of this project. The first additional task would be to find suitable positions for which to insert burnable absorber rods into the core. Burnable absorber rods are used to help account for excess reactivity and control power peaking factors in the core. Inserting burnable absorber rods in the core would add stability and allow for a more even burn-up, leading to better efficiency and safety. The second task that should be performed is an analysis of core shuffling and reloading. The analysis stated in this paper only takes into account the initial core loading and does not cover anything past the first cycle. In order to determine the feasibility of this core over an extended period of time, an appropriate refueling and shuffling procedure needs to be developed to ensure that all criteria are met for every cycle. The last additional task is to optimize the maximum possible burn-up of the core so that it is closer to the planned burn-up of a cycle. Doing this ensures that the maximum

amount of energy possible is extracted from the fuel and will decrease the amount unnecessary fuel in the core. This can be done by altering both the fuel enrichment and power level of the reactor. All of these tasks require substantial amounts of time and knowledge to complete, putting them far beyond the scope of this project, however, the possibility of tritium production in the NuScale SMR has been proven feasible and deserves a more in-depth analysis.

With respect to the thermal hydraulic analysis, this project was performed on macro scale instead of on a micro scale. The whole core was modeled while an analysis of a single channel was not. To get a better understanding of the safety factor of the core, a sub channel analysis could be performed. This would allow the designer to look into the hottest channel as well as the coolest. Another step that could be taken is to perform transient analyses on the reactor. The GOTHIC model for this project only looked into normal operating conditions. To perform a full safety analysis on this reactor disasters such as loss of coolant accidents and loss of offsite power accidents would need to be modeled.

6. REFERENCES

1. D. J. SENOR and D. M. PAXTON, Tritium Technology Program Overview and SMR Design Challenge-NUEN 406 Presentation, Pacific Northwest National Laboratory, 7 September 2012.
2. Karriem, Z. "*Non-Proprietary Data for Modeling the NuScale Reactor*." NuScale Power, LLC. <zkarriem@nuscalepower.com>
3. NuScale Power, LLC. "*NuScale Plant Design Overview*." August 2012. <www.nuscalepower.com>
4. Burns, KA. "*Tritium Technology Program Procedure: Description of the Tritium-Producing Burnable Absorber Rod for the Commercial Light Water Reactor*." Revision 19. February 02, 2012.
5. Collins, BA. "*Tritium Technology Program: Production TPBAR Inputs for Core Designers*." Revision 15. November 14, 2012.
6. Rahn, Frank. GOTHIC Thermal Hydraulic Analysis Package User Manual. Version 8.0(QA). Jan. 2012.
7. Kok, Kenneth D. *Nuclear Engineering Handbook*. Boca Raton: CRC, 2009. Print.
8. NRC. *Reactor Safety Study An Assessment of Accident Risks. in U.S. Commercial Nuclear Power Plants*. Rep. N.p.: n.p., 1975. Print. NUREG75.
9. Rosner, Robert, and Stephen Goldberg. "Small Modular Reactors – Key to Future Nuclear Power Generation in the U.S." *Www.eenews.net*. N.p., 2 Nov. 2011. Web.

7. APPENDIX

TABLE VIII. Method 1 approximation of the composition of TPBARs with a lithium-6 linear density of 0.02675 g/in.

Composition	Mass (g)	Weight Percent
B-10	0.159717	0.160636824
Natural Li	9.057715	9.109875771
O	48.935651	49.21745795
Al	41.274342	41.51202945
Total	99.427426	100.000000
New Density		2.586716182

TABLE IX. Method 2 approximation of the composition of TPBARs with a lithium-6 linear density of 0.02675 g/in.

Composition	Mass (g)	Weight Percent
Natural Li	25.68280840	22.21453231
O	48.78367644	42.19579648
Al	41.14616027	35.58967121
Total	115.61264511	100.00000000
Adjusted Density		3.00779285

TABLE X. Actual composition of TPBARs with a lithium-6 linear density of 0.02675 g/in.

Composition	Mass (g)	Weight Percent
Li-6	1.92621063	1.916349277
Li-7	8.378386337	8.335492675
O	48.93565141	48.68512235
Al	41.27434222	41.0630357
Total	100.5145906	100.000000
Actual Density		2.62

TABLE XI. Method 2 approximation of the composition of TPBARs with a lithium-6 linear density of 0.04125 g/in.

Composition	Mass (g)	Weight Percent
Natural Li	25.68280840	22.21453231
O	48.78367644	42.19579648
Al	41.14616027	35.58967121
Total	115.61264511	100.00000000
Adjusted Density		3.00779285

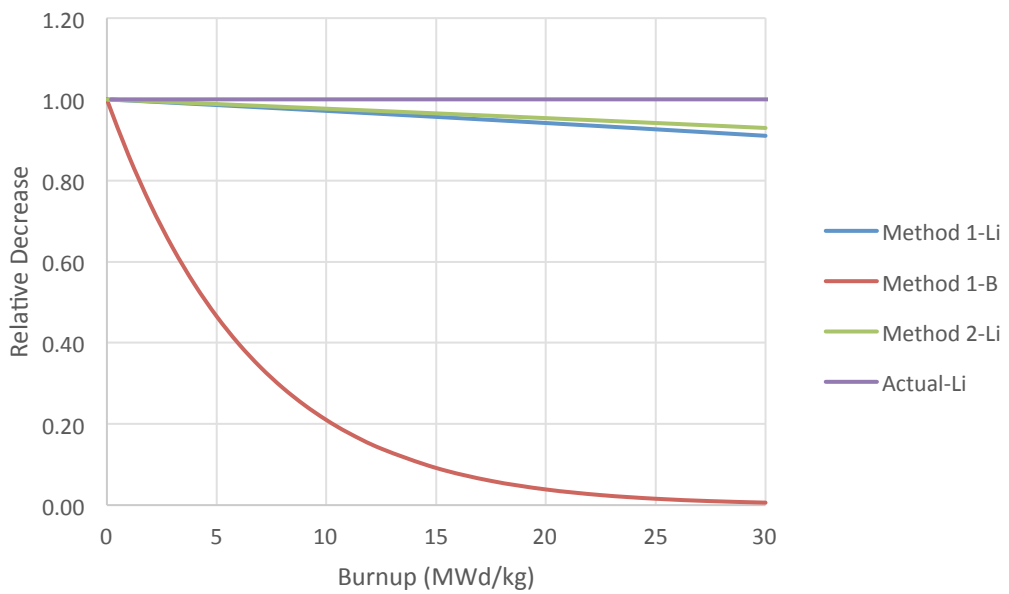

FIGURE 26. Comparison of k important isotope burn-ups for TPBAR simulation methods and actual assembly.

For full neutronics and thermal hydraulic codes, please see the appendix located in the attached flash drive.

A Feasibility Study of Tritium Production in the GE SPRISM Reactor

A Feasibility Study of Tritium Production in the GE SPRISM Reactor

Timothy Crook, Sara Loupot, Chad O'Hagan, Scott Thrower

30 April 2013

TEAM 6 Senior Design Project Final Report
Submitted in partial fulfillment of the requirements of NUEN 410
Texas A&M University, Spring 2013

A Feasibility Study of Tritium Production in the GE SPRISM Reactor

Timothy Crook, Sara Loupot, Chad O'Hagan, Scott Thrower

30 April 2013

Primary Technical Advisor: Dr. Pavel Tsvetkov

Signature: _____ Date: _____

Class Supervisor: Dr. Karen Vierow

Signature: _____ Date: _____

PNNL Advisor: Dr. David Senor

TEAM 6 Senior Design Project Final Report
Submitted in partial fulfillment of the requirements of NUEN 410
Texas A&M University, Spring 2013

1.0 Executive Summary…… 3
2.0 Introduction…… 6
2.1 Tritium Technology Program…… 6
2.2 Small Modular Reactor Application: The SPRISM…… 6
2.3 Project Objective…… 7
2.4 Project Approach…… 7
3.0 Materials…… 10
3.1 Introduction – Only Two Modifications…… 10
3.2 SPRISM Design…… 10
3.3 Fuel…… 10
3.3.1 Metal and Oxide Fuel…… 10
3.3.2 Nitride Fuel…… 11
3.3.3 Nitride Fuel Application in the Feasibility Study…… 12
3.4 Tritium Production and the TPBARs…… 14
3.4.1 Breeding Tritium…… 15
3.4.2 History…… 15
3.4.3 Tritium Breeding Candidate: Why Lithium Aluminate?…… 15
3.4.4 The TPBAR and the TPBAR Assembly and its Fabrication…… 16
3.4.5 TPBAR Performance…… 19
3.5 Conclusion…… 20
4.0 Neutronics…… 21
4.1 Goals…… 21
4.2 Methodology…… 21
4.3 Modeling…… 21
4.4 Problem Definition…… 21
4.5 Design (Parameters)…… 22
4.6 Results…… 34
4.7 Future Work…… 35
5.0 Safety Analysis…… 36
5.1 Introduction…… 36
5.2 PRISM: Five Levels of Safety…… 36
5.3 Inherently Safety Design Features, Systems, and Components…… 38
5.4 Reactivity Control…… 42
5.5 Accident Analysis…… 44
5.6 Tritium…… 44
5.7 Tritium Release from TPBARs in the SPRISM…… 46
5.8 Shielding Analysis…… 50
5.9 Conclusions…… 55
6.0 Thermal Hydraulics…… 55
7.0 Economics…… 55
8.0 Conclusions and Recommendations…… 55
Acknowledgements…… 56
References…… 57
Appendix

1.0 Executive Summary (Chad O'Hagan, Scott Thrower, Sara Loupot)

Pacific Northwest National Laboratory (PNNL) has been tasked with the mission to provide tritium for United States' thermonuclear weapon stockpile upkeep since 1995. Due to limitations of current production schemes, PNNL is exploring other means of dedicated tritium production and has asked for senior design teams at Texas A&M University (TAMU) to investigate tritium production utilizing Small Modular Reactors (SMRs). This feasibility study focused on exploring a tritium production application for the Super Power Reactor Innovative Small Module (SPRISM), a sodium-cooled, small-modular fast reactor. Today, PNNL employs unit 1 at the Tennessee Valley Authority's Watts Bar Nuclear Plant to produce tritium using tritium producing burnable absorber rods (TPBARs). Using a similar means, this study used TPBARs in the SPRISM with the objective of determining the feasibility of using the SPRISM for tritium production. The study began with the intention of choosing a fuel type, fuel composition, and a TPBAR position distribution such that tritium production is maximized. Additionally, two methods of tritium production inside the reactor were to be investigated: a breeder blanket application and a homogenous coolant mixture application. After initial background research, the investigation into the homogenous coolant mixture was halted, since its application was determined to be outside the scope of this project. A complete study should include an analysis for all three available fuel types that can be used in the SPRISM with varying TPBAR position distributions and varying lithium-6 enrichments. However, project time constraints prevented a complete study. Thus, this study focused on one fuel type, a single lithium-6 enrichment value, and two TPBAR position distributions with the object of minimizing any design changes to the TPBARs and the SPRISM and optimizing tritium production and power output.

Prior to building the computer model, decisions for input were required. Based on research, which included a timeline of tritium production beginning with its application at the Hanford site N reactor, lithium material compositions explored, TPBAR fabrication history, and TPBAR performance, the current TPBAR design was used in the SPRISM model with minimal modifications. In short, the TPBAR active length needed to be reduced to 47 inches to match that of the active core length for the selected fuel and the geometry TPBAR assembly needs to be modified from square to hexagonal in order to fit in the SPRIM core. Additionally, some TPBARs had to be modified in diameter to fit inside the assemblies. An assumption was made for the assembly: The TPBAR will replace the fuel rods in selected fuel assemblies. Regarding the fuel, of the three fuel types for the SPRISM the nitride fuel was chosen for its thermal properties. Fuel compositions for the driver fuel and blanket assemblies were also selected based on a doctoral thesis.

MCNP5 was the primary code used for modeling the SPRISM with the TPBARs. The major goals of the neutronics portion of the project were to produce 1150 grams of tritium a year in the outermost breeder blanket and to optimize power production with tritium production. These goals were chosen based upon discussion with the PNNL advisor. Modeling of the core

commenced early in the semester, however numerous problems resulting from unfamiliarity with the code prevented adequate progression throughout the semester. Four input decks were created over the course of the project that allowed computation of the flux in the core, heating ratios in the core, and the amount of tritium produced in the core. The flux in the core was found to be 1.03E15 neutrons/cm^2*s. The heating rations were passed on to the thermal hydraulics team member, Tim Crook. The flux was passed on for use by Sara Loupot in the safety and shielding analysis. In total the amount of tritium calculated to be produced in an assumed 1.5 year cycle came to less than a tenth of a gram for both TPBAR assembly core loadings analyzed.

A safety analysis was done on the SPRISM reactor and the effect tritium production will have on reactor, personnel, and public safety. The goal of the safety analysis was to analyze the extent to which the addition of TPBARs would change the behavior of the reactor with respect to the original safety criteria of the SPRISM reactor. When added to the core, TPBARs absorb neutrons, which lowers the power density of the reactor. This will also lower the temperature of the reactor in both normal operation and accident scenarios. Under this assumption, the accident scenarios analyzed in a report by Sumner should be sufficient to analyze the safety of the SPRISM core with nitride fuel. The SPRISM reactor was designed to be inherently safe. There are several features such as the Reactor Vessel Auxiliary Cooling System and the natural circulation system that ensure that all of the decay heat can be removed safely in the event of a station blackout. Reactivity control is of extreme concern in fast reactors such as the SPRISM due to the decreased importance of delayed neutrons to the reactivity coefficient. Many factors contribute to a smaller delayed neutron fraction in fast reactors than in thermal reactors which leads to a smaller margin to prompt criticality. Three transient events were analyzed including a loss of flow accident, transient over power accident, and loss of heat sink accident. An analysis by Sumner gives a worst-case estimate to what can be expected in the proposed core with TPBARs because the only modifications that are made is the addition of absorbing rods, which results in lower temperatures throughout the reactor. The loss of power accident resulted in peak fuel temperatures of 1,539 K, which decreased the margin to melting by only 25%. The transient over power accident was defined as an event in which all the control rods are withdrawn to the rod stop limit of $0.3 at the maximum rate of $0.02/s. In this transient, the power increases by 1,001 MW, but the fuel temperature increased by less than 20%. The loss of heat sink accident resulted in only a 12% increase in margin to fuel melting. Further work should be done to first characterize the flux profiles within the core and then perform a transient analysis on the core with TPBARs to confirm the hypothesis that core damage conditions would not be reached in any of these scenarios. The tritium that is produced in the TPBARs in our core is a beta emitter, so it must be managed with caution. In the proposed design, the tritium produced in the core can possibly leak into the sodium pool, diffuse into the RVACS system, and be transferred to the atmosphere. In this report, two scenarios of tritium release were analyzed. The first is based on the normal leakage rate of TPBARs. From this it was found that only 4440 TPBARs can be used in the proposed core without reaching the annual dose limit for radiation workers in the area. The public would receive doses less than background from this amount of release. A second scenario

analyzed the consequences of all of the 2,875 TPBARs required to produce 1150 g/cycle of tritium, assuming the production rate of the TPBARs in Watts Bar 1 can be reached, failing and releasing tritium. In this case, plant workers would receive 167 rem, but the annual dose limit for the public at 11 km would not be reached for six hours, which allows plenty of time for an evacuation. A shielding analysis was done using MCNP5. Since the reactor is mostly underground, the main concern for neutron dose is from neutrons that escape through the top of the vessel. In the simulation, no neutrons were able to penetrate farther than five meters under ground level. The radial distribution was similar, showing that very few neutrons are able to escape to the hot air riser system that is open to the atmosphere. Future work should be done to do a gamma ray dose analysis as well. These results show no reason to believe that the safety of the original designed SPRISM reactor will be diminished by the addition of TPBARs.

The goal of the project was to determine the feasibility of using a TPBARs in a SPRISM reactor to produce the tritium required to maintain the United States' nuclear weapons stockpile. Research on the materials to be chosen showed that the extensive research previously done on this topic has developed dimensions, materials and concentrations that are sufficiently optimized and should be kept as close to their current form as possible. From an initial neutronics analysis, it was discovered that the cross section for the reaction required to produce tritium is so small for the fast neutron energy spectrum that is characteristic of this reactor design that it is impossible to produce the target 1150 grams of tritium per cycle. A safety analysis was unable to produce any reason that the SPRISM reactor was made unsafe from the addition of TPBARs. From these results, the team recommends that PNNL does not continue investigating the use of fast reactors for tritium production at this time.

2.0 Introduction (Chad O'Hagan and Sara Loupot)

2.1 The Tritium Technology Program[1]

Tritium is a vital component of thermonuclear weapons. Its short 12.3 year half-life necessitates replenishment to maintain the US nuclear stockpile inventory. This tritium was originally produced at the Savannah River Site, but the Department of Energy (DOE) ceased production in 1988. In the following years, the DOE selected Pacific Northwest National Laboratory (PNNL) to lead a tritium production demonstration using Light Water Reactor irradiation. They developed a method of tritium production and collection in commercial Light Water Reactors using Tritium-Producing Burnable Absorber Rods (TPBARs), which replace the burnable absorber rods primarily used in Westinghouse Pressurized Water Reactors (PWR). The TPBARs are irradiated at the Tennessee Valley Authority Watts Bar Nuclear Plant Unit 1 (WBN1) for a year and a half before they are taken to an extraction plant to harvest the tritium for subsequent use in the nuclear weapons stockpile. The first irradiation cycle at WBN1 utilized 32 TPBARs. Since then the number of TPBARs per cycle has increased to 544.

The goal of the PNNL program is to increase the TPBAR quantities to around 1700 per cycle, which is comparable to about 1150 grams of tritium produced per year. However, this introduces some challenges. The number of TPBARs that can be irradiated per cycle is limited due to the amount of tritium each TPBAR releases into the environment. Adding the desired amount of TPBARs would put the system over acceptable release levels. Also, the primary mission of WBN1 is electricity generation, not tritium production. Producing tritium increases fuel costs, creates core design complications, presents public policy obstacles, and causes operational difficulties at the unit. For these reasons, PNNL is looking for alternate options for its tritium technology program. This feasibility study looks at a sodium cooled, fast spectrum, small modular reactor design for application to tritium production.

2.2 Small Modular Reactor Application: The SPRISM

Small Modular Reactors (SMR) offer a number of advantages for tritium production. A SMR can be designed primarily for dedicated tritium production, with electricity production as a secondary objective. This would relieve some of the difficulty associated with using a system that prioritizes electricity generation over tritium production. Additionally, multiple units can be constructed based on demand at greatly reduced cost compared to a commercial Light Water Reactor (LWR).[2,3] PNNL suggested several SMR design candidates, one of which is the SPRISM. This study investigates the practicality of modifying General Electric-Hitachi's (GEH) SPRISM design with the primary objective of producing tritium for maintaining the current nuclear weapon stockpile and the secondary objective of producing electricity. The results of this

study will be reviewed by PNNL for consideration in using the SPRISM for dedicated tritium production.

The SPRISM (Super-Power Reactor Innovative Small Module) is an advanced liquid metal reactor design created by GEH. It is a larger version of the PRISM, and it retains the characteristics of the PRISM, notably its passive safety systems. It is a 1000 MWt, sodium-cooled, pool-type, small modular fast reactor, and it utilizes reprocessed used light water reactor fuel, which plays a key role in reducing used nuclear fuel waste. In fact, this has the potential of reducing the waste decay times from hundreds of thousands of years to a mere few hundred, because the SPRISM can burn uranium, plutonium, and minor actinides. The SPRISM may be accompanied by the advanced recycling center on site where the fuel reprocessing will take place.

2.3 Project Objective

The project objective is to investigate the feasibility of using the SPRISM for tritium production. The study began with the intention of choosing a fuel type, fuel composition, and a TPBAR position distribution such that tritium production is maximized. Also, two methods of tritium production inside the reactor were to be investigated: a breeder blanket application and a homogenous coolant mixture application. The investigation into the homogenous coolant mixture was halted, since its application was outside the scope of this project. Also, exploring all three fuel types for the SPRISM, different fuel compositions, and various TPBAR position distributions proved to be ambitious for accomplishment within the allotted project time frame. Due to the fact that the SPRISM is a young design, and there are currently none in operation, finding the information necessary to model the reactor proved difficult, and several assumptions had to be made. For instance, for the purposes of this project when information was unavailable, the SPRISM design is assumed to be comparable to the design of the PRISM reactor. In reality, the SPRISM is slightly bigger and has a larger power density, but there is much more information available for the PRISM design. As a result of complications such as these, the objective was narrowed to analyze a single fuel type, fuel composition, and TPBAR distribution to produce tritium and the reactor core with added TPBARs was characterized based on these choices.

2.4 Approach

This project is comprised of four primary areas of study: thermal hydraulics computation and analysis, neutronics, chemical and material composition research, and safety and shielding analyses. Additionally, an economic analysis for the TPBAR application was performed. Specific goals and tasking for each area are summarized in the following paragraphs.

Scott Thrower performed the neutronics modeling and analysis. DRAGON was initially chosen for its versatility and its ability to produce accurate results for reactors operating with fast spectrums. However, DRAGON cannot perform whole-core calculations without additional software. Research later revealed a doctoral thesis that contained and modifiable MCNP input deck for the SPRISM core.[4] With this available to us, shifting from DRAGON to MCNP seemed feasible with the remaining time. Thus, MCNP was used for modeling the tritium production application for the SPRISM. Prior to modeling, materials and fuel inputs were required.

Chad O'Hagan spearheaded the research for the chemistry and materials compositions to be used in the reactor. The goal was to investigate a means of producing tritium in desired quantities while preventing a substantial loss in neutron population and maintaining reactor core integrity and safety. Additionally, a means of extracting this tritium must be considered. The two methods that were initially under consideration for producing tritium were the homogeneous coolant mixture application with a tritium-producing compound and a tritium breeder blanket application. However, the homogeneous coolant application study was later halted due to its complexity. Lithium is the primary element used for producing tritium in sufficient quantities, so a lithium compound would be required. Studies of the different compounds included lithium concentration, its state, cross section comparisons and optimization. By-products produced, tritium diffusion, and tritium extraction were also considered. The materials research and decisions based on this research are included in Section 3. This research was also used for assisting the core safety analysis.

Sara Loupot performed an extensive safety analysis. Her analysis explored tritium release effects and associated personnel exposure risks. Two scenarios were analyzed. First, the dose from the normal release rate of TPBAR leakage was determined. Second, a worst-case scenario in which all of the predicted inventory of TPBARs simultaneously fail was investigated. Dose rates to both radiation workers and the public were determined based on NRC regulatory limits. A maximum amount of TPBARs that can be used based on these release limits was determined. She also looked into the systems that make the SPRISM design inherently safe. Since none of these systems are affected by the addition of TPBARs in the core, it was assumed that the accident scenarios analyzed for the core without TPBARs by Sumner would serve as a sufficient worst-case scenario analysis. Additionally, she developed a model of the reactor based on the dimensions available for the PRISM reactor. Because the SPRISM is a young design, information about its specifics is scarce and proprietary. For this reason, the assumption must be made that a shielding analysis for the very similar, yet slightly smaller PRISM design is sufficient for this preliminary feasibility study of the SPRISM. The reactor was modeled using MCNP5. A source equivalent to the flux in the outermost assembly of the core was placed in the core and the subsequent neutron transport was calculated. Neutron absorption was then determined in the axial and radial directions to ensure that neutron dose outside the reactor was negligible.

Thermal hydraulic and application economics analyses were addressed by Timothy Crook, and are included separately.

3.0 Materials (Chad O'Hagan)

3.1 Introduction

Prior to core modeling in Dragon and MCNP, the selection of general materials used in the SPRISM core, the fuel composition to be used, and the TPBAR design were required. Since the purpose of this project was to apply tritium production to the SPRISM design, the choices in materials were relatively simple. The senior design project proposed by PNNL suggested minimal changes in the SPRISM design while integrating the TPBARs. This means that, ideally, the only modifications required would be those of the TPBARs and their assemblies. As a result, the SPRISM design will remain unchanged for the purposes of modeling, though some physical changes may be required for dedicated tritium production if this application is selected for the tritium production program. The remaining decisions involved choosing the fuel for core modeling and assessing the current TPBAR design.

3.2 SPRISM Design

Since the aim for this study is to check the feasibility of producing tritium in the SPRISM core, modifications to the SPRISM design will be minimized. The TPBAR assemblies took the place of the boron burnable absorber rods at Watts Bar 1. Since the SPRISM does not use burnable absorber rods, TPBARs will have to take the place of fuel rods in selected assemblies in the core. A model will then be used to demonstrate tritium production feasibility with these parameters.

3.3 Fuel

The SPRISM can use three different types of fuel: metal, oxide, and nitride fuel. All fuel types will be reprocessed used nuclear fuel inherent with the SPRISM-advanced recycling center concept. Thus, the fuel will contain uranium, plutonium, and minor actinides. This yields an added bonus to tritium production, since burning these heavy elements has the potential to reduce fuel waste storage times from hundreds of thousands of years to a mere few hundred years. After exploring the advantages and disadvantages of each fuel type, nitride fuel was ultimately chosen for this feasibility study. This subsection will explore the different fuel types with an emphasis on nitride fuel and the assumptions made for model development.

3.3.1 Metal and Oxide Fuel[4]

The material properties of the metal and oxide cores occupy the opposite sides of the property spectrum of the three fuels. The metal core will have a relatively high thermal conductivity compared to the other fuel types, which is about 20 W/m*K. This higher thermal conductivity will yield lower fuel centerline temperatures, a safety advantage. The fuel composition will have a lower moderation effect for neutrons compared to the other fuels – fewer moderated neutrons will increase actinide fuel utilization which maximizes tritium production. Metal fuel will not react with the sodium coolant given cladding defects or failure. However, fission gas bubble

collection in voids leads to noticeable pin swelling. The oxide core will have the smallest conductivity of the three fuel types, 5 W/m*K, which yields higher centerline temperatures. Also, oxide fuel will have the highest melting temperatures, above 3000 K. The presence of oxygen gives this fuel higher neutron moderation compared to the other fuels, which leads to a softer neutron energy spectrum. Neutron moderation may or may not have a significant effect on tritium production depending on the neutron flux distribution. A comparison analysis of the MCNP code for each fuel type should reveal any changes. However, current time constraints prevent this inquiry. Oxide fuel is prone to cracking from irradiation, and is incompatible with the sodium coolant. Stronger cladding materials will be required to avoid the risk of a violent reaction with the coolant.

3.3.2 Nitride Fuel[4]

The properties for the nitride core lie between those of the other fuels. The fuel will have a relatively good thermal conductivity, 15 W/m*K, and a melting temperature between metal and oxide fuels. See Figure 1 for a comparison between nitride and oxide fuel. The fission gas collection behaves similarly to the metal fuels, and uranium nitride theoretical density, 13.32 g/cc, lies between the oxide and metal fuels. The nitride composition provides only one moderating atom per heavy metal atom, which gives a neutron energy spectrum between the oxide and metal spectrums. This effect may or may not prove to be beneficial for tritium production. A comparison will be needed between all three fuel types to explore this. Additionally, like metal fuel, nitride fuel is chemically compatible with sodium.

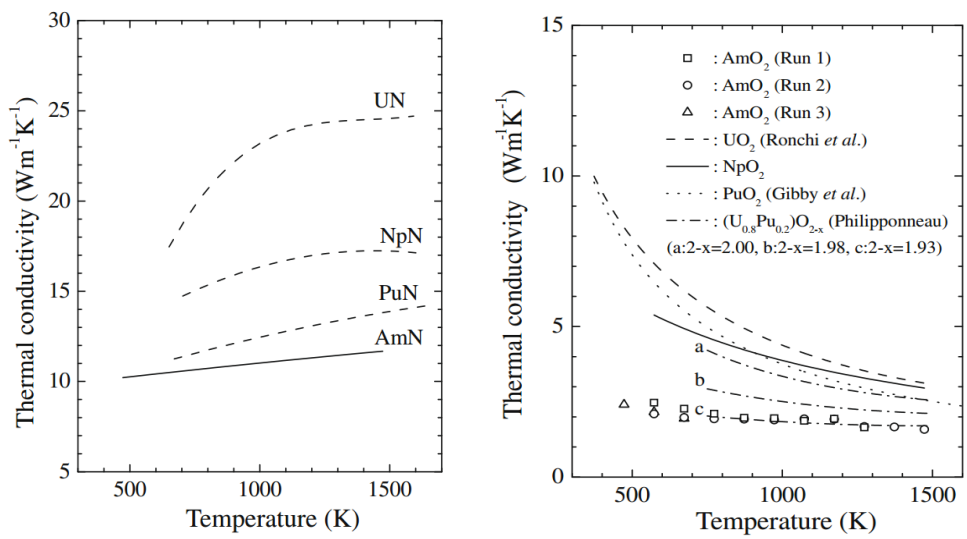

Figure 1: Thermal conductivity comparisons for Beginning of Life values[5]

Some major disadvantages of nitride fuel should be considered. Nitrogen-14 has a large cross section for neutron absorption, which will soften the neutron energy spectrum. However, the major concern is the carbon-14 formation from the ^{14}N (n, p) ^{14}C reaction. Nitrogen-14 is the

most abundant naturally occurring nitrogen isotope, and the 5730-year half-life of carbon-14 will significantly add to fuel waste radiotoxicity, thereby paralyzing the toxicity-reducing benefit of the SPRISM-advanced recycling center. This effect can be reduced by enriching the fuel with nitrogen-15, but the enrichment process is very expensive. The other disadvantage is that there is less development and utilization of nitride fuel compared to other fuels. That is, no high power level nitride-fueled reactors have been built and commercial-scale reprocessing of used light water reactor fuel into nitride fuel has not been demonstrated. This is not to say that little or no research and development have accompanied nitride fuel. On the contrary, this fuel type has been explored in parallel with oxide fuel since the 1950's, with a short lapse in interest in the 1980's and early 1990's.[6] Nitride fuel shows promise for fast reactors and several systems have been investigated. Along with its high thermal conductivity and high melting point, nitride fuel has a wide solubility between uranium nitride, plutonium nitride, and minor actinide nitrides. This results in a NaCl-type crystal structure. The current challenge is fabrication. Oxygen and carbon impurities tend to appear in the nitrides during fabrication, which will hinder fuel performance. These impurities can be significantly reduced by fabricating nitride fuel from metal fuel instead of oxide fuel.

In summary, nitride fuel shows promise for future use in fast reactors due to its thermal hydraulic properties. However, it will increase carbon-14 radiotoxicity to the environment, which will hinder radiotoxicity reduction efforts. Also, nitride fuel has limited performance experience in reactors, and it is challenging to fabricate fuel pure enough fuel to be suitable for a large-scale performance. In contrast, metal fuel has been used in reactors, is not as difficult to fabricate, and does not increase environmental radiotoxicity. This being said, nitride fuel was chosen for the SPRISM in this study, because it possesses the best qualities of both metal and oxide fuels. Nitride fuel will not react violently with sodium, it has a higher melting temperature than metal fuel, and it has a relatively high thermal conductivity. Though all aspects are to be considered, the focus of this study is tritium production. Thus, a reliable means of fabricating nitride fuel at the required purity is assumed to exist. A complete feasibility study will need to include all fuel types at different fuel compositions and different TPBAR position distributions.

3.3.3 Application of Nitride Fuel to This Feasibility Study

Limited information about the SPRISM fuel compositions is available. As a result, some assumptions needed to be made in order for a composition for use in this project to be determined. For the purposes of this study, all uranium is assumed to be natural uranium, the fuel does not contain any fission products, the internal and radial blanket assemblies have the same composition at the beginning of the cycle, and the minor actinide isotopic ratios were set equal to those of another sodium-cooled fast reactor design. Additionally, all respective assemblies will contain the same compositions. Figure 2, below shows the assembly layout of the core that was used in this project.

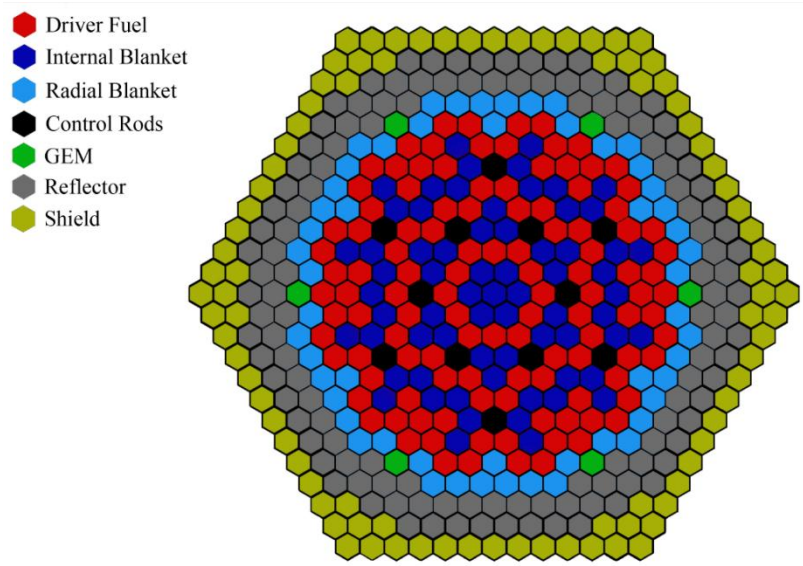

Figure 2: Assembly layout of the SPRISM core[4]

The SPRISM Nitride core contains three different fuel assemblies: driver fuel, internal (breeder) blanket, and radial (breeder) blanket. The only differences in these assemblies are their position distributions in the core and their fuel composition. For the purposes of this study of finding a critical fuel composition, the internal and radial blankets are assumed to be the same fuel compositions. The proposed fuel compositions are tabulated in Table 1. These compositions come from a study in the effects of fuel type in SPRISM safety characteristics, and were shown to yield neutron multiplication factors slightly above one. Time constraints prevent further investigation into other possible compositions for optimizing tritium production. Another feature of the SPRISM core is the Gas Expansion Module (GEM). The six modules assist in reactivity control during an accident, and will not play a vital role in this study.[4] Additionally, the control rods were assumed to be completely withdrawn for the entire study.

Table 1: Proposed nitride fuel composition[4]

Nuclide	Nitride (weight %)	
	Driver	**Blanket**
U-234	0.004	0.005
U-235	0.484	0.637
U-238	67.647	88.990
Pu-238	0.104	0.019
Pu-239	15.656	2.845
Pu-240	3.969	0.721
Pu-241	1.865	0.339
Pu-242	0.307	0.056
Np-237	2.191	0.398
Am-241	1.818	0.330
Am-243	0.372	0.068
N-14	4.989	4.997
N-15	0.594	0.595

3.4 Tritium Production and the TPBARs

This subsection reviews the tritium production process, the research and development that led to the current TPBAR design, and TPBAR design performance. Based on this research, assumptions and decisions in the SPRISM and TPBAR design were made for the purposes of this study. The model will assume pure sodium coolant, with no contaminants. Some contaminants could endanger TPBAR integrity if high enough concentrations existed. The model will also apply a TPBAR assembly design concept for use in the core. That is, TPBARs will take the place of the fuel rods in selected fuel blanket and driver assemblies. Detailed information is unavailable to develop a design for the assembly, and neglecting such a design will not violate the requirements for this study. Finally, the TPBAR length will need to be more than three times shorter than the current design due to the shorter active core length in the SPRISM.

3.4.1 Breeding Tritium

Lithium is today's primary source for tritium production. Tritium is also produced from deuterium in a conventional heavy water reactor, but the U.S. does not currently utilize heavy water reactors. Few other sources exist, such as cosmic ray interactions with the nitrogen in the atmosphere and the minute amounts produced in fission reactors, but none produce tritium on the scale required for its demand. Lithium-6 and lithium-7 transmutate into tritium using the following neutron-induced reactions:

$$^{6}_{3}Li + ^{1}_{0}n \rightarrow ^{3}_{1}H + ^{4}_{2}He$$

$$^{7}_{3}Li + ^{1}_{0}n \rightarrow ^{3}_{1}H + ^{4}_{2}He + ^{1}_{0}n$$

Lithium-6 and lithium-7 will mostly absorb neutrons of lower energies. The neutron absorption cross sections may hinder tritium production in a fast reactor, but this study should confirm either way.

3.4.2 History

The research and development of tritium production technology spans decades. Much of the work took place within the Coproduct Program at the Hanford site in the mid-1960's. This program combined both tritium and plutonium production using the N Reactor, hence the name coproduct, on a large-scale. Production for both components using the same reactor was "economically attractive", and after four operational tests were conducted, scientists noted that "no fuel performance difficulty attributable to the target element performance was experienced."[7] That is, using a single reactor to produce both components instead of only plutonium was not an issue. Thus, a dual purpose reactor is not out of the question.

3.4.3 Tritium Breeding Candidate: Why Lithium Aluminate?[8]

Initially, a tritium-breeding candidate needed to be identified. The candidate would need to be a stable lithium compound, so the first task involved looking at all possible lithium compounds. Research revealed a study based on declassified results from documents regarding large-scale tritium production programs in fission reactors. This study reviewed twenty-eight lithium compounds as potential target materials, which included halides, lithium sulfate, nitrate, carbonate compounds, and several others. Organic compounds were excluded due to instability under irradiation, and intermetallic compounds were excluded due to the lack of information on them at the time. Lithium metals were considered in other studies. This research revealed that the primary candidates in the 1960's were lithium silicate and lithium aluminate.

Though the selection criteria were specific to the Hanford site N Reactor operational and production requirements, they are applicable to Watts Bar 1, and some are applicable to the SPRISM. The candidate materials were reviewed for their physical, chemical, and neutronics properties as well as the feasibility in fabricating them and extracting the tritium. The lithium

density needed to be at least 0.1 g/cc, and the melting point for the compound must exceed 250 C, or 523 K. Note that the melting temperature for sodium is 370 K, which means that the sodium coolant temperature must exceed 370 K for normal operations. Of all the halides (LiCl, LiBr, LiI, LiF), lithium fluoride had the highest density at 0.696 g/cc. Its melting point is 1113 K, and its boiling point is 1954 K. At one point, it was used for tritium production at the N reactor, but scientists found that it was prone to swelling and slug rupture. This effect was probably from the release of fluorine gas. Fluorine gas is very reactive due to its electronegativity. It would react explosively with the tritium, react with the metals used in the SPRISM reactor, and is poisonous to humans. So, lithium fluoride could not be tolerated in the system. Lithium nitrate is soluble in water, and has a melting point at 527 K. It was not stable enough for the N reactor, which used water coolant. Lithium carbonate produced the corrosive products lithium oxide and carbon dioxide when heated beyond its melting point. A number of other compounds were also rejected for their instabilities and corrosive proper ties.[1] Some of the rejection criterion do not apply to a sodium-cooled fast reactor, but the aforementioned primary candidates may still work for the SPRISM based on the chemistry. Their melting temperatures will be the limiting factors.

Ultimately, lithium aluminate was selected, and has been used for tritium production ever since, including production at Watts Bar 1. Lithium aluminate has a melting temperature of 1883 K and a lithium density of 0.268 g/cc. It is a ceramic and has a rhombohedral structure below 1173 K and tetragonal structure above 1173 K. Lithium silicates have a 0.356 g/cc lithium density and a melting point at 1473 K. However, they are relatively corrosive and are soluble in water. Again, water solubility does not apply to the SPRISM. However, since lithium aluminate is currently and successfully used in today's TPBAR's, and since extensive research and analysis in the various compounds led to lithium aluminate, continuing to explore the potential use of this compound for this project made sense.

3.4.4 The TPBAR and the TPBAR Assembly and its Fabrication

The next step is fabricating the target material and designing an absorber rod and an assembly for the rods. The fabrication and design must maintain integrity during at-power operations, handling, and shipping. Tritium extraction needs to be achievable and efficient, meaning most, if not all, tritium can be extracted, quantified, and stored. Also, effects on the reactor plant need to be considered. Indeed, this portion of the project is key. The combination of these considerations with a cost benefit analysis will be used to determine an optimal balance that maximizes the amount of tritium safely produced and extracted and minimizes the changes in the SPRISM, TPBAR, and TPBAR assembly designs.

Upon analyzing the unclassified TPBAR design basis descriptions and some performance evaluations, an interesting conclusion was made: A change in this design need not be made with the exception of its length. The TPBAR is about 152 inches from tip to tip at room temperature, and has an outer diameter of 0.381 inches. The active core length for the SPRISM is 47 inches,

3.234 times smaller than the current TPBAR design. So, the active length for the TPBAR will need to be reduced to about 47 inches. An axial layout of a single TPBAR and an isomeric section of a TPBAR are shown in Figure 3.

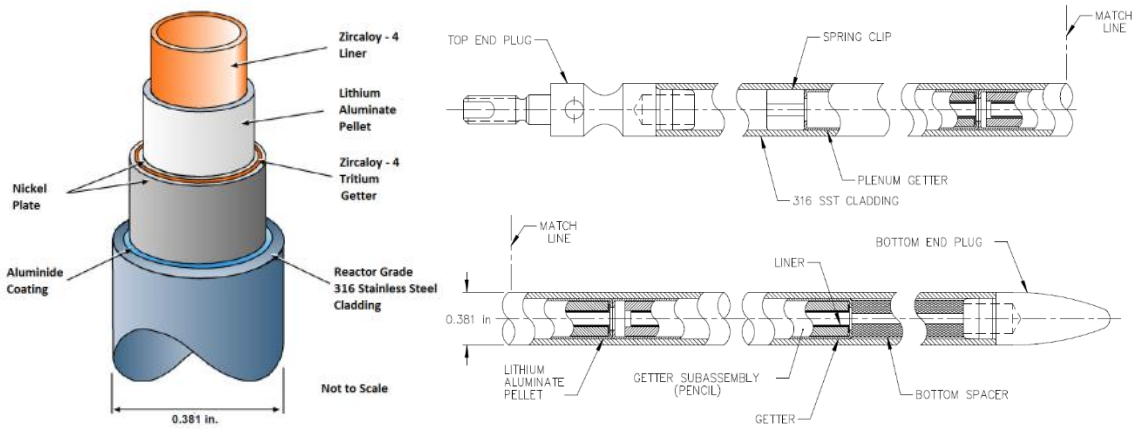

Figure 3: An Isomeric Section of a TPBAR and an Axial Layout of TPBAR Components[9]

The TPBAR is designed to produce and retain tritium, and is similar in size and nuclear characteristics to standard, commercial PWR, stainless-steel-clad burnable absorber rods. The isomeric section above shows some of the components in the rod. The inner-most piece is the Zircaloy-4 tube liner. Its purpose is to react with oxygen in any existing tritium oxide molecules. The reaction is an oxidation reaction that frees the tritium, keeping it in its pure form. Additionally, the inner liner provides mechanical support to prevent axial movement of the pellets in case any pellets crack during handling or operations. Next is the lithium aluminate pellet, the source of the tritium production. When exposed to a neutron flux, the lithium-6 isotopes absorb the neutrons, simulating the burnable absorber rods and producing tritium. Lithium's natural abundance is mostly lithium-7, so the pellet will contain enriched lithium-6 content. When the tritium is produced, it chemically reacts with the nickel plated Zircaloy-4 getter, a tube that encircles the annular ceramic lithium aluminate pellets, and becomes trapped as a metal hydride. The nickel plating prevents oxidation of the Zircaloy–4 surfaces. This oxidation would reduce the tritium absorption rate. Finally, the aluminide coating prevents tritium from diffusing outward from the TPBAR to the reactor coolant. Reactor grade 316 stainless steel cladding makes up the outer tube, which prevents hydrogen from diffusing inward from the coolant to the TPBAR getter. The SPRISM utilizes sodium for coolant, so hydrogen diffusion from water prevention is of little concern. Since the 316 stainless steel was originally developed for use as fuel cladding in a sodium-cooled fast reactor, it will suffice as a liner between the inner portions of the rod and the sodium. This conclusion is based on the other materials used in the reactor. Also, the tritium diffusion rate from the getter into the coolant might be higher without the cladding.

The composition of all these layers, with the exception of the cladding, is the "pencil." At one point, the TPBAR was composed of multiple pencils of about twelve inches in length, more or less. As of now, the TPBARs at Watts Bar 1 are constructed of a single piece, one long pencil. Both designs demonstrate the variably in the length, a very useful feature. The variability was intentional, and provides optimal flexibility in reactor core design. In effect, this feature provided additional justification to use the existing TPBAR design to produce tritium in the SPRISM reactor.

All these layers, including the cladding, are assembled with end plugs, a spring clip, and a spacer to form the entire TPBAR. The end plugs, welded to each end, provide hermetic closure of the TPBARs to keep all gasses including the tritium contained within the rod. The spring clip holds the pencils in place during the pre-irradiation handling and shipping. The upper and lower portions of the TPBAR are shown in Figure 3, above. The various pencil layers can be seen in these portions. This means of construction keeps the design simple, which reduces cost and facilitates tritium extraction at the Savanna River site. Certainly, keeping with this simple design would be ideal for the SPRISM application.

The Watts Bar 1 TPBAR assemblies hold up to twenty-four TPBARs. Due to the neutron absorption that occurs in the TPBARs, they act as a useful substitute for the boron absorber rods typically used in PWRs. In fact, the TPBAR assemblies take the place of the typical Westinghouse burnable absorber rod assemblies used in PWRs. Figure 4 shows a TPBAR assembly.

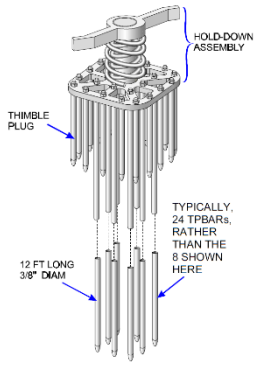

Figure 4: TPBAR Assembly[9]

These assemblies are very similar to the original absorber rods, and they fit in a 17x17 fuel assembly in the reactor. Only eight TPBARs are shown in Figure 4 along with thimble plugs acting as place holders for the other TPBAR positions. This TPBAR assembly design will need to be modified to be compatible with the hexagonal SPRISM core. Currently, few details of the core design are publically available, so a suggested design modification cannot be made. As a result, an assumption was made for the purposes of modeling and continuing with this feasibility study. TPBARs will take the place of fuel rods in selected fuel assemblies within the core, thus

the TPBAR assembly will mimic that of a fuel assembly in terms of placement and dimensions. For this to work, the TPBAR diameter will be reduced, while maintaining dimension ratios, to match the dimensions of the fuel rods. This is strictly for the purpose of replacing selected fuel rods with TPBARs in MCNP and is discussed in more detail in Section 4. In this case, the modified assembly will serve as a concept.

3.4.5 TPBAR Performance

Measured TPBAR performance further demonstrates the TPBAR design viability for use in the SPRISM application. Post-irradiation testing in the late 1990's at Watts Bar 1 and continued successful use since then have shown that these rods performed as designed. In the summer of 1997, thirty-two TPBARs were fabricated for approved irradiation testing in the Watts Bar 1 core. They underwent an irradiation period for one full cycle, a seventeen-month irradiation period. The plant experienced no unfavorable effects during its operation with the TPBARs installed. Measured tritium concentrations in the reactor coolant met design criteria of less than 6.7 Ci per TPBAR per year, and spent fuel pool tritium analyses showed no increase in tritium concentrations while the TPBARs were stored in the pool after irradiation in the reactor. Visual inspections showed no unexpected levels of corrosion, and the ease of TPBAR removal from their assemblies and installation into shipping arrays indicated that there was little change in the TPBAR dimensions. Subsequent nondestructive and destructive post-irradiation examinations at the Argonne National Laboratory near Idaho Falls and at PNNL revealed that the TPBARs performed as expected. TPBAR structural integrity withstood irradiation and post-irradiation handling and shipping. The measured amounts of tritium produced agreed with the predicted calculations, and gamma analyses showed an even power distribution in the rods. As a result of the successful irradiation testing, no design changes in the TPBAR were called for. They performed as expected.[7]

The two main differences between the SPRISM and Watts Bar 1 may or may not prove to be problematic for the current TPBAR design. The SPRISM will operate in the fast spectrum, whereas Watts Bar 1 is a thermal reactor. The TPBAR will likely perform differently at significantly higher neutron energies due to the change in cross sections. This project only demonstrates the TPBAR application with an MCNP model. An irradiation test similar to that performed at Watts Bar 1 in the late 1990's will need to be performed to confirm the TPBARs' performance in a fast reactor. Secondly, the sodium coolant has different properties than water coolant. If oxygen and chlorine were present in the sodium coolant, the hypochlorite ion (OCl^-) could attack the 316 stainless steel TPBAR cladding. So, the presence of sodium hypochlorite in the coolant will degrade the TPBARs via pitting corrosion. As with water coolants, chemistry control would be required for the PRISM.

3.5 Conclusion

For the purposes of this feasibility study, the model will assume pure sodium coolant, the fuel compositions given in Table 1, and only a few modifications to the current TPBAR design. There are two exceptions to the current TPBAR design. The active TPBAR region will need to be 47 inches in length to match that of the SPRISM active core region. Also, the TPBAR assembly will need to be hexagonal in order to be compatible with the SPRISM core. Since detailed design documents are unavailable, only a design concept for the assembly will be used. The TPBAR assembly will simply replace chosen fuel blanket assemblies in the core. This will serve as an assumption for the model. Decades of research, development, testing, and performance led to the current design and use of the TPBAR. Making any significant changes to the TPBAR for the purposes of this study would make little sense. Also, minimizing design changes adheres to the guidelines of PNNL's senior design proposal. Thus, this study applies the current SPRISM and TPBAR designs with minimal modifications.

4.0 Neutronics (Scott Thrower)

4.1 Goals

There were two main goals for the neutronics portion of the project. The first goal was to modify the loading of the SPRISM to enable the production of 1150 grams of tritium a year in the outermost breeder blanket. The second goal was to optimize power production of the reactor with its tritium production. These goals were chosen based upon discussions with the PNNL advisor, who wanted 1150 grams of tritium a year with core lifecycles of 1.5 years.

4.2 Methodology

There were four major steps necessary to accomplishing the above goals. The first step was to create a neutronics model of the core without modifications. The second step was to insert lithium for the breeding of tritium in the form of modified TPBARs into the core lattice. The third step was to determine how many modified TPBARs would be necessary to produce 1150 grams of tritium. The final step was to optimize power production in the core with the tritium production by altering the fuel composition to obtain a more favorable burn-up.

4.3 Modeling

MCNP was the primary code used for neutronics design. Originally, DRAGON was used. However, DRAGON cannot perform whole-core calculations without additional software. This was realized after DRAGON input decks for multiple assemblies were completed. Also, a MCNP input deck for the SPRISM core was found in a doctoral thesis by Ghrayeb.[10] Thus, with the recommendation of the project faculty advisor, MCNP was chosen as the primary neutronics code. The DRAGON decks that were started are included in Appendix A. MCNP is a "Monte Carlo N-Particle code."[11] It uses probabilities to predict particle interactions in a given transport problem for a three-dimensional geometry, and can be used for neutron, photon, electron, or coupled neutron/photon/electron transport. It can also be used to calculate eigenvalues for critical systems.[11] The main advantage of MCNP is that it uses continuous cross-sections, so collapsing cross-sections into energy groups is unnecessary. The generation of graphics based feedback of input decks is another useful feature in MCNP. More information on MCNP can be found in Appendix B.

4.3.1 Problem Definition

The modeling of the unmodified core began with using the MCNP input contained in "Investigations of Thorium Based Fuel to Improve Actinide Burning Rate in SPRISM Reactor, a Thesis in Nuclear Engineering," by Shadi Z. Ghrayeb.[10] After reformatting the code by removing

invisible characters, the input was changed to reflect the SPRISM core parameters. These parameters were taken from "Effects of Fuel Type on the Safety Characteristics of a Sodium Cooled Fast Reactor," a thesis by Tyler Sumner.[4] This thesis was chosen because of the specificity of the fuel loadings as well as the thermal hydraulics analysis it contained. Reproducing one of the cores contained in this thesis provides a benchmark to check the accuracy of the modeling methods chosen for both the neutronics and thermal hydraulics portions of the project. The parameters from the thesis also provided a starting place for design, which offered a time-management advantage for a focused study on tritium production instead of fuel loadings.

4.3.2 Design Parameters

The fuel in this core model uses two compositions, one for the driver fuel assemblies and the other for the radial and inner (breeder) blanket assemblies. The driver fuel composition provides the initial excess reactivity necessary to allow the core to be critical. Fuel pins for the driver fuel have an inner radius of 0.27385 cm, a gap radius of 0.3161 cm, and a cladding radius of 0.372 cm. A modeled driver fuel pin cell is shown in Figure 5.

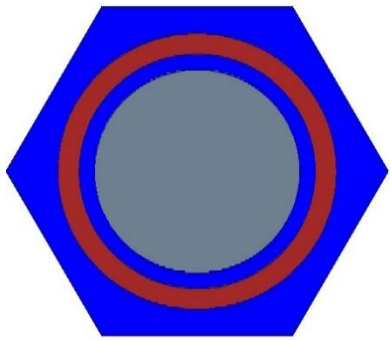

Figure 5: A graphical representation of a fuel pin cell.

Figure 5 above shows the fuel (gray), the sodium (blue), and the cladding (red) layout. The breeder fuel composition increases the k_∞ of the system late in the core's life by converting breeder material to fissile material. Breeder pins have a fuel radius of 0.5023 cm, a gap radius of 0.5446 cm, and an outer cladding radius of 0.6005 cm. A breeder fuel pin cell is shown in Figure 6.

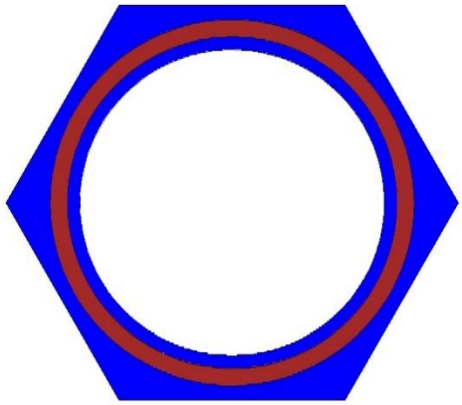

Figure 6: A graphical representation of a breeder pin cell.

Figure 6 above shows the fuel (white), the sodium (blue), and the cladding (red) layout. The driver and breeder compositions, taken from the thesis by Sumner, are shown in the following table.

Table 2: Fuel compositions for the driver and breeder fuel pins.[4]

	Weight Fraction	
Isotope	Driver	Breeder
U-234	0.00004	0.00005
U-235	0.00484	0.00637
U-238	0.67647	0.8899
Pu-238	0.00104	0.00019
Pu-239	0.15656	0.02845
Pu-240	0.03969	0.00721
Pu-241	0.01865	0.00339
Pu-242	0.00307	0.00056
Np-237	0.02191	0.00398
Am-241	0.01818	0.0033
Am-243	0.00372	0.00068
N-14	0.04989	0.04997
N-15	0.00594	0.00595

The primary components of the driver are U-238 and Pu-239, and the primary isotope in the breeder is U-238. Because cross-sections are involved, a temperature must be selected for MCNP to pull data from cross-section libraries. A temperature of 900 K was chosen for fuel regions based upon the thermal data available in the thesis by Sumner.

Other rods of importance in the core include the reflector and shield rods, shown in Figures 7 and 8, respectively.

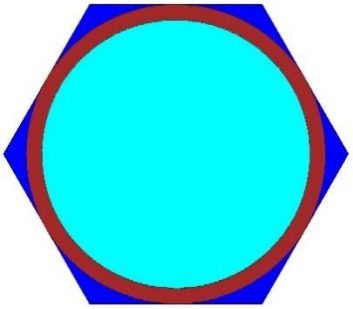

Figure 7: A graphical representation of a reflector rod cell.

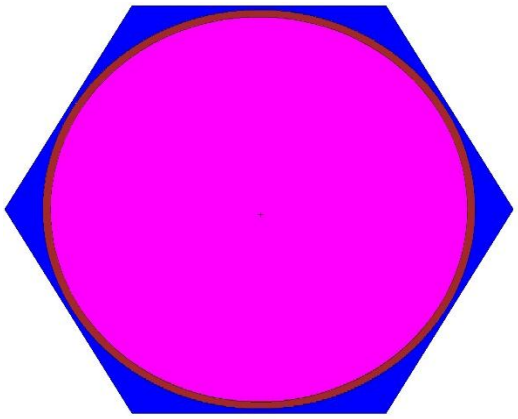

Figure 8: A graphical representation of a shield rod cell.

The reflector (teal) and cladding (red) radius for the reflector cell are 0.8393 cm and 0.9375 cm, respectively. Shield cells are significantly larger, having radii of 2.6258 and 2.724 cm for the shielding (pink) and cladding (red), respectively. The cladding and reflector materials are HT9, a type of austenitic stainless steel, and the shielding is boron carbide. Temperatures for the cross-sections were kept at 900 K for the cladding HT9 and 600 K for the reflector HT9 based upon the thesis by Sumner.[4] The weight percentages of elements contained in HT9 and boron carbide are in the following tables.

Table 3: HT9 material isotopic compositions.

	Cladding	Structure
Isotope	Weight Fraction	
Fe-56	0.8742	0.847
C-12	0.00145	0.0019
Si-0	0.001	0.0036
Mn-55	0.0045	0.0059
Ni-0	0.0046	0.0053
Cr-0	0.0979	0.1179
Mo-0	0.0123	0.0099
V-0	0.002	0.0031
Nb-93	0.0018	0.0002
P-31	0.00002	0.0049
S-32	0.00003	0.00019
N-14	0.0002	0.000005
W-0	0	0.0001

Table 4: Boron carbide material isotopic compositions.

Isotope	Weight %
B-11	0.78261
C12	0.21739

Once these individual cells had been defined they were combined into a universe to create an assembly. Differences in the cell sizes meant that a different number of cells will be contained in each assembly. Driver fuel assemblies contain 271 cells, breeder assemblies contain 127 cells, reflector assemblies contain 61 cells, and shield assemblies contain 7 cells. These assemblies are shown in Figures 9 through 12, respectively.

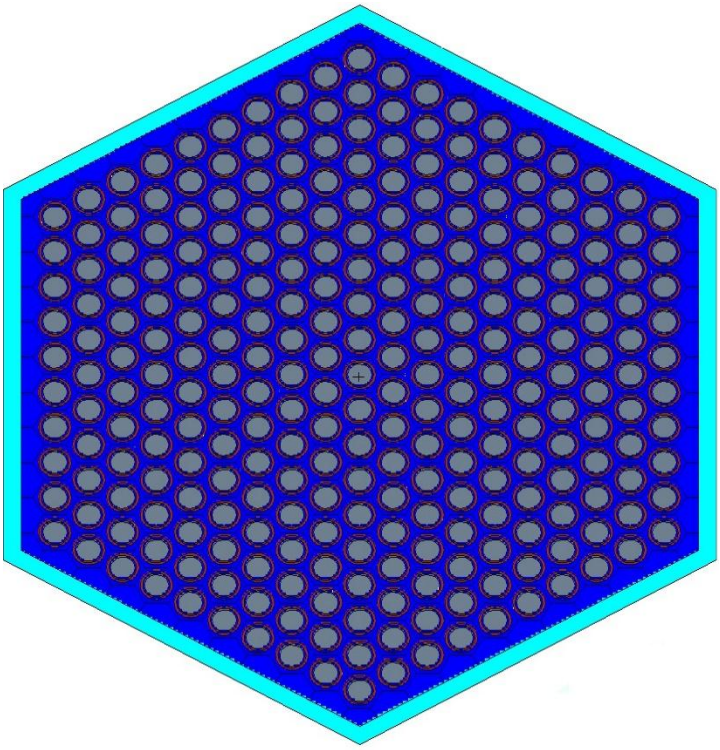

Figure 9: A graphical representation of a driver fuel assembly.

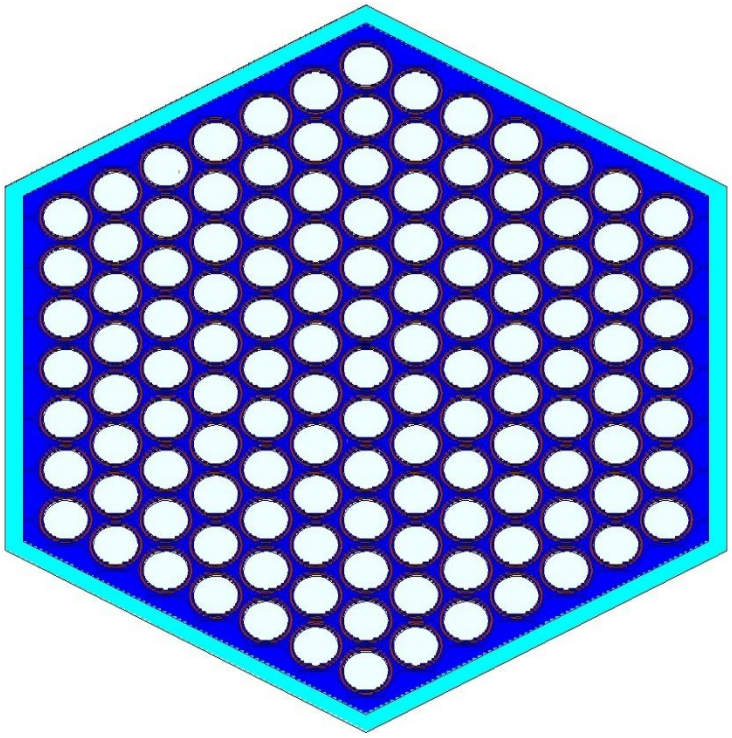

Figure 10: A graphical representation of a breeder fuel assembly.

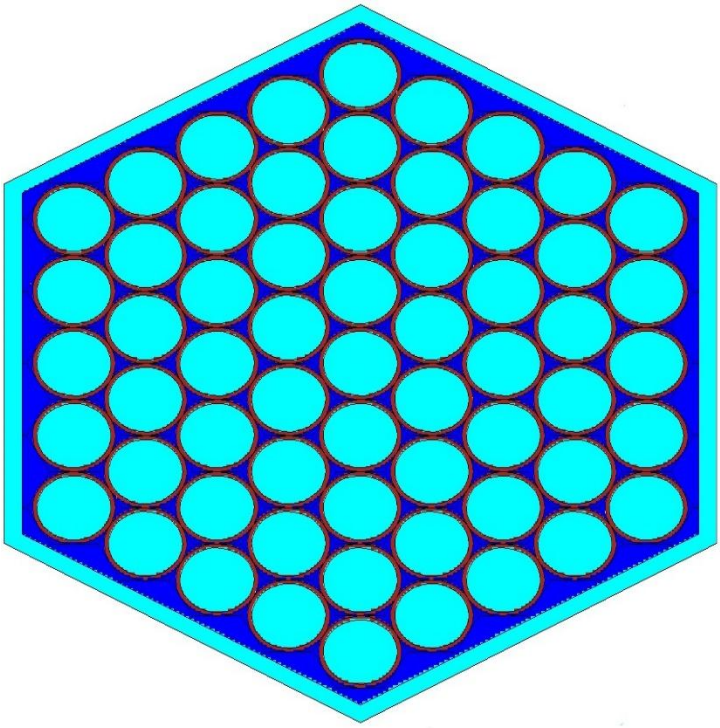

Figure 11: A graphical representation of a reflector assembly.

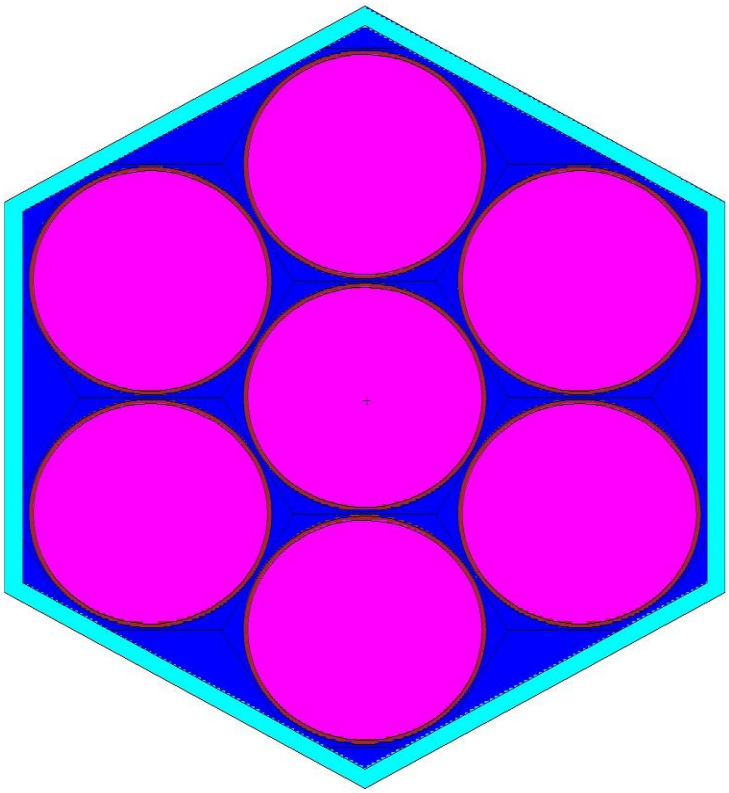

Figure 12: A graphical representation of a shield assembly.

Each of the hexagonal assemblies in the core is a right hexagonal assembly with a pitch of 16.142 cm. The height of each assembly is 1 m.

Once generated, these assemblies are combined into a 1/6th core model. The 1/6th model of the unmodified core is shown below.

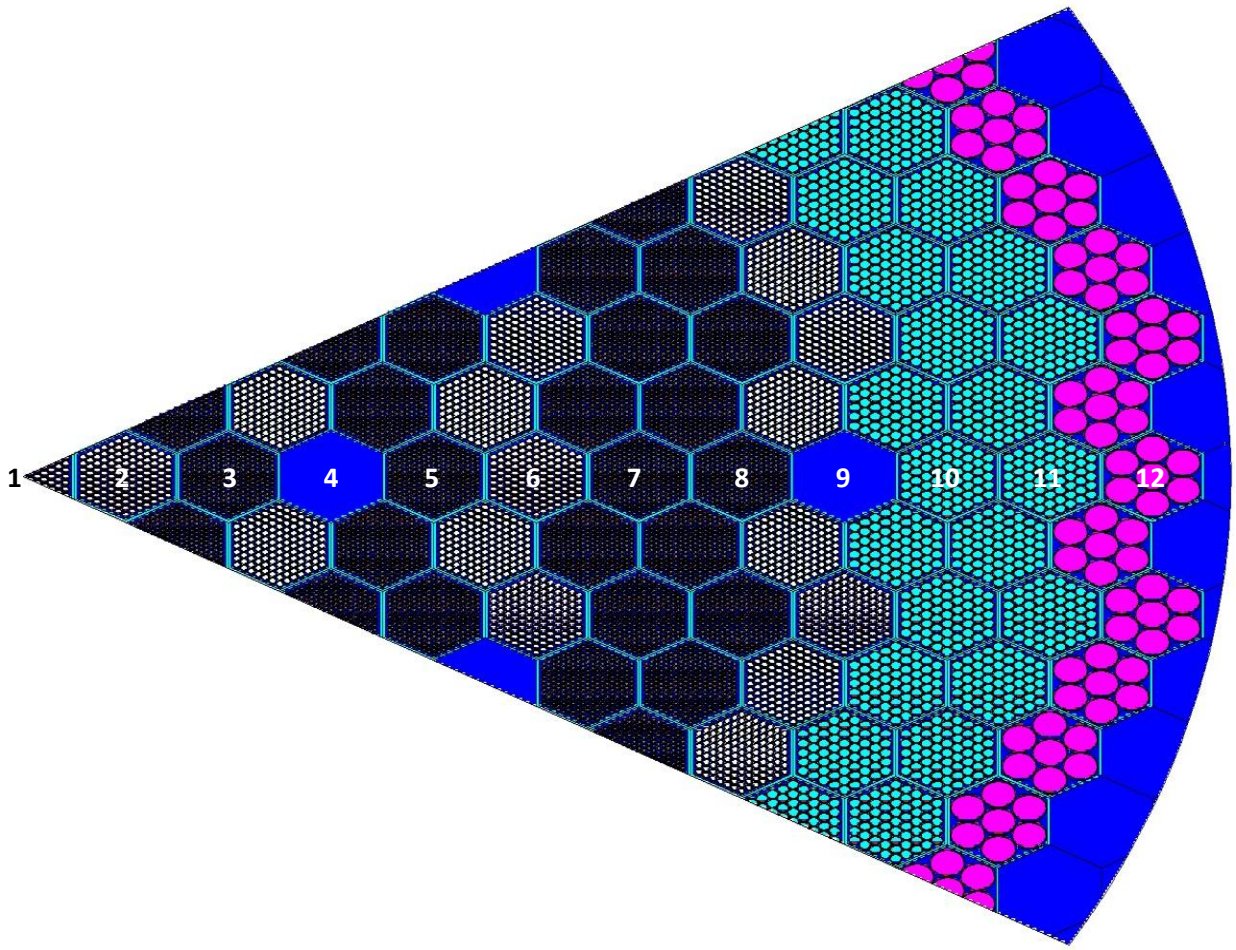

Figure 13: A graphical representation of the 1/6th core model.

The 1/6th model is comprised of a total of twelve rings. Rings 1, 2, 4, 6, and 9, as shown in Figure 13, are breeder assemblies, rings 3, 5, 7, and 8 are comprised of driver assemblies, rings 10 and 11 are made with reflector assemblies, and ring 12 contains the shield assemblies. The blue regions are the sodium coolant. Inside the 12th ring, sodium regions represent the reactivity control tubes, which could not be modeled due to a lack of information. Outside of the 12th ring sodium is used to fill empty space to prevent particles from moving through an empty space. Without the sodium fill a 'bad trouble' error, discussed in Appendix A – Problems Encountered, would result for any particle that escaped the shielding. Two reflective surfaces are defined in the radial direction to allow the simulation of the whole core while reducing processing power requirements.

The modification of the 1/6th core model required the creation of two additional assembly types, a driver TPBAR assembly type and a breeder TPBAR assembly type. To model a TPBAR in MCNP the TPBARs was simplified from nine regions into three. See Figure 14 below. This homogenization of the TPBARs is based on a declassified publication specifically for this purpose.[12] This simplification served to lower the amount of computational power required and to shorten run time for the code. Because the TPBARS are of slightly larger size than a driver fuel rod they were first inserted into the breeder assemblies to create a breeder TPBAR assembly.

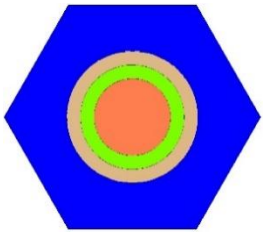

Figure 14: A graphical representation of a TPBAR cell in a breeder pin cell.

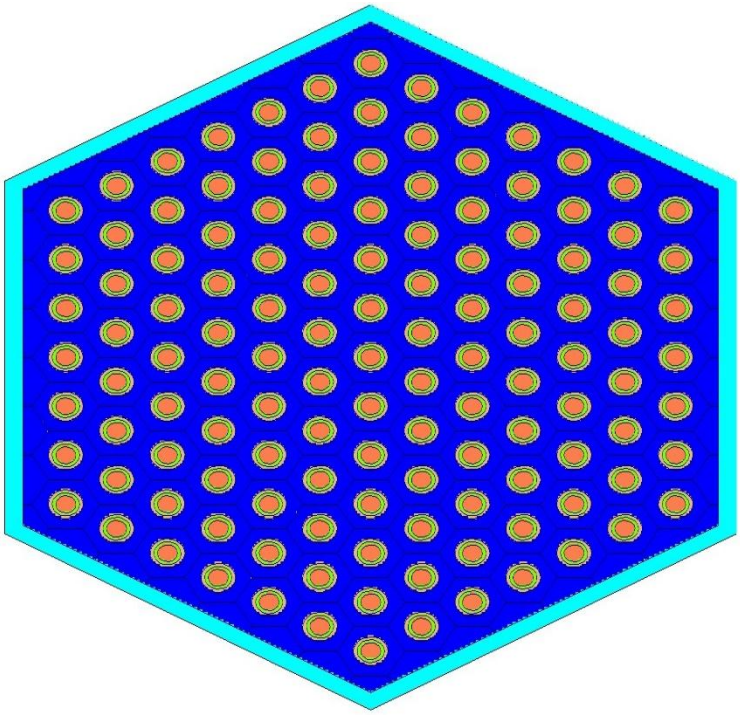

Figure 15: A graphical representation of a TPBAR breeder assembly.

The inner diameter of the gap in Figure 14 above (orange) is 0.223 cm. It is composed of the helium gap. The absorber pellet (green) outer radius is 0.302 cm, and the cladding (tan) outer radius is 0.381 cm. There are 127 TPBARs in the associated assembly.

For optimization of the number of TPBARs required to produce tritium at desirable levels, two new assemblies must be created. However, as stated earlier the TPBARS are too large to fit into a driver assembly. To overcome this limitation the TPBARS must be scaled down. The ratio of the gap to absorber pellet volume was kept the same to ensure the capture of the tritium inside the TPBAR and to prevent overpressure within the TPBAR from gas formation. To insure integrity of the TPBAR the total volume of the cladding was also conserved. A graphic of the scaled-down TPBAR and another of the associated assembly are shown in Figures 16 and 17, respectively.

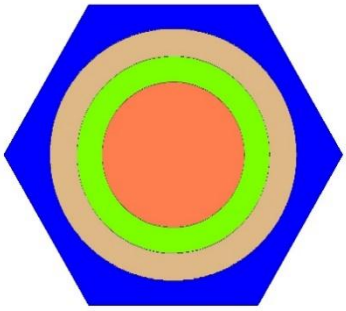

Figure 16: A graphical representation of a scaled-down TPBAR cell.

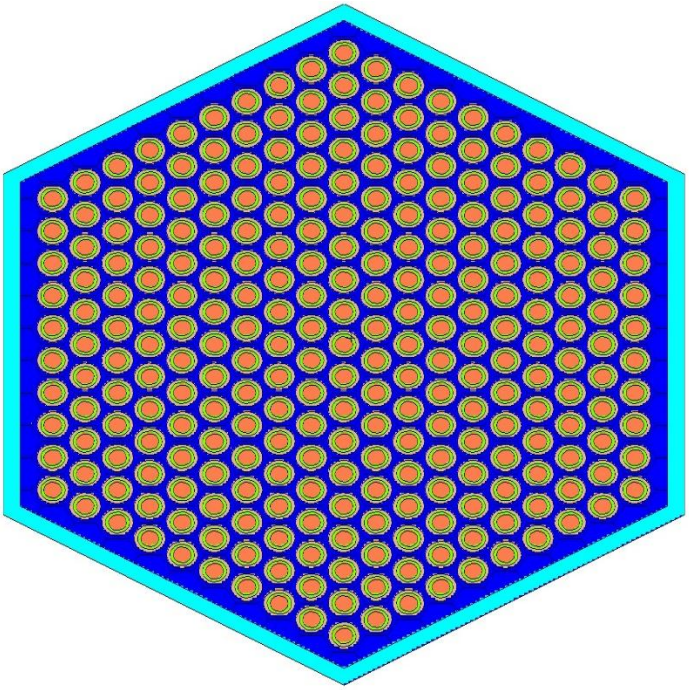

Figure 17: A graphical representation of a scaled-down TPBAR driver assembly.

The inner diameter of the gap (orange) in Figure 16 is 0.2145 cm, the absorber pellet (green) outer radius is 0.2905 cm, and the cladding (tan) outer radius is 0.372 cm. There are 272 TPBARs in the associated assembly.

After creating these assemblies they were put into desirable locations in the 1/6th core model, as shown in the Figures 18 and 19.

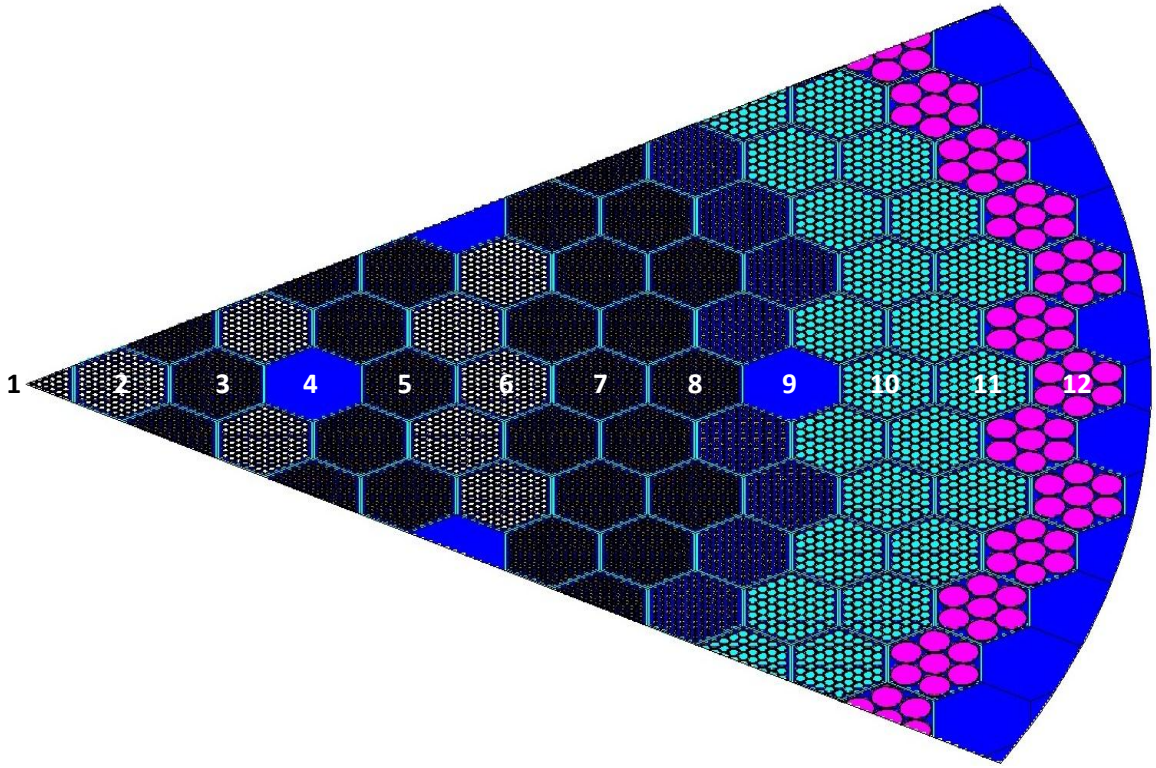

Figure 18: A graphical representation of the 1/6th core model with TPBARs in breeder assemblies.

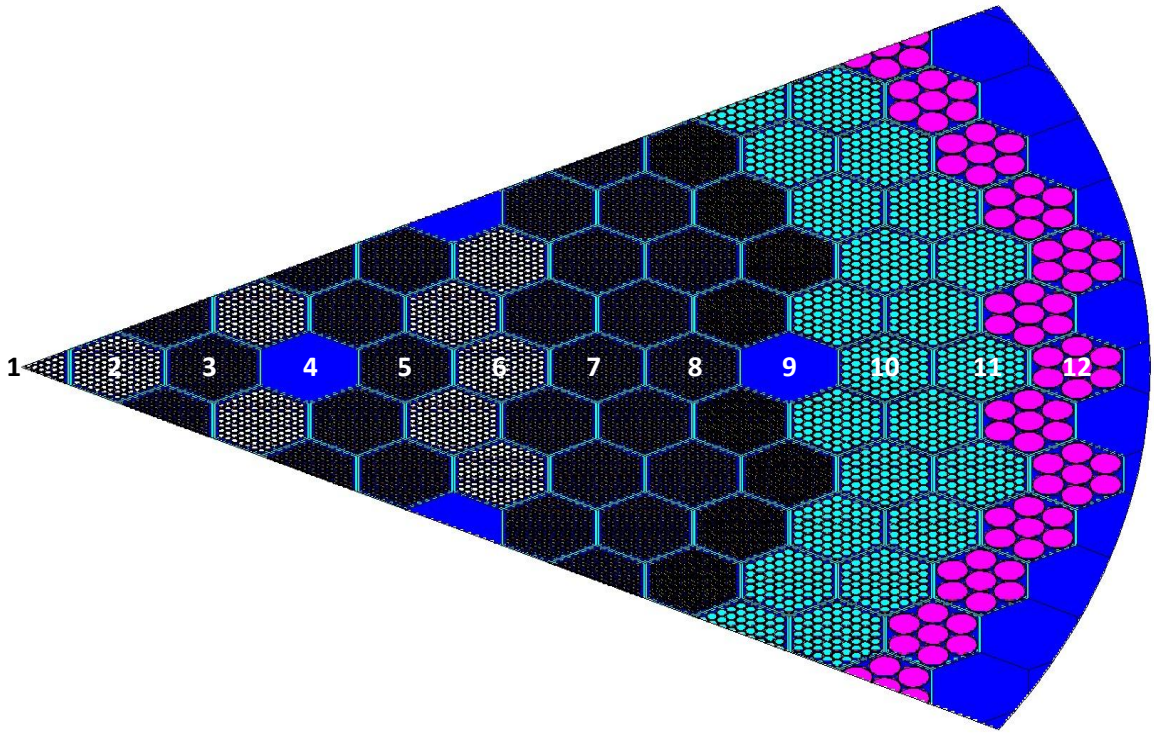

Figure 19: A graphical representation of the 1/6th core model with TPBARs in driver assemblies.

It can be seen in Figures 18 and 19 that the ninth ring in each has had the breeder fuel assemblies replaced with TPBAR breeder or driver assemblies, respectively. The MCNP decks created for the TPBARs in breeder and driver assemblies are contained in Appendix D – Breeder Assembly TPBAR Deck and Appendix E – Driver Assembly TPBAR Deck, respectively.

Based upon the data collected from the two cores with TPBARs, tritium production per unit volume can be calculated for the two TPBAR assemblies. This generation rate will show whether or not production efficiency is lowered by adding more TPBARs into an assembly. The Lithium-6 and lithium-7 cross sections are graphed below. They were generated using JANIS 3.4.

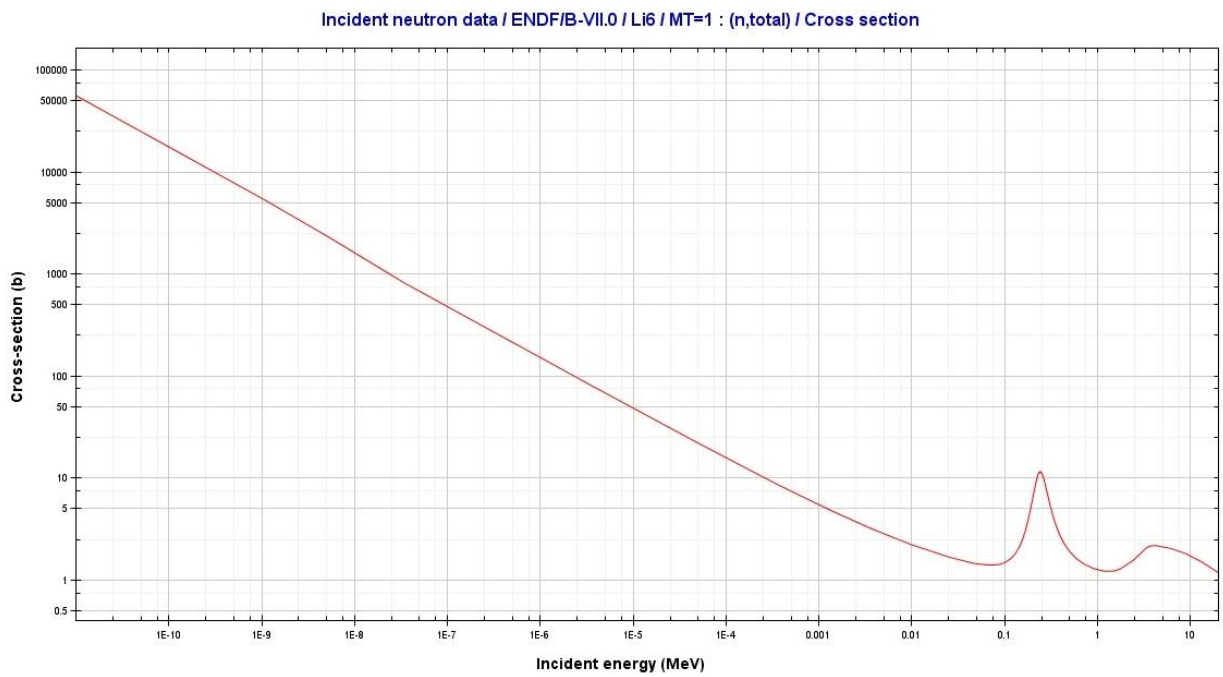

Figure 20: Cross section of Li-6 based on incident neutron energy

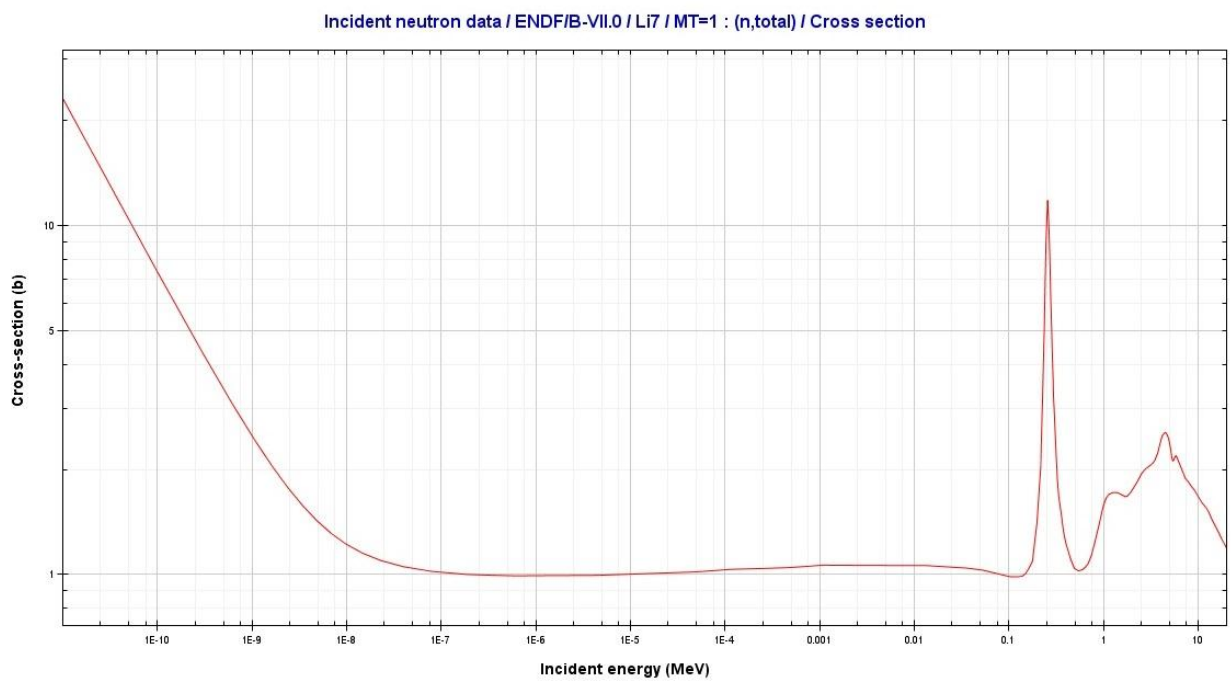

Figure 21: Cross section of Li-7 based on incident neutron energy

Based on the cross sections in the above two figures for Li-6 and Li-7, significant efficiency loss is not expected. This is because of relatively low cross sections for both isotopes when high-energy neutrons are incident.

Because MCNP is a Monte Carlo code, no data is saved unless it is indicated in the input deck that it should be. Since requiring the program to save data increases the run time drastically, specifying exactly what is needed is important. The values that were needed from MCNP are k_{eff}, heat generation rate in the fuel assemblies, the flux in the core, the neutron energy spectra in the core, and the tritium production rate in the TPBAR assemblies.

To obtain k_{eff}, a 'kcode' run is specified in the input deck. When 'kcode' is specified MCNP does criticality calculations by estimating the average number of fission neutrons produced in one generation per initiating neutron. The flux in the core, the neutron energy spectra*, the heat generation rate, and tritium production rate are recorded by MCNP when the input deck specifies for those tallies to be recorded.

Power production optimization of the core may be performed after the tritium production has been optimized. It could be achieved by varying the enrichments of fissile and breeder isotopes to increase the lifetime of the core through the increase of k_{eff}. This portion of the neutronics would require extensive collaboration with thermal hydraulics to insure that fuel and TPBAR safety limits are not reached or exceeded. PNNL has requested that the core burn for 1.5 years if possible.*

4.4 Results

The flux tally obtained from the input decks shown in Appendix F – Flux Tallies Deck, was converted into standard units (neutrons/cm^2*s) using the multiplier obtained from Equation 1 below. Appendix G – Tally Conversions was provided by Jesse Johns and it was used to solve the equation. This tally resulted in a core flux of 1.03E15 neutrons/cm^2*s. This result is reasonable when compared with neutron fluxes in other fast reactors.

$$\frac{m * P * Nu}{\sum_i^n AF_i * Q_i} \tag{1}$$

In the numerator of the equation above, *m* is the mass of fissile material in the tally cell, *P* is the power of the reactor, and *Nu* is the average number of neutrons produced per fission. The denominator is the sum of the atomic fraction, *AF*, of each fissile material multiplied by its respective value for heat produced by fission, *Q*. Because no thermal hydraulics data was available a power of 1000 MW was assumed.

The total number of TPBARS in the reactor is the number of TPBARS in the 1/6th core model multiplied by six, which comes to 6096 TPBARs in the core with breeder TPBAR assemblies and 13056 in the core with driver TPBAR assemblies. The total volume of the $LiAlO_2$ material in the breeder TPBAR assemblies is 794.29 cm^3 and the total volume in the driver TPBAR

assemblies is 1574.22 cm^3. The average neutron flux through the $LiAlO_2$ in the assemblies was calculated to be 6.26E13 neutrons/cm^2*s using the flux tally value and the spreadsheet in Appendix G. The flux is assumed to be the same for all assemblies (including driver types) because of the low Li-6 and Li-7 absorption cross sections for high energy neutrons. This assumption was made instead of determining the efficiency of each assembly type as mentioned in 4.3.2 because of the lack of results available due to time constraints and the large time required to run the code. The total tritium production rate in the core was found to be negligible using both driver TPBAR assemblies and breeder TPBAR assemblies, with a production rate of less than one gram every 1.5 years using Equation 2. A cross section of 0.33 barns was used with the spreadsheet contained in Appendix G to obtain this result.[13]

$$N_1(t) = N_{1_0} e^{-\sigma\phi t} \tag{2}$$

The equation above is a time dependent depletion calculation containing the variables N_1, σ, ϕ, and t which are the number density, microscopic cross-section, flux, and time, respectively. When $N_1(t)$ is subtracted from $N_{1_0}$the total amount of tritium produced during the time period is found. Note that this is the total amount of tritium produced and it does not account for radioactive decay.

The heating tallies collected using MCNP were given to Timothy Crook for analysis and use in the thermal hydraulics portion of the project. The flux calculated in the outermost assembly available was given to Sara Loupot for use in the safety and shielding analysis.

4.5 Future work

Work that still needs to be done includes TPBAR number optimization for tritium production, fuel optimization for power production, mapping of the neutron energy spectra, and runs with more particles and cycles to improve the statistics of data collected. It should be noted that mapping of the neutron energy spectra would allow a more reasonable cross section for Li-7 to be determined and may allow for more accurate calculation and possibly significantly larger tritium production rates.

*These portions of the neutronics were not completed due to time constrains and challenges with the MCNP decks. See Appendix A - Problems Encountered for more information on problems encountered that interfered with project completion.

5.0 Safety Analysis (Sara Loupot)

5.1 Introduction

The safety analysis analyzed the extent to which the addition of TPBARs would change the behavior of the reactor with respect to the original safety criteria of the SPRISM reactor. This analysis assumes that the core will be operated at the same power density or lower because power generation is a secondary concern. Because the power density will be lower, the core temperature in both normal operation and accident scenarios should also be lower. This assumption is necessary since an accurate characterization of the neutron flux in the core could not be determined within the project time frame. Thus, the accident scenarios analyzed by Sumner should be sufficient to analyze the safety of the SPRISM core with nitride fuel. A second significant assumption that was made is that the safety systems of the SPRISM are comparable to that of the PRISM. Due to a lack of information that is available about the SPRISM, parts of the analysis had to be based on PRISM documents. This assumption is valid because most of the safety systems remain the same between the two designs and the only significant difference between them is the SPRISM is slightly bigger.[4] This analysis will first outline some of the safety systems of the SPRISM reactor that are unchanged with the addition of TPBARs. Then it will describe the unique behavior of the reactivity in the nitrided fast reactor core and analyze several accidents outlined Sumner's thesis. It will describe some of the risks of tritium release and analyze the effects two release scenarios. Additionally, a neutron shielding analysis was performed using MCNP.

5.2 SPRISM: Five Levels of Safety[14]

The pre-application safety document for the PRISM reactor defines five levels of safety. The first level is passive, or inherent, and basic design characteristics. These characteristics include the sodium coolant properties, reactor module design, negative reactivity feedback, core inlet nozzles, and heat removal systems. Sodium coolant has excellent heat transport properties. These favorable properties allow the PRISM to be utilized at a low pressure and still remain far below the boiling point for sodium. Also, the separate reactor modules allow each unit to have better passive decay heat removal and a lower source term in the event of a catastrophic accident. Negative reactivity feedback~~s~~ decreases the power significantly when abnormal events occur. The core inlet nozzles are designed to inhibit total blockage of flow to an assembly. The passive heat removal systems have the ability to supply reliable decay heat removal, even after a loss of AC power.

The second level of safety is protection against anticipated and unlikely events, which includes the safety grade reactor protection system, non-safety grade plant control system, Auxiliary Cooling System (ACS), Reactor Vessel Auxiliary Cooling System (RVACS), and containment vessel among others. Four electromagnetic pumps with synchronous machines produce coast down during shut down. Six gas expansion modules (GEMs) in the core insert negative reactivity

during loss of flow events. A control rod stop system prevents reactivity insertion events, and the ultimate shutdown system (USS) gives additional protection if necessary.

The third level of safety is defined as protection against extremely unlikely events. It includes all of the systems listed above, as well as the reactor vessel and reactor module closure assembly which are designed to contain radioactivity released by any fuel or cladding failure.

The fourth level is protection against beyond-design basis events. This includes the passive negative feedback characteristic, and protection against loss of heat sink and loss of flow coast down. A hypothetical core disruption accident is postulated to evaluate the integrity of the reactor coolant system to test the mitigative effectiveness of the containment system. However, further investigation of this analysis is beyond the scope of this project.

The fifth level of safety is the use of PRA in evaluating the overall safety of the design and to point out areas that require improvement. PRA is used to select design basis accidents and beyond design basis accidents and to assign reliability requirements for systems and components. PRA is the only evaluation that considers beyond design basis accidents.

5.3 Inherently Safe Design Features, Systems, and Components

The SPRISM reactor is designed to be an inherently safe reactor. It takes advantage of several natural phenomena and intrinsic characteristics to avoid the release of radiation no matter what circumstances it is presented with. The reactor operates at a low pressure, close to atmospheric, so that if pressure is lost the system will remain stable, and it is less prone to explosions.[14] The core has a large heat capacity. It is structurally sound to temperatures well beyond normal operating conditions, and can remove heat extremely well in high temperature situations. The system relies on natural circulation, so in the case that the pumps fail, the reactor will continue to be cooled. It also has negative temperature coefficients of reactivity, so that as the temperature in the core rises, the reactivity will decrease, bringing the core back to a stable power level.

Normal operations are controlled by nine control rods, controlled by the plant control system (PCS). A rod stop system (RSS) prevents unprotected control rod withdrawal. The secondary shutdown system is composed of three rods. If primary rods fail to scram, the secondary system will scram by a separate Reactor Protection System (RPS). These rods will be released magnetically during under cooling or over power event in which both scram systems fail.

The inherent negative reactivity feedback response of the core will bring the core to zero fission power state at an elevated temperature. Three events it is designed to accommodate are inadvertent withdrawal of all control rods without scram, loss of primary pump power and loss of all cooling by the IHTS without scram (LOFA), and loss of coolant without scram (LOCA).[15]

The primary system consists of the reactor vessel, reactor closure, closure penetrations, below-head duct of two intermediate heat exchangers, and the primary sodium and cover gas clean up

system. During normal operation, all sodium and cover gas service lines are closed with double isolation valves, and all other penetrations in the reactor closure are seal-welded. This means the primary is totally sealed during operation.[14]

The intermediate heat transport system (IHTS) is a closed loop system that transports the reactor generated heat to the steam generator system by circulating non-radioactive sodium between the intermediate heat exchangers and the steam generator. The hot leg delivers sodium at 485 C to a single 1000 MWth steam generator, and the cold leg returns the sodium at 325 C. With the addition of TPBARs it is assumed that these temperatures would be lower. Two steam generators feed a single turbine-generator in each power block through a header arrangement.

The shutdown heat removal system (SHRS) provides post-shutdown decay heat removal. The turbine condenser normally uses the turbine bypass to remove reactor shutdown heat. Two safety grade auxiliary cooling systems are provided for cases when an alternative method of shutdown is required. The reactor vessel auxiliary cooling system and auxiliary cooling system can be used during maintenance or when the SHRS is unavailable to remove decay heat.

The reactor vessel auxiliary cooling system (RVACS) is part of the natural circulation cooling system shown in Figure 22. It can dissipate all of the reactor's decay heat through the reactor vessel and containment vessel walls by radiation and convection heat transfer to the naturally circulating air outside the containment vessel without exceeding temperature limits. Since this system does not rely on electric power, it is always operating. However since the main method of heat transfer is by radiation which is proportional to temperature to the fourth power, at normal operation temperatures it removes heat at a lower rate than in high temperature situations. Primary sodium flow is maintained through natural circulation. Decay heat generated in the core is removed by the primary sodium and transferred to the reactor vessel. From there, the heat is mostly radiated from the vessel to containment and convected to the collector cylinder. The heated air in the collected cylinder is then dissipated into the atmosphere by natural circulation.

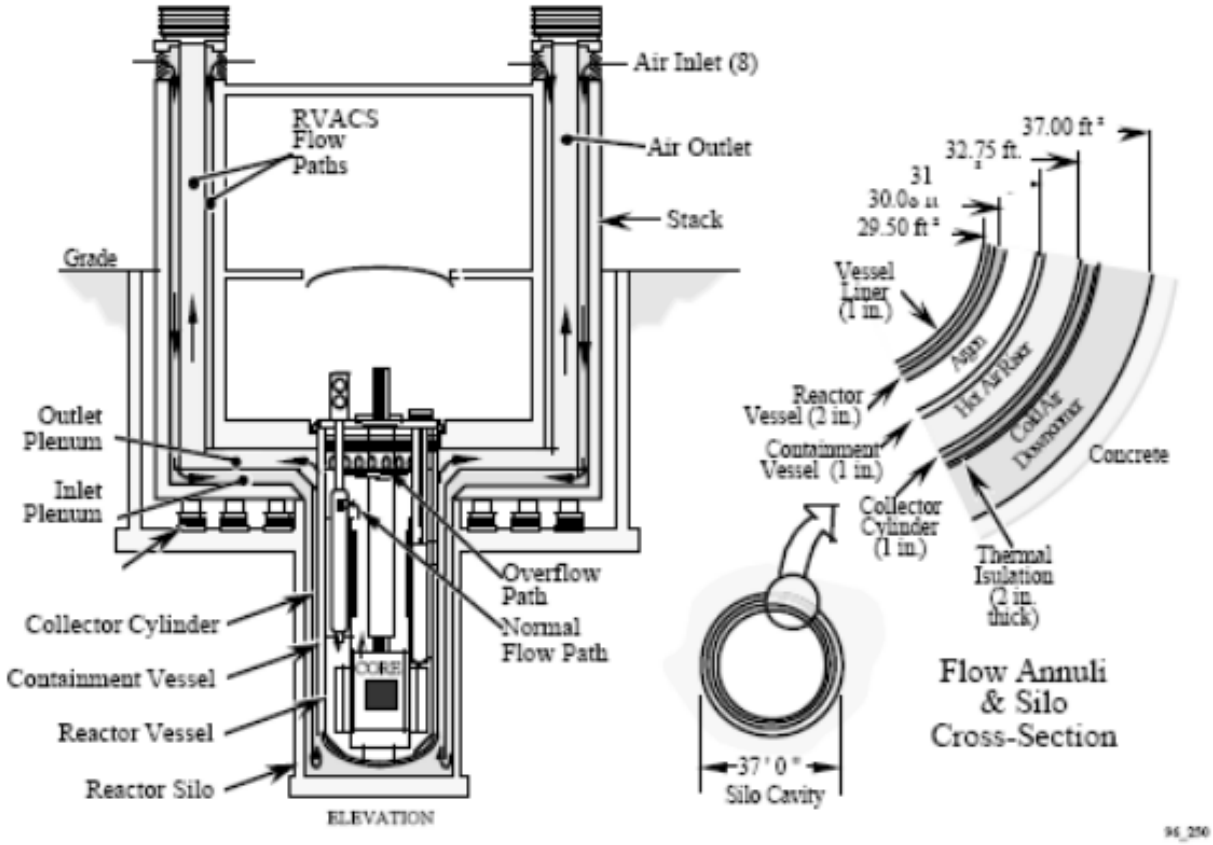

Figure 22. The SPRISM natural circulation system.[15]

The hot air riser, a perforated collector cylinder as shown in Figure 23, increases heat removal capability. When necessary, natural circulation of the primary sodium moves heat from the core to the reactor vessel. As the temperature of the sodium and reactor vessel rise, the radiant heat transfer across the argon gap to the containment vessel increases to accommodate the load. If the intermediate heat transport system becomes unavailable due to a loss of secondary sodium, RVACS can provide passive heat removal without the auxiliary cooling system.

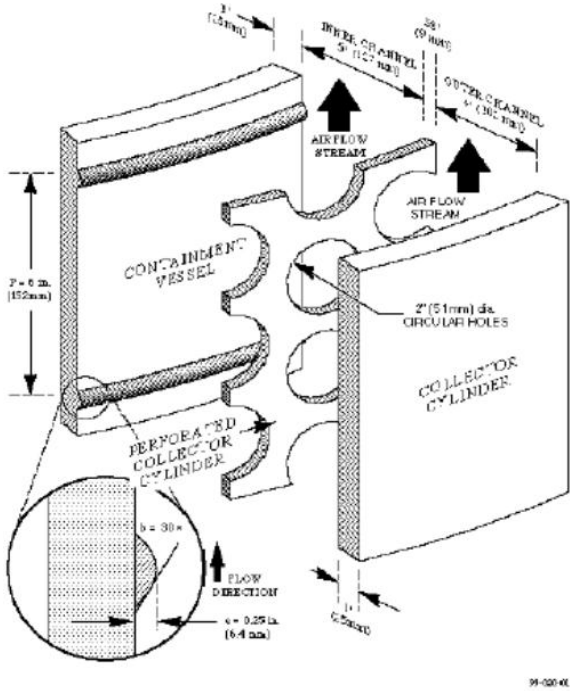

Figure 23. RVACS hot air riser with perforated cylinder for improved heat transfer.[14]

The auxiliary cooling system (ACS) uses natural circulation of the primary coolant to move heat from the core to the IHX and into the coolant. From there, natural circulation of the IHTS coolant moves the heat to the SG where natural circulation of atmospheric air past the shell side of the steam generator removes decay heat. The ACS consists of an insulated shroud around the steam generator shell with an air intake at the bottom and an isolation damper above the steam generator to prevent heat loss during normal operation. ACS is initiated by opening the exhaust damper. It's supplemented by the RVACS. An auxiliary fan located in the exhaust stack can be used to reduce cool down time for maintenance outages, but normally does not operate.

The SPRISM containment, as shown in Figure 24, is made of three successive barriers (fuel cladding, primary coolant boundary and a containment boundary) to protect from fission product release. The containment consists of a lower vessel that surrounds the reactor vessel, and a steel lined concrete upper containment structure that encloses the reactor. The reactor is also surrounded by concrete and in the ground.[15]

The upper portion is a large room. It is steel lined to limit leakage to less than 1 volume % per day at 0.35 kg/cm^2 to mitigate design basis accidents. A service room between the containments contains the primary sodium service, primary sodium storage tanks and cover gas systems. It has been designed to contain sodium spray and pool fires that would occur in a hypothetical core disruptive accident. The ability to use this additional containment volume brings the peak pressure in this situation within the containment design basis of 0.4 bar.

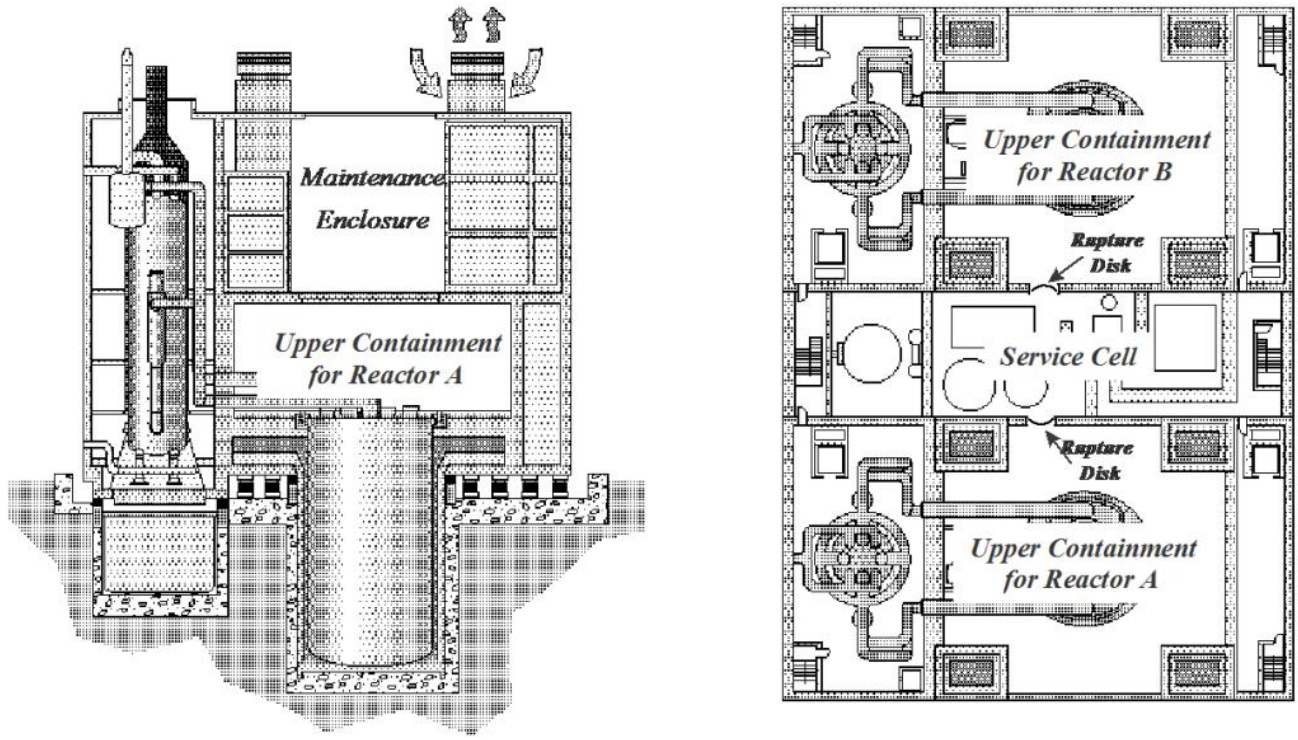

Figure 24. The SPRISM containment system[15]

The 1 inch thick steel lower level of containment is also a guard. It has no penetrations in order to remain leak tight. It is sized to be able to hold the primary sodium in the event of a reactor vessel leak such that the core, spent fuel, and inlets to intermediate heat exchangers remain covered in sodium.

A maintenance enclosure above the upper confinement serves as a secondary containment. A gas treatment system is used to maintain negative pressure during maintenance and refueling activities in this enclosure. Using multiple containment volumes reduces the peak pressure produced by a large pool and spray fire by two.

The use of rupture disks to limit peak pressures is an acceptable risk because the probability of a large pool or HCDA induced spray fire is extremely low (less than 1/10 million years).

High pressures reached in accident scenarios can be controlled by venting the containment region of one reactor to the service cell and if necessary to the next reactor.

5.4 Reactivity Control[4]

Reactivity control is of extreme concern in fast reactors, where delayed neutrons provide less benefit than in thermal reactors. Delayed neutrons are born at lower energies than prompt neutrons. At these energy levels, the importance of delayed neutrons to the reactivity coefficient is less and they are more likely to be absorbed rather than cause fissions, and thereby

diminishing their contribution to reactivity control in the reactor. Due to higher enrichments of fissile isotopes, fast reactors have less fertile isotopes, which often have extraordinarily high delayed neutron fractions. All of these factors contribute to a smaller delayed neutron fraction in a fast reactor providing a smaller margin to prompt criticality than in a thermal reactor. Other prompt reactivity feedback effects must exist to prevent rapid power increases. Three major reactivity feedback effects are of major importance and should be considered: Doppler broadening, coolant thermal expansion, and core expansion. In Doppler broadening, as the temperature increases in the reactor, the thermal motion of the nuclei increase, altering the nuclei motion relative to the neutron flux which changes the cross section of the materials in the reactor. This is of high importance for neutron fluxes in the resonant energy regions, whereas these cross sections broaden, their corresponding reaction rates will increase. In softer neutron spectra, more neutrons are in the resonant energy range and provide larger Doppler reactivity feedback effects.

As the temperature of the coolant increases during a transient event, the density decreases which has four main effects on reactivity: spectrum hardening, increased leakage, elimination of sodium parasitic absorption and changes in energy self-shielding. Decreasing coolant density decreases the moderation power that it has, and combined with the increasing number of neutrons released per fission as temperature increases this creates a positive reactivity insertion. However, the increased leakage effect acts as a negative reactivity insertion. The decreased parasitic absorption and changes in energy self-shielding have minimal effects on the overall reactivity coefficient. In the inner regions where leakage is not a factor, coolant thermal expansion generally creates a positive reactivity coefficient. The leakage component of the coolant thermal expansion tends to dominate at the edges of the reactor causing a negative reactivity coefficient. Coolant thermal expansion also hardens the neutron spectrum which leads to less effective Doppler feedback. Increasing fuel temperatures in the fuel result in fuel pin growth as well as an increase in the reactor’s height. This will increase leakage, which contributes negative reactivity.

Due to the presence of only one moderating atom per heavy metal atom, the spectrum of the nitride fuel used in our reactor tends to be harder than oxide fuels, which leads to better breeding ratios. It also has good thermal conductivity, greater than 15 W/m*K, which is higher than most oxide fuels, high density and a melting temperature at or above 2,800 K.

Three transients are of main concern for the SPRISM. These include a loss of flow accident (LOFA), transient over power accident (TOPA) and loss of heat sink accident (LOHSA). Previous investigations have characterized the behavior of the SPRISM core with nitride fuel during these transients. Since it is assumed that the operating power of the reactor will be lowered based upon power density and fuel temperatures, it will be assumed that these transient analyses are sufficient for a worst case scenario condition.

5.5 Accident Analysis[4]

A loss of flow accident will be examined first. The worst case scenario is one in which all four primary pumps lose pumping power, leading to a massive drop in coolant mass flow rate. In an analysis by Sumner it was found that reactivity feedbacks were sufficient to drop core power to decay heat levels so that only natural circulation was required to cool the core. Peak fuel temperatures reached 1,539 K and the margin to melting decreased by only 25%.

The transient over power accident occurs when all the rods are withdrawn to the rod stop limit of $0.3 at the maximum rate of $0.02/s. There is no control rod scram and reactivity feedbacks are the only thing that is responsible for bringing the power back down. In this transient, the power increases by 1,001 MW, but the fuel temperature increased by less than 20%. Power peaks at about 60 seconds into the transient and then starts to level off around 100 seconds. In a simulation in which the rod stop failed and the control rods continued to withdraw past the limit, the cladding failed at 70 seconds into the accident before the fuel reached 2,567K which is almost 500 K lower than its melting temperature.

The loss of heat sink accident was simulated similarly to the loss of flow accident except the flow is lost in the intermediate sodium loop instead of the primary sodium loop. The lower flow rates in the intermediate loop lead to inadequate heat removal across the heat exchanger which causes core temperatures to rise. The elevated core temperatures provide negative feedback to bring the power back down to steady state. In a worst case scenario, both coolant pumps in the intermediate sodium loops fail. Reactivity feedbacks were able to decrease core power to 50% where natural circulation was sufficient for cooling. At 1000 seconds into the transient natural circulation was providing a flow rate of 20% operational. Due to a large drop in reactivity at the beginning of the transient the core was able to maintain a safe margin to fuel melting. There was only a 12% increase in margin to melting.

These analyses are a worst-case scenario for our core. With the assumption of a lower power density, and thus lower temperature profiles, there will be a decrease in both normal operation and transient conditions. However, a lack of neutronics data makes this impossible to prove. Further work should be done to first characterize the flux profiles within the core and then perform transient analysis to verify that core damage conditions are not reached in any of these scenarios.

5.6 Tritium

Tritium is a beta emitter that decays into helium-3 by electron emission with maximum energies of 18.6 keV along with an anti-neutrino. It has a half-life of 12.3 years. It has an average path length of .056 micrometers, and a maximum of 6 micrometers, in water. It can be released in the form of tritiated water, liquid or vapor or as tritiated hydrogen gas. The weak beta emission and short biological half-life of tritium mean that doses calculated using standard assumptions are low. It is naturally occurring in water in the amount of 3.2 to 24 picocuries per liter.[16]

The relative biological effectiveness (RBE) is defined as the ratio of the absorbed dose of the reference radiation to the absorbed dose of the test radiation that is required to produce an identical level of biological response in a particular animal or cellular study. The equivalent dose (Sv) is defined as the average absorbed dose multiplied by a radiation weighting factor that takes into account RBE of different types of radiation at inducing malignancy or genetic damage. The ICRP assigned a weighting factor of 1 to electrons of all energies. Although there is evidence that RBE increases with decreasing photon energy, the ICRP argued a more detailed description was not necessary for the purpose of radiation protection.

Beta particles are a form of ionizing radiation, and deposit their energy in the form of highly structured tracks of ionized and excited molecules. These particles can directly ionize constituent atoms or damage them indirectly via reactions with free radicals. This ionizing radiation can cause damage to DNA. Depending on how the cell handles this damage, it can lead to an increase in mutation frequency. Tritium decay produces very low energy beta particles of short range. As a result, the average ionization density is much higher than higher energy particles or photons. Studies have reported theoretical RBE values for tritium of 3.75 compared to Co gamma rays and 1.5 compared to 250 kVp x-rays.[16]

According to the biological reasoning used by Osborne conclude that based on the assumptions made by the ICRP, the acceptable level of tritium in water to deliver less than 170 mrem/year is 1.6 micro Curies per kg. Osborne claims that this estimate is quite low, and based on his calculations up to 4.7 micro Curies per kg would still be safe. Similarly for air, the ICRP assumptions estimate a safe air concentration of 0.08 micro Curies per cubic meter, while Osborne's more realistic calculations result in a value of twice that.

According to 10 CFR 20, intro notes to Appendix B, Table 2 Column 2.[17] The NRC allows a licensee to release an amount of tritium that could result in radiation dose to a member of the public of up to 100 millirem (1 millisevert) per year, in planned air and water effluents (10CFR20.1301). This translates into one million picocuries of tritium per liter as the equivalent of 50 millirem/year.

Specific design objectives of NRC regulations are to (1) to limit the amount of radioactivity released in liquid effluents from any light-water-cooled power reactor to levels that would keep the annual exposure to an individual in an unrestricted area to not more than 3 millirems for the whole body and not more than 10 millirems to any organ, (2) to limit releases of radioactivity in gaseous effluents from any light water cooled power reactor to keep annual exposures to an individual in an unrestricted area to a maximum of 5 mr in the whole body and not more than 15 mr to the ski and (3) to limit releases of radioactive iodine and other radioactivity from any light water cooled power reactor to keep annual exposures to the thyroid of an individual in an unrestricted area to no more than 15 mr. These can be monitored through the four basic exposure pathways: air, water, food, and external radiation. The EPA set a maximum contaminant level for tritium at 20,000 pCi/L.

According to the NRC's website, in 2003, the average PWR released 725 Curies in liquid effluents and the average BWR released only 27.7. In 2007 Watts Bar 1 released 8.92 Ci of tritum in gaseous form, 6.368 Ci in liquid and 598 Ci in liquid form.[18]

In 2010, Entergy informed the NRC that it had identified tritium in a groundwater monitoring well at Vermont Yankee. It was determined that the contamination was due to a leak in the Advanced Off-Gas system, and the contamination was contained to only shallow groundwater wells in the vicinity of the known leakage source.[19] A study in 2006 conducted at Diablo Canyon Power Plant found low concentrations of tritium in two wells located near two units, and concentrations close to 17,000 pCi/L in a French drain system located about 100 feet east of the containment buildings associated with these two units. It was determined that these occurrences are likely due to washout, wherein tritiated water vapor released from the vents above both containment buildings condenses and eventually infiltrates the local subsurface.[20] In August 2005, Watts Bar 1 reported that in February of that year, groundwater monitoring revealed a significant increase of tritium in a well located in a down gradient position between the Yard Holding Pond and the Intake Pump Station for the facility. Tritium levels had jumped from 500 pCi/L to 550,000 in late January. An investigation discovered and repaired a leak at the connection of the temporary radwaste line with the permanent stainless steel radwaste line. The data also led to a new leak that may have been present in the Cooling Tower Blowdown line downstream of the liquid effluent line tie-in. After the investigation, as tritium levels in this well decreased, the levels in the next well down the gradient began to increase. This confirmed a theory that the plume caused by a leak in the radwaste line, repaired in 2003 moving along the path of the discharged line. Its natural progression will put the plume in the nearby river, but by that time the levels of tritium will be below release limits.[21]

5.7 Tritium Release from TPBARs in the SPRISM

In the proposed design, the tritium produced in the core can possibly leak into the sodium pool, diffuse into the RVACS system, and be transferred to the atmosphere. Tritium has a specific activity of 9650 Ci/g. 10 CFR 20 states that the total effective dose equivalent (TEDE) must be kept below 0.1 rem per year to any member of the public and 5 rem per year to radiation workers.[17] This is a possible limiting factor on the number of TPBARs in the core, but to carry out an accurate analysis the amount of tritium produced per TPBAR must be known. This information is unavailable at this point in time, so some assumptions must be made. In-reactor studies of TPBARs have found that they release less than 0.53 mCi per TPBAR per hour.[22] The TPBARs used in this study are three times the volume of the TPBARs in the proposed design, so the leakage considered here is one third of that, 0.177 mCi per TPBAR per hour. It is also assumed that all of this tritium escapes from the reactor vessel into the working environment. This is a conservative estimate because in reality, tritium will likely experience a chemical reaction with the sodium coolant and precipitate out of the solution as sodium hydride before it escapes the vessel. In the following analysis, a 2000 hour work year was assumed. Given the NRC limits of 5 rem per year to radiation workers this equates to this is 2.5 mrem per hour.

Inhalation rate is assumed to be $2x10^4$ mL/min as defined by the NRC's Reference Man doing light work. An analysis using HotSpot for one TPBAR that is leaking 0.177 mCi per TPBAR per hour is shown in Figure 25.[23] An explanation of the calculations done by HotSpot is available in Appendix H. The analysis simplified the problem of constant release to a release of 0.177 mCi all at once at the beginning of an hour, and considered the TEDE received from the plume that develops over the next hour. The conditions considered were a release height of 0 m, because that is where the top of our reactor is (it's underground). The receptor height was 1.5m, the height of the average person. The atmospheric stability was considered moderately stable. The terrain was a city. The wind reference height was 10 meters and a sample time of 60 minutes was taken. A detailed table of results is available for reference in the appendix.

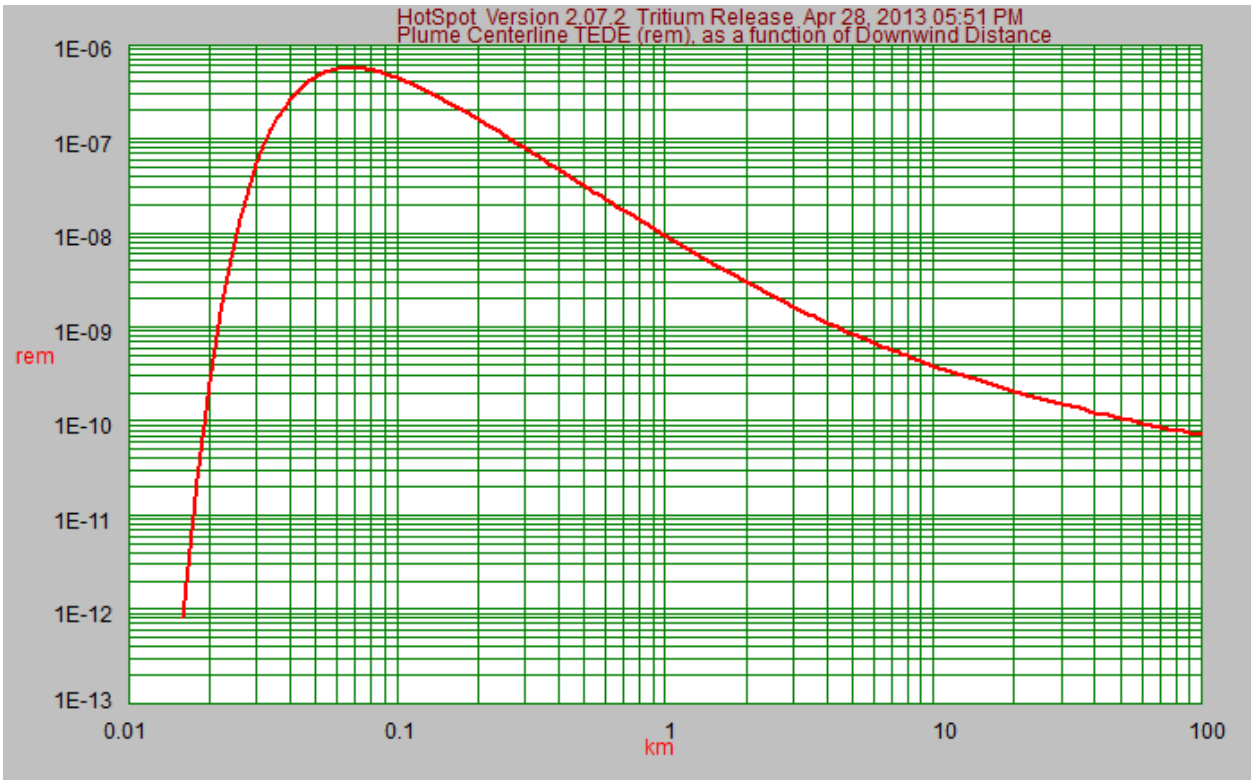

Figure 25. Tritium release from one TPBAR over one hour as a function of distance from the core.

The maximum TEDE received per TPBAR from normal in-core leakage is 0.563 µrem per hour at a distance of 100 meters from the source. This means the core would be limited to about 4440 TPBARs per cycle. Each TPBAR is assumed to be able to produce one third of the tritium of an unmodified TPBAR in the Watts Bar I plant, 0.4 g/cycle.[23] To reach our goal of 1150 g/cycle this would take 2875 TPBARS. Therefore, tritium leakage rate is not a limiting factor.

For a TPBAR that has experienced mechanical cladding failure the tritium release will be maximum of 55 Ci per TPBAR. For the smaller TPBARS used in the SPRISM core, this is assumed to be equivalent to 18.3 Ci per TPBAR. In the scenario that was analyzed, all 2875 TPBARS fail simultaneously, releasing a total of 52,612.5 Ci. The TEDE an hour later is shown in Figure 26. The maximum dose received is 167 rem at 71 meters away from the source. This is far beyond the annual dose limit for workers. Again, it is not only unlikely that all of the TPBARS would simultaneously fail, but it is also unlikely that this tritium will make it out of the sodium pool if it were to occur because of the sodium hydride production reaction.

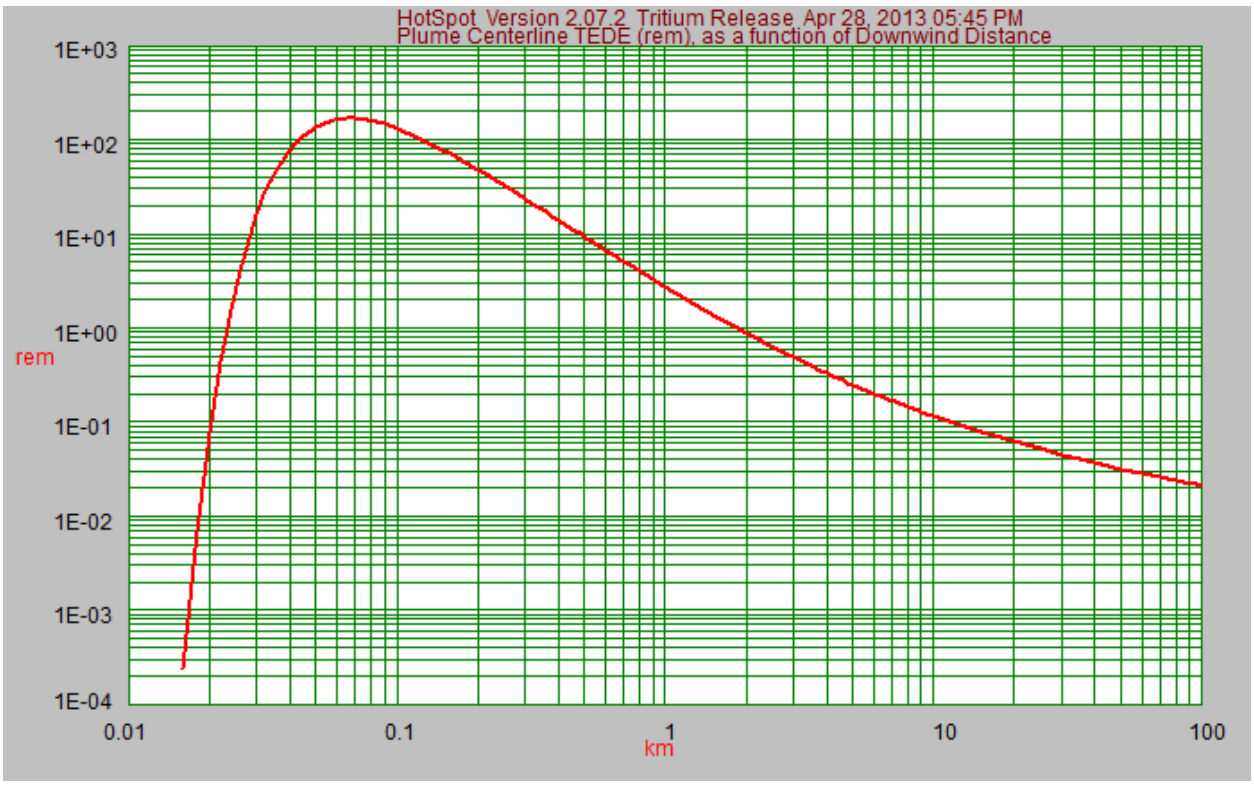

Figure 26. Tritium release TEDE rates 1 hour after the failure of 2875 TPBARs resulting in the release of 52612.5 Ci.

Figure 27 shows the plume one hour after the mechanical failure of all 2875 TPBARs and subsequent release of 52,613 Ci. The inner (red) circle represents the 5 rem yearly dose limit to radiation workers. This plume reaches 100 meters away from the source and takes four minutes to get there. This means most of the workers at the plant would have very little time to reach safety. The blue contour is the 0.1 rem yearly limit to members of the public. This plume reaches 11 kilometers from the source, but takes more than 6 hours to reach that distance. This means that there would be plenty of time to evacuate the public to safety in the case of this event.

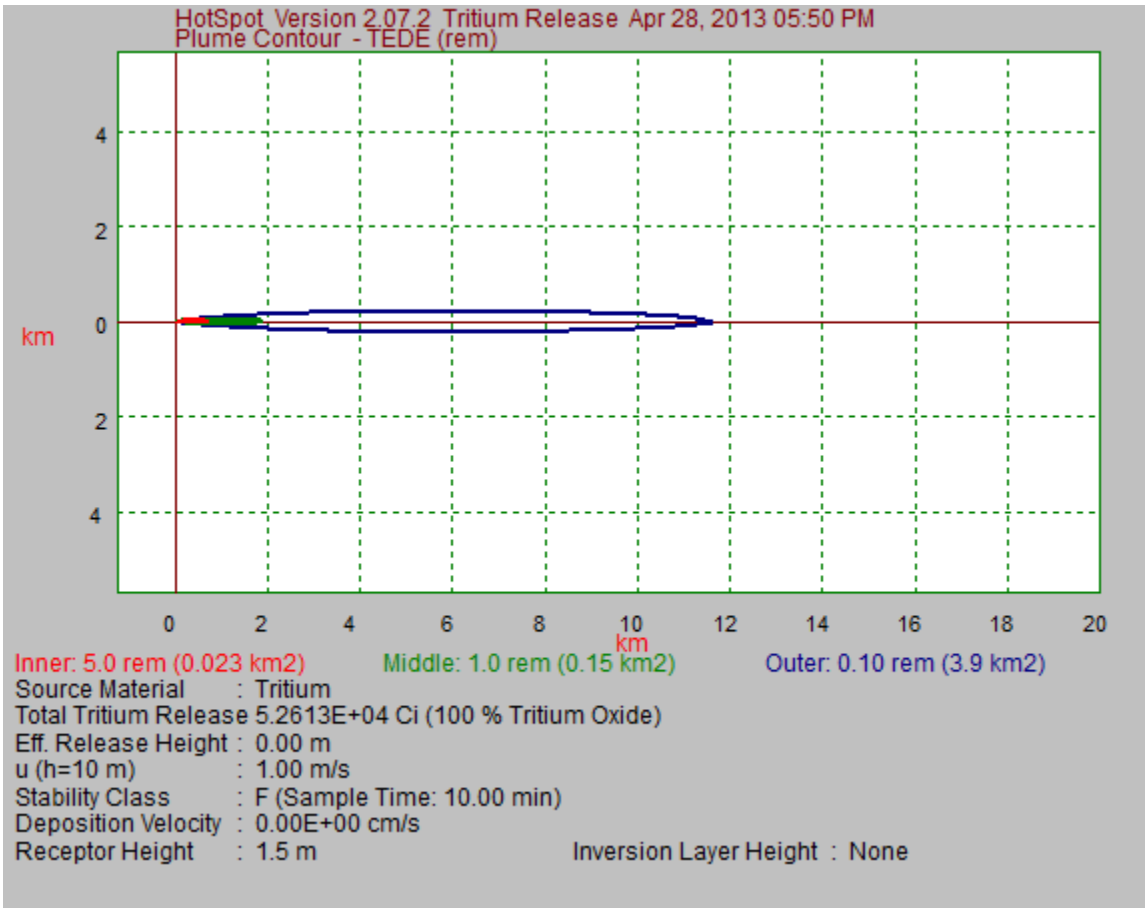

Figure 27. Gaseous release plume one hour after mechanical failure of all 2875 TPBARS resulting in a total release of 52612.5 Ci.

Table 5 summarizes the results for each scenario.

Table 5: Summary of gas release analysis

	Radiation workers- limit 5 rem/year		Public- limit 0.1 rem/year	
	Maximum dose received in 1 hour	Limit reached	Maximum dose received in 1 hour	Limit reached
Failure of all TPBARS and subsequent release 52,612.5 Ci	167 rem	Yes, in < 1 minute	Yes	11 km away from accident, > 6 hours after the event
Normal leakage of TPBARs	0.563 µrem/ TPBAR	When there are 4440 TPBARS in the core	Below background	No

5.8 Shielding Analysis

A shielding analysis was done using MCNP.[11] MCNP is a general purpose Monte Carlo N-Particle code that can be used for neutron transport. More details about the code can be found in Appendix H. In this analysis, the SPRISM reactor was modeled from the surface of the ground to the bottom of the RVACS system. The model included only the shielding features, to the best of our knowledge, and excluded the instrumentation, steam generators, fuel, and other devices in the sodium pool. This is assumed to be a conservative approximation, since these other components will only provide more shielding. The model was based on combining Figures 28 and 29 to the best of our ability, along with some estimations as necessary.

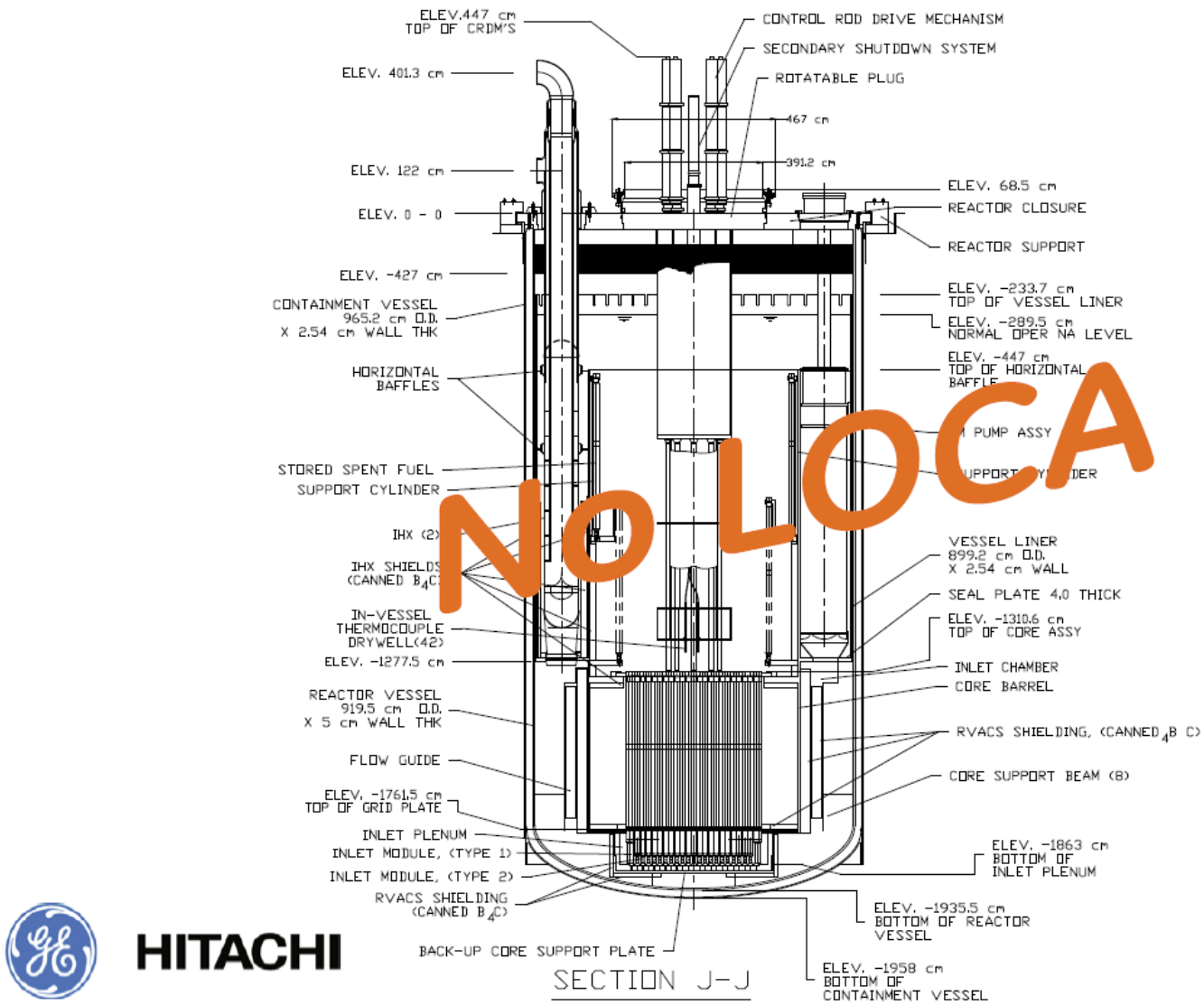

Figure 28. The best representation of the dimensions of the PRISM reactor available to develop a model.[24]

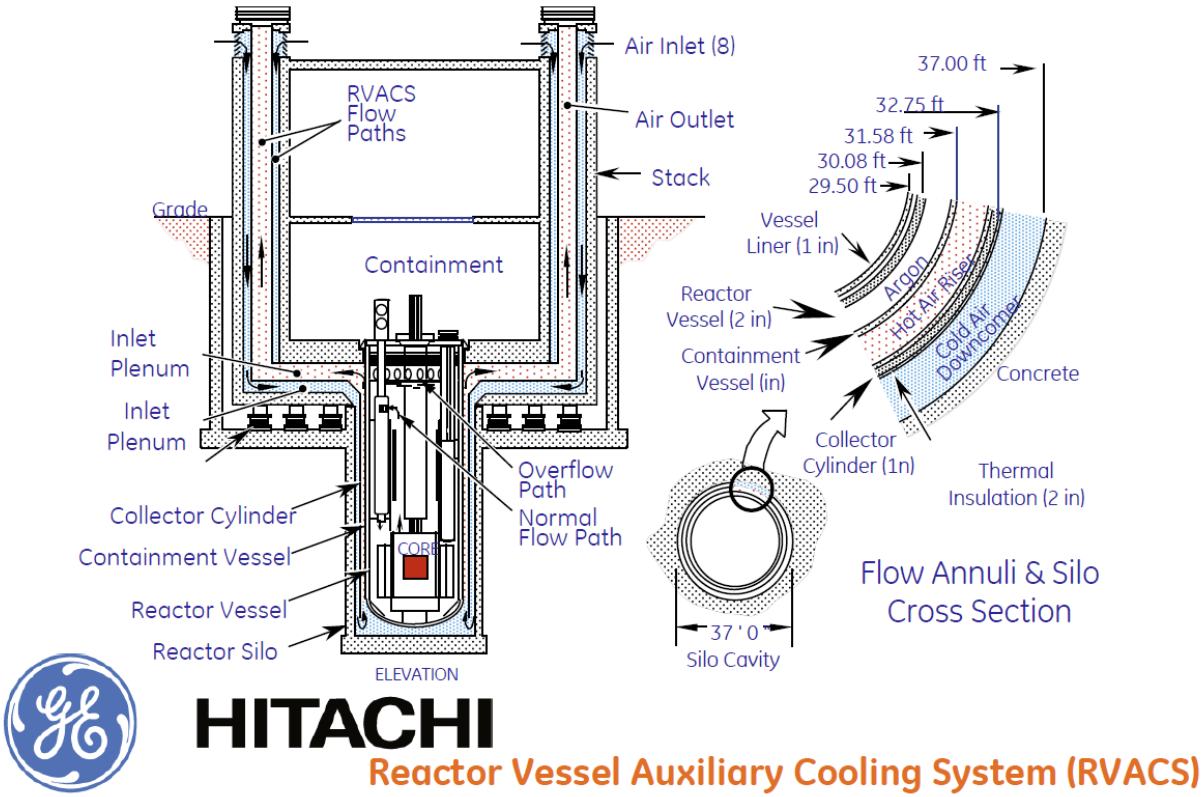

Figure 29. The best figure available to us used to determine the dimensions of the RVACS system that surrounds the core.[24]

The MCNP model developed based on these images is shown in Figure 30. A neutron source was placed in the approximate location of the core and 10,000,000 particle histories were run. Tallys of flux were taken at various points in the reactor including the core, the B_4C shields at the top and bottom of the core, the sodium surrounding the core, the support cylinder, the two B_4C shields surrounding the support cylinder, the sodium pool around the core support cylinder and shielding, the reactor vessel, the argon gap in the RVACS, the containment vessel, the hot air riser, the collector cylinder, and the hot air riser. Above the core, the sodium was divided into 14 sections to determine the release of radiation through the top of the vessel. As seen in Figure 28, most of the reactor is underground, so radiation deposition on the outside of the cold air downcomer is not of great concern. However, energy deposited in the hot air riser and cold air downcomer could potentially be released to the atmosphere. Even still, the main concern of release is through the top of the reactor.

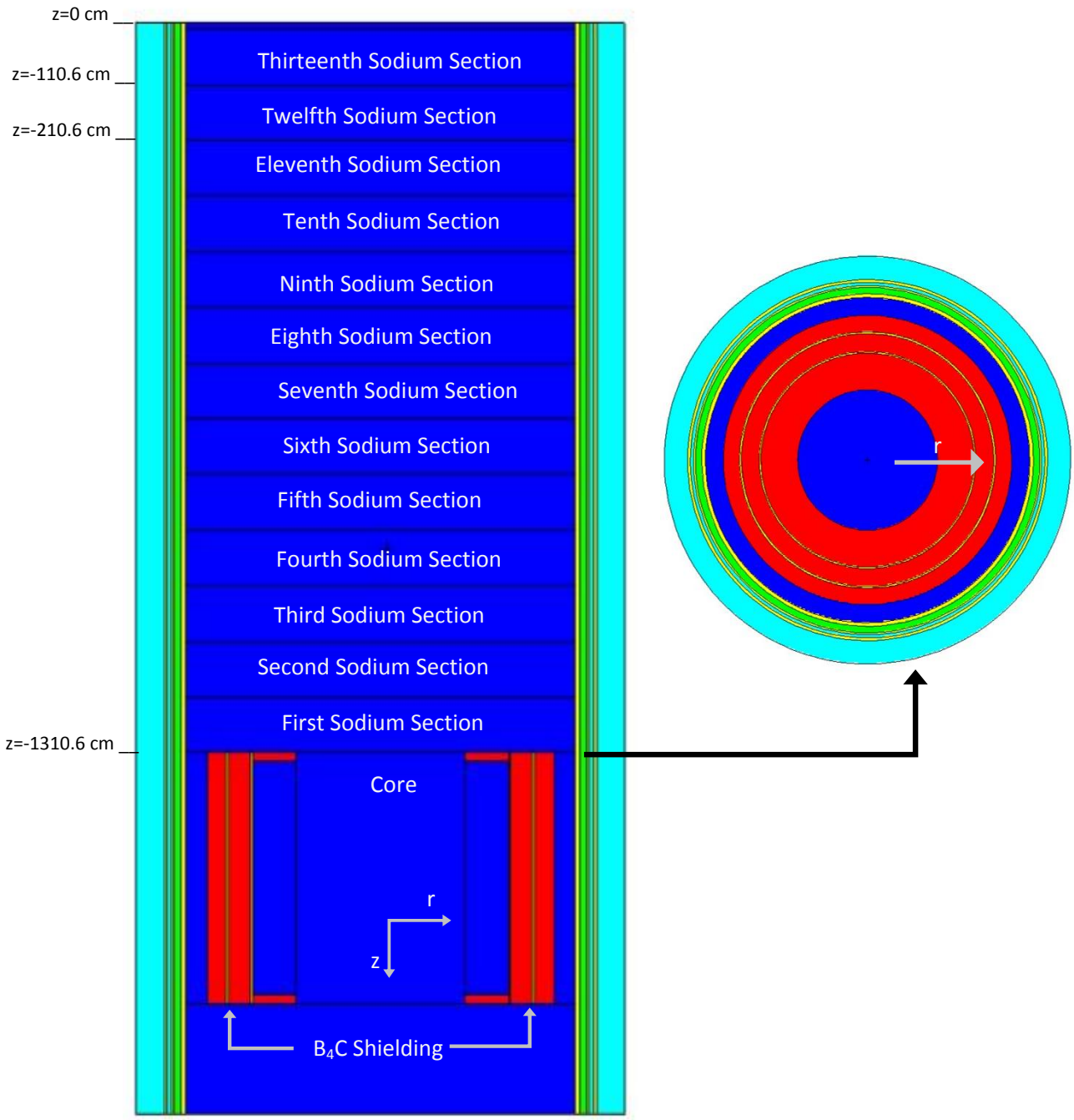

Figure 30. Cross Sectional views of the MCNP model of the shielding in the SPRISM core.

The data output by the code is normalized to neutrons absorbed in a cell per source particle. These factors were multiplied by the number of neutrons leaving in the core per unit time (a best estimate available from the neutronics analysis) to get the number of neutrons deposited per volume per unit time for the SPRISM reactor. For these results, we used a flux of 6.23E13 neutrons/second, which is the flux in the outermost breeder assembly. This is likely an over-estimation of the true flux that is leaving the core, but for a shielding analysis it will be a safe

assumption. Figure 31 shows the number of neutrons deposited in a volume per source particle in the vertical direction, from the core to the top of the reactor on a log scale, fit with an exponential.

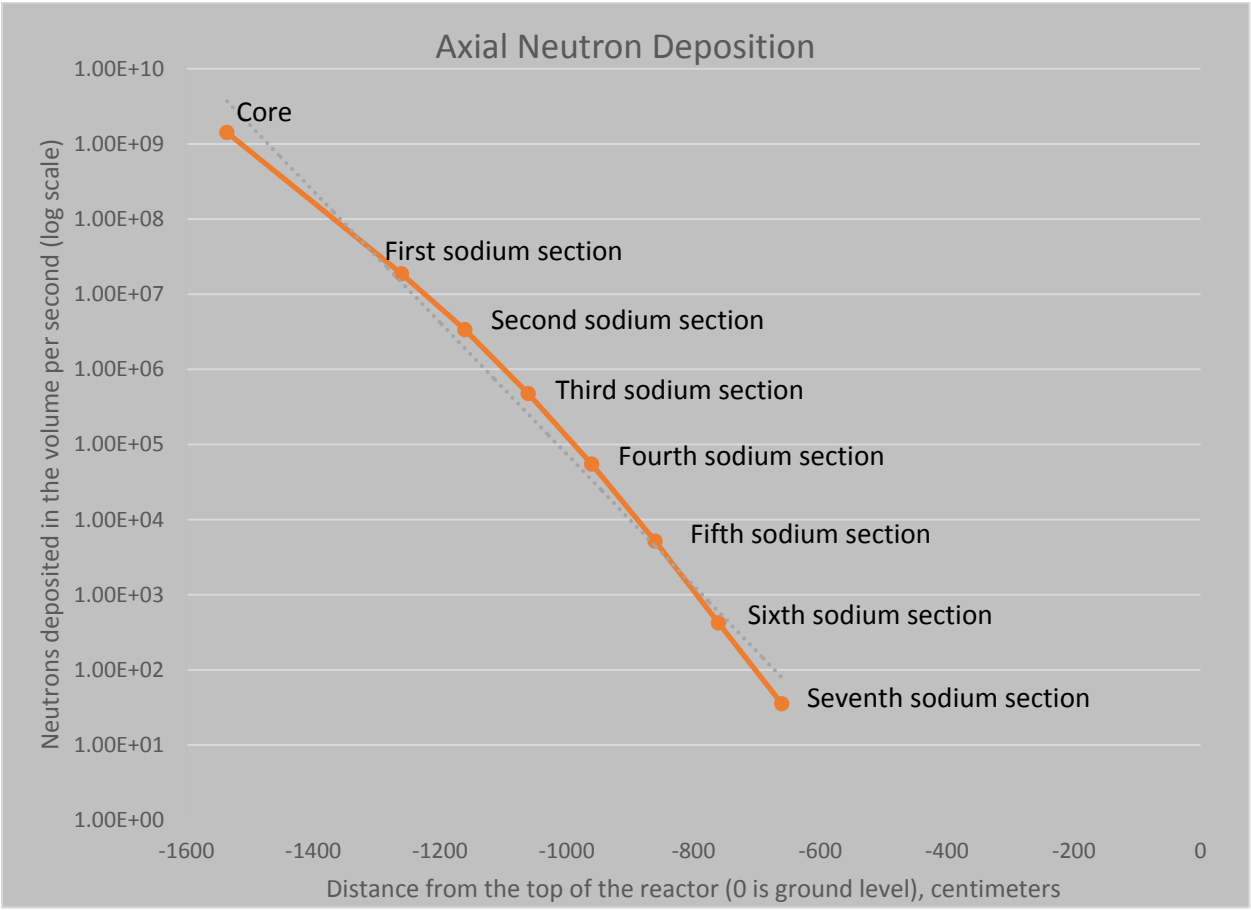

Figure 31. The results from MCNP showing an exponential decrease in number of neutrons deposited per source particle as distance from the core increases. The seventh sodium section and beyond registered no neutrons deposited.

As expected, the number of neutrons deposited per source particle decreases exponentially with distance from the core. In a run of ten million source particles, no neutrons made it beyond the sixth section of sodium, which is more than 5 meters from ground level. From this, it is safe to assume that there will be no neutron dose to the surroundings from this reactor. The radial neutron deposition is shown in Figure 32.

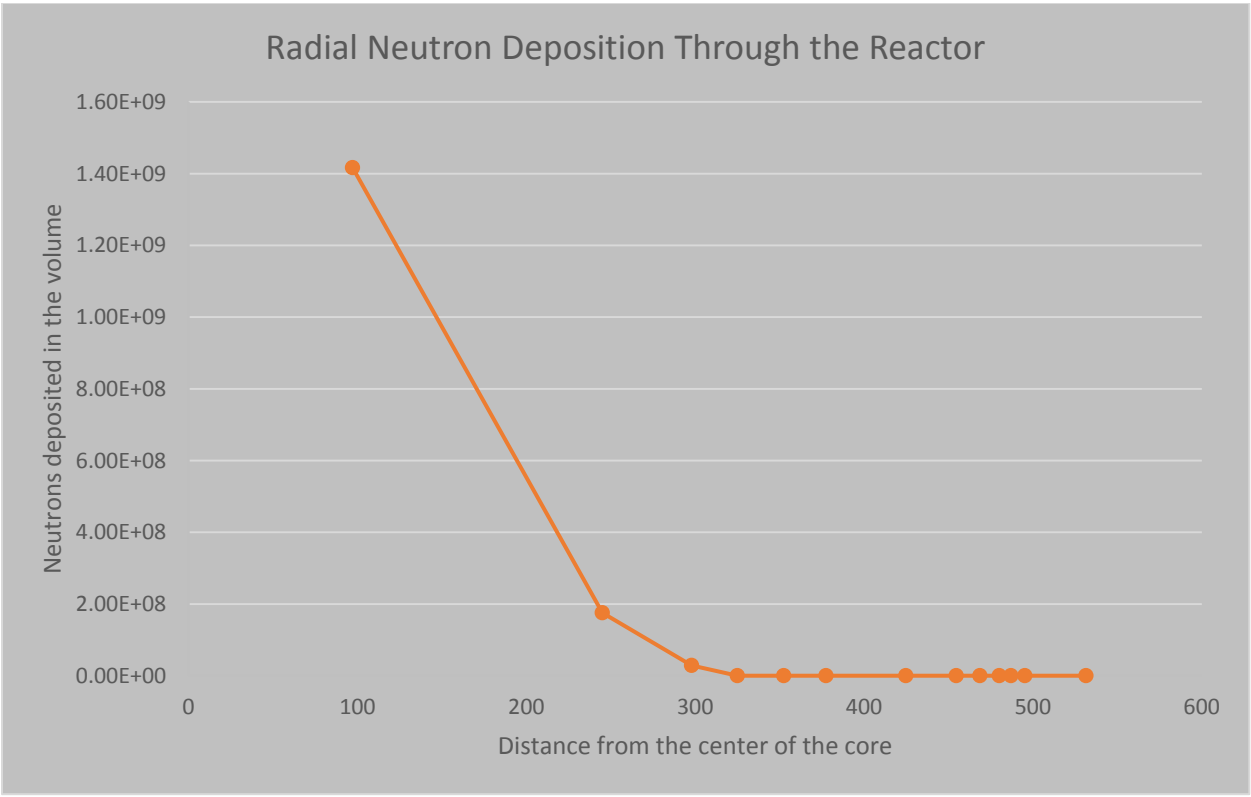

Figure 32. Number of neutrons deposited in the reactor radially.

The data shows clearly that the neutrons are well attenuated before they reach the RVACS system and risk release to the air. Future work should be done to analyze gamma radiation as well before the reactor is determined to be safe, but this is beyond the scope of this project.

5.9 Conclusions

The results of this analysis have shown no reason why the SPRISM would not retain its inherently safe characteristics with the addition of TPBARs. The addition, lowering the power density will increase its safety in accident scenarios. Tritium release from normal leakage from the TPBARs will pose no risk to the public or to radiation workers at the plant. However, the simultaneous failure of over 2000 TPBARs could result in high dose rates for workers nearby. A neutron dose assessment in MCNP showed that neutrons were properly shielded by the sodium coolant, both axially and radially. Future work should be done to examine accident scenarios and resulting transients in more detail using a code such as RELAP-3D before these results can be confirmed. A more thorough dose analysis to include gammas should be done as well. Overall, the SPRISM would offer a safe option for tritium production.

6.0 Thermal Hydraulics (Timothy Crook)

The thermal hydraulics discussion was submitted separately.

7.0 Economics (Timothy Crook)

The Economics analysis was submitted separately.

8.0 Conclusions and Recommendations (Chad O'Hagan and Sara Loupot)

This study explored the feasibility of using the SPRISM design for dedicated tritium production, applying the existing SPRISM and TPBAR designs with minimal modifications. For the purposes of this study, the model used pure sodium coolant, the fuel compositions given in Table 1, and the current TPBAR design, with two exceptions to the current TPBAR design. The active TPBAR region needed to be reduced to 47 inches in length to match that of the SPRISM active core region and the TPBAR radial dimensions were adjusted slightly to replace fuel rods in selected assemblies. The radial dimension adjustments were used for replacing fuel rods in selected assemblies with TPBARs. The core contained 13,056 TPBARs when the driver assembly fuel rods were replaced and 6,096 when the breeder assembly fuel rods were replaced. Watts Bar 1 has 544 TPBARs with active lengths of about 152 inches for the Fall 2012/Spring 2014 irradiation cycle. For the larger scale application, which is beyond the scope of this study, the TPBAR assembly will require modification for compatibility with the SPRISM core. Since detailed design documents are unavailable, only a design concept for the assembly was used, here. An average neutron flux was calculated to be 6.26E13 neutrons/cm^2 s based on core model output data. Rough calculations revealed that less than one gram of tritium produced in a 1.5 year period. Further exploration in this study may produce better results, however.

The safety analysis results indicate no challenge to the SPRISM's inherent safety with the addition of TPBARs. In fact, their addition will reduce reactor power output and neutron flux, which increases its safety in accident scenarios. Tritium release from normal TPBAR leakage pose no risk to the public or to radiation workers within the plant. However, the simultaneous failure of over 2000 TPBARs could result in high dose rates for workers nearby. A neutron dose assessment showed that neutrons were properly shielded by the sodium coolant. Future work should explore accident scenarios and transients in more detail. A more thorough dose analysis to include gammas should also be performed. Overall, the SPRISM seems to offer a safe option for tritium production.

Acknowledgements

Team 6 would like to thank Dr. David Senor and Dr. Pavel Tsvetkov for their support, guidance, advice, and assistance throughout this project. Additionally we would like to show our immense gratitude and appreciation to Jesse Johns for his patience and hours of assistance while developing, debugging, running, and analyzing the neutronics MCNP code. We also extend our thanks to Christopher Chance for his assistance with the development of the shielding MCNP code and Oluwatomi Akindele and Daniel Custead for assistance with HotSpot. Last, but not least, we would like to thank our fellow classmates for their help and support while we worked through this project.

References

1 Senor, David. *Tritium Technology Program Overview and SMR Design Challenge.* Nuclear Engineering Systems and Design, Fall 2012. Texas A&M University. 7 September 2012. PNNL Guest Lecture.

2 Makhijani and M. Boyd. *Small Modular Reactors: Fact Sheet*. Institute for Energy and Environmental Research April 2012.

3 World Nuclear Association. *Small Nuclear Power Reactors*. www.world-nuclear.org/info/inf33.html September 2012

4 Sumner, Tyler. "Effects of Fuel Type on the Safety Characteristics of a Sodium Cooled Fast Reactor." Georgia Institute of Technology, Woodruff School of Mechanical Engineering, November 2010.

5 Muta, H., "Thermal and mechanical properties of uranium nitride prepared by SPS technique," *Journal of Nuclear Materials*, vol. 43, pp. 6429-6434, October 2008.

6 Streit, M., "Nitrides as a nuclear fuel option," *Journal of the European Ceramic Society*, vol. 25, no. 12, pp. 2687-2692, 2005.

7 Lanning, D. D., Baldwin, D. L., Cunningham, M. E., Marschman, S. C. "Postirradiation Examination Report for the Tritium-Producing Burnable Absorber Rods Irradiated in the Watts Bar Nuclear Plant." Pacific Northwest National Laboratory. June 2002.

8 Johnson, A. B. Jr., Kabele, T.J., Gurwell, W. E. "Tritium Production from Ceramic Targets: A Summary of the Hanford Coproduct Program." Battell, Pacific Northwest Laboratories, August 1976.

9 Lanning D. D. "Tritium Target Qualification Project: Description of the Tritium-Producing Burnable Absorber Rod for the Commercial Light Water Reactor." Rev. 5, December 1999

10 Ghrayeb, S. Z., "Investigations of Thorium Based Fuel To Improve Actinide Burning Rate In S-PRISM Reactor: A Thesis in Nuclear Engineering." Department of Nuclear Engineering, Pennsylvania State University. December 2008.

11 "MCNP – A General Monte Carlo N-Particle Transport Code." Los Alamos National Laboratory, Volume 1, Version 5, April 2003.

12 "Production TPBAR Inputs for Core Designers." Tritium Technology Program. TTQP-1-116. November, 2012.

13 D. Redden, T. Ross, "Tritium Production and Release Path." Braidwood Operations Training. Exelon Nuclear Fuels.

14 U.S. Nuclear Regulatory Commission, "Preapplication Safety Evaluation Report for the Power Reactor Innovative Small Module (PRISM) Liquid Metal Reactor", NUREG-1368. February 1994.

15 Stachowski, Russel. "Appendix B:GE Pool-Type PRISM Fast Reactor", Fast Spectrum Reactors. Sringer 2012.

16 Health Protection Agency, "Review of Risks From Tritium." Documents of the Health Protection Agency. November, 2007.

17 United States Nuclear Regulatory Commission, "Standards For Protection Against Radiation", NRC Regulations. 56 FR 23391. May 21, 1991.
18 United States Nuclear Regulatory Commission, "Frequently Asked Questions About Liquid Radioactive Releases" December 2012. http://www.nrc.gov/reactors/operating/ops-experience/tritium/faqs.html
19 United States Nuclear Regulatory Commission, "Tritium in Groundwater at Vermont Yankee Nuclear Plant." http://www.nrc.gov/info-finder/reactor/vy/vy-groundwater-issue.pdf
20 S.M. Stoller Corporation, "Tritium Occurrence in Groundwater at Diablo Canyon Power Plant." http://pbadupws.nrc.gov/docs/ML1116/ML11166A174.pdf.
21 Watts Bar Nuclear Plant. "Groundwater Tritum Status Report" August 2005.
22 "Unclassified TPBAR Releases, Including Tritium" Tritium Technology Program, July 2012.
23 "HotSpot Health Physics Code for the PC." National Atmospheric Release Advisory Center.
24 GE Hitachi Nuclear Energy, "PRISM Technical Brief."

Design and Analysis of the Application of the B&W mPower SMR of Tritium Production

Submitted in partial fulfillment of the requirements of NUEN 410

Final Design Report

Team 9

William Cook

Leigh Ann Emerson

Connor Woolum

Pacific Northwest National Laboratory

David Senor, Ph.D.

Department of Nuclear Engineering, Texas A&M University

Karen Vierow, Ph.D.

Design and Analysis of the Application of the B&W mPower SMR for Tritium Production

April 30, 2013

Technical Advisor Approval

Team 9

William Cook

Leigh Ann Emerson

Connor Woolum

Pacific Northwest National Laboratory

_____ _____

David Senor, Ph.D. **Date**

Department of Nuclear Engineering, Texas A&M University

_____ _____

Karen Vierow, Ph.D. **Date**

EXECUTIVE SUMMARY

Written by Leigh Ann Emerson with input from Connor Woolum and Mac Cook

Tritium plays a major role in maintaining the United States' strategic nuclear weapons stockpile, and for years the United States was able to produce the tritium necessary to maintain this stockpile at the Savannah River Site (SRS). However, tritium production at the SRS was eventually ceased, and the decommissioning of old weapons became the main source of tritium. For a few years, this recycling of weapons materials allowed for the recovery of sufficient tritium to maintain the inventory (Senor & Paxton, Tritium Technology Program Overview and SMR Design Challenge, 2012). Recently though, as the tritium has decayed and the stockpile surplus depleted, it has become necessary to once again find a method to produce tritium. Currently this is done using tritium producing burnable absorber rods (TPBARs) at the Watts Bar Nuclear Power Plant in Tennessee. However, placing these TPBARs in a reactor whose main purpose is to make power has caused several issues. By placing the TPBARs in the reactor, additional negative reactivity is inserted. In order to compensate for this additional negative reactivity, the fuel must be further enriched in order to maintain the same cycle length as is achieved without the TPBARs present (Senor & Paxton, Tritium Technology Program Overview and SMR Design Challenge, 2012). This means that the federal government has had to pay the difference in the cost necessary to further enrich the fuel. Thus, the Department of Energy (DOE) is looking for a different method to maintain our nation's tritium stockpile.

One of the options to be considered is for the government to build its own small modular reactor (SMR) with the main purpose of producing tritium (Senor & Paxton, Tritium Technology Program Overview and SMR Design Challenge, 2012). To help achieve this objective, this senior design project focused on assessing the design modifications necessary to the Babcock and Wilcox (B&W) mPower SMR in order to enable the production of tritium. To accomplish this, information was obtained from various references and B&W regarding the mPower reactor (APPENDIX A). This supported the creation of thermal hydraulic and neutronic code input decks.

Thermal hydraulics analyses were performed using RELAP5—3D. The thermal hydraulic output files were used to obtain additional input for the neutronics analysis of the project. In particular, for steady state operation the average fuel temperature was found to be 909°F from the thermal hydraulics analysis. It should be noted that even during a loss of flow accident (LOFA) –the worst postulated design basis accident (DBA) for this reactor — the peak fuel and cladding temperatures were maintained within an acceptable range. The average fuel temperature was input into the neutronics analysis.

The neutronics analysis allowed for the reactor core design to be optimized and the potential amount of tritium production to be assessed. This analysis was performed using Casmo4, a lattice physics code. The optimized mPower parameters were found to be 22% lithium-6 enrichment for the TPBARs and a cycle burnup of 21 GWd/MTU, which corresponds to approximately 2 years.

The goal of this design was to produce 1150 grams of tritium per year. The tritium production calculations were performed using a code developed specifically for the project called *Team 9 Nuclide Program (T9NP).* The optimized design of the modification to the mPower reactor was found to only

produce 1116.9 grams over a two year cycle. According to the economics analysis performed, the cost of producing tritium in the mPower was calculated to be $11320 per gram, whereas the market price for buying tritium was found to be $30000 per gram. Therefore when the cost of buying versus producing tritium was considered, it was concluded that this would still be a viable way for the United States to produce tritium if two mPower SMRs were built on the same site using B&W's "twin pack" design.

TABLE OF CONTENTS

1. APPROACH 2
1.1. Thermal Hydraulics 4
1.2. Neutronics 4
1.3. Tritium Production and Modeling 5
1.4. Integration of Components 7
1.5. Economics Analysis 7
1.6. Timeline 8
2. DISCUSSION 10
2.1. Thermal Hydraulics 10
2.1.1. Design Basis 10
2.1.2. Code Choice 10
2.1.3. Coding Methodology 10
2.1.3.1. Spatial Nodalization 11
2.1.3.2. Input Data Selection 12
2.1.3.3. Loss of Flow Accident 16
2.1.4. Results 20
2.1.4.1. Steady State Analysis 20
2.1.4.2. LOFA Analysis 20
2.1.4.3. Integration 22
2.2. Neutronics 23
2.2.1. Developing an Input Model 23
2.2.2. Modeling Lithium-6 with Boron-10 24
2.2.2.1. Using Boron-10 to Simulate Lithium-6 24
2.2.2.2. Ranging the Lithium-6 Factor 28
2.2.2.3. Validation of Boron-10 Simulation Methodology 28
2.2.3. Design and Modifications 30
2.2.3.1. Determination of Cycle Length 30
2.2.3.2. Determination of Lithium-6 Enrichment for TPBAR 34
2.2.3.3. Core Loading and Fuel Enrichment 36
2.2.4. Analysis 42
2.2.4.1. Use of TPBAR in place of WABA 42

2.2.4.2. Reactivity Coefficients 44
2.2.4.3. Power Distribution in the mPower Core 46
2.3. Tritium Production and Modeling 49
2.3.1. TPBAR Design 49
2.3.1.1. Standard TPBAR Design 49
2.3.1.2. Modified TPBAR Design 50
2.3.2. Tritium Permeation and Leakage 50
2.3.3. TPBAR Activation Analysis 52
2.3.4. Dose Rates from a TPBAR 54
2.3.5. Lithium-6, Tritium, and Helium-3 Tracking 54
2.3.6. Heavy Ion Interactions 58
3. ECONOMIC ANALYSIS 61
4. CONCLUSIONS AND RECOMMENDATIONS 64
5. FUTURE WORK 65
WORKS CITED 66
APPENDIX A: DESIGN DATA RECEIVED FROM B&W 68
APPENDIX B: RELAP5-3D STEADY STATE ANALYSIS INPUT DECK 70
APPENDIX C: RELAP5-3D LOFA ANALYSIS INPUT DECK 76
APPENDIX D: PERL SCRIPT FOR TEMPERATURE EXTRACTION FROM RELAP5-3D OUTPUT FILES 83
APPENDIX E: CASMO4 INPUT DECK EXAMPLE FOR SIMPLE INFINITE ARRAY 95
APPENDIX F: CASMO4 INPUT DECK EXAMPLE FOR M X N REACTOR 97
APPENDIX G: PLOTS OF K-INFINITY VERSUS BURNUP FOR VARIOUS FUEL ENRICHMENTS AND ROD ARRANGEMENTS 101
APPENDIX H: DATA FOR VERIFICATION OF SIMULATING LITHIUM-6 USING BORON-10 106
APPENDIX I: T9NP CASES AND ANALYSIS 107
APPENDIX J: DOSE RATE DERIVATION AND CALCULATIONS 111
APPENDIX K: T9NP SOURCE CODE 117

LIST OF FIGURES

Figure 1. This shows the spatial nodalization developed for use with RELAP5-3D. 11

Figure 2. This diagram shows the various radial zones modeled in the fuel pin. The blue zones represent the fuel, the purple zone represents the helium gap, and the orange zones represent the cladding. 12

Figure 3. This shows the chopped cosine shape of axial power distribution along the fuel rod. 15

Figure 4. This diagram shows the basic layout, flow path, and penetrations of the reference design mPower. 17

Figure 5. This graph shows the radial temperature distribution through the pellet, gap, and cladding over time. 20

Figure 6. This plots shows the maximum fuel and cladding temperature as a function of time during the LOFA analysis. 21

Figure 7. This plot shows the beginning of the LOFA analysis where the maximum fuel and cladding temperature both increase as a function of time. 21

Figure 8. Basic layout of the mPower fuel assembly. (Williams, 2011). 23

Figure 9. Cross-section plot comparing boron-10 and lithium-6 total cross sections. 25

Figure 10. This plot shows the % difference in k-infinity values between TPBARs with natural lithium, and boron equivalent to natural lithium. This difference is plotted against burnup for various fuel enrichments. 29

Figure 11. This plot shows burnup versus how much lithium-6 is remaining for various lithium enrichments and fuel enriched to 3.5%. The legend on the right represents various lithium-6 enrichments ranging from 8% to 34%.....33

Figure 12. Plot of k-Infinity for various lithium-6 enrichments and U-235 enrichments. 34

Figure 13. Plot of k-Infinity for various lithium-6 enrichments and U-235 enrichments. 36

Figure 14. This plot shows k-infinity versus burnup for various fuel enrichments. The legend on the right indicates fuel enrichment. 37

Figure 15. This image shows the lower right quarter section of the core as modeled by Casmo4. It shows the individual pins in their locations, along with TPBARs shown in white, guide tubes in solid blue, and gadolium fuel pins in green. 38

Figure 16. k-infinity versus burnup for a 2-D section of the mPower core with 22% enriched Li-6 and 3.5% enriched U-235 throughout the reactor. 39

Figure 17. This image shows the multiplication factor versus burnup for a 2-D section of the mPower core. The data was generated for a core loaded with 3.5% enriched fuel assemblies, with TPBARs containing 12% helium-3. 39

Figure 18. This plot shows k-infinity versus burnup for the mPower core when modeled using 4% enriched fuel and TPBARs containing 12% helium-3. 41

Figure 19. This plot shows the k-infinity versus burnup for a 2-D section of the mPower core with 3.5% and 4.0% enriched fuel assemblies and TPBARs containing 4% helium-3. 42

Figure 20. This plot shows the k-infinity value for various rod arrangements at various burnup positions. It contains data for TPBARs for both the low and high multiplication factors used to simulate lithium in the TPBARs. 43

Figure 21. This plot shows the relative power distribution throughout the mPower core at the beginning of life. [0 GWd/MTU]. 47

Figure 22. This plot shows the relative power distribution throughout the mPower core at the middle of life. [10.5 GWd/MTU]. 47

Figure 23. This plot shows the relative power distribution throughout the mPower core at the end of life. [21 GWd/MTU]. 48

Figure 24. Diagram showing the standard TPBAR components (not to scale). 50

Figure 25. Radionuclide concentrations in a TPBAR as a function of time. 53

Figure 26. Decay heat generated in a TPBAR as a function of time. 54

Figure 27. Diagram showing the principle tritium producing reactions. 55

Figure 28. SRIM-2013 output of a triton from the (n,α) reaction of lithium-6 into the lithium aluminate pellet. 59

Figure 29. SRIM-2013 output of a beam of tritons born at the getter interface, normal to the getter. 60

Figure 30. Output of T9NP when a shutdown period is considered. 108

Figure 31. Output from T9NP for a "realistic" scenario based on the Team 9 design. 110

Figure 32. Diagram Illustrating the basic geometry for the gamma flux analysis performed here. 111

LIST OF TABLES

Table 1. This table contains data collected or received about the mPower core and was used to create neutronics and thermal hydraulics models. (Westinghouse, 2013). (Williams, 2011). (APPENDIX A). 3

Table 2. Comparison of different tritium producing targets. 6

Table 3. This table shows the relative power generated in each node along the length of a fuel pin. 16

Table 4. This table shows values for decay power versus time as input into RELAP5-3D. 19

Table 5. This table contains the molar masses of the components of lithium aluminate. 27

Table 6. This table shows the various input file combinations run in Casmo4 in order to get the data necessary to choose the optimal lithium-6 enrichment. 31

Table 7. This table contains k-infinity values for TPBARs for both the low and high factors used (see Equation 10), along with their difference for a 4% enriched fuel. 44

Table 8. This table contains k-infinity values for WABAs and average k-infinity values of the low and high factor TPBARs, along with their difference for a 4% enriched fuel. 44

Table 9. This table contains the temperature reactivity coefficients calculated for various fuel enrichments, using the low factor for lithium equivalent boron at the beginning and end of life for an mPower core. Reactivity coefficients are presented in units of [pcm/^{o}K]. 45

Table 10. This table contains the temperature reactivity coefficients calculated for various fuel enrichments, using the high factor for lithium equivalent boron at the beginning and end of life for an mPower core. Reactivity coefficients are presented in units of [pcm/^{o}K]. 45

Table 11. This table contains the temperature reactivity coefficients calculated for various fuel enrichments, using the low factor for lithium equivalent boron at the beginning and end of life for an mPower core. The TPBARs used in generating this data contained the limiting case of 12% helium-3. Reactivity coefficients are presented in units of [pcm/^{o}K]. 46

Table 12. This table contains the temperature reactivity coefficients calculated for various fuel enrichments, using the high factor for lithium equivalent boron at the beginning and end of life for an mPower core. The TPBARs used in generating this data contained the limiting case of 12% helium-3. Reactivity coefficients are presented in units of [pcm/^{o}K]. 46

*Table 13. Gamma Flux 3 feet from the center of a TPBAR (gammas/cm^2*s). 113*

*Table 14. Gamma Flux 3 feet from a point 3 feet above a TPBAR (gammas/cm^2*s). 114*

*Table 15. Unattenuated Gamma Flux 3 feet from the center of a TPBAR with a 1-foot lead shield (gammas/cm^2*s). 114*

Table 16. Source Term for a TPBAR (gammas/s/ft-TPBAR). 115

Table 17. Linear Attenuation Coefficients for Lead. 115

Table 18. Sievert Integrals of Interest for Solving the Problem given in the Text. 116

INTRODUCTION

Written by Leigh Ann Emerson with input from Connor Woolum

Nuclear weapons play a vital part in the defense of the United States of America. Therefore, as a key component of thermonuclear weapons, tritium is required for the United States' nuclear weapons stockpile. However, tritium is radioactive and has a half-life of only 12.3 years. Therefore it must constantly be produced in order maintain the nation's strategic stockpile. In 1988 the DOE ceased production of tritium at the Savannah River Site (SRS). Thus, the United States needed another method of maintaining its stockpile. From 1988 to the late 1990s the stockpile was maintained using tritium from decommissioned weapons. In 1995, Pacific Northwest National Lab (PNNL) was selected to design a process to produce tritium using light water reactors (LWRs). From 1995 to 2000, research and testing for the use of TPBARs to produce and collect tritium was performed. In 2000 this TPBAR program was selected by the DOE as the method to be used by the United States for producing tritium. In 2003 the first production core, with 240 TPBARs, was irradiated in Tennessee Valley Authority's (TVA) Watts Bar Nuclear Unit 1. Following this, design modifications were made to the TPBARs from 2005-2008 to optimize the process (Senor & Paxton, Tritium Technology Program Overview and SMR Design Challenge, 2012). Note, however, that because this method of producing tritium adds negative reactivity to the reactor core, power output of the plant is decreased. Because of this, the DOE must pay TVA for the lost electricity due to the TPBARs' presence in the reactor. Additionally, the production of weapons material at a commercial power plant has negative political considerations. Consequently the DOE's National Nuclear Security Administration (NNSA) is exploring new methods of tritium production. In an effort to help achieve this goal, this senior design project focused on modifying the design of the B&W mPower SMR for tritium production (Senor, Senior Design Project Meeting, 2012).

OBJECTIVE

The objective of this senior design project was to enable the production of tritium in an SMR in a safe, economical, and reliable manner. In order to accomplish this, B&W's mPower SMR design was modified for use with TPBARs and PNNL's tritium program.

1. APPROACH

Written by Leigh Ann Emerson; Table created by Connor Woolum

The overall design goal for this project was to assess the use and modifications to the mPower SMR to enable production of tritium. To accomplish this, there were several main areas that had to be focused on: thermal hydraulics, neutronics, and tritium production and modeling. Supporting sections include the economic analysis, integration of components and the timeline. Leigh Ann Emerson completed the thermal hydraulics analysis related to tritium production in the SMR. Mac Cook addressed the optimization of tritium production and its effects on the system, and Connor Woolum focused on the neutronics calculations. Further details about each of these tasks are explained in the sections below.

Note that the required inputs for the thermal hydraulics and neutronics sections were highly dependent on information, such as fuel assembly dimensions and the number of fuel assemblies, which is specific to the mPower reactor. Therefore because not much of the mPower design information was public knowledge, B&W was contacted in November of 2012 via Dr. David Senor to see what information they would be willing to provide. They responded in the middle of March of 2013. The requested list of parameters and B&W's response can be seen in APPENDIX A.

B&W did not provide any specific information regarding the fuel for the mPower. It was just said to be "conventional" (APPENDIX A). Because the fuel design is such an important yet complex part of reactor analysis, all fuel parameters were modeled after the Westinghouse AP 1000 (Westinghouse, 2013). A combined list of parameters as provided by B&W and as taken from the UK Westinghouse AP1000 Design Control Document are included in Table 1 below.

Table 1. This table contains data collected or received about the mPower core and was used to create neutronics and thermal hydraulics models. (Westinghouse, 2013). (Williams, 2011). (APPENDIX A).

mPower Specifications	
Operating Parameters	
Power Output	530 MW_t
Power Density	30 W/gU
Pressure	2060 PSIA
Steam Pressure	825 PSI
Design Cycle Length	4 years
Coolant Flow Rate	30 Mlbm/hr
Coolant Inlet Temperature	567 ^oF
Coolant Outlet Temperature	606 ^oF
Fuel Assemblies	
Number	69
Rod Array	17 x 17
Rod Pitch	0.496 in
Assembly Demensions	8.46 x 8.46 in
Cladding	Zircaloy-4
Burnable Absorbers	16/assembly
Guide Tube Diameter	0.442 in (ID), 0.482 in (OD)
Guide Tubes	24/assembly
Instrument Tube Diameter	0.442 in (ID), 0.482 in (OD)
Instrument Tube	1/assembly
Gadolium Doped Fuel	4/assembly, 6% Gd_2O_3
Fuel	
Enrichment	<5%
Pellet Diameter	0.3225 in
Cladding Diameter	0.3270 in (ID), 0.372 in (OD)
Rods	17,112
General	
Soluble Boron	0ppm
Pressure Vessel Dimensions	13 x 83 ft
Active Core Length	95 in

1.1. Thermal Hydraulics

Written by Leigh Ann Emerson

Major subtasks for this part of the design project included determining the temperature distribution in the fuel, helium gap, and cladding. In order to accomplish this, the equations of state, mass, momentum, and energy had to be solved. A control volume approach was determined to be the most effective way to analyze these parameters.

A discussion with Dr. Vierow last fall revealed that RELAP would be a good code to analyze this portion of the project. As RELAP5-3D is the version of RELAP available to students in the Texas A&M Department of Nuclear Engineering, it was used for the thermal hydraulics analysis portion of this project. Specifically, a spatial nodalization network was developed and the corresponding input deck created for use with RELAP5-3D in order to evaluate the mPower (Idaho National Laboratory, 2012).

RELAP5-3D was designed so that it can simulate both plant transients and a range of accidents that may occur. This includes normal transients that occur during operation as well as large and small break loss of coolant accidents (LOCAs). It also includes an automatic input check that detects input errors and inconsistencies (Idaho National Laboratory, 2012). This helps to decrease the likelihood of errors that may occur when performing analyses. This range of capabilities made RELAP5-3D ideal to model the mPower reactor. Specifically RELAP5-3D/Ver:1.1.72 was used for this analysis. This version of the code, hereafter referred to as RELAP5-3D, enabled the reactor to be modeled during both a steady state analysis as well as during a LOFA.

Variables required for creating the RELAP5-3D input deck are specific to the reactor being analyzed. Therefore a large number of specific parameters, regarding the mPower reactor, were needed as input in order to accurately model the flow through the reactor core using RELAP5-3D. These were taken from the data found in Table 1 and APPENDIX A.

RELAP5-3D has a rather large learning curve. Therefore it took quite a bit of time to understand and develop an input deck for this code. Creating a spacial nodalization network from scratch as well as running and changing the input for a steady state and transient analysis was difficult but able to be achieved. In the end, the code was successfully run and data was able to be passed from this portion of the project to the other parts of the project.

1.2. Neutronics

Written by Connor Woolum

In order to analyze the neutronic aspects of the mPower reactor, a lattice physics code was necessary. The use of Casmo4, MCNP, DRAGON and SCALE was considered. MCNP is known for having a very steep learning curve, and it also takes a significant amount of time to run due to the level of detail it tracks. While MCNP was initially an option in case any other code would not work properly, it was not the most favorable option for the reasons mentioned. SCALE is also a lattice physics code that could have been used to model the mPower reactor. While the learning curve is less significant than MCNP, it would still

take a significant amount of time to learn the capabilities of the code and how to properly run it. None of the group members had experience with SCALE, so it was not the most favorable option either. DRAGON lattice physics code should be capable of performing the necessary analyses of the mPower. However, like MCNP and SCALE, it is unfamiliar to the design team and also has a significant learning curve. All of the design team members were already familiar with Casmo4, and it was thought that it would adequately model the mPower reactor. Therefore Casmo4 was chosen to perform the neutronics analysis.

Casmo4 is a lattice physics code developed by Studsvik Scandpower. It is a multi-group, two-dimensional transport code used for analysis of PWR and BWR calculations. It models an infinite array of an input fuel assembly to determine k-infinity, along with other important variables such as burnup. Additionally, the extended version has the capability to model a 2-D section of a reactor core. This includes reflectors around the edges and specification of core configuration such as fuel assemblies with differing fuel enrichments.

Casmo4 is tailored specifically to analyze PWRs and BWRs, and since the mPower reactor is a PWR, Casmo4 is an efficient and capable tool for such an analysis. Casmo4 has the ability to accept many input parameters to accurately model the reactor. It is also a very efficient program and the code runs significantly faster than other lattice physics codes. The use of Casmo4 for modeling the mPower was discussed with Dr. Ragusa at the beginning of the design project and he believed it would adequately model the mPower. Due to the design groups' familiarity with Casmo4, and the above mentioned items, Casmo4 was chosen as the primary method to analyze the mPower reactor with TPBARs.

Note that the approach to modeling neutronics using Casmo4 was altered when it was discovered that it did not contain the cross-section definitions for lithium-6. This setback was overcome by using boron-10 in place of lithium-6 and is discussed in further detail in the neutronics section of this paper.

1.3. Tritium Production and Modeling

Written by Mac Cook

The primary objective of this design was to sustainably, economically, and safely provide tritium to the NNSA for stockpile management. Thus, many different techniques were considered for the production of tritium in the SMR. This analysis is performed in Table 2. From this, a lithium-6 target was chosen as the most effective way to create tritium.

Table 2. Comparison of different tritium producing targets.

	Thermal Cross Section		Chemical Features		Suitability for High Burnup		Cost		Score
Weighting Factor	0.3		0.3		0.3		0.1		
Helium-3	very large	10	inert	5	depletes rapidly	2	medium price	4	5.5
Lithium-6	large	9	forms many suitable compounds	9	depletes moderately	8	lower price	7	8.5
Deuterium	very small	2	chemically similar to tritium	1	deplete negligibly	4	medium price	5	2.6

Thus, the problem was approached using TPBARs, as outlined in the discussion section. The enrichment of lithium-6 determined the amount of tritium produced in each rod, as well as, the reactivity worth of the rod. Different levels of enrichment were considered for different positions in the core and different fuel assemblies. Due to the design of the mPower reactor, other methods of tritium production such as tritium producing reflectors were not feasible and therefore not considered. It has been requested that the complete design produce 1150 grams of tritium per year. This may mean the use of B&W's "twin pack" design of two coupled reactors. The team first attempted to fulfill the primary objective of tritium production before optimizing the design for electricity production, cost effectiveness, and research and development benefits.

Since the TPBARs have an impact the reactivity and thus safety of the reactor, many analyses have been performed. The TPBARs have undergone permeation and leakage analysis, activation analysis, dose rate analysis, and heavy ion modeling. These impact the structural integrity of the TPBAR and the safety of the reactor. To ensure tritium is produced effectively, CASMO along with a nuclide tracking program have been used. Within the Discussions section, the CASMO analysis is presented in the Neutronics subsection, while the nuclide tracking program is presented in the Tritium Production and Modeling subsection.

Much of the security and safety of the tritium extraction process has already been designed and is in use by PNNL. This includes the shipment of the irradiated TPBARs and their handling. Changes to these techniques were not considered.

1.4. Integration of Components

Written by Leigh Ann Emerson

The above three sections were all dependent upon each other in various ways. Results from the thermal hydraulics calculations were necessary to accurately model the reactor physics portion of the design project. The neutronics output data was then used to assess the amount of tritium being produced. In turn the amount of tritium being produced determined which enrichment and core design was to be used. Therefore an iterative process was used to determine the final core design used for this project.

Thermal hydraulics and heat removal capabilities typically serve as the limiting factor for reactor performance (Vierow, NUEN 410 Class Notes, 2013) Because of this, the thermal hydraulics analysis had to be run first. This data was then used to perform a neutronics evaluation of the reactor, with a given TPBAR configuration. This output was then used as described above to find a steady-state solution that produces tritium safely, effectively, and efficiently.

1.5. Economics Analysis

Written by Mac Cook

An economics analysis was performed towards the end of the design project. This analysis determined the differential cost of producing tritium in an mPower reactor versus simply producing electricity. The analysis of this project included all costs related to producing tritium in the mPower reactor, from initial SMR and TPBAR procurement to the production of tritium in the reactor. Costs related to transportation of TPBARs post-irradiation and tritium extraction will be very similar to current costs since the infrastructure is already in place. These costs have very little impact on design, and are required for all methods of tritium production, thus they were excluded from this analysis. It should be noted that due to the current development stage of the mPower reactor and the sensitive nature of the proprietary design, certain data was not available. When this problem was encountered, best estimates based on expert input were used.

1.6. Timeline

Written by Connor Woolum

A timeline was created initially as a rough guideline of key completion dates. Timely work was necessary and important in order to ensure a thorough and complete project by the deadline.

TIMELINE ITEM	DESCRIPTION	PROPOSED COMPLETION DATE	COMPLETION NOTES
Meet with Dr. Senor	Meet with Dr. Senor to discuss mPower SMR for tritium production	October 31, 2012	Spoke regarding mPower use for tritium production, PNNL supports this projects goals and will provide assistance as they are able.
mPower operating parameters	List of mPower parameters to get from B&W	End of November	Email sent to Dr. Senor 11/19/2012
Casmo4	Determine feasibility of using Casmo4 for model	End of November	Spoke briefly with Dr. Ragusa and he believes licensing agreement won't be an issue. Still need to determine if Casmo will accurately give us the information we need.
RELAP/TRACE Input Deck	Begin to prepare input deck for thermal hydraulics analysis of mPower reactor	January 2013	--
Casmo4 Input Deck	Begin creating Casmo input deck for mPower reactor with TPBARs	February 2013	Can't be completed until a response is received from B&W. Will use stock TPBARs as designed for the TVA WB1 reactor- these can be optimized later.
Meet with Dr. Senor	Meet with Dr. Senor when he visits TAMU mid-semester to update with progress and get input as to what PNNL wants.	Middle of Spring Semseter (determined by Dr. Senor's schedule)	--
Optimize Reactor Cycle Duration for Tritium Production	Determine what the optimal cycle length is in order to maximize tritium production and minimize costs	March 2013	This will depend upon what data PNNL and B&W is able to provide regarding current tritium production costs and costs associated to mPower reactor and fuel
Cost/Benefit Analysis	Perform economic analysis to determine estimated costs of producing tritium via the mPower SMR.	April 2013	--
Design Report	This will be started as data is available and other goals are completed.	End of April 2013	--

The timeline was followed as closely as possible, however, the project did get behind in some areas. Initially, it took longer than expected to get data regarding the mPower reactor from B&W. Because of this setback, a significant amount of time was spent data mining to find all parameters necessary to create accurate models of the reactor.

The project also ran into some difficulties with the RELAP model due to lack of familiarity with the program. RELAP has a steep learning curve and much time was spent practicing using the program and building up from simple models to the model developed to simulate the mPower.

Other than these two setbacks, the project was kept relatively in line with the timeline created in October of 2012. The setbacks faced simply meant that emphasis was refocused a few times in order to keep the project schedule on track.

2. DISCUSSION

2.1. Thermal Hydraulics

Written by Leigh Ann Emerson

2.1.1. Design Basis

The goal of the thermal hydraulics part of this project was to obtain the temperatures in the fuel and cladding to ensure fuel integrity during all reactor modes – shutdown, standby, and operation. According to the NRC the peak limit for the cladding temperature is 2200 degrees Fahrenheit (U.S. NRC, 2013). This temperature is significant because it is the approximate temperature at which the cladding reacts with the coolant, causing significant oxidation to occur. This is a highly exothermic reaction and thus should be avoided in order to prevent significantly increasing the temperature of the coolant and therefore further jeopardizing the integrity of the cladding.

The fuel temperature is limited by the melting point of the fuel (UO_2), which occurs around 5160 degrees Fahrenheit. However, the fuel temperature is a less limiting constraint on the thermal hydraulic analysis of the reactor because it will not be reached until cladding failure occurs. Therefore cladding temperature is the most limiting parameter for the thermal hydraulic analysis of the mPower.

2.1.2. Code Choice

In order to solve for the temperature distributions necessary for this analysis, the equations of state, mass, momentum, and energy needed to be solved. To do this, it was determined that a control volume analysis with a spatial nodalization network was to be used. These nodes could then be specified and parameters at each node evaluated using a code, namely RELAP5-3D.

RELAP5-3D was chosen to evaluate the thermal hydraulic portion of the reactor analysis because of its history with the NRC. The first version of the code, RELAP5/MOD3, was a code "developed by Idaho National Laboratory (for the NRC) for the analysis of transients and accidents in water-cooled nuclear power plants". Some additional versions of the code were sponsored and used by the DOE to verify the safety of its test and production reactors. Note that the code has also been experimentally validated by comparing its results to the LOFT, PBF, Semiscale, and other experimental tests (Idaho National Laboratory, 2012). Thus analysis performed using RELAP5-3D is widely accepted across the nuclear community, especially for simulating reactor system thermal-hydraulic behavior for the licensing of reactors (U.S. NRC, 2013). These reasons made RELAP an ideal choice for analyzing the thermal hydraulic state of the reactor.

2.1.3. Coding Methodology

The following sub-sections of this report explain the coding methodology used in developing the input deck for use with the RELAP5-3D code. This includes creating a spatial nodalization network, selecting appropriate input parameters, and modeling the distribution of heat generated axially in the core.

2.1.3.1. Spatial Nodalization

In order to properly model the thermal hydraulics of the core in RELAP5-3D, an appropriate spatial nodalization with respect to the core had to be developed. To do this, first the main components necessary for running the code were determined. These included the core, a heat generation mechanism (known as a heat structure), a lower holding tank (which can be likened to the lower plenum), an upper holding tank (similar to the upper plenum), and junctions between the various components. See Figure 1.

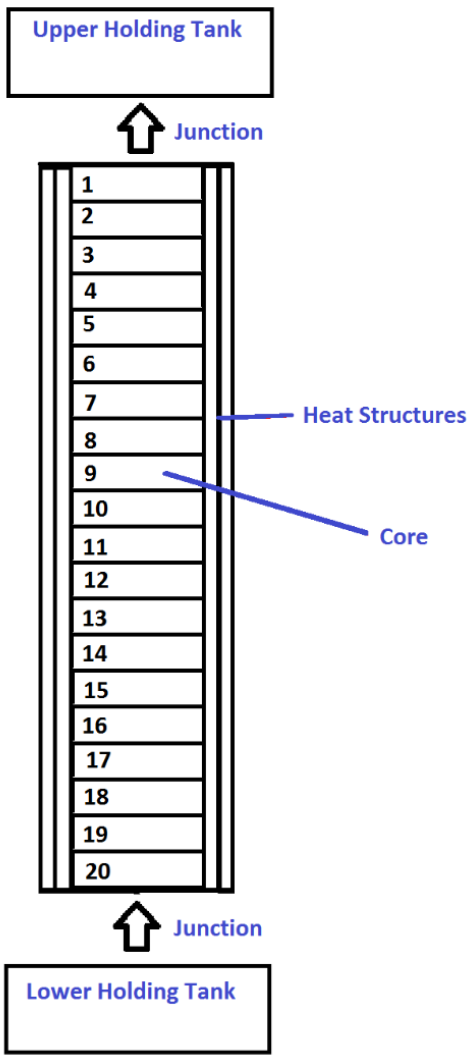

Figure 1. This shows the spatial nodalization developed for use with RELAP5-3D.

Notice in the above figure that the core is split axially into twenty nodes. This allowed the relative generation of power in each node, along the length of the fuel rods (and therefore the core) to be accounted for. Each node was also split radially into nine different zones. See Figure 2.

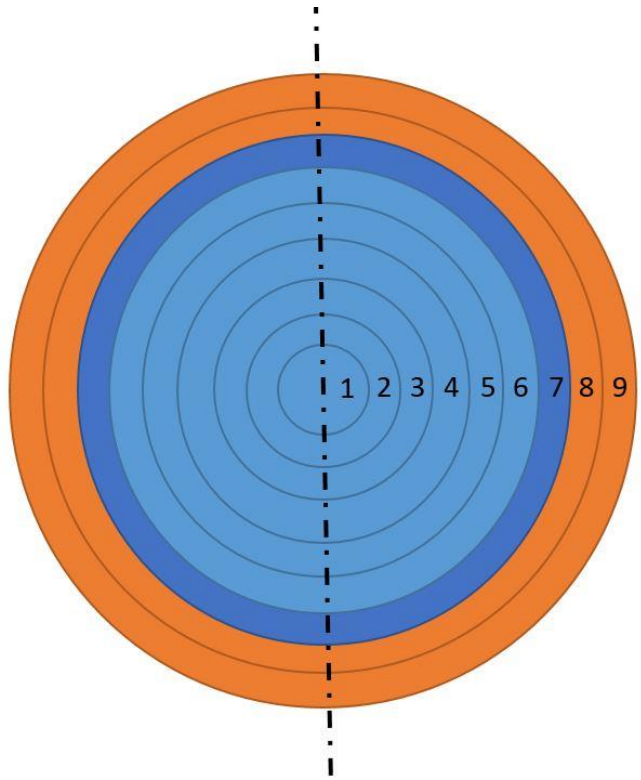

Figure 2. This diagram shows the various radial zones modeled in the fuel pin. The blue zones represent the fuel, the purple zone represents the helium gap, and the orange zones represent the cladding.

The first six radial zones are in the fuel, the seventh covers the helium gap, and the eighth and ninth are in the cladding. These zones are shown in blue, purple and orange, respectively, in Figure 2. Designating these zones along with the axial nodes allowed for a complete temperature distribution for the core to be determined. The temperature distribution was then used to analyze the maximum fuel and cladding temperatures to determine the integrity of both the cladding and fuel during various modes of operation.

2.1.3.2. Input Data Selection

Core

Data provided by B&W included the active length of the core, number of fuel assemblies in the core, and the fuel assembly array type (17x17). See APPENDIX A. Fuel dimensions given by B&W were just said to

be “conventional”. Therefore, most of the core data for the fuel assemblies and rods, including pin diameter and pitch, were taken from the Westinghouse AP1000 European Design Control Document (Westinghouse, 2013). Using these parameters, the flow area of the core was calculated from Equation 1,

$$Core\ Flow\ Area = N_{FA} * \left\{ \left[(n_p - 1) * pitch + d_p \right]^2 - {n_p}^2 * \pi * \frac{d_p}{4} \right\} \qquad \text{Equation 1}$$

where N_{FA} is the number of fuel assemblies, n_p is the number of pins on one side of the fuel assembly (for example, 17 for a 17x17 fuel assembly), $pitch$ is the distance between the centers of two consecutive fuel pins in an assembly, and d_p is the diameter of a single fuel pin.

The initial conditions for the core were established by providing a pressure and temperature on the input deck. The initial pressure, as provided by B&W, was set to 2060 PSIA, and the initial temperature was set to 586.5°F. This initial temperature is the result of averaging the inlet and outlet temperatures provided by B&W.

Tanks

Two tanks were modeled in this code. The first tank, called the lower holding tank, can be likened to the lower plenum. It was created as a massively large tank (100000 cubic feet) so that as water leaves the tank, a pressure change is not created in the tank. Such a pressure change could alter the conditions of water flowing into the core. Since the goal of this part of the project was to find the steady state conditions of the core, such changes in flow conditions were undesirable.

The second tank that was created, called the upper holding tank, can be likened to the core upper plenum. This tank is used as a sort of catch pan for the water after it travels through the core. Similar to the lower holding tank, it is a massively large tank so as to not alter the flow conditions through the core and also to enable it to catch all of the water from the lower holding tank if necessary.

Heat Structures

In RELAP5-3D the heat structures represent the solid parts of a system. They generally include fuel rods, pipe walls, heat exchanger tubing, etc. By including these solid components and their material properties in the input deck, the heat transfer between the structures and fluid can be determined (Idaho National Engineering Laboratory: Lockheed Idaho Technologies Company, 1995).Thus, the heat structures are an integral part of the thermal hydraulic analysis of a system.

For the nodal network developed for this design project, the only heat structures that needed to be included were the fuel rods. Data for the fuel rods was taken from the AP1000 European Design Control Document (Westinghouse, 2013). Note, however, that because RELAP5-3D only uses a one-dimensional form of the transient heat conduction equation, temperatures were assumed to be independent axially in each of the twenty control volumes along the length of the rod. This means that an independent radial temperature distribution was found for each of the twenty control volumes.

Component Junctions

In order to properly model the system in RELAP, junctions must exist between the various hydrodynamic components (the components through which coolant flows). There are two types: time-dependent junctions and single junctions. Time-dependent junctions are used when the flow rate or another parameter specified in the junction input changes over time. Single junctions are used when a connection with constant parameters that exist between two volumes is desired.

For this design project, a time-dependent junction was input to connect the bottom holding tank and the core. This enabled a change in flow rate over time to be designated during the LOFA analysis. Because the flow rate out of the core is only a function of flow rate through the core for this project, a single junction was used to model the junction between the core and the upper holding tank.

Axial Power Distribution

In order to accurately model the axial distribution of power along the fuel rods, a cosine shape for the power generation was assumed. For calculation purposes, the height was set to zero at the center of the rod. This assumption is relatively straightforward but assumes that there is zero power generation at both ends of the fuel rod. Since this is not true in real life, however, a method had to be developed that would allow for the power generation at the ends of the fuel rod to be accounted for.

To do this, the fuel pin was split into twenty equal volumes along the z-axis. Then two additional volumes, equivalent in height to the other twenty, were added to the length of the pin, one on the top of the pin and one on the bottom. This created a chopped cosine shape for power generation along the fuel rod. See Figure 3 below.

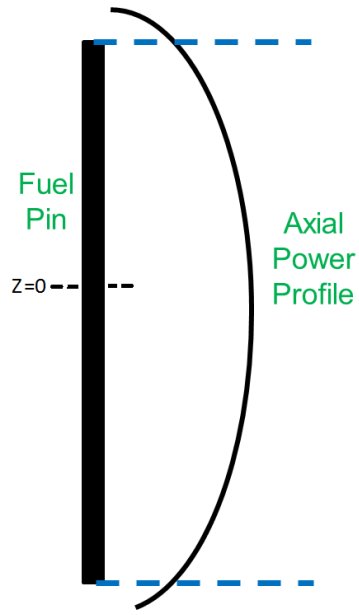

Figure 3. This shows the chopped cosine shape of axial power distribution along the fuel rod.

The value of the cosine as a function of distance from the center of the rod then had to be calculated for each volume. For RELAP, the axial peaking factors are relative and must sum to one. Therefore the values found by taking the cosine at each location along the rod had to be adjusted to find the percent of total power generated in each volume. This was done using Equation 2 below:

$$F_i^{P,Z} = \frac{cos\ (z)_i}{\sum_i \mathrm{abs}[\cos(z)_i]} \qquad \text{Equation 2}$$

where $F_i^{P,Z}$ is the axial peaking factor for volume i from i equals one to twenty, and z is the axial location of i along the fuel rod. The results of this calculation for each of the twenty volumes along the length of the fuel pin are shown in Table 3 below.

Table 3. This table shows the relative power generated in each node along the length of a fuel pin.

Node	Axial Peaking Factor
1	0.0111692
2	0.0220888
3	0.0325151
4	0.0422150
5	0.0509719
6	0.0585902
7	0.0648996
8	0.0697593
9	0.0730607
10	0.0747301
11	0.0747301
12	0.0730607
13	0.0697593
14	0.0648996
15	0.0585902
16	0.0509719
17	0.0422150
18	0.0325151
19	0.0220888
20	0.0111692

2.1.3.3. Loss of Flow Accident

For the B&W mPower design, the entire primary system loop is contained inside of the reactor pressure vessel (RPV). Therefore the only penetrations on the RPV are where the feedwater enters the vessel and steam exits. As both of these penetrations are for the secondary loop, the steam generator tubes act as a barrier to prevent losing coolant from the primary loop. According to the diagram provided by B&W both of these types of penetrations –two of each—are higher on the vessel and completely above the core. See Figure 4. That makes a LOCA unlikely and therefore less plausible than a LOFA. As such, a LOFA was briefly explored using RELAP5-3D.

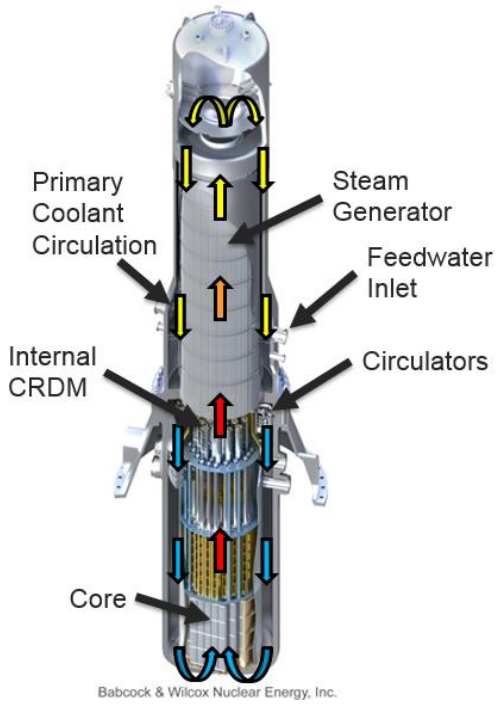

Figure 4. This diagram shows the basic layout, flow path, and penetrations of the reference design mPower.

Trips

In RELAP5-3D, trips are split into two parts. The first part involves determining the time of the trip, and the second part involves determining what the trip does (Idaho National Engineering Laboratory: Lockheed Idaho Technologies Company, 1995). For this project, only one trip card was included. It was activated five seconds into the analysis (aka the time of the trip). The second part of the trip is to designate what the trip does. For this analysis, the trip needed to simulate a loss of pump power and thus the subsequent coast down of the pumps. This was designated by changing the flow rate through the time-dependent junction between the bottom holding tank and core. Consequently, the desired change in flow rate through the reactor was achieved.

Modeling the Change in Flow Rate

Analyzing a LOFA involves determining the pump coast down and natural circulation flow rates through the core. However, because the same spatial nodalization model that was previously discussed for use with the RELAP5-3D steady state analysis was used for this part of the analysis, there is no closed flow path. Therefore due to limitations in the model that was developed and lack of time, detailed flow rate analyses were unable to be performed. Therefore several assumptions had to be made in order to assess a LOFA.

In an effort to present the most conservative case, it was assumed that all recirculation pumps simultaneously lose power, and it takes twenty-five minutes for the recirculation pumps to coast down. During this time the flow rate drops from 100% of the original total flow rate to 6% of the original total flow rate. After this point, the pumps are considered inoperable and flow through the reactor would just be the result of natural circulation. As a result, and for the purposes of this design project, flow through the core is then assumed to gradually decrease from this point to 0.6% at time equal to three hours. Flow is then held at 0.6% for the remainder of the LOFA analysis (Vierow, Associate Professor and Graduate Coordinator, 2013)

Decay Heat

For this analysis it was assumed that the reactor is scrammed five seconds after the pumps lose power and remains shut-down for the duration of the accident. Therefore, after the first five seconds of the accident, the only source of power is from the decay of fission products. This power— resulting from the deposition of energy from beta and gamma particles into the core—was found using Equation 3.

$$P = 0.066P_o[{t_s}^{-0.2} - (t_s + \tau_s)^{-0.2}] \qquad \text{Equation 3}$$

In the above equation, P is the power generated from decay heat, P_o is the power level of the reactor before shutdown, t_s is the time (in seconds) since the reactor has been shut down, and τ_s is the time the reactor was operating (in seconds) (Todreas & Kazimi, 1993). For this analysis, the reactor operating time was assumed to be eighteen months because this is the approximate time between refueling outages in currently operating US light water reactors. It should be noted though, that the decay power only changed on a small fraction of a megawatt when the operating time was changed from twelve months to eighteen months to twenty-four months. Therefore, in lieu of the other assumptions made regarding this analysis, an error in the assumption of a specific reactor operating time should only contribute slightly to the total error of the calculation.

For RELAP, decay power is input as the change in total power over time. This is included as a table where the person creating the input deck inputs the power at given times and RELAP automatically interpolates and extrapolates values as necessary. For this analysis, the decay power was input into RELAP for each hour after reactor shutdown for the first six hours then every six hours for the next thirty hours. From there power was input every twelve hours up to 72 hours. See Table 4.

Table 4. This table shows values for decay power versus time as input into RELAP5-3D.

Time	Decay Power (MW)
0	530
5 s (Shutdown)	530
Shutdown + 5 min	10.1554
Shutdown + 20 min	7.0788
Shutdown + 1 hr	5.7774
Shutdown + 2 hrs	4.8971
Shutdown + 3 hrs	4.4359
Shutdown + 4 hrs	4.1307
Shutdown + 5 hrs	3.9058
Shutdown + 6 hrs	3.7293
Shutdown + 12 hrs	3.1142
Shutdown + 18 hrs	2.792
Shutdown + 24 hrs	2.5788
Shutdown + 30 hrs	2.4217
Shutdown + 36 hrs	2.2984
Shutdown + 48 hrs	2.1129
Shutdown + 60 hrs	1.9762
Shutdown + 72 hrs	1.869

2.1.4. Results

2.1.4.1. Steady State Analysis

With the given code organization and input, a steady-state analysis was run to determine the temperature distribution through the fuel, gap, and cladding. The results are shown in Figure 5, below.

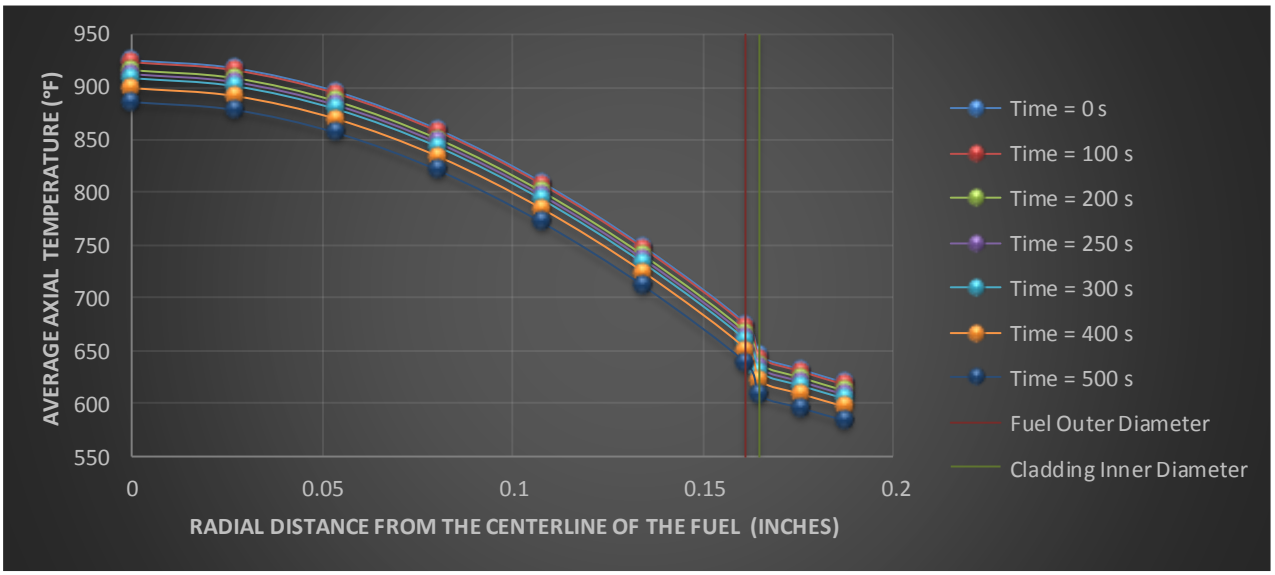

Figure 5. This graph shows the radial temperature distribution through the pellet, gap, and cladding over time.

In Figure 5 above, the shape of the temperature distribution is as expected. The low thermal conductivity of the gap— caused by a lack of convective heat transfer through the gas— caused a large temperature gradient, while the comparatively smaller thermal resistances in the fuel and cladding resulted in smaller temperature gradients (Vierow, NUEN 410 Class Notes, 2013).

While both the fuel and cladding temperatures are maintained well below temperatures that may jeopardize their integrity, the magnitude of the temperature change through each section of the fuel rod—the fuel, the gap, and the cladding— was lower than expected. Typically the change in temperature through the fuel, gap, and cladding is around 450 °F, 300 °F and 100 °F, respectively. (Vierow, NUEN 410 Class Notes, 2013). However, the results plotted above show a temperature gradient of approximately 250 °F, 30 °F, and 25 °F in the fuel, gap, and cladding, respectively. This disagreement between the accepted and calculated values for the temperature drop through each section is thought to arise from the difference in power outputs between the SMR being designed as a part of this project (540 MWth) and the typical light water reactors in operation in the United States (approximately 3000 MWth).

2.1.4.2. LOFA Analysis

The goal of the LOFA analysis for this project was the same as for the steady-state analysis—assess the fuel and cladding integrity. According to the NRC, reactors must be able to cope with a station blackout

with the use of station batteries for 72 hours. (U.S. NRC, 2013, pp. 8.4-2). Therefore, the LOFA analysis performed spanned a 72 hour (259200 seconds) time frame. The max temperature of the fuel and cladding as a function of time during this time frame can be seen in both Figure 5 and Figure 6 below.

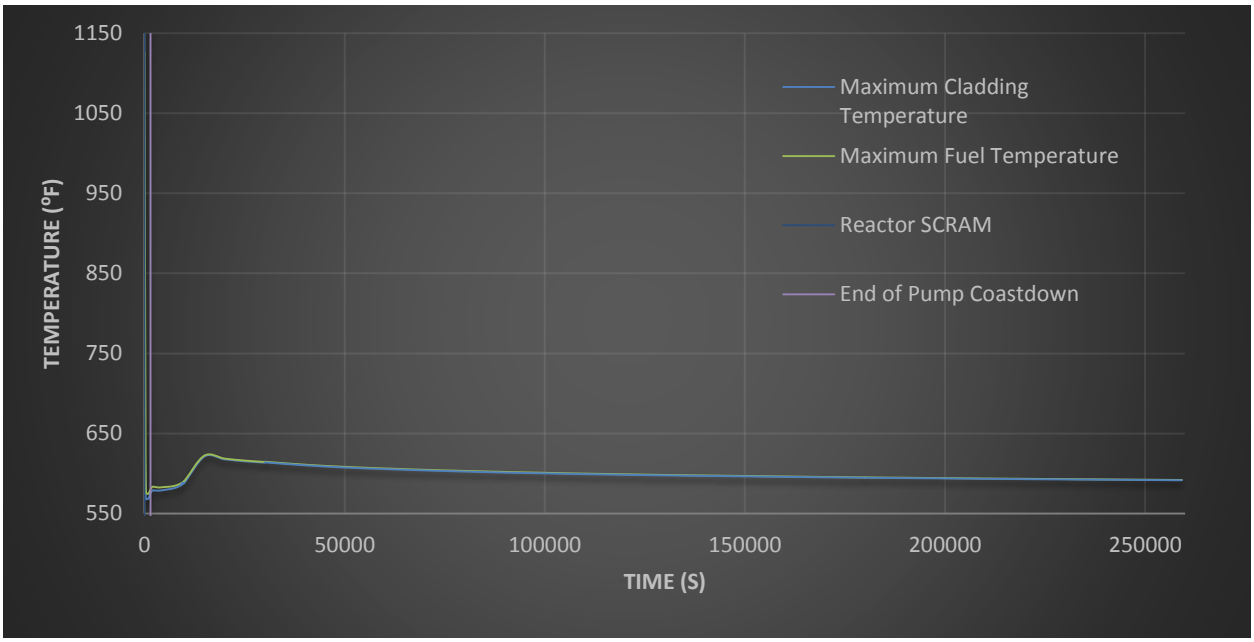

Figure 6. This plots shows the maximum fuel and cladding temperature as a function of time during the LOFA analysis.

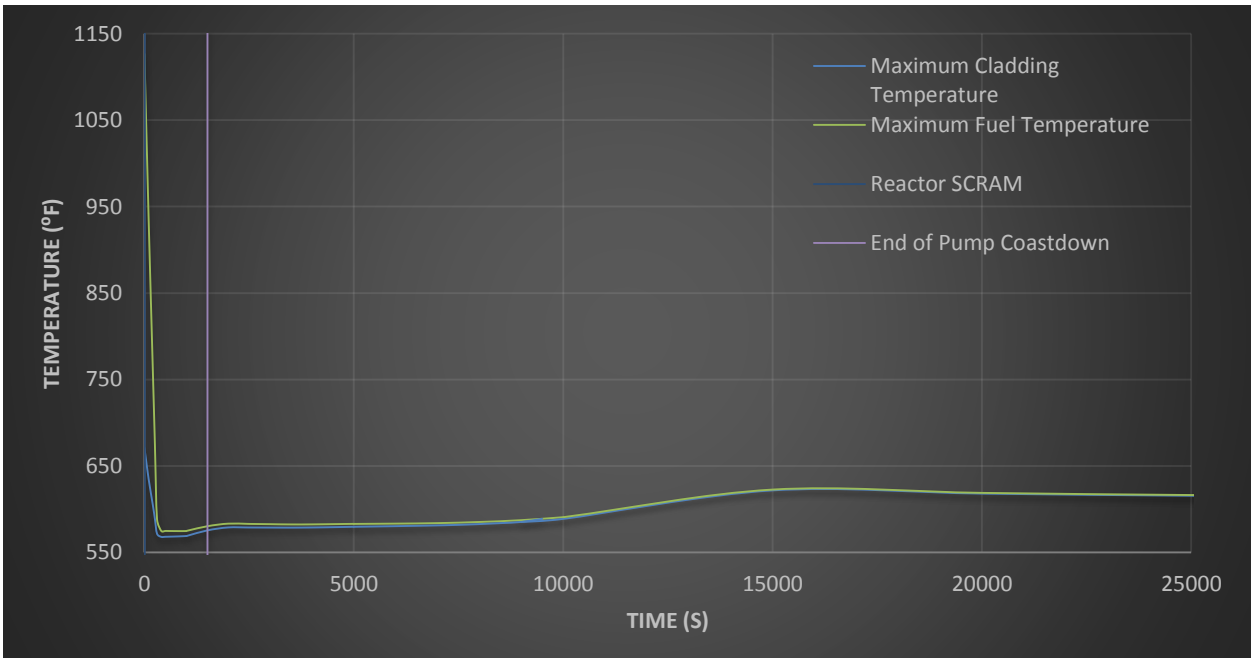

Figure 7. This plot shows the beginning of the LOFA analysis where the maximum fuel and cladding temperature both increase as a function of time.

Notice in Figure 6 and Figure 7 that there is initially a sharp decrease in the fuel and cladding temperature after the reactor is scrammed (time equal to five seconds). This is because there is a quick drop in power due to the negative reactivity insertion of the control rods. This means that the fuel is generating less heat but the pump flow rate is still at full capacity. Consequently the temperature of both the fuel and cladding will drop.

Around 300 seconds (five minutes) the fuel and cladding temperatures begin to increase over time. This is because the mass flow rate through the reactor is decreasing as the pumps coast down and eventually stop. At this point natural circulation will take over and flow will continue through the reactor but at a much smaller rate—0.6% of the original flow rate in this case. At the same time that the mass flow rate is decreasing, decay heat is being generated by the fuel in the reactor. However, because the rate at which decay heat being generated during this time is faster than the rate at which the coolant can remove the heat from the fuel pin, both the fuel and cladding temperatures rise.

The relative changes in magnitude of the rise in temperature during the first approximately 16000 seconds (about four and a half hours), is due to the different rates of change of the mass flow rate over time. During pump coast down, the change in mass flow rate is 5.2049 lbm/s/s. Then from time equal to 1500 seconds (twenty-five minutes) to 11000 seconds (about three hours), the change is mass flow rate over time is decreased to 0.0474 lbm/s/s. At that time (11000 seconds), a steady state natural circulation flow was assumed to be achieved and the mass flow rate was held constant at 50 lbm/s. During this time, the temperatures continue to rise until the decay heat decreases enough to where the coolant is removing heat from the fuel pins at a rate faster than that at which it is being generated. At this point— approximately time equal to 16000 seconds or four and half hours— the temperature of both the fuel and cladding begin to decrease.

2.1.4.3. Integration

RELAP5-3D was run until a steady state was reached within the simulated core. At this point, the temperatures were taken from RELAP5-3D, averaged axially along the length the fuel pin and input into CASMO for the neutronics analysis.

As previously mentioned, RELAP5-3D uses a one-dimensional transient heat conduction equation to determine the temperature distribution through the core. Because of this, twenty independent radial profiles are output by the code. Therefore after a steady state condition was reached in the simulated core, the temperatures were averaged axially along the length of the fuel pin to obtain an average fuel temperature of 909°F. This number was used as input for the neutronics portion of the project.

2.2. Neutronics

Written by Connor Woolum

2.2.1. Developing an Input Model

The following sections describe how the input decks were created to model the mPower reactor and TPBARs within the reactor. It was initially thought that B&W, the designer of the mPower reactor, would be willing to provide the parameters necessary to model the reactor and perform accurate analyses. However, several hold-ups were encountered in obtaining data from B&W so the reactor had to be modeled using what little data was available online. Not a lot of data was available on the mPower reactor, and a significant amount of time was spent early on collecting any that may have been available. Presentations given by B&W regarding the mPower were an important source of information. Using these presentations and other various sources such as press releases and fact sheets, a compilation of mPower parameters sufficient to model and analyze the reactors was made. The only data not found was the average fuel temperature, which was a piece of data that was generated in the RELAP5-3D analysis part of the project. Thus, it was determined that a value for this was unimportant. Table 1 in the approach section shows the values for the mPower reactor that were used to generate a model in Casmo4.

Casmo4 allows for the input of various parameters which are then used to perform an analysis. The data gathered on the fuel assemblies of the mPower were very vague and simply mentioned that the mPower used a standard 17x17 fuel assembly. Since no further information on pin pitch or assembly dimensions were available, it was assumed that the Westinghouse AP1000 fuel assembly could be accurately used to model the mPower reactor. The layout of the pins within the fuel assembly was, however, available from a B&W presentation. Figure 8 below shows the layout of an mPower fuel assembly, including the location of fuel rods, control rod guide tubes, burnable poisons, and gadolinium containing fuel rods.

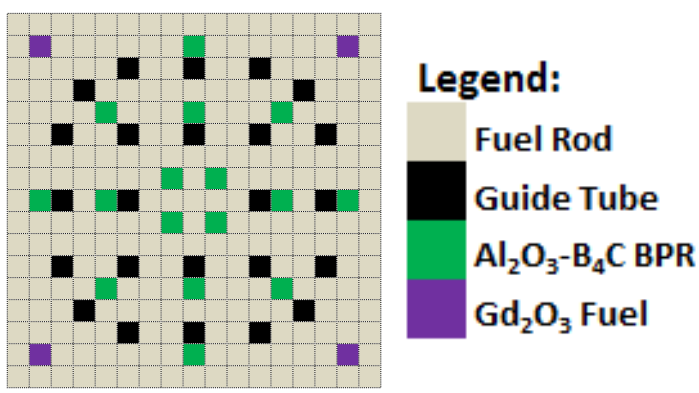

Figure 8. Basic layout of the mPower fuel assembly. (Williams, 2011).

In order to produce tritium in the mPower reactor, the burnable poisons were replaced with the standard TPBARs described elsewhere in this report. It must be noted, however, that the mPower

reactor core is only 95” tall, notably shorter than standard PWRs. Due to this, the mPower will require more TPBARs in it to produce an equivalent amount of tritium as Watts Bar I.

Most of the input data for Casmo4 was straightforward, with a few notable exceptions. The TPBARs had to be modeled as a rod, with a combination of “mixtures” in the radial direction. This modeling was done based on the design document R15TTQP-1-116, which provides number densities for modeling the TPBARs’ composition. This data is the same data used by core designers to model the TPBARs in the Watts Bar I nuclear reactor. The TPBAR was modeled with an inner portion of air, which would behave very similarly to helium in terms of neutronics properties, the next radial section was the lithium aluminate. This section was modeled using only lithium since the aluminum and oxygen that would also be found here have negligible cross sections in comparison to the lithium-6. A change had to be made in how the lithium-6 was modeled due to limitations of Casmo4, and this is described in the following section. The outer radius of the TPBAR was modeled as a homogenized cladding region, using number densities specified in the above referenced design document.

2.2.2. Modeling Lithium-6 with Boron-10

2.2.2.1. Using Boron-10 to Simulate Lithium-6

As mentioned previously, Casmo4 was chosen as the primary neutronics analysis tool for its relatively easy to use interface and its efficient computing speed. While developing the input decks to model the mPower, it was discovered that the University version of Casmo4 at Texas A&M does not have lithium-6 cross-sections in its library. In order to prevent having to learn an entirely new neutronics analysis package, alternate options were analyzed. It was found that boron-10 has very similar cross-sections to lithium-6. The image below demonstrates the “1/v” nature of the total cross-sections for both boron-10 and lithium-6. It is worth noting that the scattering cross-sections for both isotopes account for less than 5% of the total cross-section. This means that the majority of the total cross-section is due to absorption since inelastic scattering is only relevant at much higher energies for these isotopes.

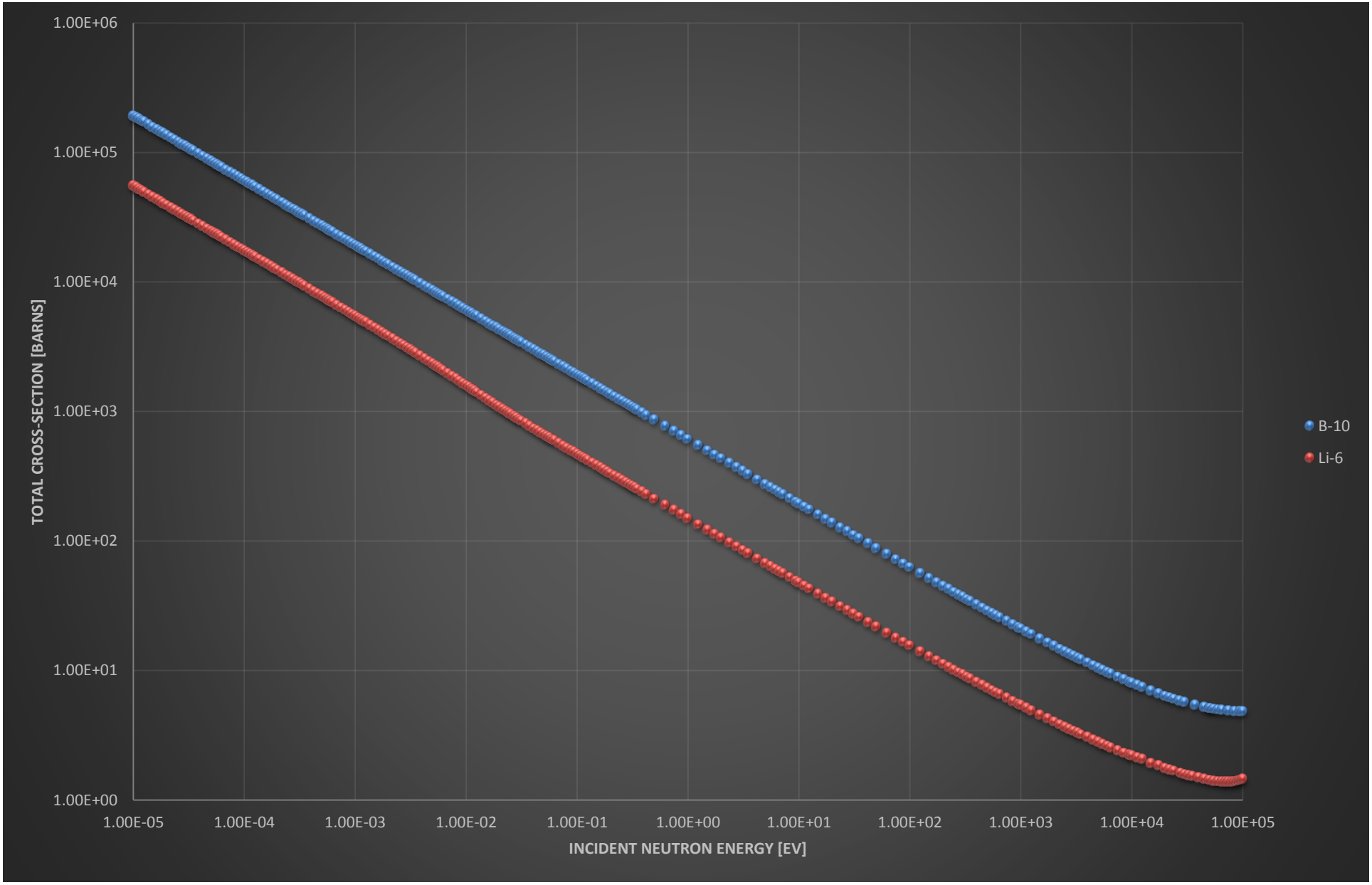

Figure 9. Cross-section plot comparing boron-10 and lithium-6 total cross sections.

As can be observed in Figure 9, both isotopes' cross-sections are proportional to "1/v" in the thermal energy range. Since the mPower is a thermal reactor, and the tritium producing reaction relies on thermal neutrons, energies above thermal are irrelevant. In the energy range of interest, the cross-sections vary by a factor of 3.47 to 4.02, with boron-10 having the larger cross-section. It was determined that boron-10 could be used to mimic lithium-6 in the reactor by adjusting the boron-10 density of the Casmo4 input file.

The methodology for adjusting the boron-10 density in Casmo4 to mimic the lithium-6 cross-section relies upon how Casmo4 uses the density input by the user. Casmo4 requires the isotope density and isotope identification. It uses the density to determine number density, which it in turn uses with microscopic cross-section to calculate a macroscopic cross section. The simple formula for macroscopic cross-section is shown below in Equation 4.

$$\Sigma = \sigma N \qquad \text{Equation 4}$$

In this equation, Σ is macroscopic cross-section, σ is microscopic cross-section, and N is number density. Number density is shown in the formula below (Equation 5).

$$N = \frac{mN_A}{M} \qquad \text{Equation 5}$$

In the equation above, N is still number density, m is mass of the isotope of interest, N_A is Avogadro's number (6.022x10^{22} atoms/gram) and M is mass of the compound containing the isotope.

In order to simulate lithium-6 with boron-10, the macroscopic cross-sections of the two isotopes were set equal, as shown in Equation 6 below.

$$\Sigma_{B-10} = \Sigma_{Li-6} \qquad \text{Equation 6}$$

It follows, from Equation 6 above, that:

$$N_{B-10}\sigma_{B-10} = N_{Li-6}\sigma_{Li-6} \qquad \text{Equation 7}$$

This relationship needs to be able to demonstrate the relationship between density and cross-sections, so Equation 5 is substituted into Equation 7, resulting in Equation 8 below.

$$\frac{\rho_{B-10}N_A}{M_{B-10}} * \sigma_{B-10} = N_{Li-6}\sigma_{Li-6} \qquad \text{Equation 8}$$

Equation 8 can then be solved for boron-10 density— the input parameter required by Casmo4.

$$\rho_{B-10} = \frac{(N_{Li-6}\sigma_{Li-6})M_{B-10}}{\sigma_{B-10}N_A} \qquad \text{Equation 9}$$

As mentioned previously, the cross-sections of boron-10 and lithium-6 vary by a multiplicative factor ranging from 3.47 to 4.02. This relationship between cross-sections is shown below in Equation 10, where x is the multiplicative factor determined from the cross-section plot in Figure 9.

$$\sigma_{Li-6} = \frac{\sigma_{B-10}}{x} \qquad \text{Equation 10}$$

This factor allows for the dependence on cross-sections in Equation 9 to be removed. This results in Equation 11 below, the final equation relating the boron-10 density to number density of lithium-6. This allows for boron-10 to be used in Casmo4 in place of lithium-6 as it scales the boron-10 cross-section to match the lithium-6 cross-section.

$$\rho_{B-10} = \frac{N_{Li-6} M_{B-10}}{x N_A} \qquad \text{Equation 11}$$

In order to vary enrichment levels of lithium-6, the number density of lithium-6 (N_{Li-6}) is changed accordingly. The rest of the variables in Equation 11 remain constant, with the exception of the x factor that can be varied as well. The relationship between lithium-6 enrichment and number density is explained below.

The general equation for number density (Equation 5) can be used to calculate the lithium-6 number density corresponding to a desired enrichment, which is then inserted into Equation 11. Lithium-6 is contained within the TPBAR as lithium aluminate, which has the chemical formula $LiAlO_2$. Lithium aluminate contains lithium-6 and lithium-7, along with oxygen and aluminum. The molar masses of these isotopes can be found in Table 5.

Table 5. This table contains the molar masses of the components of lithium aluminate.

Isotope	Molar Mass [g/mol]
Lithium-6	6.015123
Lithium-7	7.016005
Oxygen	15.9994
Aluminum	26.981539

The mass of the $LiAlO_2$ compound is calculated using Equation 12 below; it should be noted that this mass varies with lithium-6 enrichment.

$$M = e * M_{Li-6} + (1 - e) * M_{(Li-7)} + M_O + M_{Al} \qquad \text{Equation 12}$$

In the above equation, e represents the enrichment of lithium-6 in the $LiAlO_2$ of the TPBAR. The molar mass calculated in Equation 12 is used in conjunction with Avogadro's number and the density of lithium aluminate to calculate the number density of lithium for a given enrichment. This number density

represents the total number of lithium atoms, of both lithium-6 and lithium-7 isotopes. Consequently, it must be multiplied by the same lithium-6 enrichment used to calculate the molar mass to determine the number density of lithium-6 in the TPBAR.

2.2.2.2. Ranging the Lithium-6 Factor

In order to account for the variance in the multiplicative factor in Equation 10, cases were often run with both the maximum and minimum factor. This resulted in the most extreme results the reactor would face in operation. As will be shown in the following sections, the variance introduced in the results by ranging this factor is often negligible.

2.2.2.3. Validation of Boron-10 Simulation Methodology

In order to validate the use of boron-10 to simulate lithium-6 in the TPBARs, an analysis was performed using natural lithium. Casmo4 contains cross-section data for natural lithium, which is enriched to roughly 8% lithium-6. Input files were created that contained natural lithium in the TPBARs instead of the boron equivalent. Input files were also created that contained the boron-10 equivalent of 8% enriched lithium-6. These files were run, and the k-infinity values were compared. This validation method proves that boron-10 can be used as a surrogate for lithium-6 within the mPower and produce relatively accurate results.

The percent difference in k-infinity is plotted against burnup below in Figure 10. This plot allows for comparison to determine how accurately the lithium-6 simulation will model true lithium-6 in the TPBARs. It is not expected that this relationship will change much as the lithium-6 enrichment changes.

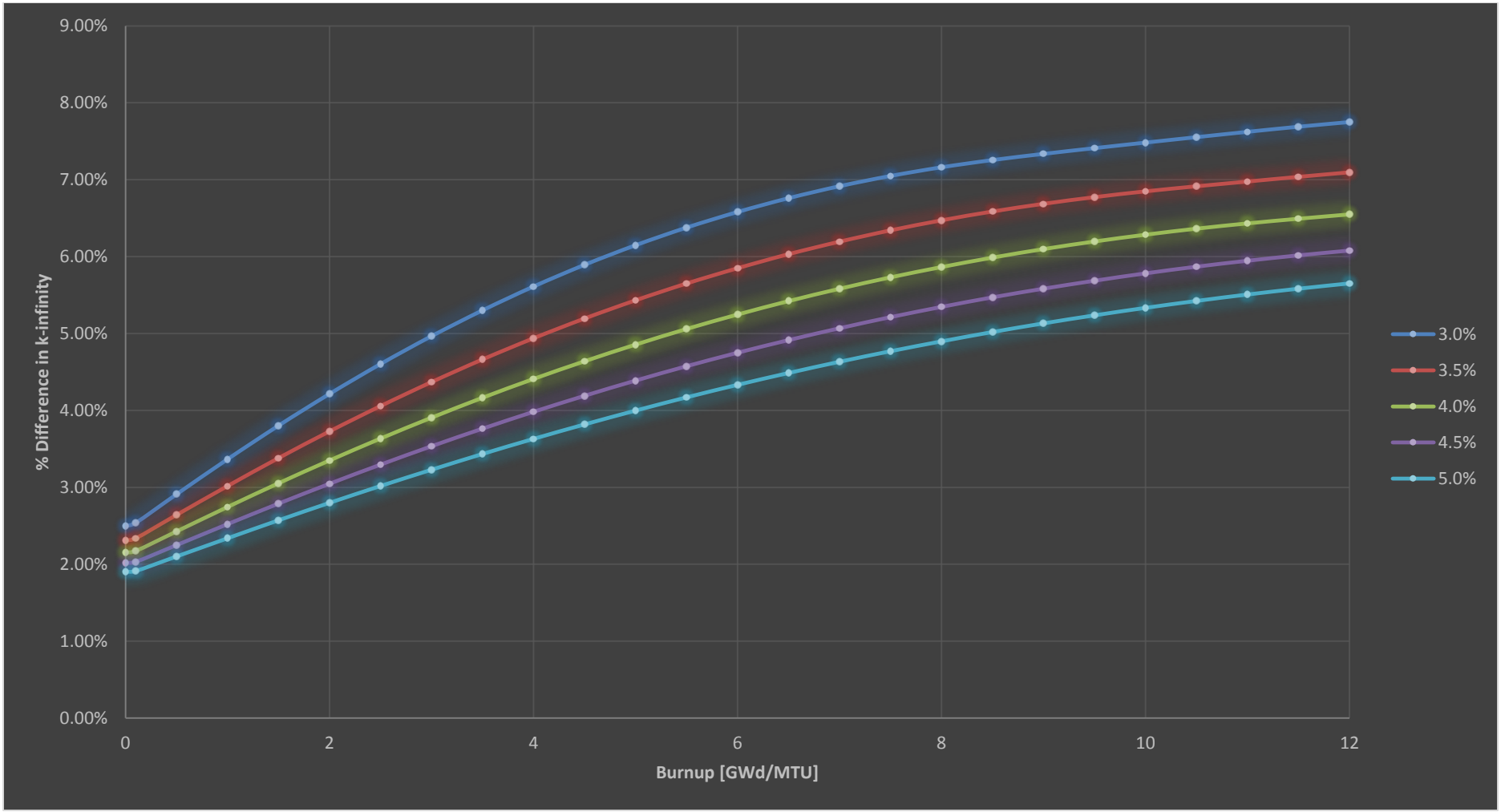

Figure 10. This plot shows the % difference in k-infinity values between TPBARs with natural lithium, and boron equivalent to natural lithium. This difference is plotted against burnup for various fuel enrichments.

The plot in Figure 10 clearly shows that there is a difference between using natural lithium, and the boron equivalent to natural lithium. This difference, however, is always under 8%. The difference tends to increase as burnup increases. This trend makes physical sense because the depletion of lithium-6 in the natural lithium would build in helium-3 to the TPBAR, thus increasing negative reactivity. This would lead to a lower k-infinity value as burnup increases. The depletion of boron equivalent to lithium-6 does not account for helium-3 buildup so the k-infinity value does not decrease as rapidly as a function of burnup. The buildup of helium-3 in the TPBAR is addressed in a subsequent section.

It was determined based on these results that using boron to mimic lithium-6 in the TPBAR will provide results sufficiently accurate to complete this study. It must be acknowledged that it is not ideal to use this surrogate, but the alternate option would be performing the study using a different lattice physics code. Due to the learning curve of another code, along with the efficiency of Casmo4 compared to other codes, it was in the best interest of the project that the use of Casmo4 was continued and issues were addressed as best as possible.

2.2.3. Design and Modifications

Once it was determined that Casmo4 would accurately provide the information needed to analyze the mPower reactor for tritium production, the analysis itself began. The neutronics analysis was used to determine or calculate several key parameters. Initially, a cycle length for the reactor was chosen. After a cycle length was chosen, the optimal lithium-6 enrichment had to be determined. Once these two parameters were chosen, several other items were addressed by the neutronics analysis. Operating the reactor in a safe manner is crucial to the feasibility of using the mPower to produce tritium. In order to ensure the reactor operates in a safe manner, the moderator and fuel temperature coefficients of reactivity were determined. Another factor important to safe operation is ensuring that the reactor operates in a region of under-moderation. This analysis was performed in the neutronics part of the project.

The goal of the design project is to optimize the mPower for tritium production, so several analyses related to tritium production had to be performed. This is addressed in several of the following sections. The neutronics calculations were used to determine how much tritium could be produced by the reactor, and at what rate. It was also important to ensure the reactor was capable of sustaining criticality throughout the cycle; the neutronics analysis addressed this. The difference in reactivity worth of a standard WABA and the TPBAR is also examined to determine how much excess negative reactivity the TPBAR adds. An entire mPower core is modeled using the standard outside-in loading approach to determine multiplication factors and again to ensure the reactor is capable of sustaining criticality throughout the proposed cycle length.

2.2.3.1. Determination of Cycle Length

The choice of cycle length was made early on in order to increase efficiency in running Casmo4 files. The time the code takes to run increases significantly with additional burnup steps. Determining the target burnup of the mPower allowed for the input files to be written so Casmo4 only does calculations to the specified burnup, thus saving computational time and allowing for a faster analysis of output.

It was determined that the most effective way to decide on a target burnup was based on depletion of lithium-6 in the TPBAR. Since the design goal is to maximize tritium production in the reactor, cycle length was based on what would most benefit this goal instead of what would necessarily be most cost effective or efficient for fuel usage. Obviously, the TPBAR serves no further purpose in the reactor when there is no longer any lithium-6 remaining to be converted to tritium. This was used as the main criteria when choosing cycle length.

Varying the lithium enrichment with fuel enrichment obviously produces differing k-infinity values for various burnup levels. Casmo4 cases were run for lithium-6 enrichments varying from 8% to 34%, in 2% increments. The lower limit of 8% enriched lithium-6 was chosen because this is the enrichment in natural lithium and would serve as a lower bound if natural lithium was used in the TPBAR. An upper limit of 34% was chosen based on input from Dr. Senor. Each of these lithium enrichments were run for fuel enrichments of 3%, 3.5%, 4%, 4.5%, and 5%. Table 6 below shows the various input combinations that had to be run in Casmo4.

Table 6. This table shows the various input file combinations run in Casmo4 in order to get the data necessary to choose the optimal lithium-6 enrichment.

Fuel Enrichment	3%													
Lithium-6 Enrichment	8%	10%	12%	14%	16%	18%	20%	22%	24%	26%	28%	30%	32%	34%
Fuel Enrichment	3.5%													
Lithium-6 Enrichment	8%	10%	12%	14%	16%	18%	20%	22%	24%	26%	28%	30%	32%	34%
Fuel Enrichment	4%													
Lithium-6 Enrichment	8%	10%	12%	14%	16%	18%	20%	22%	24%	26%	28%	30%	32%	34%
Fuel Enrichment	4.5%													
Lithium-6 Enrichment	8%	10%	12%	14%	16%	18%	20%	22%	24%	26%	28%	30%	32%	34%
Fuel Enrichment	5%													
Lithium-6 Enrichment	8%	10%	12%	14%	16%	18%	20%	22%	24%	26%	28%	30%	32%	34%

A few preliminary cases were run to determine a target range of burnup, and it was found that lithium-6 depletes to less than 1% remaining somewhere between 20 and 30 MWD/MTU for most cases. This allowed for the narrowing of burnup ranges that had to be run and increased efficiency of running Casmo4 files. The files corresponding to the combinations listed in Table 6 were then run in Casmo4 for burnup steps of 0.5 MWD/MTU, from 20 to 30 MWD/MTU. Once the files were run, the output data was analyzed to determine how fast the lithium-6 depletes in the core. This information is contained within the output files generated by Casmo4. Since tritium production is the main goal of this reactor and not power production, this allowed for the determination of the maximum cycle length. The lithium-6

depletes with burnup and this was plotted in order to determine cycle length for the reactor. The plot below was created using varying lithium-6 enrichments for a 3.5% enriched fuel. 3.5% was chosen as a minimum baseline since most new fuel assemblies are likely going to be enriched to at least 3.5%. Further analysis in the following sections shows that 3.5% and 4.0% enriched fuel yield satisfactory results.

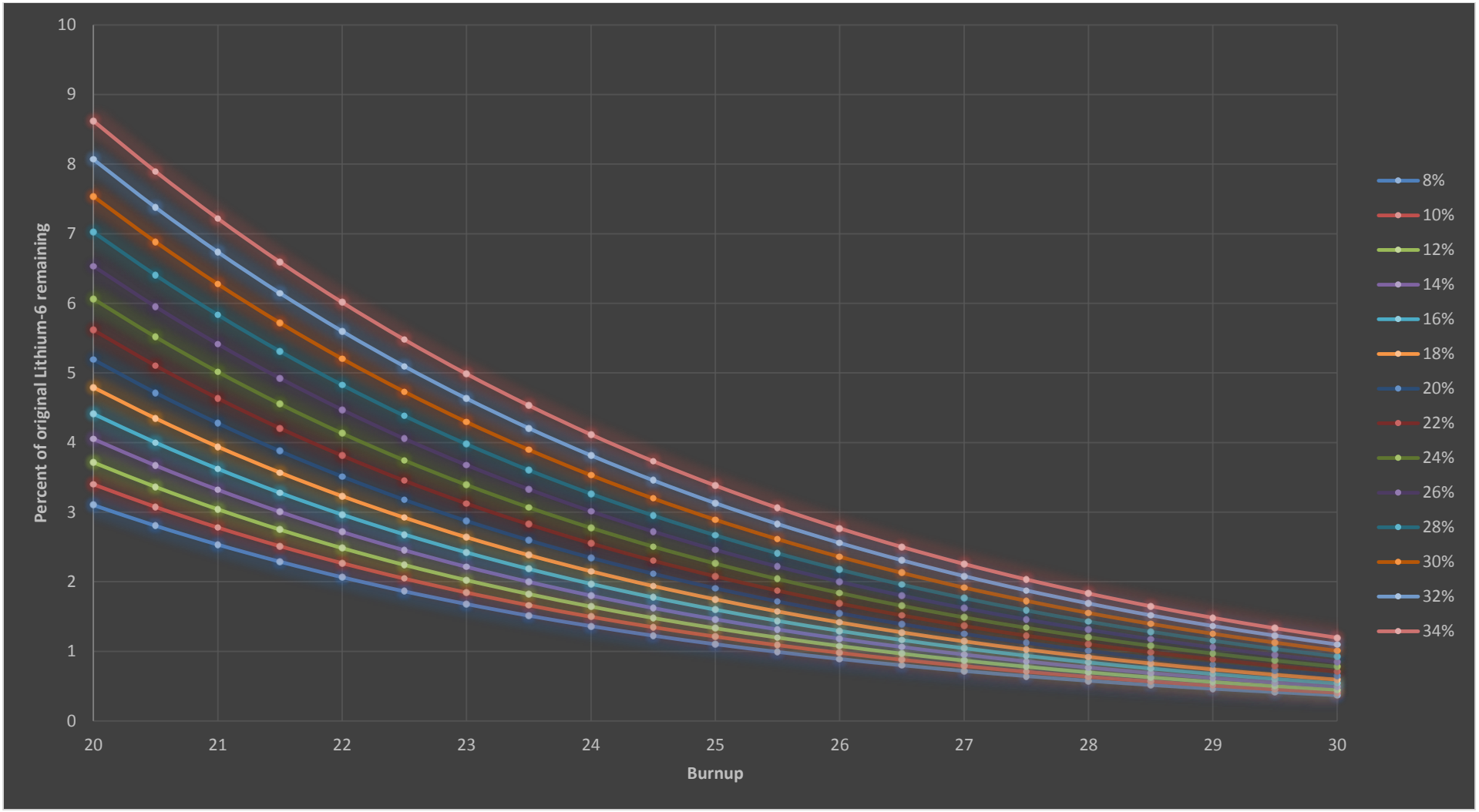

Figure 11. This plot shows burnup versus how much lithium-6 is remaining for various lithium enrichments and fuel enriched to 3.5%. The legend on the right represents various lithium-6 enrichments ranging from 8% to 34%.

As can be seen in Figure 11, the lithium depletes at a faster rate for higher initial lithium-6 enrichments. It was decided that 2% lithium-6 remaining was the point at which the TPBAR should be removed. Based on the plot, it was determined that all lithium-6 enrichments are depleted to 2% or greater of the initially loaded lithium at a burnup of 21 GWd/MTU. This was determined to be the desired cycle length in order to maximize tritium production, while limiting time the TPBARs sit in the reactor not producing tritium.

Once cycle length was determined, tritium production was to be maximized. This was done by examining the k-infinity versus lithium-6 enrichment, at the previously determined burnup level.

2.2.3.2. Determination of Lithium-6 Enrichment for TPBAR

Fuel burnup was chosen to be 21GWd/MTU as discussed in the section above. Once this was narrowed, cases were run for the same lithium enrichments and fuel enrichments as noted in Table 6. Choosing a lithium enrichment was one of the more important decisions made during the course of the design and analysis. The maximum feasible enrichment was desired in order to produce the maximum amount of tritium, and still have a viable, self-sustaining reactor. Lithium enrichment had to be chosen before further analysis of the neutronics of the reactor in order to prevent having to analyze every possible combination of fuel enrichment and lithium enrichment. The methodology chosen to determine the lithium enrichment that was used in the mPower reactor is outlined below.

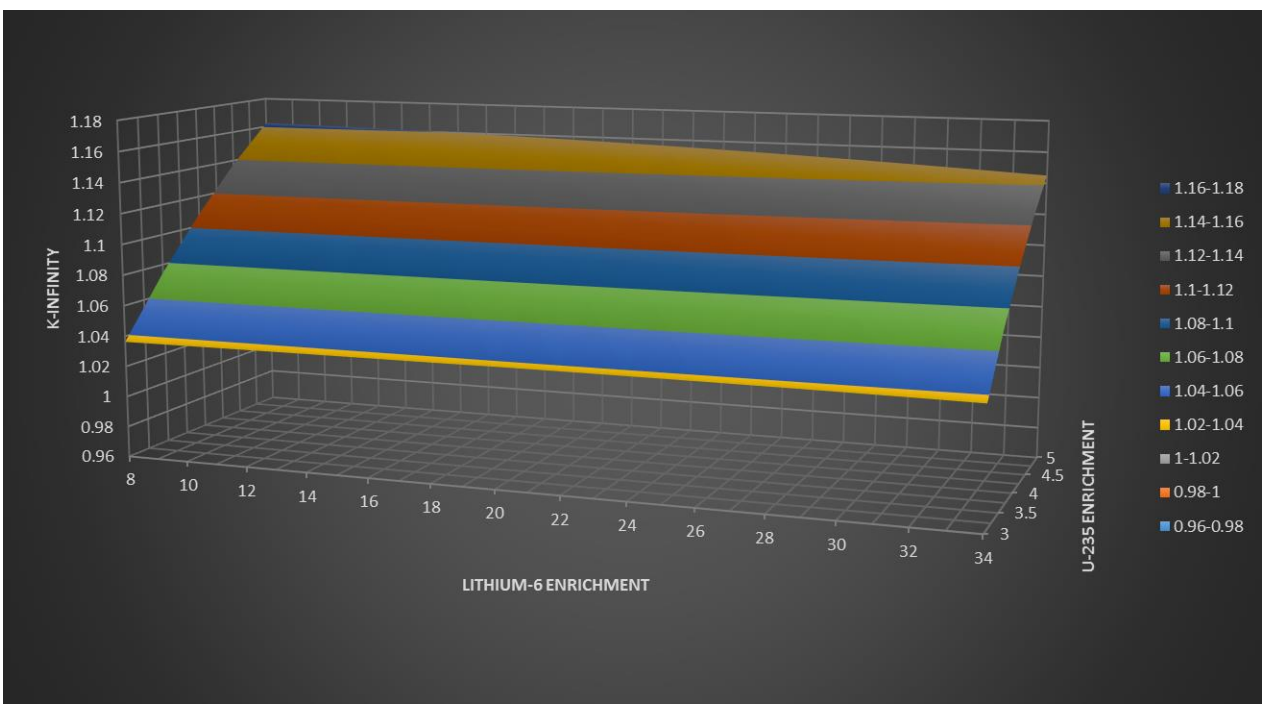

Figure 12. Plot of k-Infinity for various lithium-6 enrichments and U-235 enrichments.

The above figure clearly shows the trend of k-infinity for various combinations of lithium-6 enrichments and fuel enrichments. Close examination of the data shows that the lithium-6 enrichment doesn't appear to have much of an effect on k-infinity when combined with the lower enriched fuel. However,

for the 5% enriched fuel, increasing lithium-6 enrichments clearly decreases the k-infinity. The k-infinity seems to be somewhat stable and unchanged up until 18-22% lithium-6 enrichment.

Based on the lithium-6 enrichment starting to have a more significant effect on k-infinity around 22%, this value was chosen as the enrichment that would be used in the TPBARs in the mPower reactor. Another factor that influenced the decision to use 22% enriched lithium instead of significantly more, is that 20-22% is the current enrichment used in TPBARs at Watts Bar I nuclear power station. Using the same enrichment of lithium means that less modification of TPBAR producing equipment is necessary, and no new processes or procedures would have to be examined.

It should be noted that the above plot doesn't include the effects of helium-3 buildup as the lithium-6 reacts. Due to the limitations of Casmo4 mentioned previously, lithium is modeled with boron. This means that the helium-3 that would be produced from lithium isn't built in during the Casmo4 runs since the lithium-6 is only "simulated" in Casmo4. In order to examine how much of an effect helium-3 could have on the reactivity of the reactor with TPBARs, the TPBARs were modeled in the reactor to contain 12% helium-3. To determine feasibility, an upper helium-3 limit was established. This was done by assuming any tritium that could be produced by the TPBAR is present initially. This tritium is then allowed to decay to helium-3 for 2 years, which is the approximate maximum cycle length of the mPower reactor. Equation 13 below is the basic decay equation, where $N(t)$ is the number of atoms present at time t. N_0 is the initial number of atoms present at $t = 0$ and λ is the decay constant.

$$N(t) = N_0 * e^{-\lambda t} \qquad \text{Equation 13}$$

Equation 13 is applied to determine the maximum possible helium-3 present in a given TPBAR. Based on the maximum cycle of 2 years, $\frac{N(t)}{N_o} = 89.34\%$. This means that roughly 89% of the initial tritium remains in the reactor and the other 11% decays to helium-3. This simple analysis does not take into account the effects of neutron reactions that convert helium-3 to tritium, which may then decay back to helium-6. Helium-3 is stable so would not be removed by any other means. Neglecting the neutron absorption of helium-3 means that the 11% calculated value is an upper limit for the amount of helium-3 that can be present in the TPBAR.

In order to examine the effects of helium-3 on reactivity, the same combinations listed in Table 6 were run again. This time, 12% of the TPBAR is defined as helium-3, and the rest is the simulated lithium-6. 12% helium-3 was chosen based on the estimate provided by Equation 13, and knowing that the cycle length may vary slightly from 2 years. Rounding the helium-3 production up from 10.66% to 12% should provide a safe upper limit for the amount of helium-3 in the TPBAR. The same data that was plotted in Figure 12 was plotted for the data generated after the inclusion of helium-3 in the TPBAR. This can be found below in Figure 13. It is worth noting that this is an extremely conservative estimate, and simply included to show feasibility.

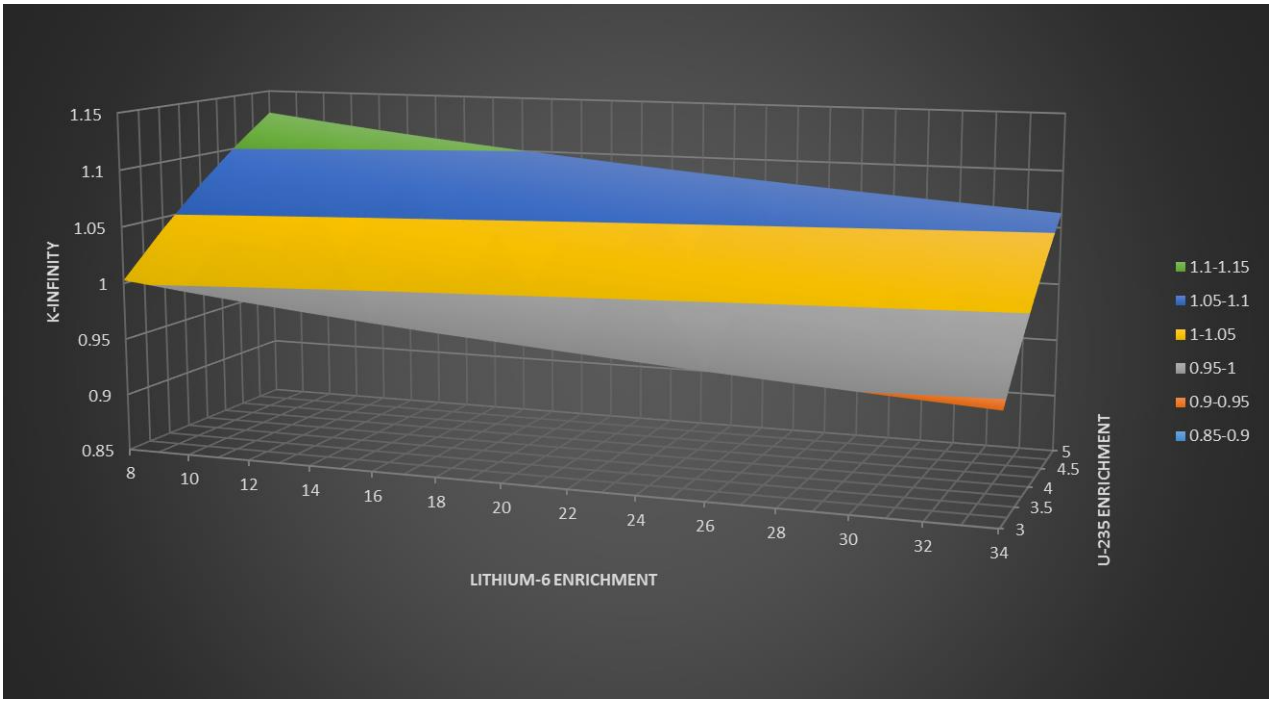

Figure 13. Plot of k-Infinity for various lithium-6 enrichments and U-235 enrichments.

Ideally, helium-3 would have been built in automatically by Casmo4 as the lithium-6 in the TPBAR depleted. Since this is not the case, an over-estimation of the maximum possible amount of helium-3 present in the core had to be made. It can clearly be seen that the effect of helium-3 is not negligible, but does not make the reactor unrealistic. It is important to keep in mind that this amount of helium-3 in the core should serve as a gross over-estimation based on assumptions, and is provided to show feasibility of the core to remain critical even if all TPBARs inside the core had the maximum amount of helium-3 throughout the cycle.

Adding 12% helium-3 to the TPBAR makes any fuel of 3% enrichment unrealistic for any lithium-6 enrichment. An increase in fuel enrichment to roughly 4-4.5% is necessary to maintain a critical configuration of the core. This data simply acts to prove that the TPBARs do not add enough negative reactivity, even considering significant helium-3 buildup, to make the mPower reactor unrealistic for use in tritium production.

Analysis in the following sections will show more realistic results regarding helium-3 inclusion. These cases were run early on in the design project before additional information regarding equilibrium helium-3 levels was available. It was meant to show upper and lower bounding cases for the mPower using the most conservative estimates possible.

2.2.3.3. Core Loading and Fuel Enrichment

The mPower adaptations to produce tritium have resulted in a 21 GWd/MTU cycle length, and the use of 22% enriched lithium-6 in the TPBAR. Once these factors were determined, along with other results yielding that the reactor is viable, the fuel enrichment and loading pattern was determined.

Since the goal of this reactor is to produce tritium effectively, cost is not the same concern as it would be at a typical power plant. This enables the reactor to be designed with a one cycle core. However, if the cost is not competitive then the mPower reactor is a lower priority option to produce tritium. In order to determine the fuel enrichment for the core, the multiplication factor versus burnup was examined for various fuel enrichments ranging from 3% to 5% U-235. This data can be found below in Figure 14.

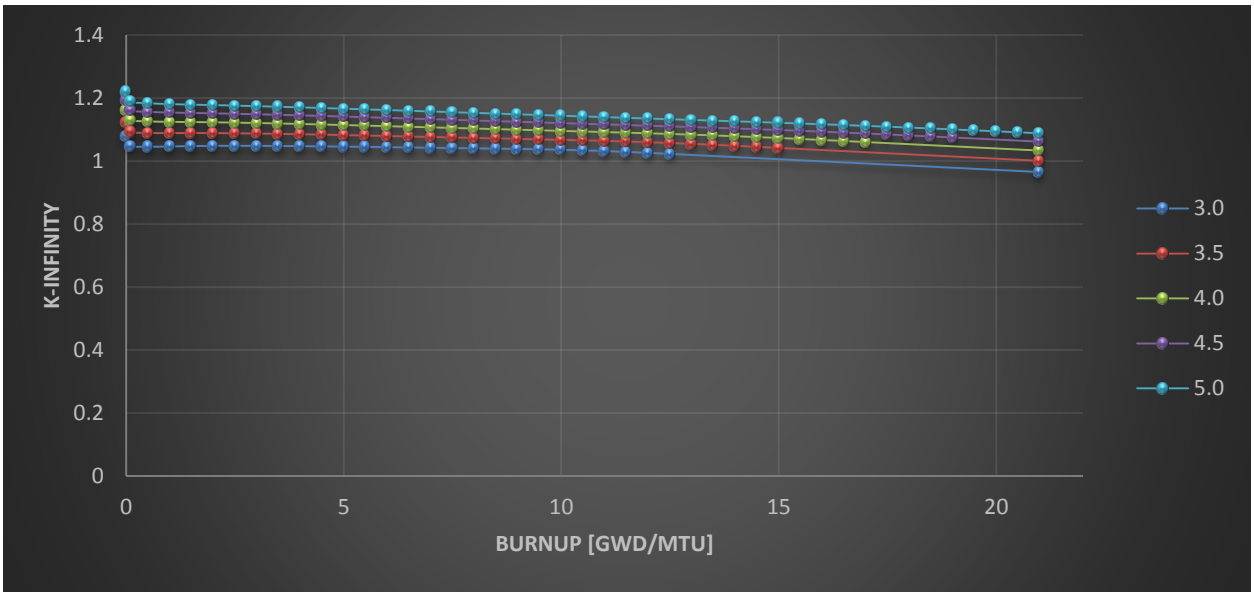

Figure 14. This plot shows k-infinity versus burnup for various fuel enrichments. The legend on the right indicates fuel enrichment.

Figure 14 above shows that for any fuel enrichment above 3% U-235, the multiplication factor remains above 1 throughout the cycle. In order to ensure that enough excess reactivity is present to maintain a critical reactor, a minimum fuel enrichment of 3.5% U-235 is necessary at the start of the cycle, though higher may be necessary.

To determine if a 3.5% enriched fuel is capable of maintaining the reactor throughout the cycle, a Casmo4 simulation of the reactor was run. As mentioned previously, Casmo4 has the capability to examine a 2-D horizontal section of the core as defined by the user. An image of the 2-D section of the core was generated by Casmo4 and included below for reference. The analysis was performed and the results can be found below in Figure 16.

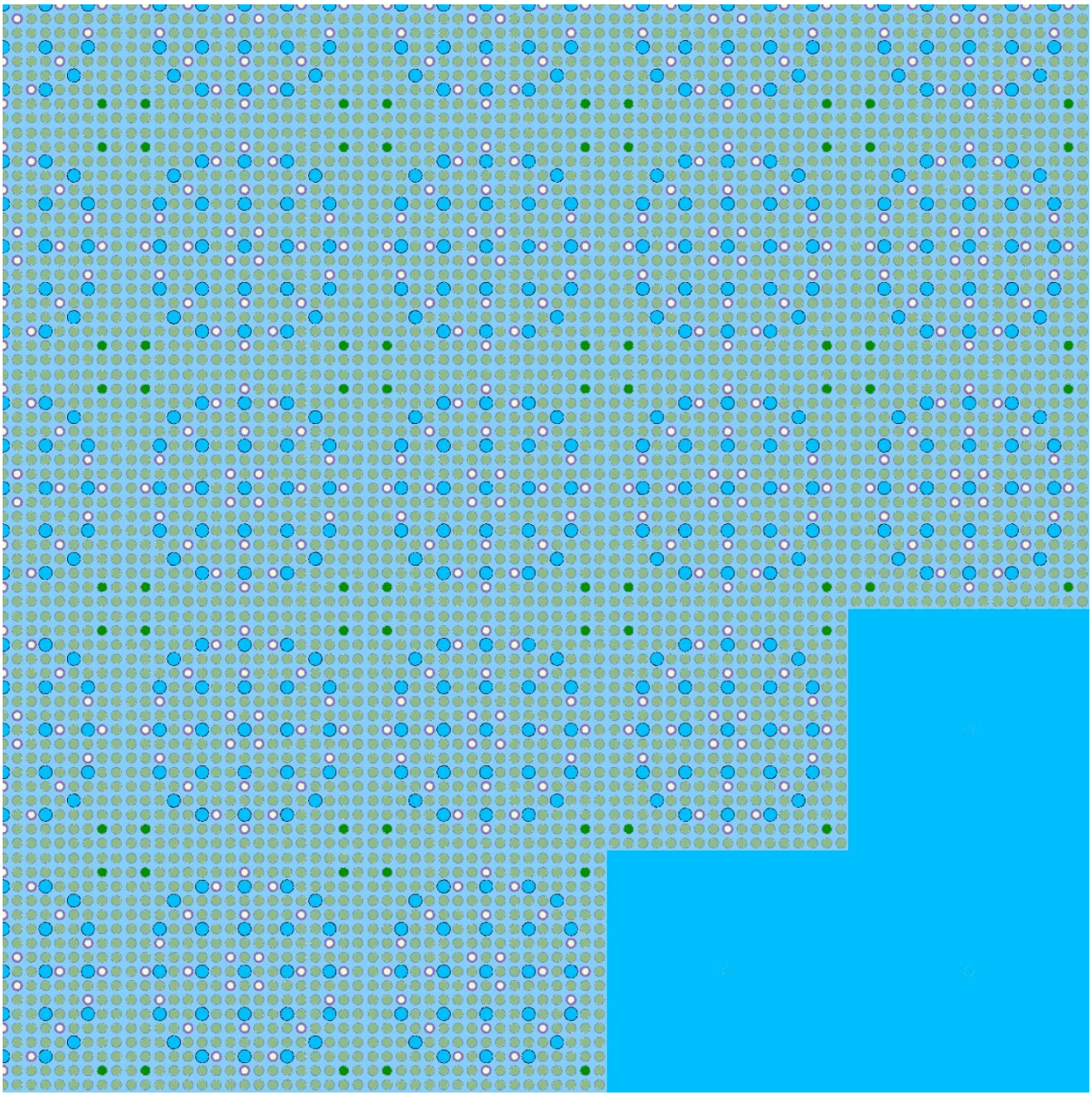

Figure 15. This image shows the lower right quarter section of the core as modeled by Casmo4. It shows the individual pins in their locations, along with TPBARs shown in white, guide tubes in solid blue, and gadolium fuel pins in green.

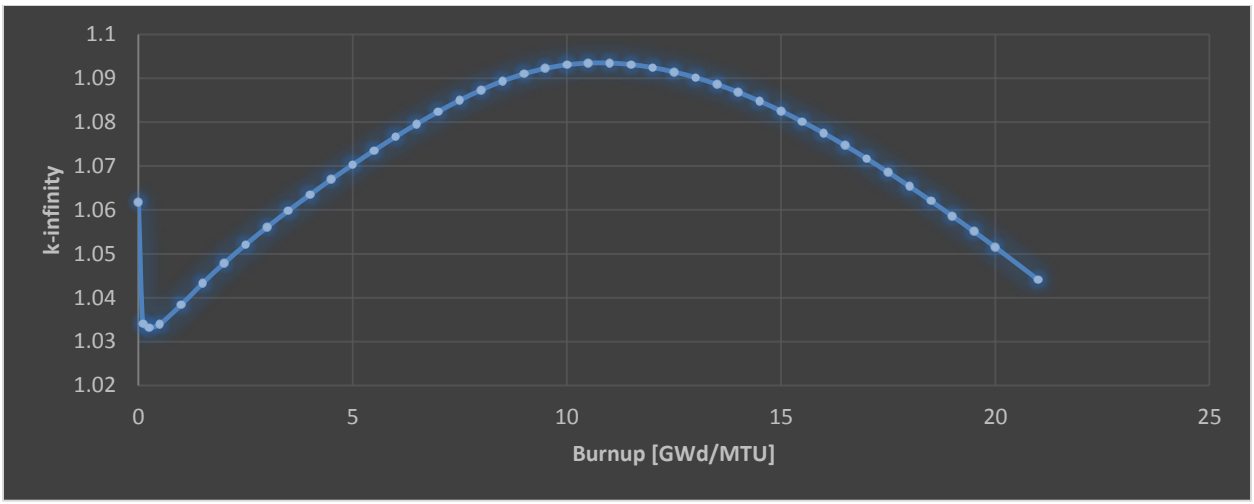

Figure 16. k-infinity versus burnup for a 2-D section of the mPower core with 22% enriched Li-6 and 3.5% enriched U-235 throughout the reactor.

This plot clearly shows an immediate drop in k-infinity which can be attributed to the immediate build up of neutron poisons such as xenon and samarium. The plot however, shows an unexpected trend when k-infinity increases with burnup to a maximum at roughly 11GWd/MTU. This feature is likely due to the burnup of neutron poisons such as the lithium in the reactor. It should be noted however, that this trend is not found in cases run in Casmo4 of infinite assemblies of the same type so this could simply be an error introduced by the more complex modeling.

Another Casmo4 case was run similar to above, except this time helium-3 was included in the calculations. As before, this data was generated as a limiting case since the helium-3 adds negative reactivity to the reactor.

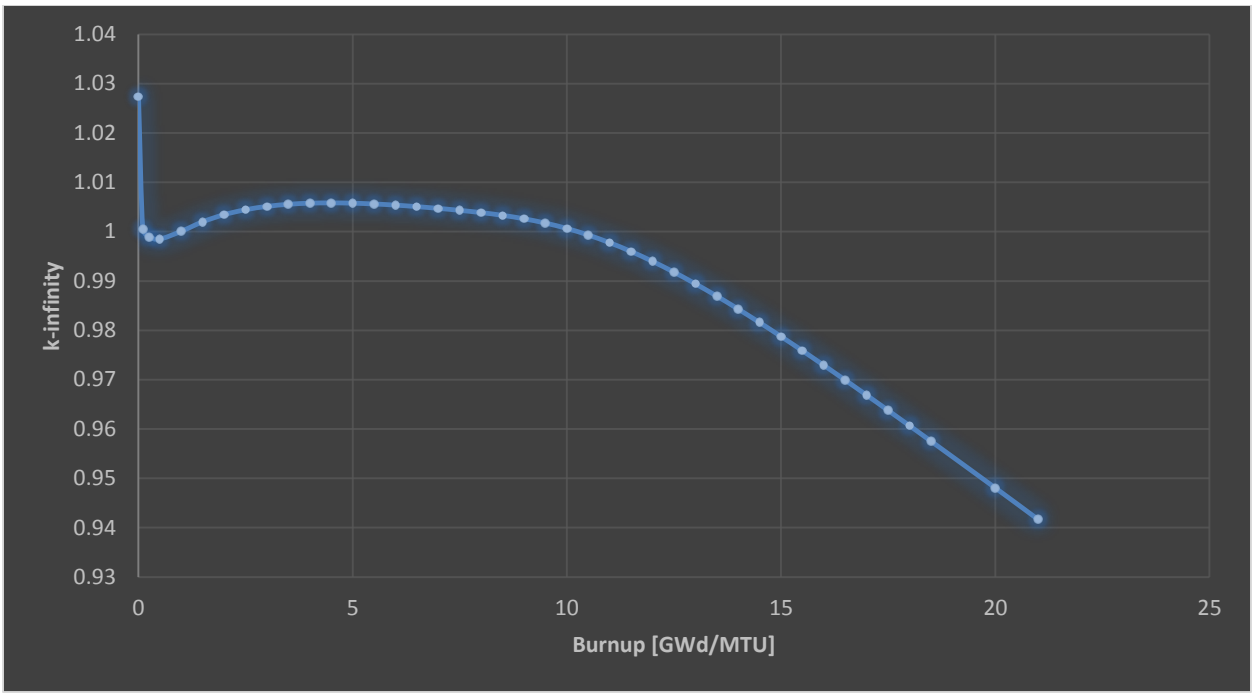

Figure 17. This image shows the multiplication factor versus burnup for a 2-D section of the mPower core. The data was generated for a core loaded with 3.5% enriched fuel assemblies, with TPBARs containing 12% helium-3.

Figure 17 above clearly shows that the use of a 3.5% enriched fuel assembly throughout the core will not allow for the target burnup of 21 GWd/MTU to be reached. The 12% helium-3 in the TPBAR has a significant effect on reactivity in the case of the full reactor core. It is important to note that this is used as a limiting case and this much helium-3 will never be present in the reactor under typical operating conditions. Based on the data generated and presented in Figure 16 and Figure 17, a Casmo4 case was run of a 2-D section of the core. This case contained 4% enriched fuel throughout, and also contained 12% helium-3 in the TPBARs. The results are presented below in Figure 18.

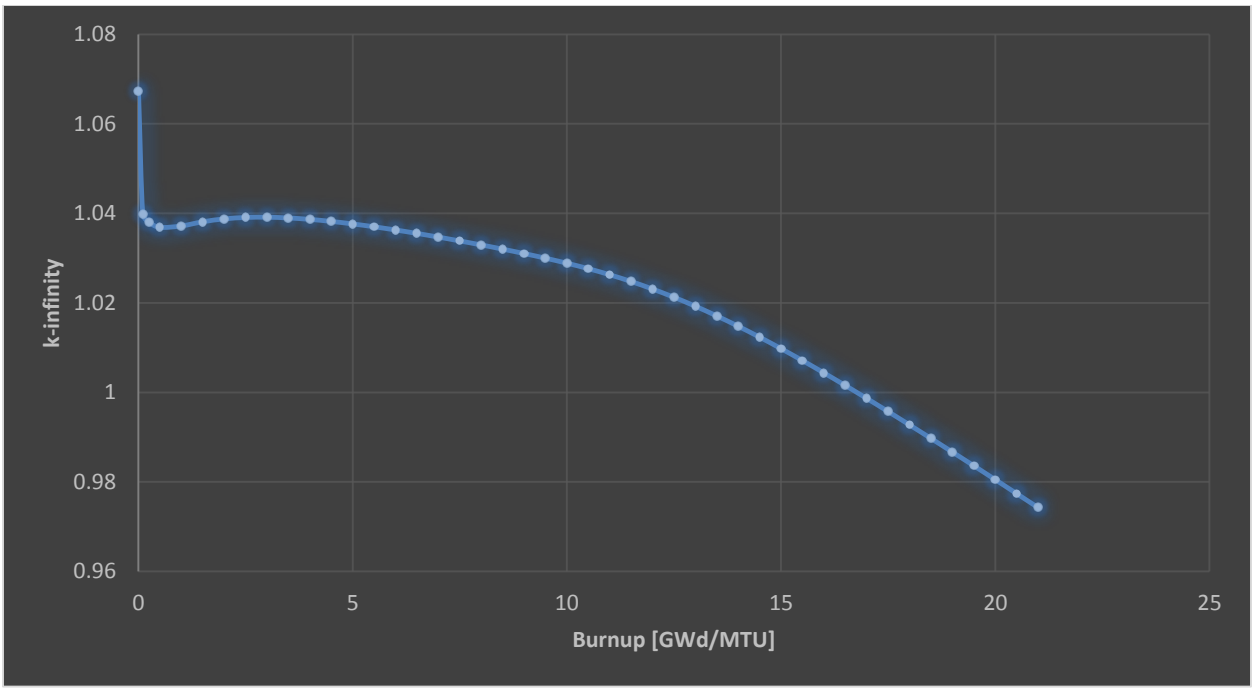

Figure 18. This plot shows k-infinity versus burnup for the mPower core when modeled using 4% enriched fuel and TPBARs containing 12% helium-3.

The above graph shows that the multiplication factor still goes below one before the end of the cycle. The use of 4% enriched fuel instead of 3.5% enriched makes a significant difference in the point at which the multiplication factor drops below one. For a 3.5% enriched fuel, this occurs initially when neutron poisons are built in whereas the 4.0% enriched fuel lasts to 17 GWd/MTU. Considering this is an extreme case and the value of 12% was calculated to be a limiting factor in terms of safety, a 4.0% enriched fuel should be sufficient to maintain the reactor core. Further analysis with better definitions that allow for proper depletion and decay of tritium may show that a core composed of 3.5% to 4.0% enriched fuel is sufficient to maintain a 21 GWd/MTU cycle length.

A final calculation was performed using this analysis method of a 2-D core. This time the core was loaded with both 3.5% and 4.0% enriched fuel in a standard checkerboard pattern, with 3.5% enriched fuel around the perimeter to decrease neutron leakage. Helium-3 was included in the TPBARs again, except only 1.5% was used for this simulation. This amount of helium-3 was determined to be the equilibrium concentration for a 21 GWd/MTU burnup based on calculations presented in the Tritium Production and Modeling section. This calculation was performed to show that a core loaded with 3.5-4.0% enriched fuel is realistic. The results are presented below in Figure 19.

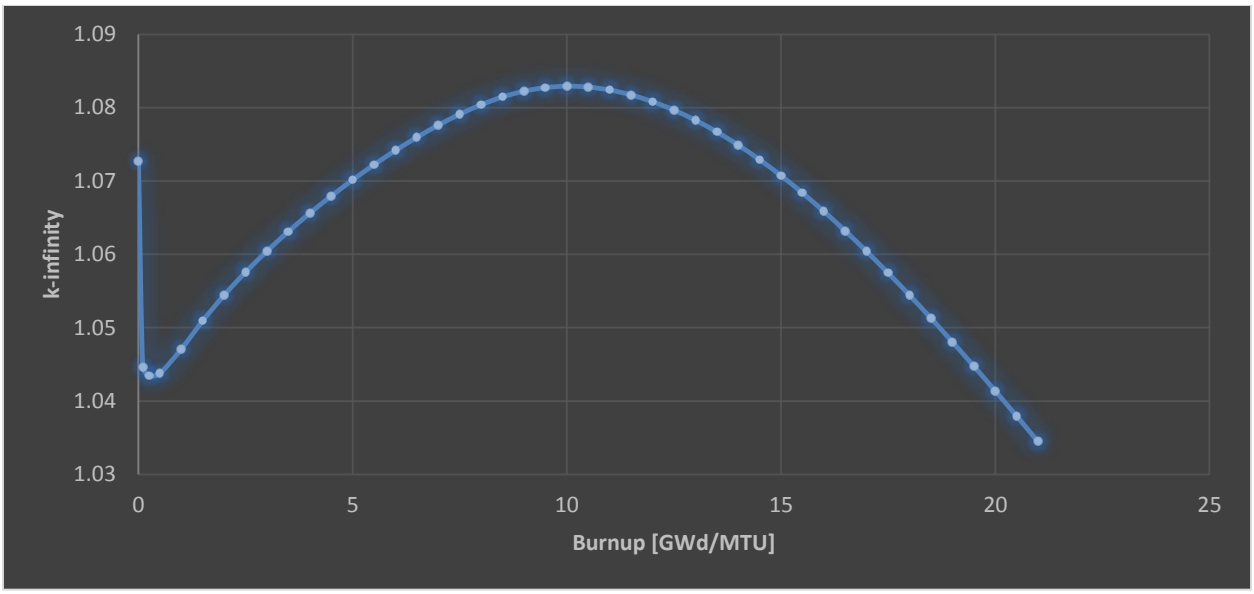

Figure 19. This plot shows the k-infinity versus burnup for a 2-D section of the mPower core with 3.5% and 4.0% enriched fuel assemblies and TPBARs containing 4% helium-3.

The results presented in the above plot clearly show that the multiplication factor remains above one throughout the life of the core. This implies that with a loading of 3.5% to 4.0% enriched fuel, the mPower core with TPBARs should be able to sustain criticality throughout the life of the cycle.

2.2.4. Analysis

2.2.4.1. Use of TPBAR in place of WABA

A wet annular burnable absorber (WABA) is a rod that is used in reactors to add additional negative reactivity. They are typically composed of boron carbide, aluminum oxide pellets (B_4C-Al_2O_3) in a zircaloy cladding. (O'Leary & Pitts, 2001). Boron has a large thermal neutron cross-section and acts to absorb some of the neutrons in the reactor core during operation. These are safety components and are critical to the safe operation of a reactor. WABAs become depleted with time as they continue to absorb neutrons. As mentioned previously, TPBARs have been located in place of the WABAs in the mPower core. These TPBARs behave very similar to the WABAs except they produce tritium, by design.

In order to examine the effect on the reactor of replacing the WABAs with TPBARs, several simulations were performed. These simulations model the reactor core with no rods in place, with WABAs in place, and with TPBARs in place. Each of these simulations were run with 22% enriched lithium, for fuel enrichments ranging from 3% to 5% U-235. As an example case, various results for 4% enriched fuel are presented below. Additional plots can be found in APPENDIX G.

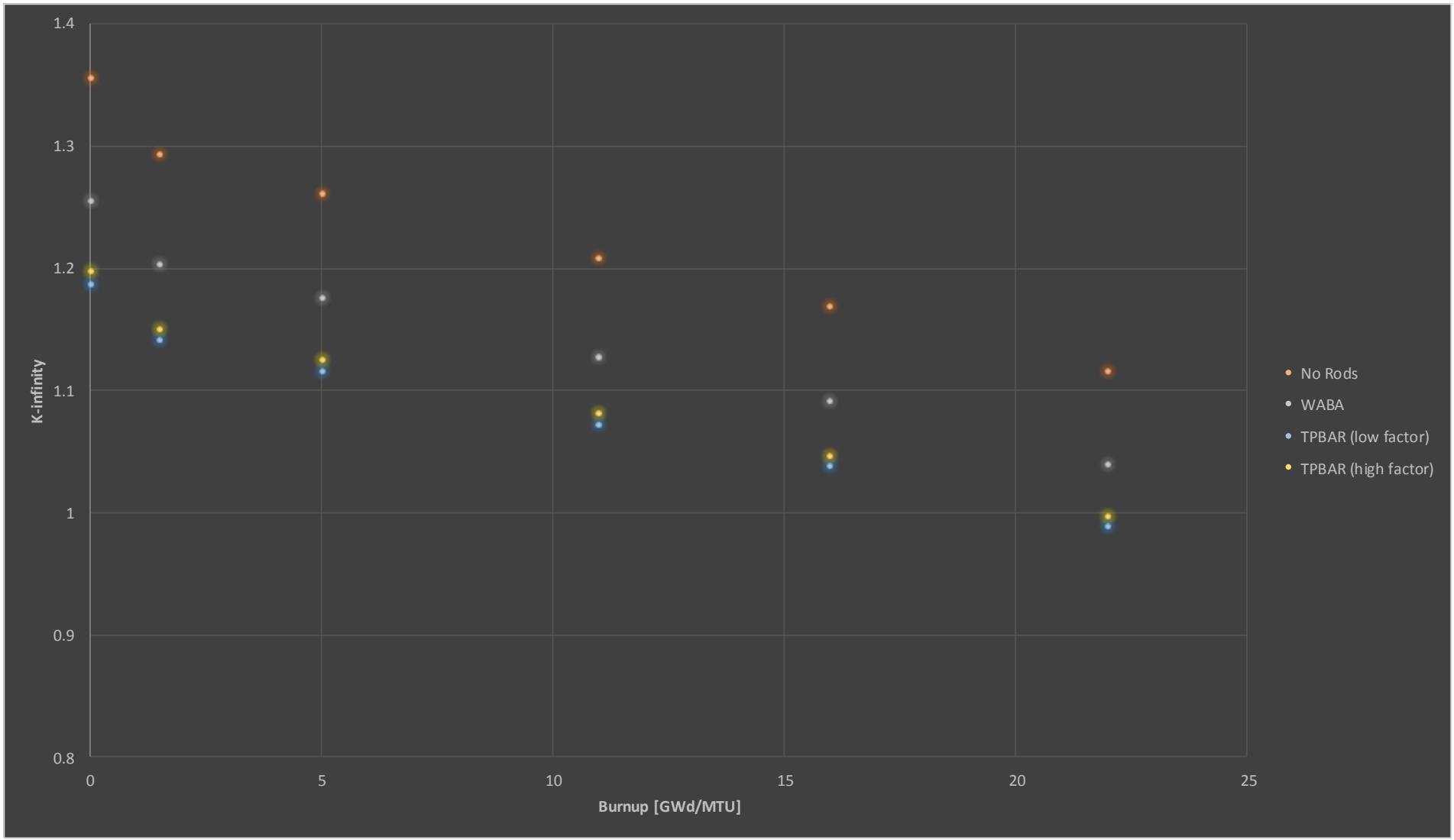

Figure 20. This plot shows the k-infinity value for various rod arrangements at various burnup positions. It contains data for TPBARs for both the low and high multiplication factors used to simulate lithium in the TPBARs.

Table 7. This table contains k-infinity values for TPBARs for both the low and high factors used (see Equation 10), along with their difference for a 4% enriched fuel.

Burnup [GWd/MTU]	TPBAR (low factor)	TPBAR (high factor)	% Difference
0	1.18734	1.1976	0.86%
1.5	1.14135	1.15079	0.82%
5	1.11624	1.12522	0.80%
11	1.07231	1.08071	0.78%
16	1.03827	1.04631	0.77%
22	0.98931	0.997	0.77%

Table 8. This table contains k-infinity values for WABAs and average k-infinity values of the low and high factor TPBARs, along with their difference for a 4% enriched fuel.

Burnup [GWd/MTU]	TPBAR (average)	WABA	% Difference
0	1.19247	1.25566	5.03%
1.5	1.14607	1.20382	4.80%
5	1.12073	1.17554	4.66%
11	1.07651	1.12769	4.54%
16	1.04229	1.09137	4.50%
22	0.993155	1.04016	4.52%

Figure 20 above contains the k-infinity values at certain burnups for calculations with no rods in place, WABAs in place, and TPBARs in place. It contains two sets of data for TPBARs, one that was generated using the low factor and one using the high factor used to simulate lithium with boron, as previously discussed. The plot clearly shows that the multiplication factor decreases with burnup with all rod arrangements, as would be expected. The use of WABAs decreases the maximum k-infinity values from what is possible without rods. The use of TPBARs further decreases these k-infinity values. The general trends shown in Figure 20 are reasonable and what would be expected for a reactor.

Table 7 shows the difference in the TPBAR k-infinity values when using the high and low factors. This comparison clearly shows that the difference is negligible when using a high or low factor to simulate lithium-6 with boron-10. Table 8 compares an average of the TPBAR k-infinity values for the low and high factor with the k-infinity values for the WABAs. This difference is not negligible in terms of reactivity, but it also not significant enough to make the use of TPBARs in the mPower unreasonable.

This data simply shows that replacing WABAs with TPBARs in the mPower reactor does result in a decreased multiplication factor. However, the additional negative reactivity added by the TPBARs is not significant enough to make the reactor unviable.

2.2.4.2. Reactivity Coefficients

Casmo4 was used to determine both the moderator and temperature coefficients of reactivity. The temperature reactivity coefficient is defined below in Equation 14.

$$\alpha_T = \frac{\partial \rho}{\partial T} \qquad \text{Equation 14}$$

In this equation, α is the reactivity coefficient while ρ is the reactivity and T is the temperature. Cases were run in Casmo4 for various fuel enrichments at varying fuel and moderator temperatures. This allowed for the determination of reactivity values at each temperature, which was then plotted. The slope of this plot represents change in reactivity with change in temperature, the equivalent of the temperature coefficient of reactivity. These coefficients were calculated and are shown below in Table 9 and Table 10.

Table 9. This table contains the temperature reactivity coefficients calculated for various fuel enrichments, using the low factor for lithium equivalent boron at the beginning and end of life for an mPower core. Reactivity coefficients are presented in units of [pcm/^{o}K].

	Beginning of Life		End of Life	
Fuel Enrichment	Coefficient of Reactivity		Coefficient of Reactivity	
(% U-235)	Moderator	Fuel	Moderator	Fuel
3.0	-19.42	-2.34	-5.85	-1.44
3.5	-18.13	-2.22	-10.51	-1.76
4.0	-17.12	-2.13	-13.55	-1.96
4.5	-16.29	-2.06	-15.51	-2.08
5.0	-15.63	-2.01	-16.74	-2.17

Table 10. This table contains the temperature reactivity coefficients calculated for various fuel enrichments, using the high factor for lithium equivalent boron at the beginning and end of life for an mPower core. Reactivity coefficients are presented in units of [pcm/^{o}K].

	Beginning of Life		End of Life	
Fuel Enrichment	Coefficient of Reactivity		Coefficient of Reactivity	
(% U-235)	Moderator	Fuel	Moderator	Fuel
3.0	-18.43	-2.32	-5.78	-1.43
3.5	-17.27	-2.2	-10.44	-1.75
4.0	-16.36	-2.11	-13.49	-1.95
4.5	-15.62	-2.04	-15.46	-2.07
5.0	-15.02	-1.99	-16.72	-2.16

The reactivity coefficients shown in the above tables demonstrate that the reactor operates safely with a negative reactivity coefficient for both moderator and fuel temperature. The coefficients are negative at both the beginning and end of the cycle, and for both lithium factors.

The same calculations were performed for fuel containing the limiting case of 12% helium-3 in the TPBARs. The results are presented below in Table 11 and Table 12.

Table 11. This table contains the temperature reactivity coefficients calculated for various fuel enrichments, using the low factor for lithium equivalent boron at the beginning and end of life for an mPower core. The TPBARs used in generating this data contained the limiting case of 12% helium-3. Reactivity coefficients are presented in units of [pcm/^{o}K].

	Beginning of Life		End of Life	
Fuel Enrichment	Coefficient of Reactivity		Coefficient of Reactivity	
(% U-235)	Moderator	Fuel	Moderator	Fuel
3.0	-22.07	-2.41	-4.93	-1.12
3.5	-20.45	-2.28	-9.92	-1.51
4.0	-19.17	-2.18	-13.19	-1.76
4.5	-16.29	-2.06	-15.51	-1.23
5.0	-17.3	-2.04	-16.67	-2.04

Table 12. This table contains the temperature reactivity coefficients calculated for various fuel enrichments, using the high factor for lithium equivalent boron at the beginning and end of life for an mPower core. The TPBARs used in generating this data contained the limiting case of 12% helium-3. Reactivity coefficients are presented in units of [pcm/^{o}K].

	Beginning of Life		End of Life	
Fuel Enrichment	Coefficient of Reactivity		Coefficient of Reactivity	
(% U-235)	Moderator	Fuel	Moderator	Fuel
3.0	-20.94	-2.38	-4.73	-1.15
3.5	-19.46	-2.26	-9.69	-1.52
4.0	-18.29	-2.16	-12.95	-1.77
4.5	-17.34	-2.09	-15.07	-1.94
5.0	-16.58	-2.03	-16.43	-2.05

The reactivity coefficients presented for cases that include helium-3 in the TPBAR are also negative for all fuel enrichments and throughout the life of the core. This means that the reactor will operate in a safe region and temperature spikes during possible transient events will not result in an addition of positive reactivity. Although these calculations were not performed for the mPower with equilibrium helium-3 levels, the fact that the reactivity coefficients are negative should not change. The magnitude may change, but since the helium-3 concentration would be somewhere between the conservative cases used, the coefficients should also fall between the calculated values for these cases.

2.2.4.3. Power Distribution in the mPower Core

The same model developed to examine a 2-D section of the core with 3.5% and 4.0% enriched assemblies was also used to gather data related to power distribution throughout the mPower core. The relative power distribution was plotted for each assembly position at the beginning, middle, and end of life of the core. These plots can be found below in Figure 21, Figure 22, and Figure 23.

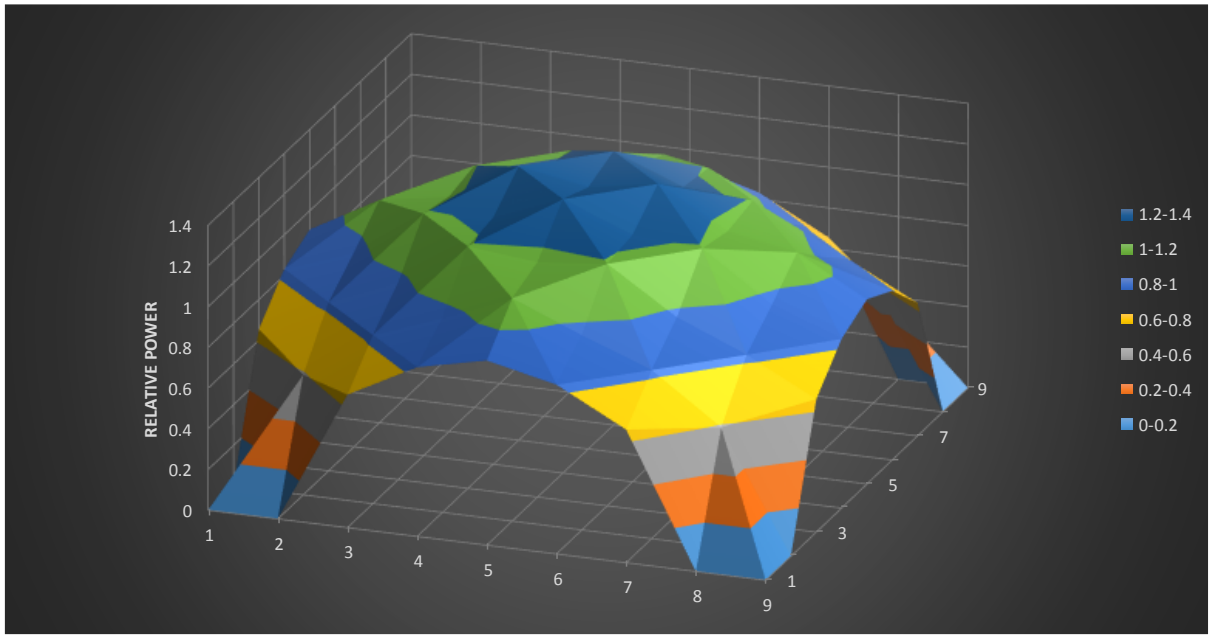

Figure 21. This plot shows the relative power distribution throughout the mPower core at the beginning of life. [0 GWd/MTU].

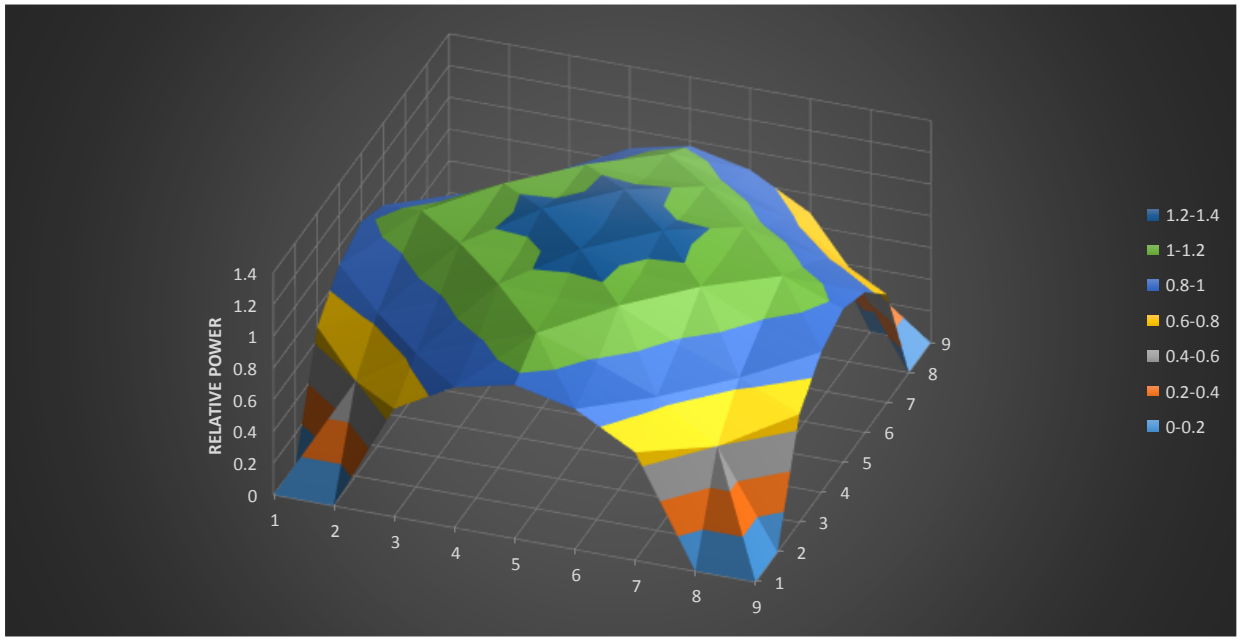

Figure 22. This plot shows the relative power distribution throughout the mPower core at the middle of life. [10.5 GWd/MTU].

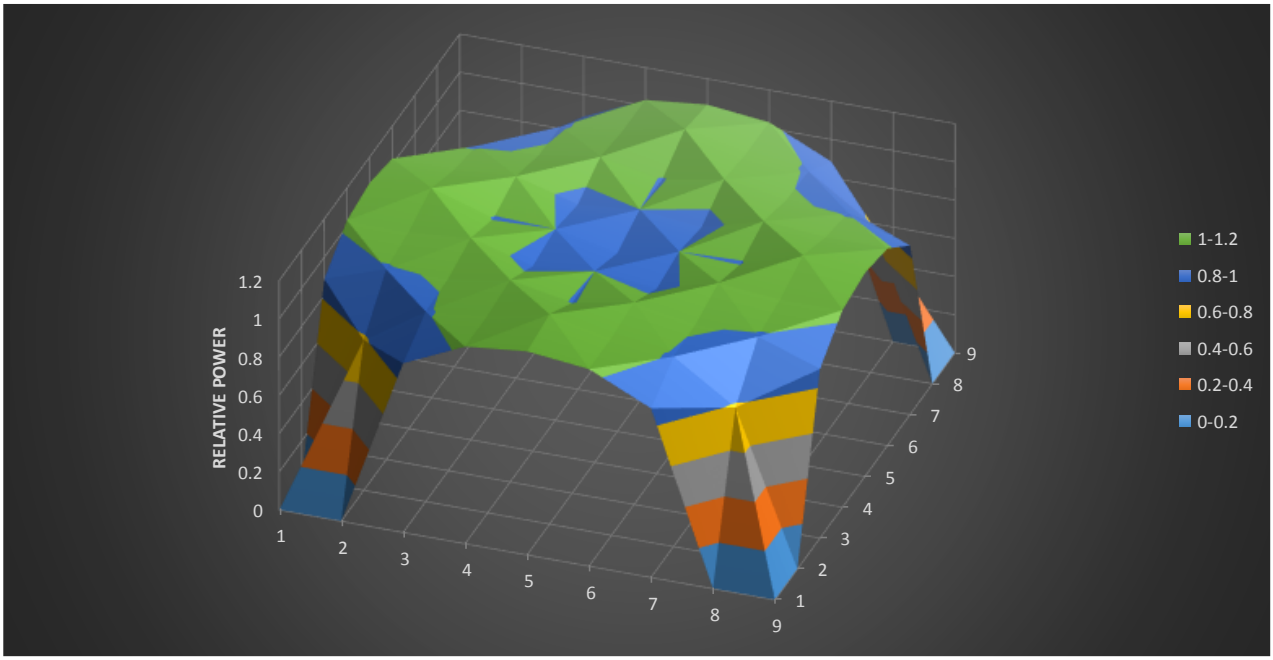

Figure 23. This plot shows the relative power distribution throughout the mPower core at the end of life. [21 GWd/MTU].

These plots of relative power distribution in the core show a higher relative power at the center of the core at the beginning of life, as would be expected with fresh fuel. The power distribution tends to move out radially with increasing burnup until the peak is no longer in the center of the reactor, but instead in a ring around the center. This is typical of reactor cores and shows that the mPower behavior with TPBARs present will behave similar to other PWRs in operation.

2.3. Tritium Production and Modeling

Written by Mac Cook

2.3.1. TPBAR Design

2.3.1.1. Standard TPBAR Design

The TPBAR is composed of several elements to ensure safety, efficiency, and reliability. Figure 24 illustrates the various components of a standard TPBAR (Burns, 2012). Each component has a specific function to help towards the goal of producing tritium safely, reliably, and efficiently. The lithium aluminate pellet is the tritium producing target. It creates tritium as shown later in Equation 23. This tritium will permeate out of the pellet and interact with the zircaloy-4 getter, which interacts according to Equation 15. The getter is nickel plated to prevent oxidation, so that this reaction will be achieved in maximum quantities.

$$\mathrm{T_2} + 2\mathrm{Zr} \rightarrow 2\mathrm{ZrT} \qquad \text{Equation 15}$$

The zircaloy-4 liner, on the other hand, is not nickel plated, and oxidation is allowed to occur, as shown in Equation 16. This oxidation layer, with a thickness of a few micrometers, serves as resistance to tritium permeation. However, some tritium may be absorbed in the liner. This tritium is recovered along with the tritium in the getter and elsewhere in the TPBAR.

$$2\mathrm{T_2}0 + \mathrm{Zr} \rightarrow \mathrm{ZrO_2} + 2\mathrm{T_2} \qquad \text{Equation 16}$$

Additionally, the zircaloy-4 liner serves as added structural integrity to the annular lithium aluminate pellets. The TPBAR is clad by Type 316 reactor grade stainless steel. This cladding provides structural integrity to the TPBAR and prevents radioactive releases to the reactor coolant system (RCS). It has an aluminide coating which acts as a barrier to the permeation of tritium out of the TPBAR and protium into the TPBAR.

The TPBAR will replace the standard burnable poison rods in the mPower reactor. The effects that will occur as a result of this design change are discussed in the following sections.

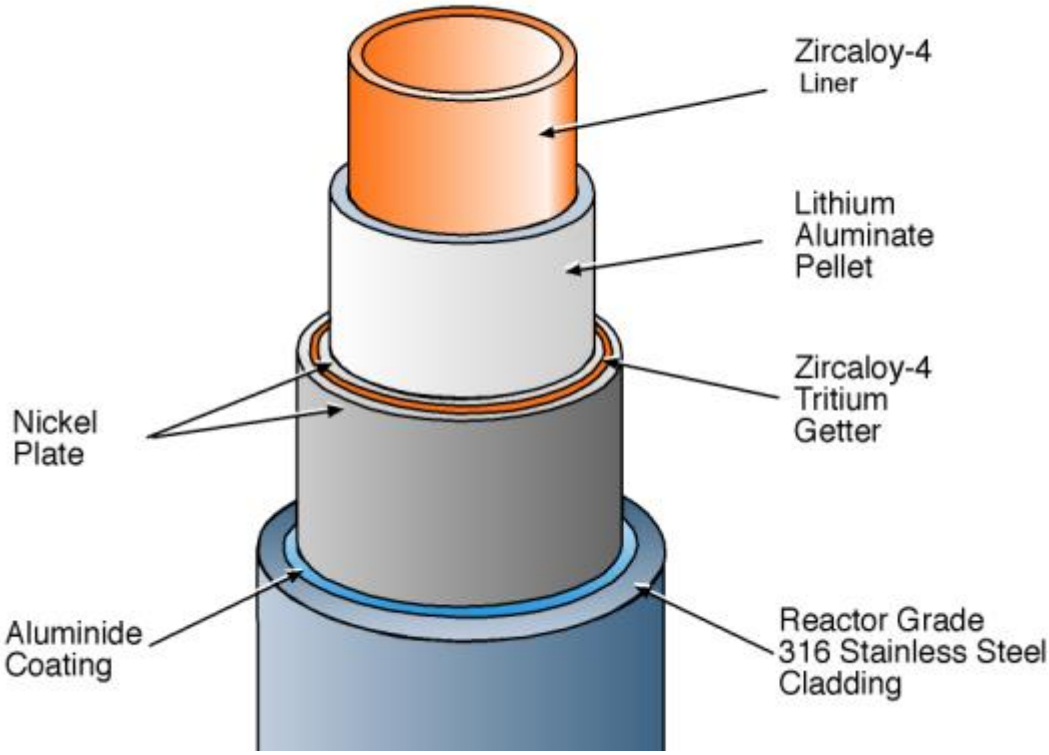

Figure 24. Diagram showing the standard TPBAR components (not to scale).

2.3.1.2. Modified TPBAR Design

The TPBAR must be modified for use in the mPower reactor. The main dimensional change is a change in the active length of absorber (lithium aluminate) by a reduction in the number of pellets. The standard active length of the pellets is 132 inches; in the mPower design, the active length will be 95 inches. The other dimensions of the TPBAR will remain the same. The reduced height is a result of core design. Since the smaller core has fewer assemblies, its width decreases. In order to minimize neutron leakage, the height must also decrease to maintain a favorable surface area to volume ratio.

Another change in the TPBAR is the enrichment of lithium-6. While a standard TPBAR can have a range of lithium-6 enrichments, the referenced value for this report is 20%. In the modified mPower design, a lithium-6 enrichment of 22% was chosen.

2.3.2. Tritium Permeation and Leakage

Permeation and leakage of tritium (and to a lesser degree helium-3) have several impacts on the system. From a safety standpoint, it is important to minimize tritium leakage into the coolant since tritium is a beta emitter and an isotope of hydrogen. As such, it forms tritiated water when exposed to the coolant. Since tritium is a low energy, “pure beta emitter,” it poses minimal health risk from external exposure. However, consumption (or absorption) of tritiated water (or inhalation of tritium gas) is a health

concern, and thus many layers of "defense in depth" towards tritium release must be in place and respected.

Permeation of tritium (and protium) involves multiple stages. Since many of the materials of interest are metallic (e.g. stainless steel, zircaloy-4), the gas will diffuse as atoms (Le Claire, 1981). First, the tritium must diffuse to the surface of the component it will travel through (Sherman & Adams, 2008). Second, it must decompose from its molecular form into a free atom and be adsorbed into the material. Third, it must travel through the material via diffusion. Fourth, it must be desorbed and recombine into a molecular structure. Lastly, it may move away from the surface. The speed of this process is limited by the slowest component. In tritium permeation, this component is diffusion within the material. (Liger & Gilardi) Because of this, permeation can be modeled by Fick's Law of Diffusion as shown by Equation 17, where D is the diffusion coefficient (diffusivity), ϕ is the concentration, and $\vec{J}$ is the diffusion flux. In the case of 2 volumes of gas separated by a wall, with one gas at high pressure, and the other at low pressure, this equation can be written as Equation 18. (Le Claire, 1981). In this equation c_h is the concentration of the gas on the high pressure side, c_l is the concentration of gas on the low pressure side, and d is the thickness of the wall. In the case of a cylindrical wall, it is clear that Equation 19 serves as an analog from Equation 18.

$$\vec{J} = -D\,\nabla\phi \qquad \text{Equation 17}$$

$$\vec{J} = D\,\frac{c_h - c_l}{d} \qquad \text{Equation 18}$$

$$\vec{J} = 2\pi D\,\frac{c_h - c_l}{\ln\left(\frac{r_h}{r_l}\right)} \qquad \text{Equation 19}$$

In Le Claire, conditions are outlined in which a simplifying case for gas dissolving only as atoms can be made. Equation 20 is Richardson's Law, where P_t is the total pressure and K_{SM} is the *molecular* Sievert (permeability) constant.

$$\vec{J} = \frac{D * K_{SM}}{d} P_t^{\frac{1}{2}} \qquad \text{Equation 20}$$

A fair amount of data exists on hydrogen permeation, including protium, deuterium, and tritium permeation, due to the conditions inside nuclear reactors, especially heavy water moderated reactors

(HWRs) and very high temperature reactors (VHTR)[1]. For example, the permeability constant for tritium in type 316 stainless steel (the TPBAR cladding material) can be obtained from Shiraishi. Using the data from Matsuyama & Redman, the permeability constant is about $5*10^{-12}$ [$mol*m/m^2*s*Pa^{1/2}$] (Shiraishi, Nishikawa, Yamaguchi, & Kenmotsu, 1999).

According to Gruel, the in-reactor permeation for a typical TPBAR of 9664 Ci (1.2 g ^3H) is less than 0.53mCi per hour. Additionally, tritium release assumptions for both transportation and non-transportation scenarios (e.g. spent fuel pool, reactor, etc.) are tabulated (Gruel, 2012).

2.3.3. TPBAR Activation Analysis

As with most materials, TPBARs undergo neutron activation when exposed to a neutron flux, such as the one present in a nuclear reactor. Thus a TPBAR becomes radioactive, and produces radiation and decay heat as a result of this radiation interacting within the TPBAR. Since the TPBAR undergoes extensive handling, it is important to understand the activation of the TPBAR to ensure safety. Additionally, knowledge of activation is needed for a complete analysis of accident scenarios, both in-core and ex-core (e.g. both a LOFA and a breach of the TPBAR transportation cask).

Radiation from the TPBAR can be broken into two groups. One is the radiation as a direct result of the tritium decay, and another is radiation as the result of activation of nuclides other than lithium-6. While tritium is the main source of radiation, it contributes very little to the expected dose from handling the TPBAR and to the decay heat generated in the TPBAR. This is a result of the fact that tritium is a "pure beta emitter," with maximum and average beta energies given by Equation 21 and Equation 22.

$$Q = \beta_{max} = 18.59\ keV \qquad \text{Equation 21}$$

$$\beta_{avg} = 5.69\ keV \qquad \text{Equation 22}$$

Activation of the TPBAR materials contributes a much larger portion to both expected dose and the decay heat generated. In order to summarize these points, Figure 25 and Figure 26 have been included below. Figure 25 illustrates the difference between the total activity of the TPBAR and the activity attributable to tritium alone, as a function of time. From this, it is shown that tritium produces 86% to >99% of the total radiation over the period of time of interest. However, as Figure 26 illustrates, the decay heat generated by the TPBAR is mostly due to other radionuclides, especially for times soon after discharge. As time progresses, tritium begins playing a larger role and eventually surpasses the other radionuclides. For long term storage of waste, the tritium is assumed to be entirely removed, and the

[1] Heavy water reactors produce fair amounts of tritium as a result of deuterium in the moderator-coolant. Additionally, the behavior of the hydrogen isotopes is of interest for material interactions. In very high temperature reactors, hydrogen permeability is often considered because hydrogen is often used as a form of energy output to boost efficiency.

activity and decay power of the TPBAR decrease greatly. In these analyses, the TPBAR is assumed to contain 1.2 g of tritium at discharge. This amount has been deemed "unsafe" for TPBARs in an mPower reactor due to a decrease in the TPBAR dimensions. This decrease is assumed to be proportional to the decrease in the active length of the absorber material, since the radial dimensions of the TPBAR are not modified from their "standard" values. Taking this into consideration, the TPBARs in this design will contain nearly 30% less tritium per rod, and thus activation and dose values must be adjusted accordingly. These analyses have been taken from Collins (2012), and the full set of data can be found within that document, as well as ORIGEN2 input files, MCNP input files, and a description of the analysis and assumptions.

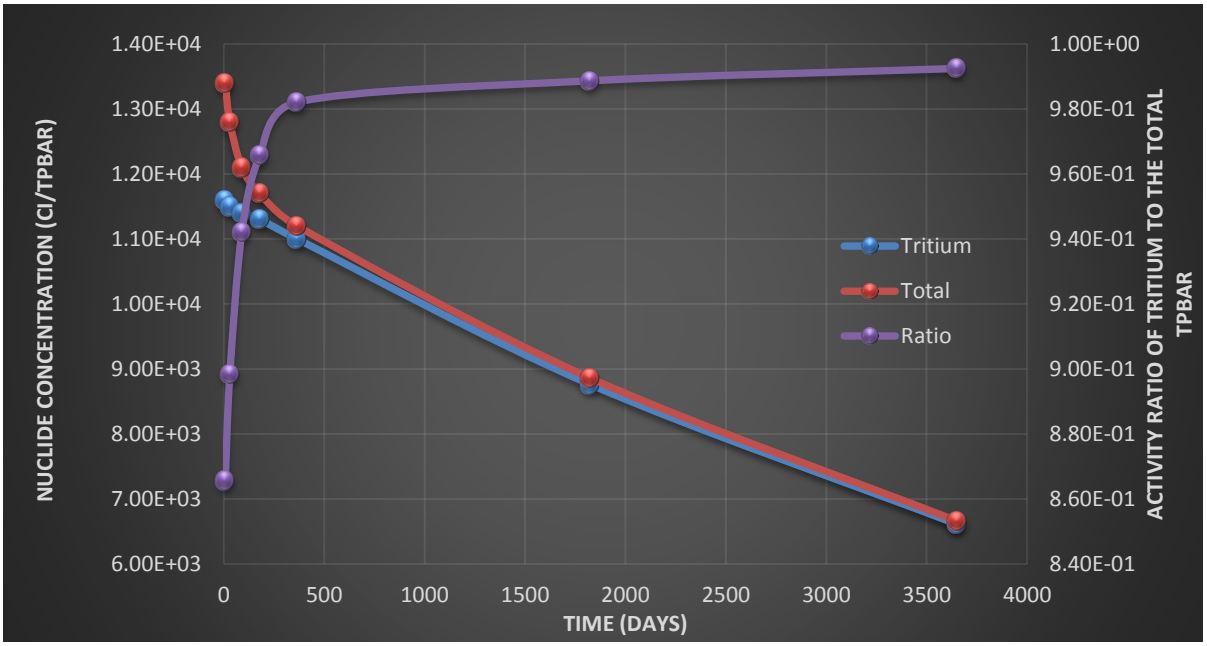

Figure 25. Radionuclide concentrations in a TPBAR as a function of time.

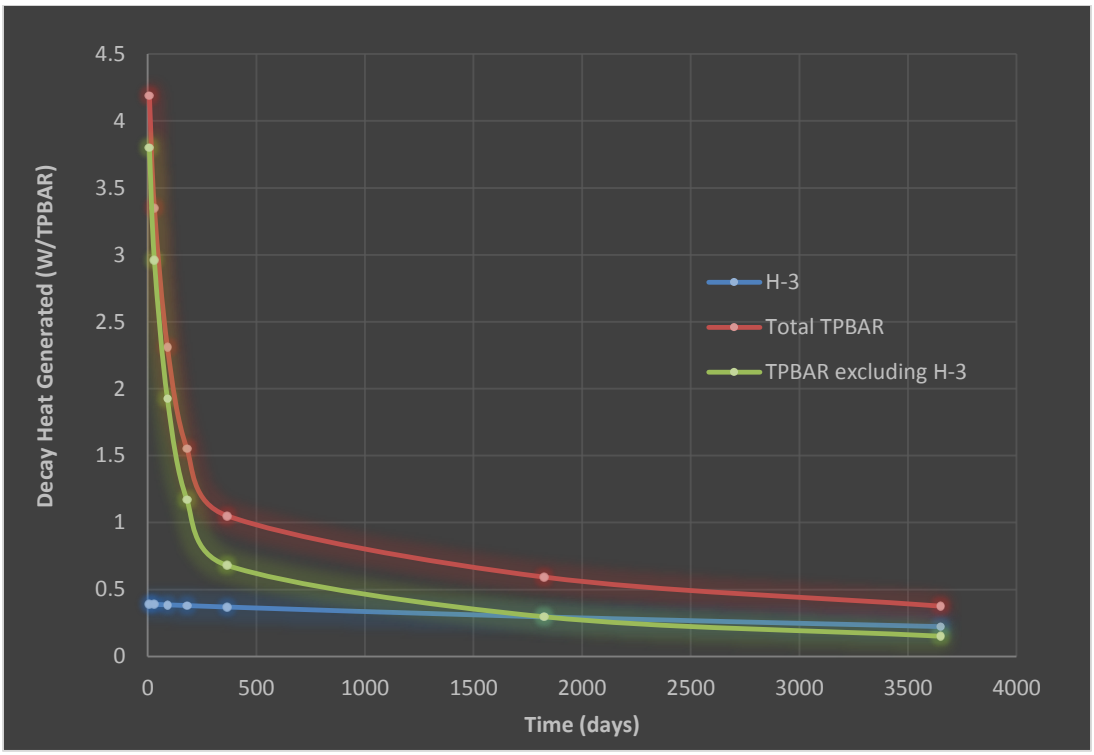

Figure 26. Decay heat generated in a TPBAR as a function of time.

2.3.4. Dose Rates from a TPBAR

Using the source terms provided in Collins (2012), it is possible to analytically calculate the multi-group gamma flux at any point, treating the TPBAR as a line source. In order to perform this analysis, a brief derivation is required. This can be found in APPENDIX J: DOSE RATE DERIVATION AND CALCULATIONS along with gamma flux calculations for three test cases.

From these results it is shown that both distance and shielding from a TPBAR serves to lower the unattenuated gamma flux. However, a TPBAR is still highly radioactive and must be given the highest level of respect. All three cases modeled show that more shielding is required before the area is safe for occupation. Just as superposition can be used to calculate the flux at a point, if multiple TPBARs are modeled, the total flux at any point is simply the sum of the flux due to each TPBAR.

2.3.5. Lithium-6, Tritium, and Helium-3 Tracking

The principle tritium producing reaction in this design is the (n,α) reaction of lithium-6. This reaction is shown in Equation 23. The lithium-6 is contained in annular lithium pellets that are stacked within a TPBAR. Tritium, as noted earlier, naturally decays and helium-3 is formed. Helium-3 is a "black" neutron absorber, and for long burnups, it plays a larger and larger role in the negative reactivity of the TPBAR. When helium-3 absorbs a neutron, an (n,p) reaction results in the creation of tritium once again. This is shown in Equation 24. The entire process is illustrated in Figure 27. Note that since both neutron

reactions are “two-body, non-relativistic” reactions, the energy of the outgoing particle can be calculated as a simple mass fraction times the reaction Q-value, as shown in Equation 25.

$$ {}^{6}_{3}Li + {}^{1}_{0}n \xrightarrow{yields} {}^{4}_{2}He + {}^{3}_{1}H + 4.78MeV \qquad \text{Equation 23} $$

$$ {}^{3}_{2}He + {}^{1}_{0}n \xrightarrow{yields} {}^{1}_{1}H + {}^{3}_{1}H + 0.764MeV \qquad \text{Equation 24} $$

$$ E_{N_1} = \frac{m_{N_2}}{m_{N_1} + m_{N_2}} * Q \qquad \text{Equation 25} $$

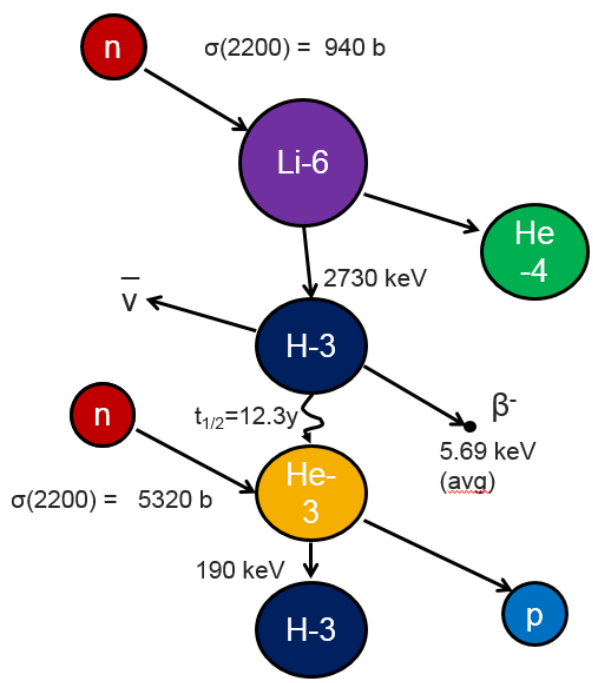

Figure 27. Diagram showing the principle tritium producing reactions.

The dynamics of this process can be modeled using ordinary differential equations (ODEs), as shown by Equation 26, Equation 27, and Equation 28. In these equations, ϕ is the neutron scalar flux, N_{Li}, N_T, and N_{He} are the atomic number densities of lithium-6, tritium, and helium-3, respectively, and σ_{Li} and

σ_{He} are the microscopic cross-sections for lithium-6 and helium-3, respectively. It is assumed that all other absorption reactions are negligible in comparison to the (n,α) reaction of lithium-6 and the (n,p) reaction of helium-3. If the scalar flux is taken to be uniform and mono-energetic, and the number densities of the various nuclides are spatially independent, this model simplifies, as shown by Equation 29, Equation 30, and Equation 31. In these equations, ϕ_0 is the "2200 m/s scalar flux." It is these equations that the program, *Team 9 Nuclide Program* (T9NP) aims to solve.

$$\frac{dN_{Li}(x,y,z,t)}{dt} = -\int_{\substack{all\ neutron\\ energies}} \phi(x,y,z,t,E)\sigma_{Li}(E)N_{Li}(x,y,z,t)\,\mathrm{dE} \qquad \text{Equation 26}$$

$$\frac{dN_T(x,y,z,t)}{dt} = -\lambda_T N_T(x,y,z,t) + \int_{\substack{all\ neutron\\ energies}} \phi(x,y,z,t,E)[\sigma_{Li}(E)N_{Li}(x,y,z,t) + \sigma_{He}(E)N_{He}(x,y,z,t)]\,\mathrm{dE} \qquad \text{Equation 27}$$

$$\frac{dN_{He}(x,y,z,t)}{dt} = \lambda_T N_T(x,y,z,t) - \int_{\substack{all\ neutron\\ energies}} N_{He}(x,y,z,t)\phi(x,y,z,t,E)\ \sigma_{He}(E)\,dE \qquad \text{Equation 28}$$

$$\frac{dN_{Li}(t)}{dt} = -\phi_0(t)\sigma_{Li}(2200)N_{Li}(t) \qquad \text{Equation 29}$$

$$\frac{dN_T(t)}{dt} = \phi_0(t)[\sigma_{Li}(2200)N_{Li}(t) + \sigma_{He}(2200)N_{He}(t)] - \lambda_T N_T(t) \qquad \text{Equation 30}$$

$$\frac{dN_{He}(t)}{dt} = \lambda_T N_T(t) - \phi_0(t)\,\sigma_{He}(2200)N_{He}(t) \qquad \text{Equation 31}$$

In order to run T9NP, initial concentrations of the three nuclides must be given. Additionally, the user must provide the time-dependent scalar flux into the flux function. The notation for the program defines an atomic number density vector and a matrix, as shown in Equation 32, Equation 33, and Equation 34 .

$$\vec{Y}(\mathrm{t}) = \begin{pmatrix} N_{Li}(t) \\ N_T(t) \\ N_{He}(t) \end{pmatrix} \qquad \text{Equation 32}$$

$$\boldsymbol{A} = \begin{pmatrix} -\phi_0(t)\sigma_{Li} & 0 & 0 \\ \phi_0(t)\sigma_{Li} & -\lambda_T & \sigma_{He}\,\phi_0(t) \\ 0 & \lambda_T & -\sigma_{He}\,\phi_0(t) \end{pmatrix} \qquad \text{Equation 33}$$

$$\overrightarrow{Y'} = \boldsymbol{A}\,\vec{Y} \qquad \text{Equation 34}$$

T9NP solves these equations using the implicit Euler method with LU factorization and an LU solve. The results are verified by using an explicit Euler method to check for consistency. The code consists of several FORTRAN files, which can be found in APPENDIX K: T9NP SOURCE CODE.

Since T9NP only solves for a homogenous TPBAR, corrections must be made for tritium and helium-3 diffusion. In order to account for this, the empirical observations from Collins (2009) are considered. According to Collins, helium-3 diffusion through the TPBAR is not well understood, but at low flux levels, helium-3 is contained in the solid components. As the flux increases, helium-3 travels to the void, but its diffusion is still a slow process. The document goes on to state that, in core physics calculations, tritium (the source of helium-3) can be assumed to remain in the lithium aluminate pellet for these purposes.

In addition to the fraction of helium-3 contained in the materials, helium-3 can collect in the void region of the TPBAR. From Collins (2009), the amount of free helium-3 in the upper plenum of the TPBAR, active length of the TPBAR, and the lower plenum of the TPBAR are shown by Equation 35, Equation 36, and Equation 37. In these equations, UP is the length from the top of the top lithium aluminate pellet to the top of the top end plug, AL is the length from the top of the top pellet to the bottom of the bottom pellet, and LP is the length from the top of the bottom end plug to the bottom of the bottom pellet. For Equation 35, Equation 36, and Equation 37 to be valid, helium-3 is assumed to fill the void region uniformly, thus these equations simply relate the void volume of a specific region to the total void volume of the TPBAR.

$$^{3}He_{UP} = \frac{1.9UP}{1.9UP + AL + 1.4LP} * {}^{3}He_{free}$$ Equation 35

$$^{3}He_{AL} = \frac{AL}{1.9UP + AL + 1.4LP} * {}^{3}He_{free}$$ Equation 36

$$^{3}He_{LP} = \frac{1.4LP}{1.9UP + AL + 1.4LP} * {}^{3}He_{free}$$ Equation 37

Additional corrections must be made for a non-uniform flux profile, and spatial self-shielding. There are a number of approaches that could be taken to perform this including assuming a cosine shaped flux profile and then performing the same calculation a number of times along a TPBAR that has been meshed axially. More complicated approaches will be investigated in future works.

Two cases of interest are examined using T9NP in APPENDIX I: T9NP CASES AND ANALYSIS. From the most realistic case modeled, it is shown that a two year cycle produces 1116.9 grams of tritium. It should be noted that a current upper limit due to internal pressure of the TPBAR is 1.2 grams per TPBAR. This would scale to roughly 0.86 grams/TPBAR for the mPower reactor because of the reduced height. This limit would result in a maximum of 949.4 grams of tritium allowed to be produced based on the current core configuration. Changes in core configuration may allow for this number to be raised by increasing the number of TPBARs in the reactor, and reconfiguring fuel enrichments as necessary to compensate.

2.3.6. Heavy Ion Interactions

The nuclear interactions in the TPBAR must not jeopardize the material integrity of the TPBAR. Much of the energy created is transferred to heavy ions following a nuclear interaction. The main reaction of interest is the (n,α) reaction of lithium-6, shown in Equation 23. This reaction has a very large Q value (4.78 MeV), which is divided among two heavy ions – an alpha particle and a triton. Like all heavy ions, most of the energy is dissipated in the final section of the ion's path. Such large amounts of energy deposition in a little volume raise concerns about damage to the material. Additionally, if the triton is sufficiently energetic, it could travel out of the lithium aluminate pellet and into other structures. To study these phenomena, the SRIM-2013 software was used.

SRIM-2013 is capable quickly creating range tables for ions in matter or modeling the actual range, transmission, energy deposition, and interactions of an ion beam into a composite target material. Figure 28 illustrates the depth that a triton goes within the lithium aluminate target pellet itself. From this, it is clear that nearly all tritons remain within the aluminate pellet, and all energy is deposited within this pellet. Conduction will transfer the heat to the clad, where it will be convected away by the

coolant. Of course, when the TPBAR is not exposed to a neutron flux, this reaction no longer occurs, and heat is produced elsewhere in the TPBAR as a result of activation as discussed earlier.

Figure 29 shows the "worst case scenario" for a heavy ion causing safety problems. This figure shows a beam of tritons that are born at the pellet-getter interface, with a direction vector normal to the surface. From this, it is shown that no tritons reach the center of the nickel plating that covers the getter and protects it from oxidation.

From these studies, it is unlikely that heavy ions would contribute to much material damage or tritium leakage. In fact, the lithium aluminate pellets maintain fair structural integrity, even with high depletion of the lithium-6 target (Senor, Senior Design Project Meeting, 2012). This is a result of favorable characteristics of the molecules that are formed as lithium is removed.

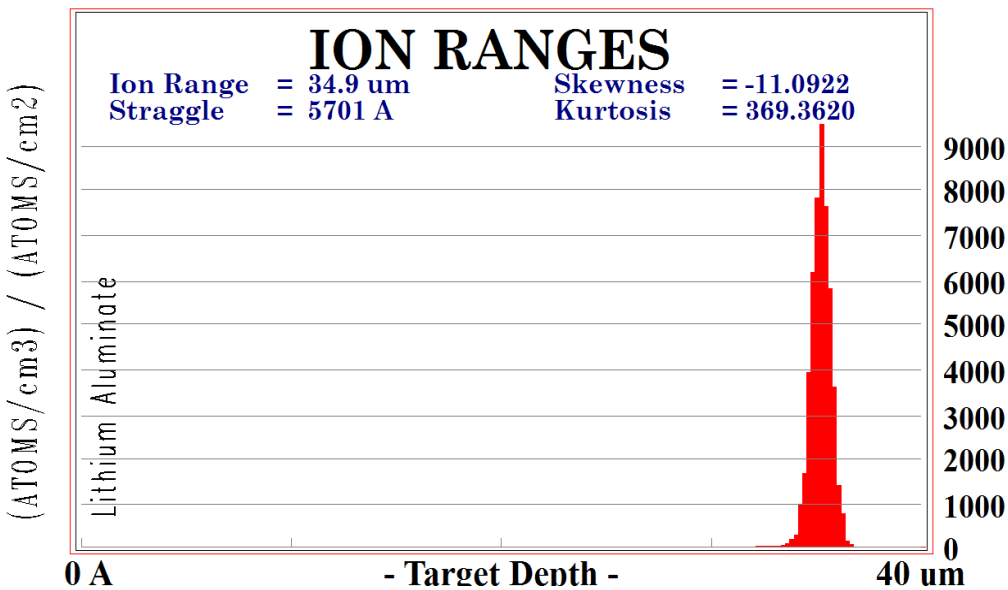

Figure 28. SRIM-2013 output of a triton from the (n,α) reaction of lithium-6 into the lithium aluminate pellet.

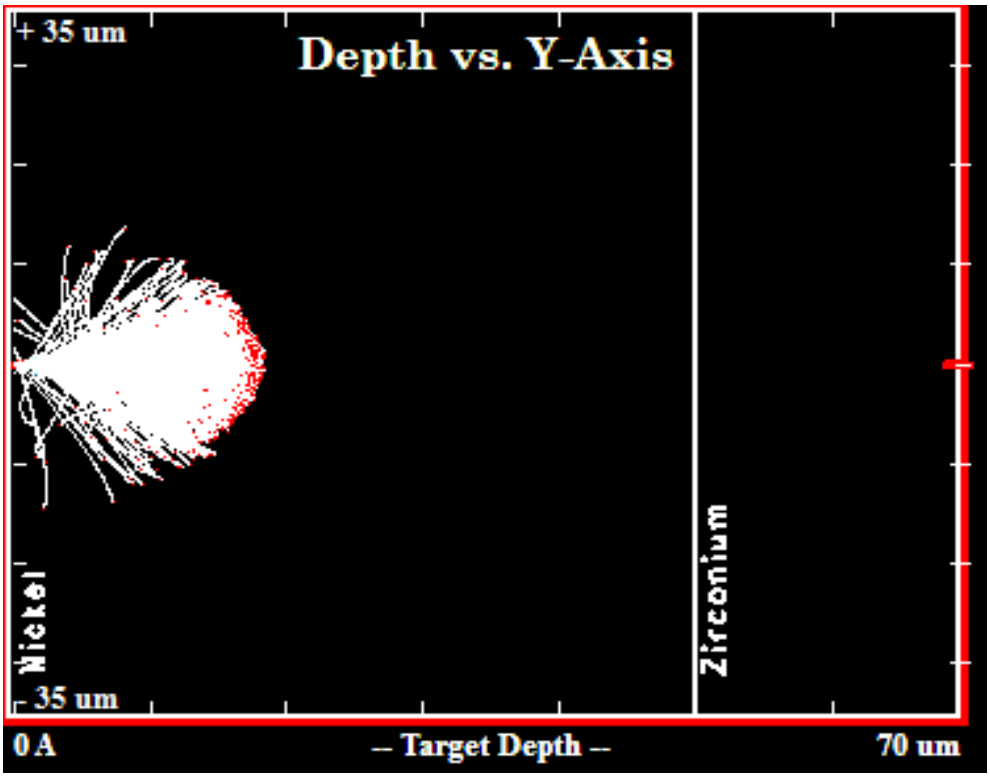

Figure 29. SRIM-2013 output of a beam of tritons born at the getter interface, normal to the getter.

3. ECONOMIC ANALYSIS

Written by Mac Cook

All engineering projects must undergo an economic analysis to ensure that the benefits of the project outweigh the costs. In this discussion, the costs and benefits of the tritium production facility described in this report will be enumerated in subdivisions.

A number of assumptions must first be taken into account before an in depth analysis can begin. Firstly, there have been a number of costs already incurred during the duration of the U.S. Department of Energy's Tritium Readiness Program. This includes, but is not limited to, production techniques and designs, safety analyses, experimental verification, system design and implementation, and various research and development efforts, including the design and application of tritium producing burnable absorber rods (TPBARs). For the analysis conducted here, all of these costs incurred are considered economic "sunk costs." Essentially, any costs that these efforts incurred do not have to be analyzed because these efforts have occurred in the past. Instead, the best economic decision must be made in the present and for the future, irrespective of previous decisions.

When viewed through this lens, it is clear why the TPBAR design was chosen from an economic standpoint. By using TPBARs, the project saves money by taking advantage of the large, detailed library of information related to the TPBAR characteristics and performance, the systems already in place for handling TPBARs, and other benefits arising from expertise and continuity of operations.

First, there are incremental costs associated with modifying a standard mPower reactor in order to produce tritium. These costs are related to the replacement of the various burnable poison rods (BPRs) in the standard design with the TPBARs used in this project. Since many burnable poisons are made of boron carbide with stainless steel or zircaloy cladding, cost of BPR's is taken to be similar to that of TPBARs (about $10000 per TPBAR) (Senor, Senior Design Project Meeting, 2012). Additionally, the fuel itself may become more expensive depending on changes in fuel enrichment and the removal of integral absorber material (Gd_2O_3). Another change in cost would come from a change in cycle length, so that the capacity factor of the plant may be altered and the burnup of the fuel may be lowered to produce a lower efficiency, and thus higher costs.

In order to calculate the differential cost of fuel, the units must be normalized to price of fuel per unit energy produced. Thus the analysis must first consider the cost of the UO_2 including the cost of enrichment. Next, this cost must be divided by the fuel burnup. The result is a price per unit energy, as summarized by Equation 40. Such an analysis ignores the time value of money (i.e. an interest rate of 0%).

For a standard mPower reactor, a cycle length is 4 years. If the reactor operates at 100% (this value may be high, but the relative cost between the two designs is the eventual desired output, so consistency is more important than accuracy) thermal power for this entire cycle, then the energy output of the core is simply 774.3 GWd, as shown by Equation 38. As shown by Equation 44, the total amount of uranium in

the core is 19.891 MTU. Thus the burnup is 38.93 GWd/MTU, as given by Equation 39. For comparison, the burnup of the core designed in this project was 21 GWd/MTU.

$$530\ MW * \frac{1}{1000}\frac{GW}{MW} * 4\ yr * 365.24\frac{d}{y} = 774.3\ GWd \qquad \text{Equation 38}$$

$$\frac{774.3\ GWd}{19.891 MTU} = 38.93\ GWd/MTU \qquad \text{Equation 39}$$

Using the uranium prices and the "enrichment equations" available at uxc.com, the price of the fuel can be obtained. On a standard mPower reactor, the core is loaded with fuels of different enrichments— all with an enrichment under 5% (LEU). In order to achieve the 4 year cycle, it is hypothesized that an approximate value for average fuel enrichment is 4.3 weight-percent (w/o). Using the tool available at uxc.com, the cost of this fuel is $1753.65/kgU. In the tritium producing design, 13.26 MTU of 3.5 w/o fuel will be used along with 6.63 MTU of 4 w/o fuel per cycle (UxC Fuel Quantity & Cost Calculator, n.d.). The prices of these fuels are $1365.04/kgU and $1607.31/kgU. Thus, the total cost of fuel per cycle for a standard mPower reactor is $34.88 million, and the total cost for the tritium producing design is $28.76 million.

With this data, a price for the thermal energy produced in the core was calculated for both designs. The energy cost for a standard design was found to be $896/MWd. The energy cost of the tritium producing design was $1369/MWd. These values were calculated using Equation 40. This is an increase in energy cost of nearly 53%. Since the thermal power of the both designs was the same, efficiencies also remain the same as this thermal energy price increase eventually presents itself as an electrical energy price increase. Since the operating, maintenance, and capital costs of the tritium producing design are similar to those of a standard mPower, the busbar cost will only change due to the increase in fuel price. Since nuclear power plants have relatively low fuel costs, when the price increase of 53% to fuel is multiplied by a rather small component of the busbar cost, the total busbar cost will rise by a percentage much lower than 53%. Note that these costs are subject to change with time as the cost of uranium ore changes and enrichment and fabrication technology improves.

$$Energy\ Cost = \frac{Fuel\ Cost}{Burnup} \qquad \text{Equation 40}$$

This project can be economically feasible, but the price the customer (i.e. the DOE/NNSA) is willing to pay for the tritium is what would eventually decide this. If 1 kg of tritium is produced in a single cycle, and the price of tritium is taken to be $30,000/g (Willms, 2003), then the net fuel cost can be lowered to only $4.88 million per cycle. This actually produces a cost savings of 83%. In Willms, the expected price of tritium for the US government is expected to rise to between $100,000/g to $200,000/g. This makes the "net fuel cost per cycle" negative costs of between ($165.1 million) and ($65.1 million). Note that

Equation 40 is still valid, but "net fuel cost" is now a function of burnup, as the amount of tritium produced depends on the burnup (this relationship is dependent on a number of factors, and tools such as T9NP are recommended).

Since the producer and consumer of the tritium is likely the US government, the price of tritium can be represented simply as the additional cost of fuel. To remain conservative in the price estimate, two two-year cycles of a tritium producing reactor are compared to one four-year cycle for the standard mPower reactor. The resulting price, P^*, is \$11320 per gram of tritium, a cost savings of 62.3% versus the market price, this is shown by Equation 41.

$$P^* = \frac{2 * \$28.76 * 10^6 - \$34.88 * 10^6}{2000\ g} = \$11320\ per\ gram\ of\ tritium \qquad \text{Equation 41}$$

If the price of the actual TPBAR is once again considered, the price P^* becomes approximately \$21320 per gram of tritium, assuming a TPBAR, on average, produces 1g of tritium, and each TPBAR costs approximately \$10000. This new price is still 29% lower than the 2003 market price of tritium and 80% to 90% lower than the anticipated cost according to Willms. This analysis is conservative, since the price of the burnable poison rods is now effectively considered zero. Thus, if a standard mPower reactor is considered economically feasible, then, all other things constant, an mPower reactor designed to produce tritium at the current market price would be even more economically competitive.

4. CONCLUSIONS AND RECOMMENDATIONS

Written by Mac Cook with input from Leigh Ann Emerson

After design and analysis, it has been shown that tritium can be safely and economically made in a modified mPower reactor. For this project, after completing the integrated design and analysis, it was found that the optimum TPBAR lithium enrichment was 22 percent and the optimum cycle length was two years. This corresponds to a burnup of 21 GWD/MTU. Note that this is less than the four year cycle and therefore less than the burnup seen by the fuel for the reference design. However this enabled the modified reactor to have a lower enriched fuel as compared to both the reference design and TVA's Watts Bar Unit 1. Thus some of the increased fuel costs that would be incurred from a reactor whose main goal is to produce power were offset.

The design goal of 1150 grams of tritium per year was not met with a single core. However, when an mPower "twin pack" design is considered, the tritium production goal is nearly met. The "twin pack" design consists of two mPower reactor connected synergistically, sharing many of the same components including a single spent fuel pool. The analysis of the design shows that approximately 1116.9 grams of tritium are produced in a two year cycle from a single core. If the two cores alternate in refueling outages (e.g. unit 1 refuels in the spring of even-numbered years, while unit two refuels in the spring of odd-numbered years) then 1116.9 grams of tritium would be produced annually, barring the pressure limit currently imposed on TPBARs. As mentioned previously, an upper limit on tritium produced by the current configuration would be 949.44 grams. This would have to be addressed by the addition of TPBARs and reconfiguration of the core to compensate for the additional TPBARs.

The deficiency in the amount of tritium produced by this design could possibly be met with more complicated TPBAR loadings, such as more TPBARs in the assemblies with the largest scalar flux. According to the neutronics analysis, there is a surplus of reactivity towards the end of the current cycle. Therefore criticality could be maintained even in this scenario. Thus the "twin pack" design is recommended in order to sufficiently meet the DOE's project goals.

The safety of such a design has also been verified. This was done by performing a thermal hydraulics analysis using RELAP5-3D, a widely accepted systems code, for the worst postulated DBA for the mPower reactor, a LOFA. In this analysis, the temperatures were shown to be well within an acceptable range. Additionally, several safety aspects of tritium production were analyzed and shown to be acceptable. The amount of tritium produced per TPBAR was less than the rated maximum, and a conservative approach was used to accommodate any inaccuracies due to the inherent heterogeneity of the core.

5. FUTURE WORK

Written by all

Future work for this project involves creating a closed flow loop in RELAP5-3D for the coolant to flow through. This would take a lot of time because all of the components involved in the primary loop would need to be modeled but would be beneficial because it would allow for a complete system analysis to be performed. Because of this the temperature and pressure drops through the entire primary loop could be established, and therefore a more accurate picture of the state of the system would be established.

It would also be beneficial to obtain the pump coast down specifications from B&W and use a computational fluid dynamics code to more accurately determine the natural circulation flow rate through the core. These parameters, combined with a closed flow loop for the RELAP5-3D simulation, would enable a more accurate and precise modeling of a LOFA. Therefore a more accurate analysis of fuel and cladding temperatures would be achieved for such an event. This is important because the flow rate through the core directly affects the amount of heat that can be removed from the fuel and consequently the temperature of the fuel and cladding. In short, a smaller pump coast down time would mean that the maximum temperatures of the fuel and cladding would rise faster because the coolant flow rate would be less with the same amount of decay heat being produced at a given time.

Regarding neutronics analyses, future work would include a more thorough model of the mPower using a lattice physics code that has a complete cross-section library. The lack of definitions for lithium-6 in Casmo4 was the limiting factor in how accurately the mPower could be modeled. Proper definitions would be able to better simulate lithium-6 interactions with neutrons, and also spatial self-shielding. The additional spatial-self shielding analysis is important since helium-3 would build up and would likely have a significant effect on flux shape within the TPBAR. This would impact the amount of tritium that is produced in the TPBAR. The Casmo4 model used was not able to simulate spatial self-shielding since the depletion chain of lithium-6 was not modeled completely in Casmo4.

Additional future work that needs to be performed in the neutronics analysis of the mPower includes further safety analyses. Determining whether the reactor operates in a region of under-moderation or over-moderation should be considered. This was not included in the scope of this project due to time constraints and the fact that the mPower reactor is already an almost complete design by B&W. It was determined that this was one of the less important factors to consider since it was not directly related to the capability of the reactor to produce tritium. Other safety parameters such as power coefficients of reactivity would also have to be examined.

Experimentation should be performed to validate the chosen methods of design and analysis, as well as the results. These experiments are crucial to ensure all safety criteria have been met. Once experimentation has been performed, the results should be verified, and any necessary changes to the design process should be implemented. A wide range of experimental data is already available for TPBARs, and this information should be used where appropriate.

WORKS CITED

Burns, K. A. (2012). *Description of the Tritium-Producing Burnable Absorber Rod for the Commercial Light Water Reactor, Revision 19. TTQP-1-015.*

Collins, B. A. (2009). *Unclassified Bounding Source Term, Radionuclide Concentrations, Decay Heat, and Dose Rates for the Production TPBAR, Revision 7. TTQP-1-111.*

Collins, B. A. (2012). *Production TPBAR Inputs for Core Designers, Revision 15. TTQP-1-116.*

Gruel, R. L. (2012). *Unclassified TPBAR Releases, Including Tritium, Revision 14. TTQP-1-091.*

Hubbell, J., & Seltzer, S. (n.d.). Tables of X-Ray Mass Attenuation Coefficients and Mass Energy-Absorption Coefficients from 1 keV to 20 MeV for Elements Z = 1 to 92 and 48 Additional Substances of Dosimetric Interest. Gaithersburg, Maryland.

Idaho National Engineering Laboratory: Lockheed Idaho Technologies Company. (1995). *RELAP5/MOD3 CODE MANUAL VOLUME II: USER'S GUIDE AND INPUT REQUIREMENTS.* Idaho Falls.

Idaho National Laboratory. (2012, November). *RELAP5-3D*. Retrieved from http://www.inl.gov/relap5/

Le Claire, A. D. (1981). *The Permeation of Gases through Solids I - Principles.* Harwell.

Liger, K., & Gilardi, T. (n.d.). *Hydrogen-Tritium Transfer in SFR Concepts.* France: CEA.

Marianno, C. (2013). NUEN 604 Class Notes. *Lecture 13: Flux Calculations*.

O'Leary, P. M., & Pitts, D. M. (2001). EFFECTS OF BURNABLE ABSORBERS ON PWR SPENT NUCLEAR FUEL. Tucson.

Senor, D. J. (2012, September 7). Senior Design Project Meeting. (L. A. Emerson, W. Cook, & C. T. Woolum, Interviewers)

Senor, D. J., & Paxton, D. M. (2012). *Tritium Technology Program Overview and SMR Design Challenge.* Pacific Northwest National Laboratory.

Sherman, S. R., & Adams, T. M. (2008). *Tritium Barrier Materials and Seperation Systems for the NGNP.* Aiken, SC: Savannah River National Laboratory.

Shiraishi, T., Nishikawa, M., Yamaguchi, T., & Kenmotsu, K. (1999). Permeation of multi-component hydrogen isotopes through austenitic stainless steels. *Journal of Nuclear Materials 273*.

Todreas, N. E., & Kazimi, M. S. (1993). *Nuclear Systems I: Thermal Hydraulic Fundamentals.* Hemisphere Publishing Corporation.

U.S. NRC. (2013, January). *About NRC.* Retrieved from U.S. NRC: http://www.nrc.gov/about-nrc/regulatory/research/comp-codes.html#th

U.S. NRC. (2013, February). *NRC Library.* Retrieved from Resolution of Generic Safety Issues: Issue 92: Fuel crumbling During LOCA (Rev. 1) (NUREG-0933, Main Report with Supplements 1-34): http://www.nrc.gov/reading-rm/doc-collections/nuregs/staff/sr0933/sec3/092r1.html

U.S. NRC. (2013, April). *NRC Library: Document Collections.* Retrieved from U.S. NRC: http://www.nrc.gov/reading-rm/doc-collections/nuregs/staff/sr1793/initial/chapter19.pdf

UxC Fuel Quantity & Cost Calculator. (n.d.). Retrieved from UxC: http://www.uxc.com/tools/uxc_FuelCalculator.aspx

Vierow, K. (2013, April 17). Associate Professor and Graduate Coordinator. College Station, Texas, United States of America.

Vierow, K. (2013). NUEN 410 Class Notes. College Station, Texas, United States of America: Texas A&M University.

Westinghouse. (2013). *AP1000 Documentation.* Retrieved from https://www.ukap1000application.com/doc_pdf_library.aspx

Williams, J. (2011). Generation mPower: Introduction to mPower. *IRUG Conference.* Salt Lake City.

Willms, S. (2003). Tritium Supply Consideration. Los Alamos National Laboratory.

APPENDIX A: DESIGN DATA RECEIVED FROM B&W

Characteristics	Importance	Value
Operating Conditions		
Power density [power/liter cold core]		Power Output - 530 Mwt (divide by core volume to get density approximation)
Specific power [power/mass U]		Power Output - 530 MWt (divide by core mass (conventional core with shorter rods) to get specific power approximation.)
Pressure		2060 PSIA / 2300 PSI design pressure
		Steam at 825 PSI
Cycle length		4 years
Coolant flow rate		30 Mlbm/hr
Neutron source type/location		
Coolant inlet/outlet/avg temp		Outlet - 606 F
		Inlet - 567 F
		Feedwater Temp - 414F
Core bypass		
Fuel		
Pellet dimensions		Conventional Fuel
Rod dimensions (Gas gap, clad thickness, etc.)		Conventional Diameters
Enrichment		<5%
Density		Conventional Fuel
Pin layout		17X17 Array
Temperatures (centerline/outer)		
Pitch		Conventional Pitch
Assembly dimensions		Same as traditional core, but 95 inches active length
Composition (UO_2??)		UO2
Cladding material (Zirc-4)		Zirc-4
Core		
Presence of burnable absorbers		Yes. Burnable poisons. No boron Shim in coolant
Control rod material		
Control rod layout		69 Control Rod Assemblies
Core loading		
Batch loading? (# cycles in core)		1
Spacer		
Active core length		95 in
Guide tube/instrument tube dimensions		
Reflector dimensions/materials		
Dimensions		13 ft diameter
		83 ft height
General		
Number of loops		N/A. Integral Reactor
Steam generator efficiency		
Other component efficiencies		
Fuel cost		
Estimated cost per unit		

Key	
	Most Important
	Least Important

http://www.generationmpower.com/pdf/sp201100.pdf

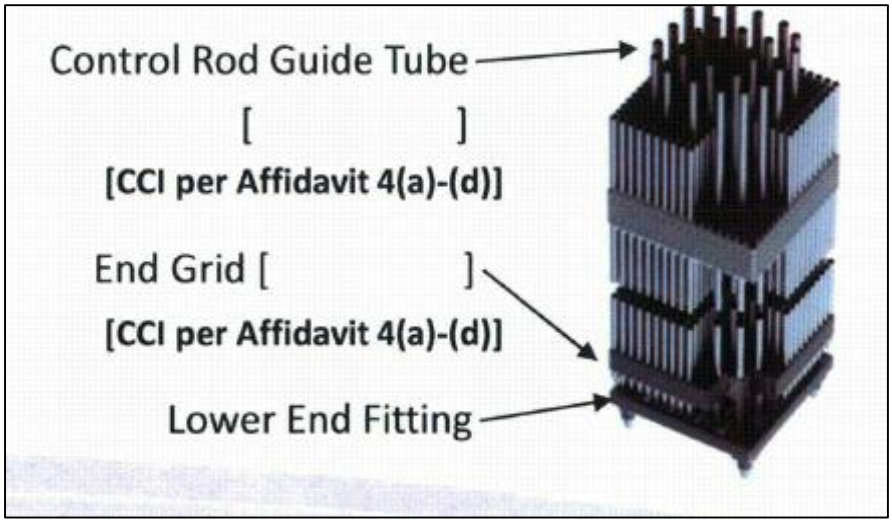
Control Rod Guide Tube
[ ]
[CCI per Affidavit 4(a)-(d)]
End Grid [ ]
[CCI per Affidavit 4(a)-(d)]
Lower End Fitting

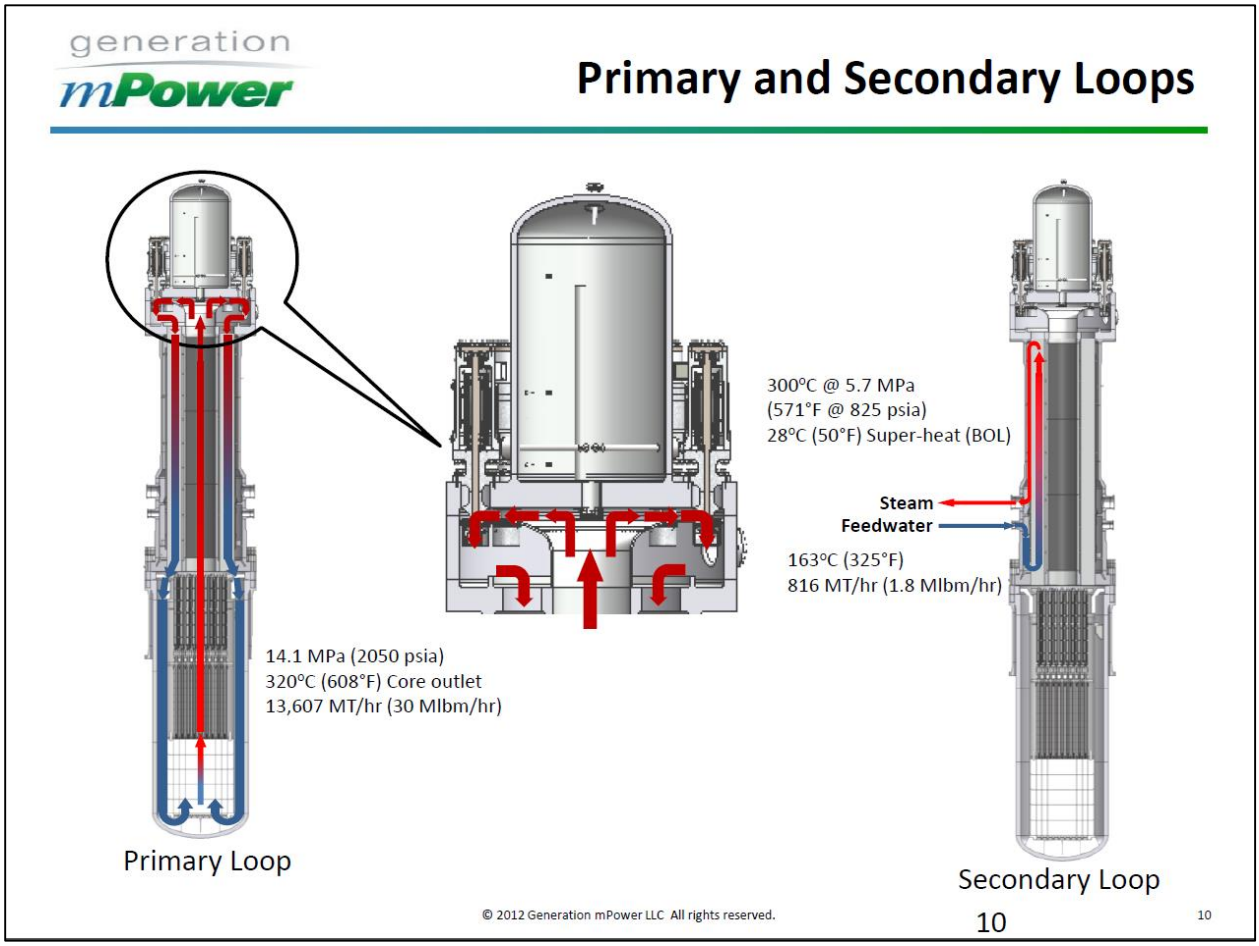
generation
mPower
Primary and Secondary Loops
300°C @ 5.7 MPa
(571°F @ 825 psia)
28°C (50°F) Super-heat (BOL)
Steam
Feedwater
163°C (325°F)
816 MT/hr (1.8 Mlbm/hr)
14.1 MPa (2050 psia)
320°C (608°F) Core outlet
13,607 MT/hr (30 Mlbm/hr)
Primary Loop
Secondary Loop
© 2012 Generation mPower LLC All rights reserved.
10
10

APPENDIX B: RELAP5-3D STEADY STATE ANALYSIS INPUT DECK

```
= MPower SMR Model
*
* * * * * * * * * * * * * * * * * * * * * * * * * * * * * * * * * * * *
100 new stdy-st *pg26
*
102  british   british *input units then output units
105  5.0 6.0 5000.0 *pg 30: CPU remaining limit, CPU remaining limit,
CPU time allocated
110 nitrogen *not sure this is needed (only needed with accumulators)
120 103010000 0.0 h2o primary *don't need this card because water is
assumed by default
*****************************************************
*                                                   *
*               time step cards                     *
*                                                   *
*****************************************************
*
201 1500.0 1.0-9 0.50 23 2 200 500 *pg35 tend, min time step, max
step, control options(??)
*
*****************************************************
*                                                   *
*              minor edit variables                 *
*                                                   *
*****************************************************
*
*none listed here; can be used for extra plots
*
***********************************************
*                                             *
*                  Core                       *
*                                             *
***********************************************
1030000 core pipe
*       nv
1030001 20
*         flArea    vn
1030101  17.87629   20 *flArea of core
*         jFlArea      jn
1030201   0.0          19
*         FlLen        vn
1030301  7.9166666     20
*         vol          vn
1030401  141.5206      20
*         vAng         vn
1030601   90.0         20
*         rough    hyd     vn
```

```
1030801   0.0    .57434    20 *hyd of FA
*1030901 -- assuming no junction loss coefficients
*         tlpvbfe nv (pg.89)
1031001   0000000 20
*         jefvcahs jn
1031101   00001000 19
*         ebt  pressure  temp
1031201   3    2060.0   586.5  0.0 0.0 0.0 20 *avg coolant temp
*junction initial condion
1031300   1
*         liqMflw vapMflw ifVel jn
1031301   8333.33   0.0    0.0  19
* 1031401 CCFL and Junction diameter
*         elCh        vn

************************************************
*                                              *
*                Bottom Tank                   *
*                                              *
************************************************
1040000 bottank snglvol *pg 77
*       FlArea FlLen  Vol AziAng InclinAng elCh rough hyd tlpvbfe
1040101 1000.   100.  0.0    0.    90.     100.  0.   0.  0
*       ebt  pressure  temp
1040200  3   2200.    567.
*       variable values
*
************************************************
*                                              *
*                Top Tank                      *
*                                              *
************************************************
1050000 toptank tmdpvol *pg 77
*       FlArea FlLen Vol AziAng InclinAng elCh rough hyd tlpvbfe
1050101  10000. 100. 0.0  0.     90.      100.   0.   0. 0
*       ebt  pressure temp
1050200  3
*       variable values
1050201 0. 1900. 606.

************************************************
*                                              *
*          Junctions                           *
*                                              *
************************************************
1120000 bot-core tmdpjun
*       from      to        area   jefvcahs
1120101 104010000 103000000 0.0
1120200  1
*     variable LiqVel VapVel IntVel
1120201 0.0   8333.33 0.0    0.0
```

```
1110000 core-top sngljun
*       from      to      area  Af Ar jefvcahs
1110101 103010000 105000000 0. 0.0 0.0 0
*     control MflowL MflowG Interface
1110201 1    8333.33 0.0 0

**********************************************************************
**
*
*
*                 Heat Structures
*
*
*
**********************************************************************
**
**********************************************
*                                            *
*           Fuel Assembly                    *
*                                            *
**********************************************
******Heat Structures******
*       nAxHS nRadP geoType HSFlgs LeftCoord Reflood
11030000  20    10    2      1       0.0       0
*         MeshLocFlg MeshFormatFlg
11030100     0         1
*         #ofIntervals RightCoord
11030101    6         .013438
11030102    1         .013708
11030103    2         .015583

******Heat Structure Composition Data(Radial)******
*       Composition# Interval#
11030201   1           6  *pellet
11030202   2           7  *air gap
11030203   3           9  *cladding

******Heat Structure Source Distribution Data (Radial)******
*       SourceValue RadInt#
11030301   1.0      6
11030302   0.0      9

*        Temp  nRadP
11030401 1100.0 3
11030402 900.0  5
11030403 620.0  7
11030404 600.0  8
11030405 570.0  10

******Left Boundary Condition******
```

```
*       vn increment BCtype SAcode SA nAxHS
11030501 0    0        0      0    0.0  20

******Right Boundary Condition******
*          vn     increment BCtype SAcode SA nAxHS
11030601 103010000  10000    1      0   1092.  20

******Source Data******
*      SourceType AxPeakF ModHeatMult HS#
11030701 1   0.011169174   0  0     1
11030702 1   0.022088847   0  0     2
11030703 1   0.032515091   0  0     3
11030704 1   0.042215002   0  0     4
11030705 1   0.050971900   0  0     5
11030706 1   0.058590170   0  0     6
11030707 1   0.064899632   0  0     7
11030708 1   0.069759344   0  0     8
11030709 1   0.073060747   0  0     9
11030710 1   0.074730094   0  0     10
11030711 1   0.074730094   0  0     11
11030712 1   0.073060747   0  0     12
11030713 1   0.069759344   0  0     13
11030714 1   0.064899632   0  0     14
11030715 1   0.058590170   0  0     15
11030716 1   0.050971900   0  0     16
11030717 1   0.042215002   0  0     17
11030718 1   0.032515091   0  0     18
11030719 1   0.022088847   0  0     19
11030720 1   0.011169174   0  0     20

******Additional Left Boundary******
*       Dh HLength HLRev GSL GSLRev GLossCoef GLCRev LBoilF HS#
11030801 0.0 15.0  15.0  0.0  0.0    0.0       0.0    1.0   20

******Additional Right Boundary******
11030900  1
*       Dh HLen HLRev GSL GSLRev GLossCoef GLCRev LBoilF NatCircL
PDiamR FoulF HS#
11030901 0.0 15.0 15.0 0.0 0.0 0.0 0.0 1.0 0.0 1.3262 1.0 20


*********************************************************************
**
*
*
*               Heat Structure Thermal Property Data
*
*
*
*********************************************************************
**
```

```
*                                        *
* composition type and data format       *
*                                        *
*****************************************
*
20100100       uo2     * core fuel
20100200       tbl/fctn       1       1     * air gap
20100300       tbl/fctn       1       1     * cladding
*
*********************************************************************
**
*
*
* thermal conductivity data (btu/sec-ft/deg f) and volumetric heat
*
* capacity  data (btu/ft**3-deg f) versus temperature for above
*
* composition
*
*
*
*********************************************************************
**
*
*
*
*
* Air gap
*
*        Temperature    Thermal Conductivity
*
20100201        32.0          2.4487788e-04
20100202      5400.0          2.4487788e-04
*
*        Temperature    Heat Capacity
*
20100251        32.0          0.000065
20100252      5400.0          0.000065
*
*
* Cladding
*
*         Temperature    Thermal Conductivity
*
20100301        32.0  2.9267e-03 392.0 2.9267e-03
20100302       752.0         1.2478e-03
20100303      1112.0         4.7297e-03
20100304      1472.0         5.0508e-03
20100305      1832.0         6.5325e-03
20100306      2192.0         4.0142e-03
20100307      2552.0         5.8169e-03
```

```
20100308      2912.0         8.7803e-03
20100309      3272.0         1.0647e-03
20100310      3632.0         1.8311e-03
20100311      3992.0         9.0918e-02
20100312      5000.0         9.0918e-02
*
*          Temperature     Heat Capacity
*
20100351         0.0         26.392
20100352      1480.3         35.476
20100353      1675.0         75.176
20100354      1787.5         44.370
20100355      3500.0         24.476
*
*
*
**********************************************************************
*
*
*  General Table 1
20200100       power
*            Time (sec)        Power(MW)
20200101        0.0             530.
20200102        1000.0          530.
*
**********************************************
*                                            *
* End of input deck                          *
*                                            *
**********************************************
.
```

APPENDIX C: RELAP5-3D LOFA ANALYSIS INPUT DECK

```
= MPower SMR Model
*
* * * * * * * * * * * * * * * * * * * * * * * * * * * * * * * * * * * *
100 new transnt *pg26
*
102  british   british *input units then output units
105  5.0 6.0 5000.0 *pg 30: CPU remaining limit, CPU remaining limit,
CPU time allocated
110 nitrogen *not sure this is needed (only needed with accumulators)
120 103010000 0.0 h2o primary *don't need this card because water is
assumed by default
*******************************************************
*                                                     *
*               time step cards                       *
*                                                     *
*******************************************************
*
201 259205.0 1.0-9 0.50 23 2 200 500 *pg35 tend, min time step, max
step, control options(??)
*
*******************************************************
*                                                     *
*              minor edit variables                   *
*                                                     *
*******************************************************
*
*none listed here; can be used for extra plots
*
*******************************************************
*                                                     *
*              trip cards                             *
*                                                     *
*******************************************************
*
507  time   0     ge   null    0      5.0      1
*
***********************************************
*                                             *
*                  Core                       *
*                                             *
***********************************************
1030000 core pipe
*       nv
1030001 20
*         flArea    vn
1030101  17.87629   20 *flArea of core
*         jFlArea      jn
1030201   0.0          19
```

```
*         FlLen        vn
1030301  7.9166666     20
*         vol          vn
1030401  141.5206      20
*         vAng         vn
1030601   90.0         20
*         rough    hyd     vn
1030801   0.0    .57434    20 *hyd of FA
*1030901 -- assuming no junction loss coefficients
*         tlpvbfe nv (pg.89)
1031001   0000000 20
*         jefvcahs jn
1031101   00001000 19
*         ebt  pressure  temp
1031201   3    2060.0   586.5  0.0 0.0 0.0 20 *avg coolant temp
*junction initial condion
1031300   1
*         liqMflw vapMflw ifVel jn
1031301   1.0   0.0    0.0  19
* 1031401 CCFL and Junction diameter
*         elCh        vn
**********************************************
*                                            *
*                Bottom Tank                 *
*                                            *
**********************************************
1040000 bottank snglvol *pg 77
*       FlArea FlLen  Vol AziAng InclinAng elCh rough hyd tlpvbfe
1040101 10000. 1000.  0.0    0.    90.     1000.  0.   0.  0
*       ebt  pressure  temp
1040200  3   2200.    567.
*       variable values
*
**********************************************
*                                            *
*                Top Tank                    *
*                                            *
**********************************************
1050000 toptank tmdpvol *pg 77
*       FlArea FlLen Vol AziAng InclinAng elCh rough hyd tlpvbfe
1050101  10000. 1000. 0.0  0.     90.     1000.   0.   0. 0
*       ebt  pressure temp
1050200  3
*       variable values
1050201 0. 1900. 606.

**********************************************
*                                            *
*          Junctions                         *
*                                            *
**********************************************
```

```
1120000 bot-core tmdpjun
*       from      to        area   jefvcahs
1120101 104010000 103000000 0.0
1120200  1 507
*     variable LiqVel VapVel IntVel
1120201 -5.0    8333.33  0.0    0.
1120202  0.0    8333.33  0.0    0.
1120203  1505.0  500.00  0.0    0.
1120204  11000.   50.00  0.0    0.
1120204  12000.   50.00  0.0    0.
*1120205  500.0    1.00  0.0    0.
*1120206  600.0    1.00  0.0    0.
*
1110000 core-top sngljun
*       from      to      area  Af Ar jefvcahs
1110101 103010000 105000000 0. 0.0 0.0 0
*     control MflowL MflowG Interface
1110201 1    1.0  0.0  0
*********************************************************************
**
*
*
*
*                 Heat Structures
*
**
*
*********************************************************************
**
**********************************************
*                                            *
*           Fuel Assembly                    *
*                                            *
**********************************************
******Heat Structures******
*       nAxHS nRadP geoType HSFlgs LeftCoord Reflood
11030000  20    10    2      1       0.0       0
*         MeshLocFlg MeshFormatFlg
11030100     0         1
*         #ofIntervals RightCoord
11030101    6         .013438
11030102    1         .013708
11030103    2         .015583

******Heat Structure Composition Data(Radial)******
*       Composition# Interval#
11030201   1           6  *pellet
11030202   2           7  *air gap
11030203   3           9  *cladding

******Heat Structure Source Distribution Data (Radial)******
```

```
*       SourceValue RadInt#
11030301   1.0      6
11030302   0.0      9

*        Temp  nRadP
11030401 1100.0 3
11030402 900.0  5
11030403 620.0  7
11030404 600.0  8
11030405 570.0  10

******Left Boundary Condition******
*       vn increment BCtype SAcode SA nAxHS
11030501 0    0        0      0    0.0  20

******Right Boundary Condition******
*          vn     increment BCtype SAcode SA nAxHS
11030601 103010000  10000    1      0   1092.  20

******Source Data******
*      SourceType AxPeakF ModHeatMult HS#
11030701 1   0.011169174   0  0     1
11030702 1   0.022088847   0  0     2
11030703 1   0.032515091   0  0     3
11030704 1   0.042215002   0  0     4
11030705 1   0.050971900   0  0     5
11030706 1   0.058590170   0  0     6
11030707 1   0.064899632   0  0     7
11030708 1   0.069759344   0  0     8
11030709 1   0.073060747   0  0     9
11030710 1   0.074730094   0  0     10
11030711 1   0.074730094   0  0     11
11030712 1   0.073060747   0  0     12
11030713 1   0.069759344   0  0     13
11030714 1   0.064899632   0  0     14
11030715 1   0.058590170   0  0     15
11030716 1   0.050971900   0  0     16
11030717 1   0.042215002   0  0     17
11030718 1   0.032515091   0  0     18
11030719 1   0.022088847   0  0     19
11030720 1   0.011169174   0  0     20

******Additional Left Boundary******
*       Dh HLength HLRev GSL GSLRev GLossCoef GLCRev LBoilF HS#
11030801 0.0 15.0  15.0  0.0  0.0    0.0       0.0    1.0   20

******Additional Right Boundary******
11030900  1
*       Dh HLen HLRev GSL GSLRev GLossCoef GLCRev LBoilF NatCircL
PDiamR FoulF HS#
11030901 0.0 15.0 15.0 0.0 0.0 0.0 0.0 1.0 0.0 1.3262 1.0 20
```

```
*********************************************************************
**
*
*
*               Heat Structure Thermal Property Data
*
*
*
*********************************************************************
**
*                                        *
* composition type and data format       *
*                                        *
*****************************************
*
20100100       uo2     * core fuel
20100200       tbl/fctn       1       1     * air gap
20100300       tbl/fctn       1       1     * cladding
*
*********************************************************************
**
*
*
* thermal conductivity data (btu/sec-ft/deg f) and volumetric heat
*
* capacity  data (btu/ft**3-deg f) versus temperature for above
*
* composition
*
*
*
*********************************************************************
*
*
* Air gap
*
*        Temperature    Thermal Conductivity
*
20100201        32.0          2.4487788e-04
20100202      5400.0          2.4487788e-04
*
*        Temperature    Heat Capacity
*
20100251        32.0          0.000065
20100252      5400.0          0.000065
*
*
* Cladding
*
```

```
*         Temperature    Thermal Conductivity
*
20100301        32.0  2.9267e-03 392.0 2.9267e-03
20100302       752.0         1.2478e-03
20100303      1112.0         4.7297e-03
20100304      1472.0         5.0508e-03
20100305      1832.0         6.5325e-03
20100306      2192.0         4.0142e-03
20100307      2552.0         5.8169e-03
20100308      2912.0         8.7803e-03
20100309      3272.0         1.0647e-03
20100310      3632.0         1.8311e-03
20100311      3992.0         9.0918e-02
20100312      5000.0         9.0918e-02
*
*          Temperature     Heat Capacity
*
20100351         0.0         26.392
20100352      1480.3         35.476
20100353      1675.0         75.176
20100354      1787.5         44.370
20100355      3500.0         24.476
*
*
*
**********************************************************************
**
*
*  General Table 1
20200100       power
*            Time (sec)        Power(MW)
20200101        0.0              530.0
20200102        5.               530.0
20200103        305.             10.1554
20200104        1505.            7.0788
20200105        3605.            5.7774
20200106        7205.            4.8971
20200107        10805.           4.4359
20200108        14405.           4.1307
20200109        18005.           3.9058
20200110        21605.           3.7293
20200111        43205.           3.1142
20200112        64805.           2.7920
20200113        86405.           2.5788
20200114        108005.          2.4217
20200115        129605.          2.2984
20200116        172805.          2.1129
20200117        216005.          1.9762
20200118        259205.          1.8690
*
**********************************************
```

```
*                                              *
* End of input deck                            *
*                                              *
************************************************
.
```

APPENDIX D: PERL SCRIPT FOR TEMPERATURE EXTRACTION FROM RELAP5-3D OUTPUT FILES

```
#!/usr/bin/perl

use strict;

# read the relap output file
my $file_in = $ARGV[0];
print "input file is $file_in \n";
open my $in,  '<', $file_in  or die "Can't open input file !!!  ";
# read the file where we will APPEND the temperature values
my $file_out = $ARGV[1];
print "output file is $file_out \n";
open my $out, '>>', $file_out or die "Can't open output file !!! ";

my $temp1;
my $temp2;
my $temp3;
my $temp4;
my $temp5;
my $temp6;
my $temp7;
my $temp8;
my $temp9;
my $temp10;
my $time;


# parse $in file line-by-line
while (<$in>){
    my $line = $_; # put current line into a clearer variable name
    chomp $line; # remove invisible ending characters

    # look for a line with a specific text
    if( ($line =~ /0   At time=/) ){
        #print "$line \n";
        #$line =~ s/\.\s+//g; # remove the dots that a followed by one
or more whitespaces
        #$line =~ s/PIN PITCH//; # remove that text
        my @a = split(/\s+/,$line); # split the remaining items into
an array
        $time = $a[3]; # grab the second value in that array
           print $out "$time \n"
    }

          if( ($line =~ / 1030-001    /) ){
        #print "$line \n";
```

```
        #$line =~ s/\.\s+//g; # remove the dots that a followed by one
or more whitespaces
        #$line =~ s/PIN PITCH//; # remove that text
        my @a = split(/\s+/,$line); # split the remaining items into
an array
        $temp1 = $a[2]; # grab the second value in that array
           $temp2 = $a[3]; # grab the value in that array
           $temp3 = $a[4]; # grab the value in that array
           $temp4 = $a[5]; # grab the value in that array
           $temp5 = $a[6]; # grab the value in that array
           $temp6 = $a[7]; # grab the value in that array
           $temp7 = $a[8]; # grab the value in that array
           $temp8 = $a[9]; # grab the value in that array
           $temp9 = $a[10]; # grab the value in that array
           $temp10 = $a[11]; # grab the value in that array
           print $out "$temp1  ";
           print $out "$temp2  ";
           print $out "$temp3  ";
           print $out "$temp4  ";
           print $out "$temp5  ";
           print $out "$temp6  ";
           print $out "$temp7  ";
           print $out "$temp8  ";
           print $out "$temp9  ";
           print $out "$temp10 \n";
     }
         if( ($line =~ / 1030-002    /) ){
        #print "$line \n";
        #$line =~ s/\.\s+//g; # remove the dots that a followed by one
or more whitespaces
        #$line =~ s/PIN PITCH//; # remove that text
        my @a = split(/\s+/,$line); # split the remaining items into
an array
        $temp1 = $a[2]; # grab the second value in that array
           $temp2 = $a[3]; # grab the second value in that array
           $temp3 = $a[4]; # grab the second value in that array
           $temp4 = $a[5]; # grab the second value in that array
           $temp5 = $a[6]; # grab the second value in that array
           $temp6 = $a[7]; # grab the second value in that array
           $temp7 = $a[8]; # grab the second value in that array
           $temp8 = $a[9]; # grab the second value in that array
           $temp9 = $a[10]; # grab the second value in that array
           $temp10 = $a[11]; # grab the second value in that array
           print $out "$temp1  ";
           print $out "$temp2  ";
           print $out "$temp3  ";
           print $out "$temp4  ";
           print $out "$temp5  ";
           print $out "$temp6  ";
           print $out "$temp7  ";
           print $out "$temp8  ";
```

```
           print $out "$temp9  ";
           print $out "$temp10 \n";
      }
            if( ($line =~ / 1030-003    /) ){
        #print "$line \n";
        #$line =~ s/\.\s+//g; # remove the dots that a followed by one
or more whitespaces
        #$line =~ s/PIN PITCH//; # remove that text
        my @a = split(/\s+/,$line); # split the remaining items into
an array
        $temp1 = $a[2]; # grab the second value in that array
           $temp2 = $a[3]; # grab the value in that array
           $temp3 = $a[4]; # grab the value in that array
           $temp4 = $a[5]; # grab the value in that array
           $temp5 = $a[6]; # grab the value in that array
           $temp6 = $a[7]; # grab the value in that array
           $temp7 = $a[8]; # grab the value in that array
           $temp8 = $a[9]; # grab the value in that array
           $temp9 = $a[10]; # grab the value in that array
           $temp10 = $a[11]; # grab the value in that array
           print $out "$temp1  ";
           print $out "$temp2  ";
           print $out "$temp3  ";
           print $out "$temp4  ";
           print $out "$temp5  ";
           print $out "$temp6  ";
           print $out "$temp7  ";
           print $out "$temp8  ";
           print $out "$temp9  ";
           print $out "$temp10 \n";
    }
                  if( ($line =~ / 1030-004    /) ){
        #print "$line \n";
        #$line =~ s/\.\s+//g; # remove the dots that a followed by one
or more whitespaces
        #$line =~ s/PIN PITCH//; # remove that text
        my @a = split(/\s+/,$line); # split the remaining items into
an array
        $temp1 = $a[2]; # grab the second value in that array
           $temp2 = $a[3]; # grab the value in that array
           $temp3 = $a[4]; # grab the value in that array
           $temp4 = $a[5]; # grab the value in that array
           $temp5 = $a[6]; # grab the value in that array
           $temp6 = $a[7]; # grab the value in that array
           $temp7 = $a[8]; # grab the value in that array
           $temp8 = $a[9]; # grab the value in that array
           $temp9 = $a[10]; # grab the value in that array
           $temp10 = $a[11]; # grab the value in that array
           print $out "$temp1  ";
           print $out "$temp2  ";
           print $out "$temp3  ";
```

```
            print $out "$temp4  ";
            print $out "$temp5  ";
            print $out "$temp6  ";
            print $out "$temp7  ";
            print $out "$temp8  ";
            print $out "$temp9  ";
            print $out "$temp10 \n";
    }
                  if( ($line =~ / 1030-005    /) ){
        #print "$line \n";
        #$line =~ s/\.\s+//g; # remove the dots that a followed by one
or more whitespaces
        #$line =~ s/PIN PITCH//; # remove that text
        my @a = split(/\s+/,$line); # split the remaining items into
an array
        $temp1 = $a[2]; # grab the second value in that array
            $temp2 = $a[3]; # grab the value in that array
            $temp3 = $a[4]; # grab the value in that array
            $temp4 = $a[5]; # grab the value in that array
            $temp5 = $a[6]; # grab the value in that array
            $temp6 = $a[7]; # grab the value in that array
            $temp7 = $a[8]; # grab the value in that array
            $temp8 = $a[9]; # grab the value in that array
            $temp9 = $a[10]; # grab the value in that array
            $temp10 = $a[11]; # grab the value in that array
            print $out "$temp1  ";
            print $out "$temp2  ";
            print $out "$temp3  ";
            print $out "$temp4  ";
            print $out "$temp5  ";
            print $out "$temp6  ";
            print $out "$temp7  ";
            print $out "$temp8  ";
            print $out "$temp9  ";
            print $out "$temp10 \n";
    }
                  if( ($line =~ / 1030-006    /) ){
        #print "$line \n";
        #$line =~ s/\.\s+//g; # remove the dots that a followed by one
or more whitespaces
        #$line =~ s/PIN PITCH//; # remove that text
        my @a = split(/\s+/,$line); # split the remaining items into
an array
        $temp1 = $a[2]; # grab the second value in that array
            $temp2 = $a[3]; # grab the value in that array
            $temp3 = $a[4]; # grab the value in that array
            $temp4 = $a[5]; # grab the value in that array
            $temp5 = $a[6]; # grab the value in that array
            $temp6 = $a[7]; # grab the value in that array
            $temp7 = $a[8]; # grab the value in that array
            $temp8 = $a[9]; # grab the value in that array
```

```
          $temp9 = $a[10]; # grab the value in that array
          $temp10 = $a[11]; # grab the value in that array
          print $out "$temp1  ";
          print $out "$temp2  ";
          print $out "$temp3  ";
          print $out "$temp4  ";
          print $out "$temp5  ";
          print $out "$temp6  ";
          print $out "$temp7  ";
          print $out "$temp8  ";
          print $out "$temp9  ";
          print $out "$temp10 \n";
    }
                if( ($line =~ / 1030-007    /) ){
        #print "$line \n";
        #$line =~ s/\.\s+//g; # remove the dots that a followed by one
or more whitespaces
        #$line =~ s/PIN PITCH//; # remove that text
        my @a = split(/\s+/,$line); # split the remaining items into
an array
        $temp1 = $a[2]; # grab the second value in that array
          $temp2 = $a[3]; # grab the value in that array
          $temp3 = $a[4]; # grab the value in that array
          $temp4 = $a[5]; # grab the value in that array
          $temp5 = $a[6]; # grab the value in that array
          $temp6 = $a[7]; # grab the value in that array
          $temp7 = $a[8]; # grab the value in that array
          $temp8 = $a[9]; # grab the value in that array
          $temp9 = $a[10]; # grab the value in that array
          $temp10 = $a[11]; # grab the value in that array
          print $out "$temp1  ";
          print $out "$temp2  ";
          print $out "$temp3  ";
          print $out "$temp4  ";
          print $out "$temp5  ";
          print $out "$temp6  ";
          print $out "$temp7  ";
          print $out "$temp8  ";
          print $out "$temp9  ";
          print $out "$temp10 \n";
    }
                if( ($line =~ / 1030-008    /) ){
        #print "$line \n";
        #$line =~ s/\.\s+//g; # remove the dots that a followed by one
or more whitespaces
        #$line =~ s/PIN PITCH//; # remove that text
        my @a = split(/\s+/,$line); # split the remaining items into
an array
        $temp1 = $a[2]; # grab the second value in that array
          $temp2 = $a[3]; # grab the value in that array
          $temp3 = $a[4]; # grab the value in that array
```

```
            $temp4 = $a[5]; # grab the value in that array
            $temp5 = $a[6]; # grab the value in that array
            $temp6 = $a[7]; # grab the value in that array
            $temp7 = $a[8]; # grab the value in that array
            $temp8 = $a[9]; # grab the value in that array
            $temp9 = $a[10]; # grab the value in that array
            $temp10 = $a[11]; # grab the value in that array
            print $out "$temp1  ";
            print $out "$temp2  ";
            print $out "$temp3  ";
            print $out "$temp4  ";
            print $out "$temp5  ";
            print $out "$temp6  ";
            print $out "$temp7  ";
            print $out "$temp8  ";
            print $out "$temp9  ";
            print $out "$temp10 \n";
    }
                  if( ($line =~ / 1030-009    /) ){
        #print "$line \n";
        #$line =~ s/\.\s+//g; # remove the dots that a followed by one
or more whitespaces
        #$line =~ s/PIN PITCH//; # remove that text
        my @a = split(/\s+/,$line); # split the remaining items into
an array
        $temp1 = $a[2]; # grab the second value in that array
            $temp2 = $a[3]; # grab the value in that array
            $temp3 = $a[4]; # grab the value in that array
            $temp4 = $a[5]; # grab the value in that array
            $temp5 = $a[6]; # grab the value in that array
            $temp6 = $a[7]; # grab the value in that array
            $temp7 = $a[8]; # grab the value in that array
            $temp8 = $a[9]; # grab the value in that array
            $temp9 = $a[10]; # grab the value in that array
            $temp10 = $a[11]; # grab the value in that array
            print $out "$temp1  ";
            print $out "$temp2  ";
            print $out "$temp3  ";
            print $out "$temp4  ";
            print $out "$temp5  ";
            print $out "$temp6  ";
            print $out "$temp7  ";
            print $out "$temp8  ";
            print $out "$temp9  ";
            print $out "$temp10 \n";
    }
                  if( ($line =~ / 1030-010    /) ){
        #print "$line \n";
        #$line =~ s/\.\s+//g; # remove the dots that a followed by one
or more whitespaces
        #$line =~ s/PIN PITCH//; # remove that text
```

```
        my @a = split(/\s+/,$line); # split the remaining items into
an array
        $temp1 = $a[2]; # grab the second value in that array
           $temp2 = $a[3]; # grab the value in that array
           $temp3 = $a[4]; # grab the value in that array
           $temp4 = $a[5]; # grab the value in that array
           $temp5 = $a[6]; # grab the value in that array
           $temp6 = $a[7]; # grab the value in that array
           $temp7 = $a[8]; # grab the value in that array
           $temp8 = $a[9]; # grab the value in that array
           $temp9 = $a[10]; # grab the value in that array
           $temp10 = $a[11]; # grab the value in that array
           print $out "$temp1  ";
           print $out "$temp2  ";
           print $out "$temp3  ";
           print $out "$temp4  ";
           print $out "$temp5  ";
           print $out "$temp6  ";
           print $out "$temp7  ";
           print $out "$temp8  ";
           print $out "$temp9  ";
           print $out "$temp10 \n";
    }
                if( ($line =~ / 1030-011    /) ){
        #print "$line \n";
        #$line =~ s/\.\s+//g; # remove the dots that a followed by one
or more whitespaces
        #$line =~ s/PIN PITCH//; # remove that text
        my @a = split(/\s+/,$line); # split the remaining items into
an array
        $temp1 = $a[2]; # grab the second value in that array
           $temp2 = $a[3]; # grab the value in that array
           $temp3 = $a[4]; # grab the value in that array
           $temp4 = $a[5]; # grab the value in that array
           $temp5 = $a[6]; # grab the value in that array
           $temp6 = $a[7]; # grab the value in that array
           $temp7 = $a[8]; # grab the value in that array
           $temp8 = $a[9]; # grab the value in that array
           $temp9 = $a[10]; # grab the value in that array
           $temp10 = $a[11]; # grab the value in that array
           print $out "$temp1  ";
           print $out "$temp2  ";
           print $out "$temp3  ";
           print $out "$temp4  ";
           print $out "$temp5  ";
           print $out "$temp6  ";
           print $out "$temp7  ";
           print $out "$temp8  ";
           print $out "$temp9  ";
           print $out "$temp10 \n";
    }
```

```
                if( ($line =~ / 1030-012    /) ){
        #print "$line \n";
        #$line =~ s/\.\s+//g; # remove the dots that a followed by one
or more whitespaces
        #$line =~ s/PIN PITCH//; # remove that text
        my @a = split(/\s+/,$line); # split the remaining items into
an array
        $temp1 = $a[2]; # grab the second value in that array
           $temp2 = $a[3]; # grab the value in that array
           $temp3 = $a[4]; # grab the value in that array
           $temp4 = $a[5]; # grab the value in that array
           $temp5 = $a[6]; # grab the value in that array
           $temp6 = $a[7]; # grab the value in that array
           $temp7 = $a[8]; # grab the value in that array
           $temp8 = $a[9]; # grab the value in that array
           $temp9 = $a[10]; # grab the value in that array
           $temp10 = $a[11]; # grab the value in that array
           print $out "$temp1  ";
           print $out "$temp2  ";
           print $out "$temp3  ";
           print $out "$temp4  ";
           print $out "$temp5  ";
           print $out "$temp6  ";
           print $out "$temp7  ";
           print $out "$temp8  ";
           print $out "$temp9  ";
           print $out "$temp10 \n";
    }
                if( ($line =~ / 1030-013    /) ){
        #print "$line \n";
        #$line =~ s/\.\s+//g; # remove the dots that a followed by one
or more whitespaces
        #$line =~ s/PIN PITCH//; # remove that text
        my @a = split(/\s+/,$line); # split the remaining items into
an array
        $temp1 = $a[2]; # grab the second value in that array
           $temp2 = $a[3]; # grab the value in that array
           $temp3 = $a[4]; # grab the value in that array
           $temp4 = $a[5]; # grab the value in that array
           $temp5 = $a[6]; # grab the value in that array
           $temp6 = $a[7]; # grab the value in that array
           $temp7 = $a[8]; # grab the value in that array
           $temp8 = $a[9]; # grab the value in that array
           $temp9 = $a[10]; # grab the value in that array
           $temp10 = $a[11]; # grab the value in that array
           print $out "$temp1  ";
           print $out "$temp2  ";
           print $out "$temp3  ";
           print $out "$temp4  ";
           print $out "$temp5  ";
           print $out "$temp6  ";
```

```
            print $out "$temp7  ";
            print $out "$temp8  ";
            print $out "$temp9  ";
            print $out "$temp10 \n";
    }
                  if( ($line =~ / 1030-014    /) ){
        #print "$line \n";
        #$line =~ s/\.\s+//g; # remove the dots that a followed by one
or more whitespaces
        #$line =~ s/PIN PITCH//; # remove that text
        my @a = split(/\s+/,$line); # split the remaining items into
an array
        $temp1 = $a[2]; # grab the second value in that array
            $temp2 = $a[3]; # grab the value in that array
            $temp3 = $a[4]; # grab the value in that array
            $temp4 = $a[5]; # grab the value in that array
            $temp5 = $a[6]; # grab the value in that array
            $temp6 = $a[7]; # grab the value in that array
            $temp7 = $a[8]; # grab the value in that array
            $temp8 = $a[9]; # grab the value in that array
            $temp9 = $a[10]; # grab the value in that array
            $temp10 = $a[11]; # grab the value in that array
            print $out "$temp1  ";
            print $out "$temp2  ";
            print $out "$temp3  ";
            print $out "$temp4  ";
            print $out "$temp5  ";
            print $out "$temp6  ";
            print $out "$temp7  ";
            print $out "$temp8  ";
            print $out "$temp9  ";
            print $out "$temp10 \n";
    }
                  if( ($line =~ / 1030-015    /) ){
        #print "$line \n";
        #$line =~ s/\.\s+//g; # remove the dots that a followed by one
or more whitespaces
        #$line =~ s/PIN PITCH//; # remove that text
        my @a = split(/\s+/,$line); # split the remaining items into
an array
        $temp1 = $a[2]; # grab the second value in that array
            $temp2 = $a[3]; # grab the value in that array
            $temp3 = $a[4]; # grab the value in that array
            $temp4 = $a[5]; # grab the value in that array
            $temp5 = $a[6]; # grab the value in that array
            $temp6 = $a[7]; # grab the value in that array
            $temp7 = $a[8]; # grab the value in that array
            $temp8 = $a[9]; # grab the value in that array
            $temp9 = $a[10]; # grab the value in that array
            $temp10 = $a[11]; # grab the value in that array
            print $out "$temp1  ";
```

```
          print $out "$temp2  ";
          print $out "$temp3  ";
          print $out "$temp4  ";
          print $out "$temp5  ";
          print $out "$temp6  ";
          print $out "$temp7  ";
          print $out "$temp8  ";
          print $out "$temp9  ";
          print $out "$temp10 \n";
    }
                if( ($line =~ / 1030-016    /) ){
        #print "$line \n";
        #$line =~ s/\.\s+//g; # remove the dots that a followed by one
or more whitespaces
        #$line =~ s/PIN PITCH//; # remove that text
        my @a = split(/\s+/,$line); # split the remaining items into
an array
        $temp1 = $a[2]; # grab the second value in that array
          $temp2 = $a[3]; # grab the value in that array
          $temp3 = $a[4]; # grab the value in that array
          $temp4 = $a[5]; # grab the value in that array
          $temp5 = $a[6]; # grab the value in that array
          $temp6 = $a[7]; # grab the value in that array
          $temp7 = $a[8]; # grab the value in that array
          $temp8 = $a[9]; # grab the value in that array
          $temp9 = $a[10]; # grab the value in that array
          $temp10 = $a[11]; # grab the value in that array
          print $out "$temp1  ";
          print $out "$temp2  ";
          print $out "$temp3  ";
          print $out "$temp4  ";
          print $out "$temp5  ";
          print $out "$temp6  ";
          print $out "$temp7  ";
          print $out "$temp8  ";
          print $out "$temp9  ";
          print $out "$temp10 \n";
    }
                if( ($line =~ / 1030-017    /) ){
        #print "$line \n";
        #$line =~ s/\.\s+//g; # remove the dots that a followed by one
or more whitespaces
        #$line =~ s/PIN PITCH//; # remove that text
        my @a = split(/\s+/,$line); # split the remaining items into
an array
        $temp1 = $a[2]; # grab the second value in that array
          $temp2 = $a[3]; # grab the value in that array
          $temp3 = $a[4]; # grab the value in that array
          $temp4 = $a[5]; # grab the value in that array
          $temp5 = $a[6]; # grab the value in that array
          $temp6 = $a[7]; # grab the value in that array
```

```
            $temp7 = $a[8]; # grab the value in that array
            $temp8 = $a[9]; # grab the value in that array
            $temp9 = $a[10]; # grab the value in that array
            $temp10 = $a[11]; # grab the value in that array
            print $out "$temp1  ";
            print $out "$temp2  ";
            print $out "$temp3  ";
            print $out "$temp4  ";
            print $out "$temp5  ";
            print $out "$temp6  ";
            print $out "$temp7  ";
            print $out "$temp8  ";
            print $out "$temp9  ";
            print $out "$temp10 \n";
    }
                  if( ($line =~ / 1030-018    /) ){
        #print "$line \n";
        #$line =~ s/\.\s+//g; # remove the dots that a followed by one
or more whitespaces
        #$line =~ s/PIN PITCH//; # remove that text
        my @a = split(/\s+/,$line); # split the remaining items into
an array
        $temp1 = $a[2]; # grab the second value in that array
            $temp2 = $a[3]; # grab the value in that array
            $temp3 = $a[4]; # grab the value in that array
            $temp4 = $a[5]; # grab the value in that array
            $temp5 = $a[6]; # grab the value in that array
            $temp6 = $a[7]; # grab the value in that array
            $temp7 = $a[8]; # grab the value in that array
            $temp8 = $a[9]; # grab the value in that array
            $temp9 = $a[10]; # grab the value in that array
            $temp10 = $a[11]; # grab the value in that array
            print $out "$temp1  ";
            print $out "$temp2  ";
            print $out "$temp3  ";
            print $out "$temp4  ";
            print $out "$temp5  ";
            print $out "$temp6  ";
            print $out "$temp7  ";
            print $out "$temp8  ";
            print $out "$temp9  ";
            print $out "$temp10 \n";
    }
                  if( ($line =~ / 1030-019    /) ){
        #print "$line \n";
        #$line =~ s/\.\s+//g; # remove the dots that a followed by one
or more whitespaces
        #$line =~ s/PIN PITCH//; # remove that text
        my @a = split(/\s+/,$line); # split the remaining items into
an array
        $temp1 = $a[2]; # grab the second value in that array
```

```
          $temp2 = $a[3]; # grab the value in that array
          $temp3 = $a[4]; # grab the value in that array
          $temp4 = $a[5]; # grab the value in that array
          $temp5 = $a[6]; # grab the value in that array
          $temp6 = $a[7]; # grab the value in that array
          $temp7 = $a[8]; # grab the value in that array
          $temp8 = $a[9]; # grab the value in that array
          $temp9 = $a[10]; # grab the value in that array
          $temp10 = $a[11]; # grab the value in that array
          print $out "$temp1  ";
          print $out "$temp2  ";
          print $out "$temp3  ";
          print $out "$temp4  ";
          print $out "$temp5  ";
          print $out "$temp6  ";
          print $out "$temp7  ";
          print $out "$temp8  ";
          print $out "$temp9  ";
          print $out "$temp10 \n";
    }
                if( ($line =~ / 1030-020    /) ){
        #print "$line \n";
        #$line =~ s/\.\s+//g; # remove the dots that a followed by one
or more whitespaces
        #$line =~ s/PIN PITCH//; # remove that text
        my @a = split(/\s+/,$line); # split the remaining items into
an array
        $temp1 = $a[2]; # grab the second value in that array
          $temp2 = $a[3]; # grab the value in that array
          $temp3 = $a[4]; # grab the value in that array
          $temp4 = $a[5]; # grab the value in that array
          $temp5 = $a[6]; # grab the value in that array
          $temp6 = $a[7]; # grab the value in that array
          $temp7 = $a[8]; # grab the value in that array
          $temp8 = $a[9]; # grab the value in that array
          $temp9 = $a[10]; # grab the value in that array
          $temp10 = $a[11]; # grab the value in that array
          print $out "$temp1  ";
          print $out "$temp2  ";
          print $out "$temp3  ";
          print $out "$temp4  ";
          print $out "$temp5  ";
          print $out "$temp6  ";
          print $out "$temp7  ";
          print $out "$temp8  ";
          print $out "$temp9  ";
          print $out "$temp10 \n\n\n";
    }y
}

exit 66;
```

APPENDIX E: CASMO4 INPUT DECK EXAMPLE FOR SIMPLE INFINITE ARRAY

```
TTL * mPower deck en-4

TFU=760.5 TMO=582.3 BOR=0.0                    *fuel temp, mod temp, boron concentration (ppm)
PRE 142                                                *pressure in bars
PDE 30                                                 *pwr density [W/gU]
DEP 1*20,20*0.5 / 'DE'

****definitions****
**TPBAR components**
MI1 0.0252675972307692/5010=100.0              *LiAlO2 equivalent in TPBAR
*MI4 is the homogenized cladding*
*homogenized per TTQP-1-116*

THE 0              *thermal expansion off

MI4 /24000=8.2E21 26000=2.83E22 28000=2.71E22
42000=6.35E20 25000=6.65E20 40000=9.74E21
************************

****FUEL****
PWR 17 1.260 21.5                        *17*17 FA, 1.26cm pin pitch
************************
* pin 1=fuel
* pin 2=guide tube
* pin 3=burnable poison (TPBAR)
* pin 4=Gd2O3 fuel pin
* pin 5=empty instrument tube
************************

FUE 1 10.374/4.0                         *fuel 1, density/enrich.
FUE 4 10.1/4.0 64016=6.0                 *fuel with 6% Gd2O3

PIN 1 0.409575 0.41524 0.47244           *pin radii [cm]
PIN 2 0.5615 0.612 / 'MOD'  'BOX'
PIN 3 0.28321 0.38354 0.48387
/ 'AIR' 'MI1' 'MI4'
PIN 4 0.409575 0.41524 0.47244
PIN 5 0.5615 0.612 / 'MOD'  'BOX'

LPI                                                    *pin layout
5                                                      *center pin
1 3
1 1 1
2 1 1 2
3 1 1 1 3
```

1 1 1 1 1 2
2 1 1 2 1 1 1
3 1 1 1 1 1 1 4
1 1 1 1 1 1 1 1 1

LFU *Layout of FUE
0
1 0
1 1 1
0 1 1 0
0 1 1 1 0
1 1 1 1 1 0
0 1 1 0 1 1 1
0 1 1 1 1 1 1 4
1 1 1 1 1 1 1 1 1

STA
END

APPENDIX F: CASMO4 INPUT DECK EXAMPLE FOR M X N REACTOR

```
MEM 400 400 400
TTL * mPower deck en-3.5

MXN 1 1
LSE 1 2 1 2 1
   2 1 2 1 1
   1 2 1 2 1
   2 1 2 1 0
   1 1 1 0 0 /5 5


BAS
TFU=760.5 TMO=582.3 BOR=0.0                    *fuel temp, mod temp, boron concentration (ppm)
PRE 142                                                *pressure in bars
PDE 30                                                 *pwr density [W/gU]
DEP -21

****definitions****
**TPBAR components**
MI1 0.025238182/5010=96.0 2003=4.0             *LiAlO2 equivalent in TPBAR
*MI4 is the homogenized cladding*
*homogenized per TTQP-1-116*
THE 0              *thermal expansion off
MI4 /24000=8.2E21 26000=2.83E22 28000=2.71E22
42000=6.35E20 25000=6.65E20 40000=9.74E21

**SS316**
MI3 8/6000=.03 24000=18 28000=12 42000=3 25000=2
14000=1 15000=.04 16000=.02 26000=63.91
***********************

****FUEL****
SEG 1  *
PWR 17 1.260 21.5,,,,,1                        *17*17 FA, 1.26cm pin pitch
***********************
* pin 1=fuel
* pin 2=guide tube
* pin 3=burnable poison (TPBAR)
* pin 4=Gd2O3 fuel pin
***********************

FUE 1 10.374/3.5                               *fuel 1, density/enrich.
FUE 4 10.1/3.5 64016=6.0                       *4.0% enr fuel with 6% Gd2O3
```

```
PIN 1 0.409575 0.41524 0.47244          *pin radii [cm]
PIN 2 0.5615 0.612 / 'MOD'  'BOX'
PIN 3 0.28321 0.38354 0.48387
/ 'AIR' 'MI1' 'MI4'
PIN 4 0.409575 0.41524 0.47244


LPI                                                          *pin layout
1 1 1 1 1 1 1 1 1 1 1 1 1 1 1 1 1
1 4 1 1 1 1 1 1 3 1 1 1 1 1 1 4 1
1 1 1 1 1 2 3 1 2 1 3 2 1 1 1 1 1
1 1 1 2 1 1 1 1 1 1 1 1 2 1 1 1
1 1 1 1 3 1 1 1 3 1 1 1 3 1 1 1 1
1 1 2 1 1 2 1 1 2 1 1 2 1 1 2 1 1
1 1 3 1 1 1 1 1 1 1 1 1 1 1 3 1 1
1 1 1 1 1 1 1 3 1 3 1 1 1 1 1 1 1
1 3 2 1 3 2 1 1 2 1 1 2 3 1 2 3 1  *center
1 1 1 1 1 1 1 3 1 3 1 1 1 1 1 1 1
1 1 3 1 1 1 1 1 1 1 1 1 1 1 3 1 1
1 1 2 1 1 2 1 1 2 1 1 2 1 1 2 1 1
1 1 1 1 3 1 1 1 3 1 1 1 3 1 1 1 1
1 1 1 2 1 1 1 1 1 1 1 1 2 1 1 1
1 1 1 1 1 2 3 1 2 1 3 2 1 1 1 1 1
1 4 1 1 1 1 1 1 3 1 1 1 1 1 1 4 1
1 1 1 1 1 1 1 1 1 1 1 1 1 1 1 1 1


LFU                                                          *Layout of FUE
1 1 1 1 1 1 1 1 1 1 1 1 1 1 1 1 1
1 4 1 1 1 1 1 1 0 1 1 1 1 1 1 4 1
1 1 1 1 1 0 0 1 0 1 0 0 1 1 1 1 1
1 1 1 0 1 1 1 1 1 1 1 1 0 1 1 1
1 1 1 1 0 1 1 1 0 1 1 1 0 1 1 1 1
1 1 0 1 1 0 1 1 0 1 1 0 1 1 0 1 1
1 1 0 1 1 1 1 1 1 1 1 1 1 0 1 1
1 1 1 1 1 1 1 0 1 0 1 1 1 1 1 1 1
1 0 0 1 0 0 1 1 0 1 1 0 0 1 0 0 1  *center
1 1 1 1 1 1 1 0 1 0 1 1 1 1 1 1 1
1 1 0 1 1 1 1 1 1 1 1 1 1 0 1 1
1 1 0 1 1 0 1 1 0 1 1 0 1 1 0 1 1
1 1 1 1 0 1 1 1 0 1 1 1 0 1 1 1 1
1 1 1 0 1 1 1 1 1 1 1 1 0 1 1 1
1 1 1 1 1 0 0 1 0 1 0 0 1 1 1 1 1
1 4 1 1 1 1 1 1 0 1 1 1 1 1 1 4 1
1 1 1 1 1 1 1 1 1 1 1 1 1 1 1 1 1

SEG 2  *
```

```
PWR 17 1.260 21.5,,,,,1                    *17*17 FA, 1.26cm pin pitch
***********************
* pin 1=fuel
* pin 2=guide tube
* pin 3=burnable poison (TPBAR)
* pin 4=Gd2O3 fuel pin
***********************

FUE 1 10.374/4.0                           *fuel 1, density/enrich.
FUE 4 10.1/4.0 64016=6.0                   *4.0% enr fuel with 6% Gd2O3


PIN 1 0.409575 0.41524 0.47244        *pin radii [cm]
PIN 2 0.5615 0.612 / 'MOD'  'BOX'
PIN 3 0.28321 0.38354 0.48387
/ 'AIR' 'MI1' 'MI4'
PIN 4 0.409575 0.41524 0.47244


LPI                                                        *pin layout
1 1 1 1 1 1 1 1 1 1 1 1 1 1 1 1 1
1 4 1 1 1 1 1 1 3 1 1 1 1 1 1 4 1
1 1 1 1 1 2 3 1 2 1 3 2 1 1 1 1 1
1 1 1 2 1 1 1 1 1 1 1 1 1 2 1 1 1
1 1 1 1 3 1 1 1 3 1 1 1 3 1 1 1 1
1 1 2 1 1 2 1 1 2 1 1 2 1 1 2 1 1
1 1 3 1 1 1 1 1 1 1 1 1 1 1 3 1 1
1 1 1 1 1 1 1 3 1 3 1 1 1 1 1 1 1
1 3 2 1 3 2 1 1 2 1 1 2 3 1 2 3 1  *center
1 1 1 1 1 1 1 3 1 3 1 1 1 1 1 1 1
1 1 3 1 1 1 1 1 1 1 1 1 1 1 3 1 1
1 1 2 1 1 2 1 1 2 1 1 2 1 1 2 1 1
1 1 1 1 3 1 1 1 3 1 1 1 3 1 1 1 1
1 1 1 2 1 1 1 1 1 1 1 1 1 2 1 1 1
1 1 1 1 1 2 3 1 2 1 3 2 1 1 1 1 1
1 4 1 1 1 1 1 1 3 1 1 1 1 1 1 4 1
1 1 1 1 1 1 1 1 1 1 1 1 1 1 1 1 1


LFU                                                   *Layout of FUE
1 1 1 1 1 1 1 1 1 1 1 1 1 1 1 1 1
1 4 1 1 1 1 1 1 0 1 1 1 1 1 1 4 1
1 1 1 1 1 0 0 1 0 1 0 0 1 1 1 1 1
1 1 1 0 1 1 1 1 1 1 1 1 1 0 1 1 1
1 1 1 1 0 1 1 1 0 1 1 1 0 1 1 1 1
1 1 0 1 1 0 1 1 0 1 1 0 1 1 0 1 1
1 1 0 1 1 1 1 1 1 1 1 1 1 1 0 1 1
```

```
1 1 1 1 1 1 1 0 1 0 1 1 1 1 1 1 1
1 0 0 1 0 0 1 1 0 1 1 0 0 1 0 0 1  *center
1 1 1 1 1 1 1 0 1 0 1 1 1 1 1 1 1
1 1 0 1 1 1 1 1 1 1 1 1 1 1 0 1 1
1 1 0 1 1 0 1 1 0 1 1 0 1 1 0 1 1
1 1 1 1 0 1 1 1 0 1 1 1 0 1 1 1 1
1 1 1 0 1 1 1 1 1 1 1 1 1 0 1 1 1
1 1 1 1 1 0 0 1 0 1 0 0 1 1 1 1 1
1 4 1 1 1 1 1 1 0 1 1 1 1 1 1 4 1
1 1 1 1 1 1 1 1 1 1 1 1 1 1 1 1 1


STA
END
```

APPENDIX G: PLOTS OF K-INFINITY VERSUS BURNUP FOR VARIOUS FUEL ENRICHMENTS AND ROD ARRANGEMENTS

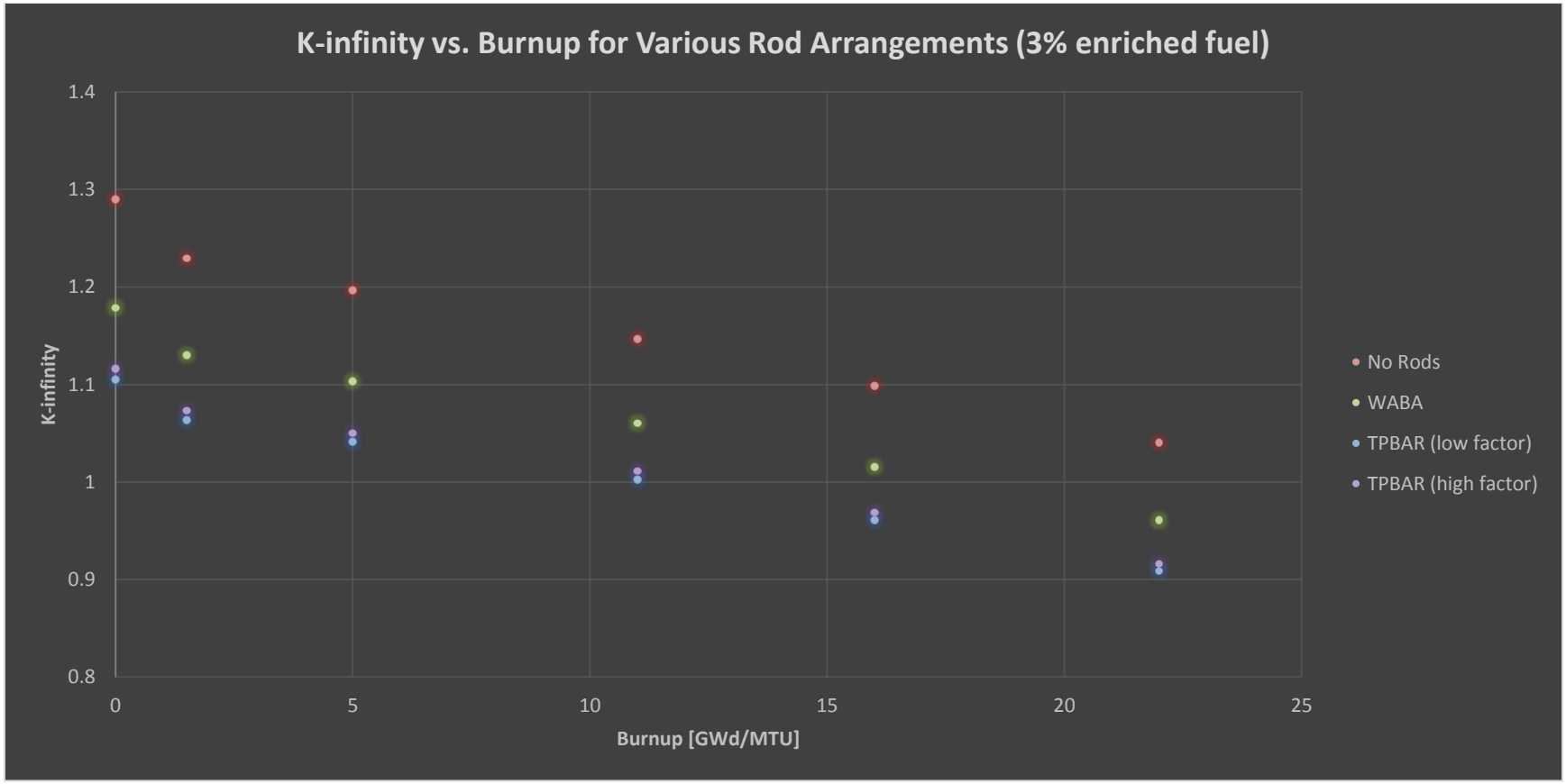

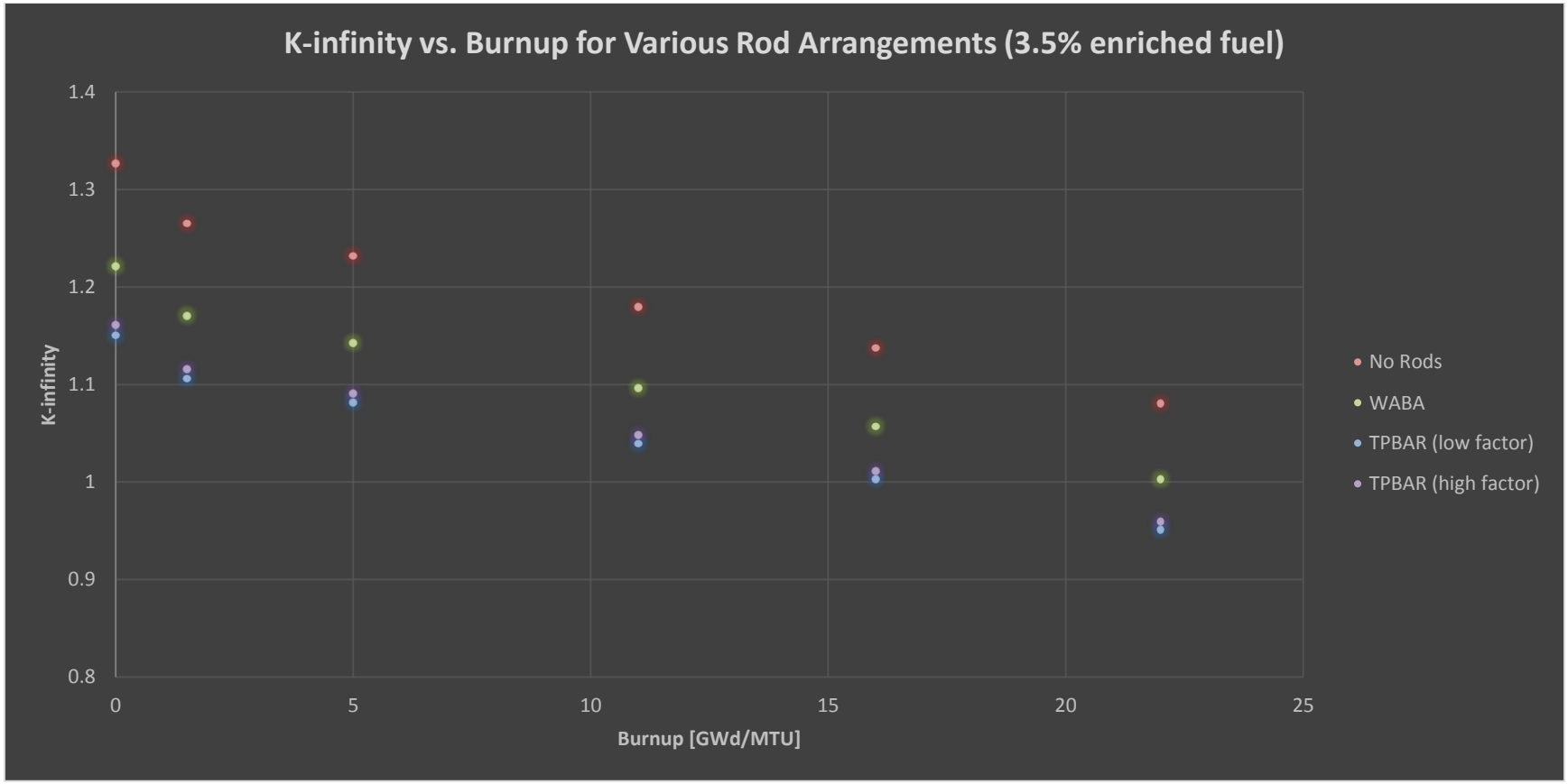
K-infinity vs. Burnup for Various Rod Arrangements (3.5% enriched fuel)
K-infinity
1.4
1.3
1.2
1.1
1
0.9
0.8
0
5
10
15
20
25
Burnup [GWd/MTU]
No Rods
WABA
TPBAR (low factor)
TPBAR (high factor)

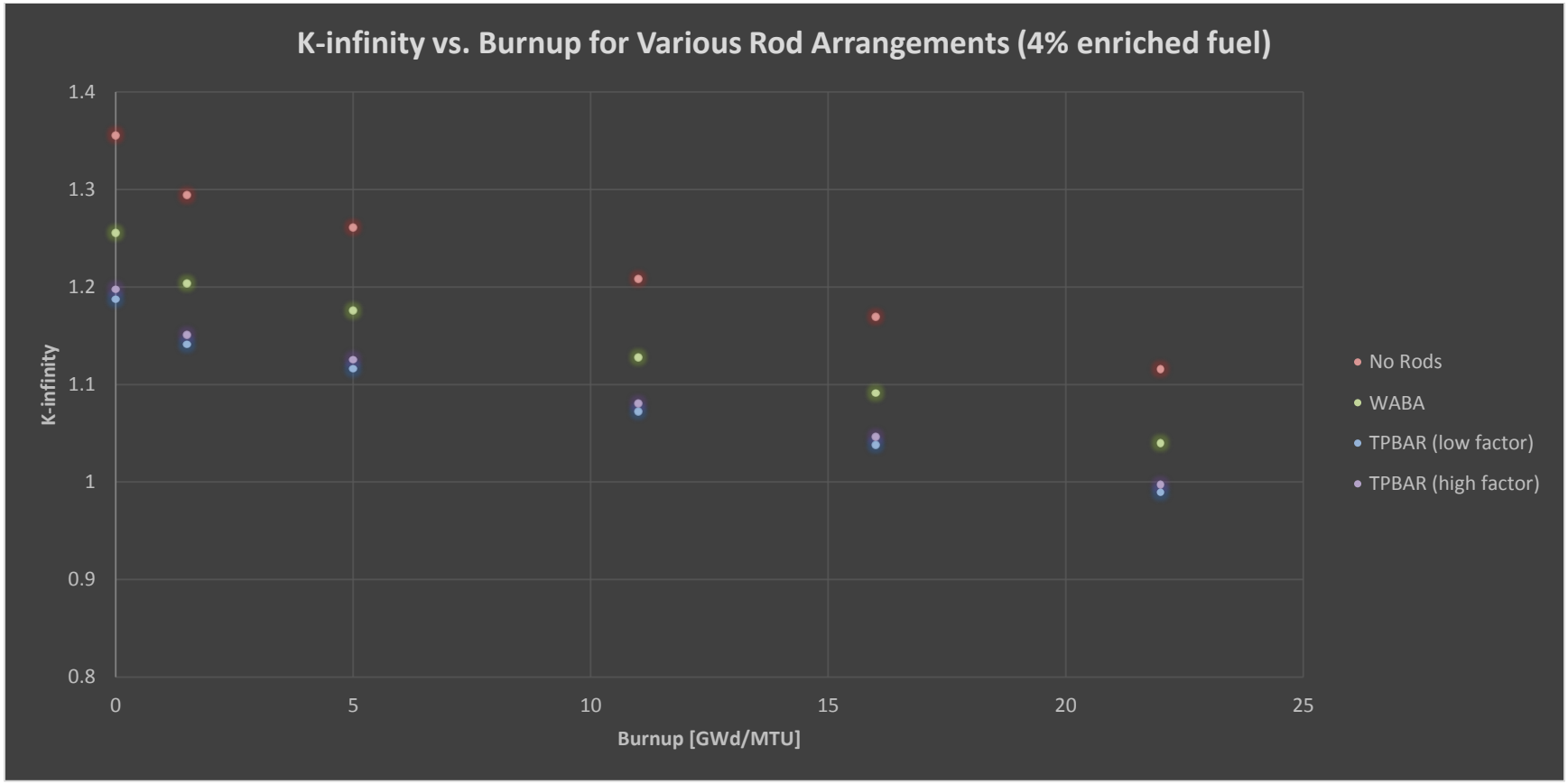
K-infinity vs. Burnup for Various Rod Arrangements (4% enriched fuel)
K-infinity
1.4
1.3
1.2
1.1
1
0.9
0.8
0
5
10
15
20
25
Burnup [GWd/MTU]
No Rods
WABA
TPBAR (low factor)
TPBAR (high factor)

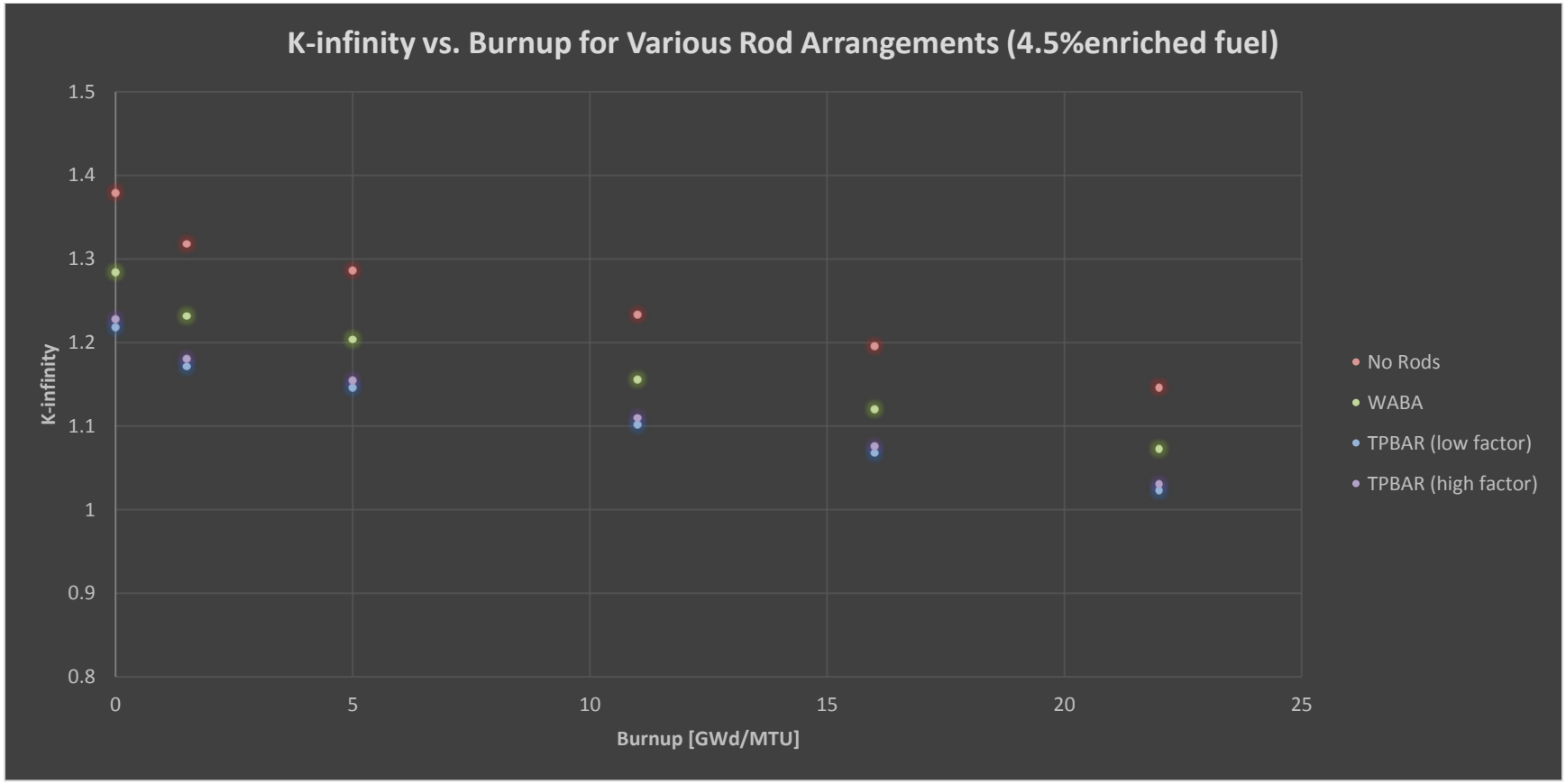
K-infinity vs. Burnup for Various Rod Arrangements (4.5%enriched fuel)
K-infinity
1.5
1.4
1.3
1.2
1.1
1
0.9
0.8
0
5
10
15
20
25
Burnup [GWd/MTU]
No Rods
WABA
TPBAR (low factor)
TPBAR (high factor)

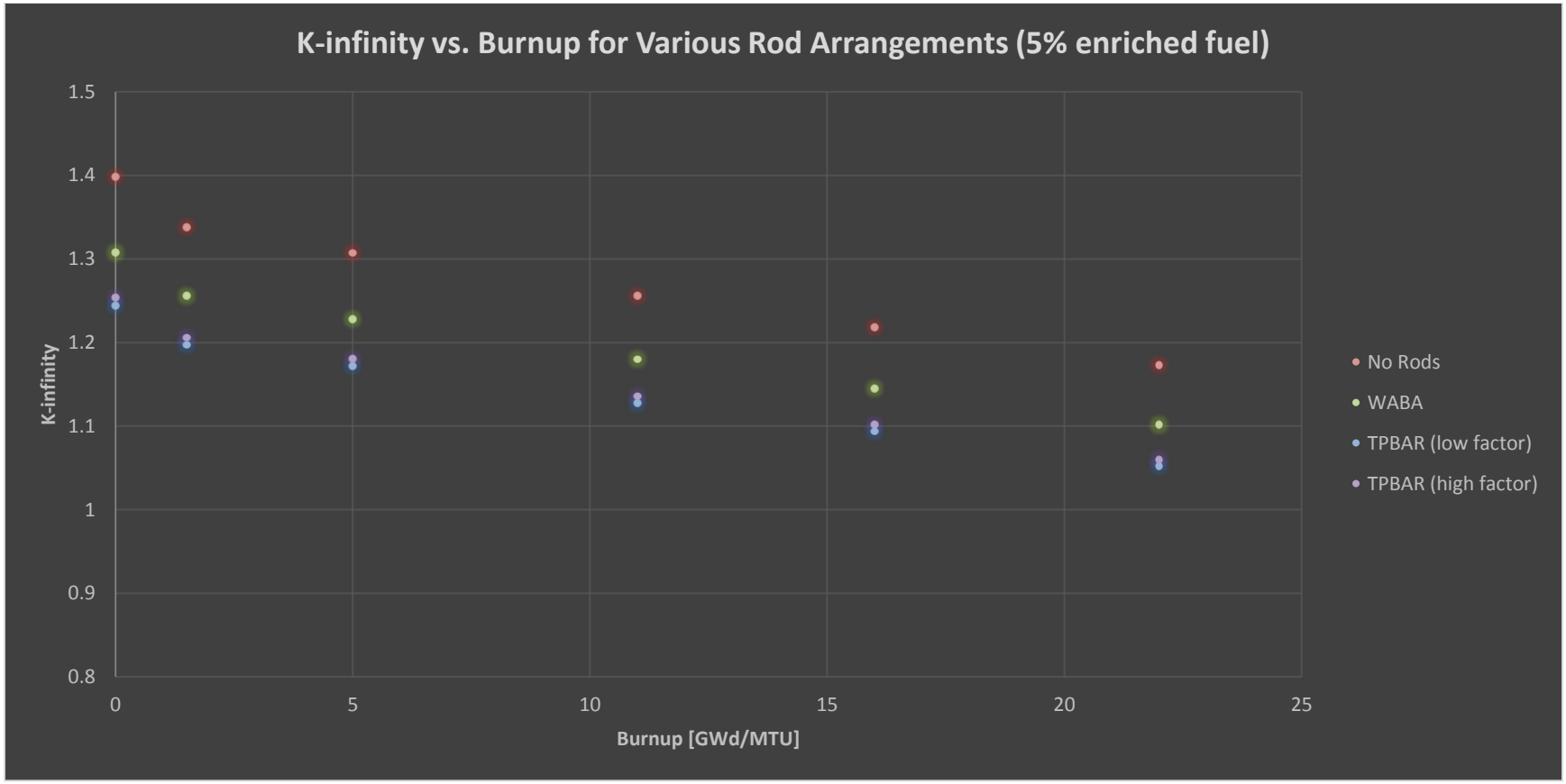
K-infinity vs. Burnup for Various Rod Arrangements (5% enriched fuel)
K-infinity
1.5
1.4
1.3
1.2
1.1
1
0.9
0.8
0
5
10
15
20
25
Burnup [GWd/MTU]
No Rods
WABA
TPBAR (low factor)
TPBAR (high factor)

APPENDIX H: DATA FOR VERIFICATION OF SIMULATING LITHIUM-6 USING BORON-10

Fuel Enrichment	3.0%			3.5%			4.0%			4.5%			5.0%		
	k-infinity		% Difference	k-infinity		% Difference	k-infinity		% Difference	k-infinity		% Difference	k-infinity		% Difference
Burnup [GWd/MTU]	Boron Equivalent	Natural		Boron Equivalent	Natural		Boron Equivalent	Natural		Boron Equivalent	Natural		Boron Equivalent	Natural	
0	1.17494	1.1463	2.50%	1.21784	1.19034	2.31%	1.25239	1.226	2.15%	1.28088	1.25552	2.02%	1.30472	1.28032	1.91%
0.1	1.14044	1.1122	2.54%	1.18263	1.15563	2.34%	1.21703	1.19117	2.17%	1.24575	1.22094	2.03%	1.27009	1.24625	1.91%
0.5	1.13813	1.10594	2.91%	1.17898	1.14865	2.64%	1.21256	1.18385	2.43%	1.24078	1.21349	2.25%	1.26485	1.23881	2.10%
1	1.14068	1.10353	3.37%	1.17974	1.1452	3.02%	1.21202	1.17966	2.74%	1.23926	1.20878	2.52%	1.26259	1.23374	2.34%
1.5	1.14333	1.10144	3.80%	1.18106	1.14245	3.38%	1.21239	1.17648	3.05%	1.2389	1.20529	2.79%	1.26167	1.23003	2.57%
2	1.14529	1.09896	4.22%	1.18196	1.13949	3.73%	1.21254	1.17325	3.35%	1.23851	1.20189	3.05%	1.26087	1.22654	2.80%
2.5	1.14662	1.09615	4.60%	1.18238	1.13629	4.06%	1.21235	1.16984	3.63%	1.23788	1.19839	3.30%	1.25992	1.22301	3.02%
3	1.14739	1.0931	4.97%	1.1824	1.13291	4.37%	1.21184	1.16629	3.91%	1.237	1.19477	3.53%	1.25878	1.2194	3.23%
3.5	1.14772	1.08993	5.30%	1.18207	1.12941	4.66%	1.21106	1.16264	4.16%	1.2359	1.19108	3.76%	1.25746	1.21571	3.43%
4	1.14766	1.08668	5.61%	1.18141	1.12582	4.94%	1.21002	1.15892	4.41%	1.23459	1.18731	3.98%	1.25596	1.21196	3.63%
4.5	1.14726	1.08341	5.89%	1.18049	1.1222	5.19%	1.20875	1.15516	4.64%	1.23309	1.1835	4.19%	1.25429	1.20816	3.82%
5	1.14656	1.08015	6.15%	1.17933	1.11858	5.43%	1.20729	1.15138	4.86%	1.23143	1.17967	4.39%	1.25249	1.20434	4.00%
5.5	1.14561	1.07693	6.38%	1.17797	1.11498	5.65%	1.20567	1.14761	5.06%	1.22963	1.17584	4.57%	1.25057	1.20051	4.17%
6	1.14444	1.07378	6.58%	1.17642	1.11142	5.85%	1.2039	1.14388	5.25%	1.2277	1.17203	4.75%	1.24853	1.19668	4.33%
6.5	1.14307	1.07069	6.76%	1.17472	1.1079	6.03%	1.202	1.14018	5.42%	1.22566	1.16825	4.91%	1.2464	1.19288	4.49%
7	1.14152	1.06768	6.92%	1.17287	1.10446	6.19%	1.19997	1.13652	5.58%	1.22352	1.1645	5.07%	1.24419	1.1891	4.63%
7.5	1.13984	1.06478	7.05%	1.1709	1.10108	6.34%	1.19785	1.13292	5.73%	1.2213	1.16079	5.21%	1.2419	1.18536	4.77%
8	1.13803	1.06197	7.16%	1.16882	1.09778	6.47%	1.19562	1.12938	5.87%	1.21899	1.15713	5.35%	1.23955	1.18167	4.90%
8.5	1.13614	1.05928	7.26%	1.16664	1.09455	6.59%	1.19332	1.1259	5.99%	1.21662	1.15352	5.47%	1.23714	1.17801	5.02%
9	1.13418	1.05666	7.34%	1.16437	1.0914	6.69%	1.19093	1.12247	6.10%	1.21417	1.14997	5.58%	1.23467	1.1744	5.13%
9.5	1.13212	1.05401	7.41%	1.16205	1.08834	6.77%	1.18846	1.1191	6.20%	1.21166	1.14647	5.69%	1.23214	1.17083	5.24%
10	1.12985	1.05119	7.48%	1.15969	1.08536	6.85%	1.18594	1.1158	6.29%	1.20909	1.143	5.78%	1.22955	1.16729	5.33%
10.5	1.12729	1.04812	7.55%	1.15726	1.08242	6.91%	1.18337	1.11256	6.36%	1.20646	1.13958	5.87%	1.22691	1.16379	5.42%
11	1.12438	1.04474	7.62%	1.15473	1.07943	6.98%	1.18075	1.10938	6.43%	1.20379	1.13623	5.95%	1.22425	1.16035	5.51%
11.5	1.1211	1.04105	7.69%	1.15206	1.07632	7.04%	1.17808	1.10624	6.49%	1.2011	1.13294	6.02%	1.22155	1.15696	5.58%
12	1.1174	1.03703	7.75%	1.14919	1.07305	7.10%	1.17539	1.10313	6.55%	1.19838	1.12971	6.08%	1.21883	1.15363	5.65%
12.5	1.11335	1.03282	7.80%	1.1461	1.06961	7.15%	1.17264	1.09999	6.60%	1.19564	1.12651	6.14%	1.21608	1.15033	5.72%
13	1.10902	1.02848	7.83%	1.14277	1.06597	7.20%	1.16977	1.09677	6.66%	1.19285	1.12334	6.19%	1.21331	1.14708	5.77%
13.5	1.10452			1.13918	1.06212	7.26%	1.16677	1.09346	6.70%	1.19004	1.1202	6.23%	1.21051	1.14387	5.83%
14				1.13536	1.05812	7.30%	1.16362	1.09003	6.75%	1.18717	1.11701	6.28%	1.2077	1.1407	5.87%
14.5				1.13133	1.054	7.34%	1.1603	1.08647	6.80%	1.18422	1.11378	6.32%	1.20487	1.13755	5.92%
15				1.12713	1.04982	7.36%	1.15683	1.08279	6.84%	1.18117	1.11047	6.37%	1.202	1.1344	5.96%
15.5				1.12282			1.15319	1.07899	6.88%	1.17801	1.10709	6.41%	1.19909	1.13123	6.00%
16							1.1494	1.0751	6.91%	1.17474	1.10362	6.44%	1.19613	1.12804	6.04%
16.5							1.14547	1.07113	6.94%	1.17136	1.10008	6.48%	1.1931	1.12479	6.07%
17							1.14143	1.06713	6.96%	1.16788	1.09646	6.51%	1.19	1.12151	6.11%
17.5							1.13731	1.06311	6.98%	1.16429	1.09277	6.54%	1.18683	1.11819	6.14%
18							1.13315			1.1606	1.08903	6.57%	1.18357	1.1148	6.17%
18.5										1.15682	1.08525	6.59%	1.18024	1.11136	6.20%
19										1.15298	1.08144	6.62%	1.17683	1.10787	6.22%
19.5										1.14908	1.07763	6.63%	1.17334	1.10432	6.25%
20										1.14514			1.16978	1.10074	6.27%
20.5										1.14118			1.16616	1.09712	6.29%
21										1.13721			1.16248	1.09349	6.31%

APPENDIX I: T9NP CASES AND ANALYSIS

A great test case to begin with for T9NP is a reactor operating at full power, performing a shutdown, and then returning to full power. This case is of interest due to a number of phenomenon that can be seen. The information that can be obtained from this case, as shown in Figure 30, is enumerated below:

1. Lithium-6 “decays” exponentially, as shown by its linear path on a semi-log plot.
2. The rate of tritium build up is always decreasing except at points where the scalar flux is discontinuous or increasing.
3. Helium-3 and tritium converge to equilibrium values at about the same time scale.
4. During a shutdown, tritium decays while helium increases since the tritium decay is independent of neutron flux and all other reactions depend on neutron flux.
5. When the flux is brought back to the same level, tritium and helium-3 approach the same equilibrium values.
6. As the flux is decreased, more helium-3 is present at equilibrium per unit tritium.
7. For the flux values in this problem, helium-3 is a small component, and the lithium-6 quickly depletes.
8. Eventually the helium-3 concentration surpasses the lithium-6 concentration, and when considering helium-3’s very large cross-section, the helium-3 can play a significant role in neutronics calculations.

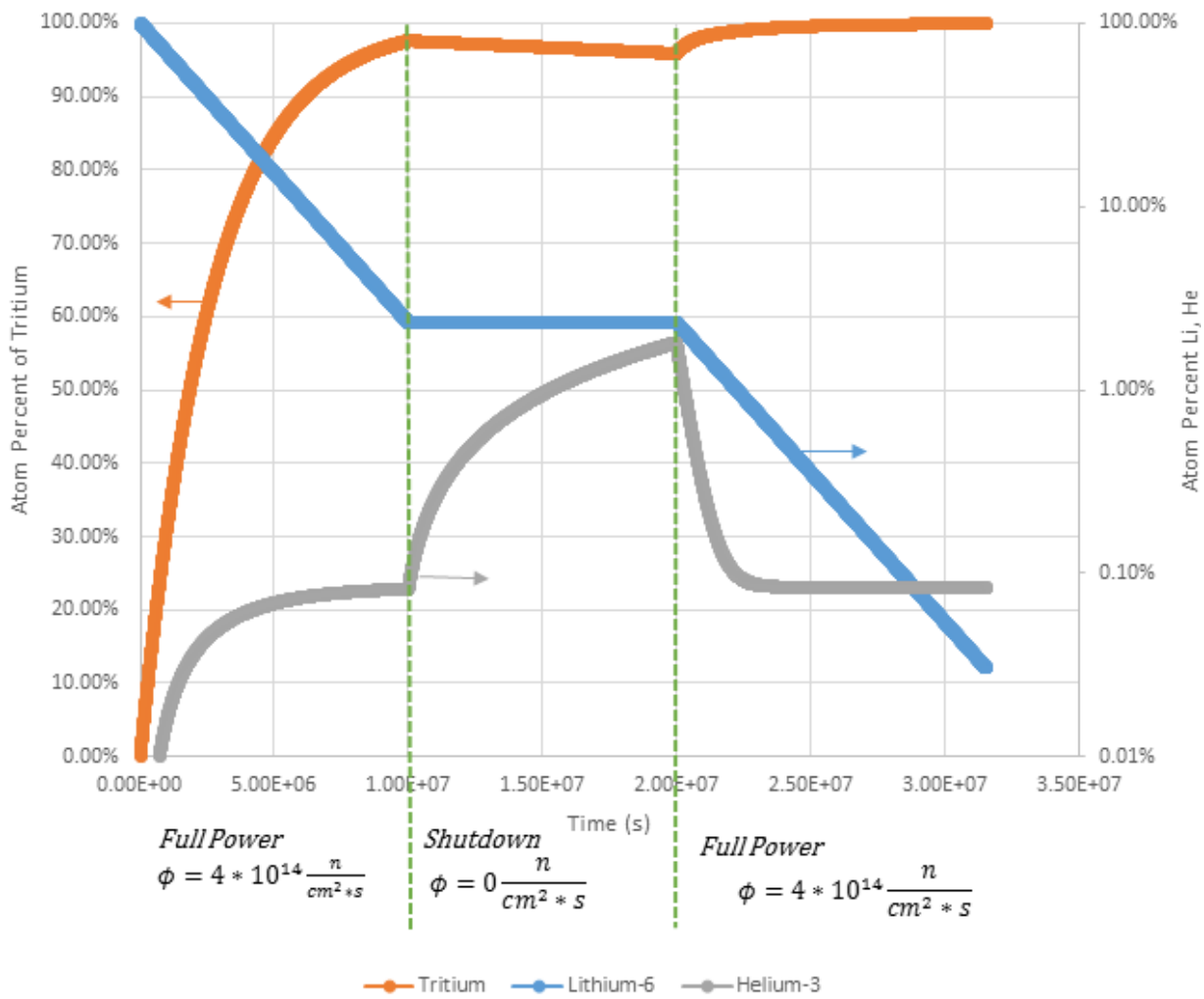

Figure 30. Output of T9NP when a shutdown period is considered.

The next case that will be demonstrated will be the case that most closely resembles a normal cycle for the mPower reactor designed here. First, the "2200 m/s scalar flux" must be found for the reactor. To do this, the thermal power is converted into fissions per second, as in Equation 42. Next, this is related to the integral of the fission rate density over the entire core, as in Equation 43. Next, the total number of ^{235}U atoms in the core is found by using Equation 44. Lastly, the all of the terms are plugged into Equation 43, with the result being Equation 45. The next parameter that needs to be solved for is the initial loading of lithium-6 for the core (alternatively, this whole process could be done for a single assembly, etc.). Lastly, the design cycle length must be known, at which time the flux becomes zero. The cycle length in the Team 9 design is 2 years.

$$P = 530\ MW * 6.2415 * 10^{18} \frac{\frac{MeV}{s}}{MW} * \frac{1\ fission}{200 MeV} = 1.654 * 10^{19} \frac{fissions}{s} \qquad \text{Equation 42}$$

$$1.654 * 10^{19} \frac{fissions}{s} \cong \iiint N_{235} \sigma(2200) \phi_0 \, dV$$ Equation 43

$$\iiint N_{235} \, dV = 69 \frac{ASM}{CORE} * 248 \frac{FR}{ASM} * (\pi * 0.409575^2 * 95 * 2.54) \frac{cm^3}{FR} * 10.37 \frac{gUO_2}{cm^3} * \frac{238}{270} \frac{gU}{gUO_2} * 0.03 \frac{g235}{gU} * \frac{1}{235} \frac{mol}{g235} * 6.0222 * 10^{23} \frac{atoms}{mol} = 1.529 * 10^{27} atoms$$ Equation 44

$$\phi_0 \cong 1.654 * \frac{10^{19} \frac{fissions}{s}}{585b} * \frac{1b}{10^{-24} cm^2} * \frac{1}{1.529 * 10^{27}} atoms = 1.849 * 10^{13} \frac{n}{cm^2 * s}$$ Equation 45

$$N_{Li6} = 69 \frac{ASM}{CORE} * 16 \frac{TPBARs}{ASM} * [\pi * (0.38354^2 - 0.28321^2) * 95 * 2.54] \frac{cm^3}{TPBAR} * 2.62 \frac{g\ LiAlO_2}{cm^3} * \frac{6.78}{6.78 + 26.98 + 32} \frac{g\ Li}{g\ LiAlO_2} * 0.22 \frac{gLi6}{gLi} * \frac{1}{6} \frac{mol}{gLi6} * 6.0222 * 10^{23} \frac{atoms}{mol} = 3.339 * 10^{26} atoms$$ Equation 46

The output from this case is plotted in Figure 31, below. From this data, $2.23*10^{26}$ tritium atoms are present when the reactor shuts down at two years. By converting this to the mass of tritium, 1116.9g of tritium are predicted. This equates to 1.012g of tritium per TPBAR. Since the design incorporates a "twin pack" of B&W mPower reactors on alternating 2 year cycles, T9NP predicts that the design goals will very nearly be met.

Equation 47

$$2.23 * 10^{26}\ T\ atoms * \frac{1\ mol}{6.022 * 10^{23}\ atoms} * 3.016 \frac{g}{mol} = 1116.9\ g\ Tritium$$

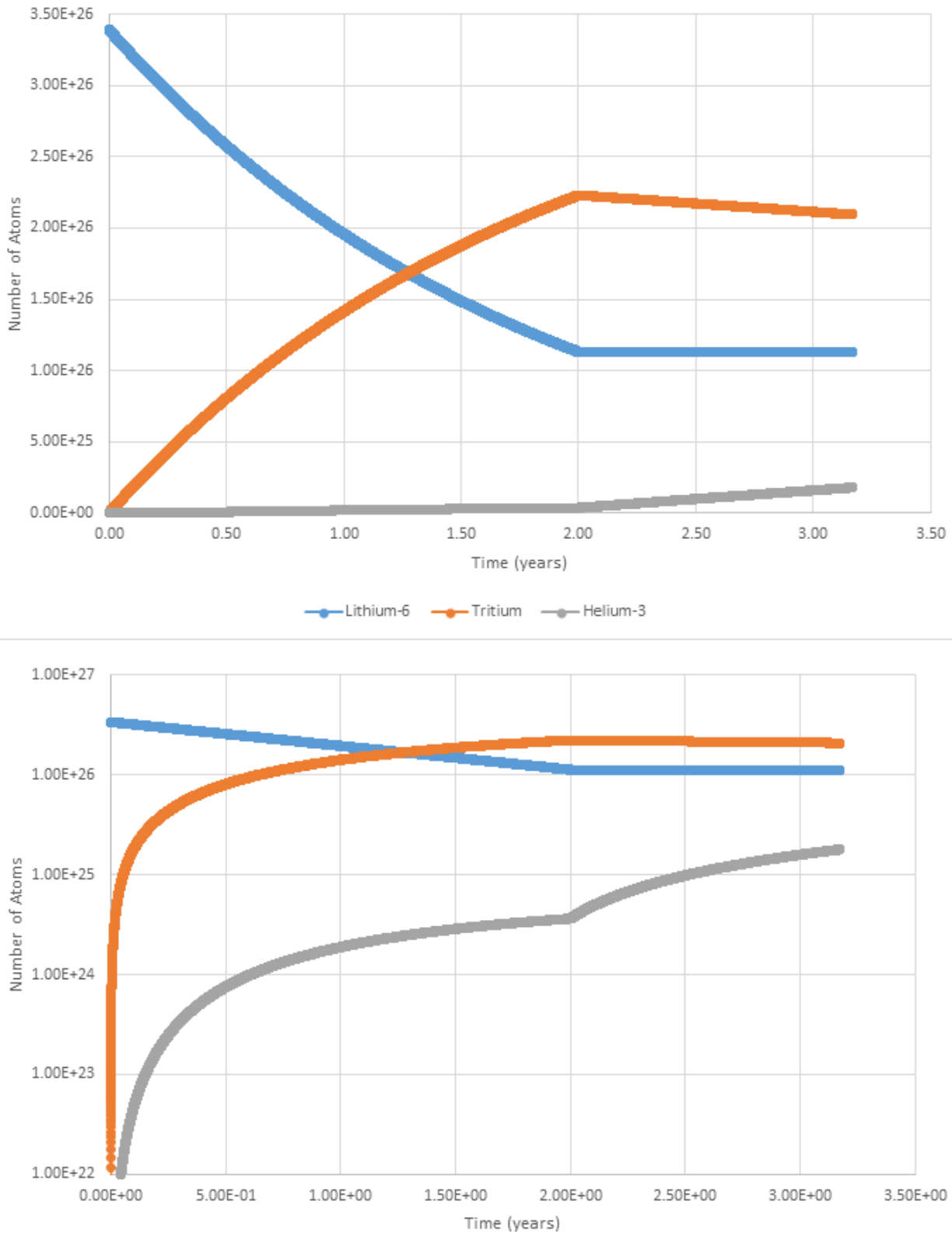

Figure 31. Output from T9NP for a “realistic” scenario based on the Team 9 design.

APPENDIX J: DOSE RATE DERIVATION AND CALCULATIONS

Consider a point source of radiation at position $\vec{r}_s$, and a target point of interest at position $\vec{r}_t$. The point kernel, G^0, is given by Equation 48 where r is defined as the distance between the radiation source and the point of interest, given by Equation 49. In Equation 48, μ is the total linear attenuation coefficient and is the sum of the attenuation coefficients for all reaction types.

$$G^0(\vec{r}_s, \vec{r}_t, \mathrm{E}) = \frac{e^{\int_r^0 \mu(s)ds}}{4\pi r^2} \qquad \text{Equation 48}$$

$$r = |\vec{r}_s - \vec{r}_t| \qquad \text{Equation 49}$$

In this analysis, radiation is not emitted from a single point, but an activated TPBAR can be modeled as line source, as shown in Figure 32.

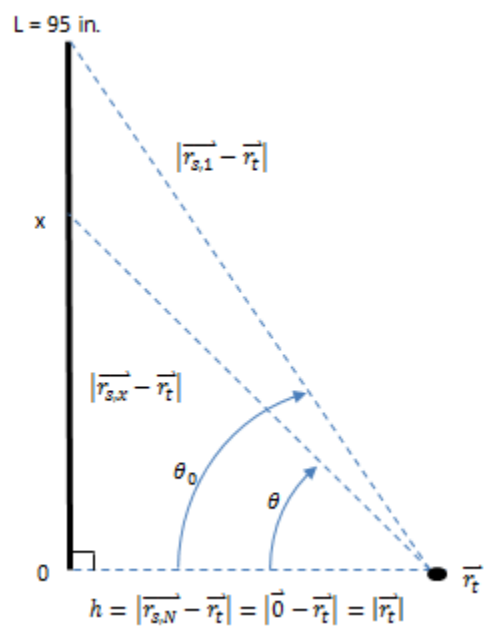

Figure 32. Diagram Illustrating the basic geometry for the gamma flux analysis performed here.

A differential component of uncollided flux at $\vec{r}_t$ can then be expressed as shown by Equation 50, in terms of the point kernel and the source strength, $S_l(x)$, in units of particles of energy E per unit length.

$$d\phi^0 = S_l(x)dx\, G^0(\vec{r}_s\,, \vec{r}_t, \mathrm{E}) \qquad \text{Equation 50}$$

If the case of no attenuation and constant source strength along the TPBAR is considered, Equation 50 can be rewritten as Equation 51. Integrating Equation 51 yields Equation 52. Using trigonometric substitution, Equation 52 can be rewritten as Equation 53, which simplifies to Equation 54.

$$d\phi^0 = \frac{S_l dx}{4\pi(x^2 + h^2)} \qquad \text{Equation 51}$$

$$\phi^0(\vec{r}_t) = \int_0^L \frac{S_l(x)dx}{4\pi(x^2 + h^2)} \qquad \text{Equation 52}$$

$$\phi^0(\vec{r}_t) = \int_0^{\theta_0} \frac{h\ \sec^2\theta\ \ d\theta}{h^2 \sec^2\theta} \qquad \text{Equation 53}$$

$$\phi^0(\vec{r}_t) = \frac{S_l\ \theta_0}{4\pi h} \qquad \text{Equation 54}$$

If the case of an attenuating medium is considered, then Equation 51 must be altered to the form of Equation 55 (Marianno, 2013). Integrating this yields Equation 56. Equation 57 defines the Sievert Integral, which is used to recast Equation 56 into Equation 58. In order to expand this analysis to other points, the principle of superposition is used.

$$d\phi^0 = \frac{S_l e^{-\mu\sqrt{x^2+h^2}} dx}{4\pi(x^2 + h^2)} \qquad \text{Equation 55}$$

$$\phi^0(\vec{r}_t) = \frac{S_l}{4\pi h}\int_0^{\theta_0} e^{-(\mu\, h\, sec\theta)} d\theta \qquad \text{Equation 56}$$

$$F(\theta, b) = \int_0^{\theta} e^{-b\, secx} dx \qquad \text{Equation 57}$$

$$\phi^0(\vec{r}_t) = \frac{S_l}{4\pi h} F(\theta_0, \mu h)$$ Equation 58

As a demonstration of these equations and their applicability to a TPBAR, three cases will be illustrated: the gamma flux 3 feet away from the center of the TPBAR in the absence of attenuation, the gamma flux 3 feet away from a point 3 feet above the TPBAR in the absence of attenuation, and the unattenuated gamma flux 3 feet away from the center of the TPBAR with the insertion of a 1-foot thick lead shield. All of these cases will ignore self-attenuation, as the TPBAR is treated as a line source. The data used for these calculations includes the source term for the TPBAR, calculated using Excel from the source data given in Collins (2012), and shown in

Table 16. Additionally, the linear attenuation coefficient for lead is available in

Table 17, and has been interpolated from the data given by NIST (Hubbell & Seltzer). Table 13,Table 14, and

Table 15 contain the approximate results of the three cases mentioned above. Table 18 contains the relevant Sievert integrals for case 3, with interpolated data.

Table 13. Gamma Flux 3 feet from the center of a TPBAR (gammas/cm^2*s).

Energy (MeV)	7 Days	30 Days	90 Days	180 Days	1 Year	5 Years	10 Years
1.00E-02	4.78E+10	3.13E+10	1.44E+10	7.05E+09	3.71E+09	1.96E+09	1.41E+09
2.50E-02	4.15E+09	2.56E+09	1.60E+09	1.09E+09	6.37E+08	1.21E+08	4.34E+07
3.75E-02	1.11E+09	6.67E+08	4.11E+08	2.30E+08	1.14E+08	4.22E+07	1.76E+07
5.75E-02	3.58E+09	2.74E+09	1.79E+09	9.89E+08	3.26E+08	1.03E+07	5.25E+06
8.50E-02	9.39E+08	6.06E+08	3.62E+08	1.81E+08	5.63E+07	1.03E+07	5.25E+06
1.25E-01	1.38E+09	7.05E+08	5.44E+08	2.88E+08	8.96E+07	4.38E+06	2.13E+06
2.25E-01	2.79E+09	1.47E+09	7.42E+08	3.99E+08	1.33E+08	8.03E+06	2.60E+06
3.75E-01	1.89E+10	1.07E+10	2.53E+09	4.05E+08	1.20E+08	4.06E+07	1.17E+07
5.75E-01	1.70E+10	1.34E+10	7.48E+09	3.19E+09	6.30E+08	5.17E+07	1.48E+07
8.50E-01	9.64E+10	7.97E+10	4.84E+10	2.33E+10	6.86E+09	1.67E+08	3.26E+06
1.25E+00	1.88E+10	1.83E+10	1.74E+10	1.63E+10	1.47E+10	7.91E+09	4.43E+09
1.75E+00	3.10E+08	2.45E+08	1.36E+08	5.62E+07	9.15E+06	5.62E+00	3.41E-02
2.25E+00	1.31E+07	2.32E+06	2.02E+05	1.14E+05	8.03E+04	4.53E+04	2.35E+04
2.75E+00	4.62E+06	4.00E+02	3.28E+02	2.77E+02	2.40E+02	1.40E+02	7.29E+01
3.50E+00	3.12E+03	1.16E-02	3.79E-04	2.90E-06	1.95E-08	1.77E-08	1.59E-08
5.00E+00	3.22E-05	3.24E-10	4.09E-11	2.61E-11	1.03E-11	6.86E-15	1.19E-17
7.00E+00	3.94E-12	3.59E-12	2.66E-12	1.70E-12	6.74E-13	4.47E-16	7.73E-19
9.50E+00	2.49E-13	2.27E-13	1.68E-13	1.08E-13	4.25E-14	2.82E-17	4.90E-20

TOTAL	2.13E+11	1.62E+11	9.58E+10	5.34E+10	2.74E+10	1.03E+10	5.94E+09

Table 14. Gamma Flux 3 feet from a point 3 feet above a TPBAR (gammas/cm^2*s).

Energy (MeV)	7 Days	30 Days	90 Days	180 Days	1 Year	5 Years	10 Years
1.00E-02	1.34E+10	8.79E+09	4.04E+09	1.98E+09	1.04E+09	5.49E+08	3.95E+08
2.50E-02	1.16E+09	7.19E+08	4.49E+08	3.05E+08	1.78E+08	3.38E+07	1.22E+07
3.75E-02	3.12E+08	1.87E+08	1.15E+08	6.45E+07	3.21E+07	1.18E+07	4.92E+06
5.75E-02	1.01E+09	7.69E+08	5.03E+08	2.77E+08	9.13E+07	2.88E+06	1.47E+06
8.50E-02	2.63E+08	1.70E+08	1.02E+08	5.08E+07	1.58E+07	2.88E+06	1.47E+06
1.25E-01	3.88E+08	1.98E+08	1.53E+08	8.08E+07	2.51E+07	1.23E+06	5.98E+05
2.25E-01	7.83E+08	4.12E+08	2.08E+08	1.12E+08	3.73E+07	2.25E+06	7.28E+05
3.75E-01	5.30E+09	3.00E+09	7.11E+08	1.14E+08	3.36E+07	1.14E+07	3.29E+06
5.75E-01	4.77E+09	3.76E+09	2.10E+09	8.94E+08	1.77E+08	1.45E+07	4.14E+06
8.50E-01	2.70E+10	2.24E+10	1.36E+10	6.53E+09	1.92E+09	4.68E+07	9.15E+05
1.25E+00	5.29E+09	5.13E+09	4.87E+09	4.56E+09	4.12E+09	2.22E+09	1.24E+09
1.75E+00	8.68E+07	6.86E+07	3.81E+07	1.58E+07	2.56E+06	1.58E+00	9.57E-03
2.25E+00	3.67E+06	6.50E+05	5.67E+04	3.19E+04	2.25E+04	1.27E+04	6.59E+03
2.75E+00	1.30E+06	1.12E+02	9.18E+01	7.76E+01	6.72E+01	3.93E+01	2.04E+01
3.50E+00	8.75E+02	3.26E-03	1.06E-04	8.15E-07	5.48E-09	4.97E-09	4.47E-09
5.00E+00	9.03E-06	9.10E-11	1.15E-11	7.31E-12	2.89E-12	1.92E-15	3.34E-18
7.00E+00	1.10E-12	1.01E-12	7.47E-13	4.77E-13	1.89E-13	1.25E-16	2.17E-19
9.50E+00	6.98E-14	6.38E-14	4.71E-14	3.02E-14	1.19E-14	7.92E-18	1.37E-20
TOTAL	5.98E+10	4.56E+10	2.69E+10	1.50E+10	7.68E+09	2.90E+09	1.67E+09

Table 15. Unattenuated Gamma Flux 3 feet from the center of a TPBAR with a 1-foot lead shield (gammas/cm^2*s).

Energy (MeV)	7 Days	30 Days	90 Days	180 Days	1 Year	5 Years	10 Years
1.00E-02	4.66E+09	3.06E+09	1.41E+09	6.88E+08	3.62E+08	1.91E+08	1.38E+08
2.50E-02	4.50E+08	2.78E+08	1.74E+08	1.18E+08	6.90E+07	1.31E+07	4.70E+06
3.75E-02	1.33E+08	7.96E+07	4.90E+07	2.74E+07	1.36E+07	5.03E+06	2.09E+06
5.75E-02	4.66E+08	3.57E+08	2.33E+08	1.29E+08	4.24E+07	1.33E+06	6.83E+05
8.50E-02	1.32E+08	8.55E+07	5.10E+07	2.55E+07	7.94E+06	1.45E+06	7.40E+05
1.25E-01	2.25E+08	1.15E+08	8.85E+07	4.68E+07	1.46E+07	7.12E+05	3.47E+05
2.25E-01	5.15E+08	2.71E+08	1.37E+08	7.36E+07	2.45E+07	1.48E+06	4.78E+05
3.75E-01	3.69E+09	2.09E+09	4.95E+08	7.90E+07	2.34E+07	7.92E+06	2.29E+06
5.75E-01	3.69E+09	2.91E+09	1.62E+09	6.92E+08	1.37E+08	1.12E+07	3.20E+06

8.50E-01	2.51E+10	2.07E+10	1.26E+10	6.06E+09	1.79E+09	4.34E+07	8.49E+05
1.25E+00	5.93E+09	5.75E+09	5.46E+09	5.11E+09	4.63E+09	2.49E+09	1.39E+09
1.75E+00	1.07E+08	8.49E+07	4.72E+07	1.95E+07	3.17E+06	1.95E+00	1.18E-02
2.25E+00	4.76E+06	8.42E+05	7.34E+04	4.13E+04	2.92E+04	1.65E+04	8.53E+03
2.75E+00	1.70E+06	1.48E+02	1.21E+02	1.02E+02	8.84E+01	5.17E+01	2.69E+01
3.50E+00	1.17E+03	4.35E-03	1.42E-04	1.09E-06	7.31E-09	6.64E-09	5.96E-09
5.00E+00	1.19E-05	1.20E-10	1.51E-11	9.67E-12	3.83E-12	2.54E-15	4.42E-18
7.00E+00	1.43E-12	1.30E-12	9.68E-13	6.17E-13	2.45E-13	1.62E-16	2.81E-19
9.50E+00	8.64E-14	7.89E-14	5.83E-14	3.73E-14	1.47E-14	9.80E-18	1.70E-20
TOTAL	4.51E+10	3.58E+10	2.24E+10	1.31E+10	7.11E+09	2.76E+09	1.54E+09

Table 16. Source Term for a TPBAR (gammas/s/ft-TPBAR).

Energy (MeV)	7 Days	30 Days	90 Days	180 Days	1 Year	5 Years	10 Years
1.00E-02	9.76E+11	6.40E+11	2.94E+11	1.44E+11	7.59E+10	4.00E+10	2.88E+10
2.50E-02	8.48E+10	5.24E+10	3.27E+10	2.22E+10	1.30E+10	2.46E+09	8.87E+08
3.75E-02	2.27E+10	1.36E+10	8.40E+09	4.70E+09	2.34E+09	8.63E+08	3.59E+08
5.75E-02	7.33E+10	5.61E+10	3.66E+10	2.02E+10	6.66E+09	2.10E+08	1.07E+08
8.50E-02	1.92E+10	1.24E+10	7.40E+09	3.70E+09	1.15E+09	2.10E+08	1.07E+08
1.25E-01	2.83E+10	1.44E+10	1.11E+10	5.89E+09	1.83E+09	8.94E+07	4.36E+07
2.25E-01	5.71E+10	3.01E+10	1.52E+10	8.16E+09	2.72E+09	1.64E+08	5.31E+07
3.75E-01	3.87E+11	2.19E+11	5.18E+10	8.27E+09	2.45E+09	8.30E+08	2.40E+08
5.75E-01	3.47E+11	2.74E+11	1.53E+11	6.52E+10	1.29E+10	1.06E+09	3.02E+08
8.50E-01	1.97E+12	1.63E+12	9.89E+11	4.76E+11	1.40E+11	3.41E+09	6.67E+07
1.25E+00	3.85E+11	3.74E+11	3.55E+11	3.32E+11	3.01E+11	1.62E+11	9.04E+10
1.75E+00	6.33E+09	5.00E+09	2.78E+09	1.15E+09	1.87E+08	1.15E+02	6.97E-01
2.25E+00	2.68E+08	4.74E+07	4.13E+06	2.32E+06	1.64E+06	9.26E+05	4.80E+05
2.75E+00	9.45E+07	8.19E+03	6.69E+03	5.66E+03	4.90E+03	2.87E+03	1.49E+03
3.50E+00	6.38E+04	2.37E-01	7.74E-03	5.94E-05	3.99E-07	3.63E-07	3.26E-07
5.00E+00	6.58E-04	6.63E-09	8.35E-10	5.33E-10	2.11E-10	1.40E-13	2.44E-16
7.00E+00	8.05E-11	7.34E-11	5.44E-11	3.47E-11	1.38E-11	9.13E-15	1.58E-17
9.50E+00	5.09E-12	4.65E-12	3.44E-12	2.20E-12	8.68E-13	5.77E-16	1.00E-18
TOTAL	4.36E+12	3.32E+12	1.96E+12	1.09E+12	5.60E+11	2.11E+11	1.21E+11

Table 17. Linear Attenuation Coefficients for Lead.

Energy (MeV)	mu/rho (cm^2/g)	mu(cm^-1)	mu(ft^-1)
1.00E-02	1.31E+02	1.48E+03	4.51E+04
2.50E-02	5.83E+01	6.62E+02	2.02E+04

3.75E-02	1.84E+01	2.08E+02	6.34E+03
5.75E-02	5.78E+00	6.55E+01	2.00E+03
8.50E-02	2.20E+00	2.49E+01	7.60E+02
1.25E-01	3.78E+00	4.29E+01	1.31E+03
2.25E-01	8.50E-01	9.64E+00	2.94E+02
3.75E-01	2.75E-01	3.12E+00	9.51E+01
5.75E-01	1.34E-01	1.52E+00	4.63E+01
8.50E-01	8.43E-02	9.56E-01	2.91E+01
1.25E+00	5.88E-02	6.66E-01	2.03E+01
1.75E+00	4.91E-02	5.57E-01	1.70E+01
2.25E+00	4.51E-02	5.12E-01	1.56E+01
2.75E+00	4.33E-02	4.91E-01	1.50E+01
3.50E+00	4.22E-02	4.78E-01	1.46E+01
5.00E+00	4.27E-02	4.84E-01	1.48E+01
7.00E+00	4.53E-02	5.14E-01	1.57E+01
9.50E+00	4.90E-02	5.55E-01	1.69E+01

Table 18. Sievert Integrals of Interest for Solving the Problem given in the Text.

	b (relaxation length or number of mean free paths)					
Θ (degrees)	**12**	**15**	**20**	**25**	**35**	**50**
50	0.39536	0.35679	0.31183	0.28048	0.23861	0.20065
60	0.32951	0.29733	0.25986	0.23373	0.19884	0.16721
52.8415	0.376649	0.339894441	0.297063	0.267196	0.227309	0.191148

APPENDIX K: T9NP SOURCE CODE

```
!-----------------------------------------------------------------------
!  TEAM 9 NUCLIDE PROGRAM (T9NP)
!  William Cook
!  04/22/2013
!  NUEN 410
!  Copyright, Team 9, 2013
!  Apply Explicit and Implicit Euler methods to solve
!-----------------------------------------------------------------------
PROGRAM T9NP

IMPLICIT NONE
INTEGER :: n,k,ndim
REAL :: L=0.
REAL, ALLOCATABLE,DIMENSION(:)   ::Y
REAL, ALLOCATABLE,DIMENSION(:)   ::B
REAL, ALLOCATABLE,DIMENSION(:,:) ::A
INTEGER :: i,j,int
INTEGER :: ierr
LOGICAL :: correct
REAL(KIND=8)::licx,hecx


!Get user input

!Choose a method
read_12:do
   write(*,'(/,A)') 'ENTER a method #,  1 for Explicit (Forward) Euler
method,  or 2 for Implicit (Backward) Euler method.'
   read (*,*,IOSTAT=ierr) int
   if(ierr/=0.OR.(int/=1.AND.int/=2.AND.int/=3)) then
      write(*,*) 'You did not enter an integer value of 1 or 2'
   else
      write(*,33) int
      read_confirm:do
         write(*,'(A)',advance='no')"Enter true (T) or false (F): "
         read (*,*,IOSTAT=ierr) correct
         if(ierr/=0) then
            write(*,'(/,A)') 'Answer T of F, please try again'
         else
            if(correct) then
               exit read_12
            else
               exit read_confirm
            endif
         endif
      enddo read_confirm
   endif
enddo read_12
```

```
33 format ('Thank you, you have entered',1x,I5,/,'Is this correct?')

!Choose the number of time steps
read_numsteps:do
   WRITE(*,*)'ENTER a positive  INTEGER for the number of time steps
to use in approximating the solution.'
   READ(*,*,IOSTAT=ierr) n
   IF(ierr/=0 .OR. n<0) then
      write(*,*) "You did not enter a POSITIVE INTEGER!"
   ELSE
      exit read_numsteps
   END IF
END DO read_numsteps

!Here, one neutron precursor group is hardcoded
!However, Allocatable arrays have been used so that later versions can
ask for user input

ndim=3

ALLOCATE(Y(ndim),STAT=ierr)
IF(ierr/=0) STOP 'Problem allocating Y! '
ALLOCATE(A(ndim,ndim), STAT=ierr)
IF(ierr/=0) STOP 'Problem allocating A! '
ALLOCATE(B(ndim), STAT=ierr)
IF(ierr/=0) STOP 'Problem allocating B! '

CALL INITIALIZEYAB(Y,A,B,ndim,licx,hecx) !This sets up the matricies
Y, A, and B

!Solve the system by calling a subroutine of the specified methodd

IF(int==1) CALL EXPLICITEULER(Y,A,B,n,ndim,licx,hecx)   !This solves
the EE problem
IF(int==2) CALL IMPLICITEULER(Y,A,B,n,ndim,licx,hecx)   !This solves
the IE problem


END PROGRAM T9NP

!-----------------------------------------------------------------------
!-----------------------------------------------------------------------

REAL(KIND=8) FUNCTION  flux(time)
IMPLICIT NONE

!REAL(KIND=8) ::  flux
! define dummy variables
REAL, INTENT(IN) :: time ! the time
! define local variables (NONE are used here)
```

```
IF(time<0)THEN
   flux=0

ELSE IF(time<10000000)THEN
   flux=4E14
ELSE IF(time<20000000)THEN
   flux=0
ELSE
   flux=4E14
END IF

END FUNCTION flux

!-----------------------------------------------------------------------
!-----------------------------------------------------------------------

SUBROUTINE InitializeYAB(Y,A,B,ndim,licx,hecx)
IMPLICIT NONE

REAL(KIND=8),EXTERNAL :: flux
!Dummys
INTEGER, INTENT (IN) :: ndim
REAL, DIMENSION(ndim), INTENT (INOUT) :: Y,B !The Matrix, and a
source, not used
REAL, DIMENSION(ndim,ndim), INTENT (INOUT) :: A !The Source/solution
REAL(KIND=8), INTENT (OUT) ::licx,hecx


!Local variable declarations
REAL(KIND=8) :: N_Li_0, N_T_0, N_He_0, dc !N_Li_0, N_T_0, N_HE_0 are
the initial number densities of lithium tritium and helium,
respectively.
!licx and hecx are the microscopic cross sections for Li and He,
respectively.  dc is the decay constant (lambda) for tritium

!INTEGER :: i=0; This line will be added for more dnp groups

!All of these dummy values will not chage w.r.t. time, so they are not
needed in the MAIN PROGRAM.

!Initialization of dummy variables

N_Li_0 = 1E24
N_T_0  = 0
N_He_0 = 0
licx   = 940E-24
hecx   = 5300E-24
dc  = 1.7858E-9
!Write(*,*) N_Li_0, "  ", N_T_0, "  ", Y(1),  "  ",  Y(2)
!Initalization of flux
```

```
!A functional form of flux could be used, but we will just use a
constant here.
!flux=4E14


!Initialization of the Vectors Y, B and matrix, A

IF (ndim==3) THEN
   Y(1)=N_Li_0
   Y(2)=N_T_0
   Y(3)=N_He_0

   A(1,1)=-(licx*flux(0.0))
   A(1,2)=0
   A(1,3)=0
   A(2,1)=(licx*flux(0.0))
   A(2,2)=-(dc)
   A(2,3)=(hecx*flux(0.0))
   A(3,1)=0
   A(3,2)=dc
   A(3,3)=-(hecx*flux(0.0))
!This is a "source free" problem
   B(1)=A(1,1)*Y(1)
   B(2)=A(2,1)*Y(1)+A(2,2)*Y(2)+A(2,3)*Y(3)
   B(3)=A(3,2)*Y(2)+A(3,3)*Y(3)

!WRITE(*,*) dnf, "  ", ngt , "  ", dc
!Write(*,*) N_Li_0, "  ", N_T_0, "  ", Y(1),  "  ",  Y(2)
!WRITE(*,*) A
ELSE
   WRITE(*,*)"This program must be modified for the correct system
size."

END IF


Return
END SUBROUTINE INITIALIZEYAB


!-----------------------------------------------------------------------
!-----------------------------------------------------------------------


SUBROUTINE EXPLICITEULER(Y,A,B,n,ndim,licx,hecx)
IMPLICIT NONE

REAL(KIND=8),EXTERNAL :: flux
!Dummys
INTEGER, INTENT(IN) :: n,ndim !choice and dimension, respectively
REAL, DIMENSION(ndim,ndim), INTENT (INOUT) :: A !The Matrix
```

```
REAL, DIMENSION(ndim), INTENT (INOUT) :: Y,B !The Source/solution
REAL(KIND=8), INTENT (IN) ::licx,hecx

!Local variable declarations
CHARACTER(LEN=30) :: filename !This will contain the name of the
output file
REAL ::max_time = 31556736, dt=0
INTEGER i,ierr

!open corresponding output file
! create filename, as needed
filename = 'T9NPoutXXXXXXXXtimestepsEE.csv'
WRITE(filename(8:15),'(I8.8)') n
! open file with logical unit number 36 and filename
OPEN(unit=36, file=filename, status='replace', iostat=ierr)
IF(ierr/=0) STOP 'Problem opening file for output.'

dt=max_time/n
!Perform the Forward Euler Method and write into a file
IF (ndim==3) THEN
   WRITE(36,329) 0., Y(1),Y(2),Y(3)
   DO i=1,n
      Y(1)=Y(1)+dt*A(1,1)*Y(1)+dt*A(1,2)*Y(2)+dt*A(1,3)*Y(3)+B(1)
      Y(2)=Y(2)+dt*A(2,1)*Y(1)+dt*A(2,2)*Y(2)+dt*A(2,3)*Y(3)+B(2)
      Y(3)=Y(3)+dt*A(3,1)*Y(1)+dt*A(3,2)*Y(2)+dt*A(3,3)*Y(3)+B(3)

        !Update the derivative according to the flux
      A(1,1)=-(flux(i*dt)*licx)
      A(2,1)=(flux(i*dt)*licx)
      A(2,3)=(flux(i*dt)*hecx)
      A(3,3)=-(flux(i*dt)*hecx)

      WRITE(36,329) i*dt,Y(1),Y(2),Y(3)
   END DO

329 FORMAT(E12.4,",", E16.8,",",E16.10,",",E16.10 )
END IF
!Close the Output File
Close(36)

Return
END SUBROUTINE EXPLICITEULER

!-----------------------------------------------------------------------
!-----------------------------------------------------------------------

SUBROUTINE IMPLICITEULER(Y,A,B,n,ndim,licx,hecx)
IMPLICIT NONE

REAL(KIND=8),EXTERNAL :: flux
!Dummys
```

```
INTEGER, INTENT(IN) :: n,ndim !number of time steps and dimension,
respectively
REAL, DIMENSION(ndim,ndim), INTENT (INOUT) :: A !The Matrix
REAL, DIMENSION(ndim), INTENT (INOUT) :: Y,B !The Source/solution
REAL(KIND=8), INTENT (IN) ::licx,hecx

!Local variable declarations
CHARACTER(LEN=30) :: filename !This will contain the name of the
output file
REAL ::max_time = 31556736 , dt=0 !The time is in seconds, thus for a
1 year lenght, max_time=31556736
INTEGER i, ierr
REAL, DIMENSION(ndim,ndim)  :: Identity,M

!Create the Identity Matrix
Identity=0
M=0
DO i=1,ndim
   Identity(i,i)=1
END DO

dt=max_time/n


!open corresponding output file
! create filename, as needed
filename = 'T9NPoutXXXXXXXXtimestepsIE.csv'
WRITE(filename(8:15),'(I8.8)') n
! open file with logical unit number 36 and filename
OPEN(unit=36, file=filename, status='replace', iostat=ierr)
IF(ierr/=0) STOP 'Problem opening file for output.'

!Perform the Forward Euler Method and write into a file? Maybe?
IF (ndim==3) THEN
   WRITE(36,329) 0., Y(1),Y(2),Y(3)
   DO i=1,n

      M(1,1)=Identity(1,1)-dt*A(1,1)
      M(1,2)=Identity(1,2)-dt*A(1,2)
      M(1,3)=Identity(1,3)-dt*A(1,3)
      M(2,1)=Identity(2,1)-dt*A(2,1)
      M(2,2)=Identity(2,2)-dt*A(2,2)
      M(2,3)=Identity(2,3)-dt*A(2,3)
      M(3,1)=Identity(3,1)-dt*A(3,1)
      M(3,2)=Identity(3,2)-dt*A(3,2)
      M(3,3)=Identity(3,3)-dt*A(3,3)


      CALL LU_Decomp(M,ndim)

      CALL LU_Solve(M,ndim,Y,B)
```

```
      A(1,1)=-(flux(i*dt)*licx)
      A(2,1)=(flux(i*dt)*licx)
      A(2,3)=(flux(i*dt)*hecx)
      A(3,3)=-(flux(i*dt)*hecx)

!  If flux changes, then it would have to be reevaluated as a function
here


      WRITE(36,329) i*dt, Y(1),Y(2),Y(3)
   END DO

329 FORMAT(E10.5,",", E16.6,",",E16.6,",",E16.6 )
END IF
!Close the Output File
Close(36)

Return
END SUBROUTINE IMPLICITEULER

!-----------------------------------------------------------------------
!-----------------------------------------------------------------------

SUBROUTINE LU_Decomp(A,ndim)
IMPLICIT NONE

!Dummys
INTEGER, INTENT(IN) :: ndim !size of square matrix
REAL, DIMENSION(ndim,ndim), INTENT (INOUT) :: A !The Matrix

!Local variable declarations
INTEGER :: i,j,k !na is the size of the matrix that is of importance
REAL :: pivot = 0


!Perform Elimination
outer_column:DO k=1, ndim-1
   row:DO i=k+1,ndim

      !Check for division by zero
      IF (A(k,k)<.0005 .AND. A(k,k)>-.0005)THEN  !Use two conditions
to account for negatives, abs also works
         WRITE(*,*) "The GE process was terminated due to a
zero"!,A(k,k), A(k,k+1) Debug
         EXIT outer_column
      END IF
      !Calculate pivot
      pivot=-A(i,k)/A(k,k)
```

```
      inner_col:DO j=k+1,ndim
         A(i,j)=A(i,j)+pivot*A(k,j)
      END DO inner_col

      A(i,k)=-pivot

   END DO row
END DO outer_column

END SUBROUTINE LU_Decomp

!-----------------------------------------------------------------------
!-----------------------------------------------------------------------

SUBROUTINE LU_Solve(A,ndim,Y,B)
IMPLICIT NONE

!Dummys
INTEGER, INTENT(IN) :: ndim !size of square matrix
REAL, DIMENSION(ndim,ndim), INTENT (INOUT) :: A !The LU Matrix
REAL, DIMENSION (ndim), INTENT(INOUT) :: Y !The solution vector
REAL, DIMENSION (ndim), INTENT(IN) :: B ! The source vector

!Local variable declarations
INTEGER :: i,j

 ! Perform the solve for Ly=b

DO i=1, ndim

!Y(i)=B(i)

   DO j=1,i-1
      Y(i)=Y(i)-A(i,j)*Y(j)

   END DO

END DO

! Perform the solve for Ux=y
  DO i=ndim, 1, -1

     DO j=i+1,ndim
        Y(i)=Y(i)-A(i,j)*Y(j)

     END DO
     IF(abs( A(i,i))<5E-5)WRITE(*,*)"Divided by zero"

     Y(i)=Y(i)/A(i,i)
  END DO
```

```
END SUBROUTINE LU_Solve
```

Modified Holtec Inherently-Safe Modular Underground Reactor (HI-SMUR) for Tritium Production

FINAL PROJECT REPORT

MODIFIED HOLTEC INHERENTLY-SAFE MODULAR UNDERGROUND REACTOR (HI-SMUR) FOR TRITIUM PRODUCTION

Senior Design Team 13

Kevin Kapka

Clay Strack

Laura Sudderth

Ryan Upton

Under advisement of Dr. Karen Vierow and Dr. David Senor

Nuclear Engineering Department

Texas A&M University

College Station, TX 77843-3133

April 29, 2012

* Submitted in Partial Fulfillment of the Requirements for NUEN 410

FINAL PROJECT REPORT

MODIFIED HOLTEC INHERENTLY-SAFE MODULAR UNDERGROUND REACTOR (HI-SMUR) FOR TRITIUM PRODUCTION

Senior Design Team 13

	SIGNATURE	DATE
Kevin Kapka	_____	_____
Clay Strack	_____	_____
Laura Sudderth	_____	_____
Ryan Upton	_____	_____
Under advisement of:		
Dr. Karen Vierow	_____	_____
Dr. David Senor	_____	_____

April 29, 2012

* Submitted in Partial Fulfillment of the Requirements for NUEN 410

Table of Contents

1. INTRODUCTION (WRITTEN BY CLAY STRACK) 7
2. PROJECT BREAKDOWN (WRITTEN BY CLAY STRACK) 9
3. REACTOR OVERVIEW (Written by Laura Sudderth) 11
4. NEUTRONIC ANALYSIS (Written By Laura Sudderth) 15
4.1 Overview 15
4.2 Core Model 16
4.3 Tritium Production 20
4.3.1 TPBAR Surface Flux Tallies 20
4.3.2 Cell Averaged Flux Tally 22
4.4 Energy Profiles 23
4.4.1 Single Fuel Pin-Averaged 23
4.4.2 Assembly- Averaged 24
4.5 Criticality and Reactivity 25
4.6 Discussion and Future Work 27
5. THERMAL HYDRAULICS (WRITTEN BY CLAY STRACK) 28
5.1 Overview 28
5.2 Natural Circulation Model 28
5.2.1 Theory 28
5.2.2 Analysis/Methodology 32
5.2.3 Results 37
5.2.4 Future Work 38
5.3 Assembly Averaged Model 38
5.3.1 Theory 38
5.3.2 Analysis/Methodology 39
5.3.3 Results 39
5.3.4 Future Work 43
5.4 DNBR Analysis 43
5.4.1 Theory 43
5.4.2 Analysis 45
5.4.3 Method 46
5.4.4 Results 47
5.5 Temperature Analysis 49
5.5.1 Theory 49
5.5.2 Analysis/Methodology 54
5.5.3 Results 56
5.5.4 Future Work 56
6. TRITIUM PRODUCTION 57
6.1 Overview (Written by Ryan Upton) 57
6.2 Decision Making Model (Written by Ryan Upton) 57
6.3 Tritium Production Model 58
6.3.1 Theory (Written by Ryan Upton and Clay Strack) 58
6.3.2 Methodology (Written by Clay Strack and Laura Sudderth) 59
6.3.3 Results (Written by Laura Sudderth) 61
6.4 TPBAR Limitations (Written by Clay Strack) 63
6.5 Cycle Length Effects (Written by Clay Strack) 64

6.6 Discussion and Future Work (Written by Laura Sudderth) 64
7. SAFETY 65
7.1 General Safety Design (Written by Kevin Kapka) 65
7.2 Shutdown Margin (Written by Laura Sudderth) 66
7.3 Safety Systems (Written by Kevin Kapka) 66
7.3.1 Reactor Wells 67
7.3.2 Spent Fuel Pool/Transfer Pool 67
7.3.3 HPCIS 67
7.3.4 ADS 68
7.3.5 Passive Heat Rejection System 68
7.4 Reasonable Failures (Written by Kevin Kapka) 68
7.5 Non Mechanistic Failures (Written by Kevin Kapka) 69
7.5.1 A Completely Dry Reactor 69
7.5.2 LBLOCA Large Break Loss of Coolant Accident 69
7.5.3 LOFA 70
7.6 TPBAR Bursting (Written by Kevin Kapka) 71
7.6.1 TPBARs reaction to LBLOCAs and an attempt at generating actual numbers. 72
7.6.2 Double Leg Break Disaster 73
7.7 Thermal Margin (Written by Clay Strack) 73
7.8 Tritium Diffusion (Written by Ryan Upton) 73
7.9 Shielding (Written by Kevin Kapka) 74
7.10 Non-Proliferation 74
7.11 Future Work (Written by Kevin Kapka) 74
8. ECONOMICS (WRITTEN BY CLAY STRACK) 76
9. RECOMMENDATIONS (WRITTEN BY CLAY STRACK) 78
10. CONCLUSIONS (WRITTEN BY CLAY STRACK) 79
11. ACKNOWLEDGEMENTS 79
12. REFERENCES 79

EXECUTIVE SUMMARY

Tritium production is necessary to maintain the nuclear weapons stockpile in the United States. Tritium is currently produced in a commercial PWR, Watts Barr Nuclear Unit 1 (WBN1). Unfortunately, the license for WBN1 expires in 2035, so it is necessary to explore future tritium production options. The Holtec Inherently-Safe Modular Underground Reactor (HI-SMUR) was chosen for this particular project. The HI-SMUR reactor core was modified to include Tritium Producing Burnable Absorber Rods (TPBARs), and evaluated using various analyses.

The neutronics analysis was performed using MCNP5. The average thermal flux in the lithium aluminate pellets of the TPBARs was calculated to be 2.316E12 n/cm^{2}s. This result, when combined with the Tritium Production Model, was used to set the TPBAR data at Li-6 enrichment of 12.2% and 24 TPBARs per assembly. Four cores are required to meet the annual production goal, resulting in 1186.7 g of tritium produced per year. The resulting core contains about $29.7 of excess reactivity and a $54.3 shutdown margin, and the shutdown margin in case of complete TPBAR loss was $29.2, maintaining the core well below the safety and operating limits. The radial fission heating distribution resulted in a power peaking factor of 1.76.

The thermal hydraulic analysis resulted in values for mass flow rate, departure from nucleate boiling ratio (DNBR), maximum fuel and cladding temperature, and an analysis proving that natural circulation is unaffected in a modified HI-SMUR core. The mass flow rate is 793 kg/s. This is within 5% of the predicted flow rate from Holtec technical documents. The departure from nucleate boiling ratio is 1.94, this is well above the acceptable limit of 1.3. The maximum fuel temperature is 745 degrees Celsius, and the maximum cladding temperature is 327 degrees Celsius. Both of these values are well within the operating limits as discussed in the thermal hydraulics section. The natural circulation analysis showed that the coolant in the center

of the reactor core for the current configuration causes boiling of the coolant. However, non-dimensional parameters were used to evaluate an unmodified and modified reactor core at some arbitrary power. This resulted in a conclusion that the natural circulation without TPBARs is almost identical to the natural circulation with TPBARs.

The safety analysis of this reactor shows that it has multiple redundant safety features, and, by current regulatory standards, is immune to non-mechanistic core failure. Aside from sabotage, the reactor, nor the TPBAR cladding would ever reach a dangerous temperature.

The economics analysis resulted in values for the differential cost of adding TPBARs to the HI-SMUR. These values were compared to estimates for the cost of producing tritium in WBN1, the current production location. The price of TPBARs per year in the HI-SMUR is $10,240,000. The price of TPBARs per year in WBN1 is $11,306,666. It is clearly less expensive to produce tritium in multiple HI-SMUR units; however, this does not take into account electricity production. Four HI-SMUR units would be necessary to produce tritium, and this would net approximately $219,000,000 per year in electricity generation. Comparatively, WBN1 nets approximately $365,000,000 per year in electricity generation. Overall, WBN1 will produce much more electricity; however, this is a secondary function of the tritium producing reactors so it should not be a problem.

The results of this project suggest a favorable recommendation be made in regards to using the HI-SMUR as a means of tritium production. The benefits of having a dedicated SMR for tritium production outweigh the increased cost of producing tritium. This project was successful in meeting its goals of producing tritium in a HI-SMUR.

1. INTRODUCTION (WRITTEN BY CLAY STRACK)

Tritium is an element needed to maintain the United States' nuclear weapon stockpile supply. The half-life of tritium is 12.3 years, which diminishes ~5% of the tritium in the nuclear weapon stockpile every year. Savannah River Site ceased production of tritium in the 1980s and in 1995, the Department of Energy (DOE) decided that it needed to resume tritium production. Two options were explored: a commercial nuclear reactor and an accelerator. Pacific Northwest National Laboratory (PNNL) was selected as the design authority for the commercial nuclear reactor program. Laboratory testing on tritium production in commercial reactors was performed from 1997-1999. After successful lab testing, the DOE selected the commercial reactor as the more viable option. Due to their experience, PNNL was selected again as the design authority for this project. PNNL is still the design authority to this day and tritium producing burnable absorber rods (TPBARs) are currently being irradiated at Tennessee Valley Authority's Watts Barr Nuclear Unit 1 (WBN1). The production goal for PNNL is 1696 TPBARs per cycle, which corresponds to approximately 1150 grams of tritium per year. PNNL is currently producing under this 1150 grams of tritium per year goal because they are limited to 704 TPBARs per cycle. This value is determined by a LOCA analysis and will be explored later. The licensing basis for WBN1 must be changed to reach the 1696 TPBARs per cycle goal. Higher tritium releases must be allowed, as well as new core designs that have acceptable reactivity margins during a LOCA prior to an increase in the allowed number of TPBARs per cycle. As a result of these factors and the fact that WBN1's license will expire in 20 years, PNNL has requested that the Texas A&M University senior design teams explore tritium production in small modular reactors (SMRs). This was the primary goal of this project, to modify an existing U.S. SMR design to see what increase in cost from an unmodified reactor would be necessary to produce

tritium in one or multiple SMRs at a rate of 1150 grams per year and to evaluate how much of the cost can be offset by electricity production.[1]

2. PROJECT BREAKDOWN (WRITTEN BY CLAY STRACK)

The project tasks were broken down as follows:

- Neutronics – Laura Sudderth
- Thermal Hydraulics – Clay Strack
- Tritium Handling and Economics – Ryan Upton
- Safety Analysis – Kevin Kapka

Each task obtained data from Holtec reactor documents and performed an analysis. The interaction between tasks can be seen below.

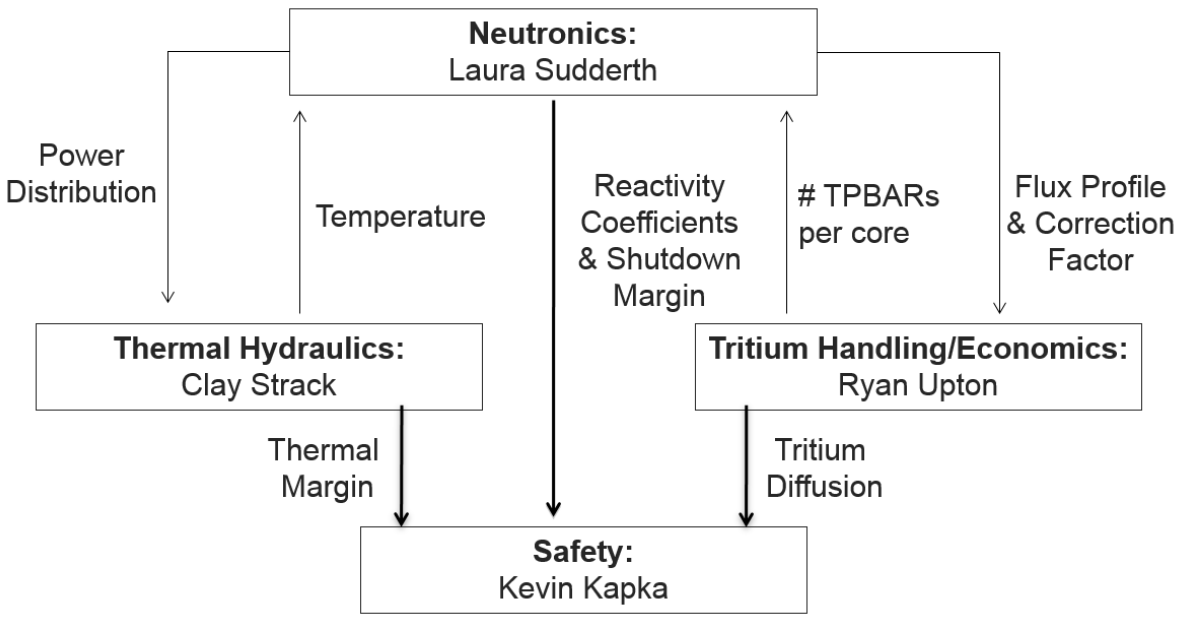

Figure 2.1. Interaction between project tasks.

It was necessary to interact between tasks to optimize the reactor core design. The LOCA safety analysis was used to impose a maximum limit on the number of TPBARs in the core. Neutronics then designed the optimal core arrangement for tritium production and cost effectiveness. Thermal hydraulics ensured that the core was operating within thermal margins.

Tritium handling and economics ensured that the amount of tritium produced was at a maximum and determined the difference in the fuel price for a HI-SMUR without TPBARs and a HI-SMUR with TPBARs. That is, the differential fuel cost with and without TPBARs.

3. REACTOR OVERVIEW (Written by Laura Sudderth)

A small modular reactor was chosen for use in this project, the Holtec Inherently-Safe Small Modular Underground Reactor (HI-SMUR). This reactor is cooled by natural convection in the primary loop. The gravity-driven circulation of the reactor coolant eliminates the need for active components, such as reactor coolant pumps and does not rely on off-site power to shut down the core or for long-term heat removal, making it a passive system. The core is contained 100 feet underground, as shown in Fig. 3.1, with all critical components, such as the steam generator and control rod drive system, accessible outside the reactor vessel as shown in Fig. 3.2. The reactor vessel is restrained to the surface of the reactor well at the bottom by a seismic restraint system, shown in Fig. 3.3. Key system parameters of the HI-SMUR are shown in Table 3.1.[2]

The core has an operating cycle of 3 years before refueling. It is loaded and refueled as a single unit, shown in Fig. 3.4, consisting of 32 full-length PWR fuel assemblies with the standard 17x17 array, lower and upper support grids, and an outer support structure to allow for handling of the cartridge. The steam system consists of two once-through steam generators with external superheaters to dry the steam produced to ensure high efficiency, shown in Fig. 3.5. Hot water enters the first steam generator, supplying steam for the high-pressure turbine, and then passes to the second steam generator where it generates steam for the low-pressure turbine.[2]

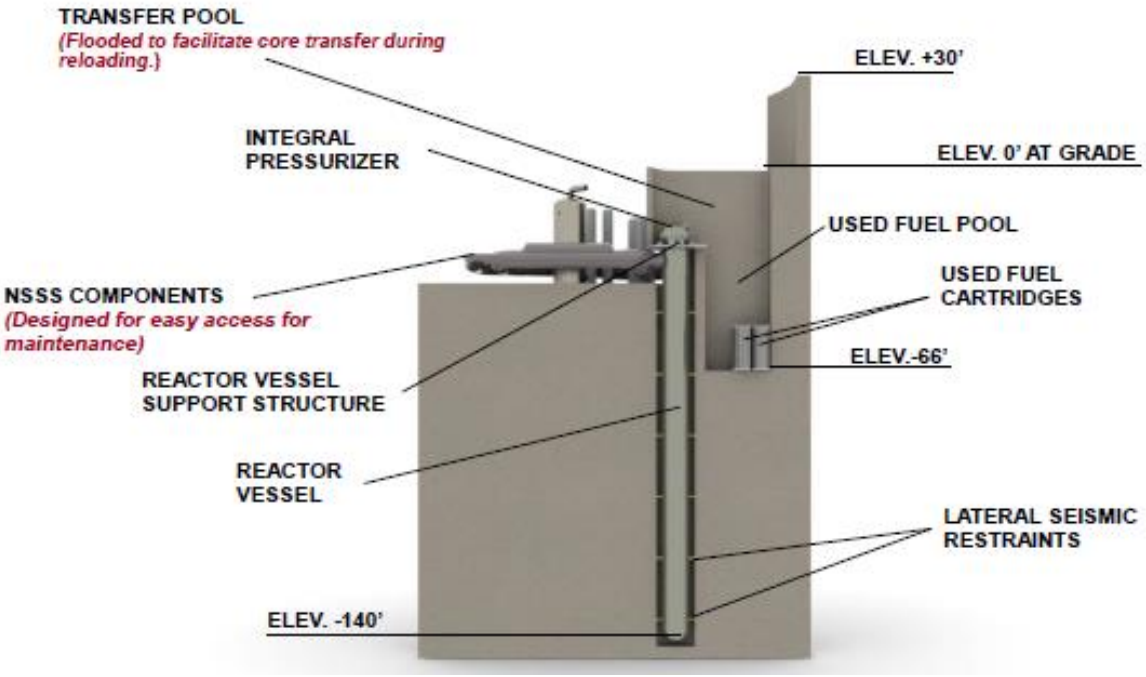

Figure 3.1. HI-SMUR reactor containment.[3]

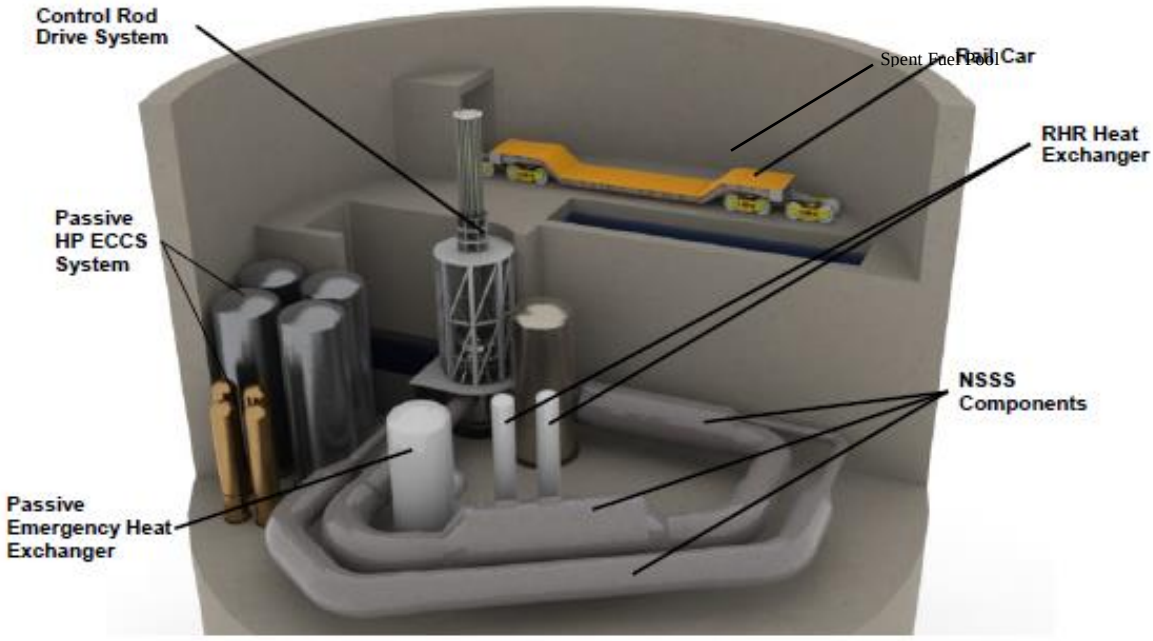

Figure 3.2. External Hi-SMUR systems.[3]

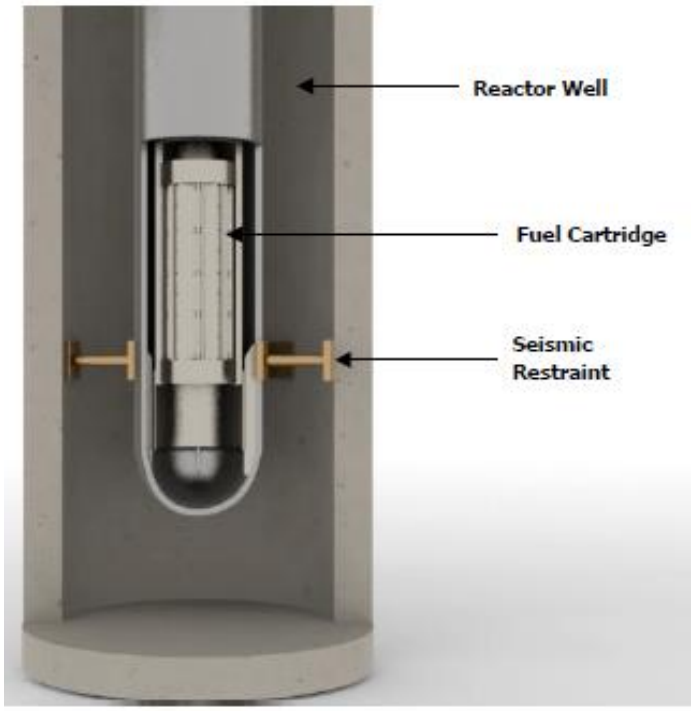

Figure 3.3. Reactor vessel restraints.[2]

Table 3.1. HI-SMUR key parameters.

Key System Parameters	Data	Units
Number of fuel assemblies in the core	32	
Nominal thermal power	446	MWt
Nominal recirculation rate	6	MLb/h
Reactor water outlet temperature	575	deg. F
Reactor water inlet temperature	350	deg. F
Reactor pressure	2250	PSIA
Water in the RV cavity	42000	gallons

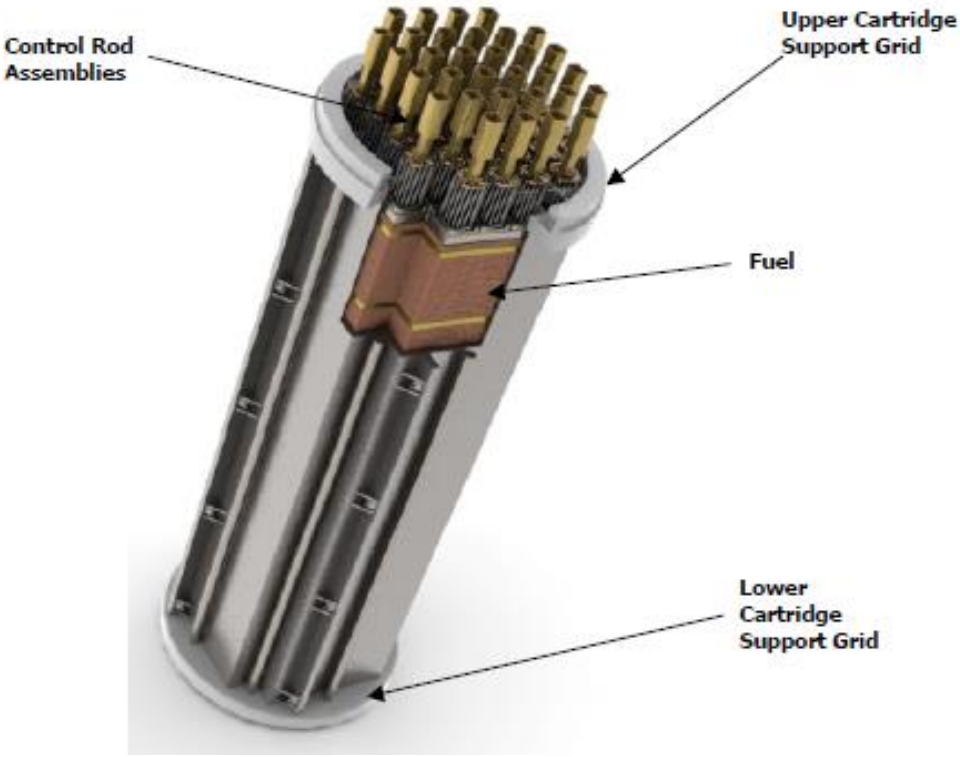

Figure 3.4. HI-SMUR core cartridge.[2]

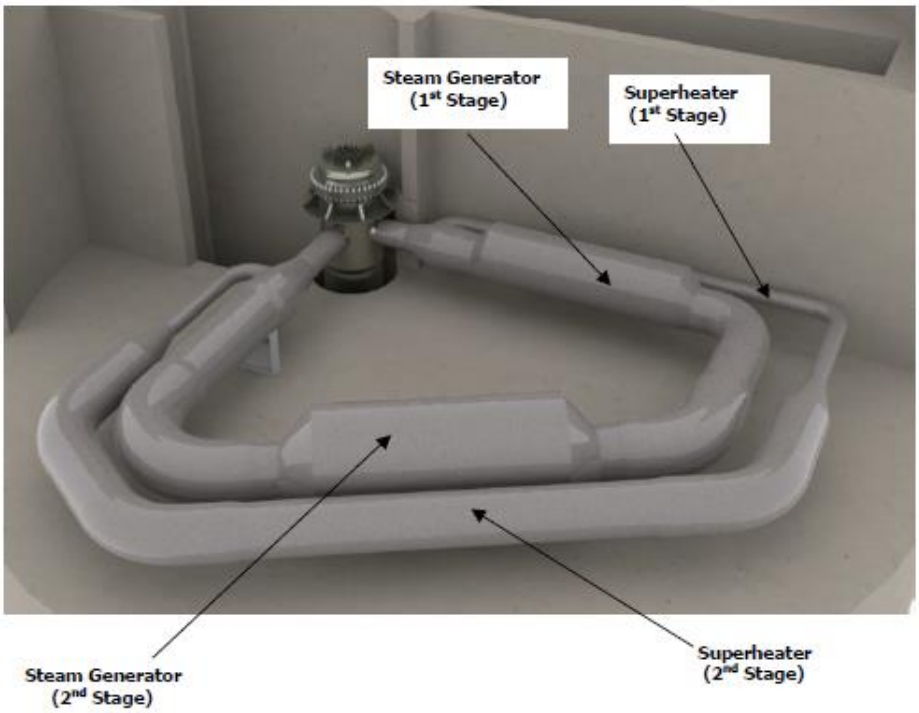

Figure 3.5. HI-SMUR steam system.[2]

4. NEUTRONIC ANALYSIS (Written By Laura Sudderth)

4.1 Overview

The objective of the neutronics analysis is to modify the layout of the HI-SMUR core and determine the locations of the TPBARs in the core to meet the tritium production goal. This process involves iteration with the thermal hydraulics, tritium production, and safety analyses as shown in Fig. 4.1. In order to simplify the analysis and iteration processes, certain parameters of the reactor were assumed to be constant. The key parameters in the analysis are shown in Table 4.1. The neutronics analysis was performed using MCNP5 and a modified HISMUR core.

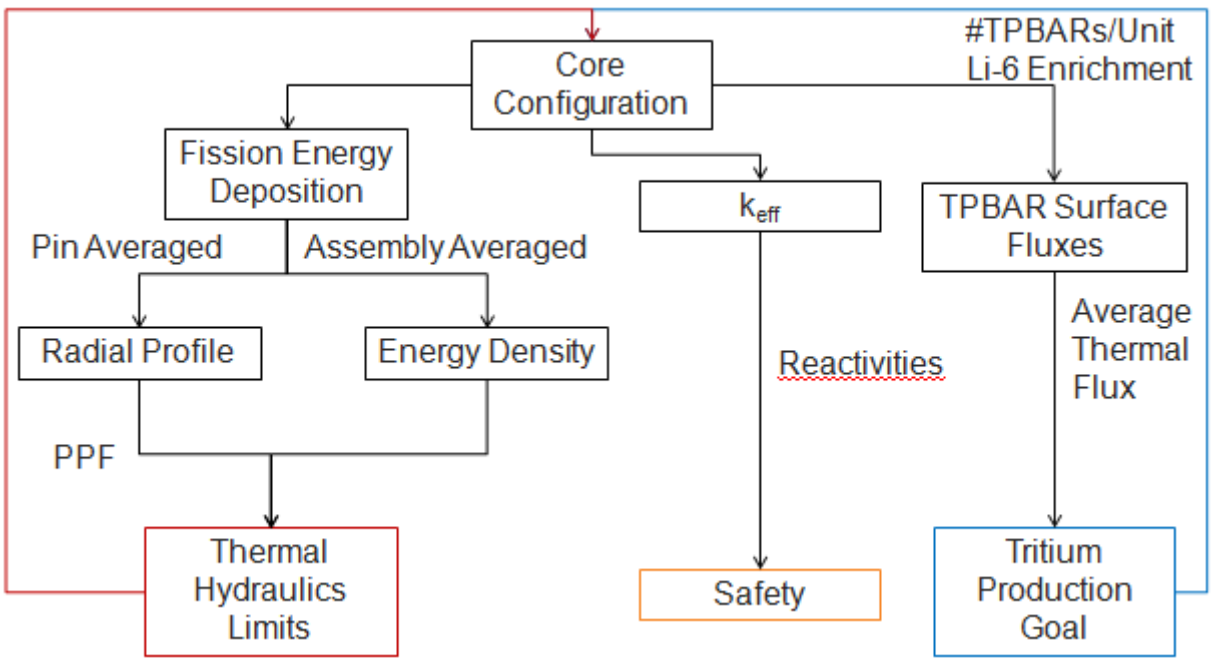

Figure 4.1. Neutronic analysis parameters and iteration.

Table 4.1. Neutronic analysis key parameters.

Parameter	**Type**	**Value**
Core Dimensions	Control	L = 4 m, 17 x 17, 32 Assemblies
# Control Rods	Control	25 per Assembly
Fuel Composition	Control	4.95%
Temperature	Input – TH	Inlet= 180 C Range= 180C and 340C Fuel T = 900K
Power	Input – TH	469 MW_{th}
TPBAR Composition	Optimize	7.5-93% Li 6
# TPBARS/Unit	Optimize	TBD
Excess Reactivity[4]	Limiting - Safety	> $2
Shutdown Margin[4]	Limiting - Safety	> $6

4.2 Core Model

The dimensions of the HI-SMUR core are considered proprietary information, so the core was modeled after the NuScale SMR, as shown in Fig. 4.2 and modified to HISMUR criteria. The length of the HISMUR core is approximately twice that of NuScale with 32 assemblies, each containing 25 control rods.[5] The fuel rod and assembly dimensions are that of a standard PWR. The Tritium Producing Burnable Absorber Rods (TPBARs) were modeled after the design from PNNL, shown in Fig. 4.3.[6] The core specifications are listed in Table 4.2. The Tritium Producing Burnable Absorber Rods (TPBARs) were modeled after the design from PNNL, shown in Fig. 4.3.[6] The cladding and getter was homogenized according to PNNL modeling criteria, shown in Table 4.3, and the annulus was filled with helium. All dimensions not available from PNNL were assumed.[7] The number of TPBARs and enrichment of Li-6 was determined by iterating the core-averaged thermal flux within the lithium aluminate pellets with the Tritium Production Model as discussed in Section 6.3. Since the radial distribution of the flux is not directly accounted for in

the Tritium Production Model, the TPBARs were evenly distributed throughout the assembly. For simplicity, all assemblies in the core are identical. The resulting core model is shown in Figs. 4.4 and 4.5.

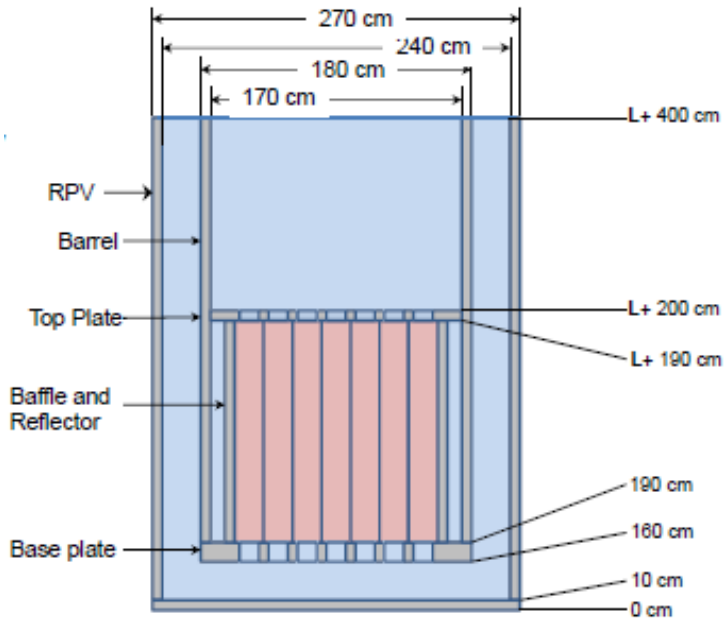

Figure 4.2. Reference model of the NuScale reactor.[5]

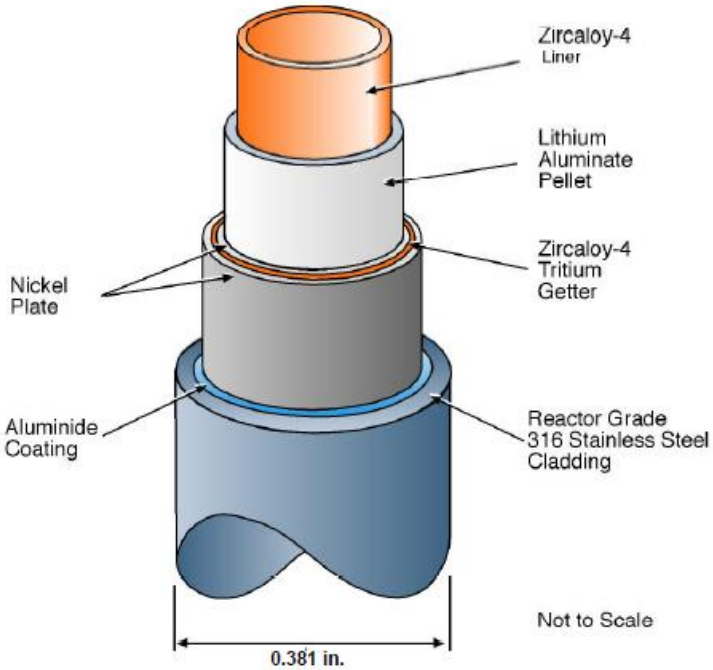

Figure 4.3. Reference model of the TPBARs.[6]

Table 4.2. Core specifications.

Core Parameters	
Core Active Length (m)	4
Core Radius (cm)	80
Number of Assemblies	32
Pressure Vessel and Barrel Material	SS-316
Assemblies	
Grid	17 x 17
Assembly Pitch (cm)	21.5
Control Rods	25
TPBARs	24
Fuel Pins	
Fuel Rod Pitch (cm)	1.265
Fuel Rod Radius (cm)	0.409
Cladding Inner Radius (cm)	0.418
Cladding Outer Radius (cm)	0.475
Fuel Enrichment	5%
Cladding Material	Zircaloy-4
Fuel Temperature (K)	900
Control Rods	
Absorber Radius (cm)	0.43
Cladding Outer Radius (cm)	0.48

Table 4.3. TPBAR parameters.

TPBARs	
Zircaloy Liner Inner Radius (cm)	0.1
Li Aluminate Inner Radius (cm)	0.112
Li Aluminate Outer Radius (cm)	0.384
Cladding Outer Radius (cm)	0.484
Li-6 Enrichment	12.2%
TPBAR Homogenized Cladding Material Number Densities[7]	
Cr (Atoms/b-cm)	8.2004E-03
Fe (Atoms/b-cm)	2.8330E-02
Ni (Atoms/b-cm)	2.7095E-02
Mo (Atoms/b-cm)	6.3490E-04
Mn (Atoms/b	6.6525E-04
Zr (Atoms/b-cm)	9.7431E-03

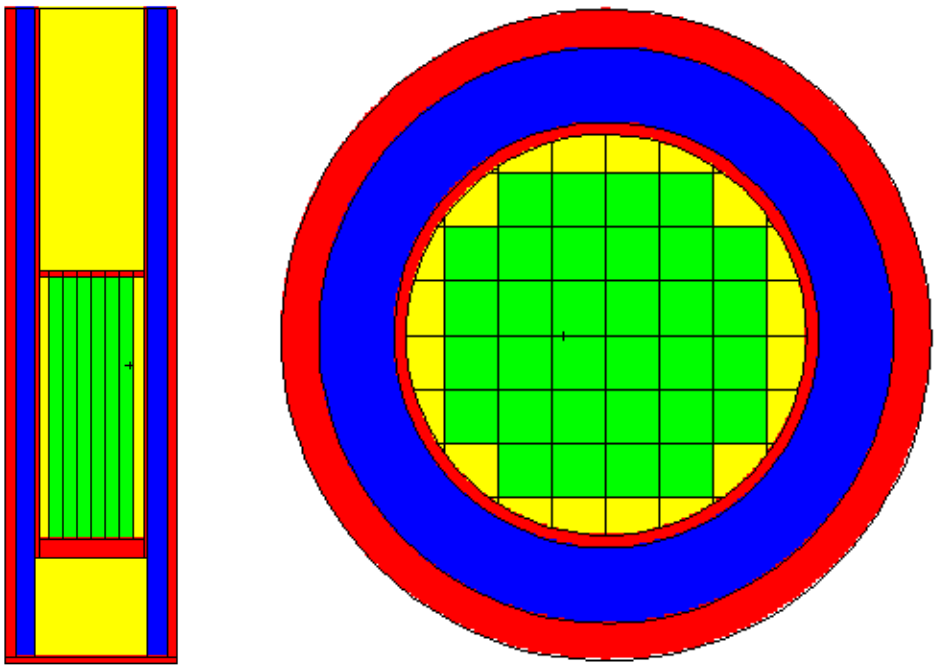

Figure 4.4. (Left) Axial Core Cross-Section and (Right) Radial Core Cross-Section. The models show identical assemblies (Green), moderator (yellow), core barrel and pressure vessel (red), and air gap (blue).

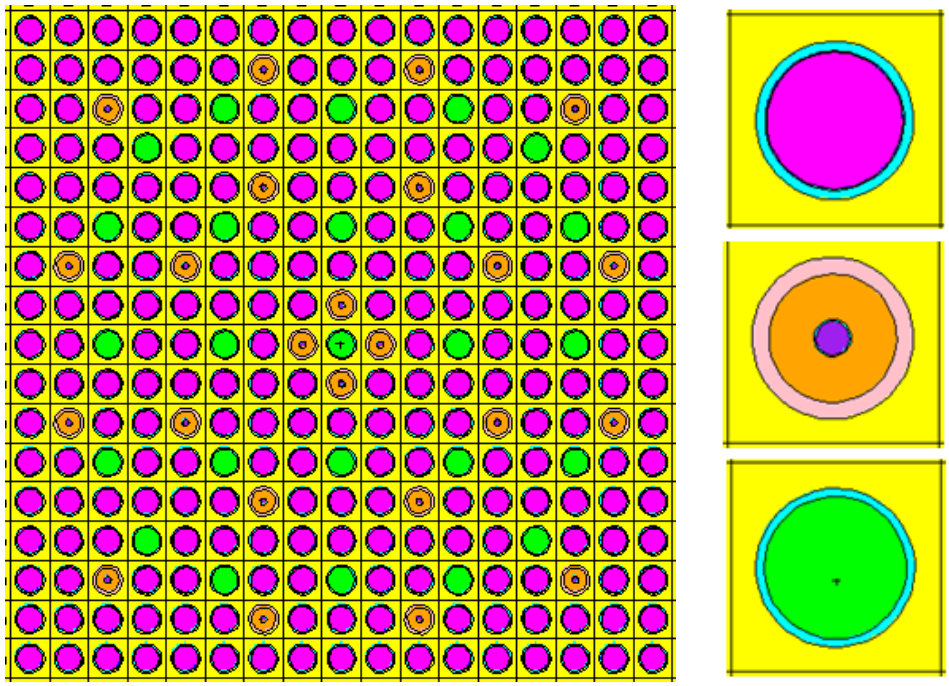

Figure 4.5. (Left) Assembly Configuration, (Right top) Fuel Pin, (Right Middle) TPBAR, and (Right Bottom) Control Rod.

4.3 Tritium Production

The tritium production rate was calculated and compared by using two methods. The first method used MCNP5 to calculate to the thermal neutron flux radial variations in the lithium pellet and iterate with the Tritium Production Model, described later in this report. This was used to determine the number of TPBARs required in each assembly to meet the goal because it accounted for depletion of lithium. The second method utilizes a cell averaged flux tally in MCNP5 coupled with a neutron reaction multiplier, not accounting for depletion, to compare with results from the Tritium Production Model.

4.3.1 TPBAR Surface Flux Tallies

The radial distribution of the flux was measured using an F2 surface flux tally along 4 evenly distributed surfaces in the lithium pellet of the TPBAR, shown in Fig, 4.6, averaged throughout the core. As the geometry of the core is input into MCNP using repeated structures,

the total surface area of each surface was input manually using and SD2 card. The tally was divided into energy bins using an E2 card, allowing for calculation of the thermal, fast, and total flux.[8] A rise in the total flux at the inner surface of the TPBAR due to the scattering of fast neutrons was observed in the helium annulus. This phenomena was not observed in the thermal region (below 0.025 eV), and only the thermal flux was considered in the calculations for tritium production. A sample of the tally input is shown below, where 302, 305, 306, 303 are the tally surfaces.

```
c TALLIES
F2:N 302 305 306 303        $part/cm2
SD2 215216.7 390227.4 565238.2 740306.8
E2 .000000025 20
```

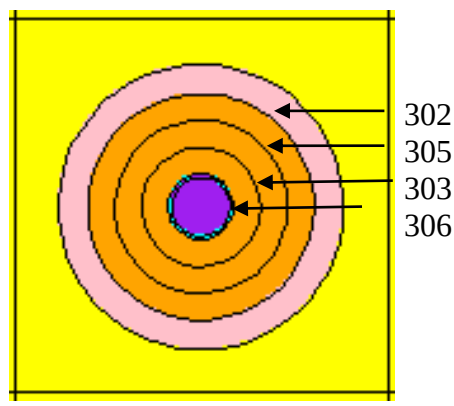

Figure 4.6. MCNP5 model of the TPBAR for surface flux calculations.

The flux was measured with the control rods fully withdrawn in units of neutrons/cm^2. In order to get the output in useable units, the flux was normalized with the power using Eq. 4.1, where S is the neutron source strength, P is the thermal power of the reactor, C is a unit conversion factor, and ν is the number of neutrons produced per fission.[8] At 469 MW_{th}, the source strength was calculated to be 4.221x10^{19} n/s. The radial distribution, shown in Fig. 4.7 was fitted with an exponential function and integrated to determine the average thermal flux, and

input into the Tritium Production Model to calculate the enrichment of Li-6 and number of TPBARs each assembly required to meet the production goal.

$$S = P\,(W) \times C\left(\frac{fiss}{W \cdot s}\right) \times \bar{\nu}\left(\frac{n}{fiss}\right) \tag{4.1}$$

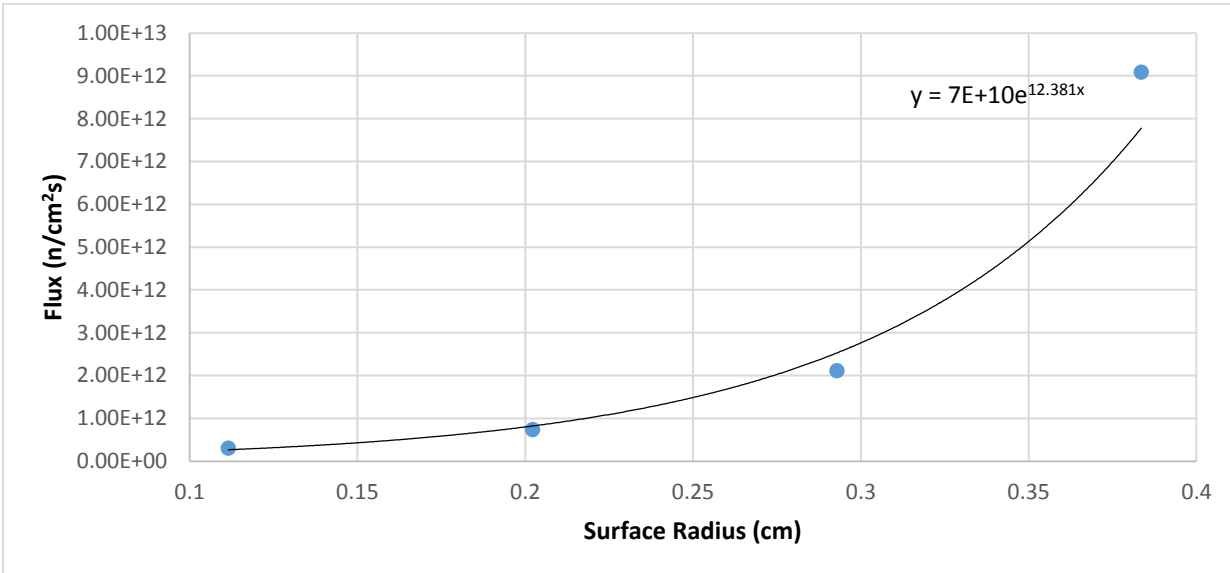

Figure 4.7. Radial distribution of the thermal flux in a TPBAR.

4.3.2 Cell Averaged Flux Tally

The volume-averaged flux in the lithium pellet of the TPBAR was measured using and F4 cell average flux tally and averaged throughout the core with control rods inserted and withdrawn. This was coupled with an FM4 multiplier for the atomic density, in $^{a}/_{barn \cdot cm}$, the material number, and code for the (n,t) reaction.[9] Similar to the previous method, an SD4 card was used to input the volume of the repeated structure for the tally. A sample of the tally input is shown below, where 302 is the cell containing lithium aluminate. The tritium production rate was calculated by Eq. 4.2, where T is the tally output of the total amount of tritium produced, S is the source strength from the power normalization as previously discussed, MW is the molar weight of tritium, and N_A is Avogadro's number. The results are shown in Table 4.4.

```
C TALLIES
F4:N 302
SD4 129970.3
FM4 0.0239 7 105
```

$$Tritium\ Production\ Rate\ \left(\frac{g}{cm^3 \cdot s}\right) = \frac{T\left(\frac{a}{cm^3}\right) MW\left(\frac{g}{mol}\right) S\left(\frac{n}{s}\right)}{N_A\left(\frac{a}{mol}\right)} \tag{4.2}$$

Table 4.4. Tritium Production Results from MCNP5 F4 Tally.

Quantity of Interest	**Value**
Amount of Tritium Produced (a/cm^3)	2.00x10^{-7}
Tritium Production Rate (g/unit - year)	694.48

4.4 Energy Profiles

The energy profiles in the core were obtained using MCNP5 with control rdos fully withdrawn for use in the thermal hydraulics analysis. The energy profiles in the core were obtained using an F7 fission heating tally and an SD7 card to input the volume of fuel in the cells for repeated structures. The output, in MeV/g, as converted to W/cm^3 using the power normalization and conversion factors combined in an FM7 card.[8] The structure in which the energy was averaged was dependent on the application of the results.

4.4.1 Single Fuel Pin-Averaged

In order to calculate the power peaking factor, the energy deposition averaged in a single fuel pin was measured at radially distributed locations in the core. Fig. 4.8 shows the energy deposition in the fuel with respect to location of the center of the fuel pin. The corresponding power peaking factor is 1.76.

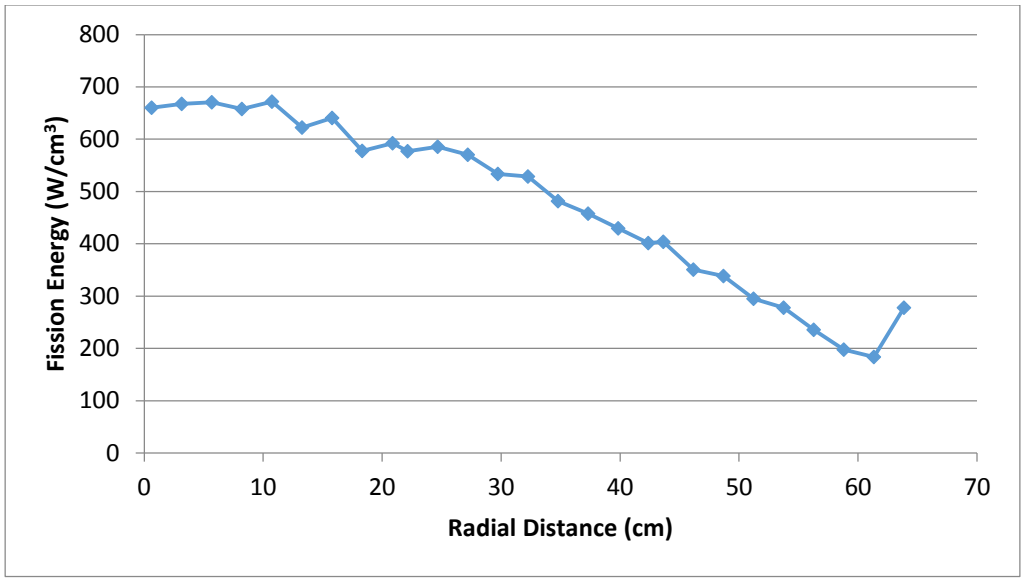

Figure 4.8. Radial energy distribution.

4.4.2 Assembly- Averaged

In order to compare assemblies in the modified and unmodified HISMUR core, the energy deposition was measured as an average in an assembly. Assuming 1/8 symmetry of the core, only 5 assemblies were tallied. The results are shown in Figs. 4.9 and 4.10.

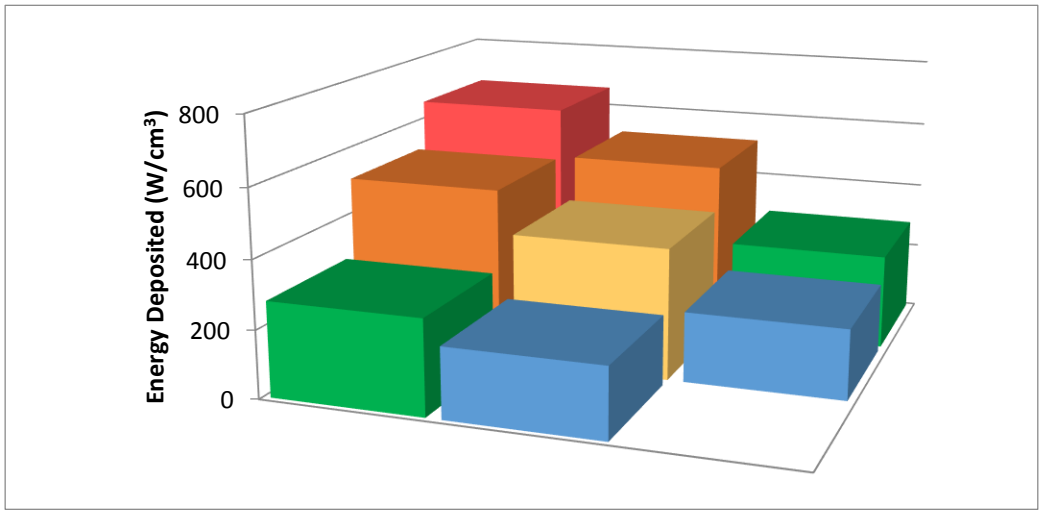

Figure 4.9. ¼ of modified HI-SMUR core.

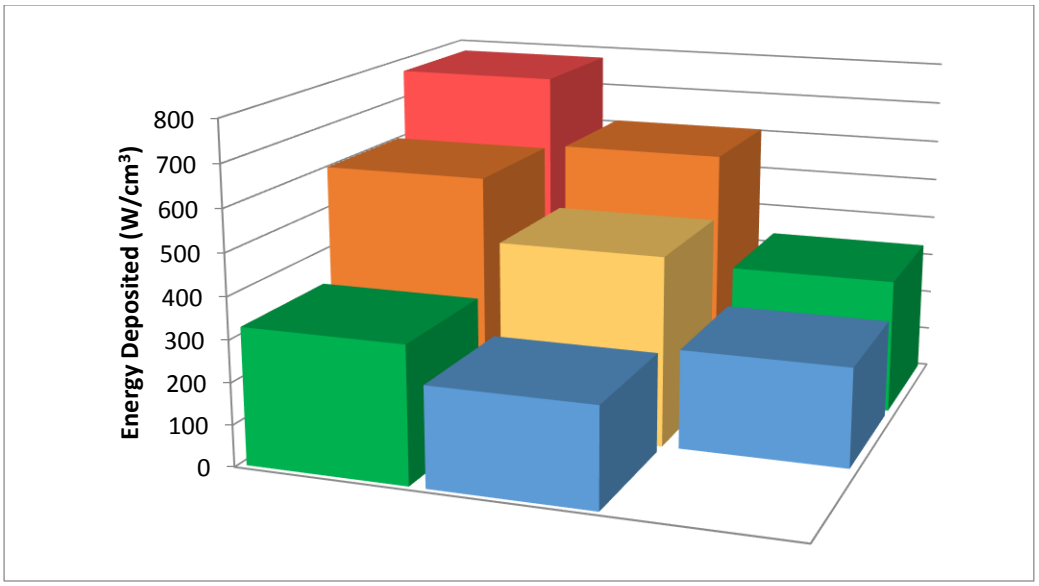

Figure 4.10. ¼ of the original HI-SMUR core.

4.5 Criticality and Reactivity

The effective multiplication factor, k_{eff}, and standard deviation, σ, was calculated at the beginning of life using the kcode card with 100,000 histories with 50 skipped cycles and 100 active cycles. The neutron source was designated in a central fuel cell using a ksrc card, as shown in the section of code shown below. In order to determine the excess reactivity in the modified HISMUR core, the k_{eff}, was calculated with the control rods fully withdrawn and fully inserted, and the shutdown margin in the modified core was calculated using the k_{eff} with rods fully inserted. The k_{eff} was also calculated in the unmodified HISMUR core to determine the amount of negative reactivity introduced by TPBARs. The last condition analyzed was the modified core with TPBARs removed and replaced with water to ensure shutdown capability without TPBARs present. The reactivities, ρ, were calculated using Eqs. 4.3-4.6, where the delayed neutron fraction of U-235, β, is 0.0065. The results are shown in Table 4.5 and 4.6.

```
c DATA CARDS********************
mode    n
kcode     100000  1  50  150
ksrc     0.6 0.6 390
```

$$\rho = \frac{k_{eff} - 1}{k_{eff}} \tag{4.3}$$

$$\rho\ (\$) = \frac{\rho}{\beta} \tag{4.4}$$

$$\rho_{TPBAR}(\$) = \frac{\rho_{Mod}(\$) - \rho_{Unmod}(\$)}{N_{TPBARs}} \tag{4.5}$$

$$Rod\ Worth\ (\$) = \frac{\rho_{out}(\$) - \rho_{in}(\$)}{N_{Control\ Rods}} \tag{4.6}$$

Table 4.5. Core neutronic properties.

Core Configuration	keff	σ
Modified, Rods Inserted	0.7393	0.00027
Modified, Rods Withdrawn	1.23943	0.00024
Unmodified, Rods Withdrawn	1.43502	0.0002
Unmodified, Rods Inserted	0.87479	0.00025
Modified, No TPBARs	0.84065	0.00025

Table 4.6. Calculated reactivities.

	ρ
Excess Reactivity ($)	29.72
Shutdown Margin ($)	54.25
Control Rod Worth ($)	0.10
TPBAR Worth ($/TPBAR)	0.04
Shutdown Margin without TPBARs	22.02

4.6 Discussion and Future Work

Due to time constraints, the depletion calculations were not performed in this analysis. To obtain more accurate flux distributions over the cycle lifetime, either MCNPX or CASMO should be used to account for burnup of the fuel. Furthermore, when the control rods were partially removed from the core in MCNP, the code started behaving unexpectedly and would not converge on the k_{eff}. This phenomena was not observed when the rods were either fully inserted or removed. Therefore, the analysis was performed with either the control rods fully inserted or removed, depending on the parameter of interest, and the tally results don't accurately reflect the behavior of an operating core. Further work is required to determine the source of the behavior and correct it to proceed with the analysis.

5. THERMAL HYDRAULICS (WRITTEN BY CLAY STRACK)

5.1 Overview

The purpose of the thermal hydraulic analysis is to evaluate natural circulation in the HI-SMUR reactor to ensure that normal operating conditions can be maintained with the addition of TPBARs in the reactor core. The primary objective was to ensure that thermal margin is maintained at steady-state operation. Namely, mass flow rate, DNBR, and peak temperatures must all be maintained within design limits. The primary side was evaluated with natural circulation models. The initial model was extremely simple and was able to calculate the mass flow rate in the core within 5% of the known correct value. The following, more complex models, also calculated mass flow rate to a very similar accuracy. The DNBR model proved that the modified HI-SMUR core can still operate well within critical heat flux constraints. Also, the peak temperature analysis yielded acceptable maximum fuel temperatures. Overall, the thermal hydraulic analysis was able to show that the core could successfully operate safely and within thermal design limits with the addition of an optimum number and arrangement of TPBARs.

5.2 Natural Circulation Model

5.2.1 Theory

Natural circulation is a phenomenon that occurs when a fluid in a closed system, a reactor in this specific case, is heated at some vertical location and subsequently cooled at a higher vertical location. The addition of heat from the reactor core to the primary coolant system causes the density of water to decrease because density decreases as temperature increases in liquid water. Subsequently, when the primary coolant system is cooled in the steam generator, the density of the water coolant increases. This heating and subsequent cooling results in a maintained density difference across the height of the natural circulation loop, the reactor core.

The density difference, under the effects of gravitational acceleration, produces a driving head, causing the primary coolant to flow. A simple natural circulation loop can be seen below in Fig. 5.1.

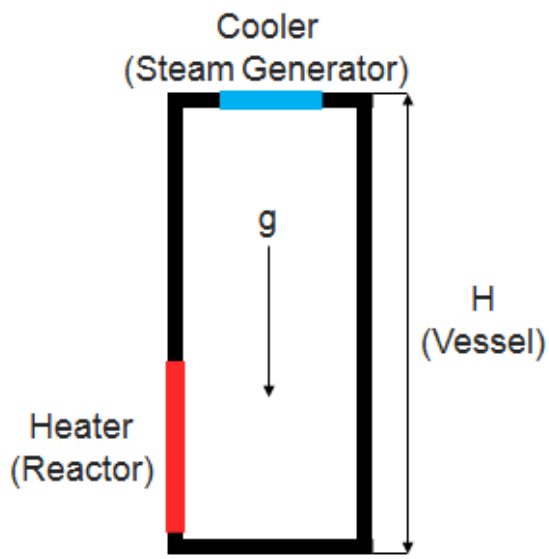

Figure 5.1. The general setup of a simple natural circulation loop.

As one can clearly see, a driving head will be produced in this natural circulation loop by the phenomena described previously.

After understanding the governing phenomena of natural circulation, it becomes necessary to evaluate how powerful the driving head actually is. The driving head will produce a mass flow rate through the primary coolant loop, and this is the quantity of interest for this analysis. By evaluating the mass, momentum and energy balance equations over a control volume in the reactor pressure vessel volume, a flow rate for the coolant water can be calculated. The natural circulation loop in the reactor itself can be seen in Fig. 5.2.[2]

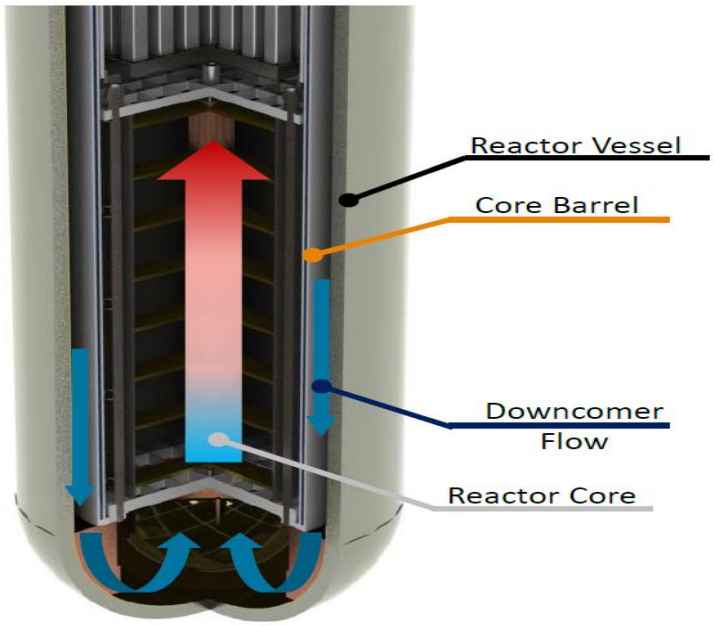

Figure 5.2. Natural circulation flow through the downcomer and up through the core.

Several assumptions are necessary to simplify this natural circulation analysis[1]:

- One-dimensional axial flow (fluid properties at a given cross-section are uniform)
- Boussinesq approximation is applicable
- Incompressible fluid
- Constant inlet temperature
- Form losses dominate the loop resistance

The Boussinesq approximation needs further justification, especially for those who are unfamiliar with natural circulation.

The Boussinesq approximation is the typically applied assumption to natural circulation loops, so it will be applied for the HI-SMUR analysis. This approximation states that density differences within the natural circulation loop are small enough that they can be neglected unless they are multiplied by the gravitational acceleration of the earth. This is an advantageous approximation because it allows one to consider a single reference density throughout the natural

circulation loop, as opposed to solving for density at each subsequent temperature throughout the length of the loop.

Prior to evaluating the natural circulation loop, the flow conditions must be understood. In natural circulation, turbulence is defined by the Grashof number, similar to the Reynolds number in forced convection. Above a Grashof number of 10^9, a turbulent flow condition exists.[14] This is the threshold of interest for this analysis. Turbulent flow conditions are most desirable for thermal hydraulics because it prevents high form losses and allows for higher heat transfer. The Grashof number is defined as follows:

$$Gr_m = \frac{D^3 \rho_0^2 \beta g \Delta T_r}{\mu^2} \tag{5.1}$$

where

Gr_m	modified Grashof number
D	hydraulic diameter
ρ_0	reference density
β	thermal expansion coefficient
g	gravitational acceleration
μ	dynamic viscosity
ΔT_r	reference temperature difference

and ΔT_r has a functional representation

$$\Delta T_r = \frac{Q_h H}{A \mu c_p} \tag{5.2}$$

where

Q_h	total heat rate
H	loop height

A flow area

c_p specific heat

It is also necessary to define the equation for hydraulic diameter.

$$D = \frac{4A}{P} \tag{5.3}$$

where

A cross sectional area

P wetted perimeter

One portion of natural circulation that will not be explored in this analysis is stability. Stability is an issue that one must be aware of in natural circulation loops. In a two-phase flow regime, natural circulation loops are susceptible to flow oscillations that perturb the system and prevent predictable cooling of the system.[3] It is of note that this may occur in an accident scenario if vapor forms in the primary. Stability analysis is extremely complex and beyond the scope of this project; however, the reader should be aware that recommendations made in this analysis do not take stability into account because the primary is in single phase, as will be confirmed in further analyses.

5.2.2 Analysis/Methodology

To begin a natural circulation analysis, one must solve the conservation of momentum and energy equations. The conservation of energy equation, integrated over the natural circulation loop of interest, is as follows[1]:

$$c_v m \frac{dT}{dt} = \dot{m} c_p (T_H - T_C) - \dot{Q}_{SG} - \dot{Q}_{loss} \tag{5.4}$$

where $\frac{dT}{dt} = 0$ because it is assumed that the reactor is operating at steady state and also, $\dot{Q}_{loss} = 0$ because the system is assumed to be well insulated and heat losses through the pipes are negligible. The above equation then simplifies to:

$$\dot{Q} = \dot{m} c_p \Delta T \tag{5.5}$$

which is the general equation that one may recognize.

where

$\dot{Q}$ heat generation rate

$\dot{m}$ mass flow rate

c_p specific heat of the coolant (assumed to be constant and determined at the inlet conditions)

ΔT temperature rise across the core

This will allow for calculations of the temperature rise through the core at a given reactor power level. Also, using known or approximated values for the temperature rise across the core, one can confirm that the mass flow rate obtained from the conservation of momentum equations is correct.

Similarly, the steady state conservation of momentum equation, integrated over the natural circulation loop of interest, is as follows[3]:

$$g \rho_0 \beta \oint T dz = \sum_{i=1}^{N_t} \left(\frac{f_i L_i}{D} \right) \frac{W_{ss}^2}{2 \rho_0 A^2} \tag{5.6}$$

This equation can be simplified into an easily solvable form.

$$g \rho_0 \beta \left(\frac{Q_h H}{W_{ss} c_p} \right) = \sum_{i=1}^{N_t} \left(\frac{f_i L_i}{D} \right) \frac{W_{ss}^2}{2 \rho_0 A^2} \tag{5.7}$$

where

z vertical coordinate

W_{ss} mass flow rate

N_t total number of pipe segments

f_i friction factor of given pipe segment

L_i length of given pipe segment

A formula was necessary to accurately calculate the friction factors for each relevant pipe segment. The Darcy friction factor formula was used.[5]

$$\frac{1}{\sqrt{f}} = -2log_{10}\left(\frac{\epsilon}{3.7D} + \frac{2.51}{Re\sqrt{f}}\right) \tag{5.8}$$

where

f friction factor

ϵ roughness height

Re Reynolds number

This equation was solved using the goal seek function in Excel.

These sets of equations were solved to complete a mass flow rate thermal hydraulic analysis of the HI-SMUR reactor core. An Excel document was created for the purposes of thermal hydraulic analysis. Initially, all unknown quantities had to be solved for using known reactor conditions and parameters prior to solving for the mass flow rate and the outlet temperature of the coolant. The flow of the excel document is as follows

- Define reactor conditions (obtained from Holtec data)
    - Inlet temperature
    - Primary pressure
- Calculate needed parameters for the analysis
    - Flow area

    - Thermal expansion coefficient
    - Reference density
    - Friction factor
    - Pipe segment lengths
    - Hydraulic diameter
    - Specific heat
- Assume lengths that are not specified in the Holtec documents
    - Steam generator length
    - Length of primary loop outside the vessel
- Input parameters from neutronics
    - Thermal power
- Determine mass flow rate
- Using an assumed inlet flow temperature designated in the Holtec technical presentation, determine the core outlet temperature

An example calculation can be seen in Table 5.1.

Table 5.1. Mass flow rate value for fully turbulent primary coolant system.

Parameter	Calculated Value	Units		
Cold Leg				
D	2.05725	m		
Flow Area	4.432030699	m^2		
Re	2235148.87			
viscosity	0.000157	Pa-s		
L	47.95	m		
Friction Factor	0.101625889			
D-W	-0.000589145			
Heat Exchanger				
D	2.05725	m		
Flow Area	4.432030699	m^2		
Re	3161426.779		**Mass Flow Rate**	**Units**
viscosity	0.000111	Pa-s	**793.0033323**	**kg/s**
L	20	m		
Friction Factor	0.101623691			
D-W	-0.000589907			
Reactor				
D	1.3715	m		
Flow Area	0.8785	m^2		
Re	10632927.75			
viscosity	0.000111	Pa-s		
L	4.058	m		
Friction Factor	0.101619963			
D-W	-0.000591199			
Hot Leg				
D	1.3715	m		
Flow Area	1.477343566	m^2		
Re	8579911.309			
viscosity	0.0000818	Pa-s		
L	32.522	m		
Friction Factor	0.101620341			
D-W	-0.000591068			

5.2.3 Results

A simple natural circulation model yielded extremely promising results. The flow areas were calculated using dimensions from neutronics. A sample calculation can be seen below:

$$A_c = N_a P^2 - \pi r_{pin}^2 N_p \tag{5.9}$$

where

A_c core flow area

N_a number of assemblies

P assembly pitch

r_{pin} fuel pin radius

N_p number of fuel pins

A similar calculation can be performed for the other flow areas, using appropriate dimensions from the neutronics analysis. The hydraulic diameters were taken from the Holtec documents, where provided, and assumed otherwise. Assuming a constant diameter pipe, the simplest model predicted an outlet temperature of 317 °C, while the actual value predicted by Holtec is 300 °C.[2] Likewise, accurate results were obtained for the mass flow rate. The predicted mass flow rate was found to be 792.73 kg/s while the actual mass flow rate is 756 kg/s. The simple analysis yielded results within 5% of the actual predicted values by Holtec. A more complex analysis was completed that predicted a mass flow rate of 793.00 kg/s and the same outlet temperature. The excel document for this analysis can be seen in the appendix. Although these numbers are slightly over-predicting, this is to be expected because the analysis used assumes form losses as the dominating pressure drops. There are other pressure drops in the system that are not accounted for, so the model would not be able to predict the flow rate much more accurately.

5.2.4 Future Work

A successful, fairly simple natural circulation model was created. Many simplifying assumptions were made; however, a more detailed analysis would be desirable for thermal hydraulic verification. Discretizing the entire core or using a verified thermal hydraulic code to supplement these results is recommended. An unmodified HI-SMUR has already been analyzed by Holtec and has been determined safe. The modified core, including TPBARs, should also pass similar rigorous testing prior to implementing TPBARs in the reactor core. RELAP could be used to verify the results from the natural circulation model and obtain more detailed analyses; however, there was insufficient time left in the semester to successfully analyze the HI-SMUR core using RELAP after developing this analysis.

5.3 Assembly Averaged Model

5.3.1 Theory

An assembly averaged analysis was performed to determine the effects of adding TPBARs to the reactor core. This was determined as the best approach because each assembly should have a fairly constant power level throughout, and it is much more efficient to evaluate on the assembly level than on the subchannel level. Also, the coolant flowing through individual subchannels in the same assembly should have similar, if not identical properties because of radial mixing in each individual assembly. As natural circulation depends on density differences that occur due to heating of the fluid, one may reasonably expect that assemblies with differing power levels may have non-negligible density differences that cause flow to prefer the hotter assemblies because of a larger density difference. To determine if this is the case, unmodified and modified HI-SMUR cores were evaluated and density differences between assemblies were compared to one another. The goal was to determine if the density differences between

assemblies would have some sort of preferential flow effect on the natural circulation through the reactor core.

5.3.2 Analysis/Methodology

To perform this analysis, the conservation of energy equation was to be employed. Given an assembly averaged heat rate, the outlet temperature for each individual assembly could be found. This can be seen in the below equation:

$$\dot{Q} = \dot{m} c_p \Delta T \tag{5.10}$$

After finding the outlet temperature for each assembly, the density at the outlet of the assembly could be found using tables of water properties. The density at the inlet of the assembly was assumed to be constant, because mixing in the lower plenum of the reactor pressure vessel should ensure that the coolant has a uniform temperature prior to entering the core.

The mass flow rate was taken from the thermal hydraulic analysis used previously, and the outlet temperatures for each individual assembly were calculated. These values corresponded to a density for the coolant at the top of the fuel assembly. Density values for water at reactor conditions and the specified outlet temperature were then compiled in a table. After compiling the density values, the plan was to evaluate differences between the hot and cold assemblies using a simple difference formula.

5.3.3 Results

The neutronics results yielded unfavorable results for this analysis. The coolant was found to be boiling in the center of the core. The boiling temperature of primary coolant in the HI-SMUR is 344 degrees Celsius.[3] This can be seen highlighted in red in Table 5.2.

Table 5.2. Assembly outlet temperature analysis. Assemblies 1 and 2 are boiling.

Input Parameters	Value	Units
Assembly Mass Flow Rate	24.772813	kg/s
Specific Heat	4180	J/kg-K
Inlet Coolant Temperature	176.7	C
Heat Generation	13937500	W
Assembly 1	662	W/cm^3
Assembly 2	514	W/cm^3
Assembly 3	387	W/cm^3
Assembly 4	280	W/cm^3
Assembly 5	207	W/cm^3
Average	410	W/cm^3
Calculated Parameters	**Value**	**Units**
Average Outlet Coolant Temperature	311.29635	C
Assembly 1 OCT	**394.02386**	C
Assembly 2 OCT	**345.43786**	C
Assembly 3 OCT	303.74582	C
Assembly 4 OCT	268.61946	C
Assembly 5 OCT	244.65474	C
Inlet Coolant	176.7	C

Therefore, the density analysis was not performed as described. Instead, dimensionless power ratios were used to compare the modified and unmodified cores. This allowed a reasonable comparison to be made between the two cores without actually calculating the density values. Ratios were taken between the average assembly power and the actual assembly power for both the modified and unmodified cores. This can be seen in equation

$$\frac{Q_A}{Q_{AVE}} \tag{5.11}$$

where

Q_A power of the selected assembly

Q_{AVE} average assembly power

This ratio gives a measure of how much the power in each assembly is changing across the core. It is proportional to the density difference across the core because the mass flow rate was assumed constant and since the density differences could not be calculated, this method was used. These ratios were compared between the unmodified and modified cores. Presumably, if they are the same, a calculated mass flow rate for the modified core similar to that of the unmodified core should yield adequate heat transfer, regardless of certain assemblies being hotter. A plot of the assembly power ratios for the unmodified HI-SMUR core can be seen in Fig. 5.3.

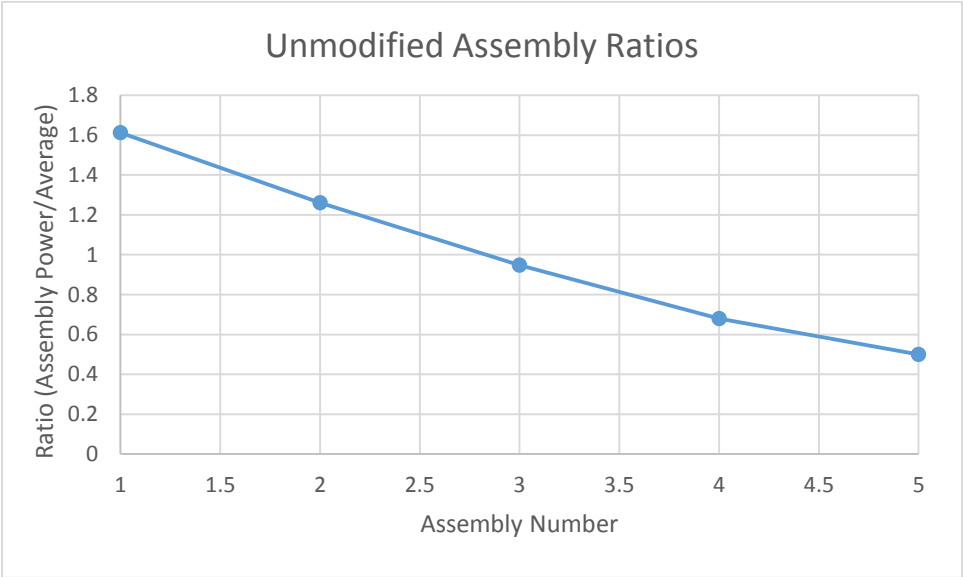

Figure 5.3. The unmodified HI-SMUR power ratios.

The ratios were also found for the modified HI-SMUR reactor core, the core of interest in this project. It was necessary to do this so that one could compare the differences in the modified core to those of the unmodified core that has been verified by Holtec to operate safely. The ratios can be seen in Fig. 5.4.

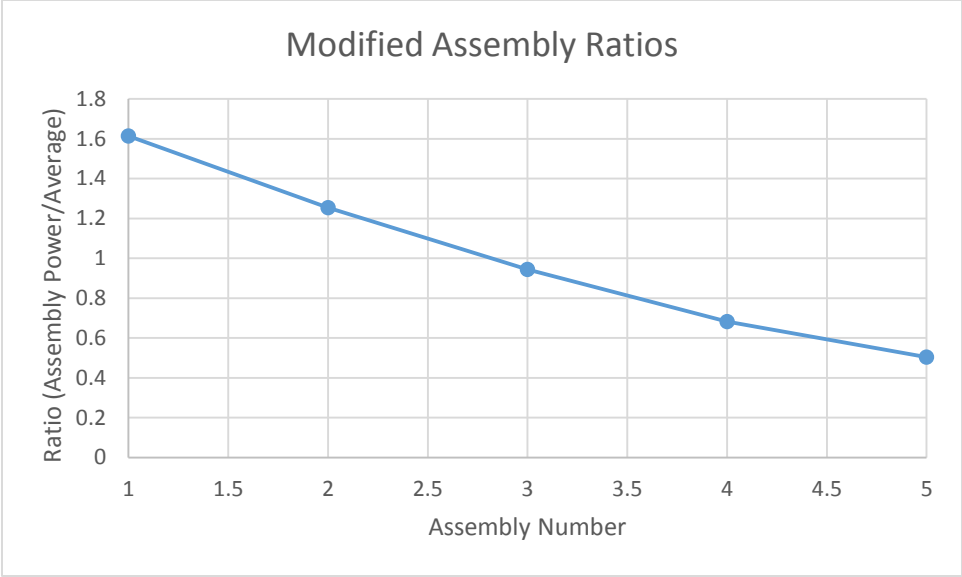

Figure 5.4. The modified HI-SMUR power ratios.

A differential plot was also created to more readily see what the differences are. This can be seen in Fig. 5.5.

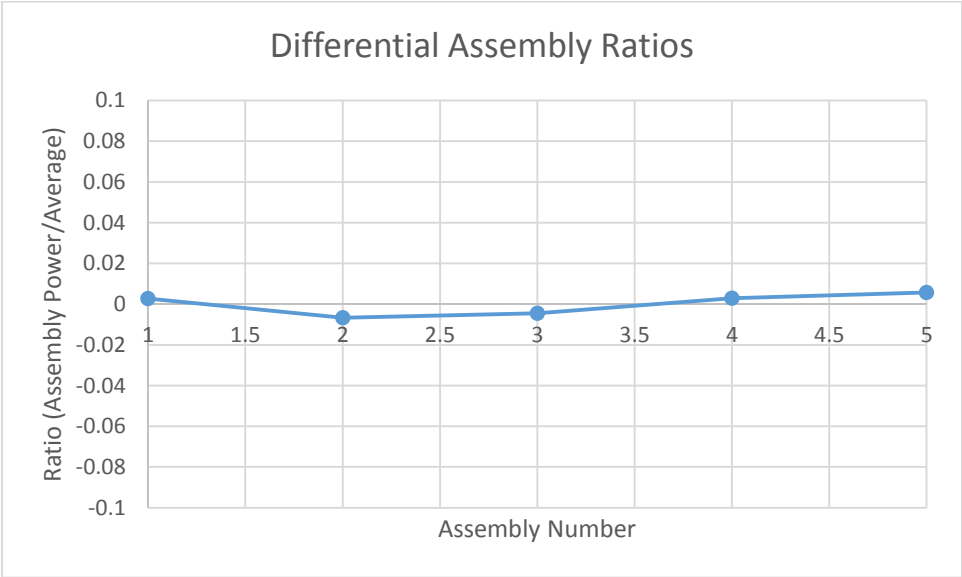

Figure 5.5. The differential HI-SMUR power ratios.

In an unmodified reactor and modified reactor, one can see that the differences between the two ratios are more or less negligible. This is a direct result of the uniform distribution of TPBARs throughout the reactor core, producing the same neutron flux distribution as the

unmodified reactor core. Since there are no striking differences between the unmodified and modified core, one may reasonably conclude that the addition of TPBARs would not have an appreciable effect on the mass flow rate beyond what has already been verified to safely operate in the unmodified HI-SMUR. Therefore, this particular issue has been resolved to some degree.

5.3.4 Future Work

Using this thermal hydraulic analysis, the TPBARs were determined to be a nonissue; however, it would be desirable to verify this result using RELAP or other reputable software. Also, a more accurate power distribution is needed to verify this analysis using the method described prior to the ratio analysis. Engineering intuition would suggest that the analysis should be sufficient, but it is always better to verify results if possible. Also, if experiments could be performed to verify the results, this would be ideal, although costly.

5.4 DNBR Analysis

5.4.1 Theory

The departure from nucleate boiling ratio (DNBR) is a quantity used to evaluate safety in the reactor core. It is a necessary thermal design limit which ensures that critical heat flux does not occur along fuel pins. If critical heat flux were to occur, a temperature excursion would result and there would be water vapor forming at a rapid rate in the primary side. This would result in huge problems for the reactor systems and likely a very severe accident. The pool boiling curve is useful to aid in understanding the departure from nucleate boiling phenomenon. The pool boiling curve can be seen below.

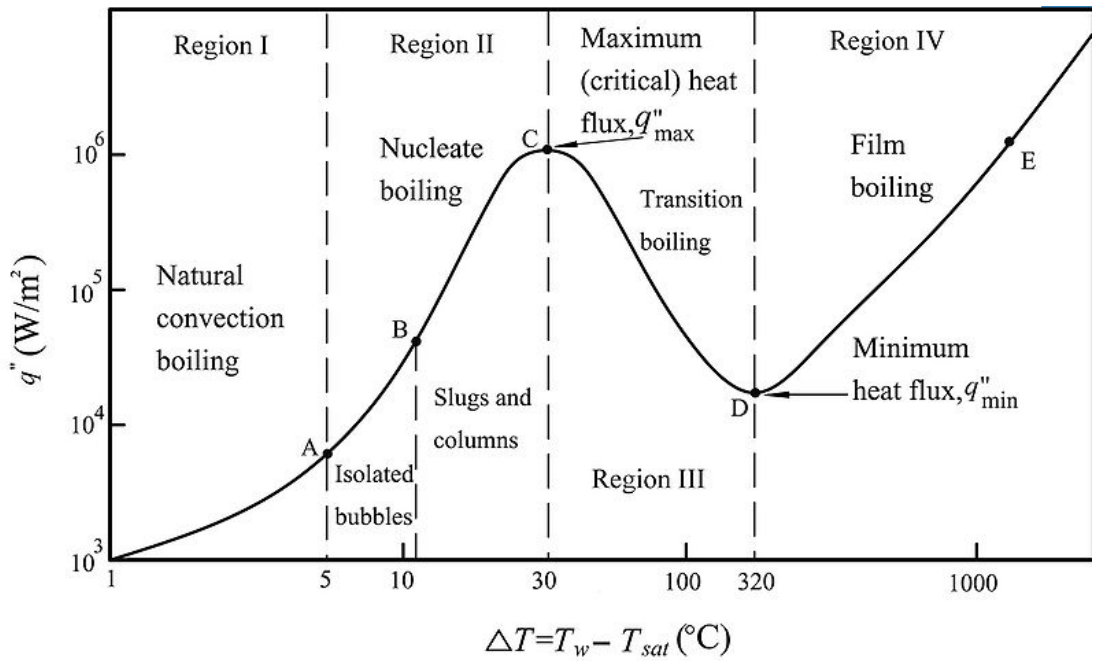

Figure 5.6. The pool boiling curve.[4]

Firstly, looking at the pool boiling curve, it is necessary to mention that in a PWR (i.e., the HI-SMUR), there is no boiling in the primary side. It is imperative; however, if boiling does occur to ensure that critical heat flux does not occur in the reactor. The critical heat flux position is denoted on the figure by C, and if the heat flux were to reach this point, there would be a temperature excursion in the reactor from point C to point E. The goal of maintaining an acceptable DNBR is to ensure that this never occurs.

The DNBR is defined as follows

$$DNBR = \frac{q''_{crit}}{q''_{actual}} \tag{5.12}$$

where

q''_{crit} critical heat flux (generally calculated by some empirical correlation)

q''_{actual} actual heat flux at this position in the core

As a result of the departure from nucleate boiling phenomena, it is necessary to calculate the critical heat flux for the HI-SMUR. Calculation of critical heat flux is typically done using the W-3 correlation.[4] The W-3 correlation is an experimental correlation derived by Westinghouse. The functional form of the W-3 correlation can be seen below:

$$\begin{aligned} q''_{crit} = \{&(2.022 - .06348p) \\ &+ (.1722 - .01427p)\exp[(18.177 - .5987p)x_e]\}[(.1484 \\ &- 1.596x_e + .1729x_e|x_e|)2.326G + 3271][1.157 \\ &- .869x_e][.2664 + .8357\exp(-124.1D_h)][.8258 \\ &+ .0003413(h_f - h_{in})] \end{aligned} \tag{5.13}$$

where

p	primary side pressure
x_e	local quality
D_h	heated diameter
G	mass flux
h_f	saturated liquid enthalpy
h_{in}	inlet enthalpy

This equation will be useful for calculating the critical heat flux for a given subchannel, using given inlet conditions.

5.4.2 Analysis

The DNBR was evaluated at the axial center of the core in the subchannel with the highest linear power. The axial flux distribution can be approximated by a chopped cosine wave, so it is assumed the peak is at the center of the core, although in reality it is slightly below the center due to density changes in the moderator as coolant rises through the core. The average

value of the cosine function will be used to calculate the peak heat flux, since the heat flux is in a cosine shape. The average value of the cosine function is calculated below.

$$\frac{1}{\pi}\int_{-\frac{\pi}{2}}^{\frac{\pi}{2}} \cos(x)\, dx = \frac{2}{\pi} \tag{5.14}$$

Using this, the peak heat flux could be found. The heat flux at the axial mid-plane of the fuel pin was found by dividing by the average flux by the average value of the cosine function, since the maximum value of the cosine function is 1. This can be seen in the equation below.

$$q''_{peak} = \frac{\pi}{2} q''_{ave} p_f \tag{5.15}$$

where

q''_{peak} peak heat flux

q''_{ave} average heat flux

p_f power peaking factor

The average heat flux must be calculated using the reactor power. The average rod power can be found by dividing the nominal thermal output of the reactor core by the number of fuel rods present in the core. The flux is subsequently found by dividing the average rod power by the surface area of the fuel pin. The peak flux in the hot channel can now be evaluated. This equation will be useful for calculating the DNBR.

5.4.3 Method

An excel document was used to calculate the DNBR. The flow for the spreadsheet is as follows:

- Define reactor conditions
    - Pressure
    - Hot channel linear power

    - Mass flow rate
- Obtain relevant quantities from steam tables
    - Inlet enthalpy
    - Saturated liquid enthalpy
    - Specific heat
- Calculate relevant quantities
    - Local coolant temperature
    - Local quality
- Calculate critical heat flux using the W-3 correlation
- Calculate the heat flux at the center axial location in the core
- Calculate DNBR and compare to an acceptable value (1.3 or above, typically want above 2)

5.4.4 Results

The DNBR value for the HI-SMUR was calculated. A sample calculation can be seen in Table 5.3.

Table 5.3. Calculated DNBR for hot channel in HI-SMUR core.

W-3 correlation	Calculated Value	Units
pressure	15.5	MPa
local quality	0	
equivalent heated diameter	0.00818	m
mass flux	797.6121183	kg/m^2-s
inlet enthalpy	756	kJ/kg
saturated liquid enthalpy	1630	kJ/kg
CRITICAL HEAT FLUX		
2641.466315	kW/m^2	
264.1466315	W/cm^2	
DNBR	**1.936647939**	
Fuel-Centered Flow Channel		
Flow Area	0.00010747	m^2
Heated Diameter	0.00818	m^2
Number of Pins	9248	
Mass Flow Rate	0.085719074	kg/s
Hot Channel		
Average Rod Power	50713.66782	W
Hot Rod Power	89256.05536	W
Rod Surface Area	1027.929116	cm^2
Hot Rod Average Heat Flux	86.83094384	W/cm^2
Hot Rod Peak Heat Flux	136.3937276	W/cm^2

This table shows the calculated DNBR for the HI-SMUR. The DNBR was found to be 1.936. According to the Nuclear Regulatory Commission, the minimum acceptable value for DNBR is 1.3.[16] Therefore, the HI-SMUR is currently within this limit and should be able to operate safely; however, one could see from the earlier analysis that according to the neutronics analysis the coolant will boil in the center of the core. This makes sense, because the only value that was taken from neutronics for this calculation was the power peaking factor, found to be 1.76. All other data was known values, while the density analysis was completely dependent on the output of the neutronics analysis, which has an inaccurate power distribution.

5.5 Temperature Analysis

5.5.1 Theory

In a commercial reactor core, it is not practical to measure fuel temperatures. The coolant temperature; however, is easily measured. Thankfully, one can work backward from the coolant temperature to determine peak fuel temperatures. To do this, one must analyze the conduction equation in cylindrical geometry.

$$\frac{1}{r}\frac{d}{dr}\left(kr\frac{dT}{dr}\right) + q''' = 0 \tag{5.16}$$

where

r	radius
k	thermal conductivity
T	temperature
q'''	volumetric heat rate

it is useful to define the linear heat rate as a function of the volumetric heat rate

$$q' = \pi R^2 q''' \tag{5.17}$$

where

q' linear heat rate

Similarly, Newton's law of cooling must be used to work backwards from coolant temperature.

$$\frac{dQ}{dt} = hA\Delta T_m \tag{5.18}$$

where

$\frac{dQ}{dt}$ rate of change of thermal energy

ΔT_m temperature difference between the wall and the mean coolant temperature

It is easy to evaluate this system by using the concept of thermal resistances. Thermal resistances are analogous to electrical resistances and allow for conduction problems to be solved in a familiar fashion. A thermal resistance circuit for a fuel rod can be seen in the figure below.

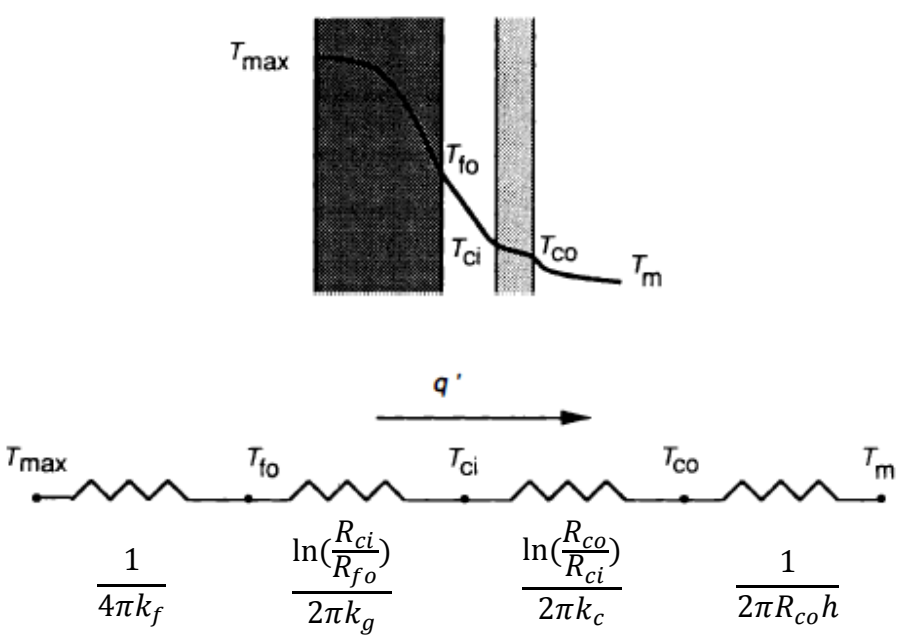

Figure 5.7. A thermal resistance circuit for a fuel rod.

This thermal resistance circuit can be used to obtain an equation for the maximum fuel temperature. The equation for maximum fuel temperature can be seen below.

$$T_{max} - T_m = q' \left[\frac{1}{4\pi k_f} + \frac{\ln\left(\frac{R_{ci}}{R_{fo}}\right)}{2\pi k_g} + \frac{\ln\left(\frac{R_{co}}{R_{ci}}\right)}{2\pi k_c} + \frac{1}{2\pi R_{co} h} \right] \tag{5.19}$$

where

T_{max} maximum fuel temperature

T_m mean coolant temperature

k_f thermal conductivity of the fuel

k_g thermal conductivity of the gas gap

k_c thermal conductivity of the cladding

h heat transfer coefficient of the coolant

R_{fo} outer fuel radius

R_{ci} inner clad radius

R_{co} outer clad radius

It is necessary to have a way to calculate the thermal conductivity of the fuel and the cladding. Similarly, one can calculate the maximum cladding temperature by removing the first two thermal resistance terms, the fuel and gas gap. Thankfully, correlations exist for such values in IAEA technical documents. The thermal conductivity of irradiated uranium dioxide is expressed as follows:

$$\lambda_f = \frac{100}{7.5408 + 17.692t + 3.6142t^2} + \frac{6400}{t^{\frac{5}{2}}} \exp\left(-\frac{16.35}{t}\right) \tag{5.20}$$

where

λ_f calculated thermal conductivity of the fuel

and

$$t = \frac{T_f}{1000} \tag{5.21}$$

where

T_f temperature of the fuel in Kelvin

This correlation allows one to iterate the thermal conductivity of the fuel as the temperature changes. Similarly, there exists an expression for the thermal conductivity of the cladding.

$$\lambda_c = 27.3952 + \frac{9687.1T_c - .126187 * 10^8}{(T_c - 1067.64)^2 + .397548 * 10^6} \tag{5.22}$$

where

λ_c calculated thermal conductivity of the cladding

T_c temperature of the cladding in Kelvin

This allows one to iterate the cladding thermal conductivity as its temperature changes until a convergent condition is reached.

All of the above quantities are known or calculated from reactor conditions. This becomes an iterative analysis because thermal conductivities are dependent on temperature. Values for the thermal conductivities of each material are assumed and iterations are performed until a convergent situation is realized. The mean coolant temperature is found using the energy balance described previously. The heat transfer coefficient of the coolant is unknown and must be found using empirical correlations for the Nusselt number. An empirical correlation for the Nusselt number could not be found for reactor conditions, so a correlation was chosen for free convection at a vertical wall. It is expected that the Nusselt number will not be correct, but the effect of changing the Nusselt number will be studied to ensure that this does not produce

terribly skewed results. Convection at a vertical wall is the closest correlation to what would be seen in a reactor from what is available. The correlation is as follows[5]:

$$Nu = 0.68 + \frac{.67Ra^{\frac{1}{4}}}{\left[1 + \left(\frac{.492}{\mathrm{Pr}}\right)^{\frac{9}{16}}\right]^{\frac{4}{9}}} \tag{5.23}$$

where

Nu	Nusselt number
Ra	Rayleigh number
Pr	Prandtl number

The governing equation for the Rayleigh number is below:

$$Ra = GrPr \tag{5.24}$$

where the calculation for the Grashof number in the reactor core was performed in the natural circulation analysis.

The Prandtl number is defined as follows:

$$Pr = \frac{c_p \mu}{k} \tag{5.25}$$

where

μ	dynamic viscosity

The Nusselt number can be calculated using the above correlation and then one can find the heat transfer coefficient for the coolant by the equation below.

$$Nu = \frac{hL}{k} \tag{5.26}$$

where

L characteristic length

The above theory allows one to calculate peak fuel temperatures using known values.

5.5.2 Analysis/Methodology

The governing equations for the temperature analysis were solved using an Excel spreadsheet. The flow for the spreadsheet is below.

- Read reactor conditions
    - Average coolant temperature
    - Grashof number
    - Specific heat
    - Dynamic viscosity
    - Thermal conductivity of coolant
    - Characteristic length of pipe
    - Thermal conductivity of gas gap
    - Thermal conductivity of cladding
    - Radii
    - Linear heat rate obtained from neutronics
- Assume a fuel thermal conductivity
- Calculate flow parameters
    - Prandtl number
    - Rayleigh number
    - Nusselt number
    - Heat transfer coefficient
- Calculate maximum fuel temperature

- Iterate on the fuel temperature and fuel thermal conductivity until a convergence
    - Convergence realized by using the Solver function in Excel

Table 5.4. The fully converged centerline fuel temperature.

Input Parameters	Calculated Value	Units
Average Coolant Temp	247.27	C
Grashof Number	4E+18	
Specific Heat	4180	J/kg-K
Dynamic Viscosity	0.000157	Pa-s
Thermal Conductivity of Coolant	0.635	W/m-K
Characteristic Length	4	m
Thermal conductivity of fuel	21.86	W/m-K
thermal conductivity of gas gap	0.28	W/m-K
thermal conductivity of cladding	25.89	W/m-K
outer fuel radius	0.475	cm
inner clad radius	0.48325	cm
outer clad radius	0.54045	cm
Thermal Power	469000000	W
Number of Pins	9248	
average rod power	50713.66782	W
hot rod power	140203.0839	W
Hot Rod Linear Heat Rate	35050.77098	W/m
Calculated Parameters		
Prandtl Number	1.033480315	
Rayleigh Number	4.13392E+18	
Nusselt Number	24127.00415	
Heat Transfer Coefficient	3830.161909	W/m^2-K
Maximum Fuel Temperature	**744.729492**	C
Maximum Cladding Temperature	**326.7990504**	C

Table 5.4 contains the fully converged centerline fuel temperature as well as the maximum cladding temperature. This value is useful when determining if the core operating conditions are within thermal margins.

5.5.3 Results

The calculated Nusselt number is very high. This is due to the fact that a correlation at the HI-SMUR reactor conditions could not be found. The maximum fuel temperature was found for a Nusselt number an order of magnitude less than the current Nusselt number, and the maximum fuel temperature rose by less than 50 degrees Celsius. It is determined that although the Nusselt number is incorrect, it is close enough to make reasonable conclusions about fuel centerline temperature. The maximum fuel temperature was found to be 745 degrees Celsius. A typical value for a PWR is 750 degrees Celsius.[12] The calculated maximum fuel temperature is slightly below the typical value, and it is still well below 1400 degrees Celsius, the temperature at which fission product gas release occurs. Therefore, it is determined that the maximum fuel temperature is within the thermal limits of a typical PWR, even if the Nusselt number was an order of magnitude wrong, the predicted fuel temperature would be less than 800 degrees Celsius. The fuel temperature has a profound effect on the cross section of the fuel, so the fuel temperature should be used to choose cross section libraries for use in the neutronics analysis. Similarly, the maximum cladding temperature was found to be 327 degrees Celsius. This is a low number; however, this is to be expected when the Nusselt number is an order of magnitude higher than it should be. A higher Nusselt number corresponds to a higher heat transfer coefficient of the fluid which causes the peak cladding temperature to decrease. Also, peaking factors from a more favorable neutronics analysis would need to be included to calculate absolute maximums.

5.5.4 Future Work

It would be desirable in future work to develop a full temperature map throughout the core to more accurately assess the neutronic behavior in the core. This analysis; however, should be sufficient to ensure safety within the core.

6. TRITIUM PRODUCTION

6.1 Overview (Written by Ryan Upton)

Tritium is produced by the decay of neutron-irradiated Lithium 6 as shown below.

$$^{6}_{3}Li + n \rightarrow {}^{4}_{2}He + {}^{3}_{1}Tritium \tag{6.1}$$

The purpose of a TPBAR is to successfully utilize this nuclear reaction to produce tritium. When inserted in a nuclear reactor the ^{6}Li will absorb neutrons and produce tritium. After the reaction occurs, the tritium must be captured, because it is a highly diffusive material, especially at reactor temperatures. Each TPBAR contains several lithium aluminate pellets enriched with ^{6}Li. The pellets are surrounded by a single nickel-coated Zircaloy-4 full length getter (FLG), which absorbs and reacts with the molecular Tritium during irradiation and forms a metal hydride. These getters prevent the tritium from diffusing into the coolant and allow future extraction of the tritium, the entire purpose of this project.

6.2 Decision Making Model (Written by Ryan Upton)

Optimization Factor	Tritium Production Weight	Cost Weight	Computational Weight	Factor Total
Number of TPBARs/Core	1.5	0.5	1	0.75
Thermal Flux (Position of TPBARS)	1.1	1	0.5	0.55
Number of Cores	1.5	0.25	1	0.375

Figure 6.1 Decision making model.

Originally it was determined that a technically rigorous decision-making model would be necessary to weight the various factors that we would be optimizing, however after initial calculations were performed it was discovered time would limit the amount of iterating we could do. This led to a significant simplification of the decision-making process, which is described in section 6.3.3.

6.3 Tritium Production Model

6.3.1 Theory (Written by Ryan Upton and Clay Strack)

The production of ^{3}T in the reactor can be modeled using a simple production and loss equation. The time rate of change of the number density of some element can be calculated by taking the production rate of this element and subtracting the loss rate. This can be seen in Eq. 6.2.

$$\frac{dN_T}{dt} = -\lambda N_T + \phi\, \sigma_a N_{Li} \tag{6.2}$$

where

N_{Li} atom number of ^{6}Li

N_T atom number of ^{3}T

ϕ thermal flux

σ_a thermal absorption microscopic cross-section

λ decay constant of ^{3}T

Similarly, the loss of ^{6}Li can be modeled with the equation

$$\frac{dN_{Li}}{dt} = -\Phi\sigma_a N_{Li} \tag{6.3}$$

Solutions to these differential equations exist, and allow for an accurate calculation of ^{3}T production and ^{6}Li depletion over some period of time. The number of ^{6}Li atoms available at any given time is as follows[17]:

$$N_{Li}(t) = N_{Li0}\exp(-\sigma_a \phi t) \tag{6.4}$$

where

$N_{Li}(t)$ lithium inventory at time t

N_{Li0} initial lithium inventory

t irradiation time

Similarly, an equation for the ^{3}T inventory can be found.[17]

$$N_T(t) = \frac{\sigma_a \phi N_{Li0}}{\lambda + \phi \sigma_a} [\exp(-\sigma_a \phi t) - \exp(-\lambda t)] \tag{6.5}$$

These equations can be solved as at any specified irradiation time to evaluate the amount of ^{3}T produced or the amount of ^{6}Li depleted.

The production and depletion of the relevant isotope inventories are of interest; however, the simple model presented above will not be sufficient to accurately calculate the tritium production rate. Lithium has a very large thermal absorption cross section, 945 barns, and this causes spatial self-shielding that cannot be neglected. The spatial self-shielding phenomenon can be understood in very simple terms. Lithium atoms near the outer radius of a TPBAR absorb thermal neutrons, causing the lithium atoms near the inner radius of the TPBAR to see a depressed thermal neutron flux. Due to the strong spatial self-shielding effects found within the TPBAR, a correction must be made for the thermal flux throughout the TPBAR. Radial flux values were found in the TPBAR. The derivation of this factor is provided in more detail in section 4.3.1.

6.3.2 Methodology (Written by Clay Strack and Laura Sudderth)

Although MCNP is capable of keeping decay product inventories during calculations, the long computing time of the program means it is simpler to calculate the ^{6}Li and ^{3}T inventories using basic production equations in Excel. The Excel program used inputs of ^{6}Li absorption cross section, half-life, and decay constant, as well as the initial atom number of ^{6}Li and the thermal flux, and gave values for the atom numbers of ^{6}Li and ^{3}T after the first sixty seconds, the first hour, and first day of full power operation, followed by time-steps of 1 week over a ~3 year time period. By changing the values of the thermal flux and atom number of ^{6}Li, which are

dependent on the position and number of TPBARs in each assembly, we use this program to iterate along with MCNP until the optimum configuration is reached using the process shown in Fig 6.2.

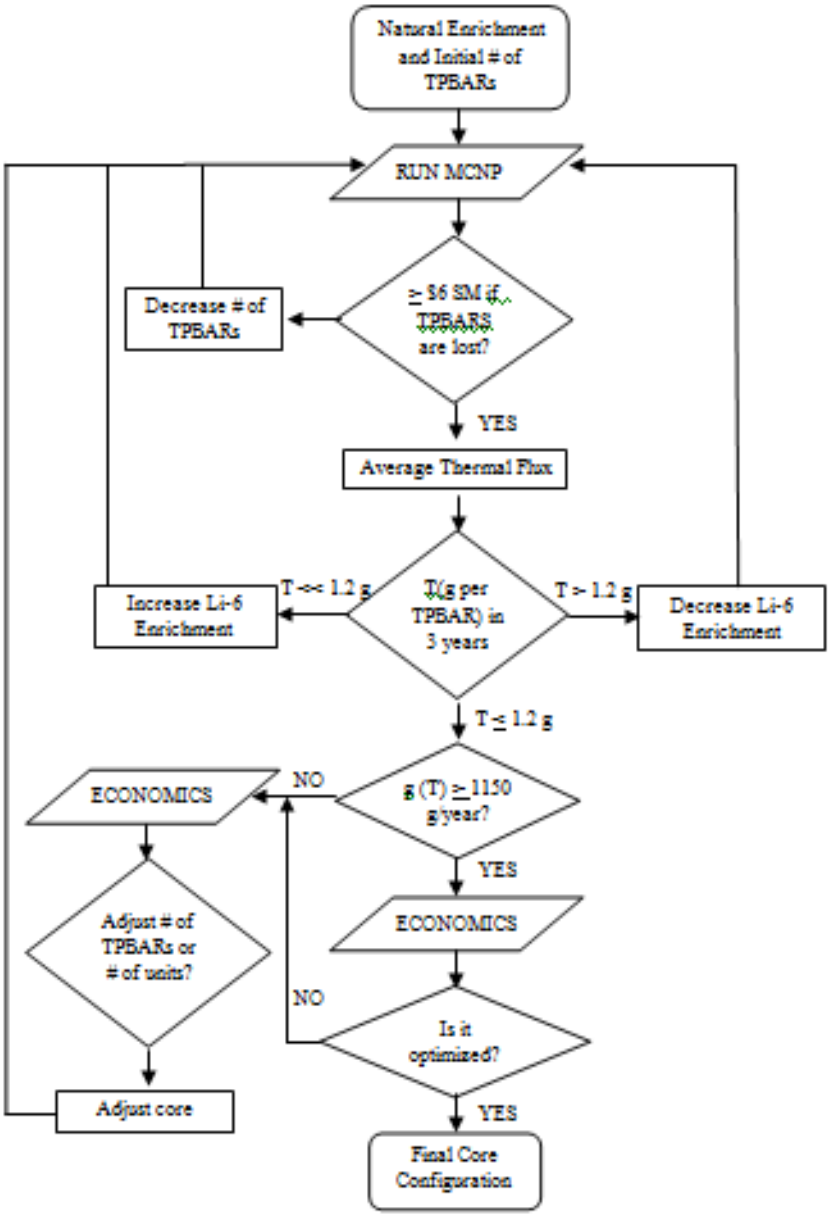

Figure 6.2. Tritium production iteration flow chart.

6.3.3 Results (Written by Laura Sudderth)

Due to the complex iteration process and integrated relationships of the parameters involved in determining the optimum configuration of the TPBARs in the core, and time constraints, the core was unable to be optimized. Instead, an approximation of the Li-6 enrichment was made to minimize the enrichment and remain below the limit of 1.2 g of tritium produced per TPBARs in the cycle lifetime of three years as discussed in Section 6.4. Next, a conservative estimate was made on the number of TPBARs each assembly could contain in order to remain below the safety limit of a minimum of $6 shutdown margin in the event of an accident in which the TPBARs are lost. The resulting estimate was 24 TPBARs per assembly. The lithium depletion and tritium production curves over the cycle lifetime are shown in Fig. 6.3.

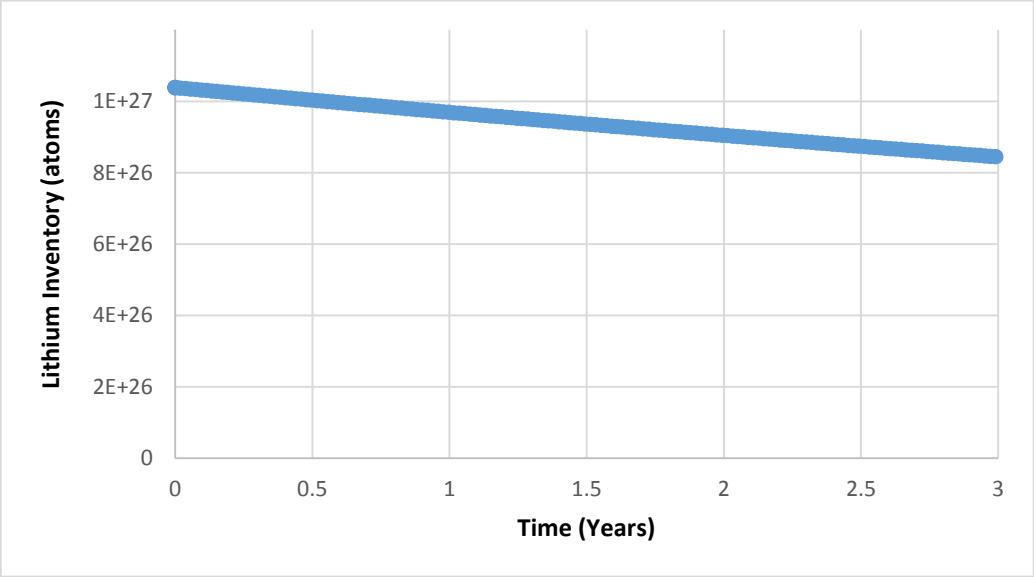

Figure 6.3. Graph of ^{6}Li inventories over 3 year cycle lifetime.

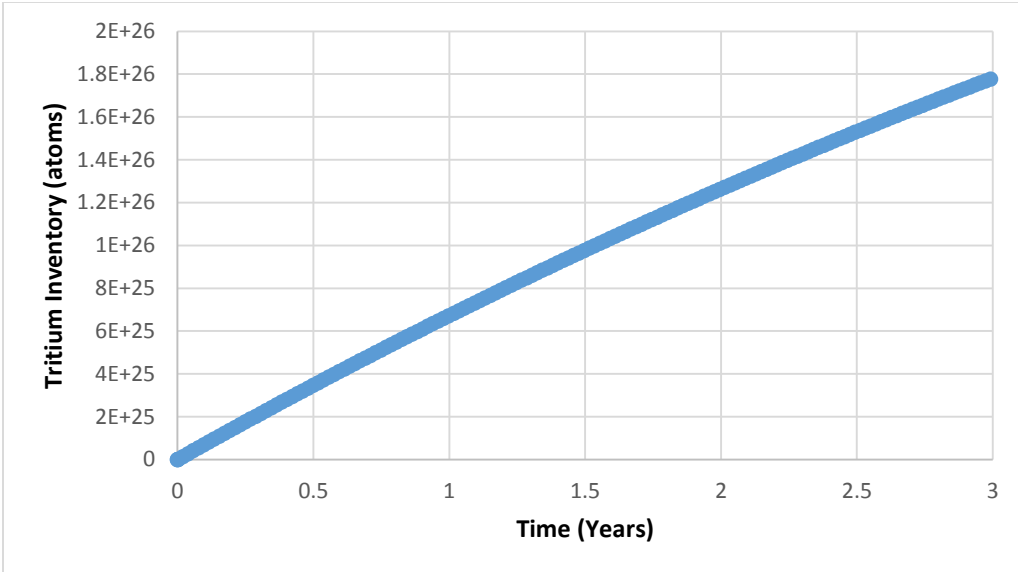

Figure 6.4. Graph of ^{3}T inventories over 3 year cycle lifetime.

The total amount of tritium produced in one unit and tritium per TPBAR produced over the cycle lifetime was calculated by Eqs. 6.6 and 6.7, respectively, where T_3 is the amount of tritium produced in three years and N is the number of TPBARs in each unit. The number of units required to meet the production goal and resulting amount of tritium produced per year were calculated using Eqs. 6.8 and 6.9, where t is the cycle lifetime. The results are listed in Table 6.1.

$$T_3\left(\frac{g}{unit}\right) = \frac{T_3\,(atoms)\,MW\left(\frac{g}{mol}\right)}{N_A\left(\frac{atoms}{mol}\right)} \tag{6.6}$$

$$T_3\left(\frac{g}{TPBAR}\right) = \frac{T_3\left(\frac{g}{unit}\right)}{N\left(\frac{TPBAR}{unit}\right)} \tag{6.7}$$

$$Number\ of\ Units\ Required = 1150\left(\frac{g}{year}\right) \times \frac{t\,(years)}{T_3\left(\frac{g}{unit}\right)} \tag{6.8}$$

$$Tritium\ Production\ Rate\ \left(\frac{g}{year}\right) = Number\ of\ Units \times \frac{T_3\ \left(\frac{g}{unit}\right)}{t\ (years)} \tag{6.9}$$

Table 6.2. Tritium Production Model Results

Quantitiy of Interest	**Value**
Average Thermal Flux (n/cm^2-s)	2.316E12
Number of TPBARs per Assembly	24
Li-6 Enrichment	12.2%
Tritium Produced per unit per cycle (g/unit)	890.01
Trtium produced per TPBAR per cycle (g/TPBAR)	1.16
Number of units required	3.88 (4)
Tritium Production Rate with 4 units (g/year)	1186.68

6.4 TPBAR Limitations (Written by Clay Strack)

Tritium diffusion out of the TPBAR into the reactor coolant and decay of tritium in the TPBAR are limiting factors associated with the TPBAR. Firstly, tritium diffuses from the TPBAR into the reactor coolant at a rate of ~0.04% of the tritium produced.[18] This is potentially problematic because tritium releases have been known to occur at nuclear power plants and they pose a threat to public safety. Tritium release limits; however, are a function of the reactor site, so this is well beyond the scope of this project. At best, the tritium diffusion could be taken into account in the tritium production model; however, the numbers that PNNL have modeled are an order of magnitude less than what is actually observed. Also, the fraction is so small it is neglected in the model and this introduces very little error.

Secondly, and more importantly, the decay of tritium presents a large technical challenge. Tritium decay is illustrated by the below equation:

$$ {}^{3}_{1}T \rightarrow {}^{3}_{2}He^{1+} + e^{-} + \overline{v_e} \quad (6.10) $$

As tritium decays in the annular TPBAR, ^{3}He gas builds up in the center of the TPBAR, causing a slow increase in pressure. The design limit for TPBARs is 1.2 grams of tritium, to curb this increase in pressure. If more than 1.2 grams of tritium are produced, there will be too much ^{3}He buildup in the TPBAR and this may cause failure. This limit was applied to the HI-SMUR design. The 1.2 grams of tritium production corresponds to 600 days of irradiation in WBN1; however, according to Dr. Senor, this 600 day irradiation limit is not absolute, while the 1.2 grams of tritium per bar is.

6.5 Cycle Length Effects (Written by Clay Strack)

With the current neutronics evaluation, the optimum cycle length for the HI-SMUR remains the full cycle length, 3 years. At 3 years, the TPBARs are still under the 1.2 grams of tritium per bar production limit and have produced a monotonically increasing amount of tritium over their lifetime. Cycle length effects are a very interesting and needed portion of future work on this project. There was insufficient time to study changing cycle length for various core configurations. As a result, it is recommended that cycle lengths be explored ranging from 1 year to 3 years, to determine the optimum cycle length for tritium production in this SMR.

6.6 Discussion and Future Work (Written by Laura Sudderth)

The results of the two methods used to estimate the tritium production rate are listed in Table 6.3. The results from the MCNP were expected to be higher than the results of the Tritium Production Model because it does not account for the depletion of Li-6. A this hold true, but the MCNP tally result is more than twice the amount calculated from the Tritium Production Model.

This large discrepancy should be further investigated to determine whether the results from the two methods are accurate or if one, or both, methods contain an error.

Table 6.3. Comparison of the tritium production rates.

Method	Tritium Production Rate (g/year-unit)
MCNP Reaction Tally	694.48
Tritium Production Model	296.67

In addition to method verification, future work required for the tritium production includes a more in-depth optimization of the core. As stated in Section 6.3.3, the core configuration used in the analysis is not the optimal configuration. Further analysis and iteration with neutronics, thermal hydraulics, and economics is needed in order to include spatial variation of TPBARs in the assemblies, varying the number of TPBARs in each assembly based on flux and energy distributions, and finally to determine the ideal number of TPBARs in each assembly, number of units, and Li-6 enrichment.

7. SAFETY

7.1 General Safety Design (Written by Kevin Kapka)

The HI-SMUR reactor is inherently safe. Due to its underground construction, and advanced nature, it has many advantages over a typical reactor. In terms of sabotage and other intentional damage, it is the spent fuel pool, and the entire pressure vessel are underground. According to Holtec the top level is even rated against missiles and commercial aircraft collisions[2] and earthquakes of greater magnitude than Fukushima. More importantly for the purpose of our analysis, HI-SMUR does not rely on any active components to circulate coolant

through the core. Instead, the flow of the reactor coolant through the reactor vessel, the steam generators, and other miscellaneous equipment occurs by the pressure head created by density differences in the flowing water in the hot and cold segments of the primary loop. The movement of the reactor water requires no pumps, valves, or moving machinery of any kind. For further examination of the mechanics behind natural convection, see section 5.2. The implications of these redundant systems will be described throughout this section.

7.2 Shutdown Margin (Written by Laura Sudderth)

The shutdown margin built into the core calculated in the neutronics analysis, was $54.25 at the beginning of life when the core contains the maximum amount of excess reactivity. The worth of a control rod was calculated to be $0.10. This shows that the core can be safely shutdown in the event of multiple control rod failures. In the event of TPBAR failure in which the TPBARs are lost and filled with water, the control rods can completely shut down the core with about a $29 shutdown margin. Therefore, even with TPBAR failure and multiple control rod failure, the core can still shutdown.

7.3 Safety Systems (Written by Kevin Kapka)

The reactor has multiply safety systems as seen on figure 3.1 The most important of these is shown in Figure 3.2 the shells of the steam generators and super heaters provide additional barriers against potential large-break LOCAs, along with the turning plenum that join the steam generators to the reactor vessel. All systems connected to the reactor vessel use a similar approach to ensure that there is no potential for a large-break LOCA that could rapidly drain the water from the reactor and uncover the core. In several of the systems, the cooling capability is reversible. I.E., if one of the legs broke, surviving one could become the inlet from the ADS. There are zero pressure vessel penetrations below the core. As long as the core is covered under

all potential conditions of operation and hypothetical accident, the release of radioactive material to the public is minimal. The Core Damage Probability (CDP) of HI-SMUR will be less than the probability level defined as non-credible in the regulatory literature (1E-06). Even with that, the reactor has a myriad of backup safety systems, just in case that break does happen.

7.3.1 Reactor Wells

The first, and most failure resistant of these is that the reactor well in figure 3.3 stays flooded during power operations. This is to assist in the passive cooling in the event of a non-mechanistic failure. Because of this, it is relatively safe to assume that a fuel burn through is almost impossible. Without the dimensions of his reactor well though, the exact cooling capacity cannot be calculated. The reactor also has several backup safety systems.

7.3.2 Spent Fuel Pool/Transfer Pool

In Fig. 3.1, the large space that is labelled as the spent fuel pool and transfer pool is flooded whenever a refueling occurs. In case of a disaster that makes the subterranean systems somehow incapacitated, on-site water tanks can fill up the gap from the top of the spent fuel pool tank, to the head of the reactor vessel.

7.3.3 HPCIS

The first of these backup systems is the HPCIS. This stands for high pressure core injection system. It is labeled as the ECCS in figure 3.2. It is used to inject borated water at high pressure into the reactor core via nitrogen tanks. This is normally the first line of defense, and in the HI-SMUR reactor, it can fill the reactor from empty to the top of the fuel[2].

7.3.4 ADS

The next feature is the ADS, or automatic depressurization system. It is the reactor blow-down system that opens a valve in the reactor vessel block to allow water and steam to escape through a pipe in the into the in-containment reactor water storage tank. The water/steam mixture is cooled and the steam is condensed by the large volume of water in water storage tank. It is approximately 300,000 gallons. This prevents high pressures and temperatures, allowing the other backup cooling systems to activate[2]. This system can actually keep the reactor post shutdown passively cooled for hours with no re-circulation.

7.3.5 Passive Heat Rejection System

The PHRS[19] uses a kettle re-boiler that removes heat from a depressurized reactor for an extended time period. This system is always connected to the reactor coolant system so that it can be used quickly in an emergency. Heat is removed by flowing water over the internal primary coolant tubes, making steam. The steam is piped through the reactor containment to an air-cooled heat exchanger at the base of a tall chimney. This system can also run through the Residual Heat Removal system shown in Fig. 3.2

7.4 Reasonable Failures (Written by Kevin Kapka)

In the case of a small break LOCA, one of the previously mentioned systems, most likely the ADS, and the HPCIS. Since the reactor operates at roughly 575 deg. F, and the response systems here are so redundant, and so fast, it is safe to assume that the cladding of the TPBAR will stay under the TPBAR in Figure 7.1.

7.5 Non Mechanistic Failures (Written by Kevin Kapka)

Since one of the primary sales points for these reactors is their ability to be "put anywhere", and their ability to use passive hair cooling systems, it is arguable that they are at a slightly elevated risk for non-mechanistic failures. Sabotage, terrorism, and celestial body impact all fall under these scenarios. In every small break LOCA scenario, it is reasonable to assume, due to the passive nature of the systems, and the reversibility of some systems, that as long as the pressure vessel is not bone dry, the core will stay well below 1000C and the TPBAR burst curve. RELAP5 models were attempted to show these scenarios, but the model of RELAP that students have access too is not very reliable at passive cooling. Rough answer could be calculated given more data and dimensions, but HOLTEC has not disclosed the capabilities of these backup systems. However, based on the amount of water that the reactor vessel is sitting in and around, this seems highly unlikely. Here we will discuss non-mechanistic incidents, and their possible consequences.

7.5.1 A Completely Dry Reactor

Since this reactor is entirely passively cooled; it is difficult to assess this scenario. There are over 500,000 gallons sitting in a pool that can be immediately dumped into the reactor, it is possible that somehow this would run out. If, both legs broke, and if containment failed so that the reactor could not force circulation throughout the building, then it is possible for the internal components to start melting. In an utterly dry situation, it would also burst the TPBARS, since they are right in the assemblies with the fuel rods.

7.5.2 LBLOCA Large Break Loss of Coolant Accident

A Large Break Loss of Coolant can only happen in a reactor like this as a means of sabotage. In normal operation, there are no valves to operate, nothing to turn on and off and legs

are strongly built into the reactor vessel. The ADS system is actually built so that it can use either leg as an input. This too could also be sabotaged though. In that case, the reactor would boil the water out, until it ran dry, albeit at a slow rate. The response of this passive cooling system to an environment where there is no water coming in is not well understood. Worth mentioning however, is that the external condensate can flood that entire room in severe circumstances, making a double break LOCA potentially irrelevant.

7.5.3 LOFA

An interesting proposal is what would happen to reactors such as these if the temperature gradient ceased to exist, since that is what is driving these reactions. Worth noting, that if the all of the water was somehow the same temperature, and drained of all of its momentum, then it would quit moving. However, if there was still a condenser or residual heat removal system, then it would begin cooling again, due to the gradient between that point, and the fuel. If there was not, the water would become heated, rise, run through the piping, and back in. Eventually, the entire water supply would reach a temperature at which it was at steady state with the fuel cladding, assuming perfectly insulated piping.

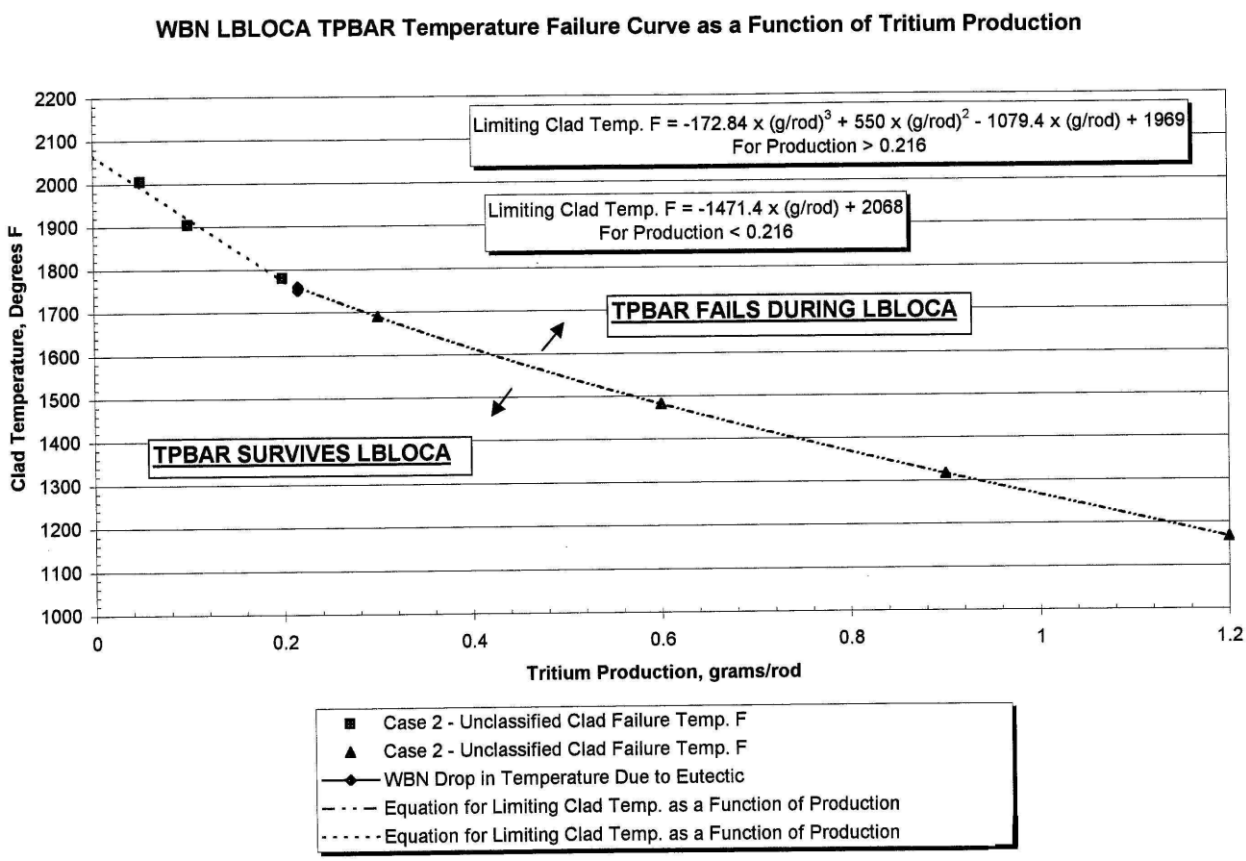

Figure 7.1. A graph of the burst rate for TPBARs versus tritium production.[1]

7.6 TPBAR Bursting (Written by Kevin Kapka)

As shown in figure 7.1, once the cladding of TPBARs reach a certain temperature they burst. In the event of TPBAR failure in which the TPBARs destroyed in the most flux critical part of the reactor, the control rods can completely shut down the core with about a $29 shutdown margin. This is $23 dollars more than the NRC set standard. With most small LOCA's this reactor's operational temperature is so high, it is safely estimated that the reactor vessel will not jump to 1200 Fahrenheit from a roughly centerline temperature of 462 Fahrenheit as long as the water is flowing, and that the various emergency heat dump systems are still connected. If, and when the TPBAR burst is a function of the material of the pipe and how much water is in

circulation. These assumption are verified by the Experimental MASLWR[20] and that even at lower power levels, the reactor maintains a very strong mass flow rate. However, in the scenario that there is no more flow, this becomes problematic, because the reactor could flush its own thermal reserves quickly.

7.6.1 TPBARs reaction to LBLOCAs and an attempt at generating actual numbers.

In the event of a double break in which external flooding is prevented, the reactor would start boiling out its water. While the assemblies stayed submerged, the cladding of the TPBAR would potentially be cooled by the water, but the radiative heat from the fuel rods. However, that radiation heat transfer would also be decreased by the water flowing through. Assuming there was water in the outer barrel when the breaks happened, as water boiled out, the cooler water would flow in from the bottom. The exact dimensions of the barrel, and the flow rates response to lower power loadings would need to be done. As shown by this extensive project at Oregon State[22], RELAP is by no means perfect in this case. For the sake of the practice, nominal values were chosen in a rough assumption that the images of the reactor vessel are drawn to size, and that the curve of flow rate matched the curve here[22]. The slope of that curve was taken, normalized to our reactor, and a value of 1.6% flow rate reduction from 40% of full load, per 1% power drop from 25% power at full load. This same model implies that our reactor would have a mass flow rate of 68 gallons per second at decay heat. This may not be reliable, because this is comparing a ~400 kW reactor to a ~ 450 Mw reactor. Other issues with this assumption are gone into in great detail by Dr. Woods of Oregon State, and Jordan Bowser in a Master's Thesis[23] written about a potential blow down at the MASLWR[23].

7.6.2 Double Leg Break Disaster

It is worth calculating the cladding temperature in a double leg break scenario. Here, I will argue that in a double leg break, with no attention and no water is added to the vessel, that it would eventually cause the cladding to exceed the right hand burst limit of 1100 F. If the reactor is safely scrammed, and both legs are broken, the reactor would burn through its own holding of 42,000 gallons at a flow rate of 68 gallons per second. The reactor would run out of water in 10 minutes. However, one of the things driving circulation, is the gravitational forces of the water in the shroud. It is safe to assume that the flow would drop dramatically without these forces, but how much so cannot be reasonably determined further modelling of a double leg break would be useful.

7.7 Thermal Margin (Written by Clay Strack)

Overall, the thermal hydraulics analysis yielded promising results. The mass flow rate for the modified HI-SMUR is within 5% of the unmodified core. The fuel centerline temperature is below the common limit for PWRs. The DNBR is well above 1.3, which is the common limiting value. Also, there are no appreciable effects on the mass flow rate from adding TPBARs to the reactor core. Thermal margin is maintained during steady state. In future work it would be desirable to determine if thermal margin is maintained during startup, shutdown, and typical expected transients. Also, analyzing accident scenarios would be desirable. Especially to see the effects of natural circulation.

7.8 Tritium Diffusion (Written by Ryan Upton)

Significant testing has been done by PNNL on the release of tritium from TPBARs in reactors as well is in spent fuel pool and dry canister storage. As shown below in figure 7.1, in all cases the release was well below NSC safety standards for non-defective TPBARs.

In-Reactor Permeation (at ~600 F)	In-Reactor Release from Defective TPBARs	Spent Fuel Pool Accident Releases (<200°F)	Tritium Releases from TPBARs in Storage Canisters (<200°F)
Less than 0.53 mCi per TPBAR per hour	Released as it is generated	The Tennessee Valley Authority take-action limit of 60 microcuries per ml of spent fuel pool water will not be exceeded following the simultaneous breach of up to 24 TPBARs. The best estimate total tritium release in this event is less than 25% of the total TPBAR tritium inventory. The release rate will be < 3% (of initial inventory) per hour. The instantaneous release of tritium from breached TPBARs (as gas within the released gas from the TPBARs) will not exceed 0.001 Ci/TPBAR. The concentration of lithium and aluminum in the spent fuel pool following a 24-TPBAR breach will not exceed 400 ppb and 50 ppb, respectively.	Tritium partial pressure within storage canisters containing LTA TPBARs and sections will not exceed 25 torr. Tritium release from extracted TPBARs will not exceed 1% of the declared tritium residual.

Figure 7.1 Summary of various ^{3}T release scenarios[21].

7.9 Shielding (Written by Kevin Kapka)

Since this reactor is buried deep underground as shown in figure 3.1, shielding is difficult to calculate. As far as shielding inside the facility, due to the lack of actual data that we had about the inside of the structure, we felt that modelling and analyzing the shielding was not the best use of our time.

7.10 Non-Proliferation

As shown by the documentation that HOLTEC has provided, this reactor, due to its underground nature, the "cartridge design"[1], which can supposedly only be opened by them, this reactor is fairly non-proliferation friendly. More study needs to be done on the ability for fuel to be taken from the cartridges.

7.11 Future Work (Written by Kevin Kapka)

The vast majority of this semester was spent proving that the student version of RELAP is inadequate at natural circulation models. RELAP could not even get a reactor like ours to exist

in its “multiphysical space”. As such one is forced to draw a lot of assumptions, because the only answers attained were ones that were obviously wrong. A lot of work needs to be done in this field. The accidental responses of passive cooling systems is not well understood [20] and it is something that IAEA is actively investing in. An accurate model for this type of reactor’s response to isolation, a “double break” needs to be developed instead of just being assumed to be impossible.

8. ECONOMICS (WRITTEN BY CLAY STRACK)

An economic analysis is of interest for any practical design to be considered. The Holtec documents contain an estimate for the HI-SMUR from 2011. They estimated that the selling price for the HI-SMUR would be $675 million.[2] This is an extremely useful number that will allow calculation of the present cost of the HI-SMUR. Since there already exists a selling price from a reputable source, it will only be necessary to correct for inflation since 2011 to obtain a very accurate approximate value for the HI-SMUR. Using the government inflation calculator, it is determined that the current cost of the HI-SMUR would be $698.51 million. For simplicity sake, it will be assumed that $700 million is a reasonable estimate. The breakdown for the cost of the HI-SMUR can be seen in Table 8.1

Table 8.1. 2011 HI-SMUR cost inflation corrected to 2013.

2011 HI-SMUR Cost	
Item	**Cost (in million dollars)**
Equipment and Systems	405
Site Construction	203
Management and Engineering	67
Total Cost	675
2013 HI-SMUR Cost	
Item	**Cost (in million dollars)**
Equipment and Systems	419.11
Site Construction	210.07
Management and Engineering	69.33
Total Cost	698.51

The only extra costs that will be incurred are from the addition of TPBARs to the core. An Excel document was created to determine the differential cost between a HI-SMUR core with TPBARs and a HI-SMUR core without TPBARs. According to Dr. Senor, a representative value

for the cost of components and assembly for a TPBAR is $10000. This will be the value assumed in this analysis. The results can be seen in Table 8.2.

Table 8.2. The cost of the HI-SMUR with TPBARs.

HI-SMUR	
Quantity of Interest	**Value**
Price of HI-SMUR	$700,000,000.00
Price of TPBAR	$10,000.00
Number of TPBARs per core	768
Number of Units	4
Total Number of TPBARs per cycle	3840
Cycle Length	3 years
Price of TPBARs per cycle	$30,720,000.00
Price of TPBARs per year	**$10,240,000.00**

It is of use to compare these numbers to those of WBN1 to see if this is an economically feasible alternative to a commercial PWR.

Table 8.3. The cost of the TPBARs in WBN1.

WBN1	
Quantity of Interest	**Value**
Price of TPBAR	$10,000.00
Number of TPBARs per core	1696
Number of Units	1
Cycle Length	18 months
Price of TPBARs per cycle	$16,960,000.00
Price of TPBARs per year	**$11,306,666.67**

As one can clearly see, operating multiple HI-SMURs for tritium production is less expensive per year in terms of TPBAR cost. Also, it is useful to calculate profit values per year. Given that WBN1 makes $1,000,000 per day, in one year WBN1 will have a profit of $365,000,000. Similarly, a HI-SMUR core is rated for 15% of the power that WBN1 so it can be assumed that the HI-SMUR would produce $150,000 worth of electricity per day. There will be 4 units

operating, so the HI-SMURs would net a profit of $219,000,000 per year. From this analysis, it is quite clear that continuing to produce tritium in commercial PWRs is the economically responsible thing to do. The cost differential over the lifetime of the plant was calculated. Essentially, choosing to build SMRs for tritium production instead of a commercial PWR would net a differential of $8,696,000,000 in electricity production. However, electricity production is not the main goal of this project, so that is not to say this is not a feasible means of tritium production.

9. RECOMMENDATIONS (WRITTEN BY CLAY STRACK)

From a purely economic standpoint, producing tritium in a HI-SMUR is more expensive than the current method of production. Although this is the case, there are several benefits of using a SMR as opposed to a commercial LWR. One benefit is that building SMRs would present a dedicated tritium production plant and electricity generation will be a secondary consideration. To produce an acceptable amount of tritium, multiple units will be necessary which will preclude any single point failure in the supply chain. Also, the incremental cost will be much lower because adding SMRs is an order of magnitude less expensive. SMRs are being actively considered by many utilities and are at the forefront of the industry. Also, it is likely that the first SMRs will be on federal property, which would lend itself well to a governmental tritium production program. Overall, it is the recommendation of this project that SMRs are a viable means of tritium production. It may be more expensive than the current method of production; however, the advantages of SMRs should offset this cost.

10. CONCLUSIONS (WRITTEN BY CLAY STRACK)

This project designed an optimized core configuration for tritium production in the HI-SMUR. The neutronics analysis designed and optimized a HI-SMUR reactor core with TPBARs. The thermal hydraulic analysis verified that natural circulation can successfully cool the core and maintain thermal margin. All thermal values were found within constraints using the base HI-SMUR case, while temperatures in the neutronic model were found to boil the coolant. The tritium production model successfully modeled the rate of tritium production over the course of the core cycle. The safety analysis ensured that all core parameters were within NRC limits. The LOCA analysis proved that the TPBARs would not fail in an any mechanistic accident scenario, so the reactor could still maintain shutdown margin. The economic analysis showed that producing tritium in a HI-SMUR will be more expensive than current methods; however, various advantages to SMRs may make this the favorable alternative. As a whole, the project was successful at making a supported recommendation on the viability of the HI-SMUR for tritium production and the majority of the project goals were reached.

11.ACKNOWLEDGEMENTS

This project was performed under the advisement of Dr. Karen Vierow and Dr. David Senor. The successful completion of this project would not be possible without them. Thank you!

12. REFERENCES

1. Senor, D. J., and D. M. Paxton. "Tritium Technology Program: Overview and SMR Design Challenge." NUEN 410 Class. Texas A&M University. 7 Sept. 2012. Lecture.
2. Holtec International. “HI-SMUR Technical Bulletin.” May 20, 2011. Obtained from Dr. Dave Senor, Pacific Northwest National Laboratories. January 2013.

3. Anton, Stefan. "HI-SMUR 140." Speech. *Presentation to NRC*. Jupiter, FL: Holtec International, 2011.
4. AP1000 Design Control Document. http://www.nrc.gov/reactors/new-reactors/design-cert/ap1000/dcd/Tier%202/Chapter%204/4-3_r14.pdf
5. Karriem, Zain. *Non-Proprietary Data for Modeling the NuScale Reactor*. NuScale Power, 2012.
6. *Tritium Target Qualification Project- Description of the Tritium-Producing Burnable Absorber Rod for the Commercial Light Water Reactor*. Rep. no. TTQP-1-015 Revision 5. Pacific Northwest National Laboratory, 1999.
7. *Tritium Technology Program- Production TPBAR Inputs for Core Designers*. Rep. no. TTQP-1-116 Revision 15. Pacific Northwest National Laboratory, 2012.
8. X-5 Monte Carlo Team. *MCNP - A General Monte Carlo N-Particle Transport Code, Version 5 - Volume 2: User's Guide*. Rep. no. LA-CP-03-0245. Los Alamos National Security, LLC, 2003.
9. X-5 Monte Carlo Team. *MCNP - A General Monte Carlo N-Particle Transport Code, Version 5 - Volume 1: Overview and Theory*. Rep. no. LA-UR-03-1987. Los Alamos National Security, LLC, 2003.
10. International Atomic Energy Agency. "Natural circulation in water cooled nuclear power plants." November 2005. Online. Accessed January 2013. http://www-pub.iaea.org/MTCD/publications/PDF/te_1474_web.pdf
11. B.T. Swapnalee, P.K. Vijayan. "A generalized flow equation for single phase natural circulation loops obeying multiple friction laws." International Journal of Heat and Mass Transfer. February 24, 2011.

12. Neil E. Todreas, Mujid S. Kazimi. “Nuclear Systems – Volume 1.” Taylor and Francis Group, LLC. 2012.
13. DeWitt, David P. “Fundamentals of Heat and Mass Transfer – 4th Edition.” New York: Wiley. 2000.
14. “Grashof number.” Princeton University. Online. 23 April 2013. <http://www.princeton.edu/~achaney/tmve/wiki100k/docs/Grashof_number.html
15. “Thermophysical properties database of materials for light water reactors and heavy water reactors.” International Atomic Energy Agency. June 2006. 23 April 2013. <http://www-pub.iaea.org/MTCD/publications/PDF/te_1496_web.pdf>
16. “Introduction to Reactor Technology – PWR.” U.S. NRC. 23 April 2013. <http://pbadupws.nrc.gov/docs/ML1215/ML12159A222.pdf>
17. R.M. Mayo. “Introduction to Nuclear Concepts for Engineers.” American Nuclear Society 1998.
18. “Backgrounder on Tritium, Radiation Protection Limits, and Drinking Water Standards.” Nuclear Regulatory Commission. February 2011. 23 April 2013. <http://www.nrc.gov/reading-rm/doc-collections/fact-sheets/tritium-radiation-fs.html>
19. “HI-SMUR 140: A safe, Secure, Economic, Small, .Modular Reactor.” U.S. Women In Nuclear. Online.25 April 2013.< <http://www.uxc.com/smr/Library/Design%20Specific/SMR-160%20(HI-SMUR)/Presentations/2011%20-%20HI-SMUR%20140%20-%20A%20Safe,%20Secure,%20Economic%20Small%20Modular%20Reactor.pdf>

20. “Passive Safety Systems and Natural Circulation in Water Cooled Nuclear Power Plants.” International Atomic Energy Agency. Online. 26 April 2013. <http://www-pub.iaea.org/MTCD/publications/PDF/te_1624_web.pdf>
21. *Tritium Technology Program- Unclassified TPBAR releases. Including Tritium.* Rep. no. TTQP-1-091 Revision 14. Pacific Northwest National Laboratory 2012.
22. MASLWR Overview and RELAP5 Simulation. Garret Ascherl. Oregon State University. Online. 2013<http://ir.library.oregonstate.edu/xmlui/bitstream/handle/1957/29308/MASLWR%20ANS%20Presentation%20Ascherl_Owen_Woods.pdf?sequence=1>.
23. RELAP5-3D Modelling of ADS blow down of MASLR facility. Bowser, C. Oregon State University. June12, 2012. Online. April 28 2013.,<http://ir.library.oregonstate.edu/xmlui/bitstream/handle/1957/30438/Thesis_Bowser_NE.pdf?sequence=1>